

GOVERNMENT OF INDIA
DEPARTMENT OF ARCHAEOLOGY
CENTRAL ARCHAEOLOGICAL
LIBRARY

CLASS _____

CALL No. **624,177** **Nov**

D.G.A. 79.

\$12.50

STRUCTURAL DESIGN FOR DYNAMIC LOADS

McGRAW-HILL CIVIL ENGINEERING SERIES

HARMER E. DAVIS, *Consulting Editor*

- BABBITT · Engineering in Public Health
BABBITT AND DOLAND · Water Supply Engineering
BENJAMIN · Statically Indeterminate Structures
CHOW · Open-channel Hydraulics
DAVIS, TROXELL, AND WISKOCIL · The Testing and Inspection of
 Engineering Materials
DUNHAM · Foundations of Structures
DUNHAM · The Theory and Practice of Reinforced Concrete
DUNHAM AND YOUNG · Contracts, Specifications, and Law for Engineers
GAYLORD AND GAYLORD · Structural Design
HALLERT · Photogrammetry
HENNES AND EKSE · Fundamentals of Transportation Engineering
KRYNINE AND JUDD · Principles of Engineering Geology and Geotechnics
LINSLEY AND FRANZINI · Elements of Hydraulic Engineering
LINSLEY, KOHLER, AND PAULHUS · Applied Hydrology
LINSLEY, KOHLER, AND PAULHUS · Hydrology for Engineers
LUEDER · Aerial Photographic Interpretation
MATSON, SMITH, AND HURD · Traffic Engineering
MEAD, MEAD, AND AKERMAN · Contracts, Specifications, and
 Engineering Relations
NORRIS, HANSEN, HOLLEY, BIGGS, NAMYET, AND MINAMI · Structural
 Design for Dynamic Loads
PEURIFOY · Construction Planning, Equipment, and Methods
PEURIFOY · Estimating Construction Costs
TROXELL AND DAVIS · Composition and Properties of Concrete
TSCHEBOTARIOFF · Soil Mechanics, Foundations, and Earth Structures
URQUHART, O'ROURKE, AND WINTER · Design of Concrete Structures
WANG AND ECKEL · Elementary Theory of Structures
WILBUR AND NORRIS · Elementary Structural Analysis

STRUCTURAL DESIGN FOR DYNAMIC LOADS

CHARLES H. NORRIS

Professor of Structural Engineering

ROBERT J. HANSEN

Professor of Structural Engineering

MYLE J. HOLLEY, JR.

Professor of Structural Engineering

JOHN M. BIGGS

Associate Professor of Structural Engineering

SAUL NAMYET

Assistant Professor of Structural Engineering

JOHN K. MINAMI

*Professor of Structural Engineering
Waseda University, Tokyo, Japan*

ALL

AT THE

MASSACHUSETTS

INSTITUTE

OF TECHNOLOGY

10893



McGRAW-HILL BOOK COMPANY, INC.

New York Toronto London

1959

STRUCTURAL DESIGN FOR DYNAMIC LOADS

Copyright © 1959 by the McGraw-Hill Book Company, Inc. Printed in the United States of America. All rights reserved. This book, or parts thereof, may not be reproduced in any form without permission of the publishers. *Library of Congress Catalog Card Number 58-11986*

II

47245

THE MAPLE PRESS COMPANY, YORK, PA.

10893
25.9.61
624.177/Nox

PREFACE

As explained in the Introduction, this book has been compiled from lecture notes prepared for a special two-week summer program surveying the field of Structural Design for Dynamic Loads. The program was planned for structural engineers principally interested in civil-engineering structures and was presented at the 1956 Summer Session of the Massachusetts Institute of Technology. The authors wish to emphasize that this book is not intended to be either a reference book or a textbook but simply a book surveying this field.

Blast-resistant design is one of the principal subjects covered herein. This material is a condensation of a portion of a manual prepared for the Office of Chief of Engineers, U.S. Army, under the supervision of three of the authors. The manual, entitled "Engineering Manual for Protective Construction, Part III, Design of Structures to Resist the Effects of Atomic Bombs," was prepared in part by the Massachusetts Institute of Technology under contract DA49-129-Eng-178 with the Office of the Chief of Engineers, U.S. Army.

Almost all the figures, charts, and tables in Chapters 7, 11, and 14 have been extracted from the manual although the text of these chapters is an abridgment of the manual presentation. Figures in Chapters 1 and 2 were also taken from the manual. Chapters 10, 12, and 13 involve material related to the manual but not used therein.

The authors take this opportunity to thank their friends, colleagues, and students who contributed in various ways to the preparation of this book. They are particularly indebted to Mrs. Bernice J. Donnelly and Misses Elizabeth P. Harris and Shirley V. Carlson, who collaborated in typing the final manuscript.

Charles H. Norris
Robert J. Hansen
Myle J. Holley, Jr.
John M. Biggs
Saul Namyet
John K. Minami

CONTENTS

<i>Preface</i>	v
<i>Introduction</i>	xv
PART 1. BEHAVIOR OF MATERIALS UNDER DYNAMIC LOADING	
1. Behavior of Steel and Steel Elements under Dynamic Loads, by John M. Biggs	3
1.1. Introduction	3
1.2. Design Properties	3
1.3. Dynamic Properties	5
1.4. Strength of Beam Sections	8
<i>a.</i> Bending Strength.	8
<i>b.</i> Shear Strength	9
<i>c.</i> Local Buckling	9
<i>d.</i> Lateral Buckling	10
<i>e.</i> Bending Resistance of I Beams in the Weak Direction	13
1.5. Strength of Axially Loaded Columns	13
<i>a.</i> Local Buckling	13
<i>b.</i> Lateral Buckling	13
1.6. Strength of Beam-columns	15
<i>a.</i> Capacity of Laterally Supported Beam-columns	15
<i>b.</i> Lateral Buckling of Beam-columns.	16
1.7. Connections	17
<i>a.</i> Welds	17
<i>b.</i> Rivets	17
<i>c.</i> Bolts	17
1.8. Fatigue	17
2. Behavior of Concrete and Concrete Structural Components under Dynamic Loading, by Myle J. Holley, Jr.	20
2.1. Introduction	20
2.2. Compressive Stress-Strain Properties of Plain Concrete.	21
<i>a.</i> Static Behavior	21
<i>b.</i> Behavior under Repeated Loading.	23
<i>c.</i> Behavior under Rapid Straining Rates.	23
2.3. Tensile Stress-Strain Properties of Concrete	24
<i>a.</i> Static Behavior	24
<i>b.</i> Behavior under Repeated Loading.	25
<i>c.</i> Behavior under Rapid Straining Rates	25

2.4. Shear Strength of Concrete	25
2.5. Stress-Strain Properties of Reinforcing Steel	25
a. Static Behavior	25
b. Behavior under Repeated Loading	26
c. Behavior under Rapid Straining Rates	27
2.6. Flexural Behavior of Reinforced Concrete	27
a. Static Behavior of Flexural Sections	27
b. Static Behavior of Flexural Members	31
c. Flexural Behavior under Repeated Loading	32
d. Flexural Behavior at Rapid Rates of Strain	33
2.7. Shear Behavior of Reinforced Concrete	34
a. Static Behavior	34
b. Dynamic Behavior	36
2.8. Behavior of Reinforced-concrete Columns	37
a. Behavior under Static Axial Load	37
b. Behavior under Static Eccentric Loads	38
c. Column Behavior under Repeated Loadings	39
2.9. Column Behavior under Rapid Strain Rates	40
2.10. Behavior of Reinforced-concrete Shear Walls and Deep Beams	40
a. Static Behavior of Shear Walls	41
b. Dynamic Behavior of Shear Walls	43
c. Shear-wall Openings	43
d. Strength of Deep Beams	43
2.11. Bond between Reinforcing Bars and Concrete	44

PART 2. CALCULATION OF RESPONSE OF STRUCTURAL SYSTEMS TO DYNAMIC LOADING

3. Dynamic Response of Systems Having One Degree of Freedom, by Charles H. Norris	51
3.1. Scope and Limitations of Application of Theory	51
3.2. Certain Fundamental Definitions	52
3.3. Undamped Free Vibration of One-degree System	55
3.4. Undamped Forced Vibration of One-degree System	56
3.5. Damped Forced Vibration of One-degree System	59
3.6. Dynamic-load Factor—Undamped One-degree System—Sinusoidal Dynamic Loading	61
3.7. Dynamic-load Factor—Undamped One-degree System—Various Typical Impulsive Loadings	64
3.8. Response Produced by Support Vibrations of Undamped One-degree System	69
3.9. Computation of Response Using Step-by-step Procedures	70
4. General Theory for Dynamic Response of Concentrated-mass Systems, by Charles H. Norris	73
4.1. General	73
4.2. Undamped Free Vibration of Two-degree Systems	74
4.3. Determination of Normal Modes of Vibration of Concentrated-mass Systems by Deflection Equations Involving Flexibility Coefficients	79
4.4. Determination of Normal Modes of Vibration of Concentrated-mass Systems by Equations of Motion Involving Stiffness Coefficients	83

4.5. Characteristic Loads and Important Properties of Shapes of Normal Modes of Vibration	84
4.6. Stodola's Procedure for Solving Equations Defining Normal Modes of Vibration	87
4.7. Use of Normalized Characteristic Loadings to Evaluate Effects Produced by Static Loading	92
4.8. Use of Normalized Characteristic Loadings to Evaluate Dynamic Response Produced by Dynamic Loading	95
4.9. Use of Normalized Characteristic Shapes to Evaluate Response Associated with Initial Motion of System	101
4.10. Solution of Reduced Equation of Motion	103
4.11. Recapitulation—Computation of Dynamic Response of Concentrated-mass Systems	103
4.12. Computation of Response Produced by Support Vibration	108
5. General Theory for Dynamic Response of Distributed-mass Systems, by Charles H. Norris	111
5.1. General	111
5.2. Differential Equation of Motion for Beams	111
5.3. Determination of Normal Modes of Vibration	113
5.4. Determination of Characteristic Shapes of Normal Modes of Vibration	114
<i>a.</i> Simple End-supported Beam	114
<i>b.</i> Two-span Continuous Beam	116
5.5. Important Properties of Characteristic-shape Functions	117
5.6. Use of Characteristic-shape Functions to Represent Deflection and Load Functions	119
5.7. Reduction and Solution of Equation of Motion for Dynamic Response of Structure Which Was Initially at Rest	121
5.8. Dynamic Response Associated with Initial Motion of Structure	122
5.9. Recapitulation—Computation of Dynamic Response of Distributed-mass Systems	123
6. Miscellaneous Considerations Regarding Dynamic-response Theory, by Charles H. Norris	124
6.1. General	124
6.2. Extension of Theory to Include General Impulsive Loads	124
6.3. Extension of Theory to Include Nonlinear Elastic and Elasto-plastic Structural Stiffness	125
6.4. Effect and Importance of Structural Damping in Response Computations	126
6.5. Dynamic Response Produced by Impact	127
7. Simplified Analysis and Design for Dynamic Load, by John M. Biggs	132
7.1. Introduction	132
7.2. Idealized Systems	132
7.3. Energy Method of Analysis (Single Degree)	135
<i>a.</i> External Work Done	136
<i>b.</i> Energy Absorbed	141
<i>c.</i> Application of Energy Method	141
7.4. Deflection Method of Analysis (Single Degree)	143
7.5. Transformation Factors	146

<i>a.</i> Load Factor K_L	148
<i>b.</i> Mass Factor K_m	148
<i>c.</i> Resistance Factor K_R	148
<i>d.</i> Maximum Resistance and Spring Constant	148
<i>e.</i> Dynamic Reaction V	149
7.6. Transformation Factors for a Simply Supported, Uniformly Loaded Beam	149
<i>a.</i> Load Factor	149
<i>b.</i> Mass Factor	151
<i>c.</i> Maximum Resistance and Spring Constant	152
<i>d.</i> Dynamic Reactions	153
<i>e.</i> Examples	153
<i>f.</i> Accuracy of Approximate Analysis	156
7.7. Other Structural Elements	158
<i>a.</i> Beams with Various Loading and Support Conditions	158
<i>b.</i> Two-way Slabs	164
<i>c.</i> Flat Slabs	164
<i>d.</i> Frames	164
<i>e.</i> Miscellaneous	167
7.8. Design Examples	167
<i>a.</i> Simple-span Steel Beam Designed for Plastic Deformation	168
<i>b.</i> Simple-span Steel Beam Designed for Elastic Behavior	170
<i>c.</i> Simply Supported Concrete Slab Designed for Plastic Deformation	172
<i>d.</i> Fixed-end Slab Designed for Elastic Behavior	175
<i>e.</i> General Conclusions Regarding Variation of Parameters	176
7.9. Multidegree Systems	177

PART 3. MODERN COMPUTATIONAL TECHNIQUES APPLICABLE TO RESPONSE CALCULATIONS

8. Introduction to Numerical-integration Methods and Their Application to Dynamic-response Calculations, by Saul Namyet	183
8.1. General	183
8.2. Differential Equations	184
8.3. Numerical Integration	185
8.4. Acceleration Methods of Numerical Integration	185
<i>a.</i> Constant-acceleration Procedure	187
<i>b.</i> Linear-acceleration Procedure	188
<i>c.</i> Constant-velocity Procedure	190
<i>d.</i> Newmark β Method	193
<i>e.</i> Numerical Example	193
8.5. Other Methods of Numerical Integration	196
<i>a.</i> Taylor Series	197
<i>b.</i> Milne's Methods	198
<i>c.</i> Method of Runge and Kutta	199
<i>d.</i> Euler's Method	202
<i>e.</i> Difference Equations	202
<i>f.</i> Methods of Finite Difference	206
8.6. General Considerations in Numerical Integration	207
<i>a.</i> Starting Procedure	207
<i>b.</i> Errors in Numerical Procedures	207
<i>c.</i> Checking Procedures	209

<i>d.</i> Selecting a Value for h	210
<i>e.</i> Selection of a Numerical-integration Method.	211
9. Introduction to Analog and Digital Computers and Their Application to Dynamic-response Calculations, by Saul Namyet	213
9.1. General	213
9.2. Analog Computers	214
<i>a.</i> Description of Electronic Indirect Analog Computers	215
<i>b.</i> Use of High-speed Analog Computer	216
<i>c.</i> Example of Analog-computer Solution of Typical Problem in Structural Dynamics.	217
9.3. High-speed Digital Computation	219
<i>a.</i> Organization of a Computer.	219
<i>b.</i> Characteristics of a Memory	220
<i>c.</i> Arithmetic Unit	221
<i>d.</i> Operation of Control Unit	221
<i>e.</i> Binary Number System.	221
<i>f.</i> Machine Operation	223
<i>g.</i> Machine Coding	223
<i>h.</i> The Use of Flow Diagrams	225
<i>i.</i> Practical Considerations in the Use of Digital Computers	226
<i>j.</i> Examples of Dynamic Analysis by Digital Computer	228

PART 4. APPLICATION OF STRUCTURAL DESIGN AND ANALYSIS TO SPECIFIC CASES INVOLVING DYNAMIC LOADING

10. Introduction to Blast-resistant Design, by Robert J. Hansen.	233
10.1. Purpose	233
10.2. Weapon Phenomena.	233
<i>a.</i> Air Blast	234
<i>b.</i> Thermal Radiation	234
<i>c.</i> Nuclear Radiation	235
10.3. The Resistant Structure.	235
<i>a.</i> Design Considerations	235
<i>b.</i> Dynamic Character of Loading.	235
<i>c.</i> Geometry of Building.	236
<i>d.</i> Fire Hazard	236
<i>e.</i> Radiation	237
10.4. Necessary Decisions	237
<i>a.</i> Site Selection	237
<i>b.</i> Level of Protection	237
<i>c.</i> Selection of Structural System—Surface Structure	238
<i>d.</i> Choice of Underground Construction	238
<i>e.</i> Type of Wall Covering	238
11. Weapons-effects Data Applicable to Blast-resistant Design, by Robert J. Hansen	239
11.1. General	239
<i>a.</i> Air Blast	239
<i>b.</i> The Blast Wave in an Infinite Homogeneous Atmosphere	240
<i>c.</i> The Blast Wave for a Finite Height of Burst.	244
<i>d.</i> Scaling Blast Phenomena	247
11.2. Loading on Structures	248

<i>a.</i> Loading on Closed Rectangular Structures	249
<i>b.</i> Loading on Exposed Structural Framework	266
<i>c.</i> Loading on Cylindrical-arch Surfaces, Cylindrical-arch Overpressure P_{cyl} , Axis Parallel to Shock Front	269
<i>d.</i> Loading on Cylindrical-arch Surfaces, Axis Perpendicular to Shock Front	276
<i>e.</i> Loading on Spherical-dome Surfaces	276
11.3. Radiation	278
<i>a.</i> Thermal Radiation	279
<i>b.</i> Nuclear Radiation	281
<i>c.</i> Fallout	285
12. Behavior of Structures under Blast Loads, by Robert J. Hansen	287
12.1. Introduction	287
12.2. Hiroshima and Nagasaki Data	287
12.3. Nuclear Experiments	290
12.4. Extrapolation to Large-yield Weapons	292
13. Blast-resistant-design Considerations, by Robert J. Hansen	294
13.1. The Problem	294
13.2. Criteria for the Building Program	294
13.3. Type of Construction	295
<i>a.</i> Buried or Semiburied Construction	295
<i>b.</i> Shear-wall Construction	295
<i>c.</i> Arch and Dome Construction	296
<i>d.</i> Rigid-frame Construction	296
<i>e.</i> Single-story vs. Multistory Construction	296
<i>f.</i> Exterior Walls	296
<i>g.</i> Windowless Construction	296
<i>h.</i> Geometry	297
<i>i.</i> Doors and Openings	298
<i>j.</i> Foundations	298
13.4. Functional Considerations	298
<i>a.</i> Space Arrangement	298
<i>b.</i> Shelter Areas	298
<i>c.</i> Building Services	298
13.5. Structural Design	299
<i>a.</i> Preliminary Layout	299
<i>b.</i> Type of Behavior	299
<i>c.</i> Blast-pressure Loading Curves	299
<i>d.</i> Dynamic Structural Design	299
13.6. Personnel Shelters	300
13.7. Deflection Criteria for Plastic Design	300
13.8. Design of Foundations	303
14. Examples of Blast-resistant Design, by Robert J. Hansen	307
14.1. General	307
14.2. Single-story Steel-frame Building	307
<i>a.</i> Loading	307
<i>b.</i> Design of Wall Slabs	307
<i>c.</i> Design of Roof Slab	308

<i>d.</i> Design of Roof Purlins	311
<i>e.</i> Preliminary Column Design	313
<i>f.</i> Design of Roof Girder	313
<i>g.</i> Final Column Design	316
<i>h.</i> Frame Connections	319
<i>i.</i> Design of Foundation	319
14.3. Single-story Reinforced-concrete Shear-wall Building	323
15. Discussion of Laboratory and Theoretical Developments for Improved Blast-resistant Design, by Robert J. Hansen	328
15.1. Introduction	328
15.2. Laboratory Studies of Blast Loading	328
15.3. Strength Properties of Structural Elements	331
15.4. Dynamic-analysis and -design Procedures	333
16. Earthquakes and Earthquake Effects on Structures, by John K. Minami	337
16.1. Earthquakes	337
16.2. Geographical Distribution of Earthquakes	338
16.3. Earthquake Waves	338
16.4. Earthquake Magnitude and Intensity	340
16.5. Earthquake Spectra and Spectrum Intensity	340
16.6. Period of Vibration of Buildings	343
16.7. Strong-motion Programs	344
16.8. Earthquake Effects on Structures	345
16.9. Failure of Daiwa Department Store Building	347
17. Earthquake Provisions in Building Codes, by John K. Minami	358
17.1. Introduction	358
17.2. Uniform Building Code	358
17.3. Japanese Building Code	362
17.4. Proposed Modifications in the Japanese Seismic Factors	372
17.5. Joint Committee Code for Lateral Forces	373
18. Earthquake-resistant-design Methods and Practice, by John K. Minami	380
18.1. Introduction	380
18.2. Dynamic Methods of Analysis	380
<i>a.</i> Earthquake-spectrum Technique	381
<i>b.</i> Phase-plane-delta Method	381
<i>c.</i> Numerical-integration Methods	381
18.3. Statical Methods of Design	382
<i>a.</i> Approximate Methods	382
<i>b.</i> The Factor Method	383
<i>c.</i> AIJ (Architectural Institute of Japan) Method	384
<i>d.</i> Exact Methods	385
18.4. Design of Actual Buildings	394
18.5. A Comparison of Aseismic Designs by Different Codes	409
18.6. Miscellaneous Considerations	414
19. Vibration of Girders under Moving Traffic Loads, by Myle J. Holley, Jr.	416
19.1. Introduction	416
19.2. Background to the Problem	416

19.3. Physical Concepts	418
19.4. Theoretical Expressions	419
a. Simply Supported Beam; Constant Force Moving at Constant Velocity; Including Damping	419
b. Simply Supported Beam; Sinusoidal Alternating Force at Constant Velocity; Neglecting Damping	421
c. Simplified Deflection Analysis	422
19.5. Verification of Simplified Deflection Analysis by Model Study and by Field Measurements	424
a. Verification by Model Study.	424
b. Verification by Field Measurements	424
19.6. Theoretical Effects of Varying the Major Parameters	430
a. Influence of β	431
b. Influence of p_B/p_v	431
c. Influence of M_v/M_B	431
19.7. Practical Application of Theory	431
20. Dynamic Effects of Wind Load, by Myle J. Holley, Jr.	434
20.1. Introduction	434
20.2. Factors Justifying the Common Design Assumption That Wind Forces Are Static.	434
a. Nonperiodic Character of Common Wind Loadings	434
b. Insensitivity of Wind-load Stresses to Local-force Variations	435
c. General Insensitivity to Rapid Changes of Wind Force	435
d. Concurrent Existence of Nonwind Forces of Significant Magnitude	435
e. Existence of Sources of Potentially Greater Error Than Is Due to Neglect of Dynamic Effects.	435
20.3. Conditions Requiring Consideration of Dynamic Effects of Wind Load	436
a. Structures Sensitive to Gusts	436
b. Structures Subject to the Periodic Forces Associated with Karman Vortices.	437
c. Structures Having Negative Slope of Curves of Lift or Moment vs. Angle of Attack	439
d. Structures Subject to Flutter	442
20.4. Sources of Positive Damping	443
20.5. Examples of Dynamic Response to Wind.	444
a. Nonguyed Towers Subject to Gusts	444
b. Singing Transmission Lines	445
c. Industrial Stacks	445
d. Girder-stiffened Suspension Bridges.	446
e. Truss-stiffened Suspension Bridges.	447
<i>Index.</i>	449

INTRODUCTION

Certain civil-engineering structures are designed to carry simply their own dead weight plus certain superimposed loads which are immovable and unvarying with time, that is, certain superimposed *static* loads. In such cases, the stress analysis involves only principles of statics. More often the design of civil-engineering structures involves not only static loads but also certain superimposed loads which are either moving or movable and may vary with time, that is, certain superimposed *dynamic* loads. In such cases, the stress analysis properly should involve principles of dynamics to determine the effects of the dynamic loading. However, in many of these cases, experience has shown that the dynamic effect makes a minor contribution to the total which must be provided for in the design and therefore that this dynamic effect need not be evaluated precisely. In such cases, the dynamic effect may be handled by use of an equivalent static load, or by an impact factor, or by a modification of the factor of safety.

In recent years, however, there have been a number of developments which have led to a growing interest in a more precise evaluation of the effects produced by the dynamic portion of the loading. Among these are the imposition of more severe live-loading conditions (that is, heavier machinery and vehicles running at higher speeds), the construction of higher towers and longer bridges involving more severe and important wind-loading conditions, the necessity of developing blast-resistant construction, and the desire to improve earthquake-resistant construction. Specific situations where it may be necessary to consider more precisely the response produced by the dynamic loading are typified by the following:

1. When a structure must be designed to resist transient and/or steady-state vibrations produced by oscillating machinery operating within
2. When a structure must be designed to resist impact loads and vibrations produced by traffic passing over the structure
3. When a structure must be designed to resist impulsive loads produced by blasts, wind gusts, or water waves
4. When a structure must be designed to resist vibrations developed by oscillating motions of its supports, produced by earthquake shocks

5. When a structure must be designed to resist self-induced vibrations (for example, vibrations produced by forces created by the vibratory motion itself, as the galloping of transmission lines or of suspension bridges caused by aerodynamic forces produced by wind blowing on the structure)

6. When a protective structure must be designed to resist the impact of projectile missiles

With the growing importance of dynamic loads in structural design, more consideration has been given to principles of dynamics in the civil-engineering curriculums of a number of engineering schools, principally at the graduate level. In recent years, several symposia and conferences have been held to bring together those particularly interested in blast-resistant and earthquake-resistant design and construction. In the summer of 1956, the Structures Division of the Department of Civil and Sanitary Engineering at the Massachusetts Institute of Technology offered a two-week special summer program on Structural Design for Dynamic Loads. The program was planned primarily for practicing structural engineers who were interested in improving their competence in this area. Thirty lectures were presented surveying this field, and notes amplifying these lectures were distributed to the enrollees.

This book has been compiled from the lecture notes. It is not presented as a textbook nor as a reference book covering the subject. The twenty chapters herein survey the field of structural design for dynamic loading and are intended as a guide to an engineer who is studying in this area. Some aspects of the subject are introduced, but existing information concerning this subject is not completely summarized as would be done in a reference book. In such cases, it is expected that the reader will extend his coverage by studying the pertinent sources cited in the References. As a textbook, this treatment is notably deficient in not having enough illustrative examples and in having no problems for solution.

Structural design, whether for static or for dynamic loading, involves the determination of the loads; the analysis (or computation) of the internal gross forces (thrust, shear, and moment), stresses, deflections, and reactions produced by the loads; and the proportioning and dimensioning of the members and connections so as to resist adequately these effects produced by the loads. The criteria used to judge whether particular proportions will result in desired behavior reflect accumulated knowledge (theory, tests, and practical experience) and judgment. For most common civil-engineering structures such as bridges, buildings, etc., the usual practice is to design on the basis of a comparison of permissible stresses with those produced by the working loads.

Depending on the type of structure, the stresses computed for the working loads may or may not be in close agreement with the stresses in the structure for the actual loads. The degree of correspondence is not important, provided the computed stresses can be interpreted in terms of previous experience. By the selection of the working loads and the permissible stresses, a margin of safety against failure is provided. The selection of the magnitude of this margin depends on the degree of uncertainty regarding loading, materials, analysis, design and construction, and on the consequences of failure.

There is a growing tendency in structural design to base the design on the ultimate strength of the structure. This approach goes under the name of *plastic theory* in reinforced-concrete-design literature and of *limit design* in steel-design literature. It is commonly used where important dynamic loadings are involved in the design of the structure. When proportioning is done on this basis, the anticipated service loading is first multiplied by a suitable "load factor" (greater than 1), the magnitude of which depends upon the same considerations as enumerated above for the margin of safety. The structure is then proportioned so that, depending on the governing conditions, the increased load would either (1) cause a fatigue failure, or (2) just produce yielding at one internal section (or simultaneous yielding at several sections), or (3) cause elastic-plastic displacement of the structure, or (4) cause the entire structure to be on the point of collapse.

In an attempt to cover the broad field of structural design for dynamic loading, the ensuing presentation is divided into four parts, covering behavior of materials, analysis of dynamic response, definition of dynamic loads, etc., as well as specific proportioning and dimensioning of structural members, as follows:

Part 1. Behavior of Materials under Dynamic Loading. This part is divided into two chapters. In Chapter 1, the behavior of steel and steel elements under dynamic loading is summarized. Chapter 2 is devoted to a similar discussion of concrete and concrete structural components.

Part 2. Calculation of Response of Structural Systems to Dynamic Loading. Chapters 3 to 7 are devoted to this portion of the book. In Chapter 3, some of the important aspects of dynamic response are introduced by considering the response of a simple one-mass system to typical dynamic loadings. This approach is expanded in Chapter 4 for application to concentrated-mass systems of any number of degrees of freedom, and further expanded in Chapter 5 to distributed-mass systems. This method involves superimposing the contributions of the normal modes of vibration and is limited to linearly elastic systems. This and other limitations of this method of analysis are discussed in Chapter 6. Even

when applicable, this general theory is very laborious to apply so that simplified methods of analysis and design such as discussed in Chapter 7 must be developed for practical design applications.

Part 3. Modern Computational Techniques Applicable to Response Calculations. Only by using numerical methods (as discussed in Chapter 8) and/or modern analog and digital computers (Chapter 9) is it possible or practicable to carry through many practical response calculations. These brief presentations must of course be supplemented by additional reading, such as the references cited.

Part 4. Application of Structural Design and Analysis to Specific Cases Involving Dynamic Loading. The remainder of the book (Chapters 10 to 20) is devoted to applications, the principal one being blast-resistant design, which is presented in Chapters 10 to 15. This material is a condensation of portions of a design manual prepared under the supervision of Professors R. J. Hansen, J. M. Biggs, and S. Namyet for the Office of Chief of Engineers, U.S. Army.

In Chapters 16 to 18, Professor J. K. Minami of Waseda University, Tokyo, has summarized some of the current thinking on earthquake-resistant design and compared current Japanese practice and codes with American codes.

Two other important types of dynamic loading are discussed in Chapters 19 and 20, vibration of girders under moving traffic loads and dynamic effects of wind load, respectively.

To the extent possible, notation and terminology are unchanged throughout the book. The reader will note certain departures from this general policy where the notation used in certain chapters is based on that used in the principal source material involved. In general, therefore, the reader should use definitions of notation within a specific chapter or portion of the book rather than attempt to correlate usages throughout the book.

PART 1

BEHAVIOR OF MATERIALS UNDER DYNAMIC LOADING

CHAPTER 1

BEHAVIOR OF STEEL AND STEEL ELEMENTS UNDER DYNAMIC LOADS

1.1. Introduction. Before beginning the discussion of structural design for dynamic loads it is desirable first to review and perhaps expand the reader's knowledge of the properties of the materials involved. This chapter is concerned with the physical properties of steel and structural elements made of steel. The first consideration will be the material properties such as yield stress and ultimate strength for rapidly applied loads in contrast to static loading. The second consideration will be the ultimate capacity of structural elements such as beams and columns. Consideration of ultimate, or "plastic," strength is of course not limited to dynamic design. However, many of the problems discussed in later chapters must be based upon ultimate strengths rather than ordinary working stresses. For this reason, it appears desirable to consider this subject at some length in this chapter. Finally, fatigue effects in structural steel will be briefly discussed. It should be noted that at no point in this chapter is a factor of safety included in the strength computations. It is assumed that the factor of safety, if any, is included in the design loads.

1.2. Design Properties. Before considering dynamic characteristics the ordinary static properties of steel will be considered. This discussion will be limited to ordinary structural carbon steel designated by ASTM Specification A 7. Figure 1.1 shows a typical stress-strain curve for this steel. Some of the important points are noted on the figure. The upper-yield-point stress is designated by f_{uy} . Up to this point the stress-strain curve is an essentially straight line and the modulus of elasticity is the ordinary value of about 30,000,000 psi. Beyond this point the stress drops to the lower-yield-point value f_{ly} . The curve is then essentially horizontal up to the point where strain hardening begins. The strain at the latter point is designated by e_s and is about fifteen or twenty times the limit of elastic strain e_y .

In some types of design, particularly blast design, it is desirable to allow for plastic deformation of the structure. Allowing the structure to deform plastically enables it to absorb more of the energy imposed by

dynamic loading. The degree of plastic deformation permitted should depend upon the function of the structure. If the structure is required to withstand this loading only once in its lifetime, the designer might permit deformation up to the point of collapse. If, on the other hand, the load is to be repeated several times, a much smaller amount of deformation would be permitted.

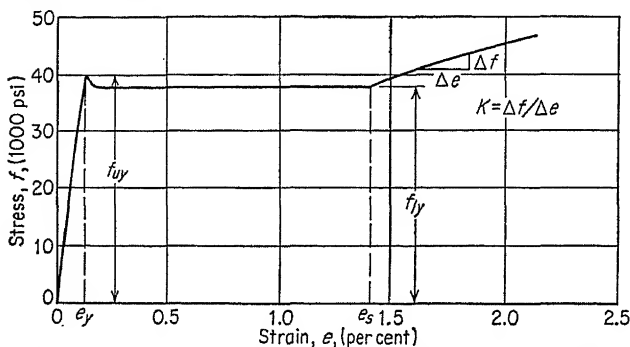


FIG. 1.1. Typical stress-strain curve for structural steel [8].

In designing for plastic deformation it is convenient to idealize the stress-strain curve as shown in Fig. 1.2. In this figure the upper yield point has been neglected and the effect of strain hardening ignored. The latter approximation is possible because in most cases plastic deformation into the strain-hardening range would permit excessive distortion of the geometry of the structure.

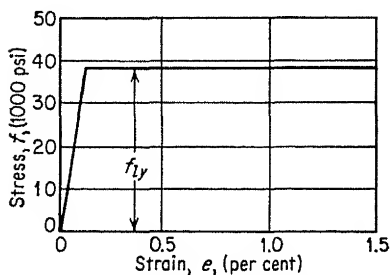


FIG. 1.2. Idealized stress-strain curve for structural steel [8].

All design computations in the following chapters will be based upon this idealized stress-strain curve.

Static design for structural carbon steel is usually based upon a yield stress of 33,000 psi. It is important to note, however, that for practical reasons there is considerable variation in this value. Figure 1.3 shows the results of nearly 4,000 mill tests representing 33,000 tons of steel [1].*

These tests were conducted according to the ASTM Standard Testing Specifications. The distribution curve indicates a considerable spread in the yield points of rolled members as delivered from the mill. The largest yield stress obtained was 82 per cent greater than the smallest value. The average value was 40,000 psi. These values are upper-

* Numbers in brackets refer to References at the end of each chapter.

yield-point stresses, which are generally about 5 per cent higher than the lower-yield-point stresses. Reducing the average upper yield stress by 5 per cent, 38,000 psi is obtained, a value which might be reasonably used for tension or compression in plastic design. This is the stress intensity which would be maintained during plastic deformation.

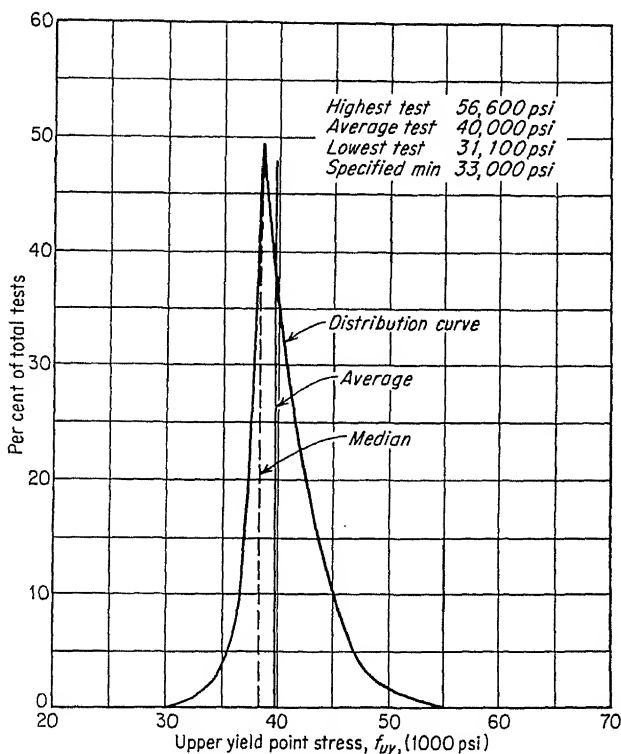


FIG. 1.3. Mill tests of structural steel. Data from 3,974 tests representing 33,000 tons of steel used on nine projects between 1938 and 1951 by Jackson and Moreland, Engineers, Boston [8].

For safety in design it might be desirable to use a yield-point value lower than the average mentioned above. This decision is the prerogative of the designer.

The average ultimate strength obtained in these same tests was 66,300 psi. This stress is not normally used for design purposes since it involves excessive strains.

The static shear yield stress of structural steel is about 55 per cent of the tensile yield stress. An average value would therefore be 21,000 psi.

1.3. Dynamic Properties. Figure 1.4 shows the effect of rate of strain on the stress-strain curve for A 7 steel. This information is based upon

a limited number of tests and should not be regarded as precise. As the rate of strain increases, the following effects take place:

1. The yield stress increases to some dynamic value f_{dy} .
2. The yield-point strain e_y increases.
3. The modulus of elasticity in the elastic range remains constant.
4. The strain at which strain hardening begins, e_s , also increases.
5. The ultimate strength increases slightly.

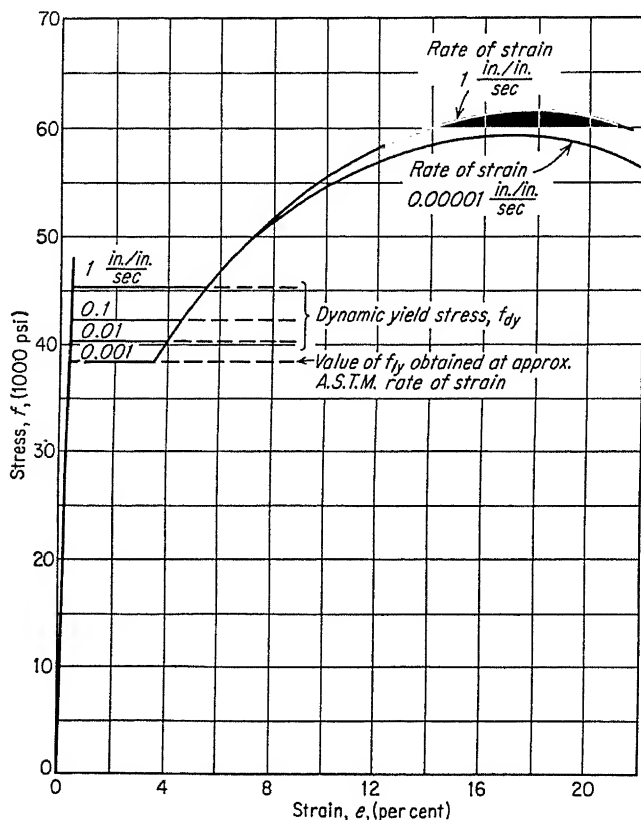


FIG. 1.4. Effect of rate of strain on stress-strain curve for structural steel [8].

Of these effects the increase in the yield stress is of most importance.

In Fig. 1.5 test results are presented giving dynamic yield stress as a function of the time required to reach that value of stress (t_{yp}). The curve is an average of these test results. Strictly speaking, the dynamic yield stress for a given case should be determined simultaneously with the analysis of the structure, which would provide a value of t_{yp} . Actually, however, this would not be justified because of the wide variation in the yield stress of the material. It is usually possible to use an average

value for the general type of structure being considered. For example, in the design of building frames to resist blast loadings it is found that the time to reach yield stresses varies between 0.01 and 0.10 sec. An average value for dynamic yield stress within this range is 41,600 psi for ASTM A 7 steel. For other types of structures appropriate averages could also be determined.

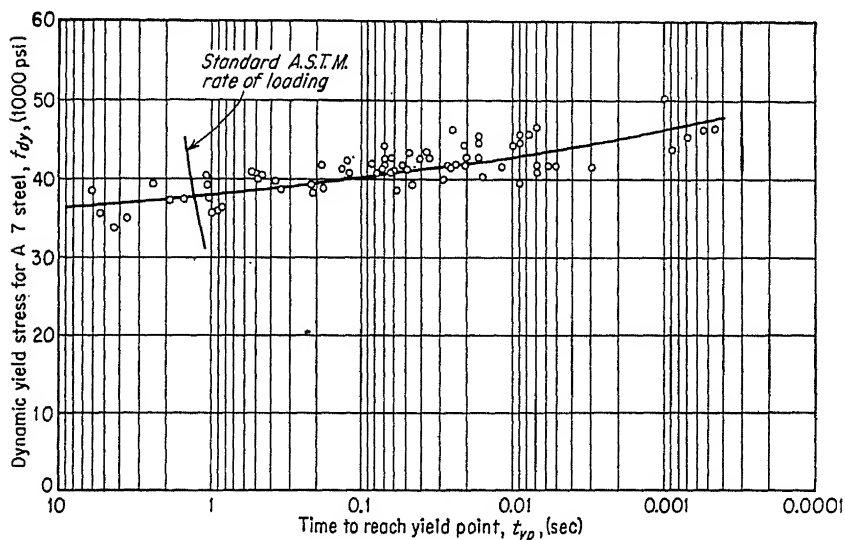


FIG. 1.5. Effect of rate of strain on yield stress.

The dynamic increase in yield stress is affected by any initial static stress that might be present. Very little test data are available on this subject. However, the increase depends upon the rate of strain at the instant when yielding begins. The effect of initial stress may be taken into account by computing an effective time to reach the yield point, as follows:

$$t_{yp} \text{ (effective)} = [t_{yp} \text{ (actual)}] \frac{f_{dy}}{f_{dy} - f_i} \quad (1.1)$$

where f_i is the initial static stress and $t_{yp} \text{ (actual)}$ is the time obtained in a dynamic analysis of the structure. The effective time can then be used in Fig. 1.5 to obtain the dynamic yield stress. Obviously, design by this method requires a trial-and-error procedure. However, because of the approximations involved, great precision is not justified.

The shear yield stress probably increases above the static value when dynamic loads are applied. However, the lack of data on this subject makes estimates of the dynamic shear yield stress questionable. For

this reason it is recommended that no dynamic increase be allowed when designing for shear.

1.4. Strength of Beam Sections. *a. Bending Strength.* In order to design for plastic deformation it is necessary to estimate the ultimate, or plastic, bending capacity of beam sections. Figure 1.6 shows the moment-curvature relationship for an I or WF steel beam laterally supported against buckling. Curvature is defined as the angle change per unit length. At the point where a plastic hinge forms, the curvature

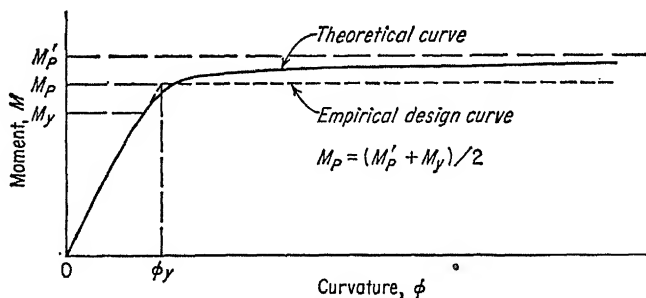


FIG. 1.6. Moment-curvature relationship for I or WF beams [8].

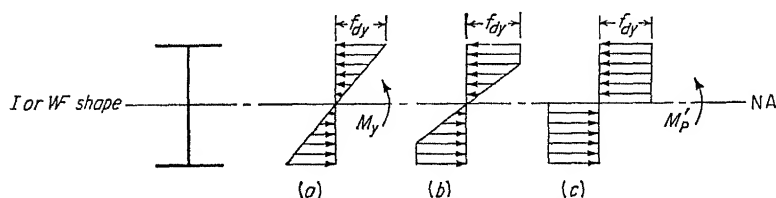


FIG. 1.7. Bending-stress distributions [8].

becomes very large, as shown in Fig. 1.6. The beam bends elastically until the yield moment M_y is reached. The curvature then increases rapidly as the moment approaches the ultimate capacity M'_P . During this process the stress distribution on the cross section changes as indicated in Fig. 1.7. In Fig. 1.7a the assumed elastic-stress distribution is shown, and if the stress on the extreme fiber is equal to the yield stress, the bending resistance is the yield moment M_y . As the moment is increased, the distribution goes through stage b and eventually approaches stage c, the latter representing the ultimate moment M'_P .

The presence of residual stresses in the beam may appreciably reduce the yield moment. Tests indicate that this is generally true. However, residual stresses have no effect on the ultimate-moment capacity and therefore need not be considered in ultimate design.

Considerable curvature is required for the section to reach its ultimate capacity, and excessive distortion of the structure would probably

result. For this reason it is recommended that a reduced capacity be used for design purposes. A reasonable value would be the average of M_y and M'_p , which is designated by M_p . It is further recommended that the moment-curvature relationship be idealized as two straight lines as indicated in Fig. 1.6.

The design-ultimate-moment capacity may be computed as follows:

$$M_p = \frac{1}{2}(M_y + M'_p) \quad (1.2)$$

$$M_y = f_{dy}S \quad (1.3)$$

$$M'_p = f_{dy}Z \quad (1.4)$$

where f_{dy} = dynamic yield stress

S = section modulus of beam

Z = plastic modulus of the section

Z is equal to twice the static moment about the centroidal axis of the cross-section area above or below the same axis. This quantity can be conveniently computed from the properties of T sections cut from the I or WF beam being considered.

The relationship between S and Z for the various standard I or WF beams does not vary appreciably. For this reason the design-ultimate-moment capacity may be approximated by

$$M_p = 1.05f_{dy}S \quad (1.5)$$

For rectangular cross sections the equation becomes

$$M_p = 1.25f_{dy}S \quad (1.6)$$

b. Shear Strength. Shear yield of a beam occurs when the average shear stress in the web equals the shear yield stress. Thus for an I section the total shear causing yield is

$$V = v_{dy}A_w \quad (1.7)$$

where v_{dy} = shear yield stress (21,000 psi)

A_w = area of web

When shear exists at the cross section of moment yielding, the ultimate-moment capacity is reduced. This may be taken into account in the computation of Z by removing from the web the area required to carry the shear force at the shear yield stress. This area, which should be symmetrical about the centroidal axis, is given by V/v_{dy} , where V is the actual shear force. The ultimate-moment capacity M'_p is then given by $f_{dy}Z'$, where Z' is the plastic modulus of the remaining area.

The presence of direct stress also reduces the ultimate-moment capacity. This is discussed in a later section.

c. Local Buckling. For the lighter standard rolled sections the web or flange may buckle soon after the yield stress is reached in compression.

As a result, the ultimate design moment M_p cannot be maintained through

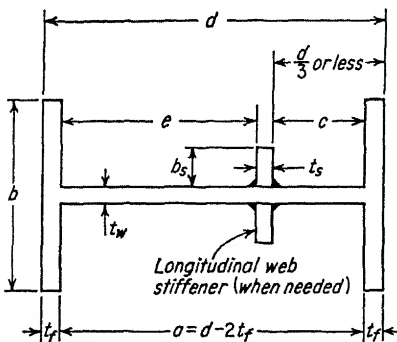


FIG. 1.8. Notation for beam cross sections [8].

local buckling (Fig. 1.8) in I beams:

Compression flange.....	b/t_f not to exceed 17
Web.....	a/t_w not to exceed 70
Load-bearing stiffeners.....	b_s/t_s not to exceed 8
Longitudinal web stiffeners.....	b_s/t_s not to exceed 7

These criteria must be satisfied if plastic-bending deformation of the beam is contemplated. If the stresses remain in the elastic range, conventional design criteria for width-thickness ratios may be used.

It will be noted that the above criteria are more severe than those used in conventional design. This is true because in conventional elastic design buckling is permitted as soon as the stress reaches the yield point.

If the web of the beam does not meet the above criteria, longitudinal stiffeners as shown in Fig. 1.8 may be added to prevent local buckling. These stiffeners should be placed inside the compression flange a distance equal to one-third the depth of the web.

d. Lateral Buckling. If a beam is to undergo plastic deformation, lateral support must be provided to prevent lateral-torsional buckling during this process. In order to prevent such buckling, it is recommended that the quantity $K'Ld/bt_f$ should not exceed 100. The notations d , b , and t_f are defined in Fig. 1.8. L is the unsupported length of the compression flange, and K' is a length-reduction factor which depends on the conditions of loading and support.

Several values of K' are given in Table 1.1 [3]. For example, in the case of a uniformly loaded simply supported beam with restraint against rotation about the longitudinal axis but not about the vertical or horizontal axes at both ends, case 5a would apply, giving a value of 0.89 for K' . For a beam with stringers framing into the web at a spacing of L such that the bending moment is essentially constant through any such length, case 7a applies and K' is 1.00.

any appreciable plastic deformation. If such deformation is desired, the cross-section proportions must be such as to prevent local buckling.

The criteria given below were derived for static-loading conditions and are probably conservative [9]. This approximation is necessary because very few data on dynamic buckling are available.

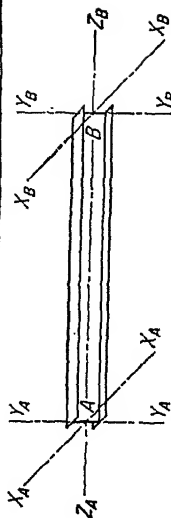
The following minimum proportions are recommended to prevent

TABLE 1.1. EQUIVALENT LENGTH COEFFICIENTS FOR Laterally UNSUPPORTED BEAMS [3, 8]

1	2	3	4	5	6	7	8	9	10	11
	Load condition	Moment diagram	Rotation * restraint		Rotation restraint at B about axis			Position * restraint		Equiv. length coeff. K'
			$X_A X_A$	$Y_A Y_A$	$X_B X_B$	$Y_B Y_B$	$Z_A Z_B$	X_B	Y_B	
1			Fixed	Fixed	Free	Free	Free	Free	Free	0.78
2			Fixed	Fixed	Free	Free	Free	Free	Free	0.49
3a 3b			Free Free	Free Fixed	Free Free	Free Fixed	Fixed Fixed	Fixed Fixed	Fixed Fixed	0.74 0.47
4			Fixed	Fixed	Fixed	Fixed	Fixed	Fixed	Fixed	0.37
5a 5b			Free Free	Free Fixed	Free Free	Free Fixed	Fixed Fixed	Fixed Fixed	Fixed Fixed	0.89 0.51
6			Fixed	Fixed	Fixed	Fixed	Fixed	Fixed	Fixed	0.53
7a 7b			Free Free	Free Fixed	Free Free	Free Fixed	Fixed Fixed	Fixed Fixed	Fixed Fixed	1.00 0.50

TABLE 1.1. EQUIVALENT LENGTH COEFFICIENTS FOR Laterally UNSUPPORTED BEAMS [3, 8] (Continued)

1	2	3	4	5	6	7	8	9	10	11
	Load condition	Moment diagram	Rotation* restraint		Rotation restraint at B about axis			Position* restraint		Equiv. length coeff. K'
			$X_A X_A$	$Y_A Y_A$	$X_B X_B$	$Y_B Y_B$	$Z_A Z_B$	X_B	Y_B	
8a 8b			Free Free	Free Fixed	Free Free	Free Fixed	Fixed Fixed	Fixed Fixed	Fixed Fixed	0.56 (0.25)
9a 9b			Fixed Fixed	Free Fixed	Free Free	Free Fixed	Fixed Fixed	Fixed Fixed	Free Free	0.56 (0.25)
10a 10b			Free Free	Free Fixed	Fixed Fixed	Free Fixed	Fixed Fixed	Fixed Fixed	Fixed Fixed	0.43 (0.18)
11a 11b 11c			Free Free Free	Free Free Fixed	Free Free Free	Free Fixed Fixed	Fixed Fixed Fixed	Fixed Fixed Fixed	Fixed Fixed Fixed	0.39 (0.31) (0.14)
12a 12b 12c			Fixed Fixed Fixed	Free Free Fixed	Fixed Fixed Fixed	Free Fixed Fixed	Fixed Fixed Fixed	Fixed Fixed Fixed	Free Free Free	0.39 (0.31) (0.14)



* Rotation restraint at A about $Z_A Z_B$ and position restraint at A in X_A , Y_A , and Z_A directions is assumed in all cases.

The quantities shown in parentheses are estimated for design purposes after qualitative consideration of restraint and load conditions and are probably conservative.

If the lateral support for a beam does not satisfy the above criteria, plastic deformation cannot be permitted in design. Beams for which $K'Ld/bt_f$ exceeds 100 should be designed for the dynamic stress at which buckling occurs. In such cases it is recommended that the following design stress be permitted [4, 8]:

$$f_b = \frac{(32)(10^6)}{600 + K'Ld/bt_f} \quad \text{psi, not to exceed } f_{dy} \quad (1.8)$$

in which f_b is the critical buckling stress. The maximum permissible design moment would then be $(f_b)(S)$.

e. Bending Resistance of I Beams in the Weak Direction. WF or I beams bent in the weak direction are not generally susceptible to lateral-torsional buckling. The recommended ultimate design moment is therefore given by

$$M_p = f_{dy}(S + \dot{Z})\frac{1}{2} \quad (1.9)$$

which may be approximated by

$$M_p = 1.25f_{dy}S \quad (1.10)$$

1.5. Strength of Axially Loaded Columns. *a. Local Buckling.* If a column is expected to develop its ultimate strength in compression, the width-thickness ratios of the web and flange must be such as to prevent local buckling. Using the notation of Fig. 1.8, the following minimum ratios are recommended:

$$\begin{array}{ll} \text{Flange} \dots\dots\dots b/t_f & \text{not to exceed 17} \\ \text{Web} \dots\dots\dots a/t_w & \text{not to exceed 43} \end{array}$$

Most standard column sections satisfy these requirements.

b. Lateral Buckling. If a column is required to develop its full ultimate compressive strength, lateral buckling must also be prevented. The recommended criterion in this case is

$$\frac{K''L}{r} \text{ not greater than 15}$$




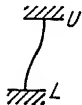
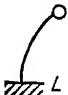
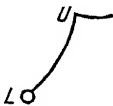
where L = unsupported length

r = least radius of gyration

K'' = a length-reduction factor which depends upon end conditions
Values of K'' are given in Table 1.2. These values are obtained from the classical elastic-buckling theory.

If the column satisfies the above criteria, the ultimate compressive

TABLE 1.2. COLUMN-LENGTH FACTORS [8]

Type of restraint	Buckled form	Condition at U		Condition at L		Length factor K''
		Rotation	Lateral position	Rotation	Lateral position	
1		Free	Fixed	Free	Fixed	1.0
2		Free	Fixed	Fixed	Fixed	0.7
3		Fixed	Fixed	Fixed	Fixed	0.5
4		Fixed	Free	Fixed	Fixed	1.0
5		Free	Free	Fixed	Fixed	2.0
6		Elastic restraint	Free	Free	Fixed	2.0-∞

strength may be computed as

$$P_p = f_{dy} A \quad (1.11)$$

where A = total cross-section area.

If the reduced slenderness ratio $K''L/r$ exceeds 15, the design capacity of the column may be computed by

$$P = f_a A \quad (1.12)$$

where

$$f_a = 44,600 - 200 \frac{K''L}{r} \quad \text{psi, not to exceed } f_{dy} \quad (1.13)$$

This expression for critical stress is empirical and differs from the conventional working stress in that no factor of safety is included. In this case no plastic deformation of the column is possible.

1.6. Strength of Beam-columns. A member subjected to combined bending and direct stress is called a beam-column. Such members are probably more common than columns carrying direct compression only.

a. Capacity of Laterally Supported Beam-columns. The interaction curve shown in Fig. 1.9 is recommended for estimating the combined capacity of WF sections in direct compression and bending. The lowest of the three curves indicates values of direct stress and bending which in combination would cause a yield stress on the extreme fiber. P_p is equal

to $f_{dy}A$, and M_p is equal to $f_{dy}S$. The upper curve is the theoretical ultimate capacity. Because of the excessive curvatures which are

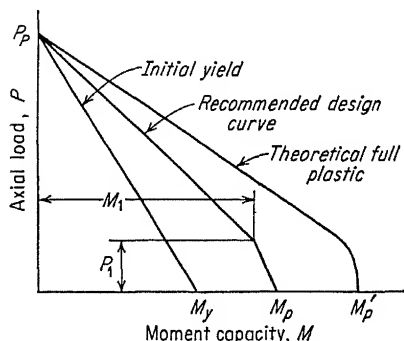


FIG. 1.9. Interaction curve for WF beam-columns [8].

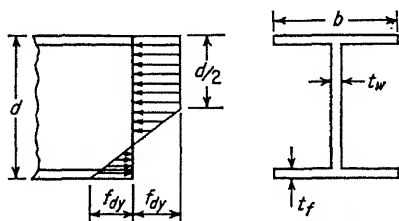


FIG. 1.10. Stress distribution for M_1 and P_1 [8].

required to reach points on the latter curve it should generally not be used for most design purposes. The intermediate empirical curve is therefore recommended. This design curve consists of two straight lines and is based upon test results [5, 6]. The intersection point of the two straight lines corresponds to the stress distribution shown in Fig. 1.10 and is defined by the quantities

$$M_1 = \frac{f_{dy}}{3d} \left[4t_w \left(\frac{d}{2} - t_f \right)^3 + bt_f(3d^2 - 6dt_f + 4t_f^2) \right] \quad (1.14)$$

$$P_1 = \frac{f_{dy}}{d} \left(2bt_f^2 + t_w \frac{d^2}{2} - 2t_w t_f^2 \right) \quad (1.15)$$

The equations for the design curve are

$$M_D = \frac{P_p - P_D}{P_p - P_1} M_1 \quad P_D > P_1 \quad (1.16)$$

$$M_D = M_p - \frac{P_D}{P_1} (M_p - M_1) \quad P_D < P_1 \quad (1.17)$$

where P_p and M_p are defined by Eqs. (1.11) and (1.2), respectively. M_D and P_D are the bending moment and direct thrust, which in combination represent the ultimate capacity of the member.

For a given WF section the design curve described above can be easily constructed. In the usual case of dynamic design the direct stress P_D is given and the designer is required to compute the bending capacity M_D of the section.

b. Lateral Buckling of Beam-columns. In order to develop the full plastic-bending and direct-stress capacity of the member, lateral-torsional buckling must be prevented. Criteria for bending and direct stress applied separately have been previously presented. In the combined case the following empirical criterion is recommended:

$$\frac{M_D}{M_p} \left(\frac{K' L d}{100 b t_f} \right) + \frac{P_D}{P_p} \left(\frac{K'' L}{15 r} \right) < 1 \quad (1.18)$$

in which the notation is as previously defined. Equation (1.18) should be applied after P_D and M_D have been determined for a given section. If the equation is satisfied, plastic deformation can take place without danger of lateral-torsional buckling.

When obtaining values of K' and K'' from Tables 1.1 and 1.2 it is important to note that it is the condition of restraint rather than loading which determines these factors. For example, a column may be bent in double curvature by the applied end moments, which might falsely indicate a value of K'' equal to 0.5. Actually, however, the column might be pin-ended, in which case K'' should be taken as 1.0.

If the column does not satisfy Eq. (1.18), its capacity is limited by buckling considerations, and plastic deformation cannot be permitted. In this case it is recommended that the capacity be determined by the interaction formula

$$\frac{f_{ad}}{f_a} + \frac{f_{bd}}{f_b} < 1 \quad (1.19)$$

where f_{ad} = average axial stress at design level = P_d/A

f_a = allowable axial stress by Eq. (1.13)

f_b = allowable bending stress by Eq. (1.8)

f_{bd} = bending stress including effect of axial load acting on deflection

In the computation of f_{bd} any rational method may be applied. As an approximation the following equation might be used:

$$f_{bd} = \frac{M}{S} \frac{1}{1 - \frac{f_{ad}}{(296)(10)^6} \left(\frac{K'' L}{r} \right)^2} \quad \text{psi} \quad (1.20)$$

where all terms are computed for the plane of bending.

1.7. Connections. *a. Welds.* Static tests show that arc welds on structural-steel members develop a strength greater than that of the base metal. When butt welds are used the base metal controls the strength of the connection, and the ultimate design stresses previously given for structural steel should be used. When fillet welds are employed in shear, failure may occur at the throat. The shear yield stress on this section may be taken as 29,000 psi.

The above recommendations do not take into account conditions involving fatigue failures.

b. Rivets. Ultimate design stresses for structural rivet steel (ASTM Specification A 141) may be taken as follows:

	<i>Psi</i>
Tension.....	40,000
Shear.....	30,000
Bearing.....	60,000 (single shear)
	80,000 (double shear)

c. Bolts. The recommended ultimate design stresses for standard bolts (ASTM A 307) are as follows:

	<i>Psi</i>
Tension.....	48,000
Shear.....	26,000
Bearing.....	60,000

High-strength bolts (such as ASTM A 325) are advantageous in conventional design because slipping is eliminated under static loads. Under dynamic loads this advantage is questionable, and it is recommended that design be based upon the strength of the bolt alone. Following current practice, which is conservative, a high-strength bolt may be considered equivalent to a rivet of the same diameter.

Under repeated loading high-strength bolts reduce the possibility of fatigue failure provided that the oscillating stress is not large enough to cause slipping [10].

1.8. Fatigue. Structures subject to repeated or oscillating stresses deserve special consideration since there is the possibility that failure may occur because of fatigue at stresses lower than those previously given. The maximum allowable stress in such cases depends upon the number of cycles of oscillation and the value of initial stress on which the oscillation is superimposed. It is also affected by stress concentrations which may be present.

Test results indicate that there is no reduction in strength if the number of cycles of repeated stress is less than about 10^4 [7]. The strength decreases, however, as the number of cycles increases. This decrease continues up to about 10^7 cycles. Beyond that point the strength is

essentially constant for any number of cycles. The latter stress level is known as the *endurance limit*. For structural carbon steel subjected to bending with complete stress reversal the endurance limit is approximately 27,000 psi. If the material is subjected to direct stress, the endurance limit is about 85 per cent of that for bending. If the stress is pure shear, the value is about one-half of that for bending.

If there is an initial static stress, the maximum allowable stress intensity is somewhat larger but the permissible amplitude of the oscillating stress is smaller. This may be approximately expressed by the empirical formula

$$f_{\max} = f_e + f_i \left(1 - \frac{f_e}{f_v} \right) \quad (1.21)$$

where f_e = endurance limit

f_i = initial stress

f_v = yield stress

The presence of stress concentrations due to any cause decreases the endurance limit. These may result from sudden changes in cross section, from surface roughness, from residual stress, or from any condition which causes nonuniform stress distribution. When designing for repeated stress every attempt should be made to avoid these stress raisers.

Information on the fatigue strength of connections is inconclusive. Most tests indicate greater reductions in strength due to repeated loading in connections than in the base material. This is true of welded, bolted, and riveted connections. However, the greater reduction is due to the stress raisers in the base material inherent in the connection detail rather than a weakness of the connecting material. For this reason connections should be detailed so as to minimize sudden changes in stress distribution and stress concentration. Even if such precautions are taken, however, connections and the surrounding base material should be designed more conservatively than the member itself.

If a member is subjected to repeated plastic deformation, failure occurs at a relatively small number of cycles. Such deformation should not be permitted in a structure subjected to repeated or oscillating loads.

REFERENCES

1. Data gathered by O. G. Julian for the ASCE Committee on Factors of Safety.
2. Bleich, F.: "Buckling Strength of Metal Structures," McGraw-Hill Book Company, Inc., New York, 1952.
3. Unpublished compilation by Prof. Bruce Johnston, University of Michigan, Ann Arbor, Mich.
4. Hechtman, Tridemann, and Styer: Second Progress Report on Lateral Buckling of Simply-supported Rolled Steel Beams, University of Washington. Seattle, 1953.

5. Ketter, Beedle, and Johnston: Column Strength under Combined Bending and Thrust, *Lehigh Univ. Progr. Rept.* 6, November, 1951.
6. Ketter and Beedle: The Moment-curvature Relation for Wide Flange Columns, *Lehigh Univ. Progr. Rept.* P, November, 1951.
7. Lessells, John M.: "Strength and Resistance of Metals," John Wiley & Sons, Inc., New York, 1954.
8. U.S. Army Corps of Engineers: "Engineering Manual for Protective Construction. Pt. III, Design of Structures to Resist the Effects of Atomic Bombs," prepared in part by the Massachusetts Institute of Technology under contract DA49-129-Eng-178 with the U.S. Army. The portions of this manual from which portions of this book have been extracted are being published by the U.S. Army Corps of Engineers as engineering manuals under the general title "Design of Structures to Resist the Effects of Atomic Weapons" and with the following specific manual numbers and subtitles:

EM 1110-345-413, Weapon Effects Data

EM 1110-345-414, Strength of Materials and Structural Elements

EM 1110-345-415, Principles of Dynamic Analysis and Design

EM 1110-345-416, Structural Elements Subjected to Dynamic Loads

EM 1110-345-417, Single-story Frame Buildings

EM 1110-345-419, Shear Wall Structures

Manuals 414, 415, and 416 were published on Mar. 15, 1957; Manuals 417 and 419 were published on Jan. 15, 1958; and Manual 413 is currently being processed for production.

9. Beedle, Thurlimann, and Ketter: "Plastic Design in Structural Steel," American Institute of Steel Construction, New York, 1955.
10. Wyly and Scott: An Investigation of Fatigue Failures in Structural Members of Ore Bridges under Service Loadings, *AREA Bull.* 524, September, 1955.

CHAPTER 2

BEHAVIOR OF CONCRETE AND CONCRETE STRUCTURAL COMPONENTS UNDER DYNAMIC LOADING

2.1. Introduction. Concrete and reinforced-concrete structures may be proportioned either on the basis of permissible unit stresses at working loads or on the basis of ultimate strengths for working loads increased by load factors. The choice of suitable permissible stresses in the first method and the choice of suitable load factors in the second method imply a knowledge of the strength behavior of concrete and reinforced-concrete structural members of various kinds under a variety of loadings.

More often than not members which have been proportioned to carry loads with a proper margin of safety will obviously be so stiff that deflections cannot be critical. In some cases, however, members proportioned for strength must be checked by an analysis of deflections. Occasionally deflections obviously are of predominant importance, and proportions may be selected directly on the basis of stiffness, possibly with a subsequent check of strength. In addition to the foregoing considerations of stiffness in relation to the proportioning of structural elements, a knowledge of the stiffness of concrete and reinforced concrete is required for the analysis of response to dynamic loading.

It is the purpose of this chapter to discuss some of the ways in which dynamic conditions may alter the static-strength properties of concrete, reinforcing steel, and the structural members comprised of these materials. As a basis for discussion of these modifications it will be necessary first to review the static properties of the basic materials and the static strength of concrete and reinforced-concrete structural elements.

Before discussing specific properties of materials and behavior of members it may be helpful to point out that dynamic loading can modify the static strength of materials in only two ways. First, failure of material can occur because of the action of a repeated cycle of stress of lesser magnitude than would cause failure in a single loading. This phenomenon, which is called *fatigue*, may occur in concrete and in steel used for reinforcement. It should be noted that the important factor in fatigue is stress repetition, not rate of strain. Thus, failures of this kind might occur under static loading (of cyclic nature) as well as under

dynamic loading. It is somewhat rare, however, for statically applied loadings to be repeated sufficiently often within the service life to produce fatigue failure. In contrast, dynamic loadings, of the oscillating kind, can easily produce millions of cycles of stress within the service life.

The second way in which dynamic loading may modify strength properties of materials is related to rate of strain. When concrete is strained at a very rapid rate its ultimate strength during that process is significantly higher than it would be at slower strain rates. Similarly, the yield stress of reinforcing steel, during extremely rapid straining, is significantly higher than for slow strain rates. This modification of strength properties obviously is important in structures proportioned to resist one (or a few) applications of high-intensity impulsive loading.

It should be understood that the experimental data bearing on the dynamic-strength properties of concrete are very limited, indeed. Consequently, there are important gaps in our knowledge of this subject, and such information as we do possess is subject to modification as additional data are accumulated. Still, it is believed that presently available information warrants the modifications of static properties for dynamic effects as indicated in later sections of this chapter.

2.2. Compressive Stress-Strain Properties of Plain Concrete. Concrete is a material comprised of fine- and coarse-stone aggregate cemented together by a paste of portland cement and water. Its physical properties depend upon a great many factors such as the properties of cement and aggregate, proportions of each, quantity of mixing water, thoroughness of mixing, care in placement (freedom from voids and segregation), curing conditions (temperature, humidity), and age. Since the degree of control of these factors is variable from job to job, and even within a single job, it is not surprising that strength properties in the concrete of a completed construction may differ from values assumed for purposes of design. Indeed, they may vary appreciably from one point to another within a single structure. Regardless of this variability the designer must assume a specific strength quality, and control measures should be established to assure that very little, if any, of the concrete placed fails to meet the specified strength.

a. Static Behavior. Strength quality of concrete usually is specified in terms of the unit compressive strength f'_c as determined from tests of standard cylinders. Concrete gains strength with increasing age, though at a decreasing rate, and it usually is specified that the cylinders shall be tested at 28 days, or at such earlier age as it is anticipated the actual structure will be subjected to the design loading. Testing machines do not apply a truly static loading but rather a slow steady stress increase (in the range 20 to 200 psi/sec from half load to failure). Since the entire test lasts only a few minutes, at most, what is determined is the

short-time strength, and under long-sustained static loadings lower strengths have been obtained. Nevertheless, it is customary to designate as *static* compressive strength those values obtained in the short-time tests.

Figure 2.1 shows a typical stress-strain curve as obtained from a standard ASTM compression test on a 6- by 12-in. plain concrete cylinder. For concretes commonly employed in construction, cylinder tests give

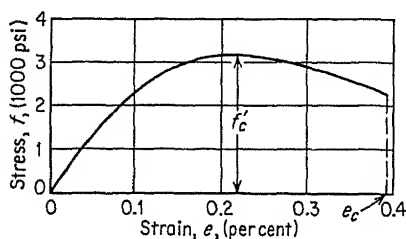


FIG. 2.1. Typical compression stress-strain diagram for concrete [Chap. 1, Ref. 8].

values of f'_c in the range 3,000 to 5,000 psi. It will be noted in Fig. 2.1 that the slope of the rising portion of the stress-strain curve is continuously decreasing; that is, there is no constant modulus of elasticity. The slope obtained from the test on any one specimen is sensitive to the rate of loading, becoming flatter as the loading rate is decreased. Nevertheless, a variety

of expressions have been proposed to relate the tangent of the initial slope to f'_c . For example, Lyse's equation (2.1) gives

$$E_c = 1,800,000 + 460f'_c \quad \text{psi} \quad (2.1)$$

From the standpoint of practical design, an effective, or secant, modulus of elasticity would be more useful. In most instances it is sufficient to approximate the effective modulus by

$$E_c = 1,000f'_c \quad (2.2)$$

Tests of concentrically loaded short columns show somewhat lower ultimate strengths than those obtained from cylinder tests of the same concrete. Based on such comparisons it is thought that the compressive strength of concrete in actual structures should be assumed equal to $0.85f'_c$.

The strain at which f'_c is reached is dependent upon the concrete itself and upon the rate of loading. For practical purposes, however, this may be taken at a constant value of 0.2 per cent.

In so far as test cylinders are concerned, the shape and extent of the descending portion of the stress-strain curve are uncertain and very difficult to measure. This may be explained partly by a uniform strain distribution which minimizes any possible stress redistribution and partly by the tendency of testing machines to release stored elastic energy. There is reason to believe, however, that the descending portion does exist, at least for stresses which are not sustained for long periods. In particular, for sections subjected to strain-depth gradients (including all cases of

reinforced concrete in flexure) it appears that the extreme fibers do indeed experience the descending stress-strain relation, to a maximum strain of approximately 0.4 per cent. At this strain, or a little less, complete failure of the concrete is to be expected. Although the descending portion of the stress-strain diagram is shown curved in Fig. 2.1, the actual shape is so uncertain that it could as well be taken as a straight line. Hognestad [2] suggests that the stress at failure be assumed to be 85 per cent of the ultimate strength.

b. Behavior under Repeated Loading. When each cycle ranges from a minimum compression stress that is essentially zero to a maximum compression stress it appears that the maximum stress, repeated for 1 or 2 million cycles, is limited to be between 50 and 65 per cent of the static ultimate strength. For any number of cycles in excess of 1 million it should be safe to assume a range from 0 to 50 per cent of static ultimate in each cycle.

As the minimum stress per cycle is increased, the maximum stress per cycle also is increased, but the tolerable range of stress decreases. For practical purposes, the variation shown in Fig. 2.2 is suggested as a conservative approximation.

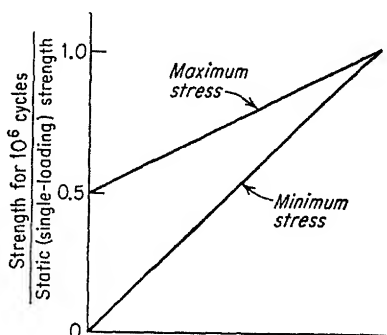


FIG. 2.2. Concrete compressive strength (>1 million cycles) as ratio of static strength.

Although it is certain that the tolerable range of cyclic stress increases with decreasing number of cycles, the available data seem insufficient to warrant proposing any mathematical relationship between these two variables at the present time.

Static tests to failure, after any number of cycles of stress below the endurance limits indicated by Fig. 2.2, show ultimate strengths as great as (or slightly greater than) those obtained from companion specimens not subjected to repeated loading.

c. Behavior under Rapid Straining Rates. Watstein [5] tested 3- by 6-in. cylinders in compression at rates of strain varying from 10^{-6} to 10 in./in.(sec). Two concretes of widely different nominal compressive strengths, namely, 2,500 and 6,500 psi, were studied.

Figure 2.3, based on results reported by Watstein [5], is a curve of DIF (*dynamic increase factor* = dynamic f'_c divided by static f'_c) vs. rate of strain. It will be noted that, for very high rates of strain, the dynamic ultimate strength can be very much greater than the static ultimate strength.

The tests referred to above also indicated increasing values of strain

at ultimate stress with increasing rates of strain. Each of these effects was substantially smaller than the effect on ultimate strength.

2.3. Tensile Stress-Strain Properties of Concrete. There is no standard test for axial tension. A variety of test specimens (cylinders and briquettes) have been used for direct tension loading, but the results obtained have varied widely. More commonly, tensile strength has been measured indirectly by the ASTM Standard Method of Test for Flexural Strength of Concrete. This test involves third-point loading

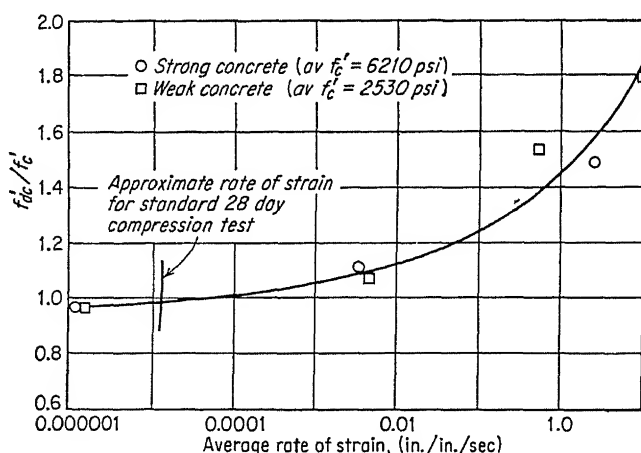


FIG. 2.3. Effect of rate of strain on concrete ultimate compression stress [Chap. 1, Ref. 8].

on plain concrete beams. End result is a *modulus of rupture* (stress in extreme fibers) computed on the assumption of a linear stress distribution. Generally speaking, tensile strengths thus computed are substantially larger than those obtained by tests of axial-tension specimens. The difference may be explained partly by the fact that the distribution of stress in the beam specimens probably is not linear. It may also be due in part to the fact that only a portion of the beam cross section is subject to maximum stress while the entire section of a tension specimen is subject to high stress. If tension failure is initiated at points of local weakness, the coincidence of points of weakness and high nominal stress is more probable in axial-tension specimens than in beam specimens.

a. Static Behavior. It is known that ultimate tensile strength of concrete does not increase in direct proportion to compressive strength. A number of expressions relating these two properties have been proposed. Perhaps as simple as any are the relations

$$\text{For uniform tension,} \quad f_t = 5 \sqrt{f'_c} \quad (2.3)$$

$$\text{For modulus of rupture,} \quad f_t = 10 \sqrt{f'_c} \quad (2.4)$$

It should perhaps be noted that tensile strengths (and maximum tensile strain) are very small. Moreover, tensile failures are abrupt.

For practical design purposes the tensile modulus of elasticity may be assumed equal to the value of the compression modulus of elasticity.

b. Behavior under Repeated Loading. Tests on plain concrete beams, involving repeated stresses varying from zero to maximum, indicate that tensile rupture moduli for a great many cycles of loading are about 50 per cent of the corresponding static values.

c. Behavior under Rapid Straining Rates. In view of the scarcity of data for tensile strength under rapid strain rates, no modification of static values appears to be justified at this time.

2.4. Shear Strength of Concrete. The strength of concrete in pure shear cannot be directly determined because a state of pure shear implies the existence of principal tensile stress of the same magnitude as the shear stress. Since concrete is weaker in tension than in shear, a specimen in pure shear always fails in tension.

An indirect indication of pure-shear strength can be obtained by biaxial and triaxial stress tests. These tests [6, 7] permit one to draw the Mohr's envelope defining all possible failure states of combined stress. This approach has indicated a theoretical ultimate strength in pure shear equal to about 20 per cent of the compressive ultimate strength.

In view of the impossibility of developing a state of pure shear of magnitude equal to the theoretical ultimate, it would be meaningless to attempt any modification for dynamic loading.

2.5. Stress-Strain Properties of Reinforcing Steel. The behavior of reinforced-concrete structural members is, of course, strongly dependent upon the amount, location, and characteristics of the steel bars used for reinforcement.

a. Static Behavior. Figure 2.4 shows typical stress-strain curves for structural-, intermediate-, and hard-grade steel bars as obtained from tests at standard testing-machine speeds. For stresses up to the yield point all grades have essentially the same modulus of elasticity E , which for practical purposes can be taken as 30,000,000 psi. For structural and intermediate grades there is a large zone of substantially constant stress between the point of yielding and the point at which strain hardening begins. For hard-grade steels the zone of constant stress is smaller, and for some hard steels the yield point may not be as pronounced as indicated in Fig. 2.4. Nevertheless, even in hard-grade steel, there is a very substantial region of plastic strain between the point where linear stress-strain behavior stops and the point of rupture. This region of plastic strain is much larger than the region of linear behavior.

Whereas the guaranteed minimum yield stresses are 33,000, 40,000, and 50,000 psi for structural-, intermediate-, and hard-grade bars, respec-

tively, mill tests indicate that average values actually are 40,000, 47,500, and 65,000 psi.

b. Behavior under Repeated Loading. Under repeated stress with a minimum value of zero per cycle the upper limit (endurance limit) for structural-grade steel is approximately equal to the yield value. Consequently, under these conditions it can be said that repeated loading has little or no effect on the useful strength of structural-grade steel. Under

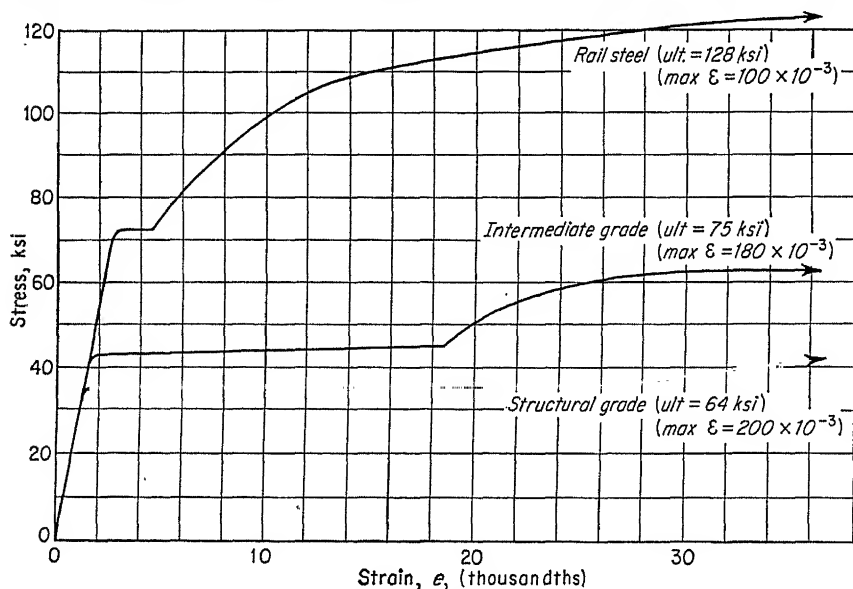


FIG. 2.4. Typical stress-strain curves for reinforcing steel.

reversed stressing (equal tension and compression maximums per cycle) the endurance limit may be as low as 60 to 70 per cent of the yield value.

As the hardness of a steel is increased, the ratio of endurance limit to yield stress tends to decrease. If one excepts those steels in which high yield is obtained by cold working, the ratio of endurance limit to yield (zero stress to maximum each cycle) might be estimated at approximately 75 per cent. In those cases where cold working is utilized to increase yield stress there is relatively little gain in endurance limit, and consequently the latter may be a small fraction (less than 50 per cent) of the yield value.

It must be noted that relatively little of the controlled fatigue testing of steels has been performed on reinforcing bars as rolled, that is, with their surface deformations. It is known that such deformations have a stress-concentrating effect which tends to reduce the fatigue resistance. Further, surface deformations should be more harmful in the harder grades of steel, particularly in steels which achieve hardness through

cold working. On the other hand, most reinforcing-steel bars used in the United States are not cold-worked. While service failures definitely attributable to fatigue of reinforcing bars may indeed have taken place, no cases of this kind are known to the authors. This would seem to imply that the margins of safety conventionally chosen for working stresses with respect to static yield automatically provide adequate margins of safety with respect to fatigue.

c. Behavior under Rapid Straining Rates. The principal effect of rapid strain rates is to increase the yield stress above values obtained in static loading. This is illustrated by Fig. 2.5, which presents curves of dynamic

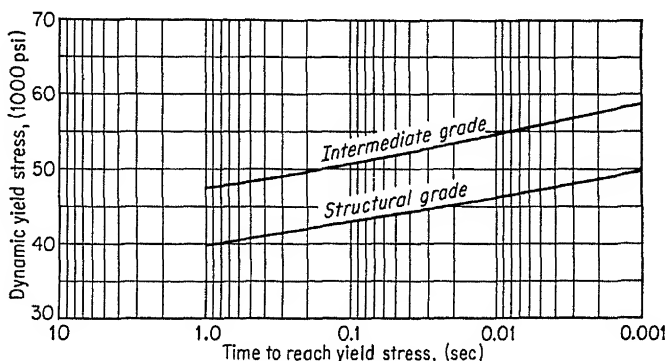


FIG. 2.5. Effect of rate of strain on yield stress in steel [Chap. 1, Ref. 8].

yield stress vs. time to reach yield for structural- and intermediate-grade steels. It will be observed that significant increases in yield stress occur at rapid rates of strain.

The ultimate (breaking) strength is not appreciably modified by speed of loading.

2.6. Flexural Behavior of Reinforced Concrete. Having discussed, briefly, certain aspects of the strength properties of concrete and steel, we proceed now to the more common structural elements. Our concern is primarily with possible modifications of behavior due to dynamic loading, but it seems necessary, first, to describe the major aspects of static behavior.

For a great variety of structures and structural elements, proportions (dimensions, amount and distribution of steel) are governed by internal moments. For this reason we start with flexural behavior, that is, the behavior of members in bending.

a. Static Behavior of Flexural Sections. At small values of moment the entire section may be uncracked, because stresses in the extreme tensile fibers are small. At a relatively low moment cracking does occur, and as the moment is further increased the contribution of concrete tensile

stresses must be neglected. In this "cracked state" the internal bending couple is comprised of equal and opposite compressive-concrete force and tensile-steel force. Figure 2.6 illustrates this condition. Tests indicate that, even after cracking, strain varies in an essentially linear manner from maximum compressive strain at one side to maximum tensile strain at the other. In the conventional *working-stress* method of proportioning, the further assumption of constant concrete modulus of elasticity leads to a linear distribution of concrete stress. This is illustrated in Fig. 2.6c.

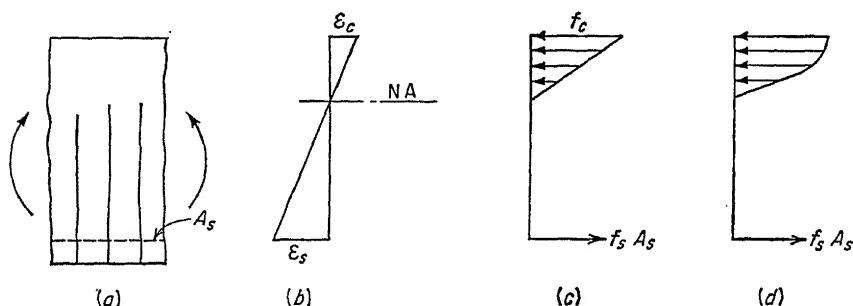


FIG. 2.6. Strain and stress in singly reinforced concrete flexural element. (a) "Cracked" state; (b) strain; (c) linear stress; (d) nonlinear stress.

Although strains can be measured with no great difficulty, it is extremely difficult to measure stresses. Consequently, only a few attempts have been made to measure, directly, the distribution of stress in the compression zone. Experimental data on this point are not yet sufficiently numerous to justify positive conclusions. Based on indirect evidence, however, it is generally believed that the compressive-stress distribution is essentially linear under normal working conditions (say, $f_c < 0.5f'_c$). At higher stress levels it is believed that the distribution is nonlinear, as in Fig. 2.6d. Indeed, some investigators think it probable that stress-strain variation in the compression zone of a flexure member would be of the same form as a portion of the cylinder-test stress-strain curve.

The mode of flexural failure depends upon the value of the reinforcing index q :

$$q = \frac{pf_y}{f'_c} \quad (2.5)$$

where f_y = static yield stress for reinforcing steel

f'_c = static ultimate stress for concrete

p = ratio of tension-steel area to concrete area defined by bd

A member is said to be overreinforced or underreinforced depending on whether q is greater or less than a critical value of about 0.45. Overreinforced members fail by crushing of the compression concrete without

yielding of the tension steel. Such failures occur with little or no warning and obviously are not desirable. In practice, however, the use of over-reinforced members is very rare. If proportioning is on the basis of working stresses, the specified permissible stresses f_c and f_s generally have such values as to render uneconomical the use of excessive steel percentages. The latest ACI Code revision permits proportioning on the basis of ultimate strength, but specifically limits q to a maximum of 0.4.

Virtually all flexural members are underreinforced and exhibit the following stages of moment-distortion behavior. First, there exists the

uncracked stage, in which the entire concrete section is effective and distortion is directly proportionate to moment. The uncracked state terminates at a value of bending moment, which is only a fraction of the working-load value. Second, there occurs the cracked, elastic stage, in which the steel stress is below yield value, and distortion increases approximately in proportion to moment but at a greater rate than in stage 1. Third, the plastic stage, which starts when the steel begins to yield, is marked by progres-

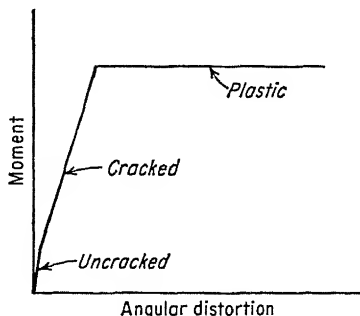


FIG. 2.7. Idealized moment-distortion behavior of underreinforced, singly reinforced flexural section.

sive movement of the neutral axis toward the compression face with consequent reduction of the compressive zone and is terminated by crushing of the concrete when the extreme fiber strain reaches a limiting value of perhaps 0.4 per cent. During the third stage the force in the steel is essentially constant ($= f_y A_s$), and since the internal arm varies but slightly, the moment is likewise practically constant. Figure 2.7 indicates the three stages of moment-distortion behavior in idealized form.

When it is necessary to supply larger moment capacity than can be obtained with a singly reinforced section of low index q , the designer may use a doubly reinforced section, that is, a section having compression reinforcement as well as tension reinforcement. As indicated in Fig. 2.8, the total moment on such a section is the sum of two couples, one involving the compressive-concrete force and a portion, T_1 , of the tensile-steel force, the other involving the compressive-steel force and the remainder, T_2 , of the tensile-steel force.

It has been determined, in tests, that the stress in compression steel is increased by shrinkage and creep strains in the concrete (time-dependent strain under sustained loading) to values substantially greater than those computed on the basis of linear strain distribution and short-term modulus of elasticity. Tests also have demonstrated that compressive steel

develops its yield stress when the section is loaded to failure. For these reasons most codes permit the working stress in compression steel to be assumed equal to twice the value computed on the basis of short-term modulus of elasticity.

For doubly reinforced sections the reinforcing index q is given by

$$q = \frac{(p - p')f_v}{f'_c} \quad (2.6)$$

where $p' =$ ratio of compression-steel area to concrete area, bd . As for singly reinforced sections, an index of approximately 0.45 divides

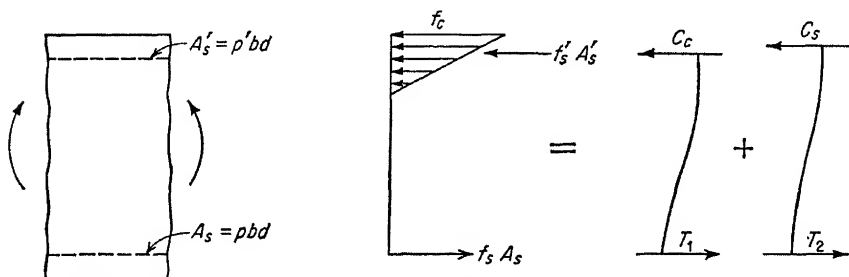


FIG. 2.8. Internal forces for doubly reinforced concrete flexural element.

underreinforced (ductile-behavior) sections from overreinforced (brittle-behavior) sections. It is apparent that the use of compression reinforcement permits retention of a low reinforcing index while using an amount of tension steel (to which moment capacity is proportionate) limited only by the practicalities of fabrication. The idealized moment-distortion behavior for a doubly reinforced section proceeds through the same stages as were described for the singly reinforced section.

Most specifications require that compression reinforcement shall be adequately secured by stirrups or ties, to prevent these bars from buckling outward. Such buckling is unlikely to occur prior to the plastic stage. However, once crushing of the concrete commences, effective ties are needed to delay buckling of the compression bars and to ensure that buckling, when it does occur, will be local rather than general. Well-tied compression steel greatly extends the range of plastic strain beyond that which can be developed by an otherwise similar section lacking compression steel.

A number of different expressions have been proposed for the yield moment of flexural sections, and these expressions owe their differences to different assumptions regarding the distribution of the concrete compressive stresses. For underreinforced sections numerous tests have indicated that the yield moment is not sensitive to assumed compressive-stress distribution. Recognizing this fact, Whitney and others have

suggested simple expressions for yield moment M_y based on a (fictitious) uniform distribution of compression stress. For rectangular sections, singly reinforced, one can use the following:

$$M_y = A_s f_y d \left(1 - \frac{p f_y}{1.7 f'_c} \right) \quad (2.7)$$

$$M_y = b d^2 \left[p f_y \left(1 - \frac{p f_y}{1.7 f'_c} \right) \right] \quad (2.8)$$

and for doubly reinforced rectangular section:

$$M_y = A'_s f_y d' + (A_s - A'_s) f_y d \left[1 - \frac{(A_s - A'_s) f_y}{1.7 f'_c b d} \right] \quad (2.9)$$

$$M_y = b d^2 \left\{ p' f_y \frac{d'}{d} + (p - p') f_y \left[1 - \frac{(p - p') f_y}{1.7 f'_c} \right] \right\} \quad (2.10)$$

where A_s = area of tension steel

A'_s = area of compression steel

b = width of rectangular section

d = depth of rectangular section to tension steel

d' = distance between tension and compression steel

$p = A_s/bd$; $p' = A'_s/bd$

f_y = static yield stress for steel

f'_c = static ultimate stress for concrete

b. Static Behavior of Flexural Members. The foregoing section (2.6a) of this chapter relates to the moment-distortion behavior of individual sections of flexure elements. In a complete flexural member the bending moment generally varies from section to section along the span. In addition, the steel percentage (and sometimes the section dimensions) may vary along the span. These factors, plus uncertainty regarding the concrete modulus of elasticity, make precise deflection computations quite impractical. If the bending moments are relatively small at all sections, so that there is little or no tensile cracking, deflection computations can be based on moment of inertia of gross concrete section. If bending moments are relatively large, there will be regions of numerous tensile cracks and it may be better to use a moment of inertia which is the average of the value for the gross concrete section and the value for the transformed section (compression concrete plus n times the reinforcing steel).

Up to the start of cracking, the load-deflection curve for a flexure member is essentially a straight line. As successive cracks form and spread, the effective stiffness of the member is gradually reduced, causing the slope of the load-deflection curve to become smaller. After the major crack pattern has formed, the load-deflection curve proceeds at an

approximately constant (though steadily decreasing) slope up to the point of yielding. If the member is statically determinate, yielding at the section of maximum moment will convert the member to a mechanism, and the load-deflection curve will be essentially horizontal from the point of yielding to final collapse. If the member is statically indeterminate, yielding at a section will in effect remove one restraint, causing a sharp decrease in the slope of the load-deflection curve. Yielding of successive sections will cause successive reductions in load-deflection shape until the member becomes a mechanism, after which the load-deflection curve will be essentially horizontal to the point of collapse.

c. Flexural Behavior under Repeated Loading. It was pointed out in Sec. 2.2b that concrete under repeated compressive stress has an endurance limit which may be as low as 50 per cent of the static ultimate stress. In considering the possible significance of this figure it must be kept in mind that flexural sections subject to repeated loading usually are proportioned for working stresses in extreme compression fibers not to exceed $0.4f'_c$. As one proceeds toward the neutral axis, from the extreme fiber, stress intensities are progressively less. Thus if extreme fibers did, in fact, sustain cumulative strain because of repeated cycles of stress, a redistribution of stress might be expected to increase the share of resistance provided by zones closer to the neutral axis.

In statically indeterminate members the division of moments between different sections may be very different from that assumed in the design, either through an erroneous evaluation of relative stiffnesses, through an unanticipated settlement of supports, or because of some other factor. This might lead to moments on one section much greater (and on another section much less) than assumed and, in consequence, to extreme compression-fiber stresses at one section much greater than the endurance limit. Although cumulative strain at the overloaded section might lead to favorable redistribution of moments, the possibility of fatigue failure under the assumed set of circumstances appears to be real. This suggests that elastic analysis of indeterminate structures to determine internal gross forces may be more important for repeated loading.

A number of investigators [4, 21-25] have tested reinforced-concrete beams under repeated loading. In some cases steel percentages very different from conventional values were used to exaggerate a particular mode of failure. For example, LeCamus [25] used very low steel percentages in beams designed to fail by fatigue of the steel and very high percentages in beams designed to fail by fatigue of the concrete. For these beams he obtained endurance limits of 60 to 65 per cent of static strength. Other investigators [23, 24], using conventional percentages of steel, have obtained higher values; for example, for beams with 0.9 per cent steel Lea obtained a 1 million cycle endurance limit of 80 per

cent of static strength and a 10 million cycle endurance limit of 70 per cent of static strength.

It should be noted that many of the reported tests were made with bars which were, from the standpoint of bond, inferior to those currently used in this country. Where structural-grade steel was used failure was not by fracture of the bars, but accumulated strain in the bars and accumulated slip were factors in final failure of the concrete. Accordingly, the superior bond characteristics of bars in current use might be reflected in higher beam-endurance limits.

In tests employing high-tensile bars it is reported that failure under repeated loading usually occurred by fracture of the bars, at stresses well below the yield stress. It should be noted, however, that the endurance limit of these steels rises with increasing values of the minimum stress per cycle. In cases involving substantial dead/live load ratio the fatigue performance of such steels might be very much better than in the zero-to-maximum cyclic loadings reported.

All evidence indicates that flexure members subjected to many cycles of loading within the usual working-stress range suffer no loss of ultimate strength in subsequent static loading.

In summary, the evidence indicates that conventional margins of safety with respect to static ultimate strength guarantee adequate safety with respect to the effects of the most common cases of repeated loading. It should be kept in mind, however, that most cases of repeated loading do not involve the full value of design working load in every cycle. For example, a bridge structure may experience several million cycles of loading of which only a few thousand cycles produce design values of working stress. Consequently, in any application involving a high live/dead ratio and for which it is known that the full live loading will be repeated many times, the level of permissible working stresses should be chosen with some caution. In these circumstances, it may be advisable to use somewhat lower stresses than are conventionally used for static loading.

d. Flexural Behavior at Rapid Rates of Strain. As was noted in Secs. 2.2c and 2.5c, very rapid straining rates have the effects of increasing the compression ultimate stress for concrete and the yield stress for reinforcing steel. Tests of beams at rapid rates of strain [26-29, 33] indicate that these effects are reflected in corresponding increases of the yield moment for flexural sections. If the dynamic values of f'_c and f_y are denoted by f'_{dc} and f_{dy} , respectively, the expressions for dynamic yield moment of an underreinforced flexural section become, for singly reinforced section,

$$M_y = bd^2 \left[pf_{dy} \left(1 - \frac{pf_{dy}}{1.7f'_{dc}} \right) \right] \quad (2.11)$$

and, for doubly reinforced section,

$$M_v = bd^2 \left\{ p' f_{dy} \frac{d'}{d} + (p - p') f_{dy} \left[1 - \frac{(p - p') f_{dy}}{1.7 f'_{dc}} \right] \right\} \quad (2.12)$$

It is likewise possible to write expressions for the dynamic moment strength of overreinforced flexural sections. Since a ductile mode of failure is even more important for dynamic loading than for static loading, overreinforced sections are to be avoided; consequently, expressions for strength of overreinforced sections are purposely omitted.

2.7. Shear Behavior of Reinforced Concrete. *a. Static Behavior.*

In Sec. 2.6 attention was focused on the behavior of flexural sections only, but members subject to bending are almost always subject to transverse shear as well. Our knowledge of shear behavior under static loading is very incomplete, and recent widely publicized shear failures in reinforced-concrete rigid frames testify that our design criteria for shear reinforcement are not completely satisfactory. Reports based on a continuing series of investigations at the University of Illinois [34-39] have shed considerable light on the mechanism of shear failure under static loading. No comparable studies have been undertaken for dynamic loading.

Shear failure, or *shear-compression failure* as it is more accurately called, involves two distinct stages. The first stage is the development of diagonal tension cracking characterized by the sudden appearance of an inclined crack (or cracks) of major importance. It is wider than any of the inclined flexure cracks, although part of its length may coincide with a previously existing crack of this kind. It starts horizontally at the level of the tension steel and extends well into the compression zone. The second stage involves the sudden failure of the compression zone at the head of a diagonal tension crack, and this failure apparently is due to a reduction of the depth of the compression zone by progression of the diagonal crack.

It will be clear from the foregoing that shear failure can occur if the principal tension stresses, associated with shear and moment, and the prior pattern of flexure cracking are such as to cause a true diagonal tension crack and if, in addition, the bending moment at the head of this crack equals some critical value. After the formation of diagonal tension cracks the beam may fail either in shear compression at the head of one of these cracks or in a flexure mode at some other section, where bending moment is maximum. Which of these failure modes is experienced will depend on the distribution of bending moment along the span, in relation to the relative moment strengths of the beam sections in shear compression and in flexure.

Because the shear-compression mode is sudden (that is, with little or no ductility) it is desirable to proportion members so that the flexure mode of failure can be developed, that is, to prevent a prior shear-com-

pression failure. To achieve this objective one must be able to predict, first, whether diagonal tension cracks will occur, and second, whether the formation of such cracks will result in shear-compression failure. In Ref. 37 a rational expression is derived for the moment strength M_s when failure is in the shear-compression mode. A function only of the concrete strength and the properties of the section, this expression is, for rectangular beams,

$$M_s = bd^2 \left[f'_c (k + np') \left(0.57 - \frac{4.5f'_c}{10^5} \right) \right] \quad \text{psi} \quad (2.13)$$

where

$$k = \sqrt{[n(p + p')]^2 + 2n \left(p + p' - p' \frac{d'}{d} \right)} - n(p + p') \quad (2.14)$$

$$n = 5 + \frac{10,000}{f'_c} \quad \text{psi} \quad (2.15)$$

If web reinforcement is present, the shear-moment capacity of the section M_{sw} is given by

$$M_{sw} = M_s \left(1 + \frac{2A_w f_{yw}}{10^3 b s \sin \alpha} \right) \quad \text{psi} \quad (2.16)$$

where M_s = moment strength, as given by Eq. (2.13)

A_w = area of web reinforcement

f_{yw} = yield stress in web reinforcement

b = width of section

s = spacing of web reinforcement

α = angle of inclination of web reinforcement with respect to beam axis

In addition to the above, Ref. 37 presents modified expressions applicable to T beams as well as expressions applicable to restrained beams when the mode of failure involves redistribution of internal forces because of local bond failure. To include these expressions in the present chapter would be to extend its scope beyond that which was intended. The reader faced with an application involving possible shear-compression failure in a restrained beam is advised to consult Ref. 37 because the modified expression for this case gives lower values of M_s than does Eq. (2.13) above.

Except in certain special cases of concentrated loads, it is difficult to predict whether diagonal tension cracks will occur and where they will occur. This difficulty applies to static loading, and it would become even more pronounced in cases of dynamic loading. However, it is shown in Ref. 37 that only moderate quantities of shear reinforcement are required to make the shear-moment capacity [Eq. (2.16)] equal to the flexure-moment capacity [Eqs. (2.9) and (2.10)]. This would appear to

be a logical and conservative method for guaranteeing flexural-failure modes for beams. It should be noted, however, that the shear-moment capacity [Eq. (2.16)] is directly dependent upon f'_c , whereas the flexure capacity for underreinforced sections is almost independent of f'_c . In view of the variability of f'_c and in view of the undesirability of the shear-compression mode of failure, it seems advisable to supply enough web reinforcement to make the computed shear-moment capacity somewhat larger than the flexure capacity.

For certain cases, such as slabs, additional test data will be required to establish the criteria for shear strength and to determine whether the shear-moment concept is applicable. For the present, it can only be recommended that ultimate unit shear stress in such elements be based on relatively simple expressions which were originally suggested for beams. One such expression, proposed by Moretto [34], is-

$$v_u = 0.10f'_c + 5,000p + Krf_y \quad \text{psi} \quad (2.17)$$

where v_u = average unit shear stress ($= V/bjd$) when web reinforcement begins to yield

p = longitudinal steel ratio $= A_s/bd$

Krf_y = shear strength of web reinforcement computed on basis of a truss analogy

b. Dynamic Behavior. It might well be argued that the procedure suggested for beams in the above section can be too conservative in some cases. This is apparent from the recognized fact that for some beam proportions and static-load configurations, diagonal cracks do not develop. Thus, the above procedure would, in such cases, result in the use of web reinforcement where it clearly is not needed. In proportioning members for dynamic loading, however, several factors suggest the desirability of conservatism with respect to web reinforcement. First, only meager data are available on dynamic shear behavior (for either cyclic loading or impact loading). Second, some investigators [25] have observed relatively low shear-endurance values under repeated loading. Third, for impulsive and impactive loadings the higher modes of vibratory response, which contribute little to bending moments, may cause relatively large transient shears, and thereby cause diagonal cracking. Fourth, several investigators have found that beams subject to impact loading must have adequate stirrups to develop their full plastic flexure capacities.

In view of the above factors it is recommended for beam members subject to heavy repeated loading, and for beam members subject to impulsive and impactive loadings, that web reinforcement be supplied in accordance with the method indicated in the next-to-last paragraph of the preceding section. In view of the relative uncertainties in shear-compression failure modes it would be well to use f'_c rather than f'_{dc} in all applications of Eqs. (2.13), (2.16), and (2.17).

Web reinforcement can be bent-up bars, inclined stirrups, or vertical stirrups. For members subject to reversible shear and bending moment (including, particularly, the effects of impulsive or impactive loadings) it is advisable to use vertical stirrups.

2.8. Behavior of Reinforced-concrete Columns. *a. Behavior under Static Axial Load.* The majority of practical reinforced-concrete columns have such small slenderness ratios that failure by buckling does not have to be considered. Slender columns have been used, of course, and they may be used more extensively in the future. Consequently, although slender columns will not be discussed in the present outline, Ref. 40 is included for those who may wish to pursue studies of such members.

There have been many tests of short columns under axial and eccentric static loading, and the literature on the behavior of such members has been widely published. In the present treatment it seems unnecessary to do any more than review a few of the major points of interest.

It has long been recognized that the unit stresses in axially loaded columns are as much dependent on the effects of shrinkage and creep as upon the immediate elastic strains due to load. For this reason it is customary to proportion columns on a modified ultimate-strength basis. At failure both the concrete and the reinforcing steel are fully developed, and the column ultimate strength can be expressed as

$$P_u = 0.85f'_c A_c + f_y A_s \quad (2.18)$$

where A_c = area of concrete

A_s = total area of reinforcing steel

As a safe working (axial) load many of the codes (see Art. 1103 of ACI Code, Ref. 20) give the following expressions:

For spirally reinforced columns,

$$P = 0.225f'_c A_g + 0.4f_y A_s \quad (2.19)$$

For tied columns,

$$P = 0.18f'_c A_g + 0.32f_y A_s \quad (2.20)$$

where A_g = area of gross column section. A comparison of Eqs. (2.19) and (2.20) with Eq. (2.18) shows a greater factor of safety with respect to concrete compressive strength than with respect to steel yield stress. This is consistent with the fact that the risk of obtaining substrength concrete is greater than the risk of obtaining steel yield values below the guaranteed minimums for particular grades. It will be noted also that the allowable working load on tied columns is only 80 per cent of the allowable load on spirally reinforced columns. This is based on the fact that spiral reinforcement restrains the concrete at failure and results in a more ductile mode of failure, whereas in tied columns failure is abrupt. It is of interest to note that in the latest revision of the ACI

Code (318-56) ultimate-strength proportioning is permitted on an optional basis, and in this optional method, Eq. (2.18) is used directly, that is, without separate factors of safety for concrete and steel.

b. Behavior under Static Eccentric Loads. Although it has been common to compute axial-working-load capacities on a modified-ultimate-strength basis, eccentric working loads have been computed on the basis of permissible working stresses, assuming a linear distribution of compression stress and zero tension stress. This approach is retained in the latest ACI Code revision [20], but an optional ultimate-strength method is introduced. For an excellent historical review of ultimate-strength theories, as well as a comparison between theory and a comprehensive series of tests, the student is referred to a paper by Hognestad [2].

Just as for members subject to flexure only, it is possible to distinguish between tension and compression modes of failure in eccentrically loaded column sections. In a tension-failure case the tension reinforcement yields first, causing the neutral axis to move toward the compression face with a consequent reduction of the compression zone and, finally, crushing of the concrete. In a compression-failure case the concrete fails in compression without yielding of the tension steel. The expressions given in Ref. 20 for ultimate eccentric-load capacity of a rectangular column section are as follows (modified slightly for notation differences):

Tension-failure case:

$$P_u = 0.85f'_c b d$$

$$\left(\sqrt{\left(1 - \frac{e}{d} + \frac{1}{2} \frac{d'}{d}\right)^2 + 2 \left\{ \left(\frac{e}{d} + \frac{1}{2} \frac{d'}{d}\right) [pm - p'(m-1)] + p(m-1) \frac{d'}{d} \right\}} + \left(1 - \frac{e}{d} + \frac{1}{2} \frac{d'}{d}\right) - (p - p')m \right) \quad (2.21)$$

Compression-failure case:

$$P_u = \frac{A'_s f_y}{e/d' + 1/2} + \frac{b t f'_c}{3te/d^2 + 1.18} \quad (2.22)$$

where A'_s = area of compression reinforcement

$$p = A_s/bd$$

$$p' = A'_s/bd$$

b = width of section

d = depth of section from compression face to tension steel

d' = distance between tension and compression steel

t = over-all depth of section

e = eccentricity of loading

$$m = f_y/0.85f'_c$$

f'_c = ultimate (cylinder) strength of concrete

f_y = yield stress of steel

By utilizing Eqs. (2.21) and (2.22) one can plot a diagram of P_u versus M_u which defines all possible combinations of ultimate load and ultimate moment that can be carried by any given section. However, diagrams of this kind are more useful if they are plotted in the dimensionless variables $P_u/f'_c b t$ versus $M_u/f'_c b t^2$. Figure 2.9 illustrates the typical shape of such a diagram.

c. Column Behavior under Repeated Loadings. Theoretically, a reinforced-concrete column could suffer fatigue failure of the concrete or steel because of the effect of large numbers of cycles of loadings. When

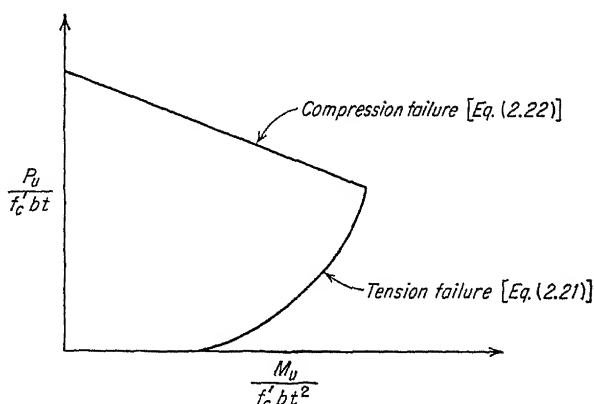


FIG. 2.9. Dimensionless diagram for static ultimate strength of column section.

the load eccentricity is large a condition of pure flexure is approached, and the previous discussion of fatigue of flexural members would apply. However, most columns are reinforced on the compression side as well as on the tension side. Thus under large loading eccentricities, their behavior should approximate that of a doubly reinforced rather than a singly reinforced flexure section and doubly reinforced sections should be more resistant to fatigue failure of the compression zone. Under small loading eccentricities the factors of safety implied by conventional working stresses [and by Eqs. (2.19) and (2.20)] are sufficiently large so that fatigue failure seems most unlikely. Finally, it might be noted that many columns carry a fairly high ratio of dead/live loading. In such members the range of cyclic stress is small; therefore the upper limit of stress to cause fatigue failure is increased. In short, it appears that fatigue failure need not be considered in reinforced-concrete columns, with the possible exception of cases in which the eccentricity is so large that the member might properly be classified as a beam. Even in the latter event fatigue need be considered only for the special circumstances noted in Sec. 2.6c.

2.9. Column Behavior under Rapid Strain Rates. As has been noted elsewhere, rapid strain rates have the effect of increasing f'_c and f_y to dynamic values of f'_{dc} and f_{dy} , where the increase depends upon the rate of strain. In practical problems involving very high rates of strain it is necessary not only that the column attain the ultimate load assumed in proportioning but that it also be able to sustain this load for a finite (though often brief) time, without buckling. For this reason it is recommended that the dynamic ultimate axial-load capacity be defined by the following expression:

$$P_u = 0.9(0.85f'_{dc})A_c + f_{dy}A_s \quad (2.23)$$

It will be noted that Eqs. (2.18) and (2.23) are similar, but the latter contains the dynamic properties of the materials plus the factor 0.9 in the first term. At 0.9 of the ultimate concrete strength the slope of the stress-strain curve (that is, tangent modulus of elasticity) is sufficient to prevent buckling of columns of typical proportions. The same analysis which led to the factor 0.9 in Eq. (2.23) led also to the following expressions for limiting the slenderness ratio L/d to avoid buckling:

For rectangular sections:

$$\frac{L}{d} \leq \sqrt{\frac{230}{1.11pm + 1.0}} \quad (2.24)$$

For circular sections:

$$\frac{L}{d} \leq \sqrt{\frac{172}{1.11pm + 1.0}} \quad (2.25)$$

where $m = f_{dy}/0.85f'_{dc}$

$$p = A_s/A_c$$

A_s = total area of steel

A_c = total area of concrete \approx gross concrete area

To obtain a diagram defining all combinations of dynamic ultimate load and dynamic ultimate moment one needs, in addition to Eq. (2.23), the following two expressions, which are obtained by substituting f'_{dc} and f_{dy} in Eqs. (2.21) and (2.22):

$$P_u = 0.85f'_{dc}bd$$

$$\left(\sqrt{\left(1 - \frac{e}{d} + \frac{1}{2} \frac{d'}{d}\right)^2 + 2 \left\{ \left(\frac{e}{d} + \frac{1}{2} \frac{d'}{d}\right)[pm - p'(m-1)] + p'(m-1) \frac{d'}{d} \right\}} + \left(1 - \frac{e}{d} + \frac{1}{2} \frac{d'}{d}\right) - (p - p')m \right) \quad (2.26)$$

$$P_u = \frac{A_s' f_{dy}}{e/d' + 1/2} + \frac{bf'_{dc}}{3te/d^2 + 1.18} \quad (2.27)$$

2.10. Behavior of Reinforced-concrete Shear Walls and Deep Beams. In buildings designed to resist large lateral forces (wind, earthquake,

blast) the shear wall is an effective element for transmitting shear between successive floors. Such walls usually are integral with floor slabs, columns, and/or similar walls oriented at 90° to the shear walls. These other elements contribute to the strength and stiffness of shear walls.

Because of their unusual proportions, and because they must be assumed to function in a cracked state, shear-wall behavior cannot be

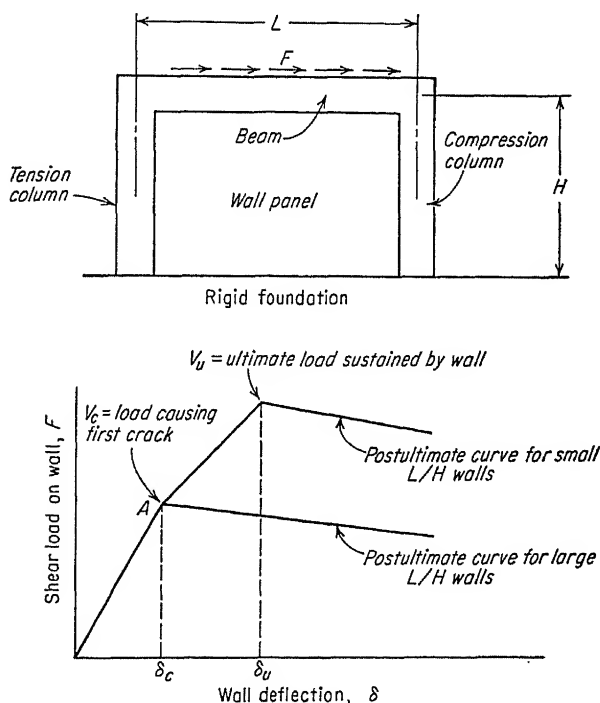


FIG. 2.10. Load-deflection behavior of shear walls [42; Chap. 1, Ref. 8].

predicted on the basis of theory derived for deep, homogeneous beams. Static tests upon scaled shear-wall models have been performed at Massachusetts Institute of Technology [41] and at Stanford University [42]. Recommendations which follow are based on the Stanford test series, which was the more extensive of the two investigations.

a. Static Behavior of Shear Walls. Figure 2.10 shows a simplified shear wall and characteristic static-load-deflection curves. It should be noted that the framing members used in the test walls correspond to integral beams or floor slabs, and columns or normal walls, in a prototype shear-wall construction. The shear wall proper is reinforced with equal percentages of vertical and horizontal steel bars, and additional longitudinal steel is placed in the perimeter members. After cracking, at point A in

Fig. 2.10, the curve is a function of the proportions of the wall and the relative proportions of reinforcing steel in the shear panel and in the perimeter members. In general, walls having a small ratio of length to height ($L/H \approx 1$) sustain an ultimate load greater than the cracking load. For large-ratio L/H (> 2) ultimate load is approximately equal to the cracking load. The ratio of ultimate to cracking load is, however, subject to modification according to the amount of steel in columns and wall panel.

The static shear load R_c for first cracking is given by

$$R_c = 0.1f'_cLt \quad (2.28)$$

where L = wall length center to center of columns

t = thickness of shear panel

The ultimate static shear load R_u is a function of P , the compression-column influence factor, and C , the panel influence factor, where P and C are given by

$$P = f_v p t (H + L) \quad (2.29)$$

$$C = A_s f'_c \left[15 + 1.9 \left(\frac{L}{H} \right)^2 \right] \quad (2.30)$$

where H = wall height to center of top beam

p = steel ratio in each direction (assumed equal)

A_s = area of column steel in column on compression edge of panel

The ratio R_u/C , which defines R_u , can be expressed as follows, for a single-story wall:

$$\frac{R_u}{C} = \frac{0.1}{P/C + 0.1} + \frac{2.1}{P/C + 0.6} \left(\frac{P}{C} \right) \quad (2.31)$$

For walls of two or more stories, the second term in Eq. (2.31) should be multiplied by 1.33.

The Stanford tests indicated that the presence of vertical load on the wall had little effect on R_u except when vertical load was greater than R_u ; therefore the effect of vertical load has been neglected.

Taking into account both shear deformation and flexural deformation, the expression for deflection at first cracking is

$$\delta_c = \frac{R_c H}{E} \left(\frac{H^2}{3I} + \frac{1}{2.2Lt} \right) \quad (2.32)$$

where E = modulus of elasticity of concrete

I = moment of inertia of gross horizontal section through shear wall and edge members

The ultimate deflection δ_u is given by

$$\delta_u = 24 \frac{H}{L} \delta_c \quad (2.33)$$

It should be noted that the above expressions are based on tests in which the parameters were varied within the following limits. Applicability of the given relations to situations outside these limits is uncertain.

Column steel ratio 0.01 to 0.033

Column steel encased in concrete

f'_c from 2,000 to 4,000 psi

L/H from 0.9 to 3.0

P/C from 0 to 3.26

f_v from 42 to 62 ksi

Shear panel p from 0 to 0.015

b. Dynamic Behavior of Shear Walls. No tests of shear walls under either repeated loading or high rates of strain have thus far been performed.

It seems inconceivable that fatigue failure could be a consideration in shear walls.

It is recommended that the effect of rapidly applied strain be taken into account by replacing f'_c and f_v by the dynamic values f'_{dc} and f_{dv} in Eqs. (2.28) to (2.31); these then become

$$R_{dc} = 0.1f'_{dc}Lt \quad (2.34)$$

$$P_a = f_{dv}pt(H + L) \quad (2.35)$$

$$C_a = A_s f'_{dc} \left[15 + 1.9 \left(\frac{L}{H} \right)^2 \right] \quad (2.36)$$

$$\frac{R_{du}}{C_a} = \frac{0.1}{P_a/C_a + 0.1} + \frac{2.1}{P_a/C_a + 0.6} \left(\frac{P_a}{C_a} \right) \quad (2.37)$$

Figure 2.11 consists of plots of C_a/R_{du} and P_a/R_{du} versus P_a/C_a . These plots may be used in computing the required reinforcement in panel and columns to resist a given-value dynamic ultimate shear load.

c. Shear-wall Openings. When there must be openings (as for corridors) it is recommended that the wall on each side of an opening be treated as an individual shear panel. These individual panels may be assumed to divide the shear load in proportion to their relative stiffnesses. At top and bottom (and if feasible along the vertical sides) of the opening, edge beams integral with the shear panel should be provided.

d. Strength of Deep Beams. Deep beams, as here considered, are structural elements loaded as beams but having very large ratios of web depth to thickness and having span/depth ratios less than 2 or 3. Roof slabs and floor slabs under horizontal load, and wall slabs under vertical load, are examples of this kind of element. Portions of intersecting elements act as flanges, preventing buckling and supplying strength and stiffness. Data obtained in shear-wall tests have applicability to deep beams of this kind.

In blast-resistant constructions those elements which may function

as deep beams usually must also carry loads normal to their surfaces. Consequently, it seems advisable to limit their deep-beam action to elastic behavior.

It is recommended that the maximum allowable shear, under dynamic loading, be taken as

$$V_m = 0.1f'_c Lt \quad (2.38)$$

The above expression assumes that the ratio of steel in each direction is

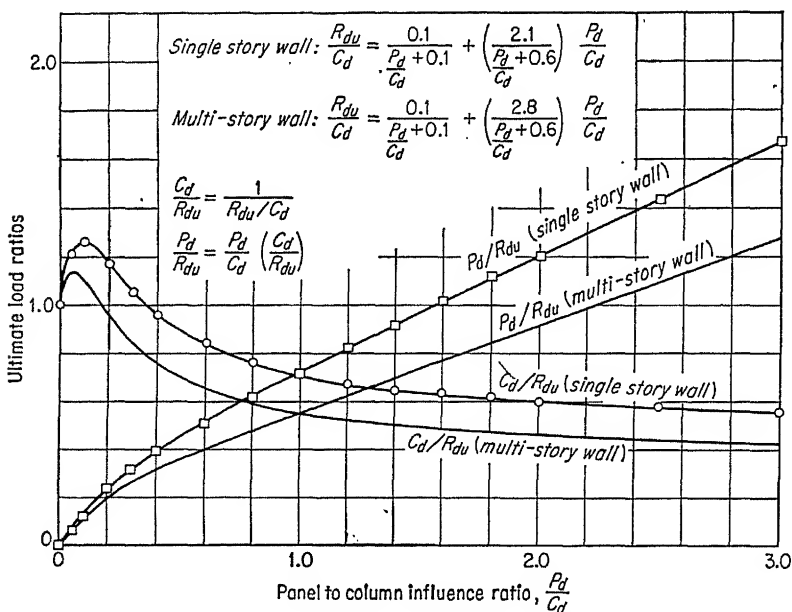


FIG. 2.11. Ultimate load ratios for shear walls [42; Chap. 1, Ref. 8].

at least 0.0025; generally the amount of steel required for loads normal to the web will exceed this minimum.

Since deep beams are almost always designed to take reversible loading, equal positive and negative bending reinforcement would be provided in the edges. The relation between maximum dynamic-moment capacity and area of steel in each edge, A_s , is

$$M_m = A_s f_{dy} d' \quad (2.39)$$

where d' = distance between tension and compression steel.

2.11. Bond between Reinforcing Bars and Concrete. The successful composite action of concrete and steel, in reinforced-concrete members, depends directly upon adequate bond between the two materials. In the majority of reinforced-concrete members the internal gross forces (thrust, shear, moment) vary from section to section; and there is a

corresponding variation of reinforcing-bar force, from section to section along the bar. Increments of bar force (from section to section) can only be provided by bond. Thus we may write

$$\frac{d}{dx} (f_s A_s) = u(O) \quad (2.40)$$

where x = distance along a reinforcing bar

$f_s A_s$ = axial force in bar, varying with position

u = intensity of bond stress along interface

(O) = bar perimeter

Significant variations in bar force from section to section occur, particularly, in flexure members. Denoting the moment by M and the internal moment arm by jd , the tension-steel force at any section is given by

$$T = f_s A_s = \frac{M}{jd} \quad (2.41)$$

For the common case of a member of constant effective depth d , jd may also be assumed constant, and substitution of Eq. (2.41) into Eq. (2.40) gives

$$u = \frac{1}{jd\Sigma O} \frac{dM}{dx} = \frac{V}{jd\Sigma O} \quad (2.42)$$

where ΣO = total perimeter of all tension bars in a section

V = transverse shear force

In order for reinforcement to perform its function in a flexure member the bar surfaces must be able to develop bond-stress intensities in accordance with Eq. (2.42) and do so without significant slip. The harmful effect of slip is to cause cracks in the concrete to widen beyond the amounts associated with longitudinal strain in the bars. As the cracks widen they spread upward, reducing the depth of the compression concrete zone, which can lead to premature crushing of the compression concrete.

In addition to its function in reinforced-concrete flexure members, bond is utilized to anchor reinforcing bars which join one member to another (beam to column, wall to footing, etc.) and to effect a (lap) splice from one bar to another. In such cases if u is the average bond stress along the anchored bar, d is the bar diameter, f_s is the bar stress to be anchored, and L is the embedment length, we may write

$$u = \frac{f_s d}{4L} \quad (2.43)$$

Again, satisfactory behavior requires that the bar surfaces be able to develop the average bond stress given by Eq. (2.43) without excessive slip.

A series of research studies undertaken in the early 1940s culminated in ASTM Specification A 305-53T covering size and spacing of ribs and lugs on reinforcing bars. All bars now in use in this country meet the requirements of A 305-53T, and their bond performance is markedly superior to that of many of the bars in use prior to the drafting of A 305-53T. In consequence the ACI Code [20] a few years ago revised upward the permissible unit bond stress at working load and decreased the requirements with respect to extension of bars beyond theoretical cutoff points. There is a rough proportionality between bond strength and f'_c for low values of f'_c , but bond strength is essentially independent of f'_c in the stronger concretes. For this reason, permissible bond stresses at working load generally are given as ratios of f'_c , but with ceiling values. In addition, it has been found that top bars which cannot follow settlement of fresh concrete develop pockets of entrapped water and air beneath their lower surfaces. This condition causes poorer bond strength for top bars, and the ACI Code [20] reduces the permissible bond stress if there is more than 12 in. of concrete below a bar. The permissible values of u are

For top bars (more than 12 in. of concrete below),

$$u = 0.07f'_c \quad \text{with ceiling of 245 psi}$$

For other bars,

$$u = 0.10f'_c \quad \text{with ceiling of 350 psi}$$

Based on repeated load pull-out tests by Muhlenbruch [43] involving old-style bars, Gilkey [44] concludes that bond fatigue should not be a serious problem provided the cyclic bond stress does not exceed 40 per cent of the static strength. It would appear that the ACI Code values provide adequate margin of safety for most common cases of repeated load. If each cycle involves practically a complete range of stress from zero to maximum, however, it would seem good judgment to use lower values.

For rapid strain rates to loads in the vicinity of ultimate (as in structures subject to blast) it is recommended that the limiting values of bond stress be taken as $0.15f'_c$. This value may not seem very high in comparison with the working-stress values specified in the ACI Code, but lack of data plus the harmful secondary effects of bond failure or excessive slip dictates a conservative attitude.

REFERENCES

1. Lyse, Inge: Der Beiwerten im Eisenbetonbald, *Beton u. Eisen*, vol. 36, no. 7, April, 1957.
2. Hognestad, E.: A Study of Combined Bending and Axial Load in Reinforced Concrete Members, *Univ. Illinois Expt. Sta. Bull.* 399.

3. Kesler, C. E., and C. P. Siess: Static and Fatigue Strength of Concrete, *ASTM Spec. Tech. Publ.* 169.
4. Probst, E.: The Influence of Rapidly Alternating Loading on Concrete and Reinforced Concrete, *Structural Engr.*, vol. 9, no. 10, October, 1931.
5. Watstein, E.: Effect of Straining Rate on the Compressive Strength and Elastic Properties of Concrete, *J. ACI*, vol. 24, no. 8, April, 1953.
6. Balmer, G.: Shearing Strength of Concrete under High Triaxial Stress-computation of Mohr's Envelope as a Curve, *Structural Research Lab. Rept.* SP-23, U.S. Bureau of Reclamation, 1949.
7. Bresler, B., and K. S. Pister: Failure of Plain Concrete under Combined Stresses, *Proc. ASCE*, separate no. 674, April, 1955.
8. Battelle Memorial Institute: "Prevention of the Failure of Metals under Repeated Stress," John Wiley & Sons, Inc., New York, 1941.
9. Graf, O.: Aus neueren Forschungsarbeiten für den Beton- und Eisenbetonbau, *Beton u. Eisen*, vol. 38, no. 11, June 5, 1939.
10. Graf, O., and G. Weil: Versuche über die Schwellzugfestigkeit von verdrehten Bewehrungsstahler, *Deut. Ausschuss Stahlbeton*, no. 101, 1948.
11. Warnock and Taylor: The Yield Phenomena of a Medium Carbon Steel under Dynamic Loading, *J. Inst. Mech. Engrs. (London)*, vol. 161, 1949.
12. Manjoine, M. J.: Influence of Rate of Strain and Temperature on Yield Stresses of Mild Steel, *J. Appl. Mechanics*, vol. 11, no. 4, December, 1944.
13. Warnock and Brennan: The Tensile Yield Strength of Certain Mild Steels under Suddenly Applied Loads, *J. Inst. Mech. Engrs. (London)*, vol. 159, 1948.
14. Broan and Edmonds: The Dynamic Yield Strength of Steel at an Intermediate Rate of Loading, *J. Inst. Mech. Engrs. (London)*, vol. 159, 1948.
15. Clark, D. S., and G. Datwyler: Stress-Strain Relations under Tension Impact Loadings, *Proc. ASTM*, vol. 38, pt. II.
16. Clark and Wood: "Influence of Rapid Load and Time at Load on Tensile Properties of Several Alloys," California Institute of Technology, 1948.
17. Whitney, C. S.: Plastic Theory of Reinforced Concrete Design, *Trans. ASCE*, vol. 107, 1942.
18. Whitney, C. S.: Application of Plastic Theory to the Design of Modern Reinforced Concrete Structures, *J. Boston Soc. Civil Engrs.*, vol. 35, no. 1, January, 1948.
19. Gaston, J. R., C. P. Siess, and N. M. Newmark: An Investigation of the Load-deformation Characteristics of Reinforced Concrete Beams Up to the Point of Failure, *Univ. Illinois Structural Research Ser.*, no. 40, December, 1952.
20. ACI Comm. 318: Building Code Requirements for Reinforced Concrete (ACI 318-56), *J. ACI*, May, 1956.
21. Austrian Fatigue Tests of Reinforced Concrete Beams, *Eng. News-Record*, May 16, 1935.
22. Fatigue Tests Reported on Reinforced Concrete Beams, *Eng. News-Record*, Oct. 31, 1935.
23. Lea, F. C.: Repeated Stresses on Structures, *Structural Engr.*, vol. 18, no. 1, January, 1940, and vol. 18, no. 2, February, 1940.
24. Vallette, R.: Endurance of Reinforced Concrete Railway Bridges: Tests of Beams with Repeated Bending, *Intern. Assoc. Bridge and Structural Eng.*, vol. 8, 1947.
25. LeCamus, B.: Recherches sur le comportement du beton et du beton armé soumis à des efforts répétés, *Ann. inst. tech. bâtiment et trav. publ.*, Circ. ser. F, no. 27, July, 1946.
26. "Behavior of Structural Elements under Impact Loads II," MIT, Dept. of Civil and Sanitary Engineering, November, 1950.

27. "Behavior of Structural Elements under Impulsive Loads," MIT, Dept. of Civil and Sanitary Engineering, April, 1950.
28. "Behavior of Structural Elements under Impulsive Loads," MIT, Dept. of Civil and Sanitary Engineering, July, 1951.
29. Wells, W. M., and R. J. Hansen: Machine for Static and Dynamic Testing of Slabs, *Proc. Soc. Exptl. Stress Anal.*, vol. 11, no. 1, 1953.
30. Simms, L. G.: Actual and Estimated Impact Resistance of Some Reinforced Concrete Units Failing in Bending, *J. Inst. Civil Engrs. (London)*, vol. 23, no. 4, February, 1945.
31. Kluge, R. W.: Impact Resistance of Reinforced Concrete Slabs, *J. ACI*, vol. 14, no. 5, April, 1943.
32. Mylrea, T. E.: Effect of Impact on Reinforced Concrete Beams, *J. ACI*, vol. 11, no. 6, June, 1940.
33. Penzien, J., and R. J. Hansen: Static and Dynamic Elastic Behavior of Reinforced Concrete Beams, *J. ACI*, vol. 25, no. 7, March, 1954.
34. Moretto, O.: An Investigation of the Strength of Welded Stirrups in Reinforced Concrete Beams, *Proc. ACI*, vol. 42, November, 1945.
35. Moody, K. G., I. M. Viest, F. C. Elstner, and E. Hognestad: Shear Strength of Reinforced Concrete Beams, pt. I, *J. ACI*, vol. 26, no. 4, December, 1954; pt. II, *J. ACI*, vol. 26, no. 5, January, 1955; pt. III, *J. ACI*, vol. 26, no. 6, February, 1955; pt. IV, *J. ACI*, vol. 26, no. 7, March, 1955.
36. Zwoyer, E. M., and C. P. Siess: Ultimate Strength in Shear of Simply-supported Beams without Web Reinforcement, *J. ACI*, vol. 26, no. 2, October, 1954.
37. Laupa, A., C. P. Siess, and N. M. Newmark: Strength in Shear of Reinforced Concrete Beams, *Univ. Illinois Eng. Expt. Sta. Bull.* 428.
38. Baron, M. J., and C. P. Siess: Effect of Axial Load on the Shear Strength of Reinforced Concrete Beams, *Univ. Illinois Structural Research Ser.*, no. 121, June, 1956.
39. Bernaert, S., and C. P. Siess: Strength in Shear of Reinforced Concrete under Uniform Load, *Univ. Illinois Structural Research Ser.*, no. 120, June, 1956.
40. Ernst, G. C., J. J. Hromadik, and A. R. Riveland: Inelastic Buckling of Plain and Reinforced Concrete Columns, Plates, and Shells, *Univ. Nebraska Eng. Expt. Sta. Bull.* 3, August, 1953.
41. Galletley, G. D.: "Behavior of Reinforced Concrete Shear Walls under Static Load," MIT, Dept. of Civil and Sanitary Engineering, August, 1952.
42. Williams, H. A., and J. R. Benjamin: Investigation of Shear Walls . . . , pts. 1 and 2, *Stanford Univ., Dept. Civil Eng., Tech. Rept.* 1, April, 1952; pt. 3, *Tech. Rept.* 1, July, 1953; pts. 4 and 5, *Tech. Repts.* 2 and 3, Aug. 1, 1953; pt. 6, *Tech. Rept.* 4, Aug. 1, 1954.
43. Muhlenbruch, C. W.: The Effect of Repeated Loading on the Bond Strength of Concrete, *Proc. ASTM*, vol. 45, 1945.
44. Gilkey, H. J.: "Bond with Reinforcing Steel," *ASTM Spec. Tech. Publ.* 169.
45. Bate, S. C. C.: "The Strength of Concrete Members under Dynamic Loading," Symposium on the Strength of Concrete Structures, Cement and Concrete Association, London, 1956.

PART 2

CALCULATION OF RESPONSE OF STRUCTURAL SYSTEMS
TO DYNAMIC LOADING

CHAPTER 3

DYNAMIC RESPONSE OF SYSTEMS HAVING ONE DEGREE OF FREEDOM

3.1. Scope and Limitations of Application of Theory. The response of a structure to dynamic loading depends upon the definition of the loading, the resistance of the structure to deflection, and, since acceleration is involved, the mass of the structure. Of course, if the supports of the structure are not immovable, their motion must also be defined in terms of time.

In general, at every point on the structure the definition of the loading must specify both the direction and the magnitude (including both the numerical value and sense) of the load at each and every instant of time. Most often, the effective load causing the response can be defined with sufficient accuracy independent of the motion or position of the structure. In other cases, the response of the structure is caused by the interacting force between it and some other body or bodies (for example, the bending of a beam when struck by a falling weight). The definition of this interacting force is then dependent on both the motion of the structure and the other body or bodies, and the solution of such problems becomes very tedious. In the flutter of airplane wings, or the "self-induced" vibration of suspension bridges, the aerodynamic loading is likewise a function of the vibratory motion of the structure. *However, in this and Chaps. 4, 5, and 6, it will be assumed that the dynamic loading producing the response of the structure is completely defined.*

The resistance of a structure to deflection can be defined more or less satisfactorily. Of course, a structure composed of a few simple elements, made of a homogeneous, isotropic, and linearly elastic material like steel (with no strains exceeding the proportional limit) and subjected to small displacements which involve no significant change in geometry of the structure, behaves very much like its mathematical idealization, and its stiffness properties can be estimated quite accurately. On the other hand, a complicated assemblage of structural elements made of a non-homogeneous, nonisotropic, and nonlinearly elastic material like concrete exhibits a behavior which is difficult to estimate. Even for the simple structure mentioned first, if the response produces strains beyond

the proportional limit and perhaps into the plastic region in excess of the yield point, computation of the stiffness becomes more difficult and more inaccurate. *In this and Chaps. 4 and 5, it will be assumed that the material exhibits linearly elastic stress-strain properties and that no strains exceed the proportional limit of the material. In Chap. 6, consideration will be given to computation of the response beyond the linearly elastic region and into the plastic region.*

Of course, the weight (and mass) distribution of a structure is easily defined. However, it would be very tedious and cumbersome to include in the computations the exact distribution of the weight. As a result, to simplify computations, *structural members usually are considered as weightless and the weights of their particles grouped together and considered as concentrated rigid masses attached to the structure at certain discrete mass points.* In Chaps. 3 and 4, weights of the structure will be handled in this manner. *In Chap. 5, however, the general theory will be developed to consider the actual distribution of the mass of the structure.*

Typical civil-engineering structures involve truss, beam, frame, slab, and shell elements. As a result, the deflection of such structures might involve the typical axial deformation of a truss member or the bending and shear deformation of a beam (and predominantly this type of deformation in a frame), or perhaps even the more complicated slab or shell behavior. The dynamic response of any of these structures could be handled by the same general approach, but the detailed computations for the various types are different. To simplify the presentation of the general theory, beams, the most common structural elements, will be depicted in the derivations and used in the applications. The extension of these ideas to another type of structure requires only a proper change in the evaluation of the resistance to deformation of that type of structure. Even a beam may be subjected to axial deformation and torsion in addition to bending in any longitudinal plane. In general, three displacements and three rotations may be involved at each cross section. *Therefore, to further simplify the discussion (but not restrict the generality of the approach) it will be assumed that the beam members depicted undergo bending and shearing deformation in the plane of the paper, and masses will be considered to undergo no rotation but simply translation in the plane of the paper.*

3.2. Certain Fundamental Definitions. To study the dynamic behavior of a structure, one must be able to define its position at any instant. If this is possible, not only can the deflection of the structure from its normal (that is, reference) position be determined, but also it is possible to evaluate the manner in which its strains, and hence stresses, vary with time.

If, at any instant, the position of a structure can be defined by *one*

number, or *one* coordinate, the structure is said to have *one degree of freedom*. Such a case is shown in Fig. 3.1a. This sketch represents a rigid* weight W attached to a spring, the mass of which is so small that it can be neglected when compared with W . Two rigid weights W_1 and W_2 as shown in Fig. 3.1b represent a structure with *two degrees of freedom* since the position of the weights can be defined by the *two* distances x_1 and x_2 . A member, such as the beam shown in Fig. 3.1c, has an *infinite number of degrees of freedom*, because the definition of its position requires

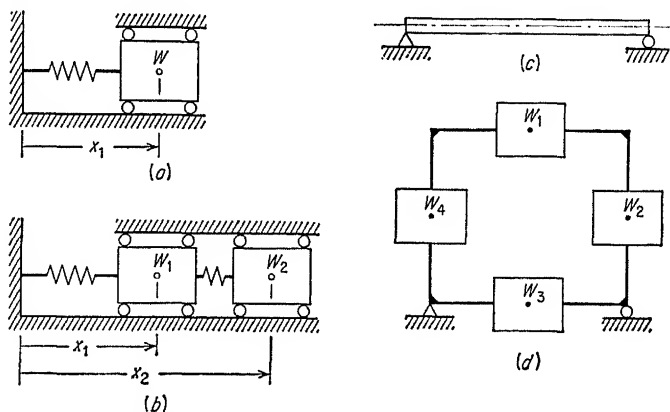


FIG. 3.1. Degree of freedom of typical systems.

enumerating the vertical ordinate of the deflection curve for every point on the beam, of which there are an infinite number.

Consider the elastic rigid frame shown in Fig. 3.1d, which is constrained to deflect in the plane of the paper. Assume that the weights of the members are small in comparison with the concentrated weights shown. Assume, therefore, that the weights of a member can be concentrated with the large mass located at mid-length of the member and that, henceforth, the elastic frame can be considered as a weightless spring. Further, assume that the axial deformations contribute little to the deflections, and therefore that only bending deflections need to be considered. On this assumption, there would be no vertical deflection of masses 4 and 2 and no horizontal deflection of mass 3. Thus, *five deflections* (horizontal deflections of masses 1, 2, and 4 and vertical deflections of masses 1 and 3) completely define the configuration of the frame, and therefore the structure is said to have *five degrees of freedom*. Note that rotation of the masses in the plane of the paper is neglected, as mentioned in the previous article.

If the motion of a body is reciprocating or oscillating in character, it is

* A rigid body is one in which there is no relative movement between any two particles of the body.

called a *vibration*. If the vibration of an elastic structure takes place in the absence of any external impressed force but in the presence of external and internal frictional forces, the motion is referred to as *damped free vibration*. In the hypothetical case where it is assumed that the frictional forces are also absent, the motion is called an *undamped free vibration*. The undamped motion is defined simply by the elastic resistances and the inertial forces of the system, by the initial conditions of the state of motion, and by the boundary conditions of the structure.

For many civil-engineering purposes, the response for the hypothetical undamped vibration is an adequate approximation of the actual damped vibration experienced by real structures, which always have more or less internal friction. This is very fortunate because results for the undamped vibration may be computed much more readily than for the damped case.

If a disturbing force is impressed on a structure, the resulting motion is called a *forced vibration*. If frictional effects are also included, the motion is called a *damped forced vibration*. For the hypothetical case where the effect of friction is neglected, the motion is called an *undamped forced vibration*.

Dynamic loadings applied to structures are of many different types. An unbalanced machine running at constant speed may apply a dynamic load which varies sinusoidally with time; such a load is called a *periodic load*, which undergoes a complete cycle (after which it repeats itself) regularly in a certain time interval called the *period* of the load. On the other hand, a group of looms—running at different speeds, some in phase, some out of phase, some starting up, and some slowing down—may in the aggregate apply to the structure a *nonperiodic* loading, which varies erratically with time and never repeats itself.

In Sec. 3.1, it was pointed out that sometimes the dynamic load could be defined as varying with time in a certain manner, completely independent of the motion of the structure, and that, in other cases, such as the impact of a falling weight on a beam, the effective dynamic loading on the structure is an interacting force which depends upon the motion of the structure and the striking body. It is convenient to distinguish between these two general types of loading. Herein, the first type will be called an *impulsive dynamic loading*, and the second type, an *impactive dynamic loading*. It should be pointed out that these definitions are not used consistently in the literature, and a reader should be careful to identify each author's definition.

One other general definition should be emphasized. A dynamic load applied to a structure produces a certain motion and associated with it certain stresses, strains, reactions, etc. Sometimes we use the term *response* to denote in the aggregate the over-all general effect produced by the load on the structure; the title of this chapter is an example of such

usage. Usually, however, we use the term *response* more specifically to denote the deflections produced by the dynamic load.

3.3. Undamped Free Vibration of One-degree System. Consider the simple idealized system shown in Fig. 3.2. This system is constrained so that the body can move only in a vertical direction in the plane of the paper and therefore has one degree of freedom. This rigid body of weight W is supported by a linearly elastic spring of stiffness k , where the stiffness factor k is equal to the force required to stretch the spring a unit distance. Under simply the dead weight W , the system is in static equilibrium in the position shown by the solid lines. Further, it will be assumed that there are neither external nor internal frictional forces present.

Suppose the body were displaced from this static position and then released. It would then undergo an undamped free vibration about the static position as defined below by Eq. (3.4). Similar free vibration such as given by Eq. (3.5) could be produced by the sudden application and removal of a force which thereby imparted an initial velocity to the body.

The dynamic displacement of the body undergoing such an undamped free vibration may be derived from the differential equation of motion [Eq. (3.1)], by proceeding in the following manner. Suppose at some time t the body is in the dashed-line position shown in Fig. 3.2. This position is defined by the coordinate x , which denotes the dynamic displacement of the body from the static-equilibrium position of the system under the dead weight W ; x is considered plus when measured downward from this position.*

If in accordance with d'Alembert's principle the inertia force $\ddot{x}W/g$ is applied to the body, the condition for dynamic equilibrium, $\Sigma V = 0$, for the isolated body is

$$W - (W + kx) - \frac{W}{g} \ddot{x} = 0$$

Rearranging terms, the above equation may be written as follows and in this new form is referred to as the differential equation of motion:

$$\frac{d^2x}{dt^2} + \frac{kg}{W} x = 0 \quad (3.1)$$

$$\text{Letting} \quad \omega^2 = \frac{kg}{W} \quad (3.2)$$

* dx/dt , the velocity of the body, is sometimes denoted by \dot{x} ; d^2x/dt^2 , the acceleration, by \ddot{x} .

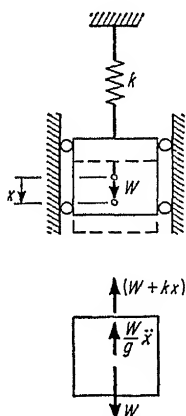


FIG. 3.2. Undamped free vibration.

the solution to Eq. (3.1) may be written

$$x = C_1 \sin \omega t + C_2 \cos \omega t \quad (3.3)$$

The arbitrary constants C_1 and C_2 may be obtained from the initial conditions of the state of motion. For example,

$$\begin{aligned} \text{If, when } t = 0, (x)_{t=0} = x_0 \text{ and } \left(\frac{dx}{dt}\right)_{t=0} = 0, \\ \text{then } C_1 = 0 \text{ and } C_2 = x_0, \text{ and } x = x_0 \cos \omega t \end{aligned} \quad (3.4)$$

$$\begin{aligned} \text{If, when } t = 0, (x)_{t=0} = 0 \text{ and } \left(\frac{dx}{dt}\right)_{t=0} = \dot{x}_0, \\ \text{then } C_1 = \frac{\dot{x}_0}{\omega} \text{ and } C_2 = 0, \text{ and } x = \frac{\dot{x}_0}{\omega} \sin \omega t \end{aligned} \quad (3.5)$$

For either case, the motion is periodic and repeats itself after the time interval T . Since $\omega T = 2\pi$, then

$$T = \frac{2\pi}{\omega} = 2\pi \sqrt{\frac{W}{kg}} \quad (3.6)$$

This time interval T is called the *period* (or natural period) of the undamped free vibration. The number of times that the motion repeats itself in one second is called the *frequency* of the vibration f , and

$$f = \frac{1}{T} = \frac{1}{2\pi} \sqrt{\frac{kg}{W}} \quad (3.7)$$

The parameter ω can now be given a physical significance, since

$$\omega = \frac{2\pi}{T} = 2\pi f \quad (3.8)$$

and is called the *circular frequency* of the vibration.

It is important to note that the constants C_1 and C_2 in Eq. (3.3) would both have values if both an initial displacement and an initial velocity were imposed on the system. However, the resulting response would still be a periodic free vibration of the same frequency and period as noted above.

Note also that the period and frequency depend only on the weight W and the spring stiffness k . The displacement at a particular time t and the amplitude of the vibration depend on the initial displacement and velocity, but these initial quantities do not affect the period and frequency.

3.4. Undamped Forced Vibration of One-degree System. Still neglecting frictional effects, consider again the simple one-degree system used in Sec. 3.3. This time, however, suppose that a sinusoidal dynamic

load P is applied to the system as shown in Fig. 3.3. The value of the dynamic load P at any time t is given by

$$P = P_1 \sin \Omega t \quad (3.9)$$

This sinusoidally varying load attains the maximum and minimum values of P_1 . The circular frequency of this periodic load is Ω , and the period of the load, T_P , is equal to $2\pi/\Omega$.

Proceeding in exactly the same manner as in Sec. 3.3, the differential equation of motion in this case may be derived from the condition of dynamic equilibrium for the isolated body:

$$W + P_1 \sin \Omega t - (W + kx) - \frac{W}{g} \ddot{x} = 0$$

and becomes

$$\frac{d^2x}{dt^2} + \frac{kg}{W} x = \frac{P_1 g}{W} \sin \Omega t \quad (3.10)$$

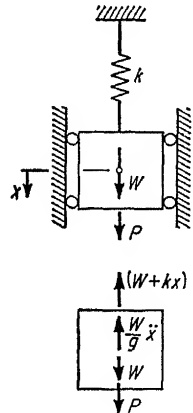


FIG. 3.3. Undamped forced vibration.

Defining ω as in Eq. (3.2), the homogeneous solution of Eq. (3.10) is given by Eq. (3.3). Adding to this the particular solution leads to the following general solution of Eq. (3.10):

$$x = C_1 \sin \omega t + C_2 \cos \omega t + \frac{P_1 g}{W(\omega^2 - \Omega^2)} \sin \Omega t \quad (3.11)$$

The first two terms of this solution are referred to as the *free part* of the solution, being vibrations with the natural period T and the circular frequency ω , but the third term is called the *forced part* of the solution since it represents a vibration having the same frequency and period as the sinusoidal load.

The arbitrary constants C_1 and C_2 may, of course, be determined from the initial conditions of the problem. For example, at $t = 0$, suppose the rigid body is at rest, that is, has no displacement ($x_0 = 0$) and no velocity ($\dot{x}_0 = 0$); then

$$C_1 = -\frac{P_1 g \Omega}{\omega W(\omega^2 - \Omega^2)} \quad \text{and} \quad C_2 = 0$$

Thus, the dynamic displacement of the body is given by

$$x = \frac{P_1 g / W \omega^2}{1 - (\Omega/\omega)^2} \left(\sin \Omega t - \frac{\Omega}{\omega} \sin \omega t \right) \quad (3.12)$$

Note, however, that

$$\frac{P_1 g}{W \omega^2} = \frac{P_1 g}{W} \frac{W}{kg} = \frac{P_1}{k} = x_{st} \quad (3.13)$$

where x_{st} = static deflection produced by P_1 (maximum value of sinusoidal load) if it were applied as a static load. Hence,

$$x = x_{st} \frac{\sin \Omega t - (\Omega/\omega) \sin \omega t}{1 - (\Omega/\omega)^2} \quad (3.14)$$

Thus, x (the dynamic displacement at any time t) is equal to x_{st} (the static displacement produced by P_1 applied as a static load) multiplied by a factor which varies with time.

Knowing the dynamic displacement at any time t , F_d , the dynamic spring force, is easily computed:

$$F_d = kx = kx_{st} \frac{\sin \Omega t - (\Omega/\omega) \sin \omega t}{1 - (\Omega/\omega)^2}$$

Note, however, that $kx_{st} = P_1$ = spring force produced by P_1 if it were applied as a static load. Hence,

$$F_d = P_1 \frac{\sin \Omega t - (\Omega/\omega) \sin \omega t}{1 - (\Omega/\omega)^2} \quad (3.15)$$

Thus, similar to the dynamic displacement, F_d (the dynamic spring force at any time t) is equal to P_1 (the spring force produced by P_1 applied as a static load) multiplied by the same time factor as is used to obtain the dynamic displacement.

The time factor common to both Eqs. (3.14) and (3.15) is called the *dynamic-load factor* (denoted by DLF) and is a function of time (that is, it varies with time).* Note that, in Eq. (3.16),

$$\text{DLF} = \frac{\sin \Omega t - (\Omega/\omega) \sin \omega t}{1 - (\Omega/\omega)^2} \quad (3.16)$$

the first term in the numerator has the same frequency as the load and is called the *forced part*; and the second term has the same frequency as the natural frequency of the system and is called the *free part*. Now using Eq. (3.16), Eqs. (3.14) and (3.15) may be written more conveniently as

$$\begin{aligned} x &= (\text{DLF})x_{st} \\ F_d &= (\text{DLF})P_1 \end{aligned} \quad (3.17)$$

Thus, dynamic-load factor could very evidently be defined as the factor by which the static deflection (or spring force) produced by P_1 applied as a static load should be multiplied in order to obtain the dynamic displacement (or dynamic spring force).

* Perhaps, to emphasize that dynamic-load factor is a factor which varies with time it should be denoted by $\text{DLF}(t)$. However, for simplicity it will be denoted as DLF.

Dynamic-load factor represents an important concept which should be discussed in detail. This will be done for the dynamic loading just considered in Sec. 3.6. The discussion will be extended to other loadings in Sec. 3.7.

3.5. Damped Forced Vibration of One-degree System. This case is discussed in detail in standard textbooks [1-3] on vibration of machinery and will be discussed only in an abbreviated manner herein. Only so-called *viscous damping* will be considered. This is the type of resisting force obtained when a body is moving through a viscous fluid with a small velocity, or if a piston forces a fluid through narrow passages, as in the case of dashpots. In the case of viscous damping, the resistance to motion by damping is assumed to be proportional to the numerical magnitude of the velocity and to act opposite to the sense of the velocity.

It is true, of course, that the damping provided by external and internal friction in structural systems is not exactly of the viscous type. However, for purposes of investigating the approximate effect of damping, it is adequate to assume that the effect of frictional resistance is equivalent to viscous damping.

Consider a simple one-degree system such as discussed in Secs. 3.3 and 3.4 and as shown in Fig. 3.4. Assume that a sinusoidal dynamic load such as defined by Eq. (3.9) is applied to the system. Assume that the damping force which opposes the velocity is proportional to it, the proportionality constant being c , the *damping coefficient*; that is, the damping force equals $-c\dot{x}$. By proceeding in exactly the same manner as in Sec. 3.4, the differential equation of motion in this case may be derived from the condition of dynamic equilibrium for the isolated body:

$$W + P_1 \sin \Omega t - (W + kx) - \frac{W}{g} \ddot{x} - c\dot{x} = 0$$

and if

$$\omega^2 = \frac{kg}{W}$$

and

$$2\beta = \frac{cg}{W} \quad (3.18)$$

it becomes

$$\frac{d^2x}{dt^2} + 2\beta \frac{dx}{dt} + \omega^2 x = \frac{P_1 g}{W} \sin \Omega t \quad (3.19)$$

If ω^2 is less than β^2 , the solution of this differential equation no longer represents a vibratory motion and is of no interest in the present discussion. When ω^2 is greater than β^2 , the solution represents the damped

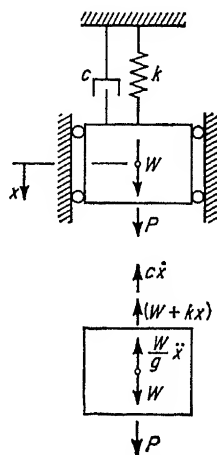


FIG. 3.4. Damped forced vibration.

vibratory motion typical of the response of structural systems. The general solution of Eq. (3.19) may be obtained in the usual manner by superimposing the homogeneous and the particular solutions. If the arbitrary constants are determined on the assumption that the *body is at rest when $t = 0$* , the solution for the dynamic displacement x and the dynamic spring force F_d may be expressed in the same form as Eq. (3.17), except that in this case the dynamic-load factor is expressed by the following complicated expression:

$$\text{DLF} = \frac{\left[\left(1 - \frac{\Omega^2}{\omega^2} \right) \sin \Omega t - 2 \frac{\beta}{\omega} \frac{\Omega}{\omega} \cos \Omega t \right] + e^{-\beta t} \left[2 \frac{\beta}{\omega} \frac{\Omega}{\omega} \cos \sqrt{\omega^2 - \beta^2} t + \frac{\Omega}{\sqrt{\omega^2 - \beta^2}} \left(2 \frac{\beta^2}{\omega^2} + \frac{\Omega^2}{\omega^2} - 1 \right) \sin \sqrt{\omega^2 - \beta^2} t \right]}{\left[1 - \left(\frac{\Omega}{\omega} \right)^2 \right]^2 + 4 \left(\frac{\beta}{\omega} \right)^2 \left(\frac{\Omega}{\omega} \right)^2} \quad (3.20)$$

Note that this DLF expression is similar to Eq. (3.16) in that the first bracketed expression in the numerator has the same frequency as the load and therefore is called the *forced part*, while the second bracketed expression has the same frequency as the natural frequency of the system and is therefore called the *free part*. Note further that the free part has the multiplier $e^{-\beta t}$ and therefore gradually dies out.

The homogeneous solution of Eq. (3.19), that is, the solution for this equation when the right-hand side is equal to zero, represents the solution for the damped free vibration of this one-degree system and is found to be

$$x = e^{-\beta t} (C_1 \sin \sqrt{\omega^2 - \beta^2} t + C_2 \cos \sqrt{\omega^2 - \beta^2} t) \quad (3.21)$$

The term in brackets is in the same form as Eq. (3.3), the solution obtained for the undamped free vibration. In this present case, however, this term represents a periodic motion with the following period:

$$T = \frac{2\pi}{\omega} \frac{1}{\sqrt{1 - (\beta/\omega)^2}} \quad (3.22)$$

Comparison of this with the period of the undamped free vibration shows that damping of the amount present in the usual structure increases the period slightly. The factor $e^{-\beta t}$ in Eq. (3.21) gradually decreases with time, and therefore the free vibration is gradually damped out.

The DLF given by Eq. (3.20) may be studied in the same manner as the expression given by Eq. (3.16). This will not be done in detail. For present purposes, it is sufficient to note that the following conclusions could be drawn from such a study:

1. The effect of damping is to decrease DLF for all values of Ω/ω .

2. As β/ω increases, DLF decreases.

3. For the usual amounts of damping present in structures, the decrease is not marked except in the vicinity of Ω/ω from 0.5 to 1.5, being greatest when $\Omega/\omega = 1$, in which case DLF is reduced to a finite but still a large value.

4. Only the forced part persists; the free part is transient and gradually disappears.

It is interesting to note that as the damping approaches zero (that is, as $\beta \rightarrow 0$) the expression for DLF in Eq. (3.20) approaches the value given in Eq. (3.16).

3.6. Dynamic-load Factor—Undamped One-degree System—Sinusoidal Dynamic Loading. The expression for DLF given in Eq. (3.16) was derived for an undamped one-degree system subjected to the sinusoidal loading represented by Eq. (3.9). It is of interest to consider in detail how DLF varies with time for several typical cases such as the following:

$$\text{Case I, } \Omega = \frac{\omega}{2}; \text{ Case II, } \Omega = 2\omega$$

The variation of the load and DLF with time for these two cases is sketched in Fig. 3.5. Note that in each case the forced and free parts of DLF are plotted separately and then superimposed to show DLF itself. These two cases are plotted on the assumption that the system is the same in both cases, but in one case the frequency of the load is lower than that of the system, and in the other case it is higher.

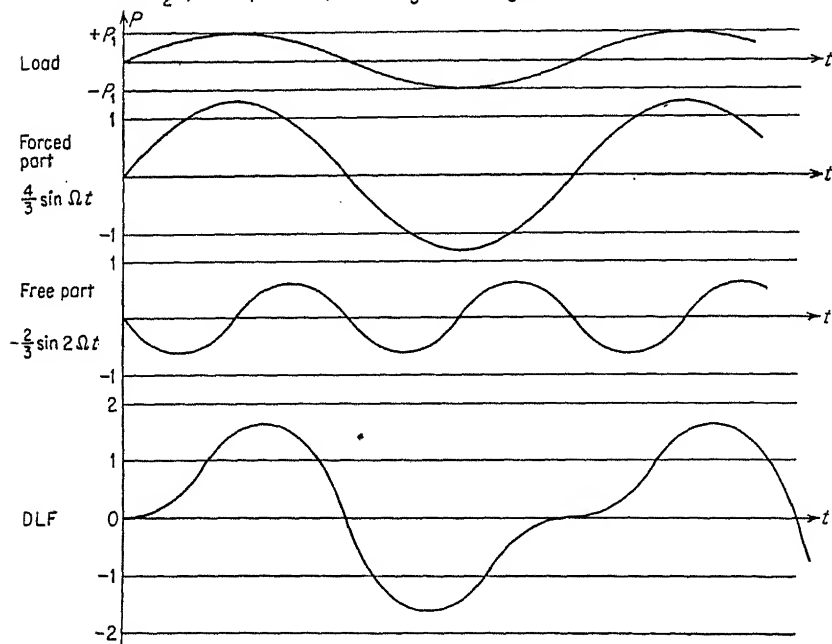
Whereas these plots of DLF vs. time are of interest in order to develop a better appreciation of dynamic response, simply the peak values of these curves are of major interest to a structural designer. Applying the usual calculus procedures to Eq. (3.16), maxima, minima, or saddle points of the DLF curve are found to occur at the following times:

$$t = \frac{\pm 2\pi n}{\Omega \mp \omega}$$

where $n = \text{an integer, } 1, 2, 3, \dots$. The maximum and minimum values of DLF are given by the following:

$$\text{DLF}_{\substack{\text{max.} \\ \text{min.}}} = \frac{\sin \frac{\pm 2\pi n}{\Omega \mp \omega} \frac{\Omega}{\omega} - \frac{\Omega}{\omega} \sin \frac{\pm 2\pi n}{\frac{\Omega}{\omega} \mp 1}}{1 - \left(\frac{\Omega}{\omega}\right)^2} \quad (3.23)$$

Case I: $\Omega = \frac{\omega}{2}$, $P = P_1 \sin \Omega t$, $DLF = \frac{4}{3} \sin \Omega t - \frac{2}{3} \sin \omega t$



Case II: $\Omega = 2\omega$, $P = P_1 \sin \Omega t$, $DLF = -\frac{1}{3} \sin \Omega t + \frac{2}{3} \sin \omega t$

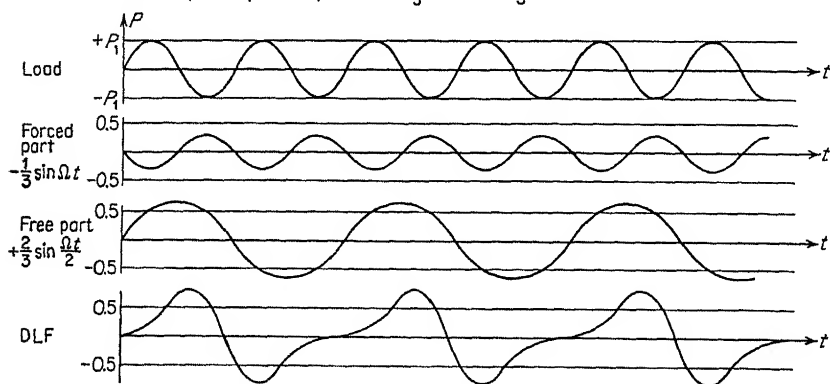


FIG. 3.5. Dynamic-load factors for sinusoidal loading.

where the value of n which gives the maximum or minimum values has to be obtained by trial. Values of DLF_{\max} obtained from Eq. (3.23) are plotted versus Ω/ω as shown by the dashed line in Fig. 3.6.

It is interesting to compare the response of the undamped and damped systems under the sinusoidal loading. While the value of β for a typical real structure is small, it still has an appreciable effect, which can be

studied by retaining only the significant parts of Eq. (3.20) when β is small, or

$$\text{DLF} \approx \frac{\sin \Omega t - e^{-\beta t} \frac{\Omega}{\omega} \sin \omega t}{1 - \left(\frac{\Omega}{\omega}\right)^2} \quad (3.24)$$

Except for the multiplier $e^{-\beta t}$ on the free part of this expression, it is identical with Eq. (3.16). Because of this multiplier the free part gradually disappears with increasing time.

In an actual structure, the free part of the response seldom persists for more than 10 or 15 times the natural period of the system. This means that in actual structures the peak values of the DLF shown in Fig. 3.5 could be realized during the initial stages of the response; but after 10 or 15 times the natural period, the peak values of the damped response are simply the peaks shown on the curve for the forced part.

The first stage of the response before the free part is damped out is called the *transient state*; the subsequent stage after the free part has been damped out is called the *steady state*. More often than not, structural engineers are interested in the peak values attained early in the transient state which are affected very little by damping. Of course, in cases where the design is controlled by fatigue conditions, the peak values in the steady state are of major interest.

Often the response of the damped one-degree system is approximated by retaining only the forced part of Eq. (3.16); that is,

$$\text{DLF} \approx \frac{\sin \Omega t}{1 - (\Omega/\omega)^2} \quad (3.25)$$

The maximum and minimum values of this expression are, obviously,

$$\text{DLF}_{\text{max. min.}} = \frac{\pm 1}{1 - (\Omega/\omega)^2} \quad (3.26)$$

Values of DLF_{max} obtained from this last expression are shown by the solid-line curve in Fig. 3.6.

It should be pointed out that the dashed-line curve in Fig. 3.6 is not completely correct. The values of DLF_{max} plotted for rational values of Ω/ω are correct. For irrational values of Ω/ω the value of n at which DLF is a maximum is laborious to find. The true DLF in such cases is not appreciably different from those indicated by this curve, and it is therefore adequate for practical purposes. Further, some of the maximum values indicated by this curve can never be attained because the free part of the response has already been damped out in actual structures. In such cases, however, the forced part is making the major

contribution to DLF, so that the values indicated by the curve are not much in error.

The solid- and dashed-line curves in Fig. 3.6 indicate the well-known resonance phenomena when $\Omega/\omega = 1$. In the discussion so far, it has been implied that the solid curve gives a good approximation of DLF_{\max} in the steady state of the response after the free part has been damped out. Actually, this is true for the usual damping found in structures, except in the vicinity of resonance where the proper inclusion of damping

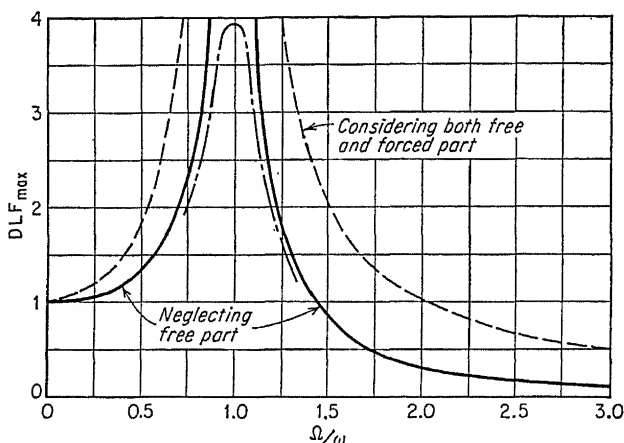


FIG. 3.6. Maximum dynamic-load factor for sinusoidal loading.

into the solution would give values of DLF_{\max} of the order indicated by the dot-dash modification of the solid-line curve.

3.7. Dynamic-load Factor—Undamped One-degree System—Various Typical Impulsive Loadings. Instead of setting up the solution for the one-degree undamped system shown in Fig. 3.3 for a sinusoidal dynamic loading as was done in Sec. 3.4, the solution could be set up in terms of any given impulsive load P . This general loading could be expressed as follows:

$$P = P_1 f(t) \quad (3.27)$$

where P_1 = maximum value attained by dynamic load. For convenience in the following derivation, let

$$q = \frac{P_1 g}{W} \quad \text{and} \quad \omega^2 = \frac{k g}{W} \quad (a)$$

By proceeding as in Sec. 3.4, the differential equation may be written as follows:

$$\frac{d^2 x}{dt^2} + \omega^2 x = q f(t) \quad (b)$$

If both sides of this equation are multiplied by $\sin \omega t$, and if $\omega \cos \omega t \, dx/dt$ is added and subtracted on the left-hand side, Eq. (b) becomes

$$\left(\sin \omega t \frac{d^2 x}{dt^2} + \omega \cos \omega t \frac{dx}{dt} \right) + \left(x \omega^2 \sin \omega t - \omega \cos \omega t \frac{dx}{dt} \right) = qf(t) \sin \omega t$$

$$\text{or} \quad \frac{d}{dt} \left(\sin \omega t \frac{dx}{dt} \right) + \frac{d}{dt} \left(-x \omega \cos \omega t \right) = qf(t) \sin \omega t$$

Integrate both sides with respect to t between limits of t_0 and t :

$$\left[\sin \omega t' \frac{dx}{dt'} \right]_{t_0}^t - \left[x \omega \cos \omega t' \right]_{t_0}^t = \int_{t_0}^t qf(t') \sin \omega t' dt'$$

where t' = any intermediate values of t between t_0 and t . If the body is known to have a displacement x_0 and a velocity \dot{x}_0 at the starting time t_0 , then

$$(x)_{t'=t_0} = x_0 \quad \text{and} \quad \left(\frac{dx}{dt} \right)_{t'=t_0} = \dot{x}_0$$

So

$$\sin \omega t \frac{dx}{dt} - \dot{x}_0 \sin \omega t_0 - x \omega \cos \omega t + x_0 \omega \cos \omega t_0 = \int_{t_0}^t qf(t') \sin \omega t' dt' \quad (c)$$

In a similar manner, but by multiplying both sides of Eq. (b) by $\cos \omega t$, and by then adding and subtracting $\omega \sin \omega t \, dx/dt$ on the left side, the following equation is obtained:

$$\cos \omega t \frac{dx}{dt} - \dot{x}_0 \cos \omega t_0 + x \omega \sin \omega t - x_0 \omega \sin \omega t_0 = \int_{t_0}^t qf(t') \cos \omega t' dt' \quad (d)$$

By multiplying Eq. (c) by $\cos \omega t$ and Eq. (d) by $\sin \omega t$ and then subtracting Eq. (c) from Eq. (d), the following equation is obtained:

$$x = x_0 \cos \omega(t - t_0) + \frac{\dot{x}_0}{\omega} \sin \omega(t - t_0) + \frac{q}{\omega} \int_{t_0}^t f(t') \sin \omega(t - t') dt' \quad (3.28)$$

However, $q/\omega^2 = P_1/k = x_{st}$ = static deflection of spring produced by P_1 if it were applied as a static load.

Hence, Eq. (3.28) may be expressed as

$$x = x_0 \cos \omega(t - t_0) + \frac{\dot{x}_0}{\omega} \sin \omega(t - t_0) + x_{st} \left[\omega \int_{t_0}^t f(t') \sin \omega(t - t') dt' \right] \quad (3.29)$$

From Eq. (3.29) it is apparent that the total dynamic displacement is simply the superposition of three separate contributions:

1. The free vibration, $x_0 \cos \omega(t - t_0)$, which would result if, at $t = t_0$, the system were displaced x_0 but had no initial velocity and subsequently were not acted upon by an impressed load P . Note that this contribution is identical with the free vibration given by Eq. (3.4) if $t_0 = 0$.

2. The free vibration, $(\dot{x}_0/\omega) \sin \omega(t - t_0)$, which would result if, at

$t = t_0$, the system were subjected to an initial velocity \dot{x}_0 but had no initial displacement and subsequently were not acted upon by an impressed load P . Note that this contribution is consistent with the free vibration given by Eq. (3.5).

3. The dynamic response which would be produced by the dynamic load P applied to a system which had neither a displacement nor a velocity at time t_0 . This contribution could be expressed as

$$\text{where} \quad \text{DLF} = \omega \int_{t_0}^t f(t') \sin \omega(t - t') dt' \quad (3.30)$$

In other words, Eq. (3.29) demonstrates that the dynamic response produced by a given dynamic load is independent of the initial motion of the system when the load is applied. The response produced simply by the given load can therefore be computed as if the system were initially at rest, and this response can then be superimposed on the free vibration caused simply by the initial displacement x_0 , and on that caused simply by the initial velocity \dot{x}_0 , to get the total dynamic displacement of a system which already has a displacement and velocity when subjected to this dynamic load.

The free vibrations associated with the initial displacement x_0 and the initial velocity \dot{x}_0 are easily computed from Eqs. (3.4) and (3.5), respectively. It is now of interest, however, to study the dynamic response produced by some typical dynamic loading applied to a system which is *initially at rest*. If $x_0 = 0$ and $\dot{x}_0 = 0$, the dynamic response produced by the loading $P_1 f(t)$ may be expressed as follows by applying Eq. (3.29):

$$x = x_{st}(\text{DLF}) \quad (3.31)$$

where DLF may be computed using Eq. (3.30).

The results of applying Eq. (3.30) to four typical dynamic loadings are summarized below:

a. Suddenly Applied Load

$$\begin{array}{lll} 0 \leq t & P = P_1 & \therefore f(t) = 1 \\ \text{DLF} = 1 - \cos \omega t & & \text{DLF}_{\max} = 2 \end{array} \quad \begin{array}{c} P_1 \\ \uparrow \\ \text{---} \\ t \end{array}$$

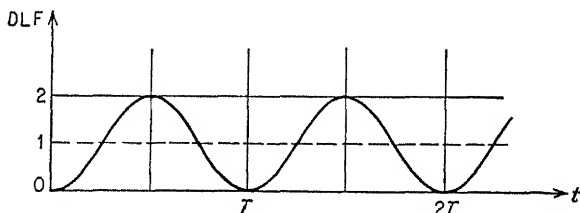


FIG. 3.7. Dynamic-load factor for suddenly applied load.

b. Gradually Applied Load

$$0 \leq t \leq t_1 \quad P = P_1 \frac{t}{t_1} \quad \therefore f(t) = \frac{t}{t_1}$$

$$t_1 \leq t \quad P = P_1 \quad \therefore f(t) = 1$$

$$0 \leq t \leq t_1 \quad \text{DLF} = \frac{t}{t_1} - \frac{\sin \omega t}{\omega t_1} = \frac{t}{t_1} - \frac{T}{2\pi t_1} \sin \omega t$$

$$t_1 \leq t \quad \text{DLF} = 1 + \frac{T}{2\pi t_1} [\sin \omega(t - t_1) - \sin \omega t]$$

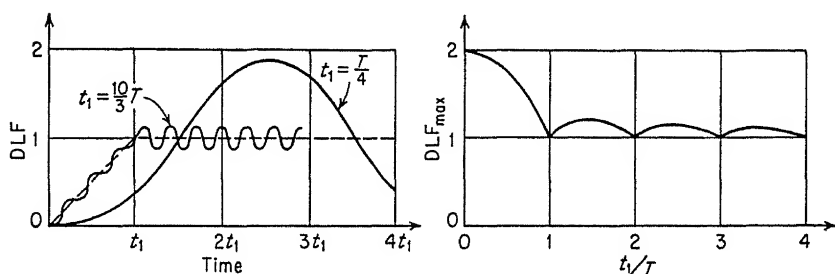
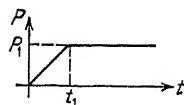


FIG. 3.8. Dynamic-load factor for gradually applied load.

c. Rectangular Pulse Load

$$0 \leq t \leq t_1 \quad P = P_1 \quad \therefore f(t) = 1$$

$$t_1 \leq t \quad P = 0 \quad \therefore f(t) = 0$$

$$0 \leq t \leq t_1 \quad \text{DLF} = 1 - \cos \omega t$$

$$t_1 \leq t \quad \text{DLF} = 2 \sin \frac{\omega t_1}{2} \sin \omega \left(t - \frac{t_1}{2} \right)$$

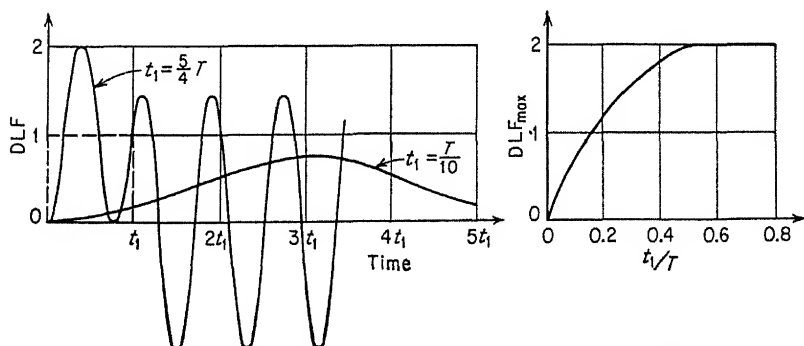
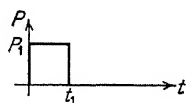


FIG. 3.9. Dynamic-load factor for rectangular pulse load.

d. Triangular Pulse Load

$$0 \leq t \leq 0.5t_1 \quad P = 2 \frac{t}{t_1} P_1$$

$$\therefore f(t) = 2 \frac{t}{t_1}$$

$$0.5t_1 \leq t \leq t_1 \quad P = \left(2 - 2 \frac{t}{t_1}\right) P_1$$

$$\therefore f(t) = \left(2 - 2 \frac{t}{t_1}\right)$$

$$t_1 \leq t \quad P = 0 \quad \therefore f(t) = 0$$

$$0 \leq t \leq 0.5t_1 \quad \text{DLF} = 2 \frac{t}{t_1} - \frac{T}{\pi t_1} \sin \omega t$$

$$0.5t_1 \leq t \leq t_1 \quad \text{DLF} = 2 - 2 \frac{t}{t_1} + \frac{T}{\pi t_1} \left[2 \sin \omega \left(t - \frac{t_1}{2} \right) - \sin \omega t \right]$$

$$t_1 \leq t \quad \text{DLF} = \frac{T}{\pi t_1} \left[-\sin \omega(t - t_1) + 2 \sin \omega \left(t - \frac{t_1}{2} \right) - \sin \omega t \right]$$

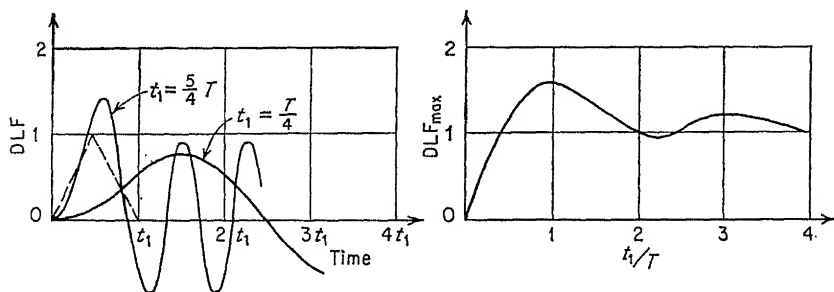
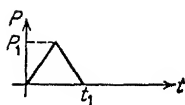


FIG. 3.10. Dynamic-load factor for triangular pulse load.

The solutions for these four cases contain a great deal of interesting and significant information and should be studied carefully. Case *a* confirms the well-known conclusion from elementary mechanics that a suddenly applied load produces twice the response of static load of the same magnitude. Note that the free part (that is, the term $\cos \omega t$) of the expression for DLF does not persist indefinitely in an actual structure when damping is present. In other words, if damping were considered, the amplitude of the oscillating curve for DLF would gradually decrease and the curve would become a substantially straight horizontal line at a value of $\text{DLF} = 1$. It would require 10 to 15 cycles (that is, 10 to 15 times the natural period T) for this damping process to occur, however. If one were interested in the maximum response, damping has no practical effect since the maximum DLF of 2 is first obtained during the first cycle.

Case *b* is also very interesting. If the rise time t_1 is equal to or greater than the natural period, there is no appreciable dynamic effect (that is,

DLF_{\max} is little greater than 1). On the other hand, if the rise time is less than one-quarter or so of the natural period, DLF_{\max} is substantially equal to 2 (in other words, in such cases, the maximum response is substantially the same as if the load were truly suddenly applied). Here again, note that damping has little influence on the important effects involved.

Case *c* is very important background to persons studying response to short violent explosive blasts or wind gusts. Note that, if the duration of a pulse is half the natural period or more, the maximum response of the system is the same as if the load P were applied to the structure for an indefinite time. On the other hand, if the duration t_1 of the pulse is less than approximately $0.15T$, the response is less than the effects produced by P_1 applied as a static load.

The reader should compare cases *c* and *d* carefully and also develop and include in the comparison the solution for a suddenly applied triangular pulse, this pulse being one where the load increases suddenly (in zero time) to its maximum value P_1 and then decays linearly to zero in the time t_1 .

3.8. Response Produced by Support Vibrations of Undamped One-degree System. As background for subsequent discussion of the effect of earthquakes on structures, it is of interest to consider the response of an undamped one-degree system caused by a vibratory motion of the supports. For purposes of this discussion, consider the system discussed previously in Sec. 3.3 and shown in Fig. 3.11.

Assume that the support undergoes a sinusoidal displacement

$$x_s = a_0 \sin \Omega_s t \quad (3.32)$$

As a result the extension of the spring is $x - x_s$ and the condition for dynamic equilibrium of the isolated body is

$$W - \frac{W}{g} \ddot{x} - [W + k(x - x_s)] = 0$$

leading to the following differential equation of motion:

$$\frac{d^2 x}{dt^2} + \omega^2 x = \omega^2 a_0 \sin \Omega_s t \quad (3.33)$$

The solution of this equation is

$$x = C_1 \sin \omega t + C_2 \cos \omega t + \frac{a_0 \omega^2}{\omega^2 - \Omega_s^2} \sin \Omega_s t \quad (3.34)$$

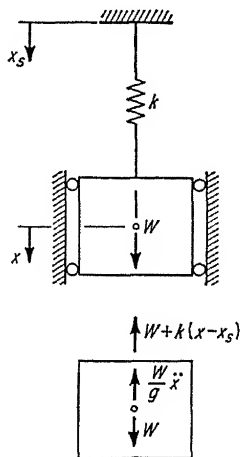


FIG. 3.11. Effect of support movement.

If the body is at rest when $t = 0$,

$$C_1 = -\frac{a_0\omega\Omega_s}{\omega^2 - \Omega_s^2} \quad \text{and} \quad C_2 = 0$$

Thus,
$$x = a_0 \frac{\sin \Omega_s t - (\Omega_s/\omega) \sin \omega t}{1 - (\Omega_s/\omega)^2} \quad (3.35)$$

The time factor in this equation is identical with the DLF for a sinusoidal load except that Ω_s has replaced Ω .

The dynamic spring force is F_d , likewise easily computed:

$$F_d = k(x - x_s)$$

Hence,
$$F_d = a_0 k \frac{(\Omega_s/\omega)^2 \sin \Omega_s t - (\Omega_s/\omega) \sin \omega t}{1 - (\Omega_s/\omega)^2} \quad (3.36)$$

There are certain features regarding this time factor which require further discussion, but this will be deferred until the next chapter, in connection with the effect of support motions of a multimass system.

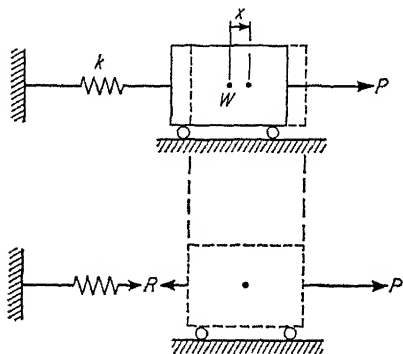


FIG. 3.12. Notation for step-by-step example.

At this time there are certain conclusions which should be noted regarding Eqs. (3.35) and (3.36):

1. When Ω_s/ω is equal to 1.0, resonance occurs.

2. When Ω_s/ω approaches zero (that is, when the spring stiffness approaches infinity), the displacement of the mass becomes identical with the displacement of the support and the stress in the spring approaches $\bar{x}_s W/g$.

3. When Ω_s/ω approaches infinity (that is, when the spring stiffness approaches zero), the mass stands still and the stress in the spring approaches ka_0 .

3.9. Computation of Response Using Step-by-step Procedures. In all the cases considered previously in this chapter, the system has deflected in a linearly elastic manner. Moreover, only the simplest types of loading have been considered. In such cases, the mathematical detail involved in the application of dynamic-response theory could be handled without difficulty. Many practical situations, however, involve inelastic behavior and very complicated loadings for which the detail of applying formal mathematical solutions becomes either impractical or, perhaps, impossible. Under these circumstances integration of the equations of motion can be performed by step-by-step numerical procedures which are designed to utilize modern computational techniques and machines.

Consider the undamped response of a one-degree system to a known dynamic load P . For purposes of this step-by-step solution, the spring force kx will be designated as R , as shown in Fig. 3.12. If, at any time t_0 , the displacement x_0 were known, thereby defining the value of the spring

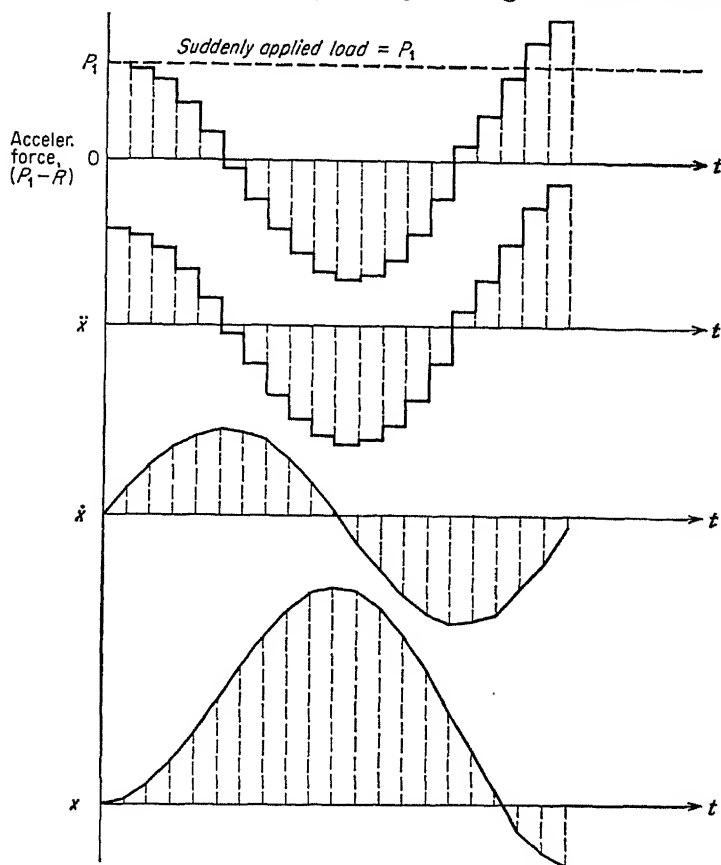


FIG. 3.13. Step-by-step analysis of response of one-degree system to suddenly applied load.

force R_0 , the net accelerating force acting on the mass would be $P - R_0$, and the acceleration \ddot{x}_0 at this instant would therefore be

$$\ddot{x}_0 = \frac{P - R_0}{W/g} \quad (3.37)$$

If the velocity \dot{x}_0 at time t_0 were also known and if, during the following short interval of time Δt , the *acceleration were assumed to remain constant* at the value \ddot{x}_0 , the velocity \dot{x}_1 at the end of this interval (that is, at time $t_0 + \Delta t$) would be

$$\dot{x}_1 = \dot{x}_0 + \ddot{x}_0 \Delta t \quad (3.38)$$

In addition, the displacement x_1 at the end of the interval would be

$$x_1 = x_0 + \dot{x}_0 \Delta t + \ddot{x}_0 \frac{(\Delta t)^2}{2} \quad (3.39)$$

Knowing the displacement x_1 defines a new value for the spring force R_1 and the accelerating force $P - R_1$ at the end of this interval. The above process could then be repeated for the next short time interval Δt to predict the velocity \dot{x}_2 and the displacement x_2 at the time $t_0 + 2 \Delta t$. By this step-by-step numerical process the motion of the mass could be tracked indefinitely.

Obviously, the accuracy of the above procedure depends on the length of the time interval Δt . This and other methods of approximating the variation of the acceleration during the time interval Δt will be discussed in Chap. 8. However, it is of interest to apply this approach in a qualitative way to get a better understanding of the manner in which a system responds to a dynamic loading.

Consider the undamped response of the above system to a suddenly applied load such as was evaluated in Sec. 3.7a. The DLF for this case is shown in Fig. 3.7. Suppose that, at $t = 0$, the system has no displacement or velocity. Consider the response for a series of intervals Δt , which are short compared with the natural period of the system. Figure 3.13 summarizes in a qualitative way step-by-step development of the response of the system. There being no displacement at $t = 0$, the spring force R is 0 and the accelerating force during the first interval is P_1 . As the displacement increases, R gradually builds up and the accelerating force, and hence the acceleration, decreases. When R exceeds P_1 , the system starts decelerating. Subsequently the velocity is reduced to zero when the displacement reaches its maximum value of $2P_1/k$. Then the mass starts rebounding and eventually reaches zero velocity and minimum deflection at its original starting position, thereby completing one complete cycle of this periodic response. Neglecting damping, the response continues indefinitely, repeating the first cycle in a periodic fashion with a period equal to the natural period of the system.

REFERENCES

1. Timoshenko, S.: "Vibration Problems in Engineering," 3d ed., D. Van Nostrand Company, Inc., Princeton, N.J., 1955.
2. Den Hartog, J. P.: "Mechanical Vibrations," McGraw-Hill Book Company, Inc., New York, 1956.
3. Thompson, W. T.: "Mechanical Vibrations," Prentice-Hall, Inc., Englewood Cliffs, N.J., 1953.
4. Frankland, J. M.: Effects of Impact on Simple Elastic Structures, *Proc. Soc. Exptl. Stress Anal.*, vol. 6, no. 2, 1948.

CHAPTER 4

GENERAL THEORY FOR DYNAMIC RESPONSE OF CONCENTRATED-MASS SYSTEMS

4.1. General. As mentioned previously in Chap. 3, the mass of an actual structure is continuously distributed over the spatial extent of the structure, and, as a result, actual structures have an infinite number of degrees of freedom as far as vibrations are concerned. Often, however, the important features of the dynamic response of an actual structure may be adequately approximated with far less tedious computations by idealizing the structure. In such an idealization, the mass of the structure is considered to be lumped or concentrated at a certain finite number of mass points and the resistance of the structure to deflection is then represented by members or elements which are considered to be weightless but to have structural strength and stiffness. Methods of idealizing actual structures will be discussed later in Chap. 7.

These idealized structures are said to be *concentrated-mass systems or structures*. In Chap. 3, the dynamic response of idealized one-mass systems was discussed. Certain additional ideas and techniques must be developed, however, in order to compute the response of a concentrated-mass system with two or more degrees of freedom. The general theory for evaluating the dynamic response of concentrated-mass systems with multiple degrees of freedom will be developed herein. This method involves first determining the frequencies and shapes of the normal modes of vibration of the system. The dynamic response of the system to a given dynamic load is then evaluated by superimposing proper contributions of the various normal modes of vibration.

The scope of this development will be limited in the following respects:

1. Only structures which deflect in a *linearly elastic* manner will be considered, that is, structures the deflection of which is directly proportional to the magnitude of the load causing the deformation. The method presented herein could be extended to approximate the response of structures which are strained through a linearly elastic region into the plastic region at certain points, but the application would be very laborious. Such extensions of this method will be discussed in Chap. 6.

2. Further, it will be assumed that the structures considered herein are

stable under static loads, though they may be either statically determinate or indeterminate. (Such structures are referred to as systems with *static coupling* in dynamics literature.) These ideas could be extended to structures which are unstable (that is, incompletely restrained) under static loads (such structures sometimes are referred to as systems with *dynamic coupling*). This extension will not be considered herein.

3. Damping will be neglected in this chapter. This is legitimate in many structural-dynamics problems where maximum effects occur early in the transient stage of response. In addition to steady-state-response

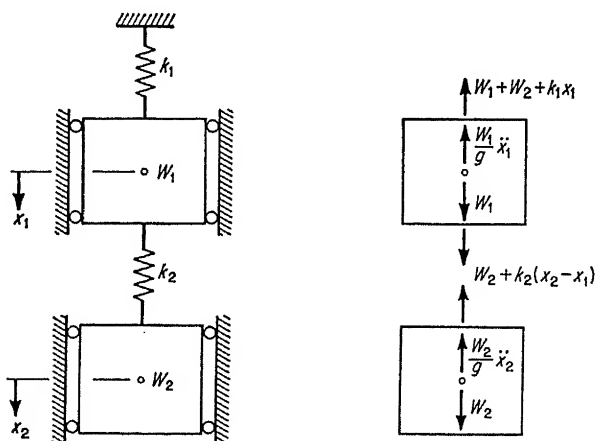


FIG. 4.1. System having two degrees of freedom.

problems, there are transient-response problems where damping is important; for example, see Ref. 1.

4.2. Undamped Free Vibration of Two-degree Systems. In order to introduce some of the new ideas involved in evaluating the response of multi-degree-of-freedom systems, consider the undamped two-degree system shown in Fig. 4.1.

As in Sec. 3.3 this is an idealized system with rigid masses and linearly elastic springs, where the masses are assumed to be constrained to move only in a vertical direction in the plane of the paper.

Assume that the system is undergoing an undamped free vibration in which the dynamic displacements of the mass centers are defined by the coordinates x_1 and x_2 , these being measured from the static-equilibrium position of the system under the dead weights of the rigid bodies W_1 and W_2 . Both x_1 and x_2 are to be considered plus when downward from this position.

If in accordance with D'Alembert's principle the inertia forces $(W_1/g)\ddot{x}_1$ and $(W_2/g)\ddot{x}_2$ are applied to the isolated bodies as shown, a condition

of dynamic equilibrium for each of the bodies, $\Sigma V = 0$, may be written as follows:

For body 1,

$$W_2 + k_2(x_2 - x_1) + W_1 - \frac{W_1}{g} \ddot{x}_1 - W_1 - W_2 - k_1x_1 = 0$$

$$\text{or} \quad \frac{W_1}{g} \frac{d^2x_1}{dt^2} + (k_1 + k_2)x_1 - k_2x_2 = 0 \quad (4.1)$$

For body 2,

$$W_2 - \frac{W_2}{g} \ddot{x}_2 - W_2 - k_2(x_2 - x_1) = 0$$

$$\text{or} \quad \frac{W_2}{g} \frac{d^2x_2}{dt^2} + k_2x_2 - k_2x_1 = 0 \quad (4.2)$$

These two equations are the two differential equations of motion which must be satisfied by any free vibration of this undamped two-degree system.

Suppose that our particular interest is in investigating whether or not a *normal mode of vibration* will satisfy these equations of motion. A normal mode of vibration, by definition, has three characteristics, namely,

1. It is an undamped free vibration.
2. It is periodic.
3. It is a vibration in which all points of the system vibrate *in phase* with one another (that is, at any two instants, the displaced positions of the system are geometrically similar).

Mathematically, a normal mode of vibration of this two-degree system would be represented as follows:

$$\begin{aligned} x_1 &= a_1 F(t) \\ x_2 &= a_2 F(t) \end{aligned} \quad (4.3)$$

Then, differentiating twice with respect to time,

$$\begin{aligned} \frac{d^2x_1}{dt^2} &= a_1 \frac{d^2}{dt^2} F(t) \\ \frac{d^2x_2}{dt^2} &= a_2 \frac{d^2}{dt^2} F(t) \end{aligned} \quad (4.4)$$

Substitution into Eqs. (4.1) and (4.2) from Eqs. (4.3) and (4.4) yields the following:

$$\begin{aligned} \frac{W_1}{g} a_1 \frac{d^2}{dt^2} F(t) + (k_1 + k_2) a_1 F(t) - k_2 a_2 F(t) &= 0 \\ \frac{W_2}{g} a_2 \frac{d^2}{dt^2} F(t) + k_2 a_2 F(t) - k_2 a_1 F(t) &= 0 \end{aligned}$$

In both of these equations, the time function $F(t)$ and its second derivative are separable, and therefore these equations may be rewritten as

$$\frac{(d^2/dt^2)F(t)}{F(t)} = \frac{-(k_1 + k_2)a_1 + k_2a_2}{(W_1/g)a_1} \quad (4.5)$$

$$\frac{(d^2/dt^2)F(t)}{F(t)} = \frac{-k_2a_2 + k_2a_1}{(W_2/g)a_2} \quad (4.6)$$

The left-hand sides of these equations are identical, and in order that the equations be satisfied for all values of t , the right-hand sides must be equal to the same constant, which will be denoted as $-\omega^2$. Thus,

$$\frac{(d^2/dt^2)F(t)}{F(t)} = -\omega^2$$

or

$$\frac{d^2}{dt^2}F(t) = -\omega^2F(t)$$

and the solution of this simple differential equation may be written as

$$F(t) = C_1 \sin \omega t + C_2 \cos \omega t \quad (4.7)$$

Thus, the time function $F(t)$ is found to represent a periodic motion having a frequency of $\omega/2\pi$ and a period of $2\pi/\omega$. The constants C_1 and C_2 could be easily found if the initial conditions of the motion at $t = 0$ were defined. For example, if at $t = 0$, both x_1 and x_2 were zero, then $[F(t)]_{t=0}$ would be zero, and therefore C_2 would have to be zero. If, in addition, the initial velocities were known, C_1 could be found to correspond. These details, however, are not necessary for the present discussion since our only interest is in showing that the motion is a periodic one.

Returning to Eqs. (4.5) and (4.6), if $-\omega^2$ is substituted for the left-hand sides, the equations may be rewritten as follows:

$$\left(\omega^2 \frac{W_1}{g} - k_1 - k_2\right)a_1 + k_2a_2 = 0 \quad (4.8)$$

$$k_2a_1 + \left(\omega^2 \frac{W_2}{g} - k_2\right)a_2 = 0 \quad (4.9)$$

In order for these equations to yield solutions for a_1 and a_2 different from zero (though the absolute values of a_1 and a_2 would still be indeterminate), the denominator determinant must be equal to zero:

$$\begin{vmatrix} \omega^2 \frac{W_1}{g} - k_1 - k_2 & k_2 \\ k_2 & \omega^2 \frac{W_2}{g} - k_2 \end{vmatrix} = 0$$

When this determinant is expanded, the following quadratic equation in ω^2 is obtained:

$$(\omega^2)^2 - g \left(\frac{k_1 + k_2}{W_1} + \frac{k_2}{W_2} \right) \omega^2 + \frac{k_1 k_2 g^2}{W_1 W_2} = 0 \quad (4.10)$$

This is the so-called *frequency equation* from which for a given system the values of the circular frequencies, ω_1 and ω_2 , can be determined. Note that there are two real roots of this equation, that is, two values of ω^2 (and therefore ω) for which the frequency equation is satisfied.

To simplify the remainder of the discussion of this solution, assume that $k_1 = k_2 = k$ and that $W_1 = W_2 = W$; then Eq. (4.10) becomes

$$(\omega^2)^2 - 3 \frac{kg}{W} \omega^2 + \frac{k^2 g^2}{W^2} = 0 \quad (4.11)$$

The two roots of this equation are

$$\begin{aligned} \omega_1^2 &= \frac{kg}{W} \frac{3 - \sqrt{5}}{2} \\ \omega_2^2 &= \frac{kg}{W} \frac{3 + \sqrt{5}}{2} \end{aligned} \quad (4.12)$$

Thus, there are two frequencies for periodic normal modes of vibration which would satisfy Eqs. (4.1) and (4.2), the differential equations of motion. Of these two frequencies, ω_1 has the smaller value and represents the frequency of the first (or so-called fundamental) normal mode of vibration, whereas ω_2 , the higher value, represents the frequency of the second normal mode of vibration. Note also that there are two sets of constants for Eq. (4.7): constants C_{11} and C_{21} corresponding to ω_1 for the first mode, and constants C_{12} and C_{22} corresponding to ω_2 for the second mode. These constants may be determined from the four initial conditions in this problem, namely, the initial displacement and the initial velocity for each of the masses.

To investigate the nature of the displacements associated with each of these modes of vibration, substitute in turn the values of ω_1 and ω_2 into Eqs. (4.8) and (4.9). First substituting ω_1 into either of these equations leads to the following relation:

$$a_{11} = \frac{2}{\sqrt{5} + 1} a_{21} \quad (4.13)$$

where the second subscript 1 of the a_{11} and a_{21} designates that these are the values of a_1 and a_2 associated with the first normal mode. Similarly, substitution of the value of ω_2 leads to the following relation:

$$a_{12} = - \frac{2}{\sqrt{5} - 1} a_{22} \quad (4.14)$$

where the second subscript 2 designates the a_1 and a_2 values for the second normal mode.

To summarize, it has been shown that there are two normal modes of vibration which satisfy the differential equations of motion, each of them

being free, and periodic vibrations having in addition the property that the masses vibrate in phase. The properties of these two normal modes are summarized in Fig. 4.2.

Note in each of these modes of vibration that the masses vibrate about their static-dead-load positions (shown by the solid outline) between the dashed-line and the dot-dash-line positions. In the first mode, both masses go down (or up) at the same time; in the second mode, when one mass is going down, the other is going up, or vice versa. The value of a_{11} , etc., is equal to the *half amplitude* of the vibratory displacement of mass point 1 in the first normal mode of vibration, etc.

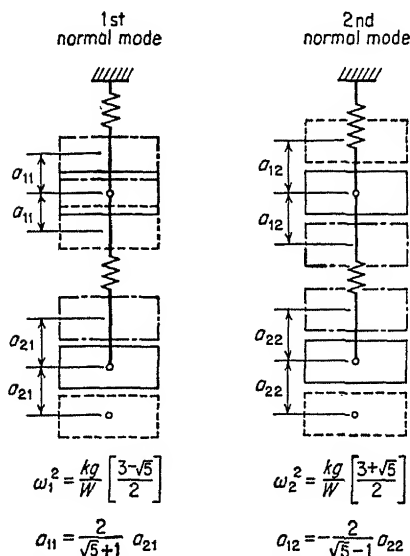


FIG. 4.2. Normal modes of vibration.

Several important properties of normal modes of vibration are illustrated by this solution and should be noted:

1. The absolute amplitude of a mode is arbitrary; for example, a_{21} could be 1 in., 12 in., or any value, but a_{11} must then be $2/(\sqrt{5}+1)$ in., $24/(\sqrt{5}+1)$ in., or $2/(\sqrt{5}+1) \times a_{21}$. Whatever the amplitude, the frequency of the vibration must be the same, which means that the velocities and accelerations involved will vary directly with the amplitude.

2. Since the absolute values of the amplitudes are arbitrary, they could be selected to have any convenient value. Later, it will be shown convenient for each mode to have the sum for all mass points of the product of each mass, and the square of the corresponding half amplitudes add up to unity. Thus, for the first mode,

$$\frac{W}{g} (a_{11}^2 + a_{21}^2) = 1$$

$$\text{or } a_{11}^2 + \frac{(\sqrt{5}+1)^2}{4} a_{11}^2 = \frac{g}{W} \quad \therefore a_{11} = A_{11} = \frac{2}{\sqrt{10+2\sqrt{5}}} \sqrt{\frac{g}{W}}$$

$$\text{and } A_{21} = \frac{\sqrt{5}+1}{\sqrt{10+2\sqrt{5}}} \sqrt{\frac{g}{W}}$$

When the amplitudes have been adjusted in such a manner, they are said to have been *normalized*. After normalization, the half amplitudes are referred to as the *normalized half amplitudes* and designated by the symbol A_{11} , A_{21} , etc. For the second mode, the following normalized half amplitudes are obtained:

$$\frac{W}{g} (a_{12}^2 + a_{22}^2) = 1$$

$$\text{or } a_{12}^2 + \frac{(\sqrt{5} - 1)^2}{4} a_{12}^2 = \frac{g}{W} \quad \therefore a_{12} = A_{12} = \frac{2}{\sqrt{10 - 2\sqrt{5}}} \sqrt{\frac{g}{W}}$$

$$\text{and} \quad A_{22} = \frac{-(\sqrt{5} - 1)}{\sqrt{10 - 2\sqrt{5}}} \sqrt{\frac{g}{W}}$$

3. Perhaps the most important mathematical property of the amplitudes of the normal modes is the following: Note that substitution of the numerical values demonstrates that

$$a_{11}a_{12} \frac{W}{g} + a_{21}a_{22} \frac{W}{g} = 0$$

and, of course, also that

$$A_{11}A_{12} \frac{W}{g} + A_{21}A_{22} \frac{W}{g} = 0$$

This is called the *orthogonality* property of the amplitudes for any two normal modes of vibration and will be seen subsequently to be the key to the use of normal modes of vibration.

The discussion of the free vibrations of this undamped system could be expanded in considerable detail; however, it is not necessary to do so for purposes of the present discussion. Whereas the above solution pertains to the normal-mode type of free vibration, it could be shown that any free vibration of this undamped system could be represented by the algebraic addition of the proper amounts of the two normal modes of vibration.

4.3. Determination of Normal Modes of Vibration of Concentrated-mass Systems by Deflection Equations Involving Flexibility Coefficients. In Sec. 4.2, an undamped two-degree system was used to introduce the concept of a normal mode of vibration and some of its important properties. The method being developed in this chapter for evaluating dynamic response involves superposition of such normal modes of vibration of the system. It is therefore important to develop workable methods for determining shapes and frequencies of the normal modes of vibration. Two such methods will be discussed herein. In this article, a method using *deflection equations* expressed in terms of *flexibility coefficients* will

be developed. In Sec. 4.4, an alternative method using *equations of motion* expressed in terms of *stiffness coefficients* will be presented.

Whereas the flexibility-coefficient method has extensive application, the ideas will be developed using as the illustrative example a simple end-supported beam with the three concentrated masses as shown in Fig. 4.3. It should be emphasized, however, that this elementary example has been used simply to expedite the presentation and that, thereby, the generality of the method has not been restricted.

Suppose that the masses are constrained to move in the plane of the paper. Since the horizontal and rotational displacements of the masses are small, they will be neglected. Only the three vertical displacements of the masses are needed, therefore, to define the configuration of the

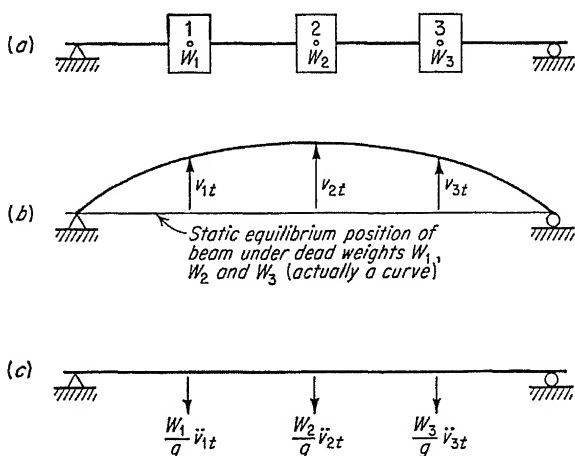


FIG. 4.3. Concentrated-mass system.

structure at any instant. The system therefore has only three degrees of freedom.

Suppose the structure is vibrating in a normal mode of vibration. The dynamic vertical displacements of the mass points during this vibration are measured from the static-equilibrium position of the masses and are designated as v_{1t} , v_{2t} , and v_{3t} for the mass points 1, 2, and 3, respectively. The vertical displacements v are to be considered plus when upward from the static-equilibrium position.

In accordance with D'Alembert's principle, the inertia forces shown in Fig. 4.3 are applied at the mass points. In this free vibration, the only forces causing dynamic displacements of the beam from the static-equilibrium position of the structure are the inertia forces. The dynamic displacements may therefore be expressed as follows:

$$\begin{aligned}
v_{1t} &= -\frac{W_1}{g} \ddot{v}_{1t} d_{11} - \frac{W_2}{g} \ddot{v}_{2t} d_{12} - \frac{W_3}{g} \ddot{v}_{3t} d_{13} \\
v_{2t} &= -\frac{W_1}{g} \ddot{v}_{1t} d_{21} - \frac{W_2}{g} \ddot{v}_{2t} d_{22} - \frac{W_3}{g} \ddot{v}_{3t} d_{23} \\
v_{3t} &= -\frac{W_1}{g} \ddot{v}_{1t} d_{31} - \frac{W_2}{g} \ddot{v}_{2t} d_{32} - \frac{W_3}{g} \ddot{v}_{3t} d_{33}
\end{aligned} \tag{4.15}$$

where the d terms are called *flexibility coefficients* and are designated in accordance with the usual notation used in statically indeterminate structural analysis, namely,

d_{ij} = upward vertical displacement of mass points i per unit upward load at mass point j , with units of distance per unit force

Assume that the initial conditions of this normal mode of vibration are that at $t = 0$, $v_{1t} = v_{2t} = v_{3t} = 0$. Then, as was found in Sec. 4.2, the displacements in this normal mode of vibration could be expressed as

$$\begin{aligned}
v_{1t} &= a_1 \sin \omega t \\
v_{2t} &= a_2 \sin \omega t \\
v_{3t} &= a_3 \sin \omega t
\end{aligned} \tag{4.16}$$

where a_1 , a_2 , and a_3 = half amplitude of vibration at mass points 1, 2, and 3, respectively. Then the accelerations of the mass points are as follows:

$$\begin{aligned}
\ddot{v}_{1t} &= -a_1 \omega^2 \sin \omega t \\
\ddot{v}_{2t} &= -a_2 \omega^2 \sin \omega t \\
\ddot{v}_{3t} &= -a_3 \omega^2 \sin \omega t
\end{aligned} \tag{4.17}$$

When the values from Eqs. (4.16) and (4.17) are substituted into Eqs. (4.15), $\sin \omega t$ will be common to all terms and, not necessarily being equal to zero, may be canceled out. Then the resulting equations may be written as

$$\begin{aligned}
\frac{g}{\omega^2} a_1 &= W_1 d_{11} a_1 + W_2 d_{12} a_2 + W_3 d_{13} a_3 \\
\frac{g}{\omega^2} a_2 &= W_1 d_{21} a_1 + W_2 d_{22} a_2 + W_3 d_{23} a_3 \\
\frac{g}{\omega^2} a_3 &= W_1 d_{31} a_1 + W_2 d_{32} a_2 + W_3 d_{33} a_3
\end{aligned} \tag{4.18}$$

Equations (4.18) could be rewritten as follows:

$$\begin{aligned}
\left(W_1 d_{11} - \frac{g}{\omega^2} \right) a_1 + W_2 d_{12} a_2 + W_3 d_{13} a_3 &= 0 \\
W_1 d_{21} a_1 + \left(W_2 d_{22} - \frac{g}{\omega^2} \right) a_2 + W_3 d_{23} a_3 &= 0 \\
W_1 d_{31} a_1 + W_2 d_{32} a_2 + \left(W_3 d_{33} - \frac{g}{\omega^2} \right) a_3 &= 0
\end{aligned} \tag{4.19}$$

These are three simultaneous equations from which the values of a_1 , a_2 , and a_3 could be determined. If there is to be any vibration, however (that is, if a_1 , a_2 , and a_3 are to have values different from zero), the denominator determinant of these equations must be equal to zero. Setting this determinant equal to zero would result in a frequency equation [analogous to Eq. (4.10)] from which three roots of ω^2 could be determined, thereby indicating that there are three different frequencies at which normal modes of vibration could occur and satisfy Eqs. (4.15). (Note that there are as many normal modes as there are degrees of freedom.) Then, by substituting each of these roots in turn back into Eqs. (4.19), the relative values of a_1 , a_2 , and a_3 corresponding to each value of ω^2 could be determined. (Note that only the relative values can be determined; the absolute values are arbitrary, as was also found for the two-degree system in Sec. 4.2.) Thus, in this way, the frequency and shape of each of the three normal modes of vibration could be found.

Note that, since in a normal mode of vibration the masses vibrate in phase with one another, the shape of the deflection curve of the structure at any instant is geometrically similar to the shape in the extreme displaced position, which is, of course, defined by the values of the half amplitudes a_1 , a_2 , and a_3 for that particular normal mode of vibration. The deflection curve of a normal mode in its extreme position as defined by the a values is usually referred to as the *characteristic shape of that mode*.

The procedure just outlined, while straightforward, is laborious, and the computations may be greatly expedited by solving Eqs. (4.18) for the shapes and frequencies by a convergent iterative procedure known as Stodola's procedure (see Refs. 1-3 in Chap. 3). This procedure will be explained and illustrated by a numerical example which is given in Sec. 4.6.

The three values of ω for which normal modes of vibration could occur are arranged in order of ascending frequencies and designated as ω_1 , ω_2 , and ω_3 , denoting the frequency of the first, second, and third normal modes of vibration, respectively. There is a separate set of values of a_1 , a_2 , and a_3 corresponding to each of these normal modes. These values of a are denoted by a double-subscript notation where the first subscript denotes the mass point and the second subscript the mode. Thus,

For first mode, frequency = ω_1 , and shape is defined by a_{11} , a_{21} , and a_{31} .

For second mode, frequency = ω_2 , and shape is defined by a_{12} , a_{22} , and a_{32} .

For third mode, frequency = ω_3 , and shape is defined by a_{13} , a_{23} , and a_{33} .

4.4. Determination of Normal Modes of Vibration of Concentrated-mass Systems by Equations of Motion Involving Stiffness Coefficients.

The evaluation of flexibility coefficients is particularly easy for statically determinate structures, and the deflection-equation method described in Sec. 4.3 is therefore particularly useful for such structures. For many indeterminate structures, this procedure is not so straightforward, however. Consider the three-story planar rigid frame shown in Fig. 4.4. Assume that the members of the frame are weightless but that large concentrated masses are supported by the frame at the locations shown. Assume also that the vertical deflections and rotations of the masses are small and can be neglected. This frame is therefore a three-degree system involving only the horizontal displacements of the mass points. To evaluate d_{11} , d_{21} , and d_{31} , for example, a stress analysis of the frame must be carried out for a unit horizontal load at mass point 1 (using moment distribution, this involves three sidesway solutions), and then the horizontal deflections at mass points 1, 2, and 3 may be computed.

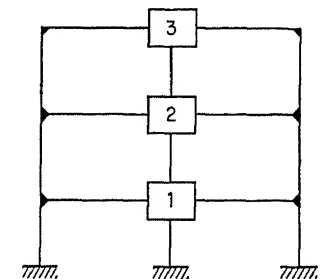


FIG. 4.4. Three-story rigid frame.

For such an indeterminate structure, however, in order to determine the frequencies and shapes of the normal modes of vibration, it is much easier to set up equations of motion for each of the mass points [instead

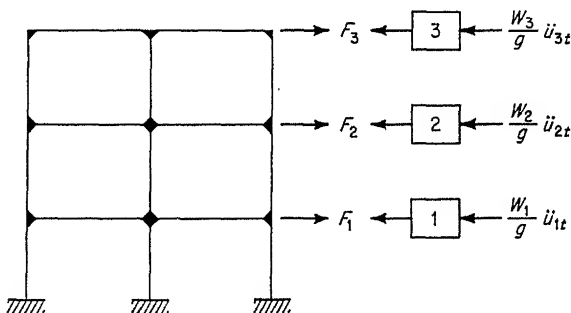


FIG. 4.5. Free-body sketches for setting up equations of motion.

of the deflection equations (4.15)]. Each of these equations of motion is simply a statement that, in a free undamped vibration, each mass is in dynamic equilibrium horizontally under the action of its inertia force and the interacting spring force between it and the structure. Considering the displacement u , and therefore the velocities and accelerations, plus when to the right and the interacting spring forces F plus when as shown in Fig. 4.5, the equations of motion may be written as

$$\begin{aligned}
-\frac{W_1}{g} \ddot{u}_{1t} - F_1 &= 0 \\
-\frac{W_2}{g} \ddot{u}_{2t} - F_2 &= 0 \\
-\frac{W_3}{g} \ddot{u}_{3t} - F_3 &= 0
\end{aligned} \tag{4.20}$$

The interacting spring forces F are uniquely determined by the deflected shape of the structure, that is, by u_{1t} , u_{2t} , and u_{3t} , and could be expressed as follows:

$$\begin{aligned}
F_1 &= k_{11}u_{1t} + k_{12}u_{2t} + k_{13}u_{3t} \\
F_2 &= k_{21}u_{1t} + k_{22}u_{2t} + k_{23}u_{3t} \\
F_3 &= k_{31}u_{1t} + k_{32}u_{2t} + k_{33}u_{3t}
\end{aligned} \tag{4.21}$$

where the coefficients k are called *stiffness coefficients* and, for example, k_{ij} is defined as the interacting spring force at mass point i per unit displacement ($u_j = 1$) at mass point j , all other displacements being zero.

If the structure is vibrating in a normal mode of vibration, the displacements and accelerations may be expressed in the same way as in Eqs. (4.16) and (4.17):

$$\begin{aligned}
u_{1t} &= a_1 \sin \omega t & \ddot{u}_{1t} &= -a_1 \omega^2 \sin \omega t \\
u_{2t} &= a_2 \sin \omega t & \ddot{u}_{2t} &= -a_2 \omega^2 \sin \omega t \\
u_{3t} &= a_3 \sin \omega t & \ddot{u}_{3t} &= -a_3 \omega^2 \sin \omega t
\end{aligned} \tag{4.22}$$

Then, by substituting in Eqs. (4.20) from Eqs. (4.21) and (4.22), the equations of motion may be converted into the following form:

$$\begin{aligned}
\frac{W_1}{g} \omega^2 a_1 &= k_{11}a_1 + k_{12}a_2 + k_{13}a_3 \\
\frac{W_2}{g} \omega^2 a_2 &= k_{21}a_1 + k_{22}a_2 + k_{23}a_3 \\
\frac{W_3}{g} \omega^2 a_3 &= k_{31}a_1 + k_{32}a_2 + k_{33}a_3
\end{aligned} \tag{4.23}$$

These equations are similar to Eqs. (4.18) and may be solved using Stodola's procedure, as will be described in Sec. 4.6. The superiority of Eqs. (4.23) over (4.18) for indeterminate structures is due to the fact that, in many cases, the stiffness coefficients are more easily obtained than the flexibility coefficients. For example, considering this frame, the stiffness coefficients, as noted in Fig. 4.6, are simply the pulling and holding forces involved in the moment-distribution-sidesway solutions, where in each case unit displacements have been introduced as noted.

4.5. Characteristic Loads and Important Properties of Shapes of Normal Modes of Vibration. In Secs. 4.3 and 4.4, methods have been discussed for computing the frequencies and characteristic shapes of the

normal modes of vibration of concentrated-mass systems. Suppose that the characteristic shapes of the modes of a system, such as the beam shown in Fig. 4.3, have been computed by one of these methods. Then suppose that static loads were applied at mass points 1, 2, and 3, the load at any particular mass point i being proportional to the product of the mass

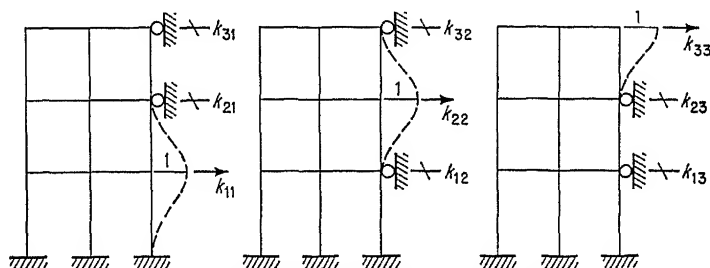


FIG. 4.6. Stiffness coefficients for rigid frame.

W_i/g and the half amplitude a_{im} of the characteristic shape of m th normal mode at that point. Such a static loading will be called the characteristic loading* for the m th mode of vibration, and the value of the characteristic load* at mass point i for mode m will be designated by ℓ_{im} . Specifically, the characteristic loads for the m th mode will be designated for mass points 1, 2, and 3 by

$$\ell_{1m} = \omega_m^2 \frac{W_1}{g} a_{1m} \quad \ell_{2m} = \omega_m^2 \frac{W_2}{g} a_{2m} \quad \ell_{3m} = \omega_m^2 \frac{W_3}{g} a_{3m} \quad (4.24)$$

or, in general, for a mass point i , as

$$\ell_{im} = \omega_m^2 \frac{W_i}{g} a_{im} \quad (4.24a)$$

The characteristic loading applied as static loads will produce the following static deflections at mass points 1, 2, and 3:

$$v_1 = \ell_{1m}d_{11} + \ell_{2m}d_{12} + \ell_{3m}d_{13}$$

and similarly for v_2 and v_3 , or

$$\begin{aligned} v_1 &= \frac{\omega_m^2}{g} (W_1d_{11}a_{1m} + W_2d_{12}a_{2m} + W_3d_{13}a_{3m}) = a_{1m} \\ v_2 &= \frac{\omega_m^2}{g} (W_1d_{21}a_{1m} + W_2d_{22}a_{2m} + W_3d_{23}a_{3m}) = a_{2m} \\ v_3 &= \frac{\omega_m^2}{g} (W_1d_{31}a_{1m} + W_2d_{32}a_{2m} + W_3d_{33}a_{3m}) = a_{3m} \end{aligned} \quad (4.25)$$

* It is important in this chapter to distinguish between the terms *loading* and *load*. As used herein (for example, see Fig. 4.9), the group of loads \mathcal{L}_{11} , \mathcal{L}_{21} , and \mathcal{L}_{31} are referred to as being "the normalized characteristic loading for the first normal mode of the structure," whereas any one of these loads, such as \mathcal{L}_{21} , is referred to as "the normalized characteristic load at mass point 2 for the first normal mode."

if substitution for the expression in brackets is made using Eqs. (4.18). By virtue of Eqs. (4.25) the following statement may be made:

The characteristic loading for the m th mode, when applied statically, deflects the structure into a curve which has the characteristic shape of the m th normal mode of vibration for the structure.

The characteristic shapes of the normal modes of vibration have several important properties, which may be demonstrated by the following consideration. First, suppose that the characteristic loading corresponding to the n th mode is acting on the structure and then the structure is subjected to a virtual displacement corresponding to the m th mode. Secondly, suppose that the characteristic loading corresponding to the m th mode is acting on the structure and then it is subjected to a virtual displacement corresponding to the n th mode. By Betti's law, the virtual work done in the first instance is equal to the virtual work done in the second instance. Thus, if there are r masses,

$$\sum_{i=1}^{i=r} \ell_{in} a_{im} = \sum_{i=1}^{i=r} \ell_{im} a_{in}$$

but $\ell_{in} = \omega_n^2 \frac{W_i}{g} a_{in}$ and $\ell_{im} = \omega_m^2 \frac{W_i}{g} a_{im}$

Therefore
$$\sum_{i=1}^{i=r} \omega_n^2 \frac{W_i}{g} a_{in} a_{im} = \sum_{i=1}^{i=r} \omega_m^2 \frac{W_i}{g} a_{im} a_{in}$$

or
$$(\omega_m^2 - \omega_n^2) \sum_{i=1}^{i=r} \frac{W_i}{g} a_{in} a_{im} = 0 \quad (4.26)$$

Thus, it may be concluded that, in order for Eq. (4.26) to be satisfied,

If $n \neq m$, $\omega_m^2 - \omega_n^2 \neq 0$

Hence
$$\sum_{i=1}^{i=r} \frac{W_i}{g} a_{im} a_{in} = 0 \quad (4.27)$$

This is called the *orthogonality condition*.

If $n = m$, $\omega_m^2 - \omega_n^2 = 0$

Hence
$$\sum_{i=1}^{i=r} \frac{W_i}{g} a_{im}^2 = \text{any arbitrary constant} \quad (4.28)$$

When the absolute values of a_{im} are selected so that the sum in Eq. (4.28) is equal to unity, the characteristic shape of the m th normal mode is said

to have been *normalized*, and Eq. (4.28) is said to be the *normalizing condition*. After normalization, let the normalized characteristic shapes be designated by A_{im} ; thus,

$$\sum_{i=1}^{i=r} \frac{W_i}{g} A_{im} A_{in} = \begin{cases} 1 & \text{if } m = n \\ 0 & \text{if } m \neq n \end{cases} \quad (4.28a)$$

Note, of course, that

$$\frac{A_{1m}}{a_{1m}} = \frac{A_{2m}}{a_{2m}} = \frac{A_{3m}}{a_{3m}} = \frac{A_{im}}{a_{im}}$$

The *normalized characteristic loads* corresponding to the normalized characteristic shapes will be designated by \mathcal{L}_{im} ; thus,

$$\mathcal{L}_{im} = \omega_m^2 \frac{W_i}{g} A_{im} \quad (4.29)$$

designating the characteristic load at the i th mass corresponding to the m th mode.

4.6. Stodola's Procedure for Solving Equations Defining Normal Modes of Vibration. It was noted in Secs. 4.3 and 4.4 that Stodola's

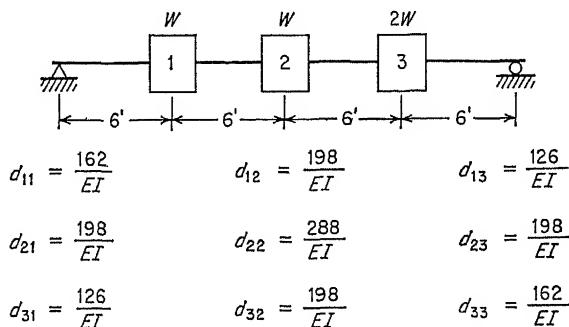


FIG. 4.7. Flexibility coefficient for three-mass beam.

procedure was the most expeditious way of computing the frequencies and characteristic shapes of the normal modes of vibration from Eqs. (4.18) or Eqs. (4.23). This method is a convergent iterative procedure which is straightforward to apply and most easily described by an illustrative example.

Consider the three-mass system shown in Fig. 4.7. In order to apply Eqs. (4.18) (the deflection equations), the flexibility coefficients must be computed. These computations are not shown in detail but may be done easily using the moment-areas theorems to obtain the values noted in the figure. Substitution of these values into Eqs. (4.18) results in the

following equations, valid for any mode m , where $\mathcal{K}_m = EIg/\omega_m^2 W$:

$$\begin{aligned}\mathcal{K}_m a_{1m} &= 162a_{1m} + 198a_{2m} + 252a_{3m} \\ \mathcal{K}_m a_{2m} &= 198a_{1m} + 288a_{2m} + 396a_{3m} \\ \mathcal{K}_m a_{3m} &= 126a_{1m} + 198a_{2m} + 324a_{3m}\end{aligned}\quad (a)$$

First Mode. In the first trial, assume $a_{11} = 0.8$, $a_{21} = 1.1$, $a_{31} = 1.0$; then insert these values into the right side of Eqs. (a), and compute the resulting improved values of the a 's:

$$\begin{aligned}\mathcal{K}_1 a_{11} &= 129.6 + 217.8 + 252 = 599.4 \\ \mathcal{K}_1 a_{21} &= 158.4 + 316.8 + 396 = 871.2 \\ \mathcal{K}_1 a_{31} &= 100.8 + 217.8 + 324 = 642.6 \quad \text{let } a_{31} = 1.0 \\ \therefore \mathcal{K}_1 &= 642.6 \quad a_{11} = 0.93 \quad a_{21} = 1.36\end{aligned}$$

In the second trial, assume $a_{11} = 0.95$, $a_{21} = 1.37$, $a_{31} = 1.0$. With these new approximations of the a 's, the right sides of Eqs. (a) now become

$$\begin{aligned}\mathcal{K}_1 a_{11} &= 154.4 + 271.26 + 252 = 677.26 \\ \mathcal{K}_1 a_{21} &= 188.1 + 394.56 + 396 = 978.66 \\ \mathcal{K}_1 a_{31} &= 119.7 + 271.26 + 324 = 714.96 \quad \text{let } a_{31} = 1.0 \\ \therefore \mathcal{K}_1 &= 714.96 \quad a_{11} = 0.948 \quad a_{21} = 1.367\end{aligned}$$

This process could be carried on to any desired degree of precision between the assumed and computed values of a . If a certain degree of precision is required for the higher modes, the calculations for the lower modes must be carried to a greater precision since some precision is lost as each mode is computed. For this example, however, the above agreement in the second trial will be considered adequate, and therefore we have the following:

First Mode

$$\begin{aligned}a_{11} &= 0.948 \\ a_{21} &= 1.367 \quad \text{and} \quad \omega_1^2 = \frac{EIg}{714.96W} \\ a_{31} &= 1.0\end{aligned}$$

Second Mode. Having determined the first mode, an orthogonality condition may be written which is valid for the first mode and any of the higher modes. Thus, applying Eq. (4.27), the first orthogonality condition becomes, for any mode m for $m = 2, 3, 4, \dots$,

$$0.948a_{1m} + 1.367a_{2m} + 2a_{3m} = 0 \quad (b)$$

Thus for $m = 2$, we may write

$$a_{32} = -0.474a_{12} - 0.6835a_{22}$$

Using this relation, we may eliminate a_{32} from the first two of Eqs. (a) and obtain the two following equations involving only a_{12} and a_{22} :

$$\begin{aligned}\mathcal{K}_2 a_{12} &= 42.552a_{12} + 25.758a_{22} \\ \mathcal{K}_2 a_{22} &= 10.296a_{12} + 17.334a_{22}\end{aligned}\quad (c)$$

These equations as written apply to the second mode, but they are likewise valid for the third mode. They may be iterated by Stodola's procedure to obtain the second mode in the same manner as was done above for the first mode.

In the first trial, assume $a_{12} = 1.0$, $a_{22} = 0.2$:

$$\begin{aligned}\mathcal{K}_2 a_{12} &= 42.552 + 5.152 = 47.704 & \text{let } a_{12} &= 1.0 & \therefore \mathcal{K}_2 &= 47.704 \\ \mathcal{K}_2 a_{22} &= 10.296 + 3.467 = 13.763 & \therefore a_{22} &= 0.29\end{aligned}$$

In the second trial, assume $a_{12} = 1.0$, $a_{22} = 0.3$:

$$\begin{aligned}\mathcal{K}_2 a_{12} &= 42.552 + 7.727 = 50.279 & \text{let } a_{12} &= 1.0 & \therefore \mathcal{K}_2 &= 50.279 \\ \mathcal{K}_2 a_{22} &= 10.296 + 5.200 = 15.496 & \therefore a_{22} &= 0.308\end{aligned}$$

In the third trial, assume $a_{12} = 1.0$, $a_{22} = 0.309$:

$$\begin{aligned}\mathcal{K}_2 a_{12} &= 42.552 + 7.959 = 50.511 & \text{let } a_{12} &= 1.0 & \therefore \mathcal{K}_2 &= 50.511 \\ \mathcal{K}_2 a_{22} &= 10.296 + 5.356 = 15.652 & \therefore a_{22} &= 0.310\end{aligned}$$

Then $a_{32} = -(0.474)(1.0) - (0.6835)(0.310) = -0.686$

using the first orthogonality condition. Therefore, scaling these results up so that $a_{32} = -1.0$, we may write as follows:

Second Mode

$$\begin{aligned}a_{12} &= +1.458 \\ a_{22} &= +0.452 & \text{and} & \quad \omega_2^2 = \frac{EIg}{50.511W} \\ a_{32} &= -1.0\end{aligned}$$

Third Mode. Now having determined the second mode, the second orthogonality condition becomes, for any mode m for $m = 3, \dots, r$ (in this case, of course, $r = 3$, so this second condition is valid simply for the third, that is, the last, mode),

$$1.458a_{1m} + 0.452a_{2m} - 2a_{3m} = 0 \quad (d)$$

or since $m = 3$,

$$a_{33} = 0.729a_{13} + 0.226a_{23}$$

But the first orthogonality condition is also valid for $m = 3$;

$$\therefore a_{33} = -0.474a_{13} - 0.6835a_{23}$$

Equating these two expressions for a_{33} yields

$$0.729a_{13} + 0.226a_{23} = -0.474a_{13} - 0.6835a_{23}$$

$$\therefore 1.203a_{13} = -0.9095a_{23}$$

Thus, if

$$a_{23} = 1.0 \quad a_{13} = -0.756$$

and

$$a_{33} = (0.729)(-0.756) + (0.226)(1.0) = -0.325$$

Thus, scaling up the results, we have

Third Mode

$$a_{13} = -2.326$$

$$a_{23} = +3.077 \quad \text{and} \quad \omega_3^2 = \frac{EIg}{8.477W}$$

$$a_{33} = -1.0$$

Since

$$\mathcal{K}_3 a_{13} = 42.552a_{13} + 25.758a_{23}$$

$$\mathcal{K}_3(-2.326) = (42.552)(-2.326) + (25.758)(3.077) \quad \therefore \mathcal{K}_3 = 8.477$$

The above calculations illustrate the application of Stodola's procedure to the computation of the normal modes of vibration using the deflection

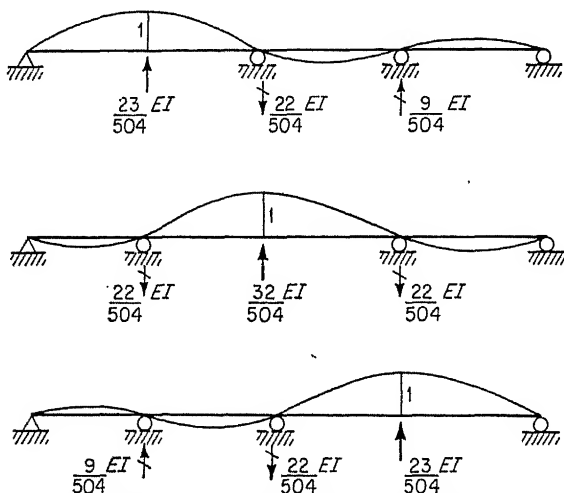


FIG. 4.8. Stiffness coefficients for the three-mass beam.

equations expressed in terms of flexibility coefficients. In a similar manner, the frequencies and characteristic shapes of the normal modes of vibration could be computed from the equations of motion (4.23), expressed in terms of stiffness coefficients. For the structure under consideration, the stiffness coefficients could be computed by the moment-distribution method and the results noted in Fig. 4.8 obtained. In applying Eqs. (4.23) to this structure, assume that the k 's are plus when

the interacting spring force acting on the beam is up. Thus the equations of motion become, letting $\mathcal{J}_m = (504W/EIg)\omega_m^2$,

$$\begin{aligned}\mathcal{J}_m a_{1m} &= 23a_{1m} - 22a_{2m} + 9a_{3m} \\ \mathcal{J}_m a_{2m} &= -22a_{1m} + 32a_{2m} - 22a_{3m} \\ 2\mathcal{J}_m a_{3m} &= 9a_{1m} - 22a_{2m} + 23a_{3m}\end{aligned}\quad (e)$$

Stodola's procedure could now be applied to find the a 's and ω for each of the modes. In this alternative solution, however, the iteration converges on the solution of the third, or highest, mode. After finding this mode, an orthogonality equation may be written and used to reduce the set of equations by one. Iteration of the reduced group of equations converges on the next lowest mode, etc. Thus the first, or fundamental, mode is the last one to be computed.

Most of the points involved in applying Stodola's procedure have been illustrated by the above example, but certain features of these calculations should be emphasized:

1. Stodola's procedure is applicable either to the deflection equations (4.18) or to the equations of motion (4.23). However, in the first case the iterative procedure converges on the lowest mode involved in the equations, and in the second case on the highest mode [3].

2. In the successive trials, the a values found in the previous trial may be assumed directly for the next trial; or, if better adjusted values can be anticipated, they may be used instead. Also, if an error is made in a given trial, this will not affect the final result (unless the error is in the last trial), but will affect only the rate of convergence.

3. After a mode has been found, an orthogonality equation may be written and used to reduce the number of working equations by one. This means that each mode is easier to compute than the previous one. The last mode to be computed can always be computed directly without iteration.

After the normal modes have been computed, the characteristic shapes can be normalized in accordance with Eq. (4.28a). In the case of the above illustrative example, the following values are obtained for the normalized characteristic shapes:

First Mode

$$\frac{W}{g} [(0.948)^2 + (1.367)^2 + 2(1.0)^2] A_{31}^2 = 1 \quad \therefore \begin{cases} A_{31} = 0.457 \sqrt{\frac{g}{W}} \\ A_{21} = 0.625 \sqrt{\frac{g}{W}} \\ A_{11} = 0.433 \sqrt{\frac{g}{W}} \end{cases}$$

Second Mode

$$\frac{W}{g} [(1.458)^2 + (0.452)^2 + 2(-1.0)^2] A_{32}^2 = 1 \quad \therefore \begin{cases} A_{32} = -0.481 \sqrt{\frac{g}{W}} \\ A_{22} = +0.217 \sqrt{\frac{g}{W}} \\ A_{12} = +0.701 \sqrt{\frac{g}{W}} \end{cases}$$

Third Mode

$$\frac{W}{g} [(-2.326)^2 + (3.077)^2 + 2(-1.0)^2] A_{33}^2 = 1 \quad \therefore \begin{cases} A_{33} = -0.243 \sqrt{\frac{g}{W}} \\ A_{23} = +0.749 \sqrt{\frac{g}{W}} \\ A_{13} = -0.566 \sqrt{\frac{g}{W}} \end{cases}$$

The normalized characteristic loads computed using Eq. (4.29) are as follows:

First Mode

$$\mathfrak{L}_{31} = 0.00128EI \sqrt{\frac{g}{W}}$$

$$\mathfrak{L}_{21} = 0.000874EI \sqrt{\frac{g}{W}}$$

$$\mathfrak{L}_{11} = 0.000606EI \sqrt{\frac{g}{W}}$$

Second Mode

$$\mathfrak{L}_{32} = -0.0191EI \sqrt{\frac{g}{W}}$$

$$\mathfrak{L}_{22} = +0.0043EI \sqrt{\frac{g}{W}}$$

$$\mathfrak{L}_{12} = +0.0139EI \sqrt{\frac{g}{W}}$$

Third Mode

$$\mathfrak{L}_{33} = -0.0573EI \sqrt{\frac{g}{W}}$$

$$\mathfrak{L}_{23} = +0.0884EI \sqrt{\frac{g}{W}}$$

$$\mathfrak{L}_{13} = -0.0668EI \sqrt{\frac{g}{W}}$$

4.7. Use of Normalized Characteristic Loadings to Evaluate Effects Produced by Static Loading. Prior to developing the theory whereby characteristic loading can be used to evaluate dynamic response, it is of

interest to show how they can be used to evaluate the effects produced by static loads. Very rarely would it be desirable to evaluate static effects in this manner, since there are much easier ways of doing static-stress analysis. The technique of using characteristic loadings for the static problem is directly applicable to the dynamic case, however, and a useful preliminary step to the subsequent discussion.

Once the characteristic loadings have been computed, it is easy to use them to evaluate the effects produced by a given static load applied to the mass points of the system. Using the previous illustrative example,

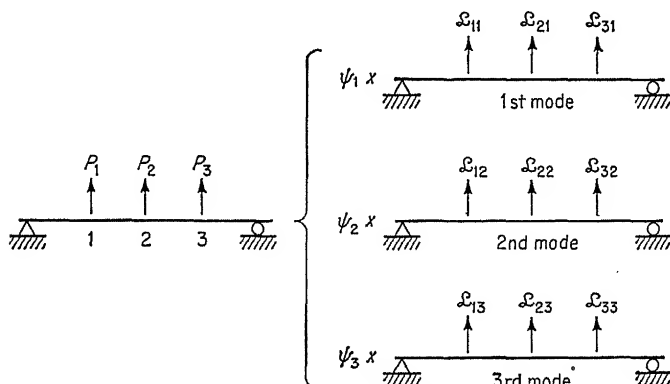


FIG. 4.9. Static-mode loads.

suppose the structure shown in Fig. 4.7 is subjected to the static loads P_1 , P_2 , and P_3 that are shown in Fig. 4.9. By taking a certain factor ψ_1 times the characteristic loading for the first mode, a factor ψ_2 times that for the second mode, and a factor ψ_3 times that for the third mode, the contributions may be superimposed (that is, added algebraically) so that the sum total is equivalent to the given loading.

The factors ψ_1 , ψ_2 , and ψ_3 are called the *participation factors* for the first, second, and third modes, respectively. Once these factors have been found, the deflection of the structure produced by the static loads P_1 , P_2 , and P_3 may be obtained by superimposing the contributions from each of the three modes, namely, ψ_1 times the deflection produced by the characteristic loading for the first mode, plus ψ_2 times that for the second mode, and plus ψ_3 times that for the third mode. Of course, not only deflection, but any effect such as bending moment, shear, etc., could be computed in this manner.

If it is noted that P_i , the given static load at mass point i , is equal to the sum for all the modes of the portions of the characteristic loads at this point, or that

$$P_i = \sum_{m=1}^{m=r} \psi_m L_{im} \quad (4.30)$$

the following simultaneous equations could be written and solved for the participation factors ψ_1 , ψ_2 , and ψ_3 :

$$\begin{aligned} P_1 &= \psi_1 \mathcal{L}_{11} + \psi_2 \mathcal{L}_{12} + \psi_3 \mathcal{L}_{13} \\ P_2 &= \psi_1 \mathcal{L}_{21} + \psi_2 \mathcal{L}_{22} + \psi_3 \mathcal{L}_{23} \\ P_3 &= \psi_1 \mathcal{L}_{31} + \psi_2 \mathcal{L}_{32} + \psi_3 \mathcal{L}_{33} \end{aligned} \quad (4.31)$$

This approach would be laborious for a system having a large degree of freedom, and it would be much easier to proceed in an alternative manner.

Suppose that we wish to find the participation factor ψ_b for the b th mode. Apply the given loads P_1 , P_2 , and P_3 to the structure and then subject the structure to a virtual displacement corresponding to the normalized characteristic shape of b th mode. The virtual work \mathcal{W}_b done by the loads P_1 , P_2 , and P_3 will then be

$$\mathcal{W}_b = P_1 A_{1b} + P_2 A_{2b} + P_3 A_{3b} = \sum_{i=1}^{i=r} P_i A_{ib} \quad (4.32)$$

However, \mathcal{W}_b could also be expressed by substituting in Eq. (4.32) from Eq. (4.30):

$$\mathcal{W}_b = A_{1b} \sum_{m=1}^{m=r} \psi_m \mathcal{L}_{1m} + A_{2b} \sum_{m=1}^{m=r} \psi_m \mathcal{L}_{2m} + A_{3b} \sum_{m=1}^{m=r} \psi_m \mathcal{L}_{3m}$$

However, substituting for \mathcal{L}_{im} from Eq. (4.29),

$$\mathcal{W}_b = \sum_{m=1}^{m=r} \psi_m \omega_m^2 \left(\sum_{i=1}^{i=r} A_{ib} A_{im} \frac{W_i}{g} \right)$$

The term in parentheses [see Eqs. (4.28a)] is equal to zero except when $m = b$, in which case it is equal to 1; thus the sum on the right-hand side is reduced to one term:

$$\mathcal{W}_b = \psi_b \omega_b^2 \quad (4.33)$$

Now, equating the right-hand sides of Eqs. (4.32) and (4.33),

$$\psi_b = \frac{\sum_{i=1}^{i=r} P_i A_{ib}}{\omega_b^2}$$

However, what has been proved for mode b could be proved for any mode m . Thus the general formula for the participation factor ψ_m for the m th mode is

$$\psi_m = \frac{\sum_{i=1}^{i=r} P_i A_{im}}{\omega_m^2} \quad (4.34)$$

which is very easily evaluated for a given loading once the shapes and frequencies of the normal modes of vibration of the system have been computed.

The loading $\psi_m \mathcal{L}_{im}$ at the various mass points i represents the portion of the characteristic loading for mode m which must be combined with similar portions for all the modes to build up the given static loading. The loading $\psi_m \mathcal{L}_{im}$ is called the *static-mode loading* for mode m and, at the various mass points i , is designated by the symbol \mathcal{P}_{im} . Thus

$$\mathcal{P}_{im} = \psi_m \mathcal{L}_{im} \quad (4.35)$$

Note that the static-mode loading for the m th mode produces deflections at the mass points equal to $\psi_m A_{im}$, since the normalized characteristic loading produces the deflections A_{im} . Thus, to summarize, the given load at mass point i , P_i , and the deflections that the given static loads produce at mass point i , v_i , may be expressed as

$$P_i = \sum_{m=1}^{m=r} \mathcal{P}_{im} = \sum_{m=1}^{m=r} \psi_m \mathcal{L}_{im} \quad (4.36)$$

and

$$v_i = \sum_{m=1}^{m=r} \psi_m A_{im} \quad (4.37)$$

In the same way, bending moments, etc., produced by the static-mode loading could be superimposed to build up the total effect produced by the given static loading acting on the structure.

To illustrate the computation of the participation factors and the static-mode loading, suppose the structure in Fig. 4.7 were acted upon by a downward static load of 10 kips at mass point 2. Thus,

$$P_1 = 0 \quad P_2 = -10 \quad P_3 = 0$$

Now the participation factors and static-mode loading for each of the three normal modes may be computed by using Eqs. (4.34) and (4.35), as shown in Fig. 4.10. The superposition of these three static-mode loadings is shown in Fig. 4.11, which obviously is equivalent to the given loading.

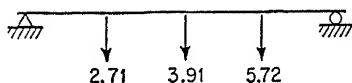
4.8. Use of Normalized Characteristic Loadings to Evaluate Dynamic Response Produced by Dynamic Loading. The extension of the theory to evaluate dynamic response is straightforward now that the application of characteristic loading to the static-loading case has been discussed. Obviously, in addition to the ideas and concepts discussed in Sec. 4.7, the dynamic case must involve certain factors which bring the time variation of the dynamic loading into the solution. The following development will demonstrate, however, that the dynamic response of a concentrated-mass system or structure to a given dynamic loading may

be evaluated by superimposing the separate dynamic contributions of the characteristic loading corresponding to each of the normal modes of vibration of the system. It will be shown that this solution satisfies

1st Mode:

$$\therefore \mathcal{Q}_{i1} = \psi_1 \mathcal{L}_{i1}$$

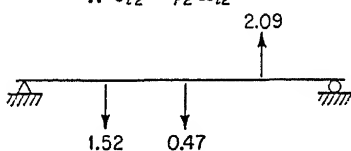
$$\begin{aligned}\psi_1 &= \frac{(-10)(0.625\sqrt{\frac{g}{W}})}{\frac{EIg}{714.96W}} \\ &= \frac{-4469}{EI\sqrt{\frac{g}{W}}}\end{aligned}$$



2nd Mode:

$$\therefore \mathcal{Q}_{i2} = \psi_2 \mathcal{L}_{i2}$$

$$\begin{aligned}\psi_2 &= \frac{(-10)(0.217\sqrt{\frac{g}{W}})}{\frac{EIg}{50.511W}} \\ &= \frac{-1096}{EI\sqrt{\frac{g}{W}}}\end{aligned}$$



3rd Mode:

$$\therefore \mathcal{Q}_{i3} = \psi_3 \mathcal{L}_{i3}$$

$$\begin{aligned}\psi_3 &= \frac{(-10)(0.749\sqrt{\frac{g}{W}})}{\frac{EIg}{8.477W}} \\ &= \frac{-63.49}{EI\sqrt{\frac{g}{W}}}\end{aligned}$$

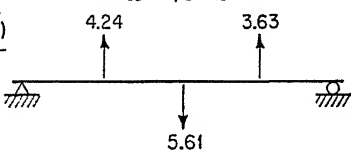
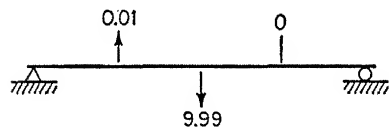


FIG. 4.10. Static-mode loads for three-mass beam.

the deflection equations which pertain and the initial conditions of the motion of the structure. The deflection equations involve the dynamic loading, the flexibility and mass characteristics of the structure, and the boundary conditions of the structure. Such a solution would therefore satisfy all the theoretical requirements of the dynamic-response problem.

FIG. 4.11. Superposition of static-mode loads for three-mass beam.



In the following development, no consideration will be given to impactive loads; that is, only impulsive loadings will be considered (see Sec. 3.2 for definitions of these loadings). Further, it will be assumed that the dynamic loading at all points of application varies with time in the same manner. In other words, if the dynamic loading involves a distributed

load or more than one concentrated load, it will be assumed that all the loading varies with time in exactly the same way. If this is not true, the response may still be computed by an extension of this approach, but the computations become very tedious. This extension will be discussed briefly in Chap. 6.

Assume that the frequencies and characteristic shapes of the r normal modes of vibration of a given concentrated-mass structure have already been computed (for convenience, think of this structure as being the beam shown in Fig. 4.3). Assume, further, that the normalized characteristic loading associated with each of these modes has been computed, and that the deflection, bending moment, shear, and other effects of interest produced by this loading have been computed and tabulated for various locations of interest on the structure.

Now suppose that this structure is subjected to a given dynamic loading which may consist of concentrated dynamic loads varying with time in some manner and applied at any or all mass points of the structure; however, as noted above, it will be assumed that all these loads are in phase with one another, that is, vary with time in the same manner. The dynamic load at any mass point i will be called P_{it} and may be represented mathematically as

$$P_{it} = P_i f(t) \quad (4.38)$$

where P_i = *maximum instantaneous value* attained by dynamic load P_{it}
 $f(t)$ = time variation of load

(Refer to Sec. 3.7 for a similar notation for a one-degree system.) However, as discussed in Sec. 4.7, the maximum value P_i could be built up or replaced by adding up the proper static-mode loadings \mathcal{P}_{im} as is expressed by Eq. (4.36). If this is done, Eq. (4.38) becomes

$$P_{it} = f(t) \sum_{m=1}^{m=r} \mathcal{P}_{im} = \sum_{m=1}^{m=r} f(t) \psi_m \mathcal{L}_{im} \quad (4.39)$$

The static deflection produced by the static-mode loading for any mode m will be $\psi_m A_{im}$ at any mass point i . Let us see if we can represent the dynamic deflection v_{it} at any mass point i caused simply by the given dynamic loading as being the superposition of the static-mode-loading deflections, each multiplied by a certain time function $\mathcal{D}_m(t)$. In other words, let us see whether or not the dynamic deflection v_{it} of any mass point i may be represented or evaluated by the following equation:

$$v_{it} = \sum_{m=1}^{m=r} \mathcal{D}_m(t) \psi_m A_{im} \quad (4.40)$$

Note that v_{it} represents the dynamic deflection which would be produced

by the loading P_{it} if it were applied to the structure when it was at rest (that is, when it had neither initial deflection nor velocity). Of course, the structure may already be in motion at time t_0 when the above dynamic loading is applied. It will be shown subsequently, in Sec. 4.9, that the dynamic deflection v_{it}^I at any mass point i produced *simply* by the initial motion of the structure may be represented by *another* superposition of the r normalized characteristic shapes, multiplied in this case by a *different time function*, $\mathfrak{D}_m^I(t)$, as follows:

$$v_{it}^I = \sum_{m=1}^{m=r} \mathfrak{D}_m^I(t) A_{im} \quad (4.41)$$

This new time function will be called the *time factor* and will be selected so as to satisfy the initial conditions at time t_0 regarding the known initial displacements and velocities of the r masses.

The total dynamic deflection v_{it}^T at any mass point i will be the algebraic sum of the deflection v_{it}^I caused by the initial motion and the additional deflection v_{it} caused by the dynamic loading P_{it} , or

$$v_{it}^T = v_{it}^I + v_{it}$$

$$\text{Hence,} \quad v_{it}^T = \sum_{m=1}^{m=r} \mathfrak{D}_m^I(t) A_{im} + \sum_{m=1}^{m=r} \mathfrak{D}_m(t) \psi_m A_{im} \quad (4.42)$$

If it is possible to complete this derivation using this expression, it will have been demonstrated that the deflection v_{it} produced by the dynamic loading is independent of the initial motion. If this is true, it will be possible to compute v_{it} and v_{it}^I separately and simply add them algebraically to obtain v_{it}^T .* In Chap. 3, it has already been shown that such a procedure is permissible for a one-degree system.

To continue the derivation and show that this approach is permissible, we must next write the equations governing the dynamic deflections of the various mass points i [similar to Eqs. (4.15)]. Continue the use of the previous illustrative example. Suppose that the dynamic loads P_{1t} , P_{2t} , and P_{3t} of the type represented by Eq. (4.38) act at the mass points 1, 2, and 3, respectively, as shown in Fig. 4.12. Then, by applying D'Alembert's principle, the dynamic deflection of the structure from its

* In some cases, it is desirable to combine the two series in Eq. (4.42) and compute v_{it}^T from the following equation:

$$v_{it}^T = \sum_{m=1}^{m=r} A_{im} [\mathfrak{D}_m^I(t) + \psi_m \mathfrak{D}_m(t)] \quad (4.42a)$$

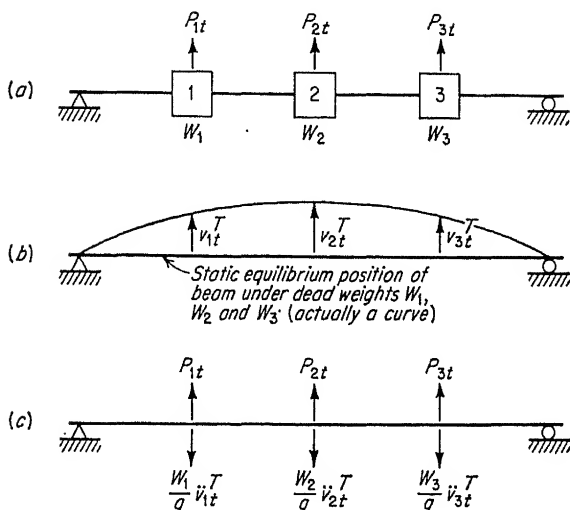


FIG. 4.12. Dynamic loading of three-mass beams.

static-dead-load position may be considered to be caused by the combined action of the three dynamic loads and the three inertia forces shown in Fig. 4.12. Assuming that the dynamic loads and dynamic deflections (and, of course, the velocities and accelerations) are plus when up, we may write, in the same manner as Eqs. (4.15),

$$\begin{aligned}
 v_{1t}T &= \left(P_{1t} - \frac{W_1}{g} \ddot{v}_{1t}T \right) d_{11} + \left(P_{2t} - \frac{W_2}{g} \ddot{v}_{2t}T \right) d_{12} + \left(P_{3t} - \frac{W_3}{g} \ddot{v}_{3t}T \right) d_{13} \\
 v_{2t}T &= \left(P_{1t} - \frac{W_1}{g} \ddot{v}_{1t}T \right) d_{21} + \left(P_{2t} - \frac{W_2}{g} \ddot{v}_{2t}T \right) d_{22} + \left(P_{3t} - \frac{W_3}{g} \ddot{v}_{3t}T \right) d_{23} \\
 v_{3t}T &= \left(P_{1t} - \frac{W_1}{g} \ddot{v}_{1t}T \right) d_{31} + \left(P_{2t} - \frac{W_2}{g} \ddot{v}_{2t}T \right) d_{32} + \left(P_{3t} - \frac{W_3}{g} \ddot{v}_{3t}T \right) d_{33}
 \end{aligned} \quad (4.43)$$

In these equations, substitute for P_{1t} , etc., from Eq. (4.39) and for $v_{1t}T$, etc., from Eq. (4.42); transpose and regroup terms to obtain the following:

$$\begin{aligned}
 &\sum_{m=1}^{m=r} \left\{ \left[f(t)\psi_m \mathcal{L}_{1m} - \frac{W_1}{g} \ddot{\mathfrak{D}}_m(t)\psi_m A_{1m} \right] d_{11} - \ddot{\mathfrak{D}}_m(t)\psi_m A_{1m} \right. \\
 &+ \left[f(t)\psi_m \mathcal{L}_{2m} - \frac{W_2}{g} \ddot{\mathfrak{D}}_m(t)\psi_m A_{2m} \right] d_{12} + \left[f(t)\psi_m \mathcal{L}_{3m} - \frac{W_3}{g} \ddot{\mathfrak{D}}_m(t)\psi_m A_{3m} \right] d_{13} \\
 &\quad \left. - \left[\frac{W_1}{g} A_{1m} d_{11} + \frac{W_2}{g} A_{2m} d_{12} + \frac{W_3}{g} A_{3m} d_{13} \right] \ddot{\mathfrak{D}}_m^I(t) - \ddot{\mathfrak{D}}_m^I(t) A_{1m} \right\} = 0
 \end{aligned}$$

$$\begin{aligned}
& \sum_{m=1}^{m=r} \left\{ \left[f(t)\psi_m \mathcal{L}_{1m} - \frac{W_1}{g} \ddot{\mathfrak{D}}_m(t)\psi_m A_{1m} \right] d_{21} - \mathfrak{D}_m(t)\psi_m A_{2m} \right. \\
& + \left[f(t)\psi_m \mathcal{L}_{2m} - \frac{W_2}{g} \ddot{\mathfrak{D}}_m(t)\psi_m A_{2m} \right] d_{22} + \left[f(t)\psi_m \mathcal{L}_{3m} - \frac{W_3}{g} \ddot{\mathfrak{D}}_m(t)\psi_m A_{3m} \right] d_{23} \\
& \quad \left. - \left[\frac{W_1}{g} A_{1m} d_{21} + \frac{W_2}{g} A_{2m} d_{22} + \frac{W_3}{g} A_{3m} d_{23} \right] \ddot{\mathfrak{D}}_m^I(t) - \mathfrak{D}_m^I(t) A_{2m} \right\} = 0 \\
& \sum_{m=1}^{m=r} \left\{ \left[f(t)\psi_m \mathcal{L}_{1m} - \frac{W_1}{g} \ddot{\mathfrak{D}}_m(t)\psi_m A_{1m} \right] d_{31} - \mathfrak{D}_m(t)\psi_m A_{3m} \right. \\
& + \left[f(t)\psi_m \mathcal{L}_{2m} - \frac{W_2}{g} \ddot{\mathfrak{D}}_m(t)\psi_m A_{2m} \right] d_{32} + \left[f(t)\psi_m \mathcal{L}_{3m} - \frac{W_3}{g} \ddot{\mathfrak{D}}_m(t)\psi_m A_{3m} \right] d_{33} \\
& \quad \left. - \left[\frac{W_1}{g} A_{1m} d_{31} + \frac{W_2}{g} A_{2m} d_{32} + \frac{W_3}{g} A_{3m} d_{33} \right] \ddot{\mathfrak{D}}_m^I(t) - \mathfrak{D}_m^I(t) A_{3m} \right\} = 0
\end{aligned} \tag{4.44}$$

Into these equations substitute $\mathcal{L}_{1m} = \omega_m^2(W_1/g)A_{1m}$, etc., and then note that Eqs. (4.18) are likewise valid for the normalized characteristic shapes A_{1m} , A_{2m} , and A_{3m} ; so

$$A_{1m} \frac{g}{\omega_m^2} = W_1 d_{11} A_{1m} + W_2 d_{12} A_{2m} + W_3 d_{13} A_{3m}$$

etc., for $A_{2m}g/\omega_m^2$ and $A_{3m}g/\omega_m^2$. In this way, we obtain

$$\begin{aligned}
& \sum_{m=1}^{m=r} \left\{ \left[f(t)\psi_m A_{1m} - \ddot{\mathfrak{D}}_m(t)\psi_m \frac{A_{1m}}{\omega_m^2} - \mathfrak{D}_m(t)\psi_m A_{1m} \right] \right. \\
& \quad \left. + \left[-\ddot{\mathfrak{D}}_m^I(t) \frac{A_{1m}}{\omega_m^2} - \mathfrak{D}_m^I(t) A_{1m} \right] \right\} = 0 \\
& \sum_{m=1}^{m=r} \left\{ \left[f(t)\psi_m A_{2m} - \ddot{\mathfrak{D}}_m(t)\psi_m \frac{A_{2m}}{\omega_m^2} - \mathfrak{D}_m(t)\psi_m A_{2m} \right] \right. \\
& \quad \left. + \left[-\ddot{\mathfrak{D}}_m^I(t) \frac{A_{2m}}{\omega_m^2} - \mathfrak{D}_m^I(t) A_{2m} \right] \right\} = 0 \\
& \sum_{m=1}^{m=r} \left\{ \left[f(t)\psi_m A_{3m} - \ddot{\mathfrak{D}}_m(t)\psi_m \frac{A_{3m}}{\omega_m^2} - \mathfrak{D}_m(t)\psi_m A_{3m} \right] \right. \\
& \quad \left. + \left[-\ddot{\mathfrak{D}}_m^I(t) \frac{A_{3m}}{\omega_m^2} - \mathfrak{D}_m^I(t) A_{3m} \right] \right\} = 0
\end{aligned} \tag{4.45}$$

Multiply the first of Eqs. (4.45) by $A_{1b}W_1/g$, the second by $A_{2b}W_2/g$, and the third by $A_{3b}W_3/g$ (where A_{1b} , A_{2b} , and A_{3b} correspond to one

particular mode b); then add the resulting equations and thereby obtain

$$\psi_b \left[f(t) - \frac{\ddot{\mathfrak{D}}_b(t)}{\omega_b^2} - \mathfrak{D}_b(t) \right] - \left[\frac{\ddot{\mathfrak{D}}_b^I(t)}{\omega_b^2} + \mathfrak{D}_b^I(t) \right] = 0$$

in view of Eqs. (4.28a), which define the orthogonality and normalized properties of the normal modes of vibration. However, what has been proved for mode b could be proved for any mode m . In Sec. 4.9, it will be demonstrated that

$$\frac{1}{\omega_m^2} \ddot{\mathfrak{D}}_m^I(t) + \mathfrak{D}_m^I(t) = 0$$

Therefore, for any mode m ,

$$\ddot{\mathfrak{D}}_m(t) + \omega_m^2 \mathfrak{D}_m(t) = \omega_m^2 f(t) \quad (4.46)$$

Equation (4.46) is called the *reduced equation of motion*, and the solution of this equation establishes the value of $\mathfrak{D}_m(t)$, which satisfies Eqs. (4.43). This value of $\mathfrak{D}_m(t)$ may be inserted in Eq. (4.40) to compute the dynamic deflection v_{it} , which is produced simply by the dynamic loading P_{it} .

It is now apparent that the theory being developed to evaluate dynamic response due to a given dynamic loading such as represented by Eq. (4.38) is very similar to the method developed in Sec. 4.7 to handle static loads. In the dynamic problem, however, the maximum values of the dynamic loading are first applied as static loads, and the participation factors ψ_m are computed, thereby defining the static-mode loads. To evaluate the modal contributions to the dynamic response at any time t , however, the effects produced by the static-mode loads must be multiplied by the factor $\mathfrak{D}_m(t)$. This factor is called the dynamic-load factor and, in Sec. 4.10, will be seen to be identical with the dynamic-load factor (DLF) discussed previously in Sec. 3.7 for the simple one-degree system. In the multidegree system, however, there is a dynamic-load factor $\mathfrak{D}_m(t)$ associated with each mode m . This varies with time, depending on the frequency of the mode, ω_m , and the time variation of the load, $f(t)$. The details of the solution of the reduced equation of motion and the development of a working formula to evaluate the dynamic-load factor will be discussed in Sec. 4.10.

4.9. Use of Normalized Characteristic Shapes to Evaluate Response Associated with Initial Motion of System. Because of previous loadings, suppose that, at the starting time t_0 , the initial motion is known and defined by the initial displacement $v_{it_0}^I$ and the initial velocity $\dot{v}_{it_0}^I$ of each mass point i . Simply as a result of this initial motion, the system will subsequently undergo an undamped free vibration denoted for each mass point i as v_{it}^I . We shall now investigate whether this vibration can be represented by Eq. (4.41).

In the absence of any impressed dynamic loading and if damping is neglected, the deflections of the structure will be caused only by the inertia forces associated with this undamped free vibration. If we continue the use of the three-mass beam as an illustration, P_{1t} , P_{2t} , and P_{3t} should be deleted from Fig. 4.12 in order to represent this present situation. The deflection equations similar to Eqs. (4.43) now become, where v_{it}^I is defined by Eq. (4.41),

$$\begin{aligned} v_{1t}^I &= -\frac{W_1}{g} d_{11} \ddot{v}_{1t}^I - \frac{W_2}{g} d_{12} \ddot{v}_{2t}^I - \frac{W_3}{g} d_{13} \ddot{v}_{3t}^I \\ v_{2t}^I &= -\frac{W_1}{g} d_{21} \ddot{v}_{1t}^I - \frac{W_2}{g} d_{22} \ddot{v}_{2t}^I - \frac{W_3}{g} d_{23} \ddot{v}_{3t}^I \\ v_{3t}^I &= -\frac{W_1}{g} d_{31} \ddot{v}_{1t}^I - \frac{W_2}{g} d_{32} \ddot{v}_{2t}^I - \frac{W_3}{g} d_{33} \ddot{v}_{3t}^I \end{aligned} \quad (4.47)$$

By manipulating these equations in the same way as Eqs. (4.43) were manipulated to obtain Eq. (4.46), we obtain

$$\ddot{\mathfrak{D}}_m^I(t) + \omega_m^2 \mathfrak{D}_m^I(t) = 0 \quad (4.48)$$

The solution of this equation may be written as

$$\mathfrak{D}_m^I(t) = \mathfrak{D}_m^I(t_0) \cos \omega_m(t - t_0) + \frac{\dot{\mathfrak{D}}_m^I(t_0)}{\omega_m} \sin \omega_m(t - t_0) \quad (4.49)$$

in which the arbitrary coefficients of these two terms are easily shown to be the initial values of the time factor $\mathfrak{D}_m^I(t_0)$ and of its first derivative $\dot{\mathfrak{D}}_m^I(t_0)$. These initial values are dependent on the initial positions and velocities of the mass points of the system, respectively.

Fortunately, $\mathfrak{D}_m^I(t_0)$ and $\dot{\mathfrak{D}}_m^I(t_0)$ are easily obtained from formulas which may be developed by the same technique that has been used several times previously. Suppose that at $t = t_0$, the displacement of all mass points ($v_{1t_0}^I$, $v_{2t_0}^I$, . . . , $v_{rt_0}^I$) and the velocities ($\dot{v}_{1t_0}^I$, $\dot{v}_{2t_0}^I$, . . . , $\dot{v}_{rt_0}^I$) are known. Then using Eq. (4.41), for the structure in Fig. 4.12,

$$\begin{aligned} v_{1t_0}^I &= \mathfrak{D}_1^I(t_0) A_{11} + \mathfrak{D}_2^I(t_0) A_{12} + \mathfrak{D}_3^I(t_0) A_{13} \\ v_{2t_0}^I &= \mathfrak{D}_1^I(t_0) A_{21} + \mathfrak{D}_2^I(t_0) A_{22} + \mathfrak{D}_3^I(t_0) A_{23} \\ v_{3t_0}^I &= \mathfrak{D}_1^I(t_0) A_{31} + \mathfrak{D}_2^I(t_0) A_{32} + \mathfrak{D}_3^I(t_0) A_{33} \end{aligned} \quad (4.50)$$

Suppose that the first of these equations is multiplied by $A_{11}W_1/g$, the second by $A_{21}W_2/g$, and the third by $A_{31}W_3/g$ and that the resulting equations are then added. In view of Eqs. (4.28a), this procedure would lead to the following result:

$$\sum_{i=1}^{i=3} v_{it_0}^I A_{i1} \frac{W_i}{g} = \mathfrak{D}_1^I(t_0)$$

However, this same procedure could be applied to a structure with r mass points, and the same manipulation accomplished for the quantities pertaining to any mode m . Therefore, by analogy,

$$\mathfrak{D}_m^I(t_0) = \sum_{i=1}^{i=r} v_{i_0}^I A_{im} \frac{W_i}{g} \quad (4.51)$$

In exactly the same manner, a similar equation could be written for $\dot{\mathfrak{D}}_m^I(t_0)$, of course starting the development with equations obtained by differentiating both sides of Eq. (4.41) with respect to time rather than starting it with Eq. (4.41) proper.

$$\dot{\mathfrak{D}}_m^I(t_0) = \sum_{i=1}^{i=r} \dot{v}_{i_0}^I A_{im} \frac{W_i}{g} \quad (4.52)$$

Thus, for any given structure in a known position and with known velocities at $t = t_0$, the initial values $\mathfrak{D}_m^I(t_0)$ and $\dot{\mathfrak{D}}_m^I(t_0)$ could be evaluated from Eqs. (4.51) and (4.52), and then the time factor $\mathfrak{D}_m^I(t)$ could be computed from Eq. (4.49). This time factor can then be inserted in Eq. (4.41) to evaluate the response associated with the known initial motion of the system.

4.10. Solution of Reduced Equation of Motion. The solution of Eq. (4.46), the reduced equation of motion, may be obtained in exactly the same manner as the solution of Eq. (3.28) in Sec. 3.7. In this case, however, v_{it} represents the dynamic displacement produced by the given dynamic loading applied to a system which is initially at rest. Therefore, at every mass point i , v_{i_0} and \dot{v}_{i_0} are both equal to zero; and therefore the initial values $\mathfrak{D}_m(t_0)$ and $\dot{\mathfrak{D}}_m(t_0)$ are likewise zero. As a result the following solution is obtained for

$$\mathfrak{D}_m(t) = \omega_m \int_{t_0}^t f(t') \sin \omega_m(t - t') dt' \quad (4.53)$$

This is identical with the expression for DLF given by Eq. (3.30).

The important conclusion to draw from this development is that the ideas regarding dynamic-load factor which were developed in Chap. 3 for the simple one-degree system likewise pertain to the multimass system. In the multimass system, however, there is a separate dynamic load factor (DLF) for each mode. Values of DLF computed in Sec. 3.7 for various types of dynamic loading are directly applicable, however, to various modal DLFs involved in the multimass system.

4.11. Recapitulation—Computation of Dynamic Response of Concentrated-mass Systems. The following will summarize the important features of the response theory which has been developed and will

suggest an itemized procedure for applying the method to response calculations. In addition, some additional notation will be introduced to emphasize the generality and flexibility of the working equations which have been developed.

It is important at this point to review the scope of this development as enumerated in Sec. 4.1. This theory is applicable to concentrated-mass systems which are linearly elastic. Damping has been neglected. Consideration is given only to dynamic loadings which vary with time in the same manner at all points on the structure. Extension of this theory to nonlinear cases and to loadings which do not remain in phase at all points will be considered later in Chap. 6.

The theory presented in this chapter for computing the normal modes of vibration and dynamic response was developed using a very simple concentrated-mass system, specifically the three-mass end-supported beam shown in Fig. 4.3. However, the theory is much more general than one might infer from this example. This beam was considered as a system in which only one coordinate was required to specify the position of each mass, namely, the vertical displacement of the mass. In general, however, six coordinates may be required to specify the position of each mass of a concentrated-mass system—three linear displacements and three angular displacements. Thus, such a system would have six degrees of freedom per mass. The frame shown in Fig. 3.1*d* illustrates, for example, a system in which there is more than one coordinate per mass required to define the configuration of the system, even though axial deformations and rotation of the masses were neglected.

The theory and working equations developed herein are completely applicable to these more complicated cases, although it is probably desirable to change the notation slightly to emphasize this generality. The revisions in notation are as follows:

1. The *displacement coordinates* required to define the configuration of the concentrated-mass system will be designated as $q_{1t}, q_{2t}, \dots, q_{rt}$, where r designates the number of degrees of freedom of the system. Note that r may be larger than the number of masses since there may be more than one coordinate per mass. Previously, in Chaps. 3 and 4, displacement coordinates were designated variously as x , u , and v .

2. The *characteristic shape* (or the half amplitude of the vibration) of the m th normal mode of vibration will be designated as $\varphi_{1m}, \varphi_{2m}, \varphi_{3m}, \dots, \varphi_{rm}$. Previously, the characteristic shapes were designated as a_{1m} , etc.

3. The *normalized characteristic shapes* (or the normalized half amplitudes of the vibration) of the m th normal mode of vibration will be designated as

$$\Phi_{1m}, \Phi_{2m}, \dots, \Phi_{rm}$$

Previously, these were designated as A_{1m} , etc.

Using this revised notation, the key equations involved in the response theory will become, where the prime on the equation number indicates that the revised notation is being used, as follows:

Deflection equations in terms of flexibility coefficients d

$$\begin{aligned} \frac{g}{\omega^2} \varphi_1 &= W_1 d_{11} \varphi_1 + W_2 d_{12} \varphi_2 + \cdots + W_r d_{1r} \varphi_r \\ \frac{g}{\omega^2} \varphi_2 &= W_1 d_{21} \varphi_1 + W_2 d_{22} \varphi_2 + \cdots + W_r d_{2r} \varphi_r \\ &\vdots \\ \frac{g}{\omega^2} \varphi_r &= W_1 d_{r1} \varphi_1 + W_2 d_{r2} \varphi_2 + \cdots + W_r d_{rr} \varphi_r \end{aligned} \quad (4.18')$$

Equations of motion in terms of stiffness coefficients k

$$\begin{aligned} \frac{W_1}{g} \omega^2 \varphi_1 &= k_{11} \varphi_1 + k_{12} \varphi_2 + \cdots + k_{1r} \varphi_r \\ \frac{W_2}{g} \omega^2 \varphi_2 &= k_{21} \varphi_1 + k_{22} \varphi_2 + \cdots + k_{2r} \varphi_r \\ &\vdots \\ \frac{W_r}{g} \omega^2 \varphi_r &= k_{r1} \varphi_1 + k_{r2} \varphi_2 + \cdots + k_{rr} \varphi_r \end{aligned} \quad (4.23')$$

Orthogonality and normalizing conditions

$$\sum_{i=1}^{i=r} \frac{W_i}{g} \Phi_{im} \Phi_{in} = \begin{cases} 1 & \text{if } m = n \\ 0 & \text{if } m \neq n \end{cases} \quad (4.28a')$$

Normalized characteristic load

$$\mathcal{L}_{im} = \omega_m^2 \frac{W_i}{q} \Phi_{im} \quad (4.29')$$

Participation factor

$$\psi_m = \frac{\sum_{i=1}^{i=r} P_i \Phi_{im}}{\omega_m^2} \quad (4.34')$$

Static-mode load

$$\mathcal{P}_{im} = \psi_m \mathcal{L}_{im} \quad (4.35)$$

Given dynamic load

$$P_{it} = P_i f(t) \quad (4.38)$$

$$P_{it} = f(t) \sum_{m=1}^{m=r} \mathcal{P}_{im} = \sum_{m=1}^{m=r} f(t) \psi_m \mathcal{L}_{im} \quad (4.39)$$

Dynamic displacement due to dynamic loading

$$q_{it} = \sum_{m=1}^{m=r} \mathfrak{D}_m(t) \psi_m \Phi_{im} \quad (4.40')$$

Dynamic displacement due to initial motion

$$q_{it}^I = \sum_{m=1}^{m=r} \mathfrak{D}_m^I(t) \Phi_{im} \quad (4.41')$$

Time factor associated with response due to initial motion

$$\mathfrak{D}_m^I(t) = \mathfrak{D}_m^I(t_0) \cos \omega_m(t - t_0) + \frac{\dot{\mathfrak{D}}_m^I(t_0)}{\omega_m} \sin \omega_m(t - t_0) \quad (4.49)$$

where
$$\mathfrak{D}_m^I(t_0) = \sum_{i=1}^{i=r} q_{it_0}^I \Phi_{im} \frac{W_i}{g} \quad (4.51')$$

and
$$\dot{\mathfrak{D}}_m^I(t_0) = \sum_{i=1}^{i=r} \dot{q}_{it_0}^I \Phi_{im} \frac{W_i}{g} \quad (4.52')$$

Dynamic-load factor associated with response due to dynamic loading

$$\mathfrak{D}_m(t) = \omega_m \int_{t_0}^t f(t') \sin \omega_m(t - t') dt' \quad (4.53)$$

Note again that r denotes the number of deflection coordinates necessary to define the configuration of the system and also the number of degrees of freedom and modes of vibration; that i denotes any particular one of the r coordinates; and that m denotes any particular one of the r modes. Note also that W_i/g designates the mass associated with the coordinate q_{it} ; therefore, when more than one coordinate is required to define the position of a mass, the same mass will be associated with more than one coordinate, and therefore the same mass may be denoted by several different subscripts. In most structural problems, the rotations of mass points can be neglected, and this discussion has therefore implied that the deflection coordinates are always linear displacements. The equations can be interpreted in a generalized sense, and q_{it} can be considered to represent also a rotation, in which case W_i/g should be interpreted to represent a corresponding mass moment of inertia.

To compute the dynamic mass response produced by a given impulsive dynamic load, the following procedure may be followed:

1. Compute the characteristic shapes φ_{im} and the circular frequencies ω_m of all the r normal modes of the system. Either the deflection equations (4.18') or the equations of motion (4.23') may be used as the basis of the solution, usually depending on whether the flexibility or stiffness coefficients, respectively, are more easily computed, and some-

times depending on whether the lowest or highest modes, respectively, are of greatest interest. The solution of either of these equations may be accomplished by Stodola's procedure.

2. Normalize the characteristic shapes Φ_{im} of all the modes and compute the normalized characteristic loads \mathcal{L}_{im} .

3. Assuming the maximum values of the given impulsive loads P_i to be applied as static loads, compute the participation factor ψ_m and the static-mode loads \mathcal{P}_{im} for each of the r modes of the system.

4. Of course the static-mode load for mode m produces the static displacements $\psi_m \Phi_{im}$. Other static effects (such as bending moments, shears, etc.) produced by the static-mode loads could also be computed at various locations on the structure and tabulated.

5. Compute the dynamic-load factors $\mathcal{D}_m(t)$ for the various modes.

6. Superimpose the contributions of the various modes at any time t by multiplying the deflection, shear, bending moment, etc., produced by a static-mode load for a given mode by the value of the dynamic-load factor for that mode at that time, and then by adding algebraically such products for all modes to get the dynamic response which would be produced by the dynamic loading applied to a structure initially at rest.

7. If at the starting time the structure has an initial motion, compute the time factors $\mathcal{D}_m^I(t)$ for the various modes.

8. Superimpose the contributions of the various modes of any time t by multiplying the deflection, shear, and bending moments produced by the normalized characteristic loading by the value of the time factor for that mode at that time, and then by adding algebraically such products for all modes to get the dynamic response which is associated with the initial motion of the structure.

9. Add algebraically the results of steps 7 and 8 to get the total dynamic response caused by both the dynamic loading and the initial motion.

10. By studying the total dynamic response at various times t compute the maximum values that they attain. To obtain maximum effects requires very tedious, laborious calculations, which time seldom permits in actual dynamic problems. Conservative results are sometimes attained by computing the maximum contributions of each mode and assuming that they can occur simultaneously and therefore be superimposed. Sometimes these absolute maximum values are good engineering approximations; other times they are too conservative.

Note that *participation factor* depends on the distribution of the load over the structure and on the characteristic shape. When the distribution of load and characteristic shapes are similar, the participation factor is large. A load applied at the node point of a mode excites none of that mode.

The dynamic-load factor for a mode depends only on the time variation of the load and on the frequency of the mode.

4.12. Computation of Response Produced by Support Vibration. The theory which has been developed to compute the response produced by dynamic loading can easily be extended to include the effect of support vibrations. Consider any structure such as the beam shown in Fig. 4.13.

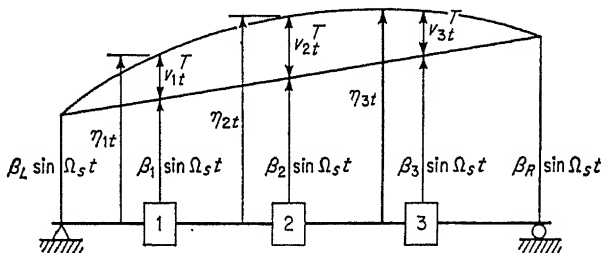


FIG. 4.13. Effect of support vibration.

Suppose that the supports vibrate sinusoidally $\beta_L \sin \Omega_s t$ at the left end and $\beta_R \sin \Omega_s t$ at the right. Neglect the small horizontal and rotational movements of the masses.

If the supports moved the specified amounts and the effect of the inertia forces were neglected, this beam would be unbent and assume a straight-line position such as the one shown at any particular time t . The displacement of the mass points to the straight unbent position could easily be computed in terms of the support movement and will be designated as $\beta_1 \sin \Omega_s t$, $\beta_2 \sin \Omega_s t$, and $\beta_3 \sin \Omega_s t$ at mass points 1, 2, and 3, respectively. However, there are accelerations, and hence inertia forces, and as a result, the structure is bent from the straight-line position by the amounts v_{1t}^T , v_{2t}^T , and v_{3t}^T . Thus the total displacements (η_{1t} , η_{2t} , and η_{3t}) from the static-equilibrium position are as follows:

$$\begin{aligned}\eta_{1t} &= v_{1t}^T + \beta_1 \sin \Omega_s t \\ \eta_{2t} &= v_{2t}^T + \beta_2 \sin \Omega_s t \\ \eta_{3t} &= v_{3t}^T + \beta_3 \sin \Omega_s t\end{aligned}\quad (4.54)$$

The bending of the beam from the straight-line position depends on the total accelerations $\ddot{\eta}_{1t}$, $\ddot{\eta}_{2t}$, and $\ddot{\eta}_{3t}$. Using the inertia forces associated with these accelerations, the following equations may be written in the same manner as Eqs. (4.15):

$$\begin{aligned}v_{1t}^T &= -\frac{W_1}{g} \ddot{\eta}_{1t} d_{11} - \frac{W_2}{g} \ddot{\eta}_{2t} d_{12} - \frac{W_3}{g} \ddot{\eta}_{3t} d_{13} \\ v_{2t}^T &= -\frac{W_1}{g} \ddot{\eta}_{1t} d_{21} - \frac{W_2}{g} \ddot{\eta}_{2t} d_{22} - \frac{W_3}{g} \ddot{\eta}_{3t} d_{23} \\ v_{3t}^T &= -\frac{W_1}{g} \ddot{\eta}_{1t} d_{31} - \frac{W_2}{g} \ddot{\eta}_{2t} d_{32} - \frac{W_3}{g} \ddot{\eta}_{3t} d_{33}\end{aligned}\quad (4.55)$$

Substitution for $\ddot{\eta}_{1t}$, $\ddot{\eta}_{2t}$, and $\ddot{\eta}_{3t}$ from Eqs. (4.54) converts Eqs. (4.55) into the following:

$$\begin{aligned}
 v_{1t}^T &= \left(\beta_1 \Omega_s^2 \frac{W_1}{g} \sin \Omega_s t - \frac{W_1}{g} \ddot{v}_{1t}^T \right) d_{11} + \left(\beta_2 \Omega_s^2 \frac{W_2}{g} \sin \Omega_s t - \frac{W_2}{g} \ddot{v}_{2t}^T \right) d_{12} \\
 &\quad + \left(\beta_3 \Omega_s^2 \frac{W_3}{g} \sin \Omega_s t - \frac{W_3}{g} \ddot{v}_{3t}^T \right) d_{13} \\
 v_{2t}^T &= \left(\beta_1 \Omega_s^2 \frac{W_1}{g} \sin \Omega_s t - \frac{W_1}{g} \ddot{v}_{1t}^T \right) d_{21} + \left(\beta_2 \Omega_s^2 \frac{W_2}{g} \sin \Omega_s t - \frac{W_2}{g} \ddot{v}_{2t}^T \right) d_{22} \\
 &\quad + \left(\beta_3 \Omega_s^2 \frac{W_3}{g} \sin \Omega_s t - \frac{W_3}{g} \ddot{v}_{3t}^T \right) d_{23} \\
 v_{3t}^T &= \left(\beta_1 \Omega_s^2 \frac{W_1}{g} \sin \Omega_s t - \frac{W_1}{g} \ddot{v}_{1t}^T \right) d_{31} + \left(\beta_2 \Omega_s^2 \frac{W_2}{g} \sin \Omega_s t - \frac{W_2}{g} \ddot{v}_{2t}^T \right) d_{32} \\
 &\quad + \left(\beta_3 \Omega_s^2 \frac{W_3}{g} \sin \Omega_s t - \frac{W_3}{g} \ddot{v}_{3t}^T \right) d_{33}
 \end{aligned} \tag{4.56}$$

Comparison of Eqs. (4.56) with Eqs. (4.43) shows that the bending displacements v_{1t}^T , v_{2t}^T , and v_{3t}^T produced by the support vibration are identical with those which would be produced by the following dynamic loads acting on a beam with immovable supports:

$$\begin{aligned}
 P_{1t} &= \frac{W_1}{g} \beta_1 \Omega_s^2 \sin \Omega_s t \\
 P_{2t} &= \frac{W_2}{g} \beta_2 \Omega_s^2 \sin \Omega_s t \\
 P_{3t} &= \frac{W_3}{g} \beta_3 \Omega_s^2 \sin \Omega_s t
 \end{aligned} \tag{4.57}$$

These loads are immediately recognized as being the inertia forces which would be produced by the accelerations associated with the straight-line displacements (that is, the rigid-body accelerations).

Note, however, that the beam is at rest initially, which means that η_{it_0} and $\dot{\eta}_{it_0}$ are both zero. According to Eqs. (4.54), this means that initially, when $t = t_0 = 0$, $v_{it_0}^T = 0$, but $\dot{v}_{it_0}^T = -\beta_i \Omega_s$. However, since $v_{it_0}^T = v_{it_0} + v_{it_0}^T$ and $\dot{v}_{it_0}^T = \dot{v}_{it_0} + \dot{v}_{it_0}^T$ and since $v_{it_0} = \dot{v}_{it_0} = 0$, then $v_{it_0}^T = 0$ and $\dot{v}_{it_0}^T = -\beta_i \Omega_s$.

The dynamic bending deflections (v_{it}^T), shears, bending moments, and stresses produced by the support vibration can be computed using Eq. (4.42) and the procedure outlined in Sec. 4.11. The loading producing these effects is given by Eqs. (4.57), which may be expressed for mass point i as

$$P_{it} = P_i \sin \Omega_s t \tag{4.58}$$

where

$$P_i = \frac{W_i}{g} \beta_i \Omega_s^2$$

There is no difficulty in evaluating ψ_m for this case. Applying Eq. (4.34),

$$\psi_m = \frac{\Omega_s^2}{\omega_m^2} \sum_{i=1}^{i=r} \beta_i \frac{W_i}{g} A_{im} \quad (4.59)$$

The dynamic-load factor for the sinusoidally varying load may be obtained from Eq. (3.16):

$$\mathfrak{D}_m(t) = \frac{\sin \Omega_s t - \frac{\Omega_s}{\omega_m} \sin \omega_m t}{1 - \left(\frac{\Omega_s}{\omega_m}\right)^2} \quad (4.60)$$

Now by substituting into Eq. (4.40), we obtain v_{it} , the dynamic deflection caused by the loads P_{it} :

$$v_{it} = \sum_{m=1}^{m=r} \left[A_{im} \frac{\sin \Omega_s t - \frac{\Omega_s}{\omega_m} \sin \omega_m t}{1 - \left(\frac{\Omega_s}{\omega_m}\right)^2} \frac{\Omega_s^2}{\omega_m^2} \sum_{i=1}^{i=r} \beta_i \frac{W_i}{g} A_{im} \right] \quad (4.61)$$

The additional dynamic deflection v_{it}^I caused by the initial motion of the beam may be computed from Eq. (4.41) after the time factor $\mathfrak{D}_m^I(t)$ is computed from Eq. (4.49) to be as follows:

$$\mathfrak{D}_m^I(t) = -\frac{\Omega_s}{\omega_m} \sin \omega_m t \sum_{i=1}^{i=r} \beta_i A_{im} \frac{W_i}{g} \quad (4.62)$$

Then,

$$v_{it}^I = \sum_{m=1}^{m=r} \left[A_{im} \left(-\frac{\omega_m}{\Omega_s} \sin \omega_m t \right) \frac{\Omega_s^2}{\omega_m^2} \sum_{i=1}^{i=r} \beta_i \frac{W_i}{g} A_{im} \right] \quad (4.63)$$

Now, v_{it} and v_{it}^I may be added to obtain v_{it}^T :

$$v_{it}^T = \sum_{m=1}^{m=r} \left[A_{im} \frac{\sin \Omega_s t - \frac{\omega_m}{\Omega_s} \sin \omega_m t}{1 - \left(\frac{\Omega_s}{\omega_m}\right)^2} \frac{\Omega_s^2}{\omega_m^2} \sum_{i=1}^{i=r} \beta_i \frac{W_i}{g} A_{im} \right] \quad (4.64)$$

When this equation is applied to the one-degree system in Sec. 3.8, the results will be identical with the solution therein.

REFERENCES

1. Clough, R. W.: Earthquake Forces in a Tall Building, *Civil Eng.*, January, 1956, pp. 54-55.
2. Kármán, T. von, and M. A. Biot: "Mathematical Methods in Engineering," McGraw-Hill Book Company, Inc., New York, 1940.
3. Bisplinghoff, R. L., H. Ashley, and R. L. Halfman: "Aeroelasticity," Addison-Wesley Publishing Company, Reading, Mass., 1955.

CHAPTER 5

GENERAL THEORY FOR DYNAMIC RESPONSE OF DISTRIBUTED-MASS SYSTEMS

5.1. General. The method developed in Chap. 4 to compute the dynamic response of concentrated-mass systems will be extended in this chapter to structures the mass of which is continuously distributed. The scope of this discussion will be limited as before to structures which are (1) linearly elastic, (2) stable under static loads, and (3) undamped.

The presentation herein will be restricted to beams. The same approach, however, could be applied to struts, cables, membranes, or plates (see Chap. 3, Ref. 1). Such extension involves no new fundamentals but simply appropriate changes in the equations of motion and the details of the solution.

5.2. Differential Equation of Motion for Beams. Consider a beam, the cross-section dimensions of which are small in comparison with the length of the member. Assume that the beam is loaded and vibrates in a plane which contains an axis of symmetry for every cross section of the member. Only the transverse bending deflections will be considered; axial change in length of the member, shear deformations, and so-called "rotary inertia" effects will all be neglected. In other words, a differential element of length of the beam between two adjacent cross sections will be assumed to move only transversely in accordance with the bending deflections of the beam; axial and rotational movement of this element will be neglected.

Let EI be the flexural rigidity of the beam in the plane of vibrations; M and S be the bending moment and shear force, respectively, at any cross section (the positive directions being as shown in Fig. 5.1); v be the displacement of any point on the axis of the beam, taken as positive when upward; and w be the intensity of the load (per foot of length) which is causing deflection of the beam from the static position, also being plus when upward. The following well-known relations from elementary beam theory exist between these quantities:

$$\begin{aligned} \frac{d^2}{dx^2} v &= \frac{M}{EI} & \text{and} & & \frac{d^2}{dx^2} M &= w \\ \frac{d^2}{dx^2} \left(EI \frac{d^2}{dx^2} v \right) &= w \end{aligned} \tag{a}$$

As written, using ordinary derivatives, these equations are, of course, applicable only when the beam is subjected to a static load, and v and w are functions only of x . If, however, a dynamic load of an intensity per foot of length $p(t, x)$ acts on the beam, then the quantities v , M , S , and w are all functions of t as well as x . Then it becomes necessary to replace the ordinary derivatives in Eq. (a) with partial derivatives and to apply D'Alembert's principle and recognize that w , the intensity of load causing deflection of the beam, now is the algebraic sum of the dynamic load

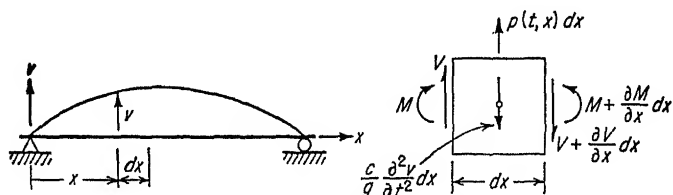


Fig. 5.1. Notation for flexural vibration.

$p(t, x)$ and the inertial load per unit length $(c/g)(\partial^2 v / \partial t^2)$, where c is the weight per foot of length of the beam. If $p(t, x)$ is taken positive when upward, Eq. (a) may be adapted to the dynamic case by substituting for w :

$$w = p(t, x) - \frac{c}{g} \frac{\partial^2}{\partial t^2} v$$

Thus,

$$\frac{\partial^2}{\partial x^2} \left(EI \frac{\partial^2}{\partial x^2} v \right) + \frac{c}{g} \frac{\partial^2}{\partial t^2} v = p(t, x) \quad (5.1)$$

Equation (5.1) is the differential equation of motion governing the transverse vibration of the beam. In any particular problem, the solution of this equation that also satisfies the initial and boundary conditions will define the displacement v at any time t and at any position x along the beam. When v is known, slopes, bending moment, and shear can be computed easily by successive differentiation with respect to x .

Implicit in this derivation is the assumption that all particles of an element of differential length of the beam undergo the same transverse motion. In other words, for the element of a beam between two adjacent cross sections located a differential distance dx from one another, there is no relative transverse motion of any two particles. In effect, the mass of this element is considered to be concentrated along the centroidal axis of this element. As a result of this implicit assumption, we are able to compute only the over-all transverse bending response of the beam. We are not able, therefore, to compute the transverse stress waves which are generated by transverse loads and which sometimes are of major importance. It is these waves, for example, which produce

scabbing on one face when high-intensity compressive forces are applied on the opposite face.

5.3. Determination of Normal Modes of Vibration. Initially this discussion will be confined to the procedure for computing the shapes and frequencies of the normal modes of vibration of beams. Since a normal mode of vibration is a free vibration, no external loads are acting on the beam, and therefore the differential equation of motion in such a case reduces to

$$\frac{\partial^2}{\partial x^2} \left(EI \frac{\partial^2 v}{\partial x^2} \right) + \frac{c}{g} \frac{\partial^2 v}{\partial t^2} = 0 \quad (5.2)$$

Since a normal mode of vibration is one in which all points along the beam vibrate in phase with one another (that is, the shape of the elastic curve remains the same at all times), a normal mode may be represented as

$$v(t, x) = F(t) \varphi(x) \quad (5.3)$$

where the function $\varphi(x)$ defines the *characteristic shape* of a normal mode of vibration. Hence

$$\begin{aligned} \frac{\partial^2 v}{\partial t^2} &= \varphi(x) \frac{d^2}{dt^2} F(t) \\ \text{and} \quad \frac{\partial^2}{\partial x^2} \left(EI \frac{\partial^2 v}{\partial x^2} \right) &= F(t) \frac{d^2}{dx^2} \left[EI \frac{d^2}{dx^2} \varphi(x) \right] \end{aligned}$$

Substitution of these expressions into Eq. (5.2) yields

$$-\frac{(d^2/dt^2)F(t)}{F(t)} = \frac{g}{c} \frac{\frac{d^2}{dx^2} \left[EI \frac{d^2}{dx^2} \varphi(x) \right]}{\varphi(x)} \quad (5.4)$$

In this equation, since the left-hand member is the quotient of two functions of t alone and the right-hand member of two functions of x alone, the two members can be equal for all values of x and t only if both sides are equal to a constant, which for convenience will be taken as ω^2 . The problem, therefore, is reduced to the solution of two ordinary differential equations:

$$\frac{d^2}{dt^2} F(t) + \omega^2 F(t) = 0 \quad (5.5)$$

$$\text{and} \quad \frac{d^2}{dx^2} \left[EI \frac{d^2}{dx^2} \varphi(x) \right] - \omega^2 \frac{c}{g} \varphi(x) = 0 \quad (5.6)$$

First consider the solution of Eq. (5.5), which is

$$F(t) = C_1 \sin \omega t + C_2 \cos \omega t \quad (5.7)$$

and therefore identical with Eq. (3.3). The values of C_1 and C_2 can easily be determined from the initial position of the member at $t = 0$.

Regardless of these values, however, it is apparent that the $F(t)$ represents a periodic function, the circular frequency of which is ω , and that

$$T = \frac{2\pi}{\omega} \quad \text{and} \quad f = \frac{\omega}{2\pi} \quad (5.8)$$

give the corresponding values of the period and frequency.

5.4. Determination of Characteristic Shapes of Normal Modes of Vibration. The characteristic shape $\varphi(x)$ of a normal mode of vibration may be obtained by finding the solution of Eq. (5.6), which also satisfies the boundary conditions of the structure. To illustrate the procedure of finding the characteristic shapes, let us consider only the cases where the beam or certain portions of it are prismatic and have constant E , I , and c over the length of such portions. In such cases, Eq. (5.6) simplifies to the following for such a portion:

$$\frac{d^4}{dx^4} \varphi(x) - a^4 \varphi(x) = 0 \quad (5.9)$$

where, for convenience,

$$a^4 = \frac{\omega^2 c}{EIg} \quad (5.10)$$

The solution of Eq. (5.9) is

$$\varphi(x) = A \sin ax + B \cos ax + C \sinh ax + D \cosh ax \quad (5.11)$$

The arbitrary constants A , B , C , and D of this solution must be selected so as to satisfy the boundary conditions at the end of the portion of the beam under consideration.

If the beam consists of simply one length over which the cross sections are unvaried, and within which there are no intermediate supports or structural connections (such as hinges, etc.), then Eqs. (5.9) to (5.11) are applicable over the entire length and only four arbitrary constants are involved. If, however, the beam cross section is changed or intermediate supports or connections are introduced, a set of these equations must be written for each portion between such interruptions. For each such portion, four arbitrary constants are introduced and four boundary conditions must be written. Thus, for example, a simple end-supported beam, a cantilever beam, or a beam clamped at both ends involves only four constants and four boundary conditions in each instance, assuming the cross section is unchanging over the entire length. In a two-span, continuous beam with constant, though perhaps different, cross sections in each span, four constants for each span, or a total of eight, must be determined simultaneously. The following examples will illustrate this procedure.

a. Simple End-supported Beam. In this case the four boundary conditions are that, at each end, both the deflection and bending moment are

equal to zero at all times. Thus, from Eq. (5.3),

At left end, $x = 0$:

$$(v)_{x=0} = F(t)[\varphi(x)]_{x=0} = 0 \quad \therefore [\varphi(x)]_{x=0} = 0 \quad (a)$$

$$\left(\frac{M}{EI}\right)_{x=0} = \left(\frac{\partial^2 v}{\partial x^2}\right)_{x=0} = F(t) \left[\frac{d^2}{dx^2} \varphi(x)\right]_{x=0} = 0 \quad \therefore \left(\frac{d^2}{dx^2} \varphi(x)\right)_{x=0} = 0 \quad (b)$$

In a similar manner, at right end, $x = L$:

$$[\varphi(x)]_{x=L} = 0 \quad (c)$$

$$\left[\frac{d^2}{dx^2} \varphi(x)\right]_{x=L} = 0 \quad (d)$$

By substituting in Eqs. (a) and (b) from Eq. (5.11), it may be shown that

$B = D = 0$. Substitution into Eqs. (c) and (d) gives

$$A \sin aL + C \sinh aL = 0 \quad (e)$$

$$-Aa^2 \sin aL + Ca^2 \sinh aL = 0 \quad (f)$$

Since $a^2 \neq 0$, it may be canceled out of Eq. (f), and the resulting equation subtracted from Eq. (e) gives

$$A \sin aL = 0 \quad (g)$$

whereas addition of it to Eq. (e) gives

$$C \sinh aL = 0$$

$$\text{Since } \sinh aL \neq 0 \quad \therefore C = 0$$

From Eq. (g), either $A = 0$ or $\sin aL = 0$. If, however, $A = 0$, there is no vibration (since then all four constants would be zero) and therefore A

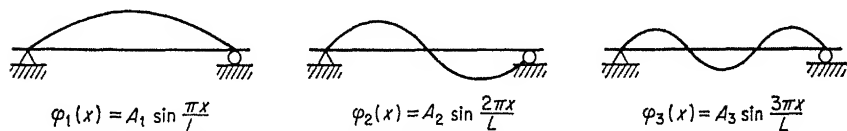


FIG. 5.3. Characteristic shapes of first three normal modes of vibration.

cannot equal zero. Therefore $\sin aL$ must be equal to zero, and this can be satisfied if aL is a multiple of π . Hence,

$$aL = n\pi \quad \text{or} \quad a = \frac{n\pi}{L} \quad (5.12)$$

Since n can be any integer from 1 to ∞ , there are an infinite number of

modes, and the characteristic shape of mode n is

$$\varphi(x) = A_n \sin \frac{n\pi x}{L} \quad (5.13)$$

where the value of A_n is arbitrary. The frequency of mode n may be obtained from Eq. (5.8) by substitution from Eqs. (5.10) and (5.12) to give

$$f_n = \frac{n^2\pi}{2} \sqrt{\frac{EIg}{cL^4}} \quad (5.14)$$

The characteristic shapes of the first three modes are shown in Fig. 5.3.

b. Two-span Continuous Beam. To express a normal mode of vibration for this beam requires separate expressions in each span:

$$v_1 = F(t)\varphi_1(x_1) \quad (a)$$

$$v_2 = F(t)\varphi_2(x_2) \quad (b)$$

where the subscripts 1 and 2 refer to spans 1 and 2. The function $F(t)$

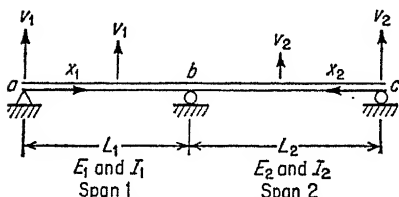


FIG. 5.4. Two-span continuous beam.

is, of course, the same for both spans since the deflections must remain in phase at all points in a normal mode. Whereas ω is the same for both spans, E , I , and c , being different, require a separate a for each, though a_1 and a_2 involve only one ω and are therefore related. Hence, applying Eq. (5.11),

these eight arbitrary constants A , B , etc., must be selected so as to satisfy the boundary conditions.

At a : Since both deflection and bending moment are zero, two equations may be set up as in the previous example, leading to the conclusion that $B_1 = D_1 = 0$.

At c : In the same way as at a , $B_2 = D_2 = 0$.

At b : Four boundary conditions are available here, namely:

1. Deflection is zero at right end of span 1:

$$[\varphi_1(x_1)]_{x_1=L_1} = 0$$

2. Deflection is zero at left end of span 2:

$$[\varphi_2(x_2)]_{x_2=L_2} = 0$$

3. Elastic curve is continuous over support so that slopes are identical here for both spans:

$$\left[\frac{d}{dx_1} \varphi_1(x_1) \right]_{x_1=L_1} = - \left[\frac{d}{dx_2} \varphi_2(x_2) \right]_{x_2=L_2}$$

4. Likewise, bending moments (and therefore curvature) are identical here for both spans:

$$\left[\frac{d^2}{dx_1^2} \varphi_1(x_1) \right]_{x_1=L_1} = \left[\frac{d^2}{dx_2^2} \varphi_2(x_2) \right]_{x_2=L_2}$$

Substitution of Eqs. (a) and (b) into these four conditions gives the following, arranged in order of conditions 1, 3, 4, and 2:

$$\begin{aligned} A_1 \sin a_1 L_1 + C_1 \sinh a_1 L_1 &= 0 \\ A_1 a_1 \cos a_1 L_1 + C_1 a_1 \cosh a_1 L_1 + A_2 a_2 \cos a_2 L_2 + C_2 a_2 \cosh a_2 L_2 &= 0 \\ -A_1 a_1^2 \sin a_1 L_1 + C_1 a_1^2 \sinh a_1 L_1 + A_2 a_2^2 \sin a_2 L_2 - C_2 a_2^2 \sinh a_2 L_2 &= 0 \\ A_2 \sin a_2 L_2 + C_2 \sinh a_2 L_2 &= 0 \end{aligned} \quad (c)$$

Since the right-hand side of these equations is zero, the numerator determinant will be zero. Therefore, for the unknown constants to have values different from zero (and therefore involve vibration), it is necessary that the denominator determinant also be equal to zero. This solution will not be carried out in detail (see Chap. 3, Ref. 1, for such a solution), but setting this determinant equal to zero gives an equation called the frequency equation. There are an infinite number of roots ω satisfying this equation and defining the infinite number of normal modes for this beam. Substitution of each ω in turn back into Eqs. (c) enables one to obtain the relative values of A_1 , C_1 , A_2 , and C_2 , although the absolute values are still arbitrary. Each set of these constants defines the characteristic shape of the normal mode having the frequency associated with that set.

5.5. Important Properties of Characteristic-shape Functions. The functions $\varphi_m(x)$ which define the characteristic shapes of the normal modes of vibration of a distributed-mass structure have several important properties which make them particularly useful in analyzing the response of such structures under dynamic loading. These properties may be developed by considering Eq. (5.6), which determines the form of the characteristic shapes $\varphi_m(x)$. The characteristic shapes $\varphi_m(x)$ and $\varphi_n(x)$ and the natural frequencies ω_m and ω_n , of any two particular normal modes m and n , must satisfy Eq. (5.6), or

$$\frac{d^2}{dx^2} \left[EI \frac{d^2}{dx^2} \varphi_m(x) \right] = \omega_m^2 \frac{c}{g} \varphi_m(x) \quad (a)$$

$$\frac{d^2}{dx^2} \left[EI \frac{d^2}{dx^2} \varphi_n(x) \right] = \omega_n^2 \frac{c}{g} \varphi_n(x) \quad (b)$$

A comparison of Eq. (a) with the well-known relationship stated in Eq. (a) in Sec. 5.2 shows that $\omega_m^2(c/g)\varphi_m(x)$ is the intensity of the load

which, when applied statically, would deflect a beam into the characteristic shape $\varphi_m(x)$. Stated another way, the *characteristic shape* is a deflection curve that is produced by a static load, the intensity of which at any point is directly proportional to the deflection at that point—the proportionality factor being such that the load intensity is $\omega_m^2(c/g)\varphi_m(x)$. Such a static load which produces a deflection curve having a characteristic shape is called a *characteristic loading*.

Proceeding now in the same manner as in Sec. 4.5, suppose a beam loaded by the characteristic loading corresponding to the m th mode were subjected to a virtual displacement corresponding to the characteristic shape of the n th mode. Then, suppose that the same beam loaded by the characterized loading corresponding to the n th mode were subjected to a virtual displacement corresponding to the characteristic shape of the m th mode. By Betti's law, the virtual work done by the m th characteristic loading in the first case is equal to the virtual work done by the n th characteristic loading in the second case, or, where the integration extends over the length of the entire structure,

$$\int_0^L \left[\omega_m^2 \frac{c}{g} \varphi_m(x) \right] \varphi_n(x) dx = \int_0^L \left[\omega_n^2 \frac{c}{g} \varphi_n(x) \right] \varphi_m(x) dx$$

or

$$(\omega_m^2 - \omega_n^2) \int_0^L \varphi_m(x) \varphi_n(x) \frac{c}{g} dx = 0 \quad (5.15)$$

If ω_m does not equal ω_n , the integral must equal zero in order to satisfy this equation. Hence, the following relationship must exist between two different characteristic shapes, which have two different frequencies:

$$\int_0^L \varphi_m(x) \varphi_n(x) \frac{c}{g} dx = 0 \quad (5.16)$$

This is the *orthogonality condition* between two different characteristic shapes.

However, if in Eq. (5.15), $m = n$, then the value of the integral is arbitrary. It would be permissible to select absolute size of $\varphi_m(x)$ so that the value of the integral was equal to unity. Selection of the size of $\varphi_m(x)$ in this manner is called *normalizing* the shape functions. Denoting the characteristic shapes after normalization by $\Phi_m(x)$, these normalized characteristic shapes have the following properties:

$$\int_0^L \Phi_m(x) \Phi_n(x) \frac{c}{g} dx = \begin{cases} 1 & \text{if } m = n \\ 0 & \text{if } m \neq n \end{cases} \quad (5.17)$$

Note that the integration extends over the entire length of the structure.

The characteristic loading associated with the normalized characteristic shape will be called the *normalized characteristic loading*, and its intensity

will be designated as $\mathfrak{L}_m(x)$, where

$$\mathfrak{L}_m(x) = \omega_m^2 \frac{c}{g} \Phi_m(x) \quad (5.18)$$

5.6. Use of Characteristic-shape Functions to Represent Deflection and Load Functions. The function $v(t, x)$, which defines the displacement of any point on a beam which was initially at rest when subjected to a dynamic loading, must satisfy the same boundary conditions at the supports of the beam as the normalized-characteristic-shape functions $\Phi_m(x)$. Therefore, if $v(t, x)$ were represented by an infinite series of terms involving an infinite number of normalized characteristic shapes $\Phi_m(x)$, the boundary conditions would automatically be satisfied and the following equation [similar to Eq. (4.40)] might be written for the dynamic deflection produced by a given dynamic loading:

$$v(t, x) = \sum_{m=1}^{m=\infty} \mathfrak{D}_m(t) \psi_m \Phi_m(x) \quad (5.19)$$

In a similar manner, the function $p(t, x)$, which defines the intensity of the dynamic loading per foot on the beam, may usually be expanded in a similar manner by an infinite series involving the normalized characteristic loadings of the normalized characteristic shapes. The given loading, however, does not have to satisfy the boundary conditions for the structure, and as a result, it sometimes is not possible to represent it in terms of the characteristic shapes. Usually, in most practical cases, it is possible to do so with sufficient accuracy, however.

Consider a dynamic loading of the type used in Sec. 4.8 and represented by Eq. (4.38), that is, a loading having the characteristic that it varies with time in the same manner at every point where it is applied (in other words, the dynamic loading is in phase with itself all over the structure). The intensity of such a loading would be represented as

$$p(t, x) = f(t)p(x)P \quad (5.20)$$

where P = *maximum instantaneous value attained by dynamic load over entire structure*

$f(t)$ = *time variation of load*

$p(x)$ = *manner in which load is distributed over structure*

Denote the intensity of load per foot of beam caused by P as $[p(t, x)]_{\max}$; then

$$[p(t, x)]_{\max} = Pp(x) \quad (5.21)$$

By proceeding in the same manner as in Sec. 4.7, $[p(t, x)]_{\max}$ could be built up or replaced by adding up proper amounts of the normalized char-

acteristic loadings, these proper amounts being called the *static-mode loadings*, denoted by $\mathcal{P}_m(x)$, where

$$\mathcal{P}_m(x) = \psi_m \mathcal{L}_m(x) \quad (5.22)$$

Thus,
$$[p(t, x)]_{\max} = Pp(x) = \sum_{m=1}^{m=\infty} \psi_m \mathcal{L}_m(x) \quad (5.23)$$

Substitution for $\mathcal{L}_m(x)$ from Eq. (5.18) gives

$$Pp(x) = \sum_{m=1}^{m=\infty} \psi_m \omega_m^2 \frac{c}{g} \Phi_m(x)$$

Multiply both sides of this equation by $\Phi_b(x)$, the normalized characteristic shape of mode b , and then integrate both sides of the equation over the entire length of the structure. Thus,

$$\int_0^L Pp(x) \Phi_b(x) dx = \sum_{m=1}^{m=\infty} \left[\psi_m \omega_m^2 \int_0^L \Phi_m(x) \Phi_b(x) \frac{c}{g} dx \right]$$

In view of Eqs. (5.17), the integral in the terms of the summation is equal to zero if $m \neq b$ and to unity if $m = b$. Thus the summation reduces simply to the b th term, and therefore

$$\psi_b = \frac{\int_0^L Pp(x) \Phi_b(x) dx}{\omega_b^2}$$

However, this same proof could be applied using any mode m instead of the mode b . Therefore, in general, the *participation factor* ψ_m for the m th mode is

$$\psi_m = \frac{\int_0^L Pp(x) \Phi_m(x) dx}{\omega_m^2} \quad (5.24)$$

This is the factor (or portion of the normalized characteristic loading) required to give the static-mode loading defined by Eq. (5.22).

The given dynamic loading of Eq. (5.20) could now be expressed as follows:

$$p(t, x) = f(t)[Pp(x)] = f(t) \sum_{m=1}^{m=\infty} \psi_m \mathcal{L}_m(x) = f(t) \sum_{m=1}^{m=\infty} \mathcal{P}_m(x) \quad (5.25)$$

an expression which is similar to Eq. (4.39). Thus, the given loading has been broken down into modal contributions, the maximum values of each being the static-mode loadings, with these contributions varying with time as defined by $f(t)$.

5.7. Reduction and Solution of Equation of Motion for Dynamic Response of Structure Which Was Initially at Rest. The response of a beam, which is initially at rest, to a dynamic loading may be computed by finding the solution to the differential equation of motion (5.1), which also satisfies the initial and boundary conditions of the problem. The solution may be facilitated by expressing the displacement and load functions $v(t, x)$ and $p(t, x)$, respectively, by infinite series involving the normalized-characteristic-shape functions $\Phi_m(x)$. The displacement boundary conditions will be satisfied exactly by such functions, and the load can usually be represented adequately. The problem is therefore reduced to satisfying the equation of motion and the initial conditions.

Suppose that the dynamic load $p(t, x)$ is broken down into the modal contributions and represented by the superposition of the static-mode loads as in Eq. (5.25). Let us assume that the dynamic response can be represented by Eq. (5.19) and then investigate whether or not such a solution will satisfy the equation of motion and the initial conditions. Substitution from Eqs. (5.19) and (5.25) into Eq. (5.1) gives

$$\begin{aligned} \frac{\partial^2}{\partial x^2} \left[EI \sum_{m=1}^{m=\infty} \mathfrak{D}_m(t) \psi_m \frac{d^2}{dx^2} \Phi_m(x) \right] + \frac{c}{g} \sum_{m=1}^{m=\infty} \psi_m \Phi_m(x) \frac{d^2}{dt^2} \mathfrak{D}_m(t) \\ = \sum_{m=1}^{m=\infty} f(t) \psi_m \mathfrak{L}_m(x) \end{aligned}$$

Now by substituting into this equation for $\mathfrak{L}_m(x)$ from Eq. (5.18), and also from the following equation,

$$\frac{d^2}{dx^2} \left[EI \frac{d^2}{dx^2} \Phi_m(x) \right] = \omega_m^2 \frac{c}{g} \Phi_m(x)$$

the following equation is obtained:

$$\sum_{m=1}^{m=\infty} \left\{ \left[\frac{d^2}{dt^2} \mathfrak{D}_m(t) + \omega_m^2 \mathfrak{D}_m(t) - \omega_m^2 f(t) \right] \frac{c}{g} \Phi_m(x) \psi_m \right\} = 0$$

Multiply this equation by $\Phi_b(x)$, the normalized shape function for mode b , and then integrate the resulting equation over the entire length of the structure:

$$\sum_{m=1}^{m=\infty} \left\{ \psi_m \left[\frac{d^2}{dt^2} \mathfrak{D}_m(t) + \omega_m^2 \mathfrak{D}_m(t) - \omega_m^2 f(t) \right] \int_0^L \Phi_m(x) \Phi_b(x) \frac{c}{g} dx \right\} = 0$$

However, this integral is equal to zero for all terms except the one when $m = b$, and for this b th term it equals unity. For this one remaining term, ψ_b is not necessarily zero; therefore the terms in brackets must add up to zero; thus,

$$\frac{d^2}{dt^2} \mathfrak{D}_b(t) + \omega_b^2 \mathfrak{D}_b(t) - \omega_b^2 f(t) = 0$$

However, this same operation could be performed for any term and therefore for any mode m :

$$\frac{d^2}{dt^2} \mathfrak{D}_m(t) + \omega_m^2 \mathfrak{D}_m(t) = \omega_m^2 f(t) \quad (5.26)$$

This equation, of course, is identical with Eq. (4.46) and is called the reduced equation of motion for the beam. The solution of Eq. (5.26) is identical with Eq. (4.53).

5.8. Dynamic Response Associated with Initial Motion of Structure. If the structure has a known initial displacement and velocity, the subsequent dynamic displacement $v^I(t, x)$ may be evaluated in the same manner as was used in Sec. 4.9 for the concentrated-mass system. Hence, for the distributed-mass system,

$$v^I(t, x) = \sum_{m=1}^{m=\infty} \mathfrak{D}_m^I(t) \Phi_m(x) \quad (5.27)$$

where, in a similar manner, the time factor $\mathfrak{D}_m^I(t)$ will be found to be the same as Eq. (4.49), or

$$\mathfrak{D}_m^I(t) = \mathfrak{D}_m^I(t_0) \cos \omega_m(t - t_0) + \frac{\dot{\mathfrak{D}}_m^I(t_0)}{\omega_m} \sin \omega_m(t - t_0) \quad (5.28)$$

In this case, new expressions must be developed in order to find the values of $\mathfrak{D}_m^I(t_0)$ and $\dot{\mathfrak{D}}_m^I(t_0)$ so as to satisfy the initial condition of the motion.

Suppose that at time $t = t_0$ the displacement and velocity of every point on the beam are known and given by the functions $r(x)$ and $s(x)$, respectively. However, from Eq. (5.27),

$$[v^I(t, x)]_{t=t_0} = \sum_{m=1}^{m=\infty} \mathfrak{D}_m^I(t_0) \Phi_m(x) = r(x) \quad (5.29)$$

$$\left[\frac{\partial}{\partial t} v^I(t, x) \right]_{t=t_0} = \sum_{m=1}^{m=\infty} \dot{\mathfrak{D}}_m^I(t_0) \Phi_m(x) = s(x) \quad (5.30)$$

Considering Eq. (5.29), multiply both sides by $(c/g)\Phi_b(x)$ and then integrate over the entire length of the structure. In the same way as in the above derivation of Eq. (5.26), this process makes all but one term of the

series disappear and ultimately leads to the following expression:

$$\mathfrak{D}_m^I(t_0) = \int_0^L r(x)\Phi_m(x) \frac{c}{g} dx \quad (5.31)$$

In the same manner, the following may be obtained from Eq. (5.30):

$$\dot{\mathfrak{D}}_m^I(t_0) = \int_0^L s(x)\Phi_m(x) \frac{c}{g} dx \quad (5.32)$$

Thus, these last two equations give the values of $\mathfrak{D}_m^I(t_0)$ and $\dot{\mathfrak{D}}_m^I(t_0)$, which satisfy the initial conditions of the problem.

5.9. Recapitulation—Computation of Dynamic Response of Distributed-mass Systems. The above development demonstrates that the theory developed in Chap. 4 to compute the response of concentrated-mass systems may be extended in its entirety to include distributed-mass systems. Naturally, the detailed working equations and procedures are different, but the fundamental ideas are identically the same.

The recapitulation and computational procedure outlined in Sec. 4.11 for the concentrated-mass system likewise pertains to the distributed-mass system, if the appropriate changes are made in the working equations, and need not be repeated here.

CHAPTER 6

MISCELLANEOUS CONSIDERATIONS REGARDING DYNAMIC-RESPONSE THEORY

6.1. General. In Chaps. 3, 4, and 5, the scope of theory has been limited to linearly elastic systems. Except for a very limited discussion in Sec. 3.5, the effect of damping on dynamic response has been neglected. In the consideration of multi-degree-of-freedom systems, only impulsive loads which varied with time in the same manner at all loaded points of the structure have been considered. No consideration whatever has been given to impact loadings.

In this chapter, all these restrictions will be discussed briefly and methods of extending the previous theory to include some of these effects will be outlined. Whereas the previous theory may be extended to include elasto-plastic and/or damped behavior under more general impulsive loadings, it will be apparent from the following discussion that calculations in accordance with this approach are very laborious and impractical. In such cases, therefore, it is often desirable and sometimes imperative to solve the equations of motion by step-by-step numerical-integration procedures which are designed to take advantage of modern computational techniques and machines. In Chaps. 8 and 9 some of these techniques and machines will be discussed.

6.2. Extension of Theory to Include General Impulsive Loads. In Chap. 4 up to Sec. 4.8, the discussion was not limited to any particular type of impulsive loading. However, in the subsequent development it was assumed that all the applied dynamic loads varied with time in the same manner. In Fig. 4.12 any or all of the loads P_{1t} , P_{2t} , and P_{3t} could be applied to the structure provided they were applied simultaneously and then varied with time in identical manner. Of course, any type of variation could be considered by the theory developed in Sec. 4.8, although the evaluation of the corresponding dynamic-load factors might be difficult and the resulting expression awkward to use.

For example, suppose that each of the loads P_{1t} , P_{2t} , and P_{3t} is applied at different times t_a , t_b , and t_c , respectively, and that each varies with time in a different manner. In addition, suppose that the structure already has some initial motion at the starting time t_0 . In such a case the total

response would be the superposition of four separate contributions. The contribution of the initial motion could be computed easily using Eq. (4.41). The separate contribution of each of the three loads could be computed by applying Eq. (4.40), separately for each load. Of course, the computation of the separate response for a particular load involves computing the participation factor, the static-mode load, and the dynamic-load factor pertaining to that load. Whereas this approach is simple enough, the detailed computations involved become tremendous.

In some cases, it might be preferable to use Eq. (4.42a) instead of proceeding as outlined in the previous paragraph. Of course, for times between t_0 and t_a , only the response due to the initial motion would be involved, and this would be computed by Eq. (4.41). Using the alternative approach between t_a and t_b would involve multiplying A_{im} by the sum of $\mathfrak{D}_m^I(t)$ for the initial motion and $\psi_m \mathfrak{D}_m(t)$ for the load P_{1i} to get the contribution of each mode. As each new load comes into action, however, the composite multiplying factor must include terms for all contributions. For example, for times t_c or greater, the multiplying factor will be the sum of $\mathfrak{D}_m^I(t)$: $\psi_m \mathfrak{D}_m(t)$ for load P_{1i} , $\psi_m \mathfrak{D}_m(t)$ for load P_{2i} , and $\psi_m \mathfrak{D}_m(t)$ for load P_{3i} .

Whereas the response theory which has been developed can be extended to handle the most general impulsive loading, the computations involved may be staggering. Anyone who had embarked on such computations would become very much interested in digital or analog computers and their potential application to such computations. Fortunately, even though the type of loading considered in Chaps. 4 and 5 is restricted, it does include a large number of practical engineering situations.

6.3. Extension of Theory to Include Nonlinear Elastic and Elasto-plastic Structural Stiffness. In Chap. 4, the theory was restricted to linearly elastic systems. This limitation was imposed at the start of the development when Eqs. (4.15) were written. For all practical purposes, it is *impossible* to extend this approach to include *nonlinearly elastic systems*. One possible approach would be to approximate a curved elastic stress-strain relation by a series of straight lines. However, the difficulties of evaluating the response of a system involving such properties would pyramid rapidly.

While the computations become cumbersome, it is possible to extend the response theory in Chap. 4 to evaluate the response of beam and frame structures having elasto-plastic stiffness characteristic involving an idealized moment-curvature relation such as represented in Fig. 1.6. Numerous investigators have studied such extensions (for example, see Refs. 1, 2). Through the elastic response, the method in Chap. 4 is applicable, of course. When the first plastic hinge is formed, however, the stiffness of the structure changes, and it is necessary to compute a

new set of normal modes for these revised stiffness factors. Using this new set, the response computations are continued as described in Chap. 4, also, of course, picking up the displacements and velocities where the response of the first set of modes left off. Subsequently, as each new hinge forms, a corresponding new set of modes must be computed. Obviously *this procedure, while possible, is impractical except for simple cases*. Recently Bleich [3] has suggested an approach which may have some merit, but no application to typical practical cases has been reported to date.

6.4. Effect and Importance of Structural Damping in Response Computations. Previously, in Sec. 3.5, brief consideration was given to the response of a damped one-degree system to a sinusoidal load. In this case, viscous damping was assumed, that is, damping in which the damping force was proportional to the velocity of the mass. The damping which is involved in structural response is partially due to external frictional effects in the supports, connections, etc., and partially due to internal frictional effects within the molecular framework of the material. No one has been able to show conclusively just what type of damping is most representative of structural damping [4-7].

Actually, in many practical problems, damping has relatively small effect on the total response involved in design, so it is not necessary to evaluate damping effects accurately. The usual procedure is to solve for the frequencies and characteristic shapes of the normal modes of vibration *neglecting damping*. The characteristic loads, participation factors, and static-mode loads are then computed as suggested in Chap. 4. The effect of damping is then approximated by altering Eq. (4.46), the reduced equation of motion [that is, the differential equation which governs the dynamic-load factor $\mathfrak{D}_m(t)$] in the following manner:

$$\ddot{\mathfrak{D}}_m(t) + 2\beta\dot{\mathfrak{D}}_m(t) + \omega_m^2\mathfrak{D}_m(t) = \omega_m^2f(t) \quad (6.1)$$

in which β is defined by Eq. (3.18). For various time variations $f(t)$ of the impulsive loading, Eq. (6.1) may be solved for $\mathfrak{D}_m(t)$ to obtain dynamic-load factors which are approximately corrected for the effect of damping. The modified dynamic-load factors are then used when superimposing the dynamic contributions of the various modes.

In some cases, the design is controlled by maximum response. If the design loading involves transient loadings (such as typical short pulse loadings similar to cases *c* and *d* in Sec. 3.7), maximum response occurs in the early stages before damping has had much effect, and therefore it can be neglected. On the other hand, if the design is controlled by fatigue conditions occurring under steady-state loadings, the maximum response during steady-state conditions may be significantly effected by damping, and the procedure outlined in the previous paragraph should be applied to

approximate this reduction. Not only should damping be considered in such steady-state cases produced by periodic loadings, but it may also be significant in response produced by relatively long nonperiodic loadings as, for example, those involved in earthquake response (Chap. 4, Ref. 1).

6.5. Dynamic Response Produced by Impact. Evaluation of dynamic response produced by the impact of a mass on a structure is the most difficult problem encountered in the field of structural dynamics. This is particularly true if one attempts to include the effect of both the directly transmitted shock waves as well as the over-all structural response. Limited solutions including over-all structural response to various approximations of the interacting force between the striking mass and the struck structure are classic problems found in numerous places in the literature (for example, Ref. 8).

Unfortunately, one of the most important practical design situations is the design of protective construction to resist harmful penetration by missile fragments. Such problems are encountered in both industrial construction and military construction. Very few theoretical or experimental fundamental investigations which are useful for practical design situations have been conducted. There is considerable empirical information on military missiles, but this is difficult to use for interpolation or extrapolation in the absence of relevant fundamental theory.

Much can be learned, however, about some important aspects of the problem by studying the simple idealized cases of elastic and of plastic impact of two rigid bodies. Consider first the case of *elastic impact*. For conservation of momentum,

$$\begin{aligned} \frac{W_1}{g} V_1 + \frac{W_2}{g} V_2 &= \frac{W_1}{g} V'_1 + \frac{W_2}{g} V'_2 \\ \therefore V_1 - V'_1 &= -\frac{W_2}{W_1} (V_2 - V'_2) \end{aligned} \quad (a)$$

For conservation of energy, assuming elastic impact and an infinite modulus of elasticity,

$$\begin{aligned} \frac{W_1 V_1^2}{2g} + \frac{W_2 V_2^2}{2g} &= \frac{W_1 (V'_1)^2}{2g} + \frac{W_2 (V'_2)^2}{2g} \\ \therefore V_1^2 - V'^2_1 &= -\frac{W_2}{W_1} (V_2^2 - V'^2_2) \end{aligned} \quad (b)$$

Dividing Eq. (b) by Eq. (a),

$$V_1 - V_2 = - (V'_1 - V'_2) \quad (c)$$

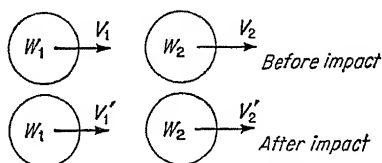


FIG. 6.1. Elastic impact.

Solving for V'_1 and V'_2 from Eqs. (a) and (c),

$$\begin{aligned} V'_1 &= \frac{2V_2W_2 + V_1(W_1 - W_2)}{W_1 + W_2} \\ V'_2 &= \frac{2V_1W_1 - V_2(W_1 - W_2)}{W_1 + W_2} \end{aligned} \quad (6.2)$$

In the special case where mass 2 is at rest, $V_2 = 0$ and

$$\begin{aligned} \frac{V'_1}{V_1} &= \frac{W_1/W_2 - 1}{W_1/W_2 + 1} \\ \frac{V'_2}{V_1} &= \frac{2(W_1/W_2)}{W_1/W_2 + 1} \end{aligned} \quad (6.3)$$

and

In a similar manner consider next the case of plastic impact of two rigid bodies, wherein, upon impact, the two bodies fuse together and move along as one combined mass (Fig. 6.2).

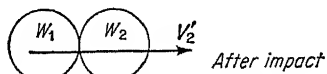
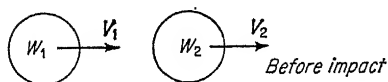


FIG. 6.2. Plastic impact.

By conservation of momentum,

$$\begin{aligned} \frac{W_1V_1}{g} + \frac{W_2V_2}{g} &= \frac{W_1 + W_2}{g} V'_2 \\ \text{If } V_2 = 0, \\ \frac{V'_2}{V_1} &= \frac{W_1/W_2}{W_1/W_2 + 1} \end{aligned} \quad (6.4)$$

This implies a loss of energy during impact:

$$\begin{aligned} \text{Loss} &= \left(\frac{W_1V_1^2}{2g} + \frac{W_2V_2^2}{2g} \right) - \left(\frac{W_1 + W_2}{2g} \right) (V'_2)^2 \\ &= \frac{W_1W_2}{(W_1 + W_2)2g} (V_1 - V_2)^2 \end{aligned} \quad (6.5)$$

Or if $V_2 = 0$,

$$\text{Loss} = \frac{W_1W_2}{(W_1 + W_2)2g} V_1^2 \quad (6.6)$$

If we now think of W_2 (the struck mass) as being the effective mass of the structure which is absorbing the impact, the energy \mathfrak{W}_E which must be absorbed by strain energy during the response of the structure will be as follows:

For plastic impact

$$\mathfrak{W}_E = \frac{W_1 + W_2}{2g} (V'_2)^2$$

Portion of kinetic energy absorbed by response of structure

$$= \frac{\mathfrak{W}_E}{W_1V_1^2/2g} = \left(1 + \frac{W_2}{W_1} \right) \left(\frac{V'_2}{V_1} \right)^2 \quad (6.7)$$

For elastic impact,

$$\mathfrak{W}_E = \frac{W_2}{2g} (V_2')^2$$

Portion of kinetic energy absorbed by response of structure

$$= \frac{\mathfrak{W}_E}{W_1 V_1^2 / 2g} = \frac{W_2}{W_1} \left(\frac{V_2'}{V_1} \right)^2 \quad (6.8)$$

In Fig. 6.3, V_2'/V_1 , V_1'/V_1 , and the *energy-absorbed ratio* [that is, $\mathfrak{W}_E / (W_1 V_1^2 / 2g)$] have been plotted against the *mass ratio* (that is, W_1/W_2)

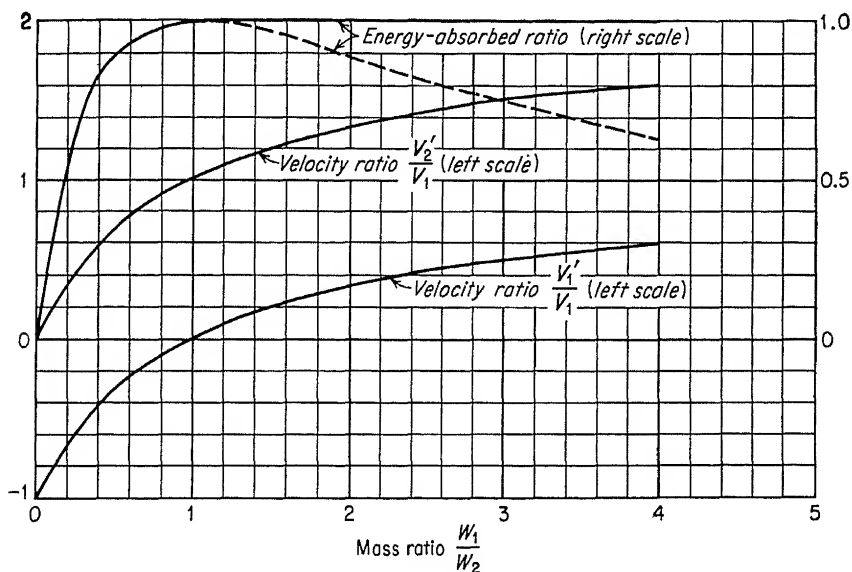


FIG. 6.3. Energy-absorbed ratio and velocity ratios vs. mass ratio, elastic impact; $v_2 = 0$.

for the case of elastic impact with the struck mass stationary. In Fig. 6.4, similar plots are shown for plastic impact also with the struck mass stationary.

In the case of elastic impact for mass ratios greater than unity, note that the struck mass has a higher velocity than the striking mass after impact. Thinking of the struck mass as representing the effective mass of the structure, note that the resistance of the structure would gradually slow it down so that the striking mass could overtake it and hit it again. In this way, through a series of impacts, the structure would eventually stop the striking mass and therefore eventually absorb as strain energy all the initial kinetic energy of the striking mass (if all the impacts were elastic). The solid horizontal line in Fig. 6.3 for mass ratio greater than

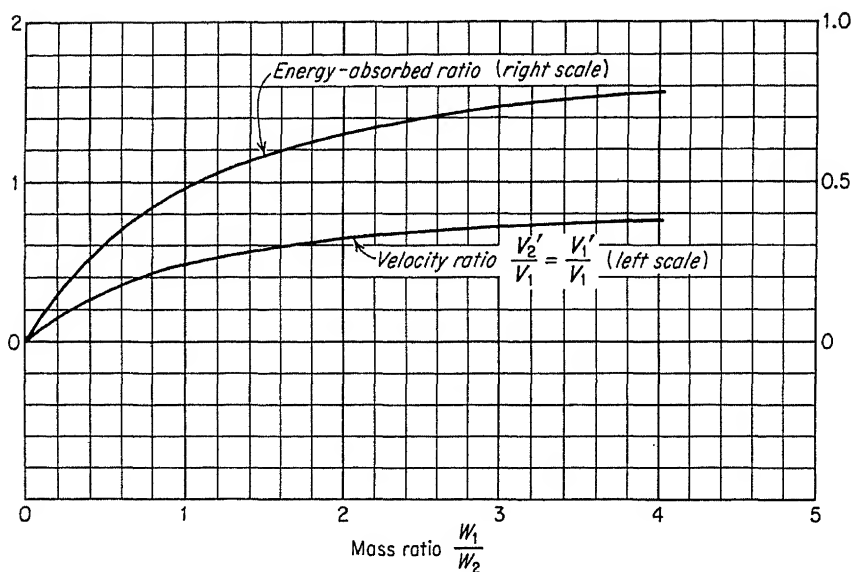


FIG. 6.4. Energy-absorbed ratio and velocity ratio vs. mass ratio, plastic impact; $v_2 = 0$.

1 represents the energy absorbed through multiple impacts; the dashed line, the energy absorbed in the initial impact.

Comparison of the curves for elastic and plastic impact leads to the following conclusions:

1. When the striking mass is large compared with the struck mass, whether the impact is elastic or plastic, the energy absorbed by the structure is essentially the same.

2. When the striking mass is small compared with the struck mass, the energy absorbed by the structural response is considerably less if the impact is plastic rather than elastic. This is due primarily to the energy loss during impact.

3. To minimize the energy absorbed by the structural response, the struck mass should be as large as practical to cut down the response of the structure.

REFERENCES

1. Cohen, E., L. S. Levy, and L. E. Smollen: Impulsive Motion of Shear Buildings Including Plasticity and Viscous Damping, *Proc. ASCE*, separate no. 676, April, 1955.
2. Bleich, H. H., and M. G. Salvadori: Impulsive Motion of Elastoplastic Beams, *Trans. ASCE*, vol. 120, p. 499.
3. Bleich, H. H.: Response of Elastoplastic Structures to Transient Loads, *Trans. N.Y. Acad. Sci.*, ser. 2, vol. 18, no. 2, pp. 135-143, December, 1955.

4. Kimball, A. L.: Vibration Problems. Part V: Friction and Internal Damping, *J. Appl. Mechanics*, vol. 8, p. 135, 1941.
5. Adamson, B.: "A Method for Measuring Damping and Frequencies of High Modes of Vibration of Beams," Publications International Association for Bridge and Structural Engineering, vol. 15, 1955.
6. Mindlin, R. D., F. W. Stubner, and H. L. Cooper: Response of Damped Elastic Systems to Transient Disturbances, *Proc. Soc. Exptl. Stress Anal.*, vol. 5, pt. 2, p. 69, 1948.
7. Schenker, L.: The Dynamic Response of Tall Structures to Lateral Loads, *Proc. ASCE*, separate no. 944, April, 1956.
8. Salvadori, M. G.: Part II: A Mathematical Treatment of the Generalized Hertz Impact of a Mass on a Simply Supported Beam, Welding Research Supplement, *J. Am. Welding Soc.*, July, 1947, p. 4093.

SIMPLIFIED ANALYSIS AND DESIGN FOR DYNAMIC LOAD

7.1. Introduction. An exact or rigorous solution for the response of a mechanical system to dynamic loads is a practical possibility only when the system consists of a simple arrangement of masses and springs and when the load-time variation is a convenient mathematical function. Actual structures and loadings often do not satisfy these conditions. For this reason, it is necessary in many problems of structural dynamics to idealize both the structure and the loading. The theoretical procedures given in Chaps. 3 to 6 then become possible without unreasonable mathematical complexity. This chapter deals with the methods by which this can be accomplished.

As an example of the difficulties involved let us consider one of the simplest of structures—a simply supported beam. Because of the distributed mass the beam has an infinite number of degrees of freedom. Obviously, the structure must be idealized by considering only a few of these degrees. Fortunately, the idealization can be quite extreme in many cases without causing large errors in the solution. Frequently only the first mode need be considered, and the system can be represented by a single concentrated mass supported by a single spring. The solution then becomes relatively simple.

When idealizing dynamic loads on structures two simplifications are generally required. The first involves the geometric distribution of the load over the structure. If for purposes of analysis the mass of the system is concentrated at certain points, the loads must be applied at the same points. This requires modification of the magnitude of the loads. The second simplification involves the load-time variation. If a numerical method of analysis is used, it is not necessary to idealize this function because any variation can be handled. However, if a direct solution is desired, the load-time curve must be taken as a simple mathematical expression which may only approximate the actual loading.

7.2. Idealized Systems. Figure 7.1 shows three simple structures together with the corresponding idealized or equivalent dynamic systems which might be used for analysis. In each case the structure is repre-

sented by an arrangement of concentrated masses supported or connected by springs. The equivalent systems have a limited number of degrees of freedom and hence can be analyzed with relative ease. The degrees of freedom must correspond to the important modes of the real structure.

The analyst is usually interested in the deflection of the structure, and it is therefore desirable to select the equivalent system such that the

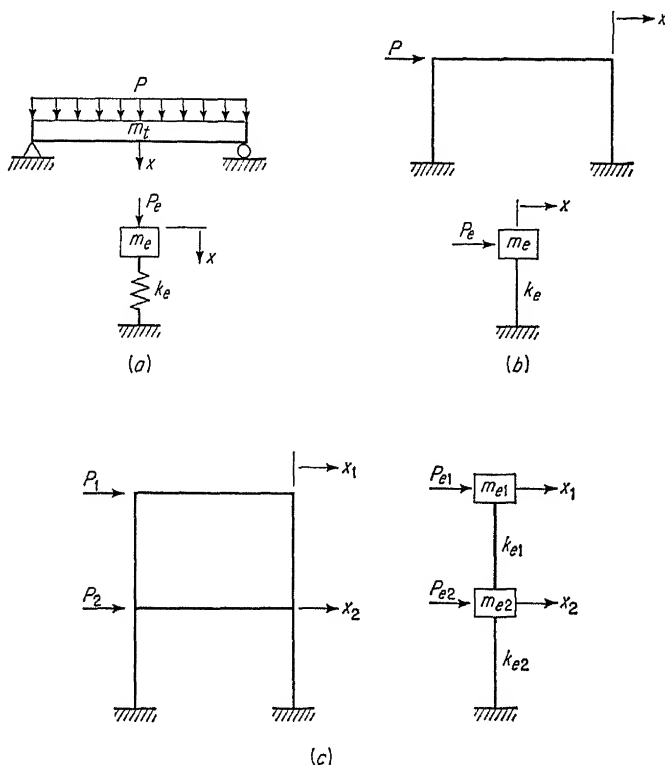


FIG. 7.1. Idealized systems.

deflections of the concentrated masses are identical with those of certain points on the actual structures. It should be noted that for a particular mode stresses may always be related to deflections. In the methods of analysis given below maximum deflections are usually determined, but it should be understood that these can readily be converted to maximum stresses. These stresses are in error by the amount which would have been contributed by the neglected modes of vibration.

In Fig. 7.1a the simply supported beam subjected to a uniformly distributed dynamic load is represented by the equivalent system shown. This system is selected such that the deflection of the concentrated mass is at all times equal to the mid-span deflection of the actual beam.

Neglecting the higher modes, this may be accomplished if the equivalent parameters P_e , m_e , and k_e are determined according to certain energy relationships, as discussed in Sec. 7.6. It is obvious that the static deflection and the natural frequency of the equivalent system must be the same as the actual structure. If the beam undergoes plastic deformation, the spring must also have plastic characteristics.

Again considering the fundamental mode only, the resistance of the actual beam or the equivalent system may be expressed in terms of the displacement x . In the elastic range the resistance is given by

$$R = kx \quad (7.1)$$

for the structure, or

$$R_e = k_e x \quad (7.2)$$

for the equivalent system. If plastic deformation is considered, the complete resistance function may be any one of the three curves shown in Fig. 7.2a. Curve *A* corresponds to a brittle material, while curve *B*

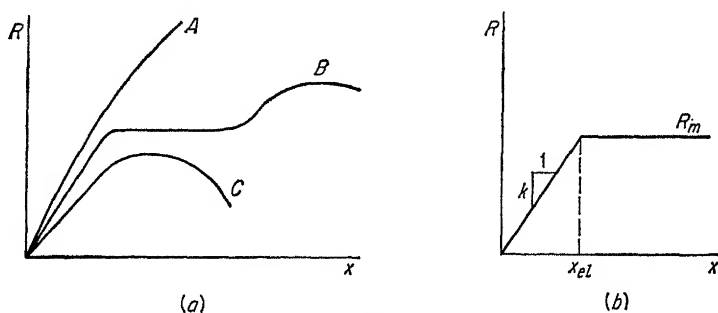


FIG. 7.2. Resistance functions.

would apply to a structure made of a ductile material with marked yielding such as steel or reinforced concrete. For curve *C* the resistance decreases above a certain value of deflection. This is generally not a property of the material but is caused either by a combination of direct stress and bending in the member providing the resistance or by plastic buckling. The resistance function for most of the structures discussed herein can be idealized by the curve shown in Fig. 7.2b. The resistance function of the equivalent dynamic system is given the same shape.

Equivalent systems for building frames subjected to lateral dynamic loads are shown in Fig. 7.1b and c. Since the floors and roofs translate essentially as rigid bodies and since most of the mass of the building is located at these levels, the concentrated masses of the equivalent system are placed at the same points. The columns may be replaced by springs supporting and connecting the masses.

A detailed description of the methods by which approximate equivalent

systems are selected is given in Sec. 7.5. However, simplified methods of dynamic analysis for such systems will first be discussed. The selection of equivalent parameters will then have more meaning.

7.3. Energy Method of Analysis (Single Degree). The method of analysis given here is based upon the principle that at the time of maximum deflection and zero velocity the work done by the externally applied load must be equal to the internal strain energy in the structure. It is developed for one-degree systems and when used with the equivalent system of an actual structure is no better than the approximations involved in computing the equivalent parameters. Curves are given to facilitate computation of the external work done. The strain energy can be easily determined from the resistance function. The method is applicable to both elastic and plastic behavior.

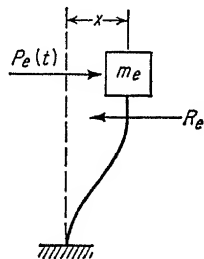


FIG. 7.3. Simple equivalent system.

Consider the simple equivalent system shown in Fig. 7.3 where the following notation is used:

$P_e(t)$ = external load as a function of time

m_e = mass of equivalent system

$R_e(x)$ = internal resistance as a function of deflection

x = deflection

The basic equation of motion is

$$m_e \frac{d^2x}{dt^2} = P_e(t) - R_e(x) \quad (7.3)$$

The equation of conservation of energy is

External work done = kinetic energy + strain energy

$$\text{or} \quad \int_0^x P_e(t) dx = \frac{1}{2} m_e \left(\frac{dx}{dt} \right)^2 + \int_0^x R_e(x) dx \quad (7.4)$$

which becomes at maximum deflection (zero velocity)

$$\int_0^{x_m} P_e(t) dx = \int_0^{x_m} R_e(x) dx \quad (7.5)$$

These are the basic equations used below to determine maximum deflection of the system under a given dynamic load.

It may be noted that in the above equations and in the following computations the effect of damping is neglected. This is possible because in most problems of structural dynamics we are interested only in the first peak value of deflection, and not in a continuous state of vibration. For this reason damping is of little importance.

a. *External Work Done.* A typical dynamic load is shown in Fig. 7.4, where T is defined as the duration of the load. If this load is applied to the dynamic system shown in Fig. 7.3, $\mathfrak{W}_e(t)$, the external work done up to any time t , is given by

$$\mathfrak{W}_e(t) = \int_0^{x(t)} P_e(t) dx = \int_0^t P_e(t) \frac{dx}{dt} dt \quad (7.6)$$

In order to evaluate the work done, the velocity dx/dt must be determined by integration of Eq. (7.3).

$$\frac{dx}{dt} = \frac{1}{m_e} \int_0^t [P_e(t) - R_e(x)] dt \quad (7.7)$$

Thus the expression for work done becomes

$$\mathfrak{W}_e(t) = \int_0^t P_e(t) \left\{ \frac{1}{m_e} \int_0^t [P_e(t) - R_e(x)] dt \right\} dt \quad (7.8)$$

In the energy method of analysis this expression is integrated between

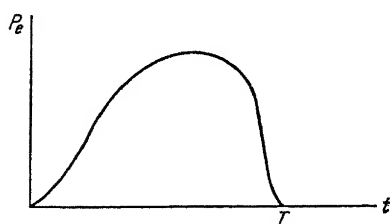


FIG. 7.4. Typical dynamic load.

$t = 0$ and $t = t_m$, the time of maximum deflection, in order to obtain \mathfrak{W}_{me} , the work done by the load during this time interval. It is evident that the work done depends not only upon the external load but also upon the mass and resistance function of the dynamic system.

If the time of maximum deflection t_m is greater than the duration of the load T , Eq. (7.8) need only be integrated up to the latter time. Thereafter the work done remains constant. If t_m is much greater than T , the resistance $R_e(x)$ is small during the application of the load and may be neglected. The expression for work done then becomes

$$\mathfrak{W}_{P_e} = \int_0^T P_e(t) \left[\frac{1}{m_e} \int_0^t P_e(t) dt \right] dt \quad (7.9)$$

which when integrated becomes, where \mathfrak{W}_{P_e} is the work done ignoring the contribution of the resistance,

$$\mathfrak{W}_{P_e} = \frac{H_{me}^2}{2m_e} \quad (7.10)$$

in which $H_{me} = \int_0^T P_e(t) dt$.

H_{me} is the total impulse of the external load and is equal to the area under the load-time curve. The external force in this case may be termed a *pure impulsive load*, and during its application the resistance

and internal strain energy of the system may be assumed to be zero. After the application of the load the mass has acquired a kinetic energy equal to the work done:

$$\frac{H_{me}^2}{2m_e} = \frac{1}{2} m_e V^2 \quad (7.11)$$

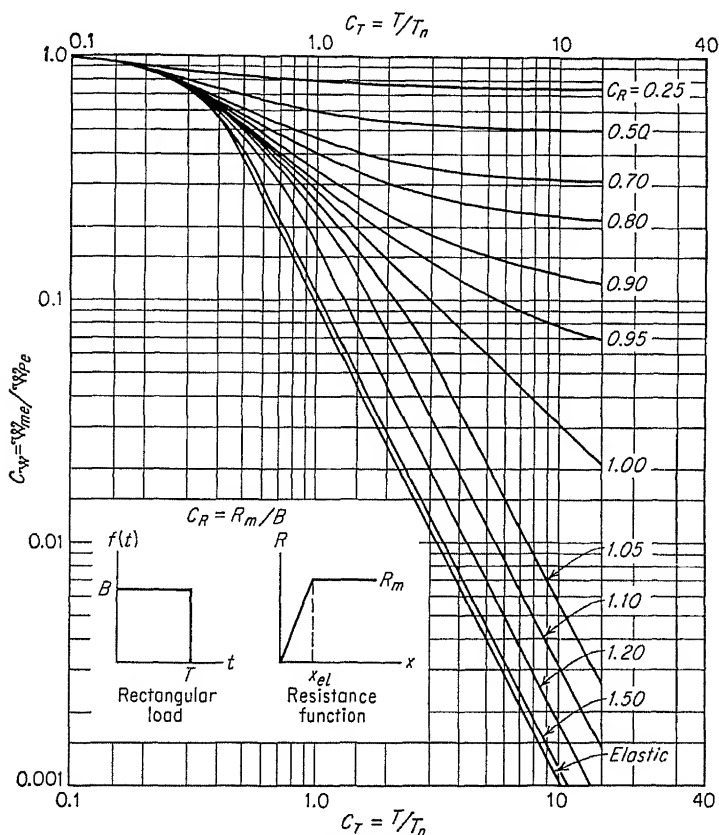


FIG. 7.5. Work-done ratios for rectangular loads and one-degree systems [1].

The initial velocity is therefore given by

$$V = \frac{H_{me}}{m_e} \quad (7.12)$$

At maximum deflection this kinetic energy is completely transferred into internal strain energy. In the case of a pure impulsive load the work done depends only upon the area under the load-time curve and is independent of the shape of that curve and the properties of the dynamic system.

In most cases the resistance $R_e(x)$ cannot be neglected in the time interval between 0 and T . From Eq. (7.8) it may be seen that the internal resistance always acts to reduce the work done on the system. Therefore the work given by Eq. (7.10) may be considered to be the

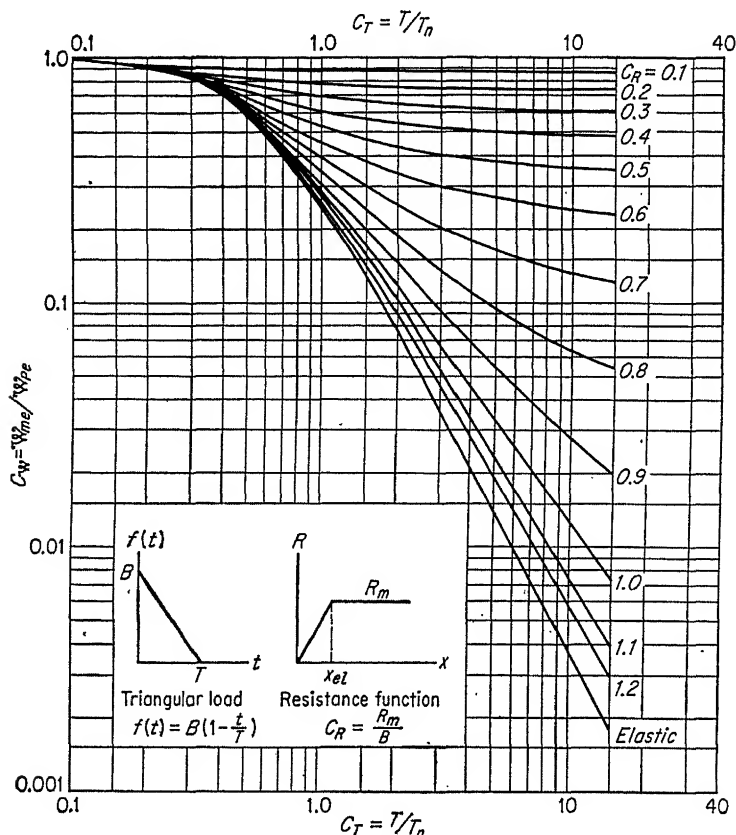


FIG. 7.6. Work-done ratios for triangular loads and one-degree systems [1].

absolute maximum work which could be done by a given load on a dynamic system.

$$\text{Absolute maximum work} = W_{Pe} = \frac{H_{me}^2}{2m_e} \quad (7.13)$$

The energy method of analysis consists in part of a determination of the ratio W_{me}/W_{Pe} , which is the actual work done divided by the absolute maximum work. This ratio depends upon the shape of the load-time curve and the properties of the dynamic system and is called the work-done ratio, C_W .

Curves giving the work-done ratio C_W for two simple load-time func-

tions and for the one-degree-of-freedom system shown in Fig. 7.3 are contained in Figs. 7.5 and 7.6. The system is assumed to have the idealized resistance function shown in Fig. 7.2b. These curves were obtained by evaluation of Eq. (7.8) for variations in the parameters involved and required determination of the deflection-time function using the basic

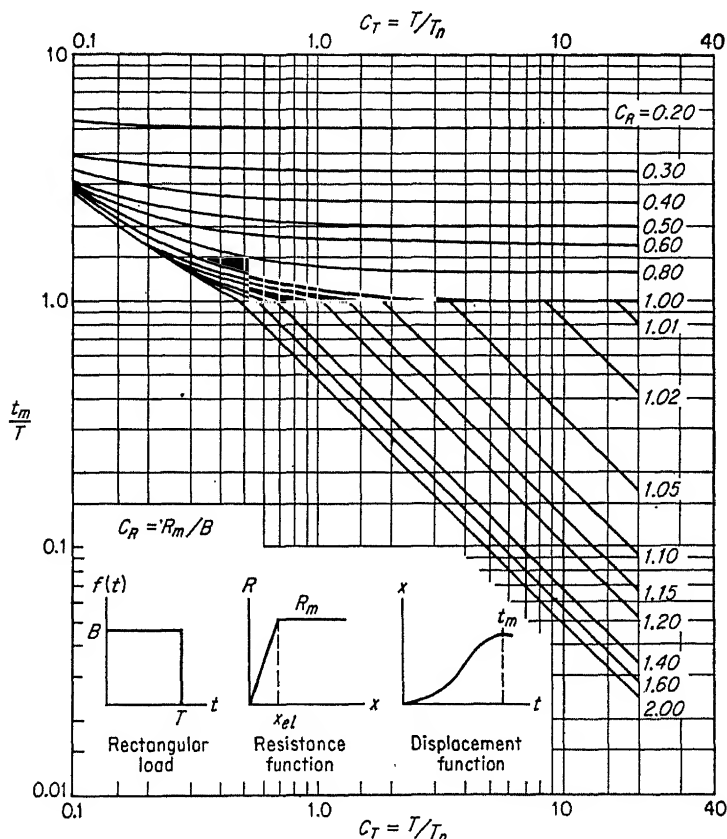


FIG. 7.7. Time of maximum deflection for rectangular loads and one-degree systems [1].

principles presented in Chap. 3. For convenience the results are given in terms of the ratios

$$C_R = \frac{R_{ms}}{B_e} \quad C_T = \frac{T}{T_n}$$

where R_{ms} = maximum or plastic resistance of system

B_e = peak value of external load

T = duration of load

$$T_n = \text{natural period of system} = 2\pi \sqrt{\frac{m_e}{k_e}}$$

For a given loading and dynamic system these ratios can be easily computed and the work-done ratio obtained from the curves presented. Having the work-done ratio, the absolute maximum work is computed by Eq. (7.13), and \mathcal{W}_{me} , the actual work done, by $C_W \mathcal{W}_{Pe}$. Detailed application of these curves is described in Sec. 7.3c.

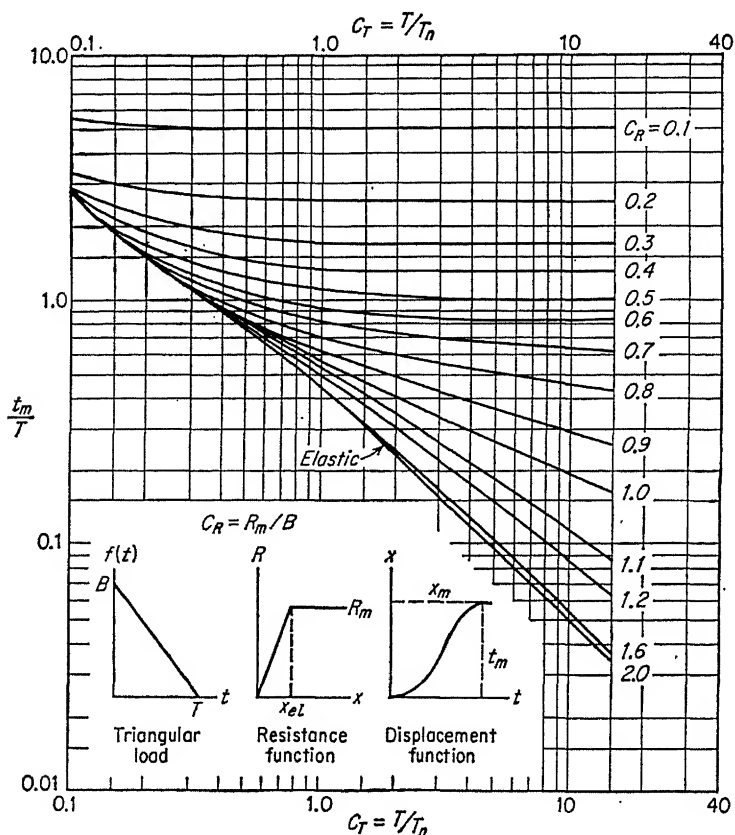


FIG. 7.8. Time of maximum deflection for triangular loads and one-degree systems [1].

It may be observed in the figures that as the ratio T/T_n decreases, the load becomes more nearly a pure impulse and the work-done ratio approaches unity. It may also be observed that as C_R increases, the behavior becomes more nearly elastic and the bottom curve applies to the completely elastic case.

In many cases it is also necessary to determine the time of maximum deflection. This may be obtained by the curves given in Figs. 7.7 and 7.8.

Although the curves described above were derived for rectangular and triangular load-time functions, they may be applied to a wide range of structural dynamic problems. In many cases the actual load on the structure may be idealized into one of these simple shapes.

b. Energy Absorbed. The energy absorbed by the dynamic system shown in Fig. 7.3 may be determined as the area under the resistance-deflection curves shown in Fig. 7.2b. If the behavior is completely

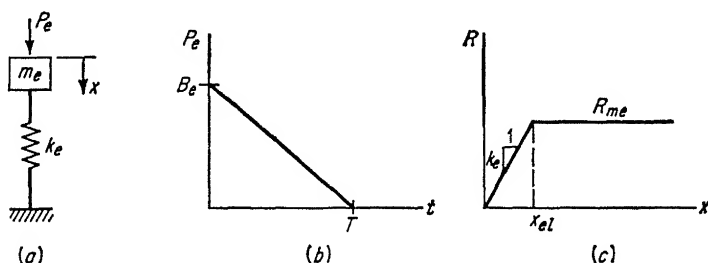


FIG. 7.9. One-degree system.

elastic, the absorbed energy is equal to the strain energy and is given by

$$SE = \frac{1}{2}k_e x_m^2 = \frac{1}{2}R_e x_m \quad (7.14)$$

where x_m = maximum deflection of system. If the deflection continues into the plastic range, the absorbed energy is given by

$$SE = R_{me}(x_m - \frac{1}{2}x_{el}) \quad (7.14a)$$

where x_{el} = limiting elastic deflection = R_e/k_e .

c. Application of Energy Method. Analysis by the energy method simply consists in equating the work done by the applied load to the energy absorbed by the system at maximum deflection. As an example consider the one-degree system shown in Fig. 7.9a. The dynamic load is triangular in shape with an initial peak value of B_e and a duration of T . The resistance function is as shown in Fig. 7.9c, where k_e is the elastic spring stiffness, R_{me} is the maximum elastic (or the plastic) spring resistance, and x_{el} is the limiting elastic deflection. This is the case for which the curves of Fig. 7.6 were derived. It is desired to determine the maximum deflections x_m and time of this deflection t_m .

The following data are given:

$$\begin{aligned} m_e &= 100 \text{ lb-sec}^2/\text{ft} & T &= 1.0 \text{ sec} \\ k_e &= 10,000 \text{ lb/ft} & R_{me} &= 1,600 \text{ lb} \\ B_e &= 2,000 \text{ lb} \end{aligned}$$

The natural period of the system is

$$\begin{aligned}
 T_n &= 2\pi \sqrt{\frac{m_e}{k_e}} = 2\pi \sqrt{\frac{100}{10,000}} = 0.628 \text{ sec} \\
 C_T &= \frac{T}{T_n} = \frac{1}{0.628} = 1.59 \\
 C_R &= \frac{R_{me}}{B_e} = \frac{1,600}{2,000} = 0.8 \\
 H_{me} &= \frac{1}{2} B_e T = \frac{1}{2} \times 2,000 \times 1 = 1,000 \text{ lb-sec} \\
 \mathcal{W}_{Pe} &= \frac{H_{me}^2}{2m_e} = \frac{(1,000)^2}{2 \times 100} = 5,000 \text{ lb-ft}
 \end{aligned}$$

From Fig. 7.6,

$$\begin{aligned}
 \frac{\mathcal{W}_{me}}{\mathcal{W}_{Pe}} &= 0.23 \\
 \mathcal{W}_{me} &= 5,000 \times 0.23 = 1,150 \text{ lb-ft} \\
 x_{el} &= \frac{R_{me}}{k_e} = \frac{1,600}{10,000} = 0.16 \text{ ft} \\
 \mathcal{W}_{me} &= SE. \\
 1,150 &= R_{me}(x_m - \frac{1}{2}x_{el}) = 1,600[x_m - (\frac{1}{2})(0.16)] \\
 x_m &= 0.80 \text{ ft} \quad \text{Ans.}
 \end{aligned}$$

From Fig. 7.8,

$$\begin{aligned}
 \frac{t_m}{T} &= 0.63 \\
 t_m &= 0.63 \times 1.0 = 0.63 \text{ sec} \quad \text{Ans.}
 \end{aligned}$$

As an example of elastic behavior the data are changed so that R_{me} is much greater than B_e . The maximum resistance (or force) developed in the spring is to be determined. Using the "elastic" curve in Fig. 7.6, we obtain

$$\begin{aligned}
 \frac{\mathcal{W}_{me}}{\mathcal{W}_{Pe}} &= 0.12 \quad \text{for } C_T = 1.59 \\
 \mathcal{W}_{me} &= 0.12 \times 5,000 = 600 \text{ lb-ft} \\
 \mathcal{W}_{me} &= SE = \frac{1}{2} k_e x_m^2 = \frac{1}{2} \times 10,000 x_m^2 = 600 \\
 x_m^2 &= 0.12 \quad x_m = 0.346 \text{ ft} \quad \text{Ans.} \\
 \text{Max } R_e \text{ developed} &= R_{me} = k_e x_m \\
 &= 10,000 \times 0.346 = 3,460 \text{ lb} \quad \text{Ans.}
 \end{aligned}$$

From Fig. 7.8,

$$\begin{aligned}
 \frac{t_m}{T} &= 0.30 \\
 t_m &= 0.30 \times 1.0 = 0.30 \text{ sec} \quad \text{Ans.}
 \end{aligned}$$

In the design of a structure one must proceed by trial and error since both R_{me} and k_e are functions of the structure selected. Design examples are given in Sec. 7.8.

7.4. Deflection Method of Analysis (Single Degree). The deflection method is basically the same as the energy method given in the preceding section. The primary difference in the two methods is the form in which

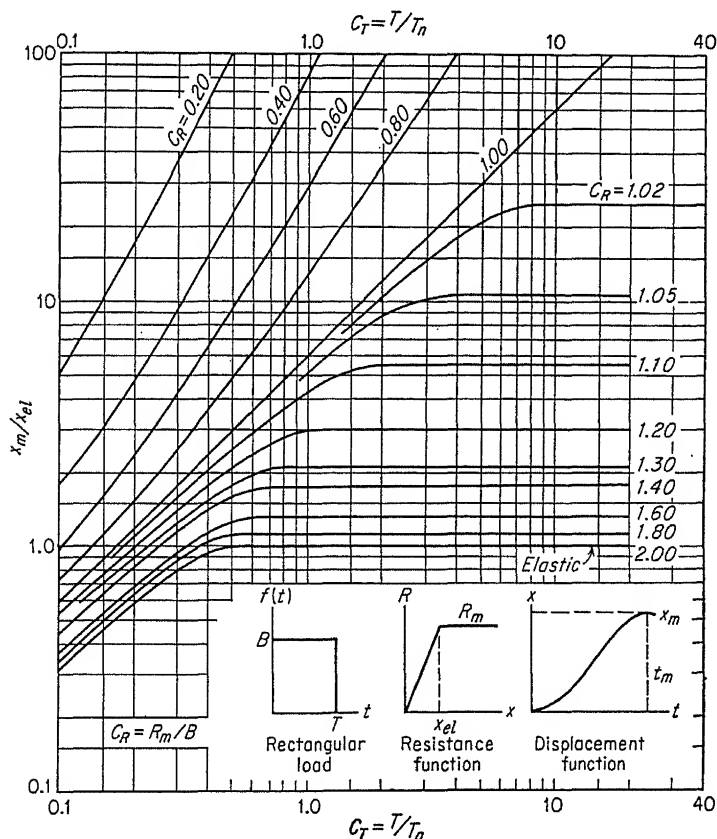


FIG. 7.10. Deflection ratios for rectangular loads and one-degree systems [1].

the data are given. It is largely a matter of personal opinion as to which is the most convenient approach.

In the deflection method the results are given in terms of maximum deflection ratio, x_m/x_{el} , rather than in terms of energy ratio. These results are shown in Figs. 7.10 and 7.11 for rectangular and triangular load-time functions. Values of x_m/x_{el} are obtained using the same basic parameter ratios as in the energy method. It may be observed that as C_R increases, the deflection ratio decreases, and that for values of C_R of

2 or greater the behavior must be purely elastic. For short load durations, the behavior may be elastic for smaller values of C_R .

As an illustration of this method consider the same example given in the preceding section in which a one-degree system is subjected to a triangular

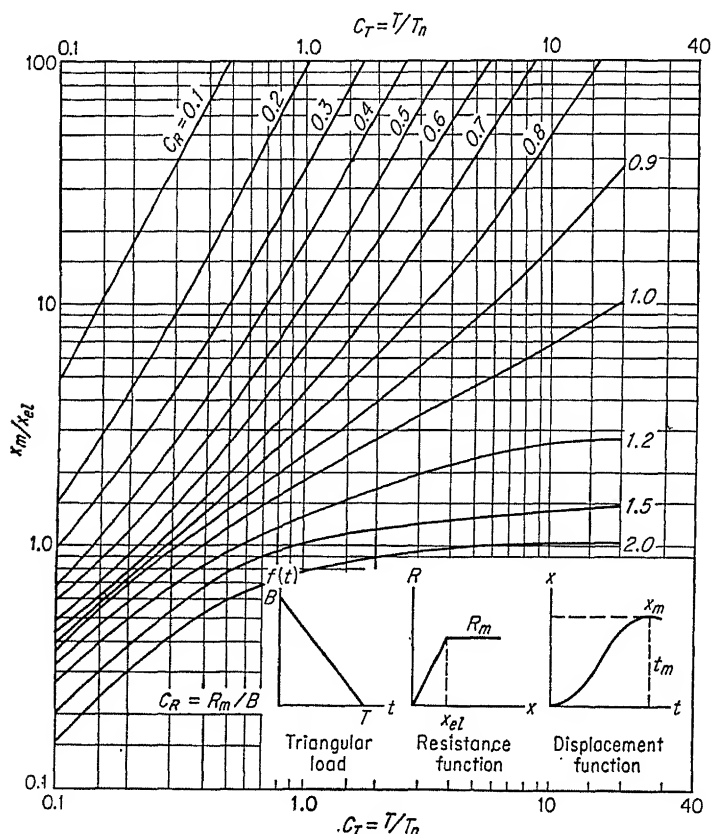


FIG. 7.11. Deflection ratios for triangular loads and one-degree systems [1].

load. In that example, the following were computed:

$$\begin{aligned} C_T &= 1.59 \\ C_R &= 0.8 \\ x_{el} &= 0.16 \text{ ft} \end{aligned}$$

From Fig. 7.11,

$$\begin{aligned} \frac{x_m}{x_{el}} &= 5.0 \\ \therefore x_m &= 5.0 \times 0.16 = 0.80 \text{ ft} \quad \text{Ans.} \end{aligned}$$

This is the same answer as obtained previously. The time of maximum

deflection is obtained from Fig. 7.8 as before. It may be noted that in this example the deflection method requires somewhat less computation than the energy method. However, in design, rather than analysis, this is not necessarily true.

In applying these curves to the elastic case, R_{me} is arbitrarily taken as twice the peak load B_e . The result obtained will hold also for any larger value of R_{me} .

$$C_T = 1.59$$

$$C_R = 2.0$$

From Fig. 7.11,

$$\frac{x_m}{x_{el}} = 0.86$$

$$x_{el} = \frac{R_{me}}{k_e} = \frac{4,000}{10,000} = 0.40 \text{ ft}$$

$$\therefore x_m = 0.40 \times 0.86 = 0.344 \text{ ft} \quad Ans.$$

As an alternative method of solving problems involving only elastic behavior the curves of Figs. 7.12 and 7.13 are given. It is evident in the elastic examples above that the maximum deflection is independent of the resistance ratio C_R . It is therefore possible and more convenient to give the results in terms of C_T only. This has been done in Fig. 7.12 for rectangular and triangular loads. In this case the results are given in terms of the maximum dynamic-load factor, which may be defined as the ratio of the maximum resistance developed to the peak value of the applied load. It may also be defined as the ratio of the maximum deflection to x_{Bs} , that which would be caused by the peak load applied statically. Thus,

$$DLF_{\max} = \frac{R_{me}}{B} = \frac{x_m}{x_{Bs}}$$

More obviously, perhaps, this factor is simply the increase in the static stress or deflection due to the dynamic character of the load. The maximum dynamic-load factor decreases as C_T decreases. For the rectangular load, however, the DLF_{\max} is 2 for all values of C_T greater than 0.5.

Using the previous example and referring to Fig. 7.12, for $C_T = 1.59$,

$$DLF_{\max} = 1.71$$

$$R_{me} = (1.71)(2,000) = 3,420 \text{ lb} \quad Ans.$$

$$x_m = 1.71x_{Bs} = (1.71)\left(\frac{2,000}{10,000}\right) = 0.342 \text{ ft} \quad Ans.$$

$$\frac{t_m}{T} = 0.30 \quad t_m = 0.30 \times 1.0 = 0.30 \text{ sec} \quad Ans.$$

In Fig. 7.13 results are given for an elastic system subjected to a load which begins at zero, increases linearly to a maximum value at time T_r ,

and then remains constant indefinitely. This load-time curve is useful when designing a girder or column supporting a beam which behaves plastically under a dynamic load. The curves of Fig. 7.13 are used in

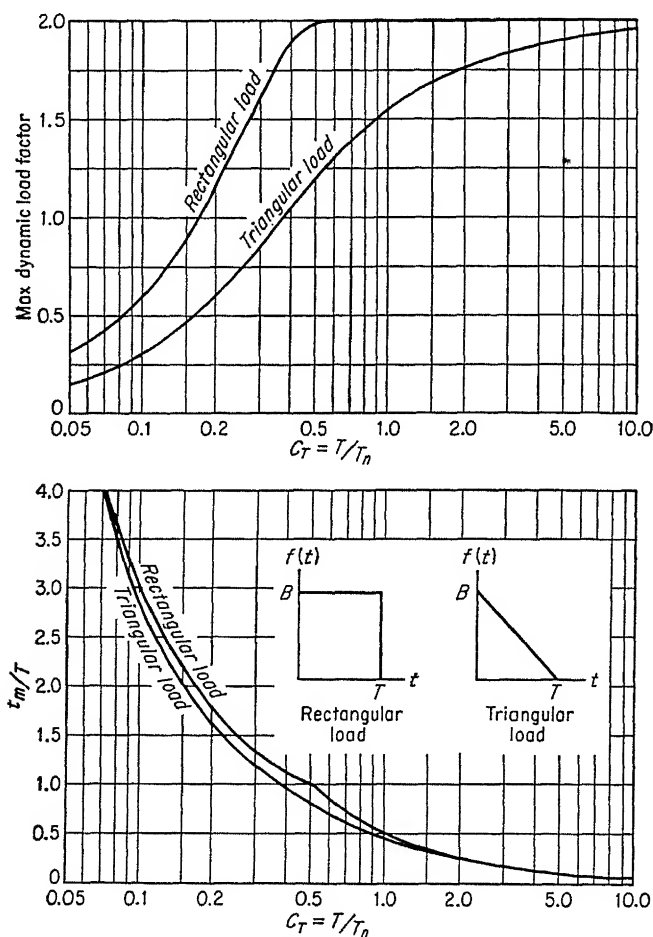


FIG. 7.12. Elastic analysis of one-degree systems [1].

exactly the same manner as those in Fig. 7.12. These curves are interesting in that the DLF_{\max} does not decrease continuously as T_r/T_n increases. The curve of DLF_{\max} has a waveform such that there is no dynamic increase when T_r is a whole multiple of T_n .

7.5. Transformation Factors. Having developed simplified methods of analysis for one-degree systems, the manner in which actual structures are converted into idealized or equivalent dynamic systems will now be dis-

cussed. This is accomplished by applying transformation factors to the dynamic parameters of the structure.

The deflection of any structural element subjected to dynamic loads is the superposition of the contributions of an infinite number of normal modes of vibration. The contribution of each mode depends upon the

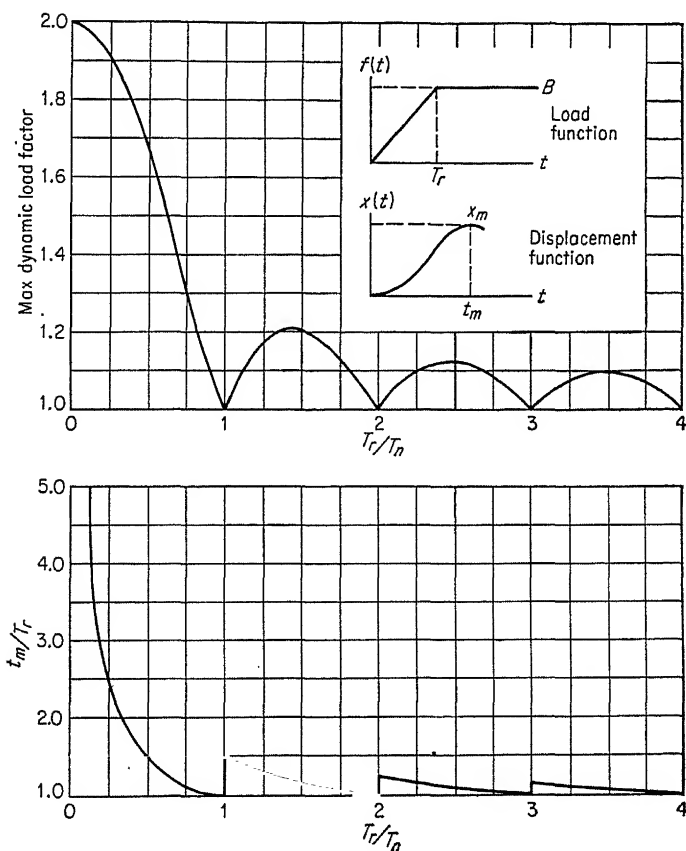


FIG. 7.13. Elastic analysis of one-degree systems [1].

spatial distribution and time variation of the load, the stiffness and mass distribution of the element, and the support conditions. Fortunately, in most cases one mode predominates, and reasonably accurate results can be obtained by considering only this mode.

The procedure used involves an assumed deflected shape corresponding to the predominant mode. This establishes a relationship between the deflections of all points on the element which is constant with time. It makes it possible to represent the element by an equivalent system having

one degree of freedom. The factors defined below provide the parameters of the equivalent system in terms of those of the actual structure (Fig. 7.1). It should be recalled that in all cases the deflection of the equivalent system is made equal to that of the real structure.

a. Load Factor K_L . The concentrated dynamic load on the equivalent system is obtained by multiplying the total load on the actual structure by the load factor. This may be expressed by the equation

$$K_L = \frac{P_e(t)}{P(t)} \quad (7.15)$$

K_L is determined by equating the external work done by P_e on the equivalent system to that done by P on the real system. Both equivalent and real loads have the same time variation.

b. Mass Factor K_m . When the total mass of the structure is multiplied by the mass factor we obtain the concentrated mass of the equivalent system.

$$K_m = \frac{m_e}{m_t} \quad (7.16)$$

This factor is obtained by equating the kinetic energy of the real and equivalent systems.

c. Resistance Factor K_R . The resistance of an element is the internal force tending to restore the element to its equilibrium position. At a given deflection the resistance is defined as numerically equal to the static load required to produce the same deflection; K_R is the factor by which the resistance of the real element is multiplied to obtain the resistance of the spring in the equivalent system. It is obtained by equating the internal strain energies of the two systems. On this basis it is found that K_R is always equal to the load factor. Thus,

$$K_R = \frac{R_e}{R} = K_L \quad (7.17)$$

d. Maximum Resistance and Spring Constant. The maximum resistance of the real element is defined as the maximum total load which can be carried. It is computed using the ultimate-strength characteristics given in Chaps. 1 and 2. When this value is multiplied by K_R we obtain the maximum resistance of the equivalent system.

The spring constant k of the real system is defined as the total static load required to cause a unit deflection. Since the deflections of the two systems are equal, the spring constant of the equivalent system is obtained by applying the resistance factor. Thus,

$$R_{me} = K_R R_m \quad (7.18)$$

$$k_e = K_R k \quad (7.19)$$

e. Dynamic Reaction V. Dynamic reactions on the element are needed both to determine shear at the supports and to determine the load applied to supporting elements. This presents a special problem since there is no force in the equivalent system which corresponds directly to the reaction on the real structure. These reactions must be obtained by a combined consideration of the resistance of the equivalent system and the actual applied load.

7.6. Transformation Factors for a Simply Supported, Uniformly Loaded Beam. In order to make the equivalent system dynamically similar to the real structure, the strain and kinetic energies and the work done by

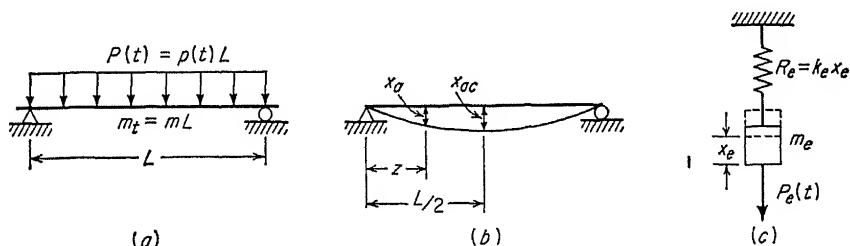


FIG. 7.14. Determination of equivalent system in elastic range. (a) Uniformly distributed load on simply supported beam; (b) assumed deflection shape; (c) equivalent single-degree system.

the external loads will be made equal. As an example, transformation factors are computed below for a simply supported beam having uniform mass and subjected to a uniformly distributed dynamic load (Fig. 7.14). It is assumed that the deflected shape is the same as that which would be caused by the load applied statically. This shape is assumed to be constant with time so that the ratio of any two ordinates of deflection along the beam is always constant. This procedure is not quite the same as considering only the first mode of vibration since the shape of the first mode is not the same as the static-deflection curve. It is believed, however, that the procedure used approximately takes into account the contribution of the higher modes and is somewhat more accurate. It should be noted that the results of these two approaches differ only slightly.

If the beam distorts into the plastic range, the transformation factors must be changed since the deflected shape changes. For this reason both elastic and plastic values are computed below. Examples of the application of these factors are given in Secs. 7.6e and 7.8.

a. Load Factor. The elastic deflected shape of the beam shown in Fig. 7.14 with the load applied statically is given by

$$x_a = \frac{pz}{24EI} (L^3 - 2Lz^2 + z^3) \quad (7.20)$$

and the deflection at mid-span is given by

$$x_{ac} = \frac{.5pL^4}{384EI} \quad (7.21)$$

Thus,
$$x_a = \frac{16}{5L^4} (L^3z - 2Lz^3 + z^4)x_{ac} \quad (7.22)$$

The total work done by the load is

$$\begin{aligned} \mathcal{W}_a &= \int_0^L \frac{px_a dz}{2} = \int_0^L \frac{16p}{5L^4} (L^3z - 2Lz^3 + z^4)x_{ac} \frac{dz}{2} \\ &= \frac{16}{25} \frac{pLx_{ac}}{2} = \frac{16}{25} \frac{Px_{ac}}{2} \end{aligned} \quad (7.23)$$

where P = total load.

In the equivalent system (Fig. 7.14c) the work done by the external load is

$$\mathcal{W}_e = \frac{P_e x_e}{2} \quad (7.24)$$

Since x_e is made equal to x_{ac} and since the work done must be the same in both cases,

$$\begin{aligned} \mathcal{W}_e &= \mathcal{W}_a \\ \frac{1}{2} P_e x_e &= \frac{16}{25} \frac{x_{ac}}{2} \\ P_e &= \frac{16}{25} P \end{aligned} \quad (7.25)$$

Thus the load factor is given by

$$K_L = \frac{P_e}{P} = \frac{16}{25} \quad (\text{elastic}) \quad (7.26)$$

Since the load-time variation is the same on both the equivalent and real systems the factor computed is not affected by the dynamic character of the load.

In the plastic range after a hinge has formed at mid-span the deflected shape is assumed to be two straight lines as shown in Fig. 7.15. In this case it is obvious that

$$\mathcal{W}_a = \frac{1}{2} \frac{Px_{ac}}{2}$$

and

$$K_L = \frac{1}{2} \quad (\text{plastic}) \quad (7.27)$$

Obviously there cannot be a sudden change in load factor when the plastic hinge forms. However, for purposes of analysis this is often assumed. Since the difference between the two factors is not great it is permissible in many cases to use an average value throughout the elasto-plastic dynamic analysis.

b. Mass Factor. In simple harmonic motion of the type assumed here the maximum velocity at any point along the beam is proportional to the ordinate of the deflection curve at the same point. The mass factor is obtained by equating the total kinetic energy of the beam to that of the equivalent system.

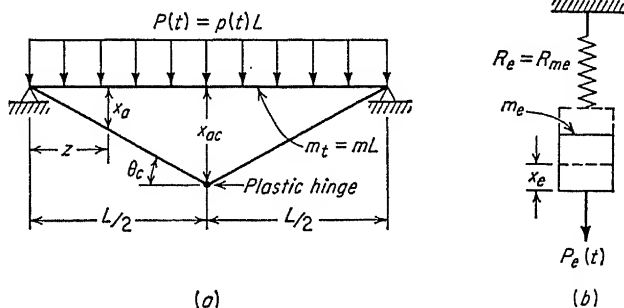


FIG. 7.15. Determination of equivalent system in plastic range. (a) Assumed deflection shape; (b) equivalent single-degree system.

In the elastic range we assume that the velocities of the beam are

$$V_a = X \frac{pz}{24EI} (L^3 - 2Lz^2 + z^3) \quad \text{and} \quad V_{ac} = X \frac{5pL^4}{384EI}$$

where X = constant relating velocity and deflection. Thus,

$$V_a = \frac{16}{5L^4} (L^3z - 2Lz^3 + z^4) V_{ac} \quad (7.28)$$

The kinetic energy of the real system is given by

$$KE_a = \int_0^L \frac{1}{2} m V_a^2 dz \quad (7.29)$$

where m = mass per unit length. When integrated, the equation produces

$$KE_a = 0.25m_t V_{ac}^2 \quad (7.30)$$

where m_t = total mass of beam.

The kinetic energy of the equivalent system is given by

$$KE_e = \frac{1}{2} m_e V_e^2 \quad (7.31)$$

Since the kinetic energies must be equal and since V_e must equal V_{ac} ,

$$\begin{aligned} KE_a &= KE_e \\ 0.25m_t V_{ac}^2 &= 0.5m_e V_e^2 \\ 0.5m_t &= m_e \end{aligned} \quad (7.32)$$

Thus the mass factor is given by

$$K_m = \frac{m_e}{m_t} = 0.50 \quad (\text{elastic}) \quad (7.33)$$

In the plastic range if we assume the same deflected shape as in the computation of load factor, we obtain

$$K_m = 0.33 \quad (\text{plastic}) \quad (7.34)$$

It is important to note that the total mass of the real beam, m_t , is not only the weight of the beam itself but also all mass which would vibrate or deflect with the beam. Normally this mass can be taken as that corresponding to the total dead weight supported by the beam.

c. Maximum Resistance and Spring Constant. The maximum resistance is defined as the maximum total distributed load which can be supported by the beam. This resistance is attained after the plastic hinge is formed at mid-span. In the elastic range the maximum moment is given by

$$M = \frac{PL}{8}$$

where P = total load. If M is equal to the maximum resisting moment M_P (Chaps. 1 and 2), then P becomes the maximum resistance R_m .

$$R_m = \frac{8M_P}{L} \quad (7.35)$$

In the equivalent system the maximum resistance is obtained by applying the resistance factor:

$$R_{me} = K_R R_m = K_L R_m = \frac{16}{25} \frac{8M_P}{L} \quad (7.36)$$

This is the limiting, or maximum, resistance in the elastic range. However, if plastic deformation occurs, the resistance of the equivalent system is changed to

$$R_{me} = \frac{1}{2} \frac{8M_P}{L} \quad (\text{plastic}) \quad (7.37)$$

The stiffness, or spring constant, of the real beam in the elastic range is defined as the total load divided by the mid-span deflection. Thus

$$k = \frac{P}{5PL^3/384EI} = \frac{384EI}{5L^3} \quad (7.38)$$

Multiplying by the load factor, the spring constant of the equivalent system is obtained.

$$k_e = K_L k = \frac{16}{25} \frac{384EI}{5L^3} \quad (7.39)$$

In the elastic range the resistance of the equivalent system is equal to $k_e x$.

d. Dynamic Reactions. The dynamic reaction of the equivalent system at any time is simply equal to the force in the spring. However, this is not representative of the dynamic reaction on the actual beam. In order to determine the latter we must consider the actual inertia forces distributed along the beam.

Referring to Fig. 7.16, it is assumed that the inertia forces are at all points proportional to the ordinates of the deflected shape. This is

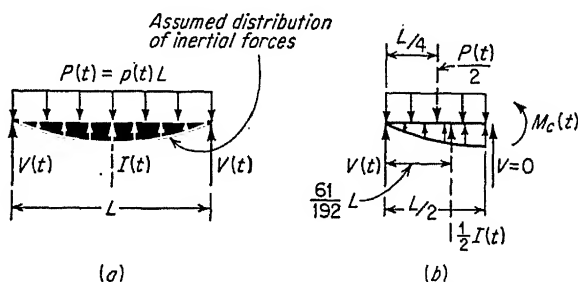


FIG. 7.16. Determination of dynamic reaction in the elastic range. (a) Load and inertia-force distribution; (b) forces on one-half of beam.

justified because if each point is in simple harmonic motion the maximum acceleration is proportional to the maximum deflection. Considering one-half of the beam as shown in Fig. 7.16b, the resultant inertia force $\frac{61}{192}I(t)$ is located at the centroid of the deflection curve. Taking moments about the inertia force,

$$V \frac{61}{192} L - M_c - \frac{1}{2} P \left(\frac{61}{192} L - \frac{L}{4} \right) = 0 \quad (7.40)$$

where M_c = bending moment at mid-span. Assuming that the resistance R is equal to $8M_c/L$ and substituting for M_c in Eq. (7.40),

$$V = 0.39R + 0.11P \quad (7.41)$$

Thus at any time the dynamic reaction depends upon both the resistance of the actual beam and the actual applied load. This resistance is equal to that of the equivalent system divided by the resistance or load factor.

In the plastic range the same procedure is followed using the assumed deflected shape for this range. In this case the dynamic reaction is given by

$$V = \frac{3}{8}R + \frac{1}{8}P \quad (\text{plastic}) \quad (7.42)$$

e. Examples. Before discussing other types of structures it will be helpful to consider an example of analysis using the principles outlined

above. The maximum elastic deflection and stress for the simple beam and load-time function shown in Fig. 7.17 is to be determined. The 16WF50 beam is laterally supported so that buckling need not be considered.

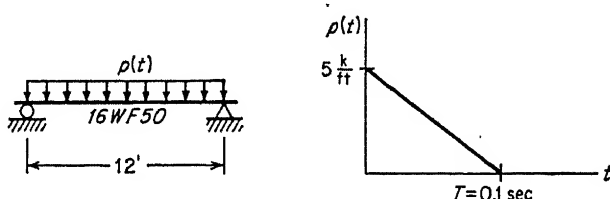


FIG. 7.17. Example.

The actual structure has the following properties:

$$\begin{aligned}
 \text{Weight per foot} &= 800 \text{ lb} \\
 \text{Total mass} &= \frac{800 \times 12}{32.2} = 298 \text{ lb-sec}^2/\text{ft} = m_t \\
 E &= 30 \times 10^6 \text{ psi} \\
 I &= 655.4 \text{ in.}^4 \\
 \text{Total peak load} &= 5,000 \times 12 = 60,000 \text{ lb} \\
 k &= \frac{384EI}{5L^2} = \frac{384 \times 30 \times 10^6 \times 655.4}{5 \times (12)^3 \times 144} = 6.07 \times 10^6 \text{ lb/ft}
 \end{aligned}$$

For the equivalent system,

$$\begin{aligned}
 \text{Mass} &= m_e = m_t K_m = 298 \times 0.50 = 149 \text{ lb-sec}^2/\text{ft} \\
 \text{Peak load} &= B_e = 60,000 \times \frac{1}{2} = 30,000 \text{ lb} \\
 k_e &= k K_R = 6.07 \times 10^6 \times \frac{1}{2} = 3.035 \times 10^6 \text{ lb/ft} \\
 \text{Natural period} &= T_n = 2\pi \sqrt{\frac{m_e}{k_e}} \\
 &= 2\pi \sqrt{\frac{149}{3.035 \times 10^6}} = 0.039 \text{ sec}
 \end{aligned}$$

Using Fig. 7.12,

$$\begin{aligned}
 \frac{T}{T_n} &= \frac{0.10}{0.039} = 2.56 \\
 \text{DLF}_{\max} &= 1.80 \quad \frac{t_m}{T} = 0.20 \\
 R_{me} &= 1.80 \times 30,000 = 54,000 \text{ lb} \\
 x_m &= \frac{R_{me}}{k_e} = \frac{54,000}{3.035 \times 10^6} = 1.78 \times 10^{-2} \text{ ft} \quad \text{Ans.}
 \end{aligned}$$

For the real beam,

$$R_m = \frac{R_{me}}{K_R} = \frac{69,100}{1.6/25} = 108,000 \text{ lb}$$

or Dynamic load = $1.80 \times 60,000 = 108,000 \text{ lb}$

$$\text{Max bending moment} = \frac{RL}{8} = \frac{108,000 \times 12}{8} = 162,000 \text{ lb-ft}$$

$$\text{Max bending stress} = \frac{M}{S} = \frac{162,000 \times 12}{80.7} = 24,000 \text{ psi} \quad \text{Ans.}$$

The dead-load stress is 2,100 psi, so the maximum total bending stress is 26,100 psi.

The shear in the beam is equal to the dynamic reaction given by Eq. (7.41). This value varies with time, but the maximum in this case occurs at t_m .

At $t_m = 0.02 \text{ sec}$,

$$R_m = 108,000 \text{ lb}$$

$$P = \frac{0.08}{0.10} \times 60,000 = 48,000 \text{ lb}$$

$$\text{Max } V = 0.39 \times 108,000 + 0.11 \times 48,000 = 47,400 \text{ lb}$$

$$\text{Dead reaction} = 4,800 \text{ lb}$$

$$\text{Max shear stress} = \frac{52,200}{16.25 \times 0.380} = 8,450 \text{ psi} \quad \text{Ans.}$$

For an example of plastic analysis let the peak dynamic load in the previous example be increased from 5 to 15 kips/ft. Using Eq. (1.5) and a dynamic yield stress of 41,600 psi, the maximum bending resistance of the cross section is given by

$$\begin{aligned} M_P &= 1.05 f_{dy} S \\ &= 1.05 \times 41,600 \times 80.7 = 3.53 \times 10^6 \text{ lb-in.} \end{aligned}$$

The maximum resistance of the beam is

$$R_m = \frac{8M_P}{L} = \frac{8 \times 3.53 \times 10^6}{12 \times 12} = 1.96 \times 10^5 \text{ lb}$$

The limiting elastic deflection is

$$x_{el} = \frac{R_m}{k} = \frac{1.96 \times 10^5}{6.07 \times 10^6} = 3.22 \times 10^{-2} \text{ ft}$$

For the transformation factors it is sufficiently accurate to use the average of the elastic and plastic values. Thus,

$$\begin{aligned} K_L &= 0.57 \\ K_m &= 0.415 \end{aligned}$$

For the equivalent system,

$$\text{Peak load} = B_e = 0.57 \times 15,000 \times 12 = 102,500 \text{ lb}$$

$$m_e = 0.415 \times 298 = 124 \text{ lb-sec}^2/\text{ft}$$

$$T_n = 2\pi \sqrt{\frac{124}{3.46 \times 10^6}} = 0.0376 \text{ sec}$$

$$R_{me} = 0.57 \times 1.96 \times 10^5 = 1.12 \times 10^5 \text{ lb}$$

Using Fig. 7.11,

$$\frac{T}{T_n} = \frac{0.10}{0.0376} = 2.66$$

$$C_R = \frac{R_{me}}{B_e} = \frac{1.12 \times 10^5}{102,500} = 1.09$$

$$\frac{x_m}{x_{el}} = 2.5$$

$$x_m = 2.5 \times 3.22 \times 10^{-2} = 8.05 \times 10^{-2} \text{ ft} \quad \text{Ans.}$$

The maximum dynamic reaction in this case cannot be determined without a more complete analysis. However, as a conservative estimate we may combine the maximum resistance with the peak load. Thus,

$$\begin{aligned} \text{Max } V &= 0.39R_m + 0.11B \\ &= 0.39 \times 1.96 \times 10^5 + 0.11 \times 15,000 \times 12 \\ &= 96,300 \text{ lb} \end{aligned}$$

$$\text{Max shear stress} = \frac{96,300}{16.25 \times 0.380} = 15,600 \text{ psi} \quad \text{Ans.}$$

Actually, the maximum shear occurs when the limiting elastic deflection is reached and is somewhat less than the value computed.

It should be noted that for these examples a rigorous solution is relatively simple to obtain and the approximate method presented has no particular merit. However, in many cases of structural analysis for dynamic loads a simplified approach of this type provides the only practical solution.

f. Accuracy of Approximate Analysis. It is apparent in the development of the simplified method that there are many approximations and possible sources of error. It is therefore of interest to compare results obtained thereby with an exact solution. This is done in Figs. 7.18 to 7.20 for the case of a simply supported beam uniformly loaded. The load-time function is triangular as in the preceding examples. The exact solution was obtained by the methods described in Chap. 5.

In Fig. 7.18 the variation of mid-span moment with time is shown up to a point slightly beyond the maximum deflection. The entire behavior is elastic. In the exact solution the effect of the higher modes is apparent. At no point, however, is the error serious.

In Fig. 7.19, a similar comparison is made for the dynamic reaction or shear at the support. The effect of the higher modes in the exact solution is even more apparent here. However, these high-frequency variations may not be of real significance. In most structures they would have little effect on elements supporting the beam which normally have long

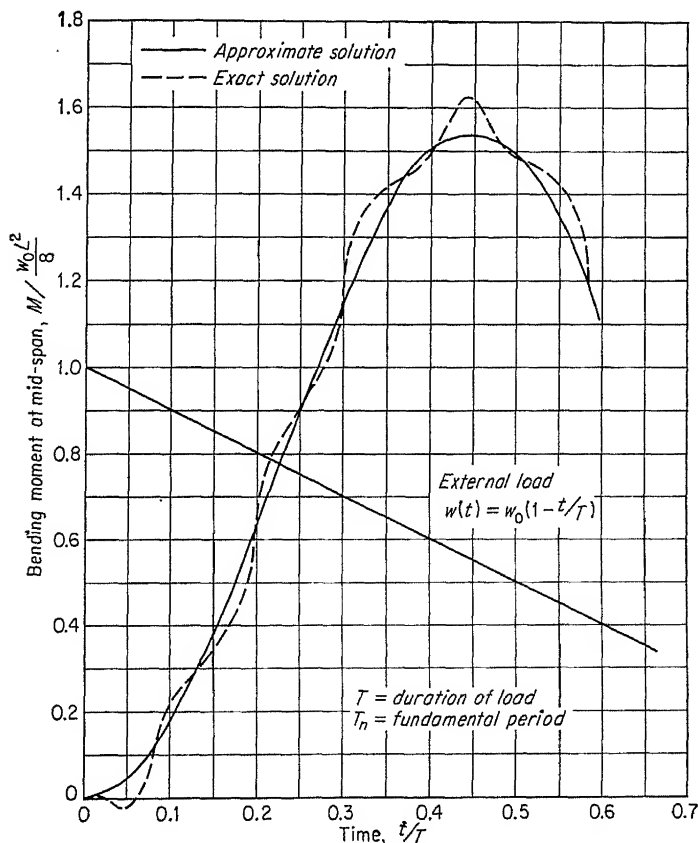


FIG. 7.18. Bending moment at mid-span for a simply supported beam under triangular load with $T/T_n = 1.0$.

natural periods. If excessive shear stresses developed in the beam itself, only a slight amount of yielding in the material would be required to quickly dampen the high frequencies. For these reasons a third curve is shown in Fig. 7.19, which is the first mode plus the average of the higher modes. This curve follows the approximate solution very closely.

The comparisons of Figs. 7.18 and 7.19 are for T/T_n equal to unity. Figure 7.20 extends the comparison to other values of this ratio. The

curves of this figure show the maximum possible error in moment, shear, and deflection as a function of T/T_n . These values were computed by adding numerically the amplitudes of all the modes and therefore represent the upper limits of error rather than actual values to be expected.

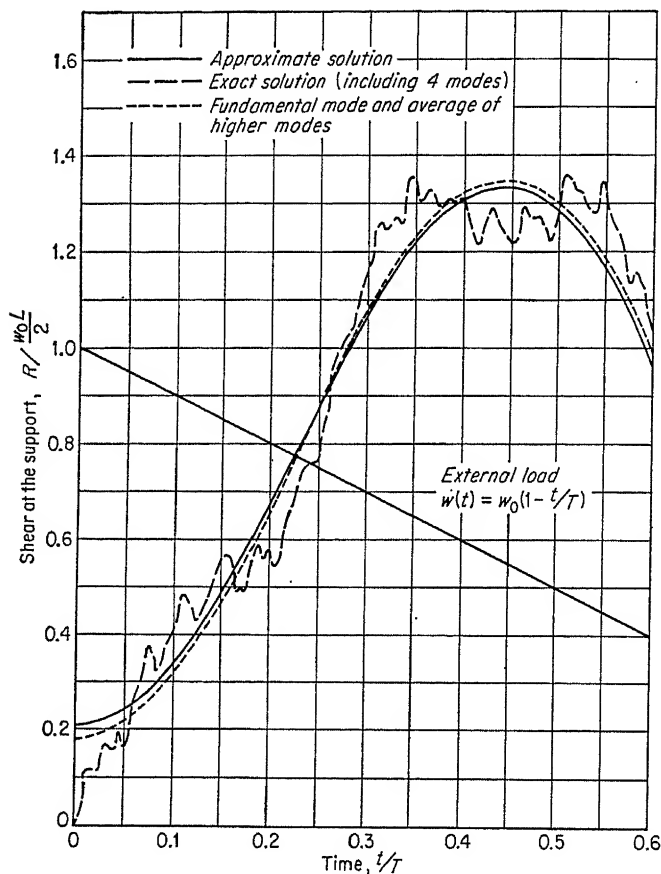


FIG. 7.19. Shear at the support for a simply supported beam under a triangular load with $T/T_n = 1.0$.

It is concluded from these curves that the only appreciable error is in the shear at the support. This error is important only for small values of T/T_n . Since in problems of structural dynamics values of T/T_n less than 0.4 are uncommon, it is concluded that the simplified method of analysis is sufficiently accurate.

7.7. Other Structural Elements. *a. Beams with Various Loading and Support Conditions.* Tables 7.1 to 7.3 contain transforming design factors for beams with various loading and support conditions. These

factors were all derived in the same manner as those for the simply supported, uniformly loaded beam which were given in Sec. 7.5. The basic difference is in the assumed deflected shape, which in each case is taken as the static-deflection curve.

In Table 7.1 values are given for simply supported beams. In addition to the factors discussed above, a load-mass factor is given which is simply equal to the mass factor divided by the load factor. Use of the

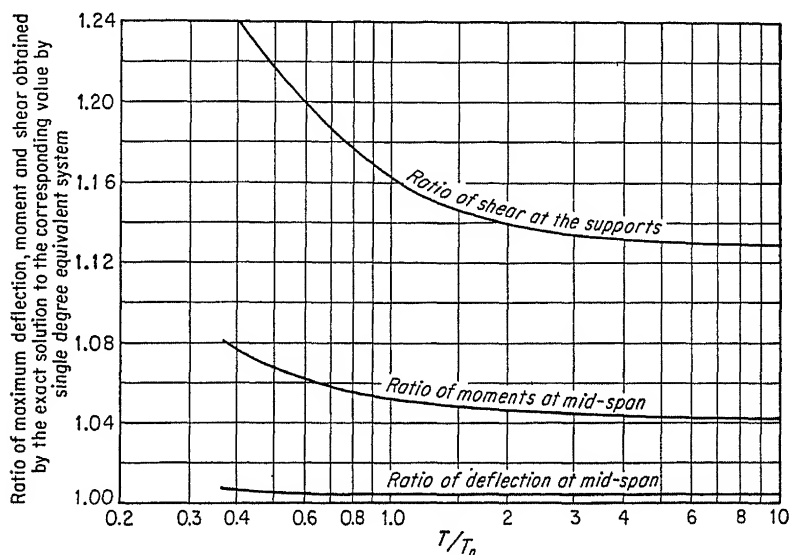
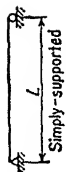


FIG. 7.20. Maximum possible errors in using an equivalent system for a simply supported beam under triangular load.

load-mass factor is sometimes convenient, especially in numerical solutions. It may be noted that the load factor is unity for a concentrated load at mid-span. This results from the fact that the deflection of the beam at the point of loading is equal to the deflection of the equivalent system. Since the work done by the real load must be equal to that done by the equivalent load the numerical values of the two loads must also be equal. For cases involving concentrated loads two mass factors are given. The first is for the case of a uniformly distributed mass, and the second is for the case of mass concentrated at the points of loading. The latter case is common and occurs when the loads are applied by other beams which are supported by the beam being analyzed. If both distributed and concentrated masses are significant, the equivalent masses should be determined separately and added together to obtain the total equivalent mass.

Table 7.2 provides factors for fixed-ended beams. For the uniformly loaded case values are given for three ranges of behavior. The necessity

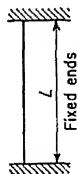
TABLE 7.1. DYNAMIC-DESIGN FACTORS FOR BEAMS AND ONE-WAY SLABS [1]



Loading diagram	Strain range	Load factor K_L	Mass factor K_m		Load-mass factor K_{Lm}		Maximum resistance R_m	Spring constant k	Dynamic reaction V
			Concentrated mass*	Uniform mass	Concentrated mass*	Uniform mass			
<p>Diagram of a beam of length \$L\$ with a point load \$P = pL\$ applied at the center.</p>	Elastic	0.64	0.50	0.78	$\frac{8M_P}{L}$	$\frac{384EI}{5L^3}$	$0.39R + 0.11P$
	Plastic	0.50	0.33	0.66	$\frac{8M_P}{L}$	0	$0.38R_m + 0.12P$
<p>Diagram of a beam of length \$L\$ with a point load \$P\$ applied at the center.</p>	Elastic	1.0	1.0	0.49	1.0	0.49	$\frac{4M_P}{L}$	$\frac{48EI}{L^3}$	$0.78R - 0.28P$
	Plastic	1.0	1.0	0.33	1.0	0.33	$\frac{4M_P}{L}$	0	$0.75R_m - 0.25P$
<p>Diagram of a beam of length \$L\$ with two point loads of magnitude \$P/2\$ applied at distances \$L/3\$ and \$2L/3\$ from the left end.</p>	Elastic	0.87	0.76	0.52	0.87	0.60	$\frac{6M_P}{L}$	$\frac{56.4EI}{L^3}$	$0.62R - 0.12P$
	Plastic	1.0	1.0	0.56	1.0	0.56	$\frac{6M_P}{L}$	0	$0.75R_m - 0.25P$

* Equal parts of the concentrated mass are lumped at each concentrated load.

TABLE 7.2. DYNAMIC-DESIGN FACTORS FOR BEAMS AND ONE-WAY SLABS [1]



Loading diagram	Strain range	Load factor K_L	Mass factor K_m		Load-mass factor K_{Lm}		Maximum resistance R_m	Spring constant k	Effective spring constant k_{eff}^\dagger		Dynamic reaction V
			Concentrated mass*	Uniform mass	Concentrated mass*	Uniform mass			Elastic	Plastic	
<p>$p = \rho L$</p>	Elastic	0.53	...	0.41	...	0.77	$\frac{12Mr_s}{L}$	$\frac{384EI}{L^3}$			$0.36R + 0.14P$
	Elasto-plastic	0.64	...	0.5078	$\frac{8}{L} (Mr_s + Mr_m)$	$\frac{384EI}{L^3}$			$0.39R + 0.11P$
	Plastic	0.50	...	0.33	...	0.66	$\frac{8}{L} (Mr_s + Mr_m)$	$\frac{384EI}{5L^3}$	$\frac{204EI}{L^3}$	$\frac{307EI}{L^3}$	$0.38R_m + 0.12P$
<p>P</p>	Elastic	1.0	1.0	0.37	1.0	0.37	$\frac{4}{L} (Mr_s + Mr_m)$	$\frac{192EI}{L^3}$			$0.71R - 0.21P$
	Plastic	1.0	1.0	0.33	1.0	0.33	$\frac{4}{L} (Mr_s + Mr_m)$	0			$0.75R_m - 0.25P$

* Concentrated mass is lumped at the concentrated load.

† See Fig. 7.21.

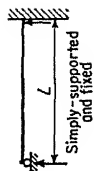


TABLE 7.3. DYNAMIC-DESIGN FACTORS FOR BEAMS AND ONE-WAY SLABS [1]

Loading diagram	Strain range	Load factor K_L	Mass factor K_m		Load-mass factor K_{Lm}		Maximum resistance R_m	Spring constant k	Effective spring constant k_{st}^\dagger		Dynamic reaction V
			Con- cen- trated mass*	Uni- form mass	Con- cen- trated mass*	Uni- form mass			Elastic	Plastic	
	Elastic	0.58	0.45	0.78	$\frac{8Mp_s}{L}$	$\frac{185EI}{L^3}$	$\frac{153EI}{L^3}$		$V_1 = 0.26R + 0.12P$ $V_2 = 0.43R + 0.19P$
	Elasto-plastic	0.64	0.50	0.78	$\frac{4}{L}(Mp_s + 2Mp_m)$	$\frac{384EI}{5L^3}$	$\frac{160EI}{L^3}$		$V_1 = V_2 = 0.38R + 0.11P$
	Plastic	0.50	0.33	0.66	$\frac{4}{L}(Mp_s + 2Mp_m)$	0	$\left(R_m\right) = \frac{14.6Mp}{L}$		$V_1 = V_2 = 0.38R_m + 0.12P$
	Elastic	1.0	1.0	0.43	1.0	0.43	$\frac{16Mp_s}{3L}$	$\frac{107EI}{L^3}$	$\frac{104EI}{L^3}$		$V_1 = 0.54R + 0.14P$ $V_2 = 0.25R + 0.07P$
	Elasto-plastic	1.0	1.0	0.49	1.0	0.49	$\frac{2}{L}(Mp_s + 2Mp_m)$	$\frac{48EI}{L^3}$	$\frac{106EI}{L^3}$		$V_1 = V_2 = 0.78R - 0.28P$
	Plastic	1.0	1.0	0.33	1.0	0.33	$\frac{2}{L}(Mp_s + 2Mp_m)$	0	$\left(R_m\right) = \frac{6.63Mp}{L}$		$V_1 = V_2 = 0.75R_m - 0.25P$
	Elastic	0.81	0.67	0.45	0.83	0.55	$\frac{6Mp_s}{L}$	$\frac{132EI}{L^3}$	$\frac{117.5EI}{L^3}$		$V_1 = 0.17R + 0.17P$ $V_2 = 0.83R + 0.33P$
	Elasto-plastic	0.87	0.76	0.52	0.87	0.60	$\frac{2}{L}(Mp_s + 3Mp_m)$	$\frac{56EI}{L^3}$	$\frac{122EI}{L^3}$		$V_1 = V_2 = 0.62R - 0.12P$
	Plastic	1.0	1.0	0.56	1.0	0.56	$\frac{2}{L}(Mp_s + 3Mp_m)$	$\left(R_m\right) = \frac{9.52Mp}{L}$		$V_1 = 0.56R_m - 0.25P$ $V_2 = 0.56R_m + 0.13P$

* Equal parts of the concentrated mass are lumped at each concentrated load.

† See Fig. 7.21.

for three ranges is apparent if the behavior of the element under a gradually increasing load is considered. As the load increases plastic hinges are first formed at the supports. Thereafter the beam behaves elasto-plastically as a simply supported element and the load and mass factors are determined accordingly. Finally, a hinge forms at mid-span and the behavior is completely plastic. The factors for the last two ranges are the same as for a simply supported beam. The values of maximum resistance given occur at the ends of the corresponding ranges of behavior. M_{P_s} is the ultimate resisting moment at the support, and M_{P_m} is that at

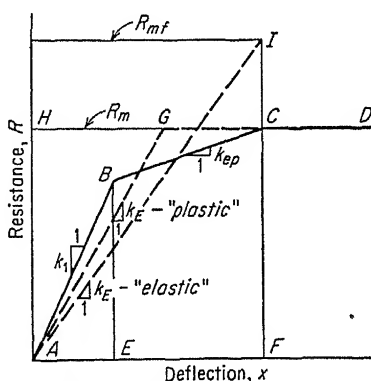


FIG. 7.21. Trilinear resistance function and effective spring constants.

mid-span. The resistance diagram for this case is trilinear, as shown in Fig. 7.21 as line $ABCD$. However, the curves for simplified analysis given in Secs. 7.3 and 7.4 are derived for bilinear resistance functions. Therefore it is necessary to replace the actual resistance curve by an equivalent bilinear shape. Two such values of "effective" spring constant are given in Table 7.2. The elastic effective value corresponds to curve AI in Fig. 7.21 and is used when the beam does not deflect beyond the actual point C . In this case a fictitious maximum resistance R_{mf} is used to replace the actual value. The plastic effective spring constant corresponds to curve AGC and is used when the beam deflects into the full plastic range. These effective constants were determined by making the areas under the resistance-deflection curves equal in the actual and assumed conditions. An example using effective spring constants is given in Sec. 7.8.

Table 7.3 gives the various factors for a beam simply supported at one end and fixed at the other.

For conditions of partial restraint at the supports intermediate values of the factors may be estimated. This is usually necessary when dealing

with continuous beams. Tables 7.1 to 7.3 may also be used for one-way slabs.

b. Two-way Slabs. Transforming design factors for simply supported and fixed two-way slabs uniformly loaded are given in Tables 7.4 and 7.5. These values were obtained using the same principles as for beams (Sec. 7.6) except that this case involves a deflected shape in three dimensions. Several ratios of the lengths of the two sides are considered.

The determination of deflected shapes and resistances for two-way slabs is obviously rather complicated. Tables 7.4 and 7.5 are based upon classical plate theory in the elastic range and idealized failure lines during plastic distortion. In the expressions for resistance the following notation is used:

M_{Pfa} = total positive plastic-bending-moment capacity along a section parallel to edge a

M_{Psa}^0 = negative plastic-moment capacity per unit width at center of edge a

M_{Psa} = total negative plastic-moment capacity along edge a

Edge a is the shorter side of the slab. The expressions for dynamic reactions give the total reaction along one of the four edges in terms of P , the total load, and R , the total resistance. In the expressions for spring constant I_a is the moment of inertia per unit width.

Once the transforming factors have been applied to the two-way slab the analysis proceeds as for any simple one-degree equivalent system.

c. Flat Slabs. Recommended factors for a square interior flat slab are given in Table 7.6. The notation used for bending moments is as follows:

M_{Pmp}, M_{Pmn} = positive and negative plastic-moment capacity per unit width in middle strip

M_{Pcp}, M_{Pcn} = positive and negative plastic-moment capacity per unit width in column strip

d. Frames. The transforming factors for rigid building frames subjected to lateral load such as shown in Fig. 7.1*b* can be easily determined. The load factor for a load concentrated at roof level is unity. For a load distributed along the side wall a factor of one-half is used. The equivalent mass may be taken as the total mass at roof level plus one-third of the mass contained in the walls. The spring constant can be determined from a conventional elastic analysis of the frame. The maximum resistance can be easily determined from the moment capacity of the columns. The same principle can be applied to the multistory frame shown in Fig. 7.1*c*.

If vertical dynamic loads are applied to the girders of the frame, these

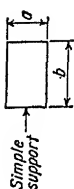


TABLE 7.4. DYNAMIC-DESIGN FACTORS FOR TWO-WAY SLABS: SIMPLE SUPPORTS—FOUR SIDES, UNIFORM LOAD [1]

Strain range	a/b	Load factor K_L	Mass factor K_m	Load-mass factor K_{Lm}	Maximum resistance	Spring constant k	Dynamic reactions	
							V_A	V_B
Elastic	1.0	0.45	0.31	0.68	$\frac{12}{a} (M_{P/a} + M_{P/b})$	$\frac{271EI_a}{a^2}$	$0.07P + 0.18R$	$0.07P + 0.18R$
	0.9	0.47	0.33	0.70	$\frac{1}{a} (12M_{P/a} + 11M_{P/b})$	$\frac{248EI_a}{a^2}$	$0.06P + 0.16R$	$0.08P + 0.20R$
	0.8	0.49	0.35	0.71	$\frac{1}{a} (12M_{P/a} + 10.3M_{P/b})$	$\frac{228EI_a}{a^2}$	$0.06P + 0.14R$	$0.08P + 0.22R$
	0.7	0.51	0.37	0.73	$\frac{1}{a} (12M_{P/a} + 9.8M_{P/b})$	$\frac{216EI_a}{a^2}$	$0.05P + 0.13R$	$0.08P + 0.24R$
	0.6	0.53	0.39	0.74	$\frac{1}{a} (12M_{P/a} + 9.3M_{P/b})$	$\frac{212EI_a}{a^2}$	$0.04P + 0.11R$	$0.09P + 0.26R$
	0.5	0.55	0.41	0.75	$\frac{1}{a} (12M_{P/a} + 9.0M_{P/b})$	$\frac{216EI_a}{a^2}$	$0.04P + 0.09R$	$0.09P + 0.28R$
Plastic	1.0	0.33	0.17	0.51	$\frac{12}{a} (M_{P/a} + M_{P/b})$	0	$0.09P + 0.16R_m$	$0.09P + 0.16R_m$
	0.9	0.35	0.18	0.51	$\frac{1}{a} (12M_{P/a} + 11M_{P/b})$	0	$0.08P + 0.15R_m$	$0.09P + 0.18R_m$
	0.8	0.37	0.20	0.54	$\frac{1}{a} (12M_{P/a} + 10.3M_{P/b})$	0	$0.07P + 0.13R_m$	$0.10P + 0.20R_m$
	0.7	0.38	0.22	0.58	$\frac{1}{a} (12M_{P/a} + 9.8M_{P/b})$	0	$0.06P + 0.12R_m$	$0.10P + 0.22R_m$
	0.6	0.40	0.23	0.58	$\frac{1}{a} (12M_{P/a} + 9.3M_{P/b})$	0	$0.05P + 0.10R_m$	$0.10P + 0.25R_m$
	0.5	0.42	0.25	0.59	$\frac{1}{a} (12M_{P/a} + 9.0M_{P/b})$	0	$0.04P + 0.08R_m$	$0.11P + 0.27R_m$

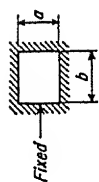


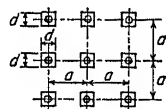
TABLE 7.5. DYNAMIC-DESIGN FACTORS FOR TWO-WAY SLABS: FIXED FOUR SIDES, UNIFORM LOAD [1]

Strain range	a/b	Load factor K_L	Mass factor K_M	Load-mass factor K_{LM}	Maximum resistance	Spring constant k	Dynamic reactions	
							V_A	V_B
Elastic	1.0	0.33	0.21	0.63	$30.2M^0r_{ab}$	$870EI_a/a^2$	$0.10P + 0.15R$	$0.10P + 0.15R$
	0.9	0.34	0.23	0.68	$27.8M^0r_{ab}$	$798EI_a/a^2$	$0.09P + 0.14R$	$0.10P + 0.17R$
	0.8	0.36	0.25	0.69	$26.0M^0r_{ab}$	$757EI_a/a^2$	$0.08P + 0.12R$	$0.11P + 0.19R$
	0.7	0.38	0.27	0.71	$26.0M^0r_{ab}$	$744EI_a/a^2$	$0.07P + 0.11R$	$0.11P + 0.21R$
	0.6	0.41	0.29	0.71	$26.4M^0r_{ab}$	$778EI_a/a^2$	$0.06P + 0.09R$	$0.12P + 0.23R$
Elasto-plastic	0.5	0.43	0.31	0.72	$25.0M^0r_{ab}$	$866EI_a/a^2$	$0.05P + 0.08R$	$0.12P + 0.25R$
	1.0	0.46	0.31	0.67	$(1/a) [12(M_{P/a} + M_{P/a}) + 12(M_{P/b} + M_{P/b})]$	$271EI_a/a^2$	$0.07P + 0.18R$	$0.07P + 0.18R$
	0.9	0.47	0.33	0.70	$(1/a) [12(M_{P/a} + M_{P/a}) + 11(M_{P/b} + M_{P/b})]$	$248EI_a/a^2$	$0.06P + 0.16R$	$0.08P + 0.20R$
	0.8	0.49	0.35	0.71	$(1/a) [12(M_{P/a} + M_{P/a}) + 10.3(M_{P/b} + M_{P/b})]$	$228EI_a/a^2$	$0.06P + 0.14R$	$0.08P + 0.22R$
	0.7	0.51	0.37	0.73	$(1/a) [12(M_{P/a} + M_{P/a}) + 9.8(M_{P/b} + M_{P/b})]$	$216EI_a/a^2$	$0.05P + 0.13R$	$0.08P + 0.24R$
Plastic	0.6	0.53	0.39	0.74	$(1/a) [12(M_{P/a} + M_{P/a}) + 9.3(M_{P/b} + M_{P/b})]$	$212EI_a/a^2$	$0.04P + 0.11R$	$0.09P + 0.26R$
	0.5	0.55	0.41	0.75	$(1/a) [12(M_{P/a} + M_{P/a}) + 9.0(M_{P/b} + M_{P/b})]$	$216EI_a/a^2$	$0.04P + 0.09R$	$0.09P + 0.28R$
	1.0	0.33	0.17	0.51	$(1/a) [12(M_{P/a} + M_{P/a}) + 12(M_{P/b} + M_{P/b})]$	0	$0.09P + 0.16R_m$	$0.09P + 0.16R_m$
	0.9	0.35	0.18	0.51	$(1/a) [12(M_{P/a} + M_{P/a}) + 11(M_{P/b} + M_{P/b})]$	0	$0.08P + 0.15R_m$	$0.09P + 0.18R_m$
	0.8	0.37	0.20	0.54	$(1/a) [12(M_{P/a} + M_{P/a}) + 10.3(M_{P/b} + M_{P/b})]$	0	$0.07P + 0.13R_m$	$0.10P + 0.20R_m$
Plastic	0.7	0.38	0.22	0.58	$(1/a) [12(M_{P/a} + M_{P/a}) + 9.8(M_{P/b} + M_{P/b})]$	0	$0.06P + 0.12R_m$	$0.10P + 0.22R_m$
	0.6	0.40	0.23	0.58	$(1/a) [12(M_{P/a} + M_{P/a}) + 9.3(M_{P/b} + M_{P/b})]$	0	$0.05P + 0.10R_m$	$0.10P + 0.25R_m$
	0.5	0.42	0.25	0.59	$(1/a) [12(M_{P/a} + M_{P/a}) + 9.0(M_{P/b} + M_{P/b})]$	0	$0.04P + 0.08R_m$	$0.11P + 0.27R_m$

elements may usually be analyzed as separate beams. The columns are then designed for the dynamic reactions of the girders.

e. Miscellaneous. Dynamic-design factors could be given for a wide assortment of structural elements. However, on the basis of the principles outlined above, the designer should be able to determine these factors as required.

TABLE 7.6. DYNAMIC-DESIGN FACTORS FOR FLAT SLABS:
SQUARE INTERIOR, UNIFORM LOAD [1]



Strain phase	d/a	Load factor K_L	Mass factor K_m	Load-mass factor K_{Lm}	Spring constant k , kips/ft	Maximum resistance R_m , kips	Dynamic column load V_c , kips
Elastic	0.05	$\frac{3}{4}$	0.34	0.64	$1.45EI_a/a^2$	$4.2\Sigma M_P$	$0.16P + 0.84R$ + load on capital
	0.10	$\frac{3}{4}$	0.34	0.64	$1.60EI_a/a^2$	$4.4\Sigma M_P$	
	0.15	$\frac{3}{4}$	0.34	0.64	$1.75EI_a/a^2$	$4.6\Sigma M_P$	
	0.20	$\frac{3}{4}$	0.34	0.64	$1.92EI_a/a^2$	$4.8\Sigma M_P$	
	0.25	$\frac{3}{4}$	0.34	0.64	$2.10EI_a/a^2$	$5.0\Sigma M_P$	
Plastic	0.05	$\frac{1}{2}$	$\frac{3}{4}$	$\frac{1}{2}$	0	$4.2\Sigma M_P$	$0.14P + 0.86R_m$ + load on capital
	0.10	$\frac{1}{2}$	$\frac{3}{4}$	$\frac{1}{2}$	0	$4.4\Sigma M_P$	
	0.15	$\frac{1}{2}$	$\frac{3}{4}$	$\frac{1}{2}$	0	$4.6\Sigma M_P$	
	0.20	$\frac{1}{2}$	$\frac{3}{4}$	$\frac{1}{2}$	0	$4.8\Sigma M_P$	
	0.25	$\frac{1}{2}$	$\frac{3}{4}$	$\frac{1}{2}$	0	$5.0\Sigma M_P$	

d = width of column capital

a = column spacing, ft

E = compressive modulus of elasticity of concrete, ksi

I_a = average of gross and transformed moments of inertia per unit width, equal in both directions, in.⁴/ft

P = total load on one slab panel, excluding capitals

R = total resistance of one slab panel, excluding capitals

$\Sigma M_P = M_{Pmp} + M_{Pmn} + M_{Psp} + M_{Psn}$

In some cases such as deep beams of reinforced concrete, shear distortion is important and should be considered when determining the deflected shape, spring constant, and maximum resistance.

The dynamic analysis of trusses may be handled in the same manner as beams except that shear distortion may also be important in this case.

The analysis of continuous reinforced-concrete T beams or composite steel beams presents complications because the effective moment of inertia varies along the span. However, reasonable approximations may be easily developed. When the beam supports a two-way slab the fact that the load and mass contributed by the slab vary along the span should also be considered.

7.8. Design Examples. This section contains design examples presented to illustrate use of the simplified analysis of this chapter and the strength properties of Chaps. 1 and 2.

a. Simple-span Steel Beam Designed for Plastic Deformation. As a first example consider the beam and loading shown in Fig. 7.22. The beam is subjected to a uniformly distributed load with a rectangular load-time function. The material is of structural carbon steel having the dynamic properties given in Chap. 1. The element supports a dead weight of 1.0 kip/ft in addition to its own weight. The maximum permitted deflection at mid-span has been determined to be 4 in. The beam is assumed to be laterally supported so that torsional buckling need not be considered.

The energy method of Sec. 7.3 will be used, and the first trial design based upon an assumed work-done ratio C_W . Since the behavior is

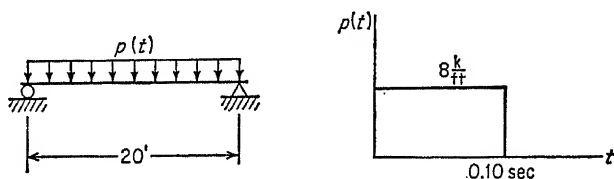


FIG. 7.22. Example.

largely plastic, the plastic-transformation factors given in Table 7.1 will be used. Actually, a weighted average of the elastic and plastic factors should be used. However, this is of secondary importance since the load-mass factor, which is the real criterion, is little different in the two ranges. Thus $K_L = 0.50$, and $K_m = 0.33$.

First determine the absolute maximum work done:

Assume weight of beam = 100 lb/ft

$$\text{Total mass} = \frac{1.10 \times 20}{32.2} = 0.684 \text{ kip-sec}^2/\text{ft}$$

$$\text{Equivalent mass} = m_e = 0.684 \times 0.33 = 0.226 \text{ kip-sec}^2/\text{ft}$$

$$\text{Total impulse} = 8 \times 20 \times 0.10 = 16.0 \text{ kip-sec}$$

$$\text{Equivalent impulse} = H_{me} = 16.0 \times 0.50 = 8.0 \text{ kip-sec}$$

$$\text{Absolute max work } \mathcal{W}_{Pe} = \frac{H_{me}^2}{2m_e} = \frac{(8.0)^2}{2 \times 0.226} = 141 \text{ kip-ft}$$

The first trial design is based on an assumed work-done ratio. A reasonable estimate can be made by a designer with experience in this type of problem.

$$\text{Assume } \frac{\mathcal{W}_{me}}{\mathcal{W}_{Pe}} = 0.2 \quad \mathcal{W}_{me} = 141 \times 0.20 = 28.2 \text{ kip-ft}$$

Since the behavior is largely plastic, the elastic range is neglected in this first trial and it is assumed that the absorbed energy is equal to

$(R_{me})(x_m)$ [Eq. (7.14)]. Thus,

$$\text{Required } R_{me} = \frac{W_{me}}{x_m} = \frac{28.2}{\cancel{4}12} = 84.6 \text{ kips}$$

For the actual beam,

$$\text{Required } R_m = \frac{84.6}{0.50} = 169 \text{ kips}$$

From Table 7.1,

$$\text{Required } M_P = R_m \frac{L}{8} = 169 \times \frac{20}{8} = 422 \text{ kip-ft}$$

In computing the required section modulus we must consider the initial dead-load stress.

$$\text{Assume } f_{\text{dead}} = 5 \text{ ksi}$$

Using Eq. (1.5) and a dynamic yield stress of 41.6 ksi,

$$\text{Required } S = \frac{M_P}{1.05(f_{dy} - f_{\text{dead}})} = \frac{422 \times 12}{1.05(41.6 - 5.0)} = 132 \text{ in.}^3$$

The most economical section for this section modulus is a 21 WF68. The section must be checked for local buckling according to Sec. 1.4c.

$$S = 139.9 \text{ in.}^3 \quad \frac{b}{t_f} = \frac{8.270}{0.685} = 12.1 < 17 \quad \therefore \text{OK}$$

$$I = 1,478 \text{ in.}^4 \quad \frac{a}{t_w} = \frac{19.76}{0.430} = 46 < 70 \quad \therefore \text{OK}$$

An analysis is now made to check the result of the first trial design.

$$\text{Equivalent mass} = m_e = \frac{1.068 \times 20}{32.2} \times 0.33 = 0.219 \text{ kip-sec}^2/\text{ft}$$

$$\begin{aligned} \text{Equivalent stiffness} = k_e &= \frac{384EI}{5L^3} \times 0.50 \\ &= \frac{384 \times 30 \times 10^3 \times 1,478 \times 0.50}{5 \times (20)^3 \times 144} = 1,290 \text{ kips/ft} \end{aligned}$$

$$\text{Equivalent peak load} = B_e = 8 \times 20 \times 0.50 = 80 \text{ kips}$$

$$\text{Dead moment} = \frac{1.068 \times (20)^2}{8} = 53.4 \text{ kip-ft}$$

$$f_{\text{dead}} = \frac{53.4 \times 12}{139.9} = 4.6 \text{ ksi}$$

$$M_P = 1.05(41.6 - 4.6) \times \frac{139.9}{12} = 452 \text{ kip-ft}$$

$$R_{me} = \frac{8 \times 452}{20} \times 0.50 = 90.4 \text{ kips}$$

$$T_n = 2\pi \sqrt{\frac{m_e}{k_e}} = 2\pi \sqrt{\frac{0.219}{1,480}} = 0.076 \text{ sec}$$

$$C_T = \frac{T}{T_n} = \frac{0.10}{0.076} = 1.32$$

$$C_R = \frac{R_{me}}{B_e} = \frac{90.4}{80} = 1.13$$

From Fig. 7.5,

$$\frac{\mathfrak{W}_{me}}{\mathfrak{W}_{Pe}} = 0.135$$

$$\mathfrak{W}_{Pe} = \frac{(8.00)^2}{2 \times 0.219} = 146 \text{ kip-ft} \quad \mathfrak{W}_{me} = 0.135 \times 146 = 19.7 \text{ kip-ft}$$

The limiting elastic deflection is

$$x_{el} = \frac{R_{me}}{k_e} = \frac{90.4}{1,480} = 0.061 \text{ ft}$$

The energy absorbed is

$$\begin{aligned} SE &= R_{me}(x_m - \frac{1}{2}x_{el}) \\ \therefore 19.7 &= 90.4(x_m - \frac{1}{2} \times 0.061) \\ x_m &= 0.249 \text{ ft} = 3.0 \text{ in.} < 4 \end{aligned}$$

This maximum is somewhat less than the design criteria of 4 in., and a lighter section might be used. However, it should be noted that the maximum deflection is very sensitive to changes in resistance and the difference obtained above is not really appreciable. A second trial if necessary might start with a new assumption for the work-done ratio.

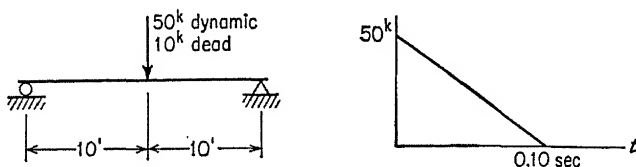


FIG. 7.23. Example.

This should be taken somewhere between the initial assumption (0.2) and the value obtained in the analysis (0.135).

The efficiency of the above design procedure depends upon the accuracy of the initial assumption for C_W . If the deflection method had been used, it would have begun with an assumed resistance ratio C_R . It is believed by those who prefer the energy method that the work-done ratio can be estimated with greater accuracy. However, this is a matter of opinion only, and either method can be applied efficiently.

b. Simple-span Steel Beam Designed for Elastic Behavior. As a second example consider the beam and loading shown in Fig. 7.23. The loads are applied at mid-span, and the dynamic-load pulse is triangular.

It is assumed that the beam is laterally supported at mid-span only. It is usually found in such cases that plastic design is impossible because of buckling considerations, and the maximum dynamic stress is limited by Eq. (1.8). The concentrated dead weight at mid-span contributes to the mass of the system. The analysis will be accomplished by the deflection method using a maximum dynamic-load factor from Fig. 7.12.

First, a preliminary design is made based upon an assumed DLF_{\max} .

Assume weight of beam = 100 lb/ft

Assume $DLF_{\max} = 1.75$

$$\text{Max bending moment} = \frac{1}{8} \times 0.10 \times 20^2 + \frac{1}{4} \times 10 \times 20 + 1.75 \times \frac{1}{4} \times 50 \times 20 = 50 + 50 + 440 = 540 \text{ kip-ft}$$

Assume a maximum stress of 35 ksi limited by buckling.

$$\text{Required } S = \frac{M}{f} = \frac{540 \times 12}{35} = 185 \text{ in.}^3$$

The most economical section for this section modulus is a 24WF84. Since the maximum stress is below the yield stress, the plastic-local-buckling criteria need not be applied and this section is satisfactory in that respect.

Try 24WF84:

$$S = 196.3 \text{ in.}^3$$

$$I = 2,364 \text{ in.}^4$$

By Eq. (1.8),

$$\text{Allow } f = \frac{32 \times 10^3}{600 + \frac{K' L d}{6 t_f}} = \frac{32 \times 10^3}{600 + \frac{0.74 \times 120 \times 24.09}{9.015 \times 0.772}} = 35.2 \text{ ksi}$$

where K' is taken from Table 1.1. This allowable stress is close to that assumed, and the section is satisfactory for the preliminary design.

For the equivalent system, $K_L = 1$ and $K_m = 1$ for the load and mass at mid-span. However, for the distributed mass of the beam itself $K_m = 0.49$ from Table 7.1. Therefore

$$\text{Equivalent mass} = m_e = \frac{10 + 0.10 \times 20 \times 0.49}{32.2} = 0.340 \text{ kip-sec}^2/\text{ft}$$

Using the stiffness from Table 7.1, since $k_e = K_L k = (1)k$,

$$k_e = \frac{48EI}{L^3} = \frac{48 \times 30 \times 10^3 \times 2,364}{(20)^3 \times 144} = 2,960 \text{ kips/ft}$$

$$T_n = 2\pi \sqrt{\frac{0.340}{2,960}} = 0.067 \text{ sec}$$

$$\frac{T}{T_n} = \frac{0.10}{0.067} = 1.49$$

From Fig. 7.12,

$$\begin{aligned} \text{DLF}_{\max} &= 1.68 \\ \text{Max } M &= 50 + 50 + 1.68 \times \frac{1}{4} \times 50 \times 20 = 520 \text{ kip-ft} \\ \text{Max } f &= \frac{M}{S} = \frac{520 \times 12}{196.3} = 31.8 \text{ ksi} < 35.2 \end{aligned}$$

Since the maximum dynamic stress is less than the allowable, the section chosen is satisfactory. If a second trial were desirable, it would start with a new assumed DLF_{\max} . A lighter section would increase T_n and decrease T/T_n . It may be observed in Fig. 7.12 that this results in a lower DLF_{\max} . Therefore the new assumed value should be somewhat less than 1.68.

The maximum shearing stress should also be checked, and for this purpose the maximum dynamic reaction must be computed. The latter is not given directly by the simplified analysis but may be estimated with sufficient accuracy. Using the 24WF84 section, first compute the time of maximum deflection.

From Fig. 7.12,

$$\begin{aligned} \frac{t_m}{T} &= 0.49 \\ t_m &= 0.49 \times 0.10 = 0.049 \text{ sec} \end{aligned}$$

This is the time of maximum resistance, R_m .

From Table 7.1,

$$V = 0.78R_m - 0.28P$$

From this equation it is obvious that the maximum reaction or shear occurs when R_m is a maximum. At $t = t_m$, $P = 25.5$ kips, and

$$R_m = 1.68 \times 50 = 84 \text{ kips}$$

Therefore

$$V = 0.78 \times 84 - 0.28 \times 25.5 = 58.3 \text{ kips}$$

Adding the dead shear of 6 kips, a total shear of 64.3 kips is obtained. The maximum stress intensity is

$$v = \frac{V}{A} = \frac{64.3}{24.09 \times 0.470} = 5.70 \text{ ksi} < 21 \quad \therefore \text{OK}$$

c. Simply Supported Concrete Slab Designed for Plastic Deformation. As a third example consider the slab with uniformly distributed load and triangular pulse shown in Fig. 7.24. The slab is to be designed for a deflection ratio x_m/x_d of 5. The deflection method will be used in the analysis. Plastic-transformation factors from Table 7.1 are used since the deflection ratio is relatively large. Dead stresses due to the weight

of the slab are ignored since they are small compared with the dynamic load.

For the preliminary design assume a resistance ratio C_R of 0.6. Thus,

$$\text{Required } R_m = 0.6(1 \times 10) = 6 \text{ kips}$$

$$\text{Required } M_P = R_m \frac{L}{8} = 6 \times \frac{10}{8} = 7.5 \text{ kip-ft}$$

A steel ratio of 0.015 is arbitrarily selected.

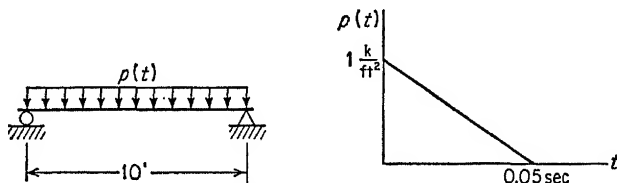


FIG. 7.24. Example.

From Eq. (2.11),

$$M_P = pf_{dy}bd^2 \left(1 - \frac{pf_{dy}}{1.7f'_{dc}} \right)$$

Using $f_{dy} = 52$ ksi and $f'_{dc} = 3.9$ ksi,

$$M_P = 0.015(52)(12)d^2 \left[1 - \frac{0.015(52)}{1.7(3.9)} \right] = 8.25d^2 \quad \text{kip-in.}$$

Equating the required and provided resistance,

$$8.25d^2 = 7.5 \times 12$$

$$\therefore d = 3.3 \text{ in.} \quad \text{Try } h = 5 \text{ in., } d = 3.5 \text{ in.}$$

The system is now analyzed for maximum deflection. For the real slab,

$$\text{Total mass} = \left(\frac{5}{12} \times 0.15 \times 10 \right) \frac{1}{32.2} = 0.0194 \quad \text{kip-sec}^2/\text{ft}$$

The stiffness is based on the average of the gross and transformed moments of inertia.

Gross moment of inertia

$$I_g = \frac{bd^3}{12} = \frac{12(5)^3}{12} = 125 \text{ in.}^4$$

Transformed moment of inertia (cracked section)

$$I_t = 38.8 \text{ in.}^4$$

Average moment of inertia

$$I_a = \frac{1}{2}(125 + 38.8) = 81.9 \text{ in.}^4$$

Stiffness

$$k = \frac{384EI}{5L^3} = \frac{384 \times 3 \times 10^3 \times 81.9}{5 \times 10^3 \times 144} = 131 \text{ kips/ft}$$

$$M_P = 8.25 \frac{d^2}{12} = 8.25 \times \frac{(3.5)^2}{12} = 8.4 \text{ kip-ft}$$

$$R_m = \frac{8M_P}{L} = \frac{8 \times 8.4}{10} = 6.7 \text{ kips}$$

For the equivalent system,

$$m_e = 0.0194 \times 0.33 = 0.0064 \text{ kip-sec}^2/\text{ft}$$

$$k_e = 131 \times 0.50 = 65.5 \text{ kips/ft}$$

$$B_e = 10 \times 0.50 = 5 \text{ kips}$$

$$T_n = 2\pi \sqrt{\frac{0.0064}{65.5}} = 0.062 \text{ sec}$$

$$\frac{T}{T_n} = \frac{0.05}{0.062} = 0.81$$

$$R_{me} = 6.7 \times 0.50 = 3.35 \text{ kips}$$

$$C_R = \frac{R_{me}}{B_e} = \frac{3.35}{5} = 0.67$$

From Fig. 7.11, $x_m/x_{el} = 4.0 < 5$. Thus the design is slightly on the conservative side. A second trial is probably unnecessary because the deflection is very sensitive to changes in d .

Before selecting steel the shear stresses and bond requirements should be investigated.

From Fig. 7.8,

$$\frac{t_m}{T} = 0.90$$

$$t_m = 0.90 \times 0.05 = 0.045 \text{ sec}$$

From Table 7.1,

$$V = 0.38R_m + 0.12P$$

Since the time at which R_m is reached is not known, the maximum reaction or shear cannot be exactly computed by this simplified analysis. This could be accomplished only by a rigorous solution or by a numerical analysis. However, it may be conservatively assumed that P has not diminished appreciably when R_m is reached. Thus,

$$V = 0.38 \times 6.7 + 0.12 \times 10 = 3.7 \text{ kips}$$

$$\text{Max } v = \frac{V}{bjd} = \frac{3,700}{12 \times \frac{7}{8} \times 3.5} = 101 \text{ psi}$$

Assuming for the allowable (ultimate) shear stress $(0.10f'_c + 5,000p)$,

$$\text{Allowable } v = 0.10 \times 3,000 + 0.015 \times 5,000 = 375 \text{ psi} \quad \text{OK}$$

Assume the allowable (ultimate) bond stress is $0.15 \times 3,000$, or 450 psi. Thus the required perimeter is given by

$$\text{Required } \Sigma o = \frac{3,700}{450 \times \frac{7}{8} \times 3.5} = 2.7 \text{ in.}$$

The required area of steel is

$$\text{Required } A_s = 0.015 \times 12 \times 3.5 = 0.63 \text{ in.}^2 \quad \left\{ \begin{array}{l} \text{Use \#5 at 6 in.} \\ A_s = 0.62 \text{ in.}^2 \\ \Sigma o = 4.7 \text{ in.} \end{array} \right.$$

In the above example the computation of stiffness based upon the average moment of inertia is obviously quite approximate. However, the error is not as serious as might appear since the maximum deflection is more sensitive to the resistance ratio C_R than to T/T_n . Thus in terms of required slab thickness the error in stiffness, and hence natural period, is not appreciable.

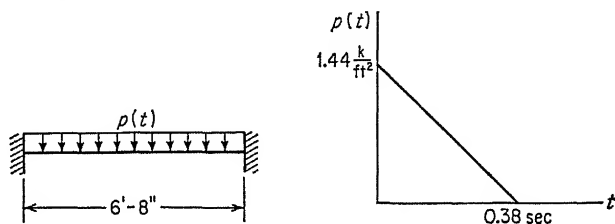


FIG. 7.25. Example.

d. Fixed-end Slab Designed for Elastic Behavior. As a final example consider the fixed-end slab with uniform-load and triangular-load pulse shown in Fig. 7.25. The slab is to be designed so that the plastic moment at mid-span is reached but not exceeded after plastic hinges have been formed at the supports. Thus the behavior is elasto-plastic, as shown in Fig. 7.21. Since the simplified analysis cannot take into account a trilinear resistance function, it is necessary to use the "elastic effective" stiffness given in Table 7.2, which represents an equivalent bilinear function. The transforming factors will be taken as the average of the elastic and elasto-plastic values given in Table 7.2. Thus $K_L = 0.585$, and $K_m = 0.455$.

The analysis is based on the DLF_{\max} by Fig. 7.12. For the preliminary design,

$$\text{Assume } \text{DLF}_{\max} = 1.5$$

$$\text{Required } R_m = 1.5(1.44 \times 6.67) = 14.4 \text{ kips}$$

$$\text{Required } M_P = R_m \frac{L}{16} = 14.4 \times \frac{6.67}{16} = 6.0 \text{ kip-ft} \quad (\text{Table 7.2})$$

Letting $p = 0.015$,

$$M_P = 8.25d^2 = 6.0 \times 12 \quad (\text{see previous example})$$

$$\text{Required } d = 2.95 \text{ in.} \quad \text{Try } h = 4 \text{ in., } d = 3 \text{ in.}$$

For the actual slab,

$$M_P = 8.25 \times \frac{(3.0)^2}{12} = 6.2 \text{ kip-ft}$$

$$R_m = 16 \frac{M_P}{L} = \frac{16 \times 6.2}{6.67} = 14.8 \text{ kips}$$

$$I_g = \frac{bh^3}{12} = \frac{12(4)^3}{12} = 64 \text{ in.}^4$$

$$I_t = 24.4 \text{ in.}^4 \quad (\text{cracked section})$$

$$I_a = \frac{1}{2}(24.4 + 64) = 44.2 \text{ in.}^4$$

Using the effective stiffness from Table 7.2,

$$k_E = \frac{264EI}{L^3} = \frac{264 \times 3 \times 10^3 \times 44.2}{(6.67)^3 \times 144} = 816 \text{ kips/ft}$$

$$\text{Total mass} = \left(\frac{4}{12} \times 0.15 \right) \left(\frac{6.67}{32.2} \right) = 0.0104 \text{ kip-sec}^2/\text{ft}$$

For the equivalent system,

$$m_e = 0.0104 \times 0.455 = 0.0047 \text{ kip-sec}^2/\text{ft}$$

$$k_e = 816 \times 0.585 = 478 \text{ kips/ft}$$

$$B_e = 1.44 \times 6.67 \times 0.585 = 5.6 \text{ kips}$$

$$T_n = 2\pi \sqrt{\frac{0.0047}{478}} = 0.0197 \text{ sec}$$

$$\frac{T}{T_n} = \frac{0.38}{0.0197} = 19.3$$

From Fig. 7.12 it is apparent that the DLF_{\max} is essentially 2.0. The preliminary design is therefore not adequate. Only one other trial is necessary since an increased slab thickness cannot reduce the DLF_{\max} below 2.0.

The correct DLF_{\max} should have been obvious at the beginning because of the short span of the element and the long duration of the load. Shear and bond stresses would be investigated as in the preceding example.

e. General Conclusions Regarding Variation of Parameters. For the economical design of a structure subjected to dynamic loads it is important that the designer understand the effect of variations in the parameters involved. It is important to note that conventional design concepts with regard to economy are not always applicable to the dynamic case.

If the duration of the load is short compared with the natural period of the structure, the load may be considered to be an impulse which represents an amount of energy which must be absorbed by the structure.

This may be observed in Figs. 7.5 and 7.6, where the ratio of load energy to required energy absorption ($\mathcal{W}_{me}/\mathcal{W}_{Pe}$) for small values of T/T_n (say, $T/T_n < 0.2$) is essentially unity. The natural period of the structure is therefore of no significance as long as it is greater than about five times the duration. The load energy, and hence the required energy absorption, is equal to $H_{me}^2/2m_e$, where H_{me} is the area under the load-time curve and m_e is the mass of the structure. Thus the required energy absorption can be decreased by increasing the mass, although this is not always a practical solution. The energy absorbed is given by $\frac{1}{2}k_e x_m^2$ for elastic design and $R_{me}(x_m - \frac{1}{2}x_{el})$ for plastic design, where x_m is the maximum deflection, x_{el} is the elastic-limit deflection, k_e is the stiffness, and R_{me} the maximum, or plastic, resistance. Thus for a given energy input x_m can be decreased only by increasing k_e in the elastic case and R_{me} in the plastic case. In the latter case an increase in stiffness alone, and hence a decrease in x_{el} , is not significant if x_m is appreciably greater than x_{el} .

If the duration of the load is long compared to the natural period of the structure, the solution is again independent of the value of the natural period. This is illustrated for the elastic case in Fig. 7.12, where for a rectangular pulse the dynamic-load factor is 2.0 for T/T_n greater than about 0.5. Thus the required resistance is twice the applied load for all larger values of T/T_n . Referring to the plastic case, it may be observed in Fig. 7.10 that each curve becomes a horizontal line above a certain value of T/T_n . Thus the ratio x_m/x_{el} depends only on the resistance R_{me} .

If the duration of the load is intermediate between the two extremes previously discussed, the value of the natural period is of considerable significance. Referring to Figs. 7.11 and 7.12 it may be observed that in both elastic and plastic cases the maximum deflection or the required resistance decreases as the natural period T_n increases. This increase in natural period can be accomplished by either increasing mass or decreasing stiffness. Thus economy can often be achieved by making the structure very flexible, reducing the required strength.

If the load-time variation is periodic, the value of the natural period is of primary importance. Referring to Fig. 3.5, which gives dynamic-load factors for a sinusoidal load, it is obvious that the designer should avoid a condition in which the natural period of the structure is close to the period of the load. A similar effect is noted in Fig. 7.13 for a load with a finite rise time where the dynamic-load factor is 1 when the ratio of rise time to natural period is an integer. For this type of load a small value of T_n is generally desirable.

7.9. Multidegree Systems. When dynamic loads are applied to a building frame or other structures consisting of an arrangement of elements it is usually possible to analyze the elements as separate one-degree systems. For example, when a floor made up of a slab-and-beam system

is analyzed, the slab is first designed assuming that the supports do not move during the response. The dynamic reaction of the slab is then applied to the beam.

Usually it is necessary to determine the dynamic reaction of the first element by a numerical integration as described in Chap. 8. However, in some cases the dynamic reaction may be idealized without actual computations. For example, if the natural frequency of the first element is much higher than that of the second, and if the first is designed plastically, it may be possible to represent the load on the second element by a rectangular pulse. The load value would correspond to the maximum resistance of the first element. In other cases it may be desirable to

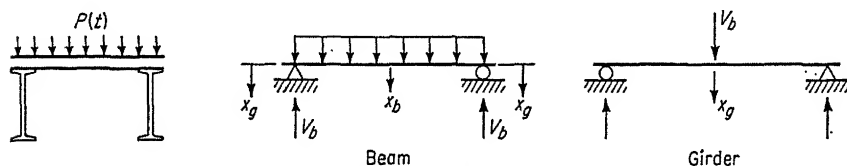


FIG. 7.26. Beam-and-girder system.

analyze the supporting member by numerical integration since the applied load cannot be idealized in any convenient manner.

Considering again the slab-and-beam floor system, the procedure described above can be used only if the deflection of the beam does not appreciably affect the resistance of the slab during its response to the load. This will be true if the beam deflections are small or take place much more slowly than those of the slab. As an approximate rule of thumb it may be stated that two connected elements can be analyzed separately if the natural frequency of one is at least two times that of the other. Generally speaking, there is less danger of error by this procedure if the elements are designed plastically than if the behavior is purely elastic.

If the two connected elements cannot be analyzed separately, they must be treated as a two-degree system. The best method in this event is numerical integration. As an example consider the beam and girders shown in Fig. 7.26. Both are assumed to be simply supported, and both elements are replaced by equivalent systems. For the beam the equation of motion is

$$m_{be}\ddot{x}_b = P_{be} - R_{be}$$

$$R_{be} = k_{be}(x_b - x_g)$$

where

In this equation all terms are for the equivalent system obtained by the factors of Table 7.1. P_{be} is the equivalent beam load which varies with time. In each time interval of the numerical solution this equation is used to evaluate x_b at the end of the interval. At the same time the

dynamic reaction is computed by

$$V_b = 0.39R_b + 0.11P_b$$

Simultaneously, the analysis of the girder proceeds, using the equation of motion:

$$m_{ge}\ddot{x}_g = V_{be} - k_{ge}x_g$$

where again all terms are for the equivalent girder system. This approach is of course approximate since the transformation factors are based on the assumption that the two elements act independently.

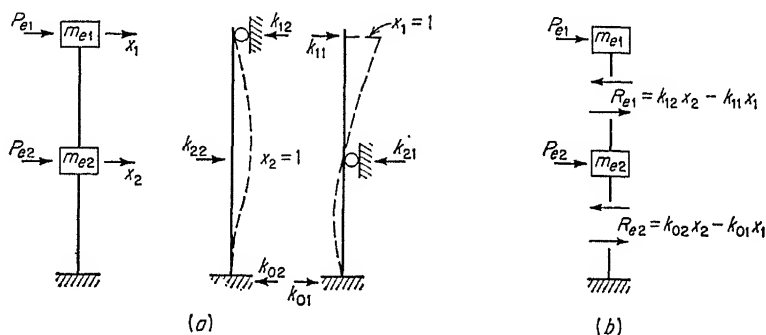


FIG. 7.27. Equivalent system for a two-story-building frame.

As a second example of two-degree analysis consider the two-story frame shown in Fig. 7.1c. Using the equivalent system of lumped masses and springs, established as described in Sec. 7.7d, the stiffness coefficients in the elastic range must first be determined. This is done by conventional elastic analysis as indicated in Fig. 7.27. Each mass is given a unit deflection, while the other is held in position and the forces k_{11} , k_{21} , . . . are determined. In the elastic range the equations of motion for the two masses are obvious from Fig. 7.27b:

$$\begin{aligned} m_{e1}\ddot{x}_1 &= P_{e1} - R_{e1} \\ m_{e2}\ddot{x}_2 &= P_{e2} + R_{e1} - R_{e2} \end{aligned}$$

where P_{e1} and P_{e2} are loads which vary with time, and R_{e1} and R_{e2} are determined at any instant from the deflections x_1 and x_2 . In the numerical integration these two equations are applied simultaneously.

If plastic deformation takes place, the values of R_{e1} and R_{e2} are limited by the plastic strength of the columns in that story. After the elastic limit has been reached in a story the corresponding R remains constant. In some cases, however, the behavior in one story may again become elastic before maximum deflections have occurred. In this event the resistance again becomes a function of the displacements.

REFERENCES

1. U.S. Army Corps of Engineers: "Engineering Manual for Protective Construction, Pt. III, Design of Structures to Resist the Effects of Atomic Bombs," prepared in part by the Massachusetts Institute of Technology under Contract DA49-129-Eng-178 with the U.S. Army. Also referred to in text as Chap. 1, Ref. 8.
2. Newmark, N. M.: An Engineering Approach to Blast Resistant Design, *Trans. ASCE*, vol. 121, 1956.
3. Whitney, C. S., B. G. Anderson, and E. Cohen: Design of Blast Resistant Construction for Atomic Explosions, *J. ACI*, March, 1955.

PART 3

**MODERN COMPUTATIONAL TECHNIQUES APPLICABLE
TO RESPONSE CALCULATIONS**

INTRODUCTION TO NUMERICAL-INTEGRATION METHODS AND THEIR APPLICATION TO DYNAMIC-RESPONSE CALCULATIONS

8.1. General. The first course in differential equations usually gives the student the impression that there are exact solutions for all types of differential equations. This is far from reality. In fact, most mathematical models that are used to describe physical situations lead to differential equations which are difficult if not impossible to solve implicitly by a direct mathematical process. Even if a direct solution does exist, its use to obtain numerical results is often tedious and time-consuming. This condition has led in recent years to the rapid development of numerical methods of analysis, computing machines, and machine methods of computation.

For many of the simple models which are adopted to represent the behavior of structural-dynamics systems, the resulting differential equations can be solved exactly in the elastic range if the loading functions are simple enough to be expressed mathematically.

If the loading function is complex, solutions can often be obtained by subdividing the load into simple segments. The solutions for these simple segments when superposed yield the solution for the complex loading if allowances are made for the varying initial conditions. However, this type of solution is much more time-consuming than most numerical-analysis methods.

A typical loading for a structure subjected to blast is shown in Fig. 8.1. Four separate equations are needed to express $f(t)$.

If this load were applied to a single-degree-of-freedom elasto-plastic system, to describe the resulting equations of motion would require eight separate differential equations. The solution of these equations by a rigorous method is generally impractical.

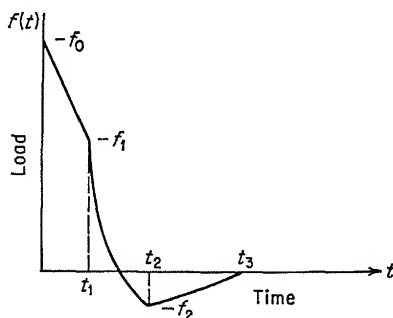


FIG. 8.1. A typical dynamic load for blast.

The rigorous method is further complicated if the resistance cannot be represented by a single mathematical function. Two practical cases are shown in Fig. 8.2*a* and *b*. Figure 8.2*a* is the idealized representation of the resistance function of a fixed-end beam, and Fig. 8.2*b* represents the lateral resistance of the columns of a single-story frame building with the vertical load taken into consideration.

Perhaps the greatest need for numerical methods of analysis arises when considering the behavior of complex structural systems beyond the elastic range. For a multi-degree-of-freedom dynamic system in the elastic range the response may be obtained by superposition of normal modes.

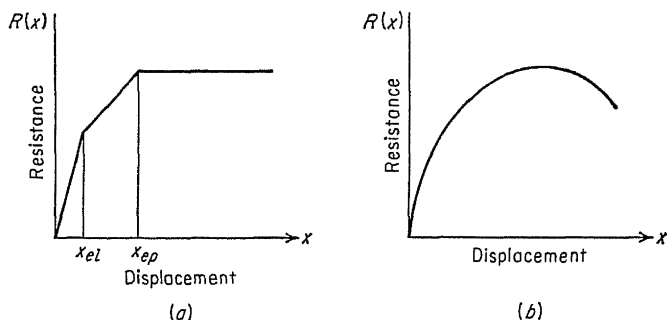


FIG. 8.2. Typical resistance functions. (a) Fixed-end beam; (b) column resisting lateral motion and subject to axial load.

Using the normal-mode procedure beyond the elastic range requires the determination of new sets of normal modes after each new plastic hinge is formed. This procedure is clearly long-winded and undesirable if an alternative procedure is available. It is the purpose of this chapter to introduce some of the better-known numerical-integration procedures and equations, to indicate their origin, their applicability to the solution of dynamic equations of motion, the errors resulting from these methods, and lastly to illustrate the use of some of them in a typical problem.

8.2. Differential Equations. Since all problems in structural dynamics reduce to the problem of solving a differential equation or a set of simultaneous differential equations, it is desirable to specify what a differential equation is.

If t is an independent variable, y a dependent variable, dy/dt , d^2y/dt^2 , d^3y/dt^3 , . . . , d^ny/dt^n the first n derivatives of y with respect to t , then a differential equation is a relation between all or some of the members:

$$y, t, \frac{dy}{dt}, \dots, \frac{d^ny}{dt^n}$$

in which at least one derivative occurs. The order of a differential equation is defined as the order of the highest derivative present in it. Thus

the differential equation of motion for a single-degree-of-freedom system,

$$\frac{d^2y}{dt^2} = f\left(y, t, \frac{dy}{dt}\right)$$

is a second-order system.

8.3. Numerical Integration. The problems encountered in structural dynamics are usually analyzed by writing a differential equation describing the motion of one or more generalized coordinates. These equations take the form of second-order differential equations with displacement as the dependent variable and time the independent variable. Generally, also, the initial conditions of velocity and displacement are known. An exact solution of such an equation implies the determination of the displacement and velocity of the system as a function of time.

A numerical solution consists in obtaining numerical values of the displacement and velocity at discrete times. These displacement and velocity values are obtained by a step-by-step integration procedure, starting with the necessary initial conditions and evaluating the conditions at the end of a discrete time interval. These values are then the basis for calculation of the velocity and displacement at successive discrete times.

Historically, the development of numerical-integration methods has resulted primarily from the efforts of individuals searching for the answers to specific problems in science or engineering. These researchers devised methods based on the physical behavior of the system of immediate interest to them with but little regard for mathematical rigor. In recent years, as the need for numerical methods of analysis has increased, mathematicians have become interested in the problem and have begun to provide a mathematical classification of the available procedures. In addition, much effort is now being applied to the subject of errors, convergence, and stability of the various numerical-integration methods.

A quick way to become acquainted with numerical-integration procedures is to derive some of the equations that result from purely physical considerations and use them in a problem or two. This is the subject of the next paragraph. In a later paragraph some of the better-known numerical-integration procedures which have been derived from a more rigorous mathematical point of view are presented.

8.4. Acceleration Methods of Numerical Integration. Consider a single-degree-of-freedom elasto-plastic system, subjected to a time-varying force as illustrated in Fig. 8.3. The differential equation of motion is

$$m\ddot{x} = f(t) - R(x) \quad (8.1)$$

The load, resistance, acceleration, velocity, and displacement are plotted against time in Fig. 8.4.

Suppose $t_0, t_1, t_2, \dots, t_{n+1}$ is a time sequence. The time interval from

t_n to t_{n+1} is denoted by Δt_n . The dynamic load is assumed to start at $t = t_0$. The acceleration, velocity, and displacement at t_n are denoted by \ddot{x}_n , \dot{x}_n , and x_n , respectively. If the acceleration in the time interval Δt_n is represented by $\ddot{x}(t)$, the velocity and displacement at t_{n+1} are given, respectively, by the following equations:

$$\dot{x}_{n+1} = \dot{x}_n + \int_{t_n}^{t_{n+1}} \ddot{x}(t) dt \quad (8.2)$$

$$x_{n+1} = x_n + \dot{x}_n(\Delta t_n) + \int_{t_n}^{t_{n+1}} \left[\int \ddot{x}(t) dt \right] dt \quad (8.3)$$

These two equations indicate that the velocity and displacement at t_{n+1} can be obtained by extrapolation from the corresponding values at t_n once the acceleration in the time interval Δt_n is known.

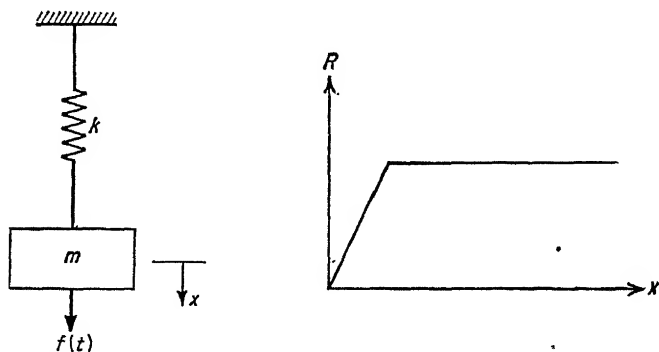


FIG. 8.3. Single-degree-of-freedom elasto-plastic system.

In the analysis of structures under dynamic load, the velocity and displacement at the initiation of load are usually known and equal to zero; that is,

$$\text{At } t = t_0 = 0, \quad x_0 = 0 \quad \text{and} \quad \dot{x}_0 = 0$$

By applying Eqs. (8.2) and (8.3), the values of x_1 and \dot{x}_1 can be obtained provided that $\ddot{x}(t)$ is known in the time interval from t_0 to t_1 . From the values of x_1 and \dot{x}_1 the values of x_2 and \dot{x}_2 can be obtained. This process can be continued until the values of x_n and \dot{x}_n are obtained. This is what is known as a step-by-step extrapolation method.

For engineering applications, simplified extrapolation formulas are often used which are obtained by assuming a simple acceleration-time relationship in any time interval Δt_n . Three procedures are developed in the following. In one case the acceleration is assumed to be constant in the time interval. In the second case the acceleration is assumed to vary linearly with time. In the third case, the acceleration is assumed to consist of a series of pure pulses.

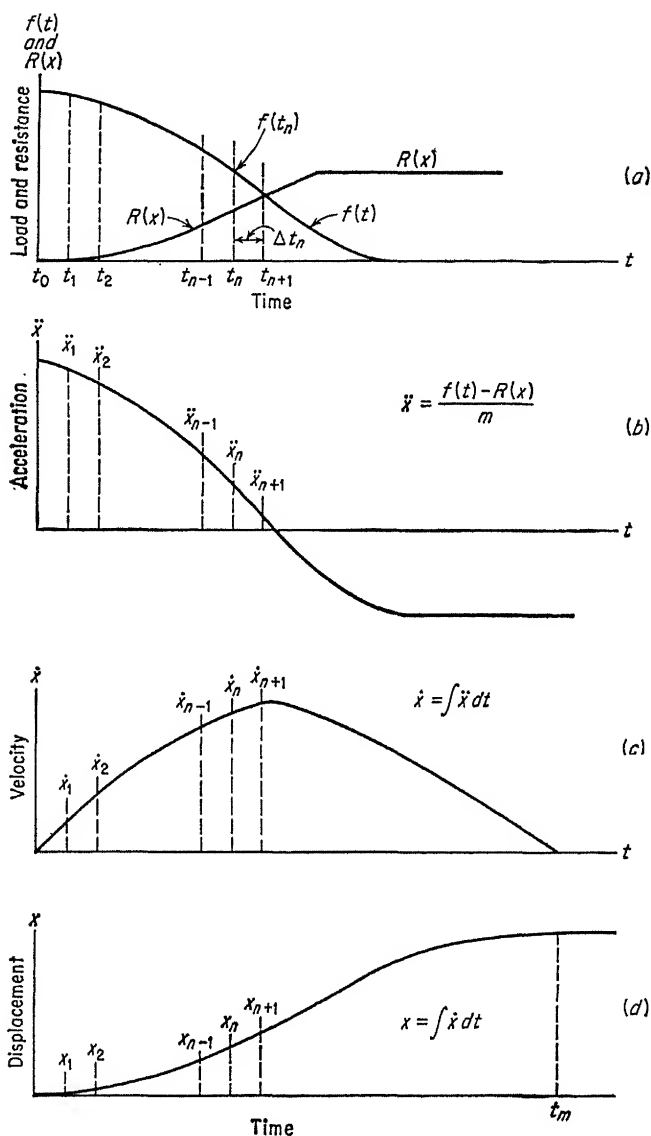


FIG. 8.4. Load, resistance, acceleration, velocity, and displacement vs. time. (a) Load and resistance; (b) acceleration; (c) velocity; (d) displacement.

a. Constant-acceleration Procedure. Consider Eq. (8.1) and Fig. 8.3, for which the initial conditions x_0 and \dot{x}_0 at $t = 0$ are known. With these data it is possible to evaluate \ddot{x}_0 at $t = 0$. Since no other data are known, a simple procedure illustrated by Fig. 8.5b is to assume that the acceleration remains constant for a finite time interval until a new value of the

acceleration is known. For most practical cases this is obviously wrong, but the error need not be very large if the time interval is made very small.

If the acceleration is constant, $\ddot{x}(t) = \ddot{x}_0$, the equations for determining the displacement and velocity at the end of the first time interval Δt obtained from Eqs. (8.2) and (8.3) are

$$x_1 = x_0 + \dot{x}_0 \Delta t + \frac{1}{2} \ddot{x}_0 (\Delta t)^2 \quad (8.4)$$

$$\dot{x}_1 = \dot{x}_0 + \ddot{x}_0 \Delta t \quad (8.5)$$

With Eqs. (8.4) and (8.5) and the value \ddot{x}_0 obtained by using the initial conditions in Eq. (8.1), it is possible to evaluate x_1 and \dot{x}_1 . A second cycle of computations begins with use of x_1 and \dot{x}_1 in Eq. (8.1) to obtain \ddot{x}_1 .

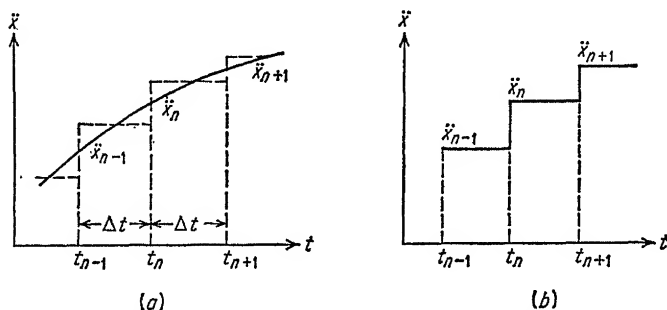


FIG. 8.5. Comparison of actual and acceleration curves used in constant-acceleration extrapolation method. (a) Actual acceleration curve; (b) approximate acceleration curve.

This is followed by the evaluation of x_2 and \dot{x}_2 in Eqs. (8.4) and (8.5), which, with properly modified subscripts, have the form

$$x_2 = x_1 + \dot{x}_1 \Delta t + \frac{1}{2} \ddot{x}_1 (\Delta t)^2$$

$$\dot{x}_2 = \dot{x}_1 + \ddot{x}_1 \Delta t$$

By repeating this procedure stepwise in Δt , the time variations of \dot{x} and x are obtainable.

b. Linear-acceleration Procedure. A closer representation of a practical case than is obtained by the constant-acceleration method is usually obtained by assuming that the acceleration varies linearly with time in any time interval Δt , as shown in Fig. 8.6. If a small enough value of Δt is used, a straight-line variation of acceleration in a time interval Δt can provide a very good approximation to a general acceleration curve.

In the time interval $\Delta t_n = t_{n+1} - t_n$, the acceleration is given by

$$\ddot{x}(t) = \ddot{x}_n + \frac{\ddot{x}_{n+1} - \ddot{x}_n}{\Delta t_n} (t - t_n) \quad (8.6)$$

Substituting Eq. (8.6) into Eqs. (8.2) and (8.3), the recurrence formulas

for displacement and velocity are given respectively by

$$x_{n+1} = x_n + \dot{x}_n \Delta t + \frac{(\Delta t)^2}{6} (2\ddot{x}_n + \ddot{x}_{n+1}) \quad (8.7)$$

$$\dot{x}_{n+1} = \dot{x}_n + \frac{\Delta t}{2} (\ddot{x}_n + \ddot{x}_{n+1}) \quad (8.8)$$

These Eqs. (8.7) and (8.8) can be utilized in two manners, depending on the time that can be devoted to the problem and the relative accuracy desired. In the less time-consuming but more approximate approach

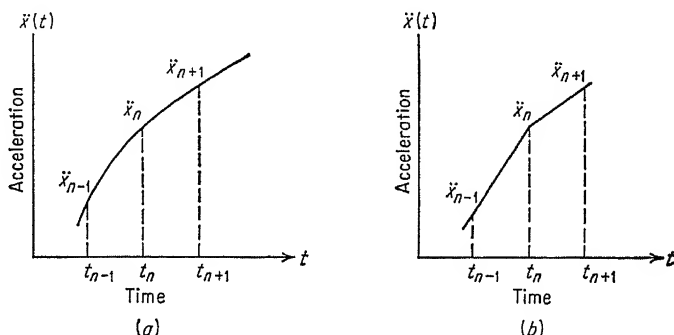


FIG. 8.6. Comparison of actual and approximate acceleration curves used in linear-acceleration extrapolation method. (a) Actual acceleration curve; (b) approximate acceleration curve.

Eqs. (8.7) and (8.8) are used as an extrapolation procedure with \ddot{x}_{n+1} determined from a supplementary Eq. (8.9) based on the assumption of linear variation of acceleration in two successive and equal time intervals.

$$\ddot{x}_{n+1} = \ddot{x}_n + (\ddot{x}_n - \ddot{x}_{n-1}) = 2\ddot{x}_n - \ddot{x}_{n-1} \quad (8.9)$$

With these equations the same procedure as described for the constant-acceleration assumption may be followed to obtain the time variation of displacement x .

A more accurate procedure, but a slower procedure than either of the two described above, uses Eqs. (8.7) and (8.8) in an iterative manner. This condition results from the fact that \ddot{x}_{n+1} is needed for the determination of x_{n+1} , but \ddot{x}_{n+1} cannot be known until x_{n+1} is known. This is the usual case where \ddot{x} is a function of x (sometimes of x and \dot{x}) [see Eq. (8.1)].

The procedure is to obtain a preliminary value of \ddot{x}_{n+1} in one of several ways, depending on the computational circumstances:

1. By letting it equal \ddot{x}_n
2. By estimating a value from a graphical variation of \ddot{x}
3. By guessing
4. By using Eq. (8.9) above
5. By assuming that $x_{n+1} = x_n + \dot{x}_n \Delta t$

In any event, this value of \ddot{x}_{n+1} and available values of x_n , \dot{x}_n , and \ddot{x}_n are substituted in Eqs. (8.7) and (8.8) to obtain x_{n+1} . (\dot{x}_{n+1} is not needed until the next time interval; therefore it is not computed until a satisfactory value of x_{n+1} has been computed.)

The value of x_{n+1} or the corresponding value of \ddot{x}_{n+1} is compared with the original estimate. If the two values do not agree within the desired limits (the limits of precision may vary with the particular problem), the calculated value of x_{n+1} or \ddot{x}_{n+1} is considered as the new estimate and the process is repeated until two successive values of x_{n+1} agree satisfactorily with each other.

In the application of the above method, the successive time intervals do not have to be equal, although they are often chosen to be equal to simplify the computations.

To determine the magnitude of the time interval to be used for a given problem, a number of factors have to be considered. First, the time interval must be chosen so that within it the acceleration can be reasonably approximated by a straight line. Secondly, the convergence of the trial-and-error procedure must be reasonably rapid. Thirdly, the number of steps necessary for the evaluation of the maximum displacement must be reasonable. For the first and second considerations, the time interval should be small, while for the third consideration, the time interval should be large. Experience indicates that a time interval $\Delta t = T_n/6$ is reasonable in the elastic range, but a larger Δt can be used in the plastic region provided that the external-load variation in the time interval is a reasonably straight line. Some writers urge that the time interval be varied with the rate of convergence of the trial-and-error procedure as follows:

1. If the solution converges in less than two trials, double the time interval.
2. If the solution converges in four or more trials, change to one-half the time interval.

c. Constant-velocity Procedure. This procedure was developed at MIT from the physical visualization of the dynamic behavior of a mass-spring system subjected to a pulse load and given the name *acceleration-pulse method*. The term derives from the basic assumption in the derivation, namely, that the area under the acceleration curve may be replaced by a train of equivalent pulses acting at time intervals Δt (Fig. 8.7b). (The resulting equations are obtainable by another approach which has been known for considerable time.)

The magnitude of the acceleration pulse at t_n is given by .

$$I(t_n) = \ddot{x}_n \Delta t \quad (8.10)$$

This is shown in Fig. 8.7b. Since a pulse is applied at t_n , there is a dis-

continuity in the value of velocity at t_n . In the time interval Δt the velocity is constant and the displacement varies linearly with time. The velocity and displacement thus obtained are shown in Fig. 8.7c and d.

Suppose t_n^- and t_n^+ indicate the time immediately before and after the application of pulse at t_n , and let $(\dot{x}_n)^-$ and $(\dot{x}_n)^+$ indicate, respectively, the velocity at t_n^- and t_n^+ . The two velocities are related by Eq. (8.11).

$$(\dot{x}_n)^+ = (\dot{x}_n)^- + \ddot{x}_n \Delta t \quad (8.11)$$

The relationship between x_{n-1} and x_n and between x_n and x_{n+1} are given by

$$\begin{aligned} x_n - x_{n-1} &= (\dot{x}_n)^- \Delta t \\ x_{n+1} - x_n &= (\dot{x}_n)^+ \Delta t \end{aligned} \quad (8.12)$$

Combining Eqs. (8.11) and (8.12), the three successive displacements are related by

$$x_{n+1} = 2x_n - x_{n-1} + \ddot{x}_n (\Delta t)^2 \quad (8.13)$$

This is the basic recurrence formula for the acceleration-pulse extrapolation method. Once the values of x at t_{n-1} and t_n are known, the value of x at t_{n+1} can be directly computed without resorting to a trial-and-error procedure.

The evaluation of x_1 by the recurrence formula needs special consideration. From Eq. (8.13), when $n = 0$, x_1 is given by

$$x_1 = 2x_0 - x_{-1} + \ddot{x}_0 (\Delta t)^2 \quad (8.14)$$

Both x_0 and x_{-1} are equal to zero, and the expression of x_1 is simplified to

$$x_1 = \ddot{x}_0 (\Delta t)^2 \quad (8.15)$$

The correct value of \ddot{x}_0 for use in Eq. (8.15) is not as indicated in Fig. 8.8a or b but is given by

$$\ddot{x}_0 = \frac{1}{2}(\ddot{x}_0)' + \frac{1}{6}[\ddot{x}_1 - (\ddot{x}_0)'] \quad (8.16)$$

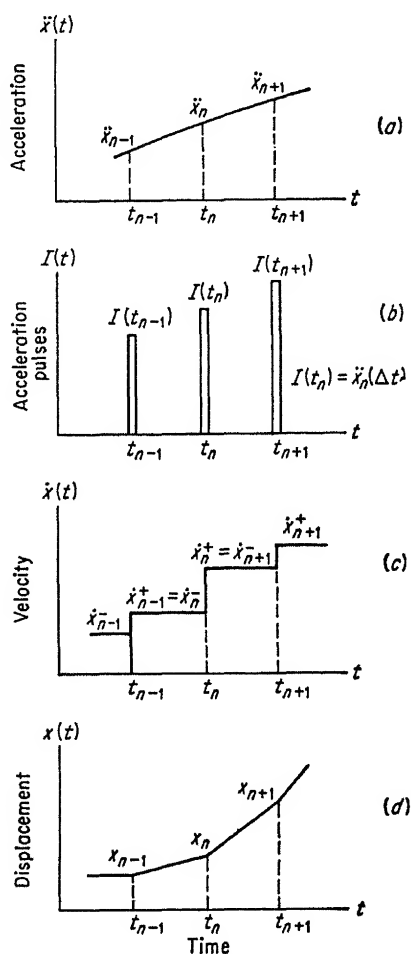


FIG. 8.7. Acceleration-pulse extrapolation method. (a) Given acceleration curve; (b) acceleration pulses to replace the given acceleration curve; (c) velocity; (d) displacement.

When Eq. (8.16) is used in Eq. (8.15) for the evaluation of x_1 , the value thus obtained is that given by Eq. (8.7), which is based on the linear-acceleration extrapolation method. In order to avoid a trial-and-error procedure for the evaluation of x_1 , the value of \ddot{x}_1 in Eq. (8.16) is taken to be $F(t_1)/m$ instead of the exact value indicated by Eq. (8.1). If $(\ddot{x}_0)' = 0$, as in Fig. 8.8c, \ddot{x}_0 from Eq. (8.16) is equal to $\ddot{x}_1/6$. If $(\ddot{x}_0)'$ and \ddot{x}_1 are approximately equal to each other as in Fig. 8.8a and b, the value $\ddot{x}_0 = (\ddot{x}_0)'/2$ may be used.

Equation (8.13) is directly applicable for the evaluation of x_2, x_3, \dots, x_{n+1} whenever the acceleration $\ddot{x}(t)$ is a continuous curve.

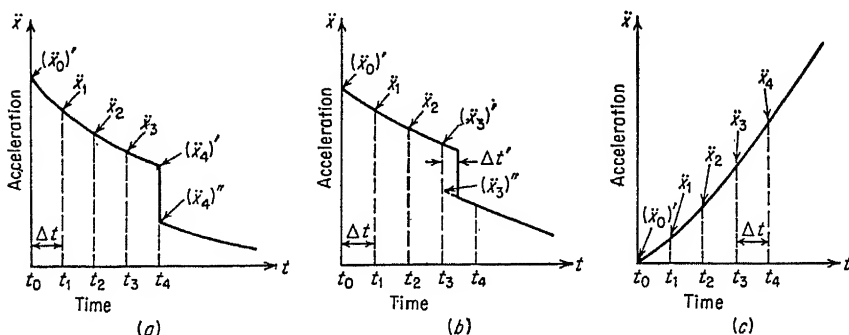


FIG. 8.8. Discontinuities in the acceleration curve.

When there is a discontinuity in the acceleration the equation is still applicable provided a modified value of the acceleration is used. This is illustrated in Fig. 8.8a and b. In Fig. 8.8a there is a discontinuity at t_4 which occurs at the end of the time interval Δt . Under this condition, the value of \ddot{x}_n used in the numerical procedure is the average value at the discontinuity, namely, $\ddot{x}_4 = \frac{1}{2}[(\ddot{x}_4)' + (\ddot{x}_4)'']$. In Fig. 8.8b, where the discontinuity occurs within the time interval Δt , a reasonable value for the acceleration term may be determined from Eq. (8.17):

$$\ddot{x}_3 = \frac{1}{2} \left\{ (\ddot{x}_3)' + (\ddot{x}_3)'' + [(\ddot{x}_3)' - (\ddot{x}_3)''] \left(\frac{\Delta t'}{\Delta t} \right)^2 \right\} \quad (8.17)$$

For a given problem if there are one or two discontinuities, the method described above can be applied conveniently. However, if the number of discontinuities is large, it is more convenient to replace the given acceleration curve by a smooth curve.

The main advantage of the acceleration-pulse extrapolation method is that the numerical computation is straightforward and involves no trial-and-error procedure. Its main disadvantage is that the result is less accurate than the linear-acceleration method. Another disadvantage of this method is that it is not self-checking and any numerical mistake in

the computation is increased by geometrical progression in subsequent steps. Hence one must be extremely careful to avoid any numerical mistakes, especially in the early stages of computation.

d. Newmark β Method. A versatile method of numerical integration is the β method originated by Prof. N. M. Newmark. This is a method in which a parameter β is introduced which can be changed to suit the requirements of the problem at hand. The net effect of β is to change the form of the variation of acceleration in the time interval Δt . For the second-order differential equation of motion

$$x_{n+1} = x_n + \dot{x}_n \Delta t + (\frac{1}{2} - \beta) \ddot{x}_n (\Delta t)^2 + \beta \ddot{x}_{n+1} (\Delta t)^2 \quad (8.18)$$

$$\text{and} \quad \dot{x}_{n+1} = \dot{x}_n + \frac{1}{2}(\ddot{x}_n + \ddot{x}_{n+1}) \Delta t \quad (8.19)$$

When β is assigned certain values, the equations reduce to the form of procedures advanced by other writers. For example, if $\beta = \frac{1}{6}$, Eq. (8.18) becomes

$$x_{n+1} = x_n + \dot{x}_n \Delta t + \frac{1}{3} \ddot{x}_n (\Delta t)^2 + \frac{1}{6} \ddot{x}_{n+1} (\Delta t)^2 \quad (8.20)$$

which was introduced earlier as the linear-acceleration method [Eq. (8.7)].

A very thorough investigation of this method covering its error, stability, and convergence for various values of β is presented in Refs. 6 and 7.

e. Numerical Example. An example is given to illustrate the actual application of some of the methods of numerical integration described above. The same example is evaluated by three different methods:

1. The rigorous method
2. The linear-acceleration extrapolation method
3. The acceleration-pulse extrapolation method

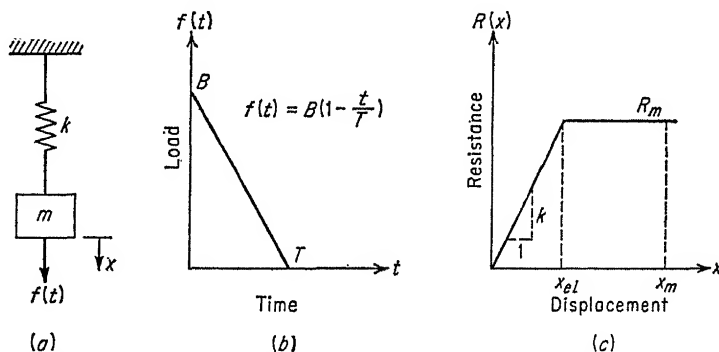


FIG. 8.9. External load and resistance function for one-degree illustrative example. (a) 1° system; (b) load function; (c) resistance function.

A single-degree-of-freedom system is considered with the external load and the resistance function for the example as shown in Fig. 8.9b and c, respectively.

The assumed dimensional parameters of the dynamic system are:

$$\begin{aligned} m &= 2.5 \text{ kip-sec}^2/\text{ft} \\ k &= 9,860 \text{ kips/ft} \\ R_m &= 750 \text{ kips} \\ x_{el} &= 0.076 \text{ ft} \\ T &= 0.10 \text{ sec} \\ B &= 1,000 \text{ kips} \\ T_n &= 2\pi \sqrt{m/k} = 0.10 \text{ sec} \end{aligned}$$

By the rigorous method of Sec. 3.7 the displacement, in the time

TABLE 8.1. COMPARISON OF RESULTS OBTAINED BY DIFFERENT METHODS OF ANALYSIS

Time t , sec	Displacement function x		
	Linear- acceleration extrapolation method	Acceleration- pulse extrapolation method	Rigorous method
0	0	0	0
0.01	0.0181	0.0200	0.0186
0.02	0.0633	0.0683	0.0651
0.03	0.1182	0.1216	0.1203
0.04	0.1713	0.1729	0.1718
0.05	0.2184	0.2182	0.2184
0.06	0.2556	0.2535	0.2548
0.07	0.2787	0.2748	0.2785
0.08	0.2839	0.2781	
0.09	0.2671	0.2594	$t_m = 0.077 \text{ sec}$ $x_m = 0.2825$
Maximum displacement...	0.2839	0.2781	0.2825

interval from 0 to T , is given by

$$x = x_s \left[\sqrt{1 + \left(\frac{T_n}{2\pi T} \right)^2} \sin \left(2\pi \frac{t}{T_n} - \phi \right) + \left(1 - \frac{t}{T} \right) \right] \quad (8.21)$$

where $x_s = B/k$ = static deflection produced by peak load B

$$\phi = \tan^{-1} (2\pi T/T_n)$$

Substituting into Eq. (8.21) we obtain the time t_{el} to reach the maximum elastic deflection x_{el} .

$$x_{el} = 0.076 \text{ ft}$$

$$t_{el} = 0.22 \text{ sec}$$

TABLE 8.2. EXAMPLE OF COMPUTATION BY THE LINEAR-ACCELERATION EXTRAPOLATION METHOD

n	Trial no.	t_n , sec	x_n , ft	\dot{x}_n , ft/sec	$\ddot{x}_n = \frac{P_n - R_n}{m}$, ft/sec ²	Assumed x_{n+1} , ft	P_{n+1} , kips	R_{n+1} , kips	$\ddot{x}_{n+1} = \frac{P_{n+1} - R_{n+1}}{m}$, ft/sec ²	\dot{x}_{n+1} , ft/sec	Computed x_{n+1} , ft
0	1	0	0	0	+400	0.0150	900	145	+282	0.0180
	2	0	0	0	+400	0.0180	900	177	+289	0.0181
	3	0	0	0	+400	0.0181	900	180	+288	+3.44	0.0181
1	1	0.01	0.0181	+3.44	+288	0.0525	800	518	+113	0.0640
	2	0.01	0.0181	+3.44	+288	0.0640	800	631	+68	0.0632
	3	0.01	0.0181	+3.44	+288	0.0633	800	624	+70	+5.23	0.0633
2	...	0.02	0.0633	+5.23	+70	*	700	750	-20	+5.48	0.1182
3	...	0.03	0.1182	+5.48	-20	*	600	750	-60	+5.08	0.1713
4	...	0.04	0.1713	+5.08	-60	*	500	750	-100	+4.28	0.2184
5	...	0.05	0.2184	+4.28	-100	*	400	750	-140	+3.08	0.2556
6	...	0.06	0.2556	+3.08	-140	*	300	750	-180	+1.48	0.2787
7	...	0.07	0.2787	+1.48	-180	*	200	750	-220	-0.52	0.2839
8	...	0.08	0.2839	-0.52	-220	*	100	750	-260	0.2671

* The displacement is larger than the maximum elastic deflection. R_{n+1} is a constant equal to 750 kips. The computation of \ddot{x}_{n+1} and x_{n+1} becomes straightforward without resorting to a trial-and-error procedure.

$$\text{NOTE: } P_n = f(t_n) = 1,000 \left[1 - \frac{n(\Delta t)}{0.1} \right] \quad \Delta t = 0.01 \text{ sec}$$

$$R_n = kx_n = 9,860x_n \quad \text{for } x < x_d = 0.0760 \text{ ft}$$

$$R_n = R_m = 750 \text{ kips} \quad \text{for } x_n \geq 0.0760 \text{ ft}$$

$$\dot{x}_{n+1} = \dot{x}_n + \frac{\ddot{x}_n + \ddot{x}_{n+1}}{2} \Delta t$$

$$x_{n+1} = x_n + \dot{x}_n \Delta t + \left(\frac{\ddot{x}_n}{3} + \frac{\ddot{x}_{n+1}}{6} \right) (\Delta t)^2$$

Differentiating Eq. (8.21) and evaluating at t_{el} gives

$$\dot{x}_{el} = 5.44 \text{ ft/sec}$$

With these results as initial conditions for the plastic-resistance region the rigorous method yields

$$x_m = 0.2825 \text{ ft} \quad \text{at } t_m = 0.077 \text{ sec}$$

The displacements computed from the rigorous-method equations are tabulated in column 4 of Table 8.1.

The detailed computations of the linear-acceleration and acceleration-pulse extrapolation methods are given in Tables 8.2 and 8.3, respectively. The displacements obtained by the three methods are listed in Table 8.1. It is seen that the error in using the numerical methods in the evaluation of the maximum displacement is less than 1.5 per cent.

TABLE 8.3. EXAMPLE OF COMPUTATION BY ACCELERATION-PULSE
EXTRAPOLATION METHOD

n	t , sec	P_n , kips	R_n , kips	$P_n - R_n$, kips	$\ddot{x}_n = (P_n - R_n)/m$, ft/sec ²	$\ddot{x}_n(\Delta t)^2$, ft	$2x_n$, ft	x_{n-1} , ft	x_{n+1} , ft
0	0	+1,000/2	0	+500	+200	+0.02	0	0	0
1	+0.01	+ 900	+197	+703	+283	+0.0283	+0.0400	0	+0.0200
2	+0.02	+ 800	+674	+126	+ 50.4	+0.0050	+0.1366	+0.0200	+0.0683
3	+0.03	+ 700	+750	- 50	- 20	-0.0020	+0.2432	+0.0683	+0.1216
4	+0.04	+ 600	+750	-150	- 60	-0.0060	+0.3458	+0.1216	+0.1729
5	+0.05	+ 500	+750	-250	-100	-0.0100	+0.4364	+0.1729	+0.2182
6	+0.06	+ 400	+750	-350	-140	-0.0140	+0.5070	+0.2182	+0.2535
7	+0.07	+ 300	+750	-450	-180	-0.0180	+0.5496	+0.2535	+0.2748
8	+0.08	+ 200	+750	-550	-220	-0.0220	+0.5562	+0.2748	+0.2781
9	+0.2594

NOTE: $P_n = f(t_n) = 1,000 \left(1 - n \frac{\Delta t}{0.1} \right)$

$P_0 = 1,000/2$ (starting approximation)

$R_n = \begin{cases} kx_n & \text{for } x_n < x_{el} = 0.0760 \text{ ft} \\ R_m = 750 & \text{for } x_n \geq x_{el} \end{cases}$

$x_{n+1} = 2x_n - x_{n-1} + \ddot{x}_n(\Delta t)^2$

$\Delta t = 0.01$

8.5. Other Methods of Numerical Integration. In the previous sections the discussion is devoted to numerical-integration methods that are derived on the basis of assumed variations of acceleration in a time interval. The remainder of this chapter is devoted to a general description of various other methods of numerical integration with comments on their usefulness in integrating second-order differential equations with known initial conditions. This is by no means intended to be a comprehensive treatment (see References). In the following sections the time increment is designated by the symbol h .

a. Taylor Series. The Taylor-series method is one of the most direct methods for starting the solution of a differential equation. In fact, if the range of the independent variable is limited, the Taylor series can be used to obtain the complete solution. For problems in structural dynamics, however, it is the starting ability that should be most useful.

When a Taylor series is found, the range for which it has a specified accuracy can be determined by equating the first neglected term to the allowable error. This is shown below.

The Taylor series of $y(t + h)$ about t is given by

$$\begin{aligned} y(t + h) &= y(t) + hy'(t) + \frac{h^2}{2!} y''(t) + \frac{h^3}{3!} y'''(t) + \cdots \quad (8.22) \\ &= \sum_{n=0}^{n=\infty} \frac{h^n}{n!} y^n(t) \end{aligned}$$

where $y^n(t)$ stands for $d^n y/dt^n$, $y^0(t) = y(t)$, and $0! = 1$. Consider the equation

$$\ddot{y} = f(y, t, \dot{y}) \quad (8.23)$$

subject to $t = t_0 = 0$, $y = y_0$, $\dot{y} = \dot{y}_0$.

By substitution of $y = y_0$ and $\dot{y} = \dot{y}_0$ in Eq. (8.23), \ddot{y}_0 may be calculated at $t = 0$.

Differentiation of Eq. (8.23) gives

$$\ddot{y} = g(y, t, \dot{y}, \ddot{y}) \quad (8.24)$$

and by substitution in Eq. (8.24), \ddot{y}_0 is evaluated at $t = 0$.

Thus by successive differentiation and evaluation the terms for the Taylor series [Eq. (8.22)] are determined for the value of y in the neighborhood of $t = t_0 = 0$.

The range of t for which the Taylor series is valid depends on the accuracy required in the value of y . If the accuracy can be specified initially, the number of derivatives to consider is easily determined by direct substitution.

For example, consider the second-order equation

$$\ddot{y} + 3ty = 6y$$

Subject to $t = 0$, $\dot{y}_0 = 0.1$, $y_0 = 1$,

$$\begin{aligned} \ddot{y}_0 &= -3t\dot{y} + 6y = -3(0)(0.1) + 6(1) = 6 \\ \ddot{\dot{y}}_0 &= -3t\ddot{y} - 3\dot{y} + 6\dot{y} = -3t\ddot{y} + 3\dot{y} = -3(0)(6) + 3(0.1) = 0.3 \\ y_0^{IV} &= -3t\ddot{\dot{y}} - 3\dot{\dot{y}} + 3\ddot{y} = -3t\ddot{\dot{y}} = -3(0)(0.3) = 0 \\ y_0^V &= -3ty^{IV} - 3\ddot{y} = -3(0)(0) - 3(0.3) = -0.9 \\ y_0^{VI} &= -3ty^V - 3y^{IV} - 3y^{IV} = -3(0)(-0.9) - 6(0) = 0 \\ y_0^{VII} &= -3ty^{VI} - 3y^V - 6y^V = -3(0)(0) - 9(-0.9) = +8.1 \end{aligned}$$

From Eq. (8.22) the Taylor series is

$$y = 1 + 0.1h + \frac{6h^2}{2!} + \frac{0.3h^3}{3!} + (0)h^4 - \frac{0.9h^5}{5!} + (0)h^6 + \frac{8.1h^7}{7!}$$

To find the range of h for which this series represents y correct to 0.0001 up to the term in h^5 , we write the first neglected term (in this case the last term) equal to or less than $\frac{1}{2}(0.0001) = 0.00005$; thus

$$\begin{aligned}\frac{8.1h^7}{7!} &\leq 0.00005 \\ \therefore h &\leq 0.6\end{aligned}$$

This procedure is quite straightforward and ideally suited for starting a numerical integration. It is only necessary to be able to determine the derivatives at a given time. If one equation does not apply to the complete range of time that is of interest, the time range may be divided into parts and a separate series developed for each interval.

Since this procedure requires evaluation of a number of derivatives for each time interval, it becomes too tedious to use if numerical results are of interest at very many points. In these cases other methods are preferred.

This self-starting character of the Taylor-series method makes it a convenient method for handling discontinuities that are not handled satisfactorily by some of the commonly used methods. Any method that utilizes previous values of displacement, velocity, or acceleration implies that the function is continuous at the point of integration. In some applications the effect of the discontinuities is erroneously neglected and the procedure is considered to yield a certain theoretical accuracy in terms of some power of h . To be correct it is necessary to evaluate between discontinuities, restarting the procedure by a Taylor-series expansion at the discontinuity.

b. Milne's Methods. In a paper published in 1949 [8], Milne presents a list of numerical-integration formulas based on the Taylor-series expansion. The most accurate formula is one with a residual of order of magnitude of h^7 . Lotkin [9] discovered the same equation independently. Tung [6] derives the formulas for second-order equations, obtaining (in the above notation)

$$\begin{aligned}y_1 = y_0 + \dot{y}_0 h + \frac{h^2}{2} (\ddot{y}_0 + \ddot{y}_1) + \frac{h^3}{20} (\ddot{y}_0 - \ddot{y}_1) + \frac{h^4}{240} (y_0^{IV} + y_1^{IV}) \\ - \frac{509h^5 y^{VIII}(s)}{806,400} \quad t_0 \leq s \leq (t_0 + h) \quad (8.25)\end{aligned}$$

If this type of equation is to be used only for starting purposes, Eq. (8.25) is sufficient by itself, since y_0 and \dot{y}_0 are the known initial conditions and

the other derivatives are obtainable from the differential equation of motion. However, if it is proposed to use the Milne method for integration over a large range of t , it is necessary to provide an equation for evaluating the velocity term \dot{y}_n for use in Eq. (8.25).

Tung [6] derives this equation, which takes the form (in revised notation)

$$\dot{y}_1 = \dot{y}_0 + \frac{h}{2} (\ddot{y}_0 + \ddot{y}_1) + \frac{h^2}{10} (\dddot{y}_0 - \dddot{y}_1) + \frac{h^3}{120} (y_0^{IV} - y_1^{IV}) - \frac{h^7 y^{(7)}(s)}{100,800} \quad t_0 \leq s \leq t_0 + h \quad (8.26)$$

A complete integration scheme involves Eqs. (8.25) and (8.26). This method is a very-high-accuracy method, as can be seen from the remainder terms in h^7 and h^8 . If the derivatives of y are known, the truncation error can be estimated. Also the interval h is not fixed in length as required for some other procedures. Of course, the accuracy varies with h .

This procedure, unlike the application of the Taylor series in Sec. 8.5a, has the disadvantage of being an iterative procedure, since it contains terms at both t_0 and $t_1 = t_0 + h$.

In addition, any procedure based on the use of derivatives has the disadvantage, in multi-degree-of-freedom systems, that computation of the derivatives is tedious and time-consuming.

c. Method of Runge and Kutta. This method is another good starting procedure, which has the advantage that it does not include the complication of evaluating derivatives that is basic to the Taylor-series method. However, the procedure is based on the Taylor-series expansion of the integrand (which is the foundation of practically all numerical methods) in that an expression is obtained that is equivalent to the Taylor-series expansion, although having a form that requires successive evaluation of the integrand itself rather than derivatives of the integrand.

Since the function rather than its derivatives is evaluated, there is no need for an analytical expression at starting (the Taylor-series method requires an analytical expression for the integrand so that derivatives can be obtained). This procedure is derived for first-order differential equations. When applied to second-order differential equations of motion it is necessary to replace the second-order equation by two first-order equations. Consider the equation

$$\ddot{y} = G(t, y, \dot{y})$$

The equivalent set of simultaneous single-order equations is

$$\begin{aligned} \dot{y} &= z = G(t, y, \dot{y}) \\ \dot{z} &= F(t, y, \dot{y}) \end{aligned}$$

The Runge approximation of the Taylor-series expansion has the form of Eq. (8.27):

$$y_{n+1} = y_n + \alpha_0 k_0 + \alpha_1 k_1 + \alpha_2 k_2 + \cdots + \alpha_n k_n \quad (8.27)$$

where $k_0 = hF(t_n, y_n)$

$$k_1 = hF(t_n + \mu_1 h, y_n + \lambda_{10} k_0)$$

$$k_2 = hF(t_n + \mu_2 h, y_n + \lambda_{20} k_0 + \lambda_{21} k_1)$$

$$\dots\dots\dots$$

$$k_n = hF(t_n + \mu_n h, y_n + \lambda_{n0} k_0 + \lambda_{n1} k_1 + \cdots)$$

and where the α , μ , and λ terms vary with the accuracy required and complication that is acceptable for a particular solution.

One of the formulas due to Kutta that is correct through the h^3 term (third-order accuracy) has the form

$$y_{n+1} = y_n + \frac{1}{6}(k_0 + 4k_1 + k_2) + 0(h^4) \quad (8.28)$$

where $k_0 = hF(t_n, y_n)$

$$k_1 = hF(t_n + \frac{1}{2}h, y_n + \frac{1}{2}k_0)$$

$$k_2 = hF(t_n + h, y_n + 2k_1 - k_0)$$

A second equation with third-order accuracy is due to Heun and is of the form [1]

$$y_{n+1} = y_n + \frac{1}{4}(k_0 + 3k_2) + 0(h^4) \quad (8.29)$$

where $k_0 = hF(t_n, y_n)$

$$k_1 = hF(t_n + \frac{1}{3}h, y_n + \frac{1}{3}k_0)$$

$$k_2 = hF(t_n + \frac{2}{3}h, y_n + \frac{2}{3}k_1)$$

As indicated, each of these formulas has limited but generally equal accuracy. The Kutta equation reduces to Simpson's rule if F is independent of y .

By retaining an additional k in the general equation (8.27), Kutta derives the following fourth-order-accuracy formula [6]:

$$y_{n+1} = y_n + \frac{1}{6}(k_0 + 2k_1 + 2k_2 + k_3) + 0(h^5) \quad (8.30)$$

where $k_0 = hF(t_n, y_n)$

$$k_1 = hF(t_n + \frac{1}{2}h, y_n + \frac{1}{2}k_0)$$

$$k_2 = hF(t_n + \frac{1}{2}h, y_n + \frac{1}{2}k_1)$$

$$k_3 = hF(t_n + h, y_n + k_2)$$

This particular form was found by Gill [10] to require minimum storage capacity when used for high-speed digital-computer operation.

When applied to simultaneous single-order equations of the form

$$\begin{aligned} \dot{y} &= \frac{dy}{dt} = F(t, y, u) \\ \dot{u} &= \frac{du}{dt} = G(t, y, u) \end{aligned} \quad (8.31)$$

where y and u are given as initial conditions at $t = t_0$ (as a preliminary to the treatment of second-order equations), the so-called Kutta-Gill method results in

$$\begin{aligned} y_{n+1} &= y_n + \frac{1}{6}(k_0 + 2k_1 + 2k_2 + k_3) + 0(h^5) \\ u_{n+1} &= u_n + \frac{1}{6}(m_0 + 2m_1 + 2m_2 + m_3) + 0(h^5) \end{aligned} \quad (8.32)$$

where $k_0 = hF(t_n, y_n, u_n)$

$$k_1 = hF(t_n + \frac{1}{2}h, y_n + \frac{1}{2}k_0, u_n + \frac{1}{2}m_0)$$

$$k_2 = hF(t_n + \frac{1}{2}h, y_n + \frac{1}{2}k_1, u_n + \frac{1}{2}m_1)$$

$$k_3 = hF(t_n + h, y_n + k_2, u_n + m_2)$$

$$m_0 = hG(t_n, y_n, u_n)$$

$$m_1 = hG(t_n + \frac{1}{2}h, y_n + \frac{1}{2}k_0, u_n + \frac{1}{2}m_0)$$

$$m_2 = hG(t_n + \frac{1}{2}h, y_n + \frac{1}{2}k_1, u_n + \frac{1}{2}m_1)$$

$$m_3 = hG(t_n + h, y_n + \frac{1}{2}k_2, u_n + \frac{1}{2}m_2)$$

Now if $F = u$, so that Eq. (8.31) is equivalent to

$$\ddot{y} = \frac{d^2y}{dt^2} = G(t, y, \dot{y}) \quad (8.33)$$

Eqs. (8.32) become

$$\begin{aligned} y_{n+1} &= y_n + h\dot{y}_n + \frac{h}{6}(m_0 + m_1 + m_2) + 0(h^5) \\ \dot{y}_{n+1} &= \dot{y}_n + \frac{h}{6}(m_0 + 2m_1 + 2m_2 + m_3) + 0(h^5) \end{aligned} \quad (8.34)$$

where $m_0 = hG(t_n, y_n, \dot{y}_n)$

$$m_1 = hG(t_n + \frac{1}{2}h, y_n + \frac{1}{2}h\dot{y}_n, \dot{y}_n + \frac{1}{2}m_0)$$

$$m_2 = hG(t_n + \frac{1}{2}h, y_n + \frac{1}{2}h\dot{y}_n, \dot{y}_n + \frac{1}{2}m_0)$$

$$m_3 = hG(t_n + h, y_n + h\dot{y}_n, \dot{y}_n + m_2)$$

In many structural-dynamics problems the \dot{y} term is not involved because damping is neglected. In these cases the evaluation of this formula is simplified significantly.

It should be noted that in the literature there are many more versions and variations of these formulas based on the original work of Runge, some having special utility for special problems.

Just as for the Taylor-series methods, the Runge-Kutta methods have the advantage of being self-starting methods and flexible with regard to length of successive time intervals. However, the methods have two important disadvantages:

1. The procedure does not have a simple means for estimating the error although an upper bound on the error can be computed by a procedure due to Bieberbach [9]. In addition, arithmetical mistakes are detected only by repetition of the calculation.

2. Each step requires several substitutions into the differential equation, which makes it a relatively slow procedure for a given time interval.

However, the error term might permit an increase in the time interval to offset the numerous substitutions required. In any application of numerical-integration formulas the attempt should be made to use the largest time interval h consistent with obtaining the proper accuracy.

d. Euler's Method. This method is related to the Runge-Kutta methods in that both are designed to determine increments of y corresponding to increments of the independent variable t by substitution into the differential equation. The Euler (modified) method has an advantage in that it includes an automatic checking routine.

The Euler approximation is based on the assumption that if

$$\dot{y} = f(t, y) \quad (8.35)$$

the increment of y corresponding to a time increment h is given approximately by

$$\Delta y = f(t, y)h \quad (8.36)$$

the value of $f(t, y)$ being at the beginning of the interval h . Thus, if the initial conditions are t_0 and h_0 , the first increment is $y_1 = f(t_0, y_0)h_1$. A second increment $y_2 = f(t_0 + h_1, y_0 + \Delta y)h_2$, where h_2 is the second increment of time. These give

$$y_1 = y_0 + \Delta y_1$$

and

$$y_2 = y_1 + \Delta y_2 = y_0 + \Delta y_1 + \Delta y_2$$

This procedure is very slow and to be reasonably accurate must utilize very small h values because it has only a second-order accuracy.

To offset the basic difficulty of the regular Euler method, the practice is to modify the procedure, essentially by taking the true average of the integrand at the beginning and end of the time interval. Starting from the basic Euler procedure, y_1 is determined at t_1 . From y_1 the integrand will yield \dot{y}_1 , which is then averaged with \dot{y}_0 for use in determining a second value:

$$y_{11} = y_0 + \frac{1}{2}[f(t_0, y_0) + f(t_1, y_1)]h \quad (8.37)$$

This value may be refined by repeating the step to obtain a third approximation y_{111} .

The modified method is considerably more accurate (third-order) than the basic Euler method and is much faster in reaching the possible accuracy. However, both are subject to serious error propagation and are therefore useful for a limited range of the independent variable.

e. Difference Equations. Since difference equations are the basis of many of the efficient numerical-integration procedures that are discussed in the literature, it is desirable to define what is meant by a difference equation and to show how it is related to a differential equation.*

* Δ = forward-difference symbol

∇ = backward-difference symbol

δ = central-difference symbol

The change in a function $f(t)$ may be calculated when t is increased from an initial value t_0 by a positive amount h . This change in f is known as the *first forward difference* of f , relative to the increment h , and is denoted by

$$\Delta f(t_0) = f(t_0 + h) - f(t_0) \quad (8.38)$$

By the same definition

$$\Delta f(t_0 + h) = f(t_0 + 2h) - f(t_0 + h) \quad (8.39)$$

The second forward difference of f associated with t_0 is then

$$\Delta^2 f(t_0) = \Delta f(t_0 + h) - \Delta f(t_0) \quad (8.40)$$

Substituting Eqs. (8.38) and (8.39) into Eq. (8.40) gives

$$\begin{aligned} \Delta^2 f(t_0) &= f(t_0 + 2h) - f(t_0 + h) - f(t_0 + h) + f(t_0) \\ &= f(t_0 + 2h) - 2f(t_0 + h) + f(t_0) \end{aligned} \quad (8.41)$$

Succeeding forward differences are defined by iteration, and a general expression for any forward difference is

$$\Delta^{r+1} f(t) = \Delta^r f(t + h) - \Delta^r f(t) \quad (8.42)$$

The beginning of a difference table is indicated in Fig. 8.10, where f_k is written in place of $f(t_k)$.

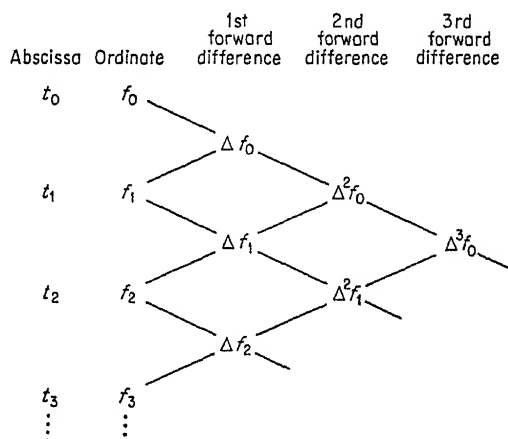


FIG. 8.10. Forward-difference table.

From the difference table it can be seen that the difference $\Delta^r f_k$ depends on the ordinates $f_k, f_{k+1}, \dots, f_{k+r}$.

For many problems the concept of backward differences is very useful. Here the *first backward difference* is

$$\nabla f(t) = f(t) - f(t - h) \quad (8.43)$$

and the general equation is

$$\nabla^{r+1}f(t) = \nabla^r f(t) - \nabla^r f(t-h) \quad (8.44)$$

The end of a backward-difference table is indicated in Fig. 8.11, from which it can be seen that $\nabla^r f_k$ depends on the ordinates $f_{k-r}, f_{k-(r-1)}, \dots, f_k$.

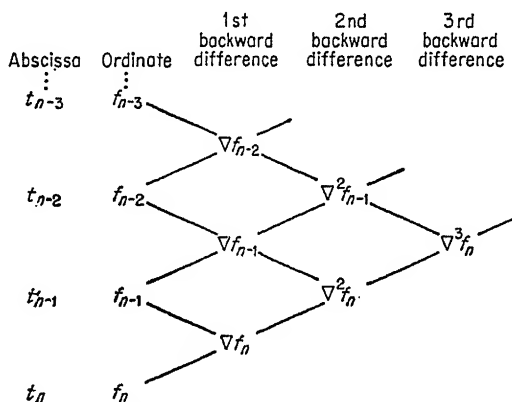


FIG. 8.11. Backward difference table.

For some calculations the notation of so-called central differences is most convenient. In the *central-difference notation*, one writes

$$\delta f(t) = f(t + \frac{1}{2}h) - f(t - \frac{1}{2}h) \quad (8.45)$$

for which the general relation is

$$\delta^{r+1}f(t) = \delta^r f(t + \frac{1}{2}h) - \delta^r f(t - \frac{1}{2}h) \quad (8.46)$$

It is seen that the first central difference $\delta f(t)$ does not involve data at even increments of the abscissa. However, the second central difference,

$$\begin{aligned} \delta^2 f(t) &= \delta f(t + \frac{1}{2}h) - \delta f(t - \frac{1}{2}h) \\ &= [f(t + h) - f(t)] - [f(t) - f(t - h)] \\ &= f(t + h) - 2f(t) + f(t - h) \end{aligned} \quad (8.47)$$

does involve data at even abscissa increments, and the same is true of all central differences $\delta^{2mf}(t_k)$ of even order and $\delta^{2m+1}f(t_{k+\frac{1}{2}})$.

The portion of the corresponding difference table in the neighborhood of a point t_0 is indicated in Fig. 8.12. Here the subscript remains constant along horizontal lines of the table, which pass through differences of only even or only odd orders.

Thus once a set of adjacent entries in a difference table has been numbered, three different sets of notations are available for the differ-

ences themselves, as may be seen from Fig. 8.13. Any one of the notations would suffice. However, each has certain advantages, depending on the application.

A differential equation is replaced approximately by a finite-difference equation.

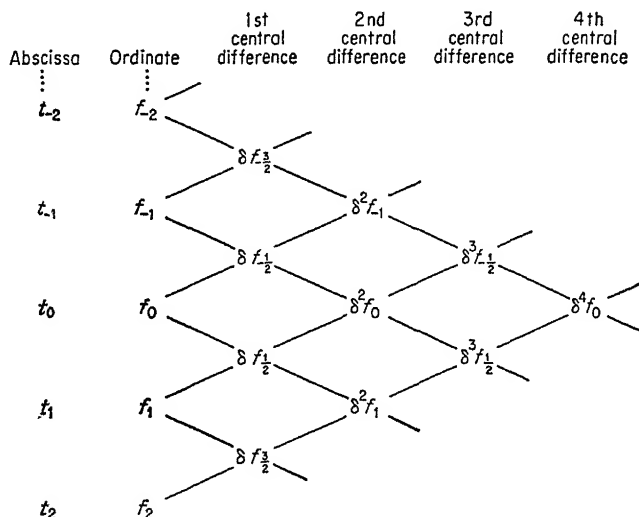


FIG. 8.12. Central-difference table.

Abscissa	Ordinate	1st difference	2nd difference
t_0	f_0		
		$\Delta f_0 = \delta f_{\frac{1}{2}} = \nabla f_1$	
t_1	f_1		$\Delta^2 f_0 = \delta^2 f_{\frac{1}{2}} = \nabla^2 f_2$
		$\Delta f_1 = \delta f_{\frac{3}{2}} = \nabla f_2$	
t_2	f_2		

FIG. 8.13. Composite difference table.

As an example, consider the equation $\dot{y} = t$, which satisfies the initial conditions $y(0) = 0$, $\dot{y}(0) = 1$. The finite-difference approximation is

$$\frac{y(t+h) - 2y(t) + y(t-h)}{h^2} = t$$

and the initial conditions are

$$y(0) = 0 \quad \dot{y}(0) = \frac{y(t+h) - y(t)}{h} = \frac{y(h) - y(0)}{h} = 1$$

As the increment h tends to zero the difference equation tends to the

differential equation, and the solution of the difference equation tends to the solution of the differential equation it replaces.

f. Methods of Finite Difference. We consider a special group of equations for the handling of the second-order equation

$$\ddot{y} = G(x, y) \quad (8.48)$$

in which \dot{y} is not explicitly involved because this is a very common equation in structural dynamics. If \dot{y} is not part of the integrand, it is just as well to have a method which does not require its computation, since \dot{y} seems to increase the truncation error.

These equations in terms of the *backward differences* of \ddot{y}_n are

$$y_{n+1} = 2y_n - y_{n-1} + h^2(1 + 0\nabla + \frac{1}{12}\nabla^2 + \frac{1}{12}\nabla^3 + \frac{19}{240}\nabla^4 + \frac{3}{40}\nabla^5 + \cdots)\ddot{y}_n \quad (8.49)$$

and

$$y_{n+1} = 2y_n - y_{n-1} + h^2(1 - \nabla + \frac{1}{12}\nabla^2 + 0\nabla^3 - \frac{1}{240}\nabla^4 - \frac{1}{240}\nabla^5 + \cdots)\ddot{y}_{n+1} \quad (8.50)$$

The first equation is classified as an *open type* since the expression for the unknown displacement y_{n+1} contains only the current and previous values of y and \ddot{y} . The most serious drawback to both Eq. (8.49) and Eq. (8.50) is that the solution is not self-starting and the difficulty in starting a solution increases as the number of backward differences retained in the equation increases.

If r backward differences $\nabla^r \ddot{y}_n$ are retained, then $r - 1$ previous values of \ddot{y} must be known before starting because $\nabla^r \ddot{y}_n$ is determined by $\ddot{y}_n, \ddot{y}_{n-1}, \dots, \ddot{y}_{n-r}$. As indicated previously, these points can be determined by Runge-Kutta methods or Taylor-series expansion.

Equation (8.50) is classified as a closed type because the expression for y_{n+1} contains the unknown \ddot{y}_{n+1} explicitly and implicitly, and the equation must be solved by iterative methods.

After determining sufficient starting points, the integration is continued by either of the two equations. This is known as the Adams-Stormer method.

Formulas (8.49) and (8.50) are representative of a whole class of similar open- and closed-type difference formulas. One other which is quite useful and well known is

$$y_{n+1} = y_n + y_{n-2} - y_{n-3} + 3h^2(1 - \nabla + \frac{5}{12}\nabla^2 + 0\nabla^3 + \frac{17}{720}\nabla^4 + \frac{17}{720}\nabla^5 + \cdots)\ddot{y}_n \quad (8.51)$$

In both Eqs. (8.50) and (8.51) the coefficient of the third backward difference is zero.

If only second differences are retained, the resulting equations (limi-

nating the backward-difference notation) are

$$y_{n+1} = y_n + y_{n-2} - y_{n-3} + \frac{h^2}{4} (5\ddot{y}_n + 2\ddot{y}_{n-1} + 5\ddot{y}_{n-2}) + \frac{17}{240} h^6 y_n^{VI} \quad (8.52)$$

$$\text{and} \quad y_{n+1} = 2y_1 - y_{n-1} + \frac{h^2}{12} (\ddot{y}_{n+1} + 10\ddot{y}_n + \ddot{y}_{n-1}) - \frac{h^6}{240} y_n^{VI} \quad (8.53)$$

If only first differences are retained, Eq. (8.49) reduces to

$$y_{n+1} = 2y_n - y_{n-1} + h^2 \ddot{y}_n \quad (8.54)$$

which is the same as the acceleration-pulse method discussed earlier.

If the same operation is performed on Eq. (8.50), the resulting equation is also the same as the acceleration-pulse equation.

Theoretically the use of higher-order differences should result in smaller truncational errors. Several investigators seem to obtain contrary results. Part of the difficulty results from the fact that higher-order differences raise the order of the difference above the order of the differential equation of which it is an approximation, thus introducing extraneous roots. However, methods have been proposed [6, 12] for correcting this difficulty. If these methods are used, the resulting procedures have a very high accuracy.

8.6. General Considerations in Numerical Integration. The following sections are intended to provide a summary and a rough guide to the questions that must be considered in selecting a numerical-integration procedure and performing the actual numerical integration. Some of the subjects which can only be pointed to as worthy of further investigation by the reader are the effect of stability, convergence, damping, and negative spring constant.

a. Starting Procedure. When a method expresses the future ordinate on the basis of past ordinates and slopes or differences of slopes it cannot be used to start a numerical solution. To obtain a good starting method one may choose among several methods, among which are the Runge-Kutta methods (Sec. 8.5c) and the Taylor-series approach (Sec. 8.5a). To use the Taylor series it is necessary that the higher derivatives of the function be readily obtainable.

b. Errors in Numerical Procedures. There are two types of errors involved in any numerical procedure. They are errors of *approximation* and errors from *rounding off*. Whenever differential equations are solved, there is inherently a need for integration. The fact that one must infer the value of the integral of a function from the samples of that function implies *approximation*. If one knows the analytic form of the function being integrated, he can infer the integral by interpolating the integrand

by Taylor's series to any accuracy desired. Usually, he would commit a *truncation* error.

Other errors of approximation come from function evaluation. A numerical process can evaluate only polynomials or ratios of polynomials. If one needs to evaluate a function numerically, he usually does this by evaluating a series or a rational approximation to the function and thereby commits an error which is like a truncation error.

The second type of errors are round-off errors. These errors must be treated by statistical methods, and the results are usually presented in terms of probability functions. Round-off errors are not considered herein.

Truncation errors can be evaluated in general by the use of the Taylor series. If one has an integration formula already established, one expands the appropriate terms in power series and collects terms. The lowest-order term on the right-hand side of the equation which has no counterpart on the left side is the error term.

As an example of this procedure, consider the integration equation for the linear-acceleration method:

$$x_{n+1} = x_n + \dot{x}_n h + \frac{h^2}{6} (2\ddot{x}_n + \ddot{x}_{n+1}) \quad (8.55)$$

The power-series expansions that are useful are

$$\begin{aligned} x_{n+1} &= x_n + \frac{h\dot{x}_n}{1!} + \frac{h^2\ddot{x}_n}{2!} + \frac{h^3\ddot{\ddot{x}}_n}{3!} + \frac{h^4x_n^{IV}}{4!} \\ \ddot{x}_{n+1} &= \ddot{x}_n + \frac{h\ddot{\ddot{x}}_n}{1!} + \frac{h^2x_n^{IV}}{2!} \end{aligned}$$

Rewriting Eq. (8.55) we obtain

$$x_{n+1} - x_n - h\dot{x}_n - \frac{h^2\ddot{x}_n}{3} = \frac{h^2}{6} \ddot{x}_{n+1} + \text{error term}$$

Substituting the power-series expressions gives

$$\begin{aligned} \frac{h^2}{6} \ddot{x}_n + \frac{h^3}{3!} \ddot{\ddot{x}}_n + \frac{h^4}{4!} x_n^{IV} &= \frac{h^2}{6} \left(\ddot{x}_n + \frac{h\ddot{\ddot{x}}_n}{1!} + \frac{h^2x_n^{IV}}{2!} \right) + \text{error term} \\ \text{Error term} &\approx -\frac{h^4x_n^{IV}}{24} \end{aligned}$$

To obtain the "true" truncation error for the linear-acceleration method [Eq. (8.8)] it is necessary to consider the error in the subsidiary equation from which the velocity term is obtained. For the equation

$$\dot{x}_{n+1} = \dot{x}_n + \frac{h}{2} (\ddot{x}_n + \ddot{x}_{n+1})$$

the truncation error is $\sim(h^3/12)x_n^{IV}$. Thus the over-all truncation is probably slightly greater than $(h^4/24)x_n^{IV}$.

By the same procedure the error term for the acceleration-pulse method is found to be $\sim(h^4/24)x_n^{IV}$ and the error term for the constant-acceleration method is $\sim(h^3/4)\ddot{x}_n$.

From these values of the truncation error it would appear that the linear-acceleration method has slightly larger truncation error than the acceleration-pulse method. However, the acceleration-pulse method is

Ordinate	Δ	Δ^2	Δ^3	Δ^4	Δ^5
y_0					$+\epsilon$
y_1				$+\epsilon$	-5ϵ
y_2		$+\epsilon$	$+\epsilon$	-4ϵ	
$y_3 + \epsilon$	$+\epsilon$		-3ϵ		$+10\epsilon$
	$-\epsilon$	-2ϵ	$+3\epsilon$	$+6\epsilon$	-10ϵ
y_4		$+\epsilon$	$-\epsilon$	-4ϵ	
y_5				$+\epsilon$	$+\epsilon$
					$-\epsilon$

FIG. 8.14. Propagation of error in a difference table.

not a self-starting method, being dependent on x_{-1} at $t = 0$, and is therefore subject to a different error by assuming, as indicated above, that in the first computation x_{-1} is zero. Other advantages of the linear-acceleration method were described above.

It should be noted that it is easier to formulate a numerical-integration method than it is to determine its error. However, the subject of errors has been treated in the literature (specific references are contained in paragraph 6.20 of Ref. 1), and one should consider this material carefully before accepting a method of numerical integration.

c. Checking Procedures. A complete and systematic method for numerical integration should include a checking procedure at each step of the integration. If an integration formula does not contain an automatic check, a check should be devised. This is an area in which difference methods can be of great value.

Differences of higher orders change in a very orderly manner if a numerical integration is carried out correctly. Thus any irregularity in the higher difference is a sure sign of an error in the calculations, and what is equally useful, the irregularity provides a very good indication of the source of the error.

Figure 8.14 illustrates the way in which an error affects the difference table. Only the error term ϵ is shown. The violent oscillation of the

error term in the higher-order differences is clearly seen, and the largest values are the central-difference terms through the original error term.

If the method of integration utilizes higher-order differences, a check of the calculations is very conveniently achieved merely by observing if the higher-order differences are consistent. However, in many circumstances it is also worthwhile to calculate the higher differences for the sole purpose of obtaining a check of the integration.

Another very good way to check previous calculations is embodied in the methods of successive approximations because the corrections should change very slowly and uniformly. Irregularities in the corrections should indicate an error in the calculations.

d. Selecting a Value for h . Experience indicates that it is better to use a small time interval h and a simple procedure than an elaborate and complex formula which would permit a longer time interval. The accuracy of difference formulas increases rapidly as the increment h is decreased. In addition, when methods of successive approximation (closed methods) are used, the fullest accuracy is usually obtained from the formulas in a small number of steps. This convergence of successive approximations is of considerable importance because it serves to reduce the amount of labor.

If the methods of successive approximations converge too quickly (less than two trials) or too slowly (more than four trials), it is desirable from the point of view of time consumption and accuracy to modify the time interval h . Rapid convergence implies too small a time interval, and therefore many more intervals than are required in a given range of time. This results in a slow computation and a large propagation of error. Slow convergence implies a large time interval and low accuracy. If, for example, an integration with fourth-order accuracy converges in four trials for $h = 0.1$ and in two trials for $h = 0.05$, the calculating time is the same for both procedures but the ratio of error in one step is

$$\frac{2 \text{ trials}}{4 \text{ trials}} = \left(\frac{0.05}{0.10}\right)^4 = 1/16$$

Another reason for changing the value of h during an integration is related to the rate of change in the value of y . If the change in y decreases, the accuracy may be maintained with an increased h ; and vice versa, if the change in y increases, it may be necessary to decrease the value of h .

The usual variations in h are either doubling or halving. For purpose of decreasing the value of h it is necessary to use an interpolation formula. One that is recommended in [4] is

$$q_{1/2} = 1/2(q_0 + q_1) - 1/16(\Delta^2 q_0 + \Delta^2 q_1) + 3/256(\Delta^4 q_{-1} + \Delta^4 q_{-2})$$

The process of adding interpolated values must be performed with accuracy at least equal to that used in obtaining the original values. To increase the interval no interpolation is needed for the usual case of doubling the interval.

e. Selection of a Numerical-integration Method. Although this chapter has introduced a large number of methods for numerical integration, we have only skimmed the surface of the literature and given a few examples of each major class. The problem of deciding which procedure to use in a specific problem is not easily dismissed because of the many considerations involved, some of which are only poorly delineated.

First, probably, comes the question of what method of computation is to be used, slide rules, logarithms, desk calculators, medium or large digital computers. A method which is convenient for a desk calculator may be inconvenient for hand calculation because of the size of the numbers, or it may even be difficult for a high-speed digital computer because of the large storage requirements or the type of operation required of the arithmetic and control units. On the other hand, a procedure that requires a very large number of iterations of a simple type may be perfectly adapted to the high-speed digital computer, but just too time-consuming for hand or desk calculation.

Stability considerations may be very important when a large number of steps are necessary, but may be much less significant if the number of steps can be reduced to a small number.

The advantages of a simple procedure with large truncation error must be weighed against the fact that a large truncation error implies the need of a short time interval h , and therefore a larger number of steps with the attendant increased importance of round-off errors. One might prefer to use a simple procedure for which an upper bound of error can be estimated with confidence, rather than use an elaborate procedure for which such a bound is not available.

This chapter covers four broad classes of numerical-integration methods:

1. Methods based on an assumed variation of the acceleration in a time interval
2. Methods which express the future ordinate as a linear combination of present and/or past ordinates and slopes
3. Methods which also involve the calculation of higher derivatives
4. Methods in which the determination of the future ordinate does not depend on knowledge of the past ordinates

The first class might be included with the second class and considered as the moderate-accuracy group in this category.

The Euler procedure and its modifications are the simplest methods of

the second type. The Adams method is the most frequently used high-order-of-accuracy procedure in this class. Except for the basic Euler method, these procedures are not self-starting.

The methods of the third type are useful only when the differential equation is of such form that higher derivatives are readily obtained from the given differential equation. The Taylor-series method described is a very good starting device for other numerical-integration procedures that are not self-starting.

The fourth class, typified by the Runge-Kutta methods, are not dependent on previous information and are therefore self-starting. In addition, they are particularly well suited to digital-computer operations because they require small memory [10]. However, they do have the disadvantages mentioned previously.

REFERENCES

1. Hildebrand, F. B.: "Introduction to Numerical Analysis," McGraw-Hill Book Company, Inc., New York, 1956.
2. Milne, W. E.: "Numerical Solution of Differential Equations," John Wiley & Sons, Inc., New York, 1953.
3. Salvadori, M. G., and M. L. Baron: "Numerical Methods in Engineering," Prentice-Hall, Inc., Englewood Cliffs, N.J., 1952.
4. Levy, H., and E. A. Baggott: "Numerical Solution of Differential Equations," Dover Publications, New York, 1950.
5. Scarborough, J. B.: "Numerical Mathematical Analysis," Johns Hopkins Press, Baltimore, 1950.
6. Tung, T. P., and N. M. Newmark: A Review of Numerical Integration Methods for Dynamic Response of Structures, *Univ. Illinois Civil Eng. Studies, Structural Research Ser.*, no. 69, 1954.
7. Newmark, N. M., and S. P. Chan: A Comparison of Numerical Methods for Analyzing the Dynamic Response of Structures, *Univ. Illinois Civil Eng. Studies, Structural Research Ser.*, no. 36, 1952.
8. Milne, W. G.: The Remainder in Linear Methods of Approximation, *J. Research Natl. Bur. Standards Rept.* 2401, vol. 43, pp. 501-511, 1949.
9. Bieberbach, L.: "Theorie der Differentialgleichungen," Dover Publications, New York, 1946.
10. Gill, S.: A Process for the Step-by-step Integration of Ordinary Differential Equations in an Automatic Digital Computing Machine, *Proc. Cambridge Phil. Soc.*, vol. 47, pp. 96-108, 1951.
11. U.S. Army Corps of Engineers: "Engineering Manual for Protective Construction. Pt. III, Design of Structures to Resist the Effects of Atomic Bombs," prepared in part by the Massachusetts Institute of Technology under Contract DA49-129-Eng-178 with the United States Army. Also referred to in text as Chap. 1, Ref. 8, and Chap. 7, Ref. 1.
12. Fox, L., and E. T. Goodwin: Some New Methods for the Numerical Integration of Ordinary Differential Equations, *Proc. Cambridge Phil. Soc.*, vol. 45, pp. 373-388, 1949.

CHAPTER 9

INTRODUCTION TO ANALOG AND DIGITAL COMPUTERS AND THEIR APPLICATION TO DYNAMIC-RESPONSE CALCULATIONS

9.1. General. In Chap. 8 it is indicated that the difficulty or tediousness of obtaining direct solutions to the differential equations of motion of complex physical systems has led to the development of numerical methods of analysis, computing machines, and machine methods of computation. As progress is made in the various fields of engineering the problems tend to become more complex, especially since rough approximations previously considered acceptable are discarded in favor of more precise analyses. As the complexity has increased, the use of desk calculators has become prohibitive for many problems because of time and cost; and new computing machines and instruments have been developed to satisfy the changing requirements.

Computers are now available in a variety of sizes, speeds, cost, and types. The two principal categories are called *digital* and *analog*. The digital deals in numbers, and the analog is concerned with continuous physical variables. The digital output is generally a number, whereas the analog output is usually a curve. In the digital computer the accuracy is limited only by the mathematical method of analysis and the time devoted to solution. In the analog computer the accuracy is limited by the agreement between the physical analog and the actual problem.

Increasing the precision of a digital computer is a straightforward problem involving only a proportional increase in the size of computer. In the analog computer, however, increased precision is attainable only by use of more precise components, the cost of which increases sharply with increasing precision requirements.

How much precision to buy in an analog or digital computer is a problem governed mainly by the problem to be solved. For the solution of some structural dynamic problems where the system parameters are not well known and the fabrication is rough, it would hardly be conceivable to purchase analog or digital equipment with a precision of 0.01 per cent.

It is frequently desirable to employ more than one type of computer on

a given problem, since each is most effective for certain phases. In general, analog and digital computers work well together in sequence, the analog indicating the region of interest and the digital operating in the indicated region to the necessary precision. Indeed, considerable effort is being devoted to the development of analog-to-digital converters, which should probably lead to the combination of analog and digital machines into so-called "hybrid" computers.

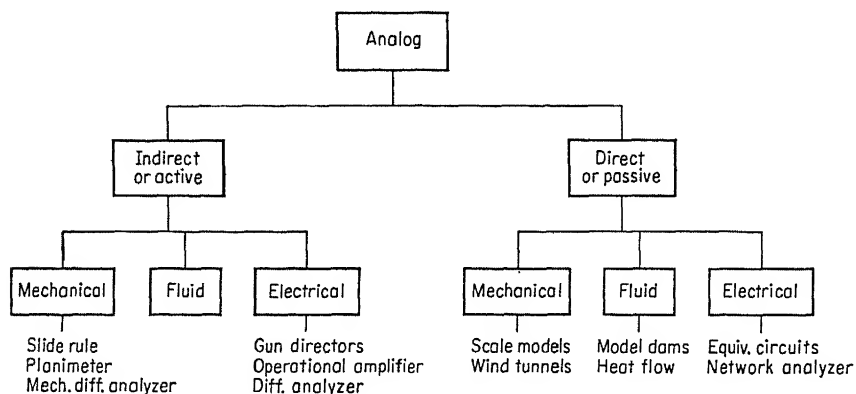


FIG. 9.1. Classification of analog computers.

In the sections which follow, separate discussions are presented of analog computers and digital computers and their application to the solution of dynamic equations of motion for physical systems.

9.2. Analog Computers. Analog computers can be divided into two basic groups (Fig. 9.1). The direct analogy is characterized by those cases where problem variables and parameters are represented directly by corresponding units on the machine. The mechanical direct analog computers are most generally scale models such as wind-tunnel models. The electrical direct analogs include such instruments as the network analyzers and equivalent circuits. In the fluid analog are found such devices as model dams and stream beds found in many hydraulic laboratories. Some of the electrical direct analog computers may be classified as general-purpose computers because they can be used to solve a class of mathematical problems.

The indirect analog computers are of a type which can carry out the solution of algebraic or differential equations. The most common example of a mechanical indirect analog computer is the slide rule. At the other end of the spectrum in size and complexity is the differential analyzer. Currently the electronic indirect analog computer is probably

the most common of the indirect type. The following section is limited to a discussion of this type of analog computer.

a. Description of Electronic Indirect Analog Computers. This type of analog computer is divided into two categories: real-time and high-speed (repetitive) machines. Compared on the basis of problems which are amenable to both high-speed and real-time computation, real-time computer installations are much more expensive for both basic and nonlinear components, operating costs are comparable, but maintenance cost is greater for real-time.

Although individual solution times are nominally in the ratio of 1,600 or 3,000 for high-speed to 1 for real-time, reports of experience indicate complete solution time to be in the order of 1 day for high-speed to 1 week for real-time. However, accuracy and precision of the real-time computer is generally one order better than the high-speed.

A commercial example of a real-time computer is the REAC manufactured by the Reeves Instrument Company. Some representative repetitive computers are the GAP/R by G. A. Philbrick Researches, Inc., and the General Purpose Simulator (GPS) by G. P. S. Instrument Co.

The following is limited to the *repetitive type of indirect analog computer*. Within limits the discussion is applicable to most of the commercially available computers.

The electronic indirect analog computer normally employs high-gain amplifiers which, when applied in appropriate feedback loops, will perform many mathematical operations. The basic components which are of primary interest and utility are the adder, or summing amplifier; the coefficient unit, or potentiometer, which is capable of multiplying by a constant (in many machines equal to or less than 1.0, but in some machines between 0 and 100); and the integrator, which is capable of integrating with respect to time. These operations are performed automatically between input and output voltages. Thus voltage is considered to be the analog of the dependent variable, with time as the independent variable.

In its physical form each component is unidirectional; that is, information flows only from input to output. The output-signal capacity of each component is such that the load imposed by the input of another component is negligible. Any component may therefore instruct any number of others without correction.

The three basic units, adder, integrator, and coefficient unit, are all that are required to simulate any linear system. However, there are many types of nonlinear components that have been developed.

Some typical components that are analogous to nonlinear relationships or mechanical motions are known as bounding, backlash, inert-zone,

squaring, square-root, and absolute-value components. The bounding component transmits the input directly or inversely within a limiting plus or minus voltage that can be adjusted by a dial from zero to 100 per cent. The backlash component transmits the input signal only after there has been a sufficient change, and then the output lags the input by the prescribed amount. If the input is reversed, the output is stationary until the input has proceeded the prescribed amount in the opposite direction. This unit may be used to represent lost motion, or backlash, in mechanical systems. The inert-zone component suppresses a central band of variation of the input signal beyond which it transmits the surplus at unit sensitivity. The names of the last three listed units are self-explanatory.

It is often necessary to represent functional relationships between two variables which cover an unlimited variety of shapes and forms and which perhaps are known only empirically. For this purpose components are available which can fit such curves by linear segmented polygons with angles and lengths adjustable. These are known as function generators, or function fitters.

Perhaps the most important nonlinear operation in computing systems is that involving the multiplication of two varying voltage signals. In recent years some very reliable high-speed electronic multipliers have been developed.

A complete high-speed electronic computing installation requires, in addition to the above-mentioned computing components, auxiliary equipment to supply initial conditions, calibrating devices, timing signal, display oscilloscopes with the necessary controls, and a power supply.

b. Use of High-speed Analog Computer. The process involved in the solution of a problem by high-speed-analog methods is described by the following steps:

1. Express the relationships at each point in the prototype system by writing the differential equations.
2. Construct a causal block diagram from the relationships expressed in step 1. A block diagram is a pictorial equation which describes the indirect model of a system. The general technique of forming a block diagram is to:
 - a. Establish the highest derivative in each local differential equation as a function of the lower-order derivatives and of known quantities.
 - b. Integrate successively, using blocks until the term of lowest required order is attained in each equation.
 - c. Perform other functional operations that are necessary to obtain the functions needed for the highest-order derivatives.

- d. Introduce initial conditions where they occur in the physical system.
- e. Connect all blocks into loops to satisfy the differential equations.

An example illustrating this technique is presented later.

- 3. Convert the numerical quantities in the problem to a suitable form for computation by scaling or normalizing.
- 4. From the block diagram set up the analog by interconnecting components and verify by checking against some known or expected solution.
- 5. Explore the problem by varying parameters.
- 6. Check results and conclusions against digital-computer or hand-computed results.

With experience some systems may be modeled directly, with a minimum of equations or diagrams. Many problems of a high degree of complexity may be dealt with in thorough fashion by first studying an elementary system. Then, constantly checking against known solutions, one gradually adds more and more orders of complexity, verifying results at each step until the whole problem is solved. On a repetitive computer this method leads to rapid solutions because parameters can be changed continuously and the system is altered with minimum effort. A very desirable feature in this procedure is the degree of understanding that comes to the researcher as the system is developed.

High-speed electronic-analog techniques utilize voltage ranges of ± 50 volts and maximum computing times of several milliseconds. The physical system might have any units; however, to obtain useful results the physical-system data must be scaled to the machine units. There are many ways of doing this, all of which should lead to the same result.

It is desirable to choose scales which result in close to full-scale operation of the components without overloading, principally because maximum accuracy is obtained at full scale. (Most components are equipped with overload lights.)

c. *Example of Analog-computer Solution of a Typical Problem in Structural Dynamics.* The description of the high-speed analog computer and the method of setting up a problem on the computer are best understood if a typical problem is investigated.

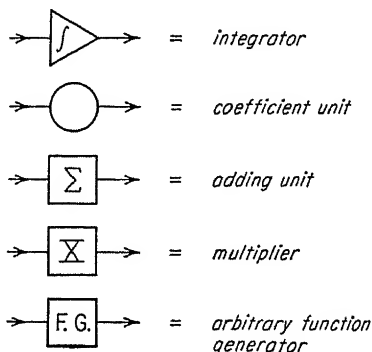
Consider the differential equation for the dynamic-load factor, as presented in Eq. (4.46).

$$\ddot{\mathfrak{D}}_m(t) + \omega_m^2 \mathfrak{D}_m(t) = \omega_m^2 f(t)$$

Rewriting the equation with the highest-order term on the left side and all other terms on the right side gives

$$\ddot{\mathfrak{D}}_m(t) = -\omega_m^2 \mathfrak{D}_m(t) + \omega_m^2 f(t) = \omega_m^2 [-\mathfrak{D}_m(t) + f(t)]$$

The block diagram (Fig. 9.2) for this equation is readily constructed, using the following symbols:



The voltage entering integrator A (input) is assumed to be $\ddot{\mathfrak{D}}_m(t)$; therefore the output must be $\dot{\mathfrak{D}}_m(t)$. If this is introduced as input to a second integrator B , the minus output for this integration is $-\mathfrak{D}_m(t)$. Refer to the line where a constant voltage is introduced as input to a function generator (which is capable of producing an output voltage of considerable complexity to match a known function), from which the output is the function $f(t)$. Both $f(t)$ and $-\mathfrak{D}_m(t)$ are combined in an adder. The adder output $f(t) - \mathfrak{D}_m(t)$ is multiplied by the coefficients ω_m^2 , thus giving $\dot{\mathfrak{D}}_m(t)$, which is what is assumed as input for integrator A . Thus the output of the coefficient unit is properly the input for the integrator A .

Since the coefficient unit for this particular computer is limited to multiplying by numerical factors from 0 to 1.0 (some computers have a range from 0 to 100), it is necessary to divide ω_m^2 by a convenient factor K so that $\omega_m^2/K < 1$. In this example it is assumed that $10 < \omega_m^2 < 100$, a convenient coefficient, therefore, being $\omega_m^2/100$. To obtain the correct relationship it is necessary to introduce gain factors of 10 in both integrators so that the analogous equation that is blocked out is

$$\frac{\ddot{\mathfrak{D}}_m(t)}{100} = \frac{\omega_m^2}{100} [-\mathfrak{D}_m(t) + f(t)]$$

It is not good practice to operate at low voltages because the accuracy attributed to any electronic component is based on full-scale operation. However, each electronic component also has a limiting voltage. If a component voltage exceeds the allowable limit, an overload light indicates that the solution is fictitious. Thus to achieve a voltage range that is as high as permissible it is only necessary to try increasing values of $f(t)$ until an overload light indicates that the selected value is too high. If the

input to function generator is 25 volts or 1 volt, the basic block diagram is the same except that $\mathcal{D}_m(t)$ for 1-volt input may be read directly, whereas $\mathcal{D}_m(t)$ for the 25-volt input must be divided by 25 (Fig. 9.2).

A few precautionary remarks are in order. A coefficient box should not follow another coefficient because they are subject to large errors in this arrangement. Similarly, cascading of more than two amplifiers should

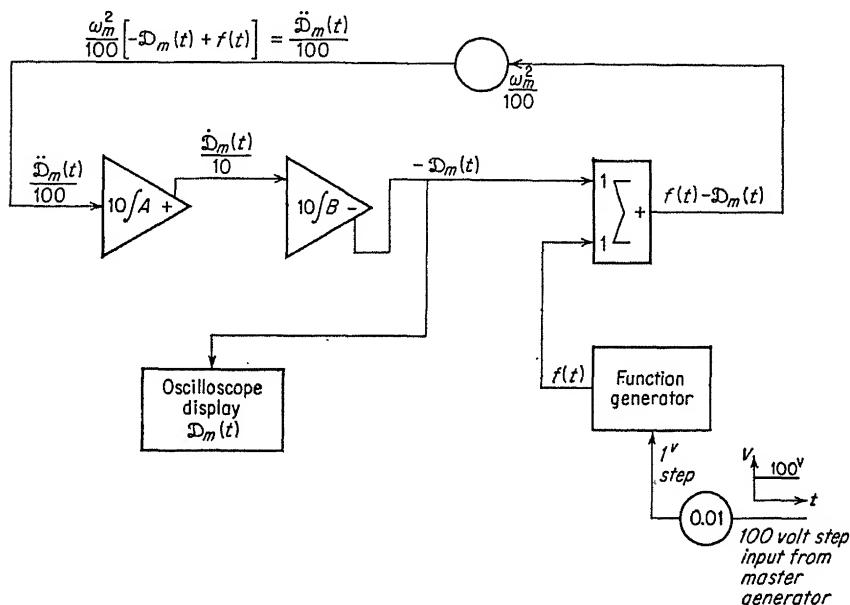


FIG. 9.2. Block diagram for analog-computer solution of $\mathcal{D}_m(t) + \omega_m^2 \mathcal{D}_m(t) = \omega_m^2 f(t)$.

be avoided to prevent amplification of the internal noise, which is additive and might tend to build up and distort the solution.

In some computers the components have built-in inverters so that the output signal may be taken as positive or negative. In others it is important to note that certain operations invert the signal, and the signs of the voltages must be considered carefully.

9.3. High-speed Digital Computation. This section describes the organization and use of high-speed electronic digital computers. This treatment is necessarily restricted to a brief description of the highlights since the primary purpose of this section is to provide an introduction to digital computers and the common techniques used to solve problems by digital computation.

a. Organization of a Computer. The modern automatic computer consists of four main elements and several possible subsidiary units, depending on the size and complexity of the installation. The basic elements are

the *memory unit*, *control unit*, *arithmetic unit*, and *input-output devices*. In the memory are stored numbers and instructions, either initially or as computing proceeds. The control unit interprets and carries out the instructions. The arithmetic unit performs the arithmetic operations on numbers delivered to it by the control unit. The input-output system is comprised of devices which place numbers and instructions in the memory unit and obtain results from the memory for reproduction by automatic typewriter, punched tape, or pictures of an oscilloscope screen, to mention a few possibilities.

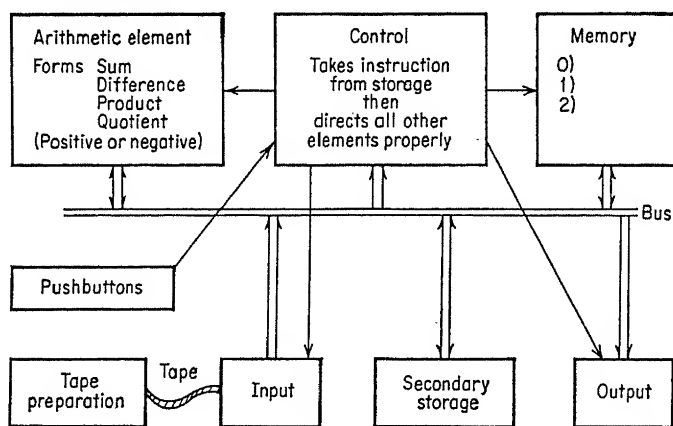


FIG. 9.3. Automatic digital computation.

The most fundamental operation of a digital computer is the transfer of information from a memory location to the arithmetic unit, where it is operated on and then returned to a particular location in the memory. Figure 9.3 gives a simple diagram of a digital computer relating the basic components to each other.

b. Characteristics of a Memory. A memory unit consists of memory cells or locations, which in turn are subdivided into memory elements. A memory element is the smallest section of the memory which can be altered by the transfer process without regard to its contents and without altering any other section. In most machines, information is stored in the element in the form of *binary digits* (scale of 2).

A word is a group of digits which may be transferred together. A word occupies one memory location. Locations are arranged in sequence and assigned a location number or address. A memory switch can locate a location by its address.

The most popular memory devices utilized today are based on magnetic principles. They may be magnetic cores, drums, tapes, or disks. The magnetic-core memory may be described as stationary in contrast to the tape and drum, which must be moving for information to be obtainable.

Thus the information in the core memory is available immediately, whereas the moving units must come around to the reading station. The speed with which information can be obtained from the memory is a very important factor in determining the speed of the computer.

The large computers have cores for primary memory and magnetic tapes and drums for secondary memory. The medium-size computers are generally drum machines with the slower tapes for secondary storage. Some of the smaller computers have only a drum without secondary storage.

c. Arithmetic Unit. The only important difference between the arithmetic unit of a digital computer and a conventional desk calculator is the extremely high speed of computation of the former. Otherwise a digital-computer arithmetic unit operates on two numbers, adding, subtracting, multiplying, and dividing, just as in the desk calculator.

It should be evident that multiplication of two n -digit numbers results in a number at least $2n - 1$ digits long. Before the number may be stored in an n -element memory cell it must be rounded off down to n bits. Therefore provision is made for an accumulator register (AC), which is a special storage place for intermediate results in a sequence of arithmetic operations or a place where a number waits to be operated on. The AC has twice as much space as an ordinary memory cell for convenience in rounding off the results of a multiplication or for use in double-precision operations. Digital computers usually perform the rounding automatically. In some cases the accumulation of round-off errors may become serious and should be considered carefully.

d. Operation of Control Unit. The memory of the digital computer is analogous to the notebook of the numerical analyst and the arithmetic unit to his desk calculator. To be complete, a computing system must also simulate the activities of the human operator as he controls the transfers and arithmetic operations. This is the role of the control unit.

One of the more important aspects of modern computers is that the control information is stored in the memory with the data that are being processed. The information for the control unit is stored in memory cells as instructions. An instruction in general consists of two basic parts: one part indicates the operation to be performed; the second part is an address portion which indicates the memory location or locations involved. Some systems indicate the location of the next instruction, and others operate sequentially.

The control unit picks up the instructions and interprets them by activating specific circuits, each instruction being a series of binary digits that determine the circuit to be selected.

e. Binary Number System. It is almost universal practice to base the operation of digital computers on the number system, having 2 as the

base. This results from the fact that many electronic devices operate best when required to distinguish between the fewest possible number of different conditions, namely two. Because of this a brief comment on the binary system (base 2) is presented. Before proceeding it should be noted that there are some decimal computers; however, the basic operation is still based on the binary system.

In the binary system each digit is either a 0 or a 1. Digits are coefficients of powers of 2 rather than powers of 10 as in the decimal-number system. Instead of a decimal point a binary point is used.

In general, the sequence of digits

$$a_{n-1} \cdot \cdot \cdot a_1 a_0 \cdot a_{-1} a_{-2} \cdot \cdot \cdot a_{-(m-1)} a_{-m}$$

with the binary point between a_0 and a_{-1} , is the binary representation of the number

$$a_{n-1}2^{n-1} + \cdot \cdot \cdot + a_12^1 + a_02^0 + a_{-1}2^{-1} + a_{-2}2^{-2} + \cdot \cdot \cdot + a_{-(m-1)}2^{-(m-1)} + a_{-m}2^{-m}$$

where each a is either 0 or 1. This is exactly comparable to decimal arithmetic wherein the decimal representation

$$78.5 = 7 \times 10^1 + 8 \times 10^0 + 5 \times 10^{-1}$$

A typical binary number is 1,001.1, which in decimal notation is 9.5. To verify this identity we note that there are $n = 4$ binary digits to the left of the binary point, making $n - 1 = 4 - 1 = 3$ the largest exponent of 2 that is involved. The number is then

$$1 \times 2^3 + 0 \times 2^2 + 0 \times 2^1 + 1 \times 2^0 + 1 \times 2^{-1} = 8 + 0 + 0 + 1 + 0.5 = 9.5$$

It can be readily seen that approximately three binary digits are required to represent one decimal digit.

The length of the binary number varies from machine to machine, anywhere from 16 to 50 binary digits (bits) being used in contemporary machines. Each number or word is stored in a register or memory cell. The position of the binary point may be *floating* or *fixed*. In *floating-point arithmetic* the word or number consists of two parts, one indicating the position of the binary point and the other containing the significant digits of the number. This arrangement permits storage of both very large and very small numbers. In *fixed-point arithmetic* the binary point is fixed between specific bits, which results in a much smaller range of numbers that the machine can accept. Some computers are designed to handle both kinds of arithmetic in one problem; others require special programming subroutines to do this.

To overcome the limitations on the size of numbers in a fixed-point

machine, it is possible to introduce scale factors which adjust the numbers within the machine limits. This phase of programming requires special skill and can be quite difficult in nonlinear problems where the range of some terms cannot be predicted.

f. Machine Operation. When a human operator solves a problem using a desk calculator he must start out with a set of instructions which specify how the computations are to be performed. In like manner the digital computer must be provided with a program of instructions which must be in the machine code so that it can be understood by the machine.

Preparation of a program consists of two basic parts: (1) planning the sequence of elementary steps, and (2) coding the sequence of steps. Coding of a problem requires detailed knowledge of the particular computer on which the problem is to be solved, because only certain codes can be understood by each computer. However, planning a solution, generally, may be accomplished without special knowledge of the computer to be used, although a given problem may frequently be solved more efficiently if planned for a specific computer. Large problems from the point of view of storage requirements are more readily performed on machines having large primary memory.

Once a program is available in the code of the particular machine, it is prepared for reading into the machine by the available input device. This may be a photoelectric punched-tape reader, a punched-card reader, or a directly connected typewriter. Whatever the input system, in the usual case the form of the input is decimal rather than binary, in order to simplify the task of the user. The computer contains conversion circuits or programs that can convert decimal input into binary machine language and, conversely, convert binary information to decimal for output.

The data and instructions may be stored sequentially or, as in some computers, in accordance with predetermined locations associated with each word.

The starting location for computation is controlled by the last information stored or by the console of the computer.

g. Machine Coding. Some of the basic instructions that are available in almost all digital computers are tabulated below to indicate the type of operations that can be performed. To simplify the explanation of the instruction, use is made of the notation $c(x)$ to represent the word contained on register x , reading it as the "contents of x ," where x is the address of a memory cell. A real understanding of the potentialities of these few instructions can be obtained only by attempting to solve some programming problems. Of course, the large machines have many more instructions wired in, which means that they can do some things faster because the small computer usually requires several of the basic instructions to perform the more involved operations. An example of this is

the operation to determine the square root of a number, which is available on some computers in machine language but which is usually determined by the iteration of a relationship such as

$$R_{i+1} = \frac{1}{2} \left(R_i + \frac{N}{R_i} \right)$$

where N = number

R_i = approximate root of N

R_{i+1} = closer approximate root of N

i = iteration number

The alphabetical symbols are actually read into the computer in some cases and then translated by the computer into the proper binary or decimal code. This is very convenient because it permits the use of mnemonic symbols that make the operations easy to remember. In some computers decimal operation codes are read in to be translated into binary operation codes.

BASIC INSTRUCTIONS FOR A DIGITAL COMPUTER

Instruction		Explanation
Operation	Address	
CAD	x	CLEAR (AC) and ADD $c(x)$ to (AC)
CSU	x	CLEAR (AC) and SUBTRACT $c(x)$ from (AC)
ADD	x	ADD $c(x)$ to $c(\text{AC})$ and store sum in (AC)
SUB	x	SUBTRACT $c(x)$ from $c(\text{AC})$ and store difference in (AC)
TRS	x	TRANSFER $c(\text{AC})$ to STORAGE register x
TRD	x	TRANSFER address DIGITS of $c(\text{AC})$ to address digit position in x
MPR	x	MULTIPLY $c(\text{AC})$ by $c(x)$ and ROUND OFF the product in (AC)
DIV	x	DIVIDE $c(\text{AC})$ by $c(x)$, storing quotient in AC
UTR	x	UNCONDITIONAL TRANSFER of control to register x
CTR	x	CONDITIONAL TRANSFER of control to register x If $c(\text{AC})$ is negative, transfer control to register x If $c(\text{AC})$ is positive, transfer control to next register

It should be noted that a word placed in the memory remains intact except when the transfer instructions (TRS and TRD) are used.

An important capability of the modern computer is the ability to program changes in the instructions in accordance with the results of computations. It is possible to reduce virtually any criterion for choice among a number of possible routines to a sequence of yes-no decisions. The CTR instruction is designated to accomplish this by comparing a known quantity with a computed quantity. This same operation is basic

to counting in a computer. Since digital computers are inherently desirable for problems that are repetitive, most problems require counting in some form.

h. The Use of Flow Diagrams. Perhaps the most important consideration in programming is learning to make a program outline or logical flow

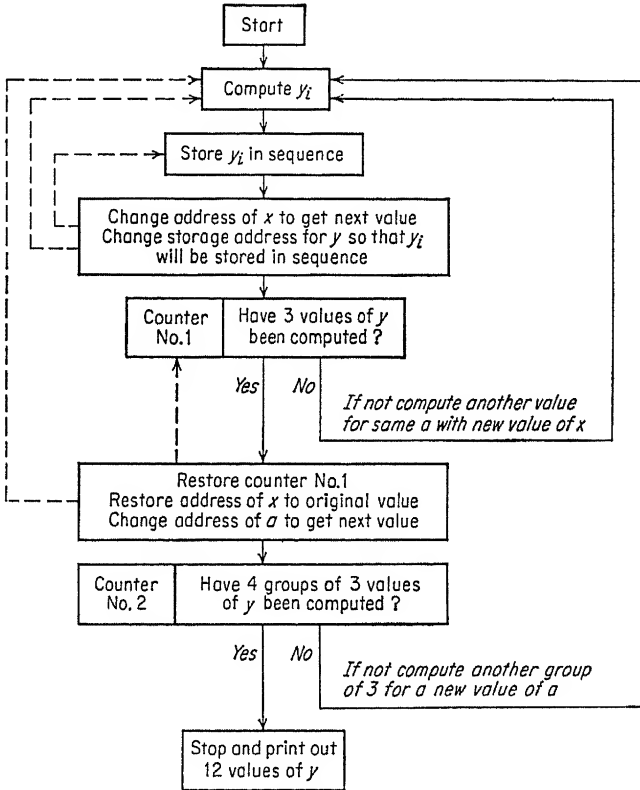


FIG. 9.4. Flow-diagram example.

chart of the problem. The function of a flow chart is to reduce a complex problem into a set of simpler units. If there is no break in the sequence of instructions, the logical flow is simple. However, if a jump results from a conditional transfer instruction, the alternatives are best illustrated by a flow diagram.

A flow diagram constructed in the planning stage before much of the coding has been performed will save considerable time in all phases of the programming.

Figure 9.4 illustrates the use of a flow chart for the computation of $y = ax^2 + bx + c$ for three different values of x and four values of a . The diagram should be self-explanatory.

Flow diagrams are very important in the "debugging" of a problem. It is very difficult to maintain a clear mental picture of the loops within loops that often develop in computer programming, and a written graphical record is of tremendous assistance. Furthermore, a flow diagram is a must if someone other than the original programmer is to attempt to understand the program.

i. Practical Considerations in the Use of Digital Computers. It should be emphasized that the digital computer is only another aid, although a very powerful one, for solving engineering problems. The engineer should list the digital computer with the slide rule and the desk calculator. In fact, for many problems in engineering the other two devices are better suited than the digital computer for obtaining solutions. The primary utility of the digital computer lies in its ability to repeat a series of simple operations at fantastic speed. Thus digital computers are best suited for problems that require numerous repetitive solutions of the same equations or relationships. Some problems can be solved once by the use of desk calculator for a given set of conditions much more rapidly than they can be programmed to the point where answers can be obtained. An obvious advantage of the digital computer is that once a program for a problem has been completed satisfactorily, in general it requires no more calendar days to obtain 100 answers than 1 answer. In production computations, that is, computations using an established program, an engineering office can save considerable time, or, what is often more desirable, make a more thorough analysis than is customary because of the time required to obtain a solution by conventional desk computers. If a problem is solved by conventional procedures and a change in basic data is introduced near the end of the process, a revised set of computations will ordinarily require the expenditure again of a large percentage of the man-hours and calendar-days required for the original calculations, whereas with the digital computer, although the original programming might require a year, new sets of answers can be obtained overnight after the time required to punch the revised data on tapes.

Each computer has a library of subroutines that are designed to fit into any program coded for the particular machine. Subroutines are usually available to calculate trigonometric functions, take square roots, etc. A well-organized computing center collects new programs that are likely to be of use in future problems and provides an explanation to go with each one. A well-run office that does programming should collect subroutines that are of special interest in its special field of application.

It requires considerable time to achieve a satisfactory program for apparently simple problems. This statement can be made with complete confidence, especially if the problem consists of a large number of decision-making routines which introduce counting and address changing. Each

of these operations is straightforward and easily understood by itself, but as they intertwine with each other and grow in number the possible mistakes multiply. Mistakes are mostly in omission—leaving out a necessary instruction or symbol, or, what is more difficult to detect, omitting a possible alternative.

Analyzing a problem for a digital computer is a procedure that may be unusual and unfamiliar to many engineers. Analysis for a digital computer must be comprehensive; no possible alternative can be overlooked. If, for example, a term is usually positive but may in rare circumstances be negative, the program must be written to consider the unusual case as well. The engineer analyzing the same problem by conventional means would not be concerned about the negative sign until it turned up, and if it did not, would be saved the trouble of considering its implication. An engineer performing an analysis can observe the sequence of events and, if the sequence is significant, can treat the analysis accordingly. However, the computer must be programmed to record the sequence of events and provide a different routine to handle each significant sequence of events.

Unless a comprehensive preliminary analysis can be prepared, programming is best done by a person who knows the engineering problem intimately. As the program develops, if alternatives have been previously overlooked, the engineer working on his own program will probably recognize the omission, the professional programmer will probably not.

One of the most important problems in digital-computer operation and one to which considerable effort has been devoted is the development of procedures for detecting and preventing mistakes. Some of these that are built into the computers analyze the input before computation begins in order to check, among other things, if the symbolic addresses are consistent, if only legitimate instruction symbols are used, if the program fits the limited capacity of the machine. Others operate during the computations to ensure against transient malfunctioning of the machine. If the built-in mistake-detection systems denote a mistake, an "alarm" results which stops the machine and indicates the type of mistake involved. An important system for program-error detection is a "post-mortem" system that records, for the benefit of the programmer, the condition of the machine memory at the time of an alarm, and some of the steps preceding the alarm. It should be possible also to obtain quickly a complete post-mortem showing the contents of each register at the time of the alarm.

The programmer can build into the program certain arithmetic or logical checking procedures (if any exist) that are appropriate to the problem. One good procedure is to use two different machine techniques for performing a computation. Spot checks, by hand calculation or by an analog computer, should also be used to verify results. Of course, none of these methods is foolproof, but disagreement between analog and digital

solutions should be the basis for a careful review of both solutions. A very important procedure that should be followed by programmers in the fight against program errors is the breakdown of the program into as many logical subdivisions as appear to exist and to test-run each for arbitrary data that are calculated to cause unusual results to develop, thus testing all the conditional responses of the program. Test runs to be verified by hand computations should be planned early in the process to provide the hand computer some lead time in competing with the programmer and the digital computer. Although proving each section of the program before incorporating it into the total program does not guarantee that the combined program will operate correctly, the sources of error are more readily detected.

Although the previous remarks are devoted mainly to the theme that programming for an engineering problem can be complex and tedious, there is no greater satisfaction, once a program has been written and "debugged," than watching a production run produce answers that previously could be achieved only by a much greater expenditure of man-hours, if at all.

j. Examples of Dynamic Analysis by Digital Computer. Useful applications for digital computers can be found in every branch of civil engineering; however, this list includes only structural dynamic applications. Some of the recent applications are:

1. A study of the theoretical dynamic behavior of a series of reinforced-concrete shear walls subjected to various impulsive loadings [18]. As many as 77 degrees of freedom were considered.

2. A study of the behavior of a single-span girder bridge under the action of a moving truckload [20]. In this problem an analog computer was used to determine the effect of various parameters, and the digital computer was used to pin-point the results. The objective of this study was to obtain curves of maximum displacements for reasonable variations of the several pertinent parameters so that a bridge designer could estimate the dynamic displacements and stresses.

3. A program to analyze a multistory building frame that has been distorted into the elasto-plastic range. Such an analysis procedure is amenable to use in the study of the effects of earthquakes and winds as well as the effects of blast loads [21].

4. Many blast-effect analyses for one- and two-degrees-of-freedom systems [21].

5. Many earthquake-effect analyses for various types of models [22, 24-26].

6. Vibration analysis of a ship propeller shaft to determine critical whirling frequencies [23].

In each of these problems use is made of one or more of the numerical

methods of integrating a second-order differential equation with known initial conditions described in Chap. 8. In some of the multidegree problems the man-hours required to obtain one complete hand solution is about equal in order of magnitude to the time required to program for the computer. In the proper circumstances, digital computers repay manyfold the effort required to get acquainted.

REFERENCES

Analog Computers

1. Korn, G. A., and T. A. Korn: "Electronic Analog Computers," McGraw-Hill Book Company, Inc., New York, 1952.
2. Flight Control Laboratory, MIT: The High Speed Analog Computer in System Engineering, *Rept. FCL-7231-R5*, Cambridge, 1954.
3. Wilts, C. H., and G. D. McCann: "New Electric Analog Computers and Their Application to Aircraft Design Problems," California Institute of Technology, 1953.
4. Soroka, W. W.: "Analog Methods in Computation and Simulation," McGraw-Hill Book Company, Inc., New York, 1954.
5. McCann, G. D., and R. H. MacNeal: Beam Vibration Analysis with the Electric-analog Computer, *J. Appl. Mechanics*, vol. 17, pp. 13-26, 1950.
6. Reswick, J. B.: Scale Factors for Analog Computers, *Product Eng.*, March, 1954.
7. Engineering Research Associates, Inc.: "High-speed Computing Devices," McGraw-Hill Book Company, Inc., New York, 1950.
8. Howe, C. E., R. M. Howe, and L. C. Rauek: Application of the Electronic Differential Analyzer to the Oscillation of Beams, Including Shear and Rotary Inertia, *Univ. Michigan Eng. Research Inst. UMM-67*, January, 1951.
9. Ragazzini, J. P., R. H. Randall, and F. A. Russell: Analysis of Problems in Dynamics by Electronic Circuits, *Proc. IRE*, vol. 35, no. 5, May, 1947.
10. Paynter, H. M., and G. A. Philbrick: Electronic Analogy as a Lab Tool, *Industrial Labs.*, vol. 3, no. 5, May, 1952.
11. Nolan, J. E.: Analog Computers and Their Application to Heat Transfer and Fluid Flow—Part 3, *Computers and Automation*, January, 1955.
12. Paynter, H. M. (ed.): "A Palimpsest on the Electronic Analog Art," Geo. A. Philbrick Researches, Inc., Boston, 1955.
13. Thomson, W. T., and J. A. Cheney: Response of Elastic Beams to Impulsive Loading, *Univ. Calif. (Los Angeles) Rept. 51-13*, December, 1951.
14. Thomson, W. T.: Plastic Behavior of Beams under Long Duration Impulsive Loads, *Univ. Calif. (Los Angeles) Rept. 54-92*, October, 1954.

Digital Computers

15. Engineering Research Associates, Inc.: "High-speed Computing Devices," McGraw-Hill Book Company, Inc., New York, 1950.
16. Hartree, Douglas R.: "Calculating Instruments and Machines," University of Illinois Press, Urbana, Ill., 1949.
17. Wilkes, Wheeler, and Gill: "The Preparation of Programs for an Electronic Digital Computer," Addison-Wesley Publishing Company, Reading, Mass., 1951.
18. Finerman, A.: Dynamic Behavior of Shear Walls, Sc.D. thesis, MIT, 1956.
19. *Indust. Math.*, vol. 3, 1953.

20. Bridge Vibration, Joint Highway Research Project, MIT and Commonwealth of Massachusetts Dept. of Public Works, *Progr. Rept. 2, Research Rept. 10*, 1956.
21. Classified research at MIT by Civil and Sanitary Engineering Dept.
22. Tung, T. P., and N. M. Newmark: Numerical Analysis of Earthquake Response of a Tall Building, *Univ. Illinois Structural Research Ser.*, no. 110, 1955.
23. Brandt, C. R., J. C. Snyder, and C. R. Thompson: Investigation of Adapting Naval Architecture and Marine Engineering Design Processes to Digital Computer Solutions, thesis, MIT, 1956.
24. Clough, R. W.: Earthquake Forces in a Tall Building, *Civil Eng.*, January, 1956.
25. "Proceedings of the World Conference on Earthquake Engineering," Earthquake Engineering Research Institute, San Francisco, Calif., 1956.
26. *Bull. Seismological Soc. Am.*
27. *J. Assoc. Computing Machinery.*
28. *Computers and Automation.*

PART 4

**APPLICATION OF STRUCTURAL DESIGN AND ANALYSIS
TO SPECIFIC CASES INVOLVING DYNAMIC LOADING**

CHAPTER 10

INTRODUCTION TO BLAST-RESISTANT DESIGN

10.1. Purpose. The purpose of Chaps. 10 to 15 is to describe methods and to present factual information whereby structures can be designed to resist the effects of atomic- or hydrogen-bomb explosions. The principles of dynamic analysis and design which have been described in other chapters will be used, along with factual information on (1) dynamic loading, as developed by the air-blast pressure wave, (2) thermal radiation and fire hazards, (3) instant nuclear radiation, and (4) radioactive fallout.

While it is *difficult* to resist the effects of atomic weapons, it is *possible* at even relatively close distances from the bomb. Whether or not it is desirable is, of course, a function of the criticality of the installation and the cost of protection. However, it is not possible to protect a surface structure from a direct hit of any size atomic or hydrogen bomb; but there are large areas surrounding an explosion in which conventional structures would collapse or suffer severe damage while blast-resistant structures would suffer little or no damage and offer protection to contents. It is for structures to be built in these regions that the following information is presented.

10.2. Weapon Phenomena. Atomic weapons are rated in terms of their energy yield, and it is customary to express this yield as the weight of TNT which would give the same total energy release. A convenient unit is the energy equivalent of 1,000 tons of TNT, and this is expressed briefly as 1 KT (1 kiloton). The so-called nominal bomb is one whose approximate yield is 20 KT. It was this size bomb that was dropped over Hiroshima and Nagasaki. The hydrogen bombs that have been detonated in the tests at the Pacific Proving Grounds have had energy yields equivalent to millions of tons of TNT, expressed as megatons (MT).

By the use of simple scaling laws, the effects of bombs of other sizes may be related to the known effects of a given-size bomb, as described in Sec. 11.1*d*.

An atomic bomb may be exploded in the air or at or near the surface of the earth. The medium in which the bomb is burst determines to a large extent the relative magnitudes of the various damaging effects. This text will be limited to air-burst or surface-burst weapons.

The detonation of an atomic weapon releases a large amount of energy in a fraction of a second. During this time the bomb components are volatilized into a sphere of hot compressed gas at a temperature of millions of degrees and a pressure of the order of hundreds of thousands of atmospheres. This sphere of intensely hot gas expands and radiates thermal energy in a band of short wavelengths. Air is nearly opaque in this range of wavelengths; consequently, the shell of air surrounding the

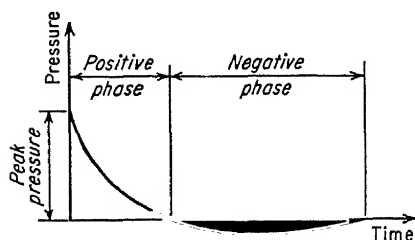


FIG. 10.1. Blast-pressure curve.

parent gas sphere absorbs radiated energy until it is approximately as hot as the sphere. Then it in turn radiates to another shell of air, and so on, until the temperature is reduced to a value at which this process is less rapid than the transmission of energy by atomic and molecular collision. Thereafter, energy transmission is by a shock-

wave or rapid-pressure rise, which moves radially outward from the point of detonation.

a. Air Blast. At any point along the path of the shock front (except in the near vicinity of the bomb) the pressure-time variation in air will be of the form shown in Fig. 10.1. This phenomenon is characterized by an instantaneous or very rapid rise to a maximum pressure followed by a decline to subatmospheric pressure and then a gradual return to normal. The portion of the wave in which the pressure is above atmospheric is termed the positive phase, while the part below atmospheric is the negative phase. The peak pressure and the duration of the positive phase of the pressure wave vary as functions of size of weapon, height of burst of weapon, and distance from point of detonation.

An effect associated with the presence of high air pressures in the blast wave is the mass movement of air commonly called the blast wind. This high-velocity surge of wind blows in the direction of the propagation of the air blast during the positive phase. The wind velocity decays to zero, and then is reversed during the negative phase. The velocity is a function of the pressure in the blast wave. The pressure exerted by this blast wind is commonly called dynamic pressure.

b. Thermal Radiation. In addition to the blast, or shock-wave, effects, the exploding bomb emits instantaneous radiation of two types, thermal and nuclear. The thermal radiation is caused by temperatures which are nearly as high as the interior of the sun, occurring in the early stages of the explosion of the atomic bomb. This radiation is capable of causing severe burns in human beings and animals and of starting fires in combustible material and structures exposed to direct rays. Roughly about

one-third of the total energy release of an atomic bomb appears in the form of thermal radiation.

c. Nuclear Radiation. The nuclear radiation consists of gamma rays and neutrons and is capable of causing serious injury to human beings and animals. If the burst is not well above the surface of the earth, residual nuclear radiation becomes an additional hazard, since all matter near the explosion will emit beta particles and gamma radiation for some time afterward. If the burst is well above the surface of the earth, most of the products of fission are rapidly dissipated and have no serious effects except for very-large-yield weapons. Radioactive fallout can be an intense hazard extending over very large areas.

10.3. The Resistant Structure. The resistant structure obviously may take any one of many forms, dependent on the function of the structure, its location, importance, etc. It may be a small boxlike personnel shelter buried underground designed for very-high-pressure levels (100 psi or more), or a large boxlike above-ground hospital designed for a relatively low-pressure level (10 psi), or an extensive low-rise-surface dome designed for high-pressure levels to protect some critical military equipment or function.

a. Design Considerations. A number of considerations enter into the design problem of blast-resistant structures. Some of the more important ones are as follows:

1. The magnitudes of forces imposed on a structure subject to attack are very large in comparison with the forces for which the structure would normally be designed.

2. The forces are dynamic in character with a duration of from one to several seconds.

3. The geometry of the building, the amount and arrangement of openings, and the type of wall covering affect the magnitude of blast forces imposed on the structure.

4. The danger of fire caused either by the radiation effects of the atomic bomb or by such secondary effects as the shorting of electrical circuits or the rupture of heating units or fuel lines is so great that special precaution should be taken to reduce fire risks.

5. The thermal and nuclear radiation hazards to human beings must be considered.

6. The distance at which windows will be broken by blast pressure is so very large that special precautions are necessary for the protection from flying glass of personnel housed in windowed structures.

b. Dynamic Character of Loading. The facts that blast forces are large in magnitude and dynamic in character introduce several new aspects to the design problem which require other than normal design procedures.

First, for example, it is desirable, whenever the function of the structure

permits, to design the building to resist the intense blast forces with plastic yielding (permanent distortion) of the framing members. If this is not done and the structure is designed to resist the dynamic blast forces with stresses in all structural members remaining within the elastic range (below the yield point), then the resulting structure would be more costly, as compared with the structure in which plastic yielding of reasonable amounts is permitted.

The amount of plastic distortion permitted in a structure must be kept small enough (1) to provide a margin of safety against collapse of the structure, (2) to limit damage of building services, and (3) not to interfere with the function of the building.

Secondly, the dynamic character of the loading, coupled with the fact that plastic yielding of structural members may be permitted, requires that the design procedure be based on a dynamic analysis. Equivalent static loadings may be substituted in certain special cases for the dynamic blast loads, and conventional static methods of analysis and design may be used. However, the indiscriminate application of such methods may result in erroneous or uneconomical designs.

c. Geometry of Building. The external shape of the building influences in a complex way the magnitude and distribution of blast forces imposed on the building. For example, certain shapes such as the arch or dome tend to reduce the magnitude of blast loads compared with the box-type building; and then, for the box-type building, the magnitude of the translational blast force is a function of the length of the building in the direction of the propagation of blast, the longer building having the larger load. This arises from the fact that the translational load is the difference between the pressures on the front and rear walls of the building. If the rear wall is farther from ground zero, then it is subjected to lower blast forces at a later time than if it were closer to ground zero.

The presence of windows or openings in the building adds further complication. First, the blast is permitted to enter and act on interior partitions, personnel, or contents. Second, the magnitude of forces causing distortion of the structure may not be reduced at all below that affecting the windowless structure. Third, the prediction of the lateral forces is less certain than for a windowless structure.

d. Fire Hazard. The thermal effects of an atomic weapon are defined in terms of amounts of radiant energy, in calories per unit area, that will be imposed on surfaces at any distance from an atomic bomb. The interpretation of thermal energy delivered per unit area as to whether or not a surface of a particular material will char or burn can be done for a variety of materials. However, the probability of setting fire to a combustible structure cannot be estimated with any degree of reliability at the present time. It is sufficient to note, however, that great fires

resulted at Hiroshima and Nagasaki and that fires are likely to occur in other targets of A-bombs unless the targets are noncombustible. For this reason, even more rigid control of fire-safety standards are recommended for the blast-resistant structure than for conventional construction.

e. Radiation. The instantaneous thermal and nuclear radiations from a detonating atomic weapon can cause injury or death to human beings if the radiation is sufficiently intense.

Protection against nuclear and thermal radiation can be furnished by the provision of shielding walls of concrete, steel, lead, or other material of sufficient thickness to reduce radiation intensities to tolerable levels.

10.4. Necessary Decisions. The objective of the architect-engineer of a blast-resistant structure is to design it so that the structure itself, its equipment, contents, and occupants are as invulnerable to the effects of atomic weapons as is physically and economically practicable.

The over-all planning of a resistant structure must recognize the potential damaging effects of an atomic explosion on a building and its contents, both equipment and personnel. Details of design, which recognize these effects once a given structural system of resistance has been selected, will be illustrated in Chap. 14.

Prior to the detailed design of a structure to resist given effects of blast and radiation, some basic planning must be made. Chapter 13 considers factors which may affect these decisions, which are briefly referred to in this section as follows.

a. Site Selection. In general, the cheapest method of securing protection against the effects of atomic weapons is to use defense by space, or dispersal. Greater safety may also be achieved by location in a non-critical area. Frequently this may be impossible, in which case a blast-resistant design is required.

If dispersal is not permissible and construction in built-up or critical areas is mandatory, then other factors should be considered. For example, structures should not be located in areas of densely built-up combustible buildings because of the great hazard from fire; or if they are, in such areas special precautions must be taken to ensure insulation from the intense heat and to provide sufficient air for occupants of shelters.

The potential hazard of radioactive fallout extends over extremely large areas (thousands of square miles from one large-yield detonation), making it potentially possible for any structure to be subject to intense radiation levels.

b. Level of Protection. The primary decisions as to whether or not protective construction should be employed in a new project, and the level of protection needed, is an extremely complex problem.

Considerations which will contribute to the formation of these decisions

involve (1) the probability of attack, (2) the size of weapon and likely distance to the structure, (3) the vulnerability of the installation to attack, (4) the evaluation of the relative importance of the activity or operation to be housed, and (5) the feasibility and cost of various levels of protective construction. Information on items 1 to 4 is not available in this treatment.

c. Selection of Structural System—Surface Structure. A number of factors affect the selection of the structural system. The function of the structure determines, of course, the required space and its arrangement. In addition, function may affect the selection of type of wall covering used, which in turn affects the decision on choice of structural framing system. For example, it may be possible to use a frangible wall covering, that is, one that breaks readily under blast. On the other hand, the contents of the building may require that the wall panels offer protection against blast and flying debris. This requirement would force the use of resistant wall panels, which in turn affects the design of the framing system and perhaps the choice of type.

An additional consideration affecting the selection of the structural system is the advantage to be gained by the use of geometric shapes of building which tend to reduce the intensity of blast loads on the building. Shapes such as the arch and dome offer some advantage when compared with the box-type structure.

d. Choice of Underground Construction. The magnitude of blast forces to be resisted by the blast-resistant structure can be materially reduced by the use of underground construction. In addition, the problem of shielding against the nuclear radiation becomes simpler since earth is effective as a shield (two-thirds as effective as concrete) in reducing radiation intensity. These two facts may result in the underground structure being a more economical solution to the problem. However, separate designs for cost comparisons will probably be required until more experience is gained in blast-resistant construction.

e. Type of Wall Covering. Certain types of construction, notably industrial structures, can be adapted to frangible-wall-type construction. Frangible walls would fracture under relatively low blast pressure, reducing the areas exposed to blast pressure, thus minimizing the cost for maximum chance for structural survival. Such construction would be suitable only for cases in which no personnel are exposed (separate shelters could be provided for personnel) and for cases in which the contents of the structure can withstand the missile hazard of the broken walls and the weathering problem should an attack materialize.

Other structures obviously will require blast-resistant walls and generally will be windowless.

CHAPTER 11

WEAPONS-EFFECTS DATA APPLICABLE TO BLAST-RESISTANT DESIGN

11.1. General. The air burst of an atomic bomb is the most likely form of attack against surface structures. It is very efficient in producing a destructive air blast which is propagated through the atmosphere to great distances with small energy losses. In contrast, in an underground burst, energy is absorbed in cratering and melting of the ground, and energy is dissipated in overdestruction of the structures located in the immediate vicinity of the burst. An additional advantage to the attacker of the air burst over the underground burst is the minimization of the shielding of one surface structure by another surface structure when the shock source is located at an elevation greater than that of the structures being attacked. Air-burst bombs are also used to attack buried structures which are vulnerable to the ground pressures induced by the air blast on the earth's surface.

In addition to the mechanical effects noted above, atomic weapons produce other effects due to thermal and nuclear radiation emitted at the time of the explosion. Thermal radiation refers to heat waves, and nuclear radiation refers to gamma rays and neutrons. The phenomena of radiation and the conditions under which they are fatal to people and destructive to property are discussed in Sec. 11.3.

a. Air Blast. The loads on an above-ground structure resulting from the air blast produced by a bomb burst may be discussed under the general headings of diffraction loading and drag loading.

Diffraction loading is the term given to the forces on a structure resulting from the direct and reflected pressure associated with the air blast in the initial phases of the envelopment of the structure. The finite time required for the air blast to surround the structure completely and the presence of large pressures on only the front face cause net lateral loads to exist on the structure in the direction of travel of the air blast. The local and differential forces thus determined as acting on the structure are defined as the diffraction loading.

Drag loading is the term given to the forces on a structure resulting from the high velocity of the air particles in the air blast acting as a high-

velocity wind. This type of loading is most important on truss-type structures such as bridges, tall chimneys, and buildings in which the wall panels fail, leaving the structural frame exposed to the air blast.

In general, diffraction loading can be neglected and only the drag loading considered if the minimum dimension of the structure perpendicular to the direction of travel of the blast wave and the dimension of the structure parallel to the direction of travel of the blast wave are less than approximately 5 ft.

For a structure subject to the air blast resulting from the detonation of a nominal-size atomic bomb, the impulse of the drag loading will predominate over the impulse of the diffraction loading if the minimum dimension of the loaded portion of the structure transverse to the direction of travel of the air blast is less than 10 ft. The larger the loaded portions of the structure become, and hence the greater the time required for the blast to reach the relatively steady condition of drag loading, the more important is the impulse of the diffraction loading relative to the drag loading. In most cases, except when a precursor exists, the maximum pressure on any portion of the structure existing during the diffraction period is at least as great, and in most cases greater than, those pressures existing during the drag period.

In the following sections the presentation of the load exerted on structures by the air blast is preceded by a description of the formation and propagation of the air-blast phenomena from a source located in an infinite homogeneous atmosphere (Sec. 11.1*b*). The effect on the air blast of the presence of the surface of the earth is then introduced for a surface-burst weapon in Sec. 11.1*c*.

The basic relations involved in scaling the given data of one size of weapon to another desired size of weapon is presented in Sec. 11.1*d*. The loading produced on various types of structures by a given air blast is discussed in detail, and procedures are presented for computing the loads on surface structures under Sec. 11.2.

b. The Blast Wave in an Infinite Homogeneous Atmosphere. It is necessary to evaluate various aspects of the air-blast phenomena associated with the detonation in air of an atomic bomb in order to determine the air-blast loading on a structure. To simplify the presentation of these phenomena the initial discussion considers the explosion of a nominal-size atomic weapon in a fictitious normal homogeneous atmosphere of infinite extent.

Almost immediately after the detonation occurs, the expansion of the hot gases initiates a pressure wave in the surrounding air, as represented very roughly by the curve in Fig. 11.1*a*. This shows the general nature of the variation of the air overpressure (or pressure above atmospheric) with distance from the explosion at a given instant. As the pressure wave

is propagated away from the center of the explosion, the following (or inner) part moves through a region which has been previously compressed and heated by the leading (or outer) parts of the wave. The disturbance moves with the velocity of sound, and since this velocity increases with the temperature and pressure of the air through which the wave is moving, the inner part of the wave moves more rapidly and catches up with the outer part, as shown in Fig. 11.1*b*. The wavefront thus gets steeper and steeper, and within a very short period it becomes abrupt, as indicated in Fig. 11.1*c*. At the advancing front of the wave, called the shock front, there is a very sudden increase of pressure from normal atmospheric to the peak shock pressure. The shock front thus behaves like a moving wall of highly compressed air.

Initially, in the hot central region of the bomb, the pressure exceeds atmospheric by perhaps a factor of many hundred thousand. The pressure distribution behind the shock front is somewhat as illustrated in Fig. 11.1*c*. It shows the peak overpressure (air pressure above atmospheric) at the shock front, indicated by P_{so} , dropping rapidly in a relatively small distance to a value about one-half the shock-front overpressure. The magnitude of the overpressure is uniform in this interior portion.

As the expansion proceeds, the pressure distribution in the region behind the shock front gradually changes. The overpressure is no longer constant but drops off continuously nearer the center. At later times when the shock front has progressed some distance from the center, a rarefaction develops at the center, causing a drop in pressure below the initial atmospheric value. Thus a suction phase develops. The front of the shock wave weakens as it progresses outward, and its velocity drops toward the velocity of sound in the initial cooler air. The sequence of events just described for increasing times t_1 to t_6 is depicted in Fig. 11.2. This shows the overpressure distribution in the shock wave as a function

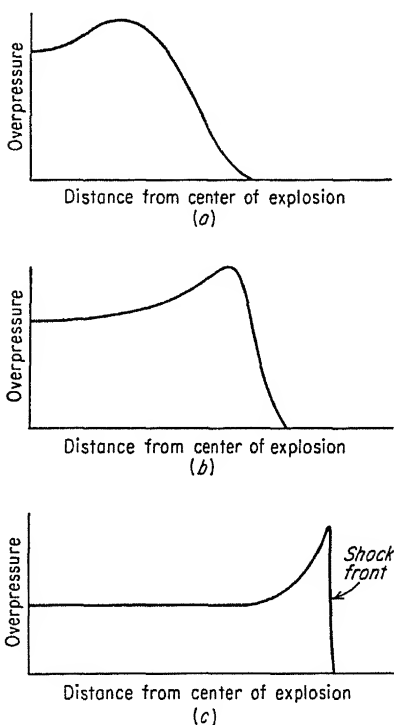


FIG. 11.1. Overpressure distribution in early stages of shock-front formation [Chap. 1, Ref. 8].

of the distance from the explosion at different stages in the expansion. When the negative overpressure (or suction phase) is well developed, the overpressure in the shock wave resembles the heavily drawn curve in Fig. 11.2.

The behavior of the shock wave from this time on can be considered in two different ways, as shown in Figs. 11.3 and 11.4. First, in Fig. 11.3,

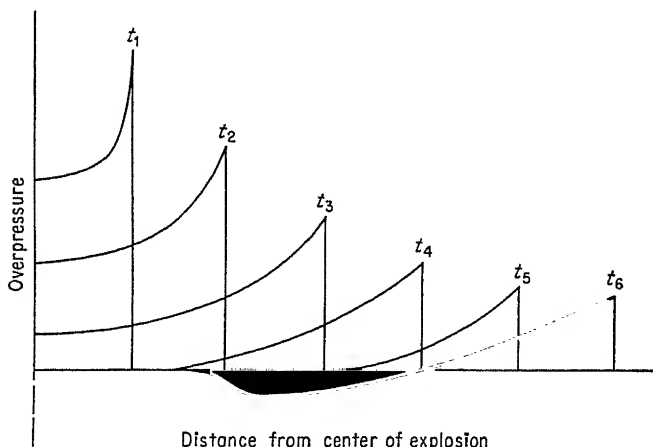


FIG. 11.2. Variation of overpressure with distance from center of explosion at various times [Chap. 1, Ref. 8].

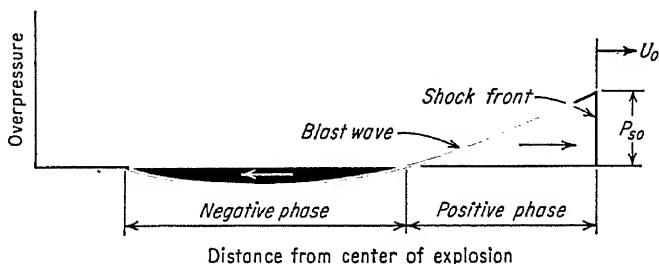


FIG. 11.3. Variation of overpressure with distance at a given time [Chap. 1, Ref. 8].

the heavy curve of Fig. 11.2 is redrawn and, as before, shows the variation of shock overpressure with distance at a given time. The symbol P_{so} represents the peak overpressure, or shock intensity, in pounds per square inch. U_o is the velocity of the shock front in feet per second. The arrows adjacent under the curve show the direction of movement of the air mass or blast wind, in the positive and negative phases. The peak overpressure in the positive phase is higher than the maximum overpressure in the negative phase. Consequently, the blast wind is of higher velocity and shorter duration in the positive phase than in the negative, or suction, phase. Second, the same wave may be considered alternatively by plotting

the variation of overpressure with time at a fixed location, as shown in Fig. 11.4. The symbol t_a is the time of arrival, or the time in seconds for the shock front to travel from the explosion to the given location; t_o is the duration in seconds of the positive phase; and P_{so} is as previously defined.

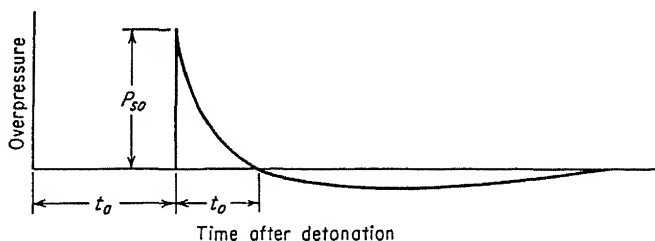


FIG. 11.4. Variation of overpressure with time at a given location [Chap. 1, Ref. 8].

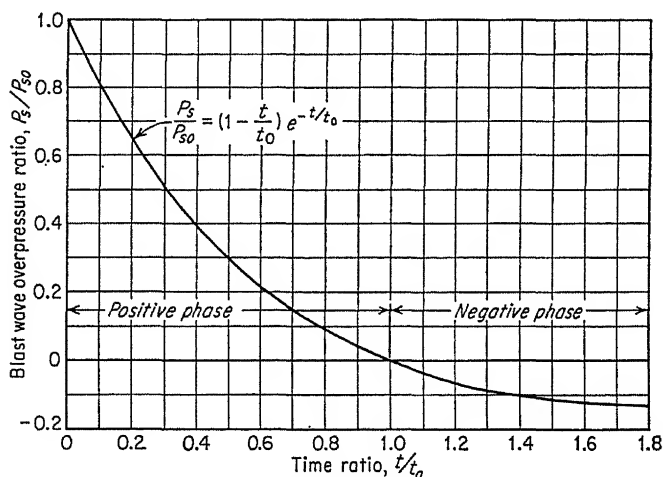


FIG. 11.5. Blast-wave overpressure ratio vs. time ratio [Chap. 1, Ref. 8].

The overpressure P_s at time t after the arrival of the shock front is given by the expression

$$P_s = P_{so} \left(1 - \frac{t}{t_o} \right) e^{-t/t_o} \quad (11.1)$$

where e = base of natural system of logarithms = 2.7182.

This expression, which is plotted in Fig. 11.5, is valid only for the positive phase of the air blast and the portion of the negative phase shown. The peak negative overpressure is approximately one-eighth of the peak positive overpressure, and the duration of the negative phase is approximately four times the duration of the positive phase of the air blast for low overpressures.

c. *The Blast Wave for a Finite Height of Burst.* The discussion in Sec. 11.1b deals with the air blast from an atomic bomb exploded in an atmosphere of infinite extent. This section considers the influence of the height of the burst on propagation and attenuation of the air blast.

If the bomb is detonated at a distance h above the surface of the earth, the shock wave will have the general configuration indicated in Fig. 11.6 during the brief time interval before it impinges upon the surface. The shock wave is, so to speak, unaware of the presence of the plane surface below and is behaving as if propagated in an atmosphere of infinite extent.

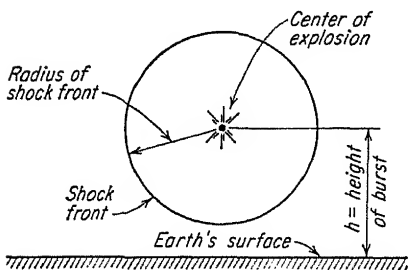


FIG. 11.6. Shock front when its radius is less than the height of burst [Chap. 1, Ref. 8].

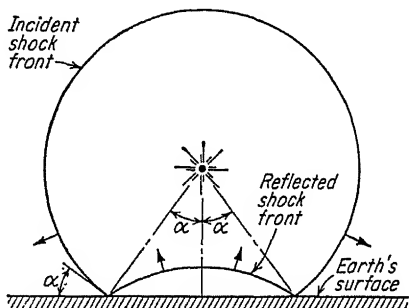


FIG. 11.7. Illustration of shock reflection where α is less than $45^\circ \pm$ [Chap. 1, Ref. 8].

A short time later the radius of the shock front becomes greater than h , and that portion of the incident shock wave which impinges upon the earth's surface is reflected back, forming the reflected shock wave illustrated in Fig. 11.7. The arrows at the incident and reflected shock fronts indicate the direction in which the shock waves are traveling. The location of the reflected shock front is roughly determined by drawing an arc, with center located a distance h below the earth's surface and directly under the point of detonation, joining the points of intersection of the incident shock with the reflecting surface. The symbol α represents the angle of incidence of the shock wave with the earth's surface. The reflected shock-wave overpressure $P_{r-\alpha}$ is a function of the incident shock overpressure P_{so} and the angle of incidence α .

The reflected shock front in Fig. 11.7 travels through the atmosphere at a higher velocity than the incident shock and gradually overtakes and merges with it to form a single shock front called the Mach stem, as shown in Fig. 11.8. The fused shock front thus formed is normal to and travels parallel to the earth's surface. The Mach-stem formation is initiated when the angle of incidence α of the shock wave becomes greater than approximately 45° . Once formed, the height of the Mach stem gradually increases as the radius of the shock wave becomes greater.

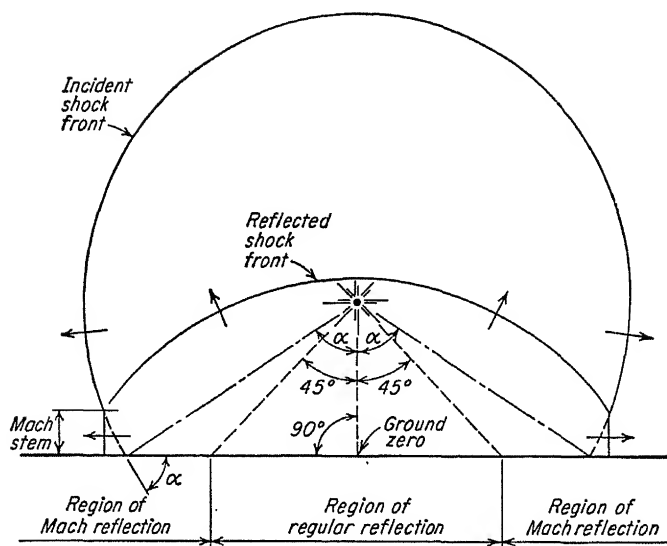


FIG. 11.8. Shock-reflection phenomena in region where α is greater than $45^\circ \pm$ [Chap. 1, Ref. 8].

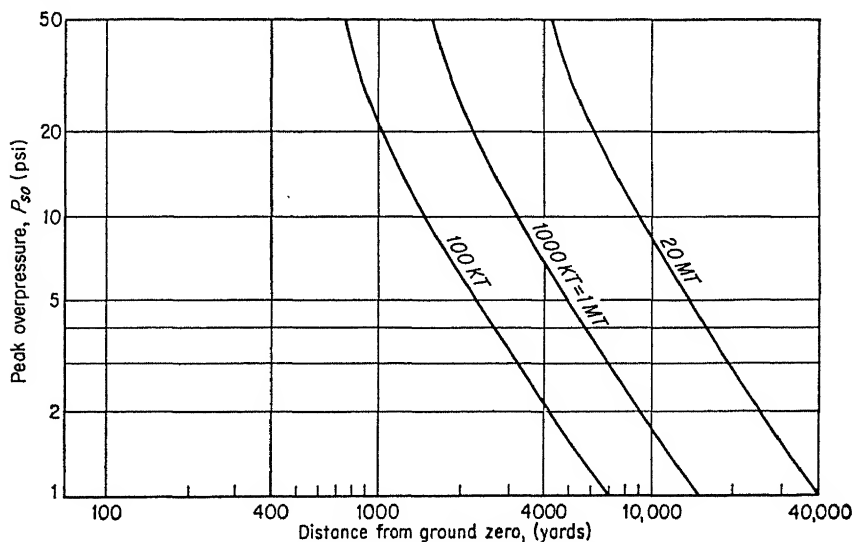


FIG. 11.9. Peak overpressure P_{so} versus distance.

The region on the earth's surface within which α is less than approximately 45° and no Mach stem is present is called the region of regular reflection, while the region for which α is greater than approximately 45° and a Mach stem is present is called the region of Mach reflection. The importance of the Mach-stem phenomenon is that it causes two shock

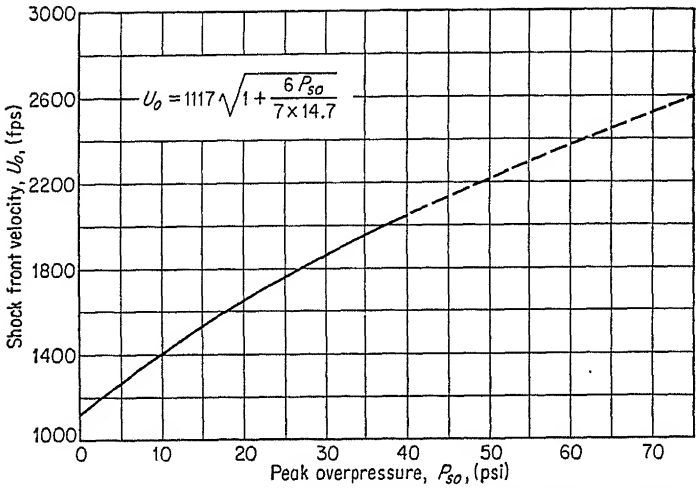


FIG. 11.10. Shock-front velocity vs. peak overpressure. (Validity of dashed portion of curve is uncertain.) [Chap. 1, Ref. 8]

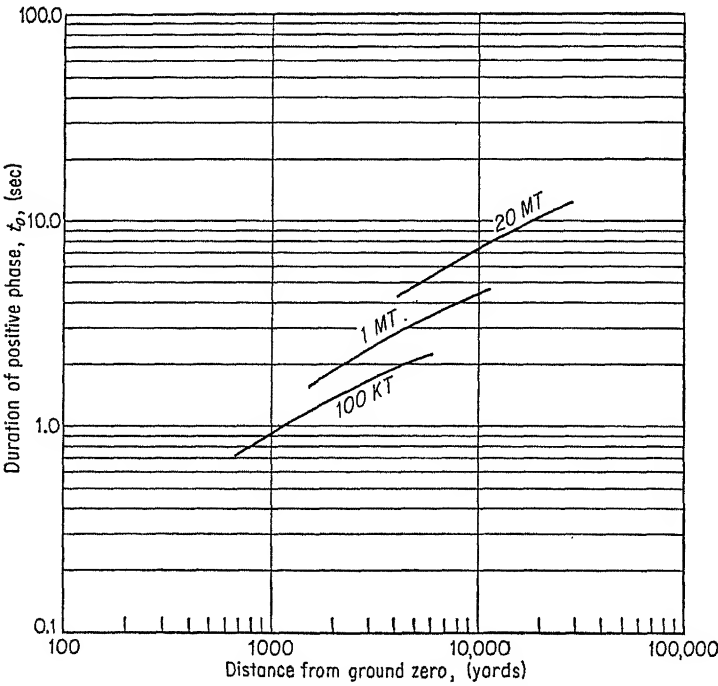


FIG. 11.11. Duration of positive phase vs. distance.

waves to fuse into a single shock wave of higher overpressure and of greater destructive power to structures located in its path.

The peak overpressure P_{so} existing in the shock wave adjacent to the ground surface is a function of the distance from the point of burst and the yield of the weapon; its value is plotted in Fig. 11.9 for three weapon sizes, 100 KT, 1 MT, and 20 MT. These curves are for weapons burst at ground surface. The shock-front velocity U_o is a function of peak overpressure P_{so} . Its value for standard atmospheric conditions is plotted

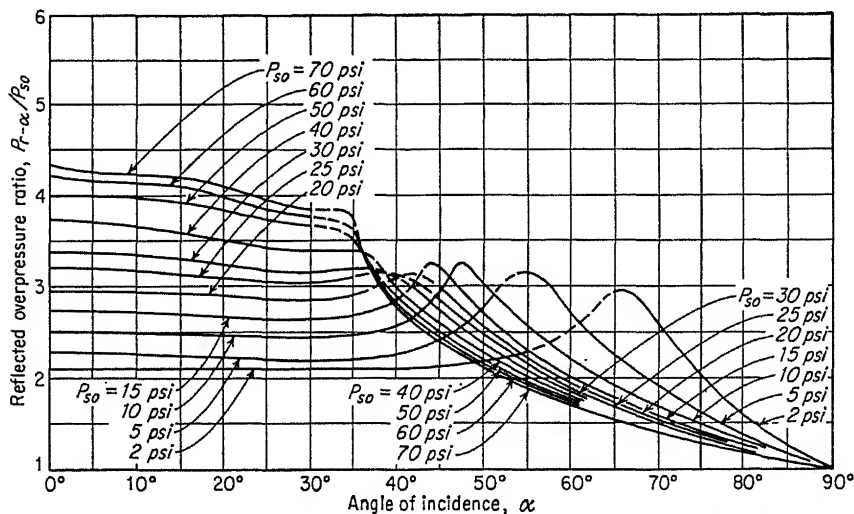


FIG. 11.12. Reflected overpressure ratio vs. angle of incidence for various peak overpressures [Chap. 1, Ref. 8].

in Fig. 11.10. The duration of the positive phase, t_o , of the blast wave is a function of the peak overpressure P_{so} and the total energy yield of the weapon; its value is plotted in Fig. 11.11 for three weapon sizes, 100 KT, 1 MT, and 20 MT, burst at ground surface. Durations for other weapon yields may be calculated using the scaling relations of Sec. 11.1*d*. The reflected overpressure ratio, $P_{r-\alpha}/P_{so}$, is plotted in Fig. 11.12 as a function of angle of incidence α of the shock front. This figure applies to both an inclined shock front striking the surface of the earth and a vertical shock front striking a vertical surface at an angle of incidence α .

The peak dynamic overpressure q_o of the blast wave at ground surface is plotted in Fig. 11.13 for three weapon sizes, 100 KT, 1 MT, and 20 MT.

d. Scaling Blast Phenomena. It has been found that air-blast phenomena such as the pressure and duration at different distances are related for different-strength bombs according to the ratio of the cube root of the equivalent weights of TNT. These relationships are referred to as the scaling laws.

These scaling laws state that if a given peak overpressure is experienced at distance r_1 from an explosion of a bomb of total energy yield \mathfrak{W}_1 , the same peak overpressure will be experienced at distance r_2 from the explosion of a bomb of total energy yield \mathfrak{W}_2 , where

$$r_2 = r_1 \left(\frac{\mathfrak{W}_2}{\mathfrak{W}_1} \right)^{1/3} \quad (11.2)$$

The same scaling laws also state that while the peak pressures from the

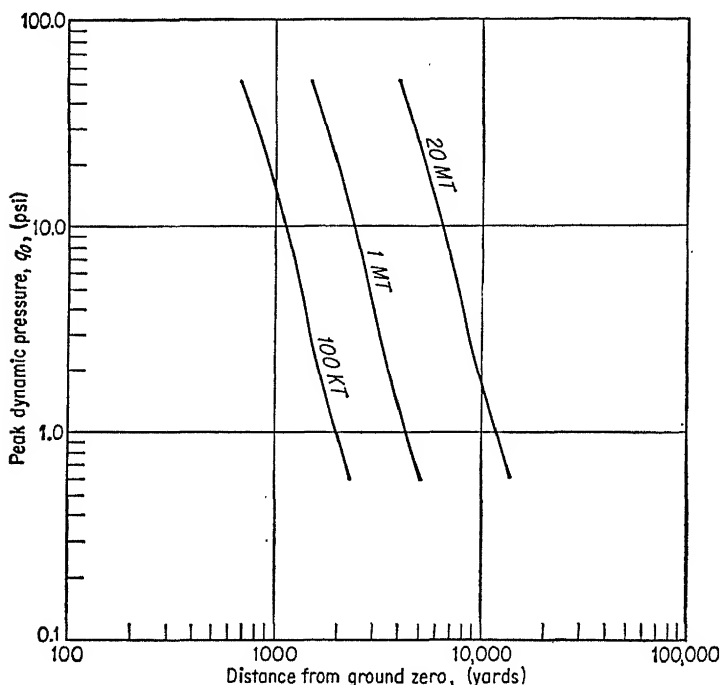


FIG. 11.13. Peak dynamic pressure vs. distance.

two bombs are equal at the two radii r_1 and r_2 , the durations of the blast-pressure waves at the two points are different. If, for example, the duration of the positive phase of the pressure wave from the first bomb is t_{01} at distance r_1 , the duration of the positive phase of the pressure wave from the second bomb at distance r_2 will be

$$t_{02} = t_{01} \left(\frac{\mathfrak{W}_2}{\mathfrak{W}_1} \right)^{1/3} \quad (11.3)$$

11.2. Loading on Structures. The manner in which the blast wave loads a structure is a function of the distance of the structure from ground zero, the height of burst of the weapon, and the weapon size.

The loading on a structure, located within the region of regular reflection (Fig. 11.14), is somewhat different in character from that for a structure located beyond this region. The procedures presented in this chapter for the determination of loads are restricted to structures outside the region of regular reflection and in the region of Mach reflection (Fig. 11.15).

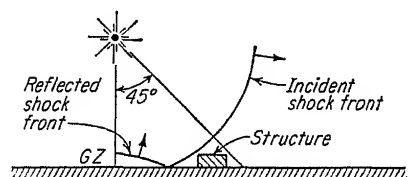


FIG. 11.14. Structure located in region of regular reflection [Chap. 1, Ref. 8].

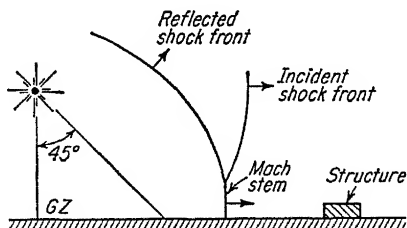


FIG. 11.15. Structure located in region of Mach reflection [Chap. 1, Ref. 8].

The problem is that of computing the loading on a structure due to the impingement upon it of a shock wave traveling parallel to the surface of the earth. The structure is considered as being oriented with one face normal to the direction of propagation of the shock wave, since such an orientation produces the most severe loading on the structural elements. For the design of a structure so located, it is necessary to predict the air overpressures existing on various portions of the structure as a function of time t , measured after the shock front strikes the front wall.

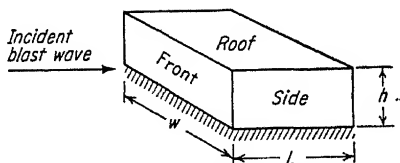


FIG. 11.16. Closed rectangular structure.

a. Loading on Closed Rectangular Structures. The type of structure for which the loading predictions of this section are applicable is illustrated in Fig. 11.16. The behavior of a shock wave upon striking a closed rectangular structure is depicted in Fig. 11.17*a* to *d*. This figure shows the position of the shock front and the behavior of the reflected and diffracted wave over the center portion of the structure of Fig. 11.16. As the shock front strikes the front face of the building (Fig. 11.17*a*) a reflected shock wave is formed, and the overpressure on this face is raised to a value in excess of the peak overpressure in the incident shock wave. This increased overpressure is called the reflected overpressure and is a function of the peak overpressure in the incident shock front and the angle of incidence of the shock front with the front wall, which is zero degrees in this case. At the instant the reflected shock front is formed, the lower overpressure existing in the incident blast wave and adjacent to the top edge of the front face initiates a rarefaction wave (Fig. 11.17*b*),

or a wave of lower overpressure than that which exists in the reflected shock wave. This rarefaction wave travels with the speed of sound in the reflected shock wave toward the bottom of the front face. Within a short time, called the clearing time, the rarefaction wave causes the reflected shock wave to disintegrate and reduces the overpressure existing on the front face to a value which is in equilibrium with the high-velocity air stream associated with the incident shock wave. The overpressure on the front face, when equilibrium with the high-velocity air stream is

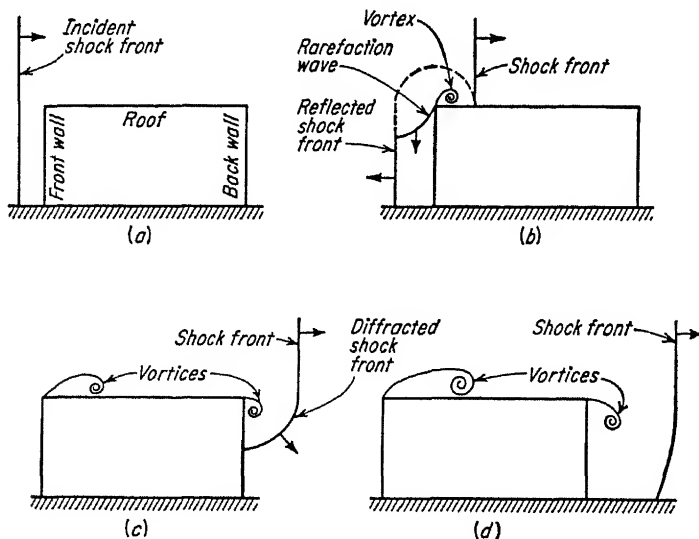


FIG. 11.17. Behavior of blast wave along center portion of closed rectangular structure [Chap. 1, Ref. 8].

reached, is equal to the stagnation overpressure at the base of the front face and an overpressure somewhat less than that in the blast wave at the top edge of the front face. The stagnation overpressure is defined as that overpressure existing in a region in which the moving air has been brought completely to rest, causing the pressure intensity to be increased by the amount of the kinetic energy of motion.

At some time after the shock wave strikes the front wall of the structure, a time equal to the length of the structure divided by the shock-front velocity, the shock front reaches the rear edge of the structure and starts spilling down toward the bottom of the back wall (Fig. 11.17c). The back wall begins to experience increased pressures as soon as the shock front has passed beyond it. The effect is first observed at the top portions of the back wall and proceeds toward the bottom. A vortex, which is a region of air spinning about an axis at a high speed with low overpressures existing at its center because of the Venturi effect, is created

on the back wall and grows in size, traveling toward the base from the top edge and also moving away from the wall (Fig. 11.17c). The maximum back-wall overpressure develops slowly as a result of (1) vortex phenomena and (2) the time required for the back wall to be enveloped by the blast wave.

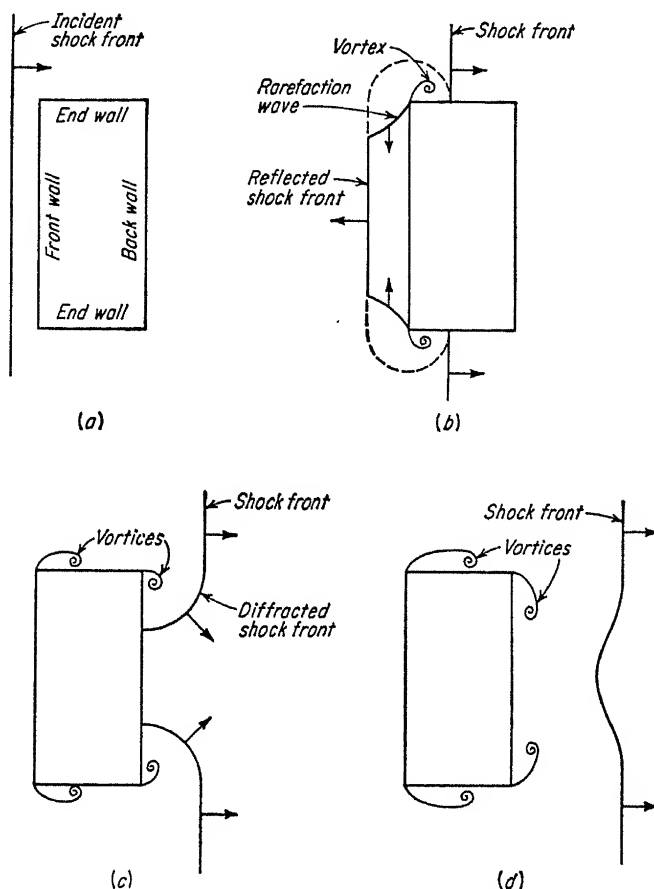


FIG. 11.18. Behavior of blast wave along horizontal section through closed rectangular structure [Chap. 1, Ref. 8].

As the shock front passes beyond the front wall the overpressure exerted on the roof of the structure is initially raised to a value nearly equal to the overpressure existing in the incident shock wave. However, the pressure difference between the reflected overpressure on the front wall and blast-wave overpressure on the roof causes the formation of a vortex along the top edge of the front wall. The vortex travels with a gradually decreasing intensity along the roof of the structure (Fig. 11.17c) at a

slower rate than the shock-front velocity. It causes a decay of the overpressures built up by the incident shock wave. After the passage of this vortex, the higher overpressure in the shock wave again becomes dominant and causes a second build-up of overpressures along the roof.

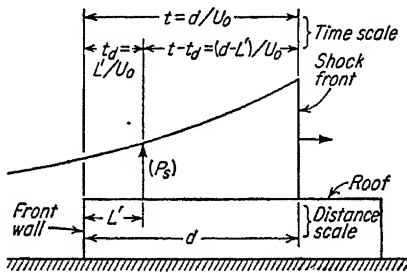


FIG. 11.19. Illustrative sketch of time-displacement-factor convention [Chap. 1, Ref. 8].

If a horizontal section through the structure is examined, it is evident that the effect of these phenomena on the roof of the structure is similar to that which the sides experience, and hence the general discussion in the preceding paragraph describes the action of the shock wave on the sides as well as on the roof of the structure. Figure 11.18 illustrates this phenomenon.

In determining the loads on a structure, it is convenient to use the instant at which the shock front impinges on the front face as a reference time ($t = 0$). In adopting this convention, it is necessary to introduce a time-displacement factor t_d , which is the time required for the shock front to travel from the front face of the structure to the surface or point under consideration. Figure 11.19 illustrates this convention.

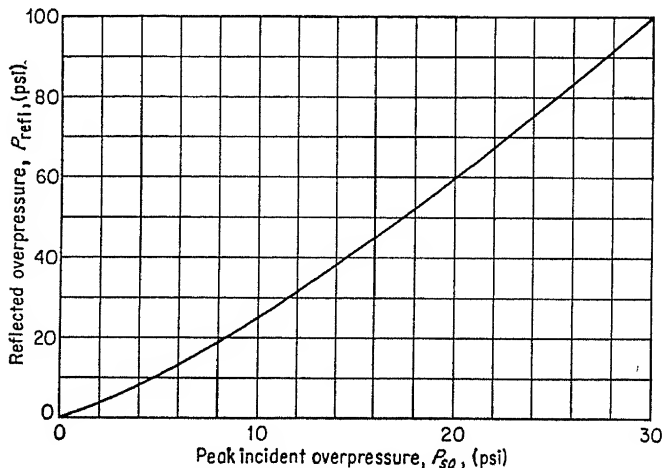


FIG. 11.20. Reflected overpressure vs. peak incident overpressure for normal reflection [Chap. 1, Ref. 8].

LOADING ON FRONT WALL. At the moment the incident shock wave strikes the front face, the overpressure on the front wall is immediately raised from zero to the reflected overpressure P_{refl} (which is higher than

the peak overpressure of the incident shock wave). Reflected overpressure is plotted in Fig. 11.20 for zero angle of incidence as a function of the peak overpressure of the incident shock wave. The value of P_{refl} from Fig. 11.20 is the same as $P_{r-\alpha}$ for $\alpha = 0^\circ$, using Fig. 11.12. The incident shock front continues its motion over the top of the structure, while the reflected shock front moves away from the front of the building in the opposite direction. Initially, the air pressure between the reflected shock

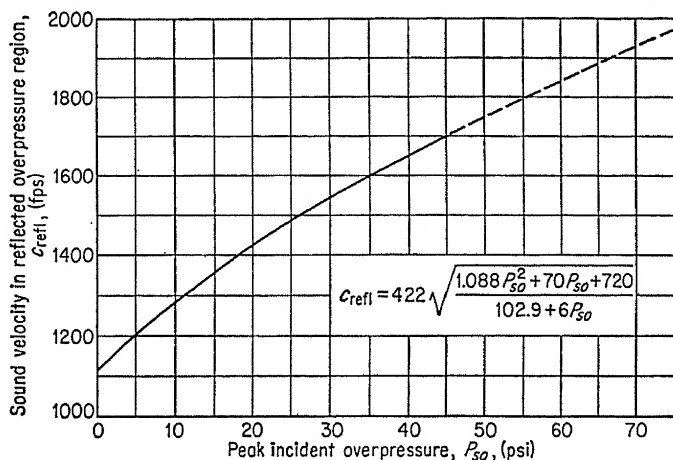


FIG. 11.21. Velocity of sound in reflected-overpressure region vs. peak incident overpressure. (Validity of dashed portion of curve is uncertain.) [Chap. 1, Ref. 8]

front and the front wall is higher than the pressure behind the incident shock. This causes air to move around to the sides and over the top of the structure into the lower-pressure zone behind the incident shock. The rarefaction wave thus caused moves from the edges toward the center of the front wall with the speed of sound for the pressure existing in this region of reflected overpressure.

For the range of shock strengths used in the Princeton shock-tube experiments [2], which correspond to peak shock overpressures of 2 to 50 psi in a standard atmosphere, it has been found that the time required to clear the front face of reflection effects is determined by the dimensions of the front face and the peak overpressure of the incident shock wave. This clearing time t_c is given by the relation

$$t_c = \frac{3h'}{c_{\text{refl}}} \quad (11.4)$$

where h' = clearing height, taken as either half the width or full height of front face, whichever is smaller

c_{refl} = velocity of sound in reflected region, plotted as a function of peak overpressure of incident shock wave in Fig. 11.21

TABLE 11.1. INCIDENT OVERPRESSURE VARIATION WITH TIME

$\frac{t - t_d}{t_o}$	$\frac{P_s}{P_{so}}$	$\frac{t - t_d}{t_o}$	$\frac{P_s}{P_{so}}$	$\frac{t - t_d}{t_o}$	$\frac{P_s}{P_{so}}$
0.00	1.000	0.35	0.458	0.70	0.149
0.01	0.980	0.36	0.447	0.71	0.143
0.02	0.961	0.37	0.435	0.72	0.136
0.03	0.941	0.38	0.424	0.73	0.130
0.04	0.922	0.39	0.413	0.74	0.124
0.05	0.904	0.40	0.402	0.75	0.118
0.06	0.885	0.41	0.392	0.76	0.112
0.07	0.867	0.42	0.381	0.77	0.106
0.08	0.849	0.43	0.371	0.78	0.101
0.09	0.832	0.44	0.361	0.79	0.095
0.10	0.814	0.45	0.351	0.80	0.090
0.11	0.797	0.46	0.341	0.81	0.085
0.12	0.780	0.47	0.331	0.82	0.079
0.13	0.764	0.48	0.322	0.83	0.074
0.14	0.748	0.49	0.312	0.84	0.069
0.15	0.732	0.50	0.303	0.85	0.064
0.16	0.716	0.51	0.294	0.86	0.059
0.17	0.700	0.52	0.285	0.87	0.054
0.18	0.685	0.53	0.277	0.88	0.050
0.19	0.670	0.54	0.268	0.89	0.045
0.20	0.655	0.55	0.260	0.90	0.041
0.21	0.640	0.56	0.251	0.91	0.036
0.22	0.626	0.57	0.243	0.92	0.032
0.23	0.612	0.58	0.235	0.93	0.028
0.24	0.598	0.59	0.227	0.94	0.023
0.25	0.584	0.60	0.220	0.95	0.019
0.26	0.571	0.61	0.212	0.96	0.015
0.27	0.557	0.62	0.204	0.97	0.011
0.28	0.544	0.63	0.197	0.98	0.008
0.29	0.531	0.64	0.190	0.99	0.004
0.30	0.519	0.65	0.183	1.000	0.000
0.31	0.506	0.66	0.176		
0.32	0.494	0.67	0.169		
0.33	0.482	0.68	0.162		
0.34	0.470	0.69	0.155		

During the time required to clear the front face of reflection effects, the average overpressure on the front face decreases from the reflected overpressure to a value which is given by the following equation [2, 3]:

$$\bar{P}_{\text{front}} = P_s + 0.85q \quad (11.5)$$

where P_s = overpressure in incident blast wave at front wall at any time $t - t_d$, as given by the equation

$$\frac{P_s}{P_{so}} = \left(1 - \frac{t - t_d}{t_o}\right) e^{-(t-t_d)/t_o} \quad (11.6)$$

Equation (11.6) is tabulated in Table 11.1.

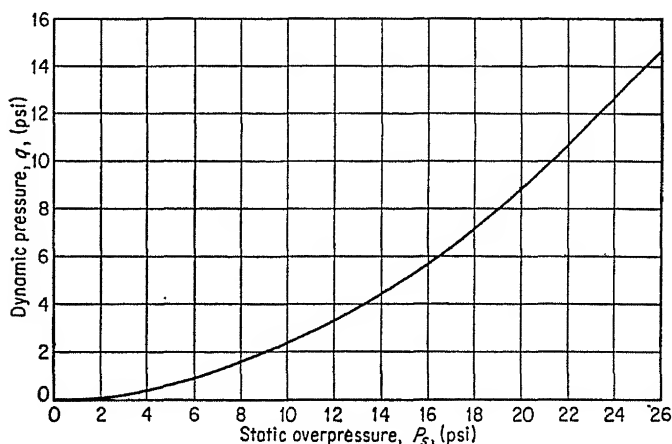


FIG. 11.22. Dynamic pressure vs. static overpressure.

The dynamic pressure q is given by $q = \rho u^2/2$, where ρ is the mass per unit volume of air, and u is the velocity of the air particles. The peak value of q is given as a function of distance from ground zero and weapon size in Fig. 11.13, based on weapons tests. The dynamic pressure q may be related theoretically to the static overpressure P_s by the following equation:

$$q = 14.7 \left[\frac{5/14 (P_s/14.7)^2}{1 + 1/7 (P_s/14.7)} \right] \quad (11.7)$$

This relationship is plotted in Fig. 11.22.

The peak dynamic overpressure q_o is given by Eq. (11.7) using P_{so} for P_s . To obtain q as a function of time it is convenient to use the ratio q/q_o , which is tabulated in Table 11.2 and given by the following expression:

$$\frac{q}{q_o} = \left(1 - \frac{t - t_d}{t_o}\right) e^{-3.5(t-t_d)/t_o} \quad (11.8)$$

TABLE 11.2. DYNAMIC PRESSURE VARIATION WITH TIME

$\frac{t - t_d}{t_o}$	$\frac{q}{q_o}$	$\frac{t - t_d}{t_o}$	$\frac{q}{q_o}$	$\frac{t - t_d}{t_o}$	$\frac{q}{q_o}$
0.00	1.000	0.35	0.191	0.70	0.026
0.01	0.956	0.36	0.182	0.71	0.024
0.02	0.914	0.37	0.173	0.72	0.022
0.03	0.873	0.38	0.164	0.73	0.021
0.04	0.835	0.39	0.156	0.74	0.020
0.05	0.798	0.40	0.148	0.75	0.018
0.06	0.762	0.41	0.141	0.76	0.017
0.07	0.728	0.42	0.133	0.77	0.016
0.08	0.695	0.43	0.127	0.78	0.014
0.09	0.664	0.44	0.120	0.79	0.013
0.10	0.634	0.45	0.114	0.80	0.012
0.11	0.606	0.46	0.108	0.81	0.011
0.12	0.578	0.47	0.102	0.82	0.010
0.13	0.552	0.48	0.097	0.83	0.009
0.14	0.527	0.49	0.092	0.84	0.008
0.15	0.503	0.50	0.087	0.85	0.008
0.16	0.480	0.51	0.082	0.86	0.007
0.17	0.458	0.52	0.078	0.87	0.006
0.18	0.437	0.53	0.074	0.88	0.006
0.19	0.417	0.54	0.070	0.89	0.005
0.20	0.397	0.55	0.066	0.90	0.004
0.21	0.379	0.56	0.062	0.91	0.004
0.22	0.361	0.57	0.059	0.92	0.003
0.23	0.344	0.58	0.055	0.93	0.003
0.24	0.328	0.59	0.052	0.94	0.002
0.25	0.313	0.60	0.049	0.95	0.002
0.26	0.298	0.61	0.046	0.96	0.001
0.27	0.284	0.62	0.043	0.97	0.001
0.28	0.270	0.63	0.041	0.98	0.001
0.29	0.257	0.64	0.038	0.99	0.000
0.30	0.245	0.65	0.036	1.000	0.000
0.31	0.233	0.66	0.034		
0.32	0.222	0.67	0.032		
0.33	0.211	0.68	0.030		
0.34	0.201	0.69	0.028		

Using the above quantities the curve of average front-wall overpressure, \bar{P}_{front} , versus time may be determined. Figure 11.23 shows a typical front-face average-overpressure curve. The curve abc is defined by Eq. (11.5). Point d , the reflected overpressure, is connected by a straight line to point b , the average overpressure at time $t - t_d = t_c$. Since the resulting discontinuity at point b is not compatible with actual behavior of the loads on the front face, these two curves are smoothed by fairing in curve ef as shown. The curve of average overpressure vs. time on the front face is then defined as curve $0-defc$.

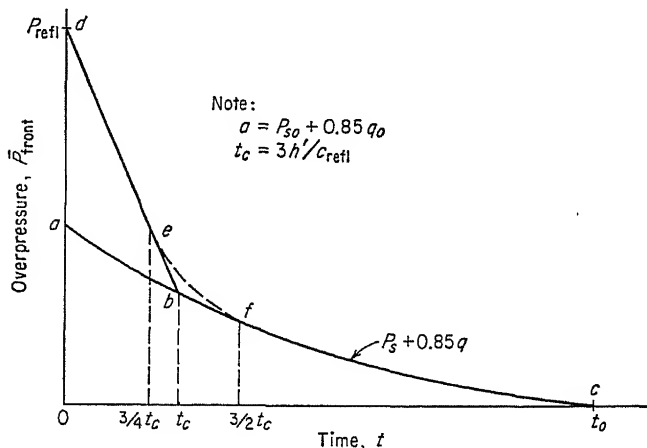


FIG. 11.23. Average front-wall overpressure vs. time, closed rectangular structure [Chap. 1, Ref. 8].

The overpressure on the front face of a structure is not uniformly distributed. The maximum value occurs at the mid-point of the base, and the minimum value occurs along the edges. Those portions of the front face nearest to the edges are cleared or relieved of the reflection effects in a shorter time than the remainder of the front face, and the overpressure existing at those points is lower, following the clearing stage. The net effect of this vertical and horizontal variation is of questionable value for design purposes. Hence, the front-wall loading is assumed to be distributed uniformly over the front-wall surface. For the same reasons, the rear-wall loading given next is assumed to be uniformly distributed over the rear wall.

LOADING ON BACK WALL. For the back wall, the time-displacement factor t_d is L/U_o , where L is the length of the building in the direction of propagation of the shock.

When the shock front crosses the rear edge of the structure, the foot of the shock spills down the back wall. The overpressures on the back wall behind this differential wave are considerably less than those in the

incident blast wave because of the vortex which develops at the top and travels down the wall. A period of time longer than that required for the passage of this diffracted shock to the bottom of the wall must pass before the back-wall average overpressure reaches its peak value. The time required for this build-up to occur, t_b , measured from the instant at which the shock wave reaches the back wall, is equal to $4h'/c_o$, where h' is the clearing height of the back wall, taken equal to either the full height

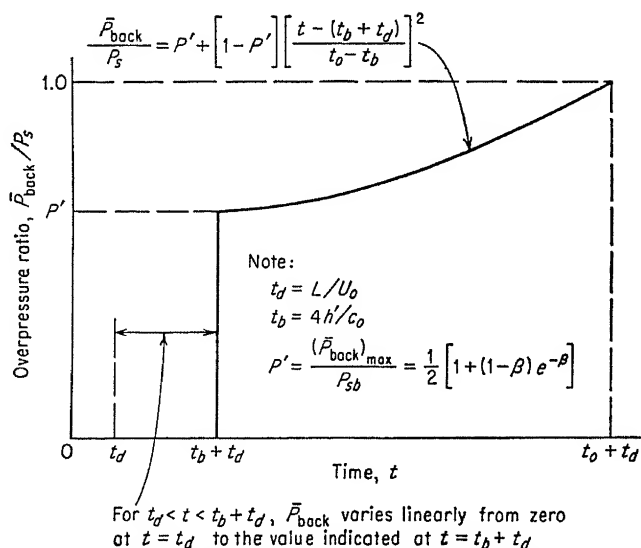


FIG. 11.24. Average back-wall overpressure ratio vs. time, closed rectangular structure [Chap. 1, Ref. 8].

of the back wall or half the width of the building, whichever is smaller, and c_o is the velocity of sound in undisturbed air, 1,115 ft/sec.

The peak value of the average overpressure on the back wall after this build-up has been completed is

$$(\bar{P}_{back})_{max} = P_{sb}(\frac{1}{2})[1 + (1 - \beta)e^{-\beta}] \quad (11.9)$$

where P_{sb} = incident blast-wave overpressure at back face at time $t - t_d = t_b$

$(\bar{P}_{back})_{max}$ = peak value of average overpressure on back wall which occurs at time $t = t_d + t_b$

$$\beta = 0.5P_{so}/14.7$$

$$e = 2.7182 = \text{base of natural logarithms}$$

It is assumed that P_{so} in the incident blast wave does not diminish in strength as the wave passes over the structure.

Figure 11.24 illustrates the variation of the ratio \bar{P}_{back}/P_s with time, for

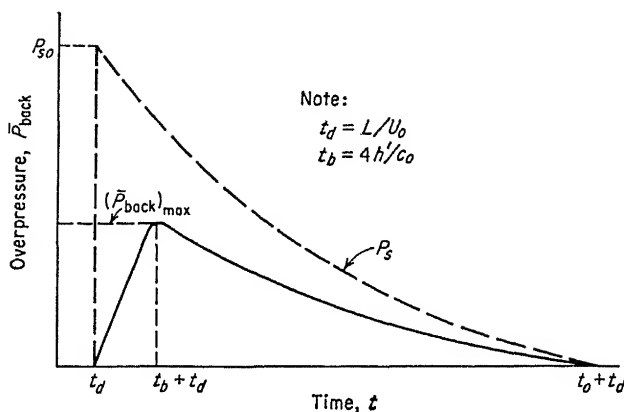


FIG. 11.25. Average back-wall overpressure vs. time, closed rectangular structure [Chap. 1, Ref. 8].

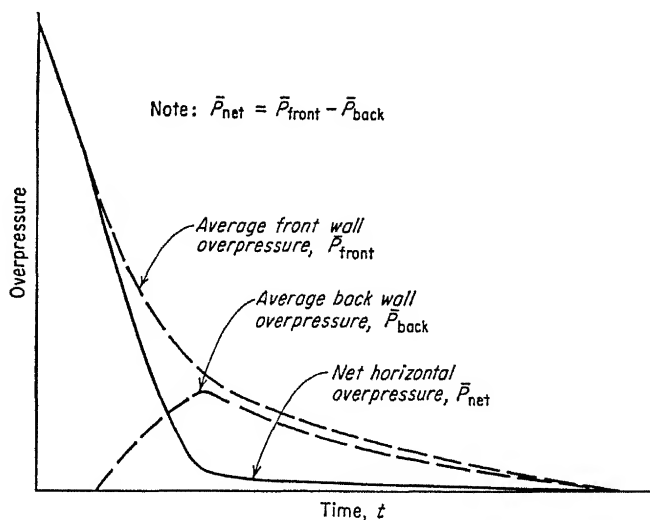


FIG. 11.26. Net horizontal overpressure vs. time, closed rectangular structure [Chap. 1, Ref. 8].

times in excess of $t - t_d = t_b$, given in the following equation:

$$\frac{\bar{P}_{\text{back}}}{P_s} = \frac{(\bar{P}_{\text{back}})_{\text{max}}}{P_{sb}} + \left[1 + \frac{(\bar{P}_{\text{back}})_{\text{max}}}{P_{sb}} \right] \left[\frac{t - (t_d + t_b)}{t_o - t_b} \right]^2 \quad (11.10)$$

where t_o = duration of positive phase. Figure 11.25 shows a typical back-wall average-overpressure curve.

AVERAGE NET HORIZONTAL LOADING \bar{P}_{net} . Considering as positive all overpressures exerted on the structure and directed toward the interior,

$$\bar{P}_{\text{net}} = \bar{P}_{\text{front}} - \bar{P}_{\text{back}} \quad (11.11)$$

where \bar{P}_{net} , \bar{P}_{front} , and \bar{P}_{back} are given in terms of time. Figure 11.26 illustrates graphically the variation of net average horizontal overpressure with time.

LOCAL ROOF OVERPRESSURE P_{roof} . The procedure developed for prediction of overpressures on the roof of a structure is predicated primarily on a curve-fitting technique with the Princeton and Michigan shock-tube data [2, 4, 8] providing the basis for the method.

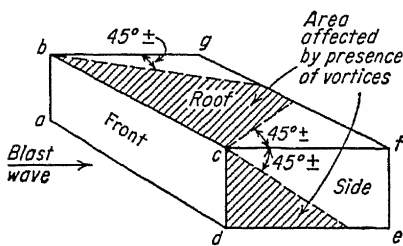


FIG. 11.27. Areas on roof and sides most affected by vortex action [Chap. 1, Ref. 8].

with gradually increasing speed. Vortices are formed all along the line $abcd$ of Fig. 11.27. At corners b and c where they are aligned at 90° to each other, the vortices tend to interfere with each other and to move away from the roof and wall surfaces. This results in a diminution of the effects of the vortices at these edges which proceeds along the axis of the

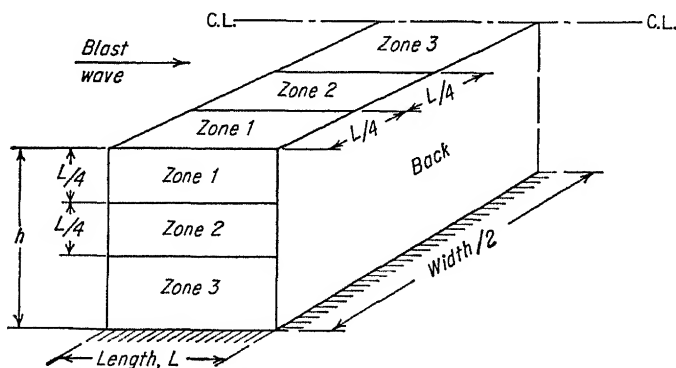


FIG. 11.28. Location of loading zones on roof and sides of structure [Chap. 1, Ref. 8].

vortices from corners b and c as the vortices move toward the rear of the building. Consequently the regions on the roof and side walls which are strongly affected by the vortices do not extend to all edges of the roof, but are triangular or trapezoidal in shape, as indicated in Fig. 11.27.

These observed results indicate a variation of overpressures on the roof in a direction parallel to the shock front in addition to that variation along the roof in the direction of propagation of the wave. Although this

lateral variation is a smooth one, the roof has been divided into three zones as illustrated in Fig. 11.28.

Zone 1: This zone is a strip on the roof extending from the sides toward the centerline a distance equal to one-quarter of the length L of the building.

Figure 11.29 is a plot of the ratio P_{roof}/P_s , the ratio of the local overpressure at any point on the roof in terms of time t , to the incident air

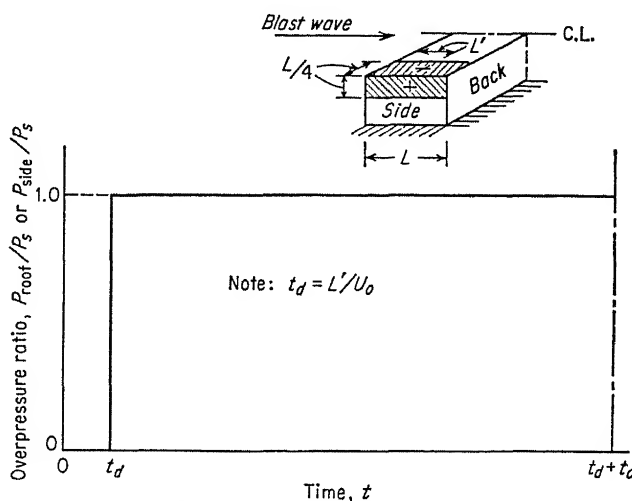


FIG. 11.29. Local roof or side-wall overpressure vs. time, zone 1, closed rectangular structure [Chap. 1, Ref. 8].

pressure, where $t_d = L'/U_0$ is the time displacement and L' the distance from the front edge of the roof to the point under consideration.

Figure 11.29 reveals that the local-overpressure-vs.-time curve for any point in zone 1 is the incident free-air overpressure curve displaced in time by a factor $t_d = L'/U_0$. This is consistent with observed vortex disintegration as illustrated in Fig. 11.27.

Zone 2: This zone is a strip on the roof of width equal to one-quarter of the length of the structure measured from the edge of zone 1 toward the center of the roof.

Figure 11.30 is a plot of the ratio P_{roof}/P_s for any point a distance L' from the front edge of the roof. Here again, P_{roof} and P_s incorporate the time displacement $t_d = L'/U_0$. t_m is given by Eq. (11.12) below.

Zone 3: This zone includes all points on the roof not included in zones 1 and 2. Figure 11.31 is a plot of the ratio P_{roof}/P_s for all points in this zone.

The effects of the vortex traveling across the roof of the structure are

confined to zones 2 and 3. The difference in the overpressures existing in these zones is due to the severity of vortex effects.

As the shock front passes over the point being considered, the local overpressure is raised to the overpressure in the incident shock wave. This equality between local and incident blast-wave overpressures is

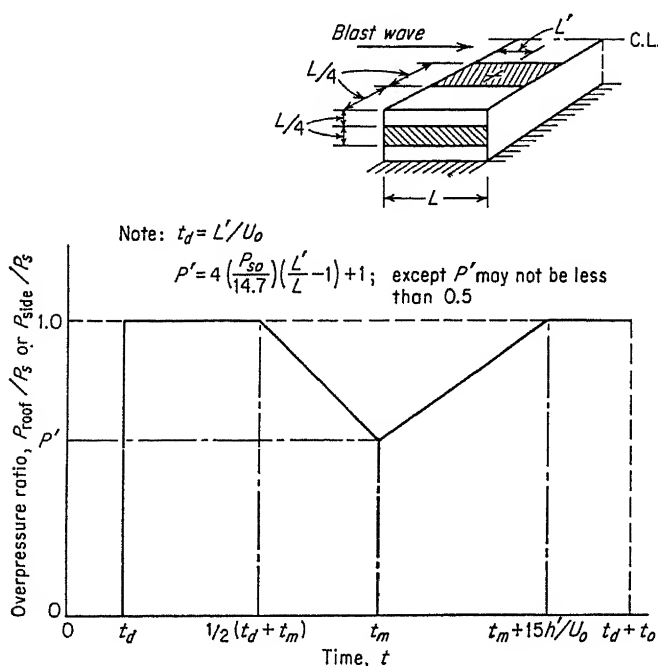


FIG. 11.30. Local roof or side-wall overpressure ratio vs. time, zone 2, closed rectangular structure [Chap. 1, Ref. 8].

maintained until the vortex developed at the front edge of the roof detaches itself and moves toward the rear edge, causing a decrease from the overpressure in the incident blast wave at the point being considered. The local overpressure reaches its minimum value at the time that the vortex is over the point in question. The time required for the vortex to travel the distance L' is

$$t_m = \frac{L'}{v} \quad (11.12)$$

where v = vortex velocity, obtained from reduction of data [2] and given by the relation

$$v = \left(0.042 + \frac{0.108L'}{L} \right) U_0 \quad (11.13)$$

The value of the ratio of $\bar{P}_{\text{roof}}/P_s$ at time $t = t_m$ is

$$P' = \frac{\bar{P}_{\text{roof}}}{P_{sm}} = 4 \frac{P_{so}}{(14.7)} \left(\frac{L'}{L} - 1 \right) + 1.0 \quad (11.14)$$

For points located in zone 2 the minimum value of Eq. (11.14) is 0.5; for points located in zone 3 the minimum value is zero.

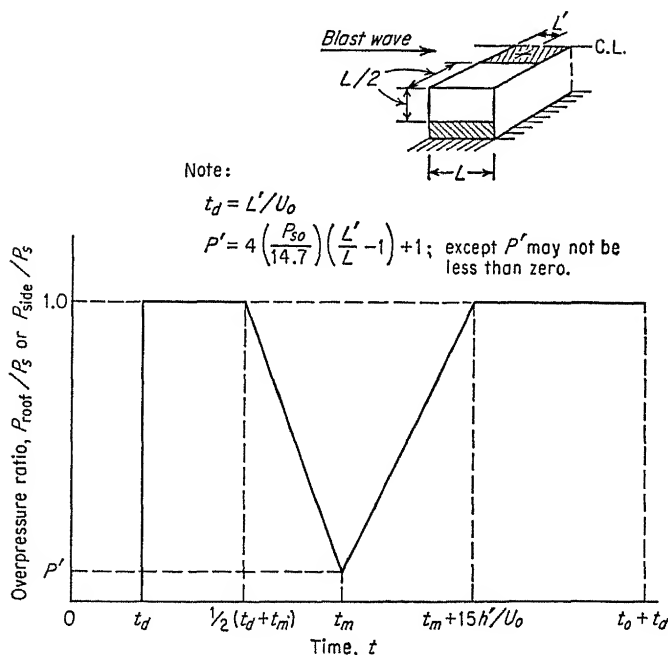


FIG. 11.31. Local roof or side-wall overpressure ratio vs. time, zone 3, closed rectangular structure [Chap. 1, Ref. 8].

As soon as the vortex has passed the point in question, the local overpressure starts to build up until at time $t = t_m + 15h'/U_o$ (where h' is the clearing height of the structure) it is once again equal to the overpressure in the incident shock wave.

AVERAGE OVERPRESSURE ON THE ROOF \bar{P}_{roof} . Having established the variation of local overpressure, the average overpressure on the roof at any time is correctly obtained through the summation of the local overpressure curves over the entire roof at a given time t . If there were no lateral variation of local overpressures, such a method would be used to develop a general procedure applicable to all structures. However, the presence of this lateral variation complicates any procedure to such a degree that only the limiting case zone 3 is considered. The ratio of the average roof overpressure \bar{P}_{roof} is plotted in Fig. 11.32 for times in

excess of time $t = L/U_o$, where P_s incorporates the time displacement $t_d = L/2U_o$. The average overpressure on the roof varies linearly from zero at time $t = 0$ to the value of \bar{P}_{roof} given in Fig. 11.32 at time $t = L/U_o$. The assumption that \bar{P}_{roof} can be expressed as a proportion of P_s is valid only if the time required for the shock front to travel the length of the

Note: $P'' = 0.9 + 0.1 \left(1.0 - \frac{P_{s0}}{14.7}\right)^2$; except P'' may not exceed 1.0.

$$P' = 2.0 - \left(\frac{P_{s0}}{14.7} + 1\right) \left(\frac{t'}{L}\right)^{1/3} \text{ or } 0.5 + 0.125 \left(2 - \frac{P_{s0}}{14.7}\right)^2$$

whichever is smaller; except P' may not be less than zero.

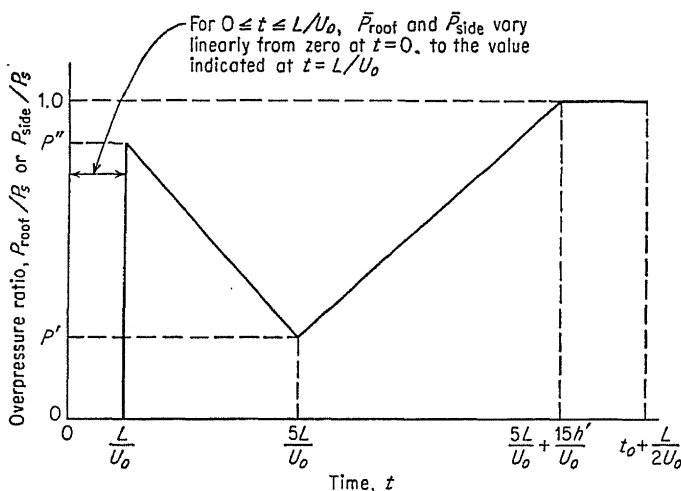


FIG. 11.32. Average roof or side-wall overpressure ratio vs. time, zone 3, closed rectangular structure [Chap. 1, Ref. 8].

building is small compared with the duration of the positive phase. For values of $(L/U_o)/t_o$ less than 0.1 this assumption is reasonable.

A further restriction which must be imposed is due to the importance of the lateral variation of overpressures on the roof. If the width of the structure normal to the direction of travel of the shock wave is greater than twice its length, the average roof overpressures as determined by Fig. 11.32 are satisfactory. For structures whose width is less than their length, the average roof overpressure for times greater than time $t = L/U_o$ is more correctly given by the relation


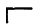



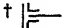
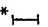
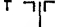

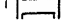

$$\bar{P}_{\text{roof}} = P_s \quad (11.15)$$

where P_s incorporates the time displacement $t = L/2U_o$. The average roof overpressure varies linearly from time $t = 0$ to the value calculated by Eq. (11.15) at time $t = L/U_o$. For structures which are approxi-

mately square in roof plan, neither method is more correct and an average of the two should be used.

LOCAL AND AVERAGE SIDE-WALL OVERPRESSURES P_{side} AND \bar{P}_{side} . The sides of a structure are loaded in the same manner as is the roof; accordingly Figs. 11.29 to 11.31 determined for the roof of a structure apply equally well to the sides.

DRAG COEFFICIENTS, C_D , FOR VARIOUS STRUCTURAL CROSS-SECTIONS

Direction of wind \longrightarrow			
Shape	C_D	Shape	C_D
	2.0		2.0
	2.0		1.0
* 	2.0	† 	2.0
* 	1.8	† 	2.0
	2.0	† 	2.2
	1.8		

* Standard or wide flange sections

† Built up sections, either riveted or welded

DRAG COEFFICIENTS, $(C_D)_w$, FOR WINDWARD (UNSHIELDED) TRUSS OF BRIDGES

$(C_D)_w$ is given as a function of the solidity ratio, $G = A'/A$, where A is the total area included within the limiting boundaries of the truss, A' is the actual area of the members in a plane normal to the wind direction.

For single span trusses:

$$G < 0.25 \quad (C_D)_w = 1.8$$

$$G > 0.25 \quad (C_D)_w = 1.6$$

For multiple span or very long span trusses:

$$0.00 < G < 0.20 \quad (C_D)_w = 2.0$$

$$0.20 < G < 0.30 \quad (C_D)_w = 1.8$$

$$0.30 < G < 0.90 \quad (C_D)_w = 1.6$$

$$0.90 < G < 1.00 \quad (C_D)_w = 2.0$$

FIG. 11.33. Drag coefficient for various structural shapes and trusses [Chap. 1, Ref. 8].

The side walls are divided into three zones, as shown in Fig. 11.28, for the determination of local overpressures P_{side} . Figures 11.29 to 11.31 present these local overpressures in the form P_{side}/P_s , where P_{side} and P_s incorporate the time displacement $t_d = L'/U_o$. L' is the distance from the front edge of the side wall to the point under consideration.

The average overpressure on the side is given as the ratio $\bar{P}_{\text{side}}/P_s$ in Fig. 11.32, where P_s is the overpressure in the incident shock wave with a time displacement $t_d = L/2U_o$. This figure is applicable only if the height h of the side wall is greater than half the length L . If this restriction is not satisfied, the average overpressure on the side is more correctly

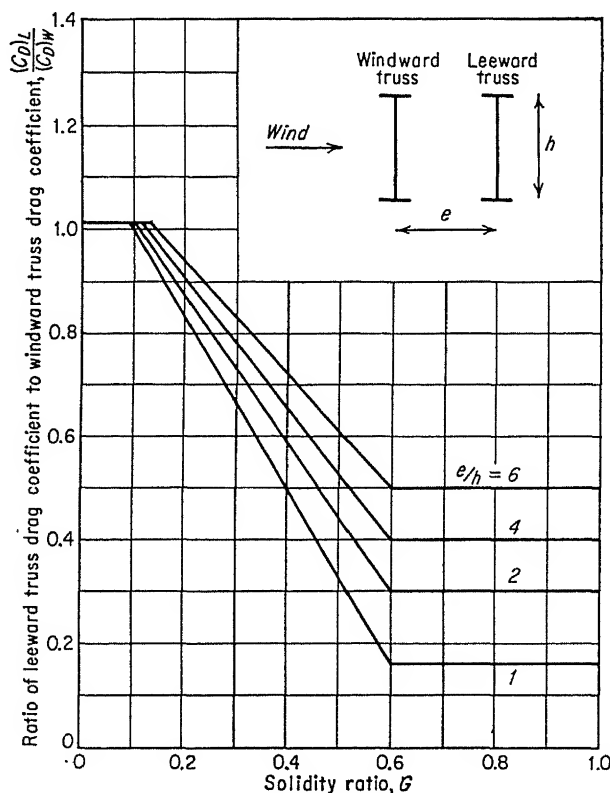


FIG. 11.34. Drag coefficients for leeward trusses [Chap. 1, Ref. 8].

given by the relation

$$\bar{P}_{\text{side}} = P_s \quad (11.16)$$

b. Loading on Exposed Structural Framework. The blast-wave loading on structures such as bridge trusses, open steel framework, or steel industrial structures following the destruction of frangible walls is caused almost entirely by the drag pressure resulting from the high-velocity blast wind which follows directly behind the shock front. The load due to the unbalanced pressures resulting from reflection and diffraction of the shock front can be neglected because of the extremely short duration of these effects.

A structure of this type consists of structural elements whose dimensions are so small that their front-face clearing times are less than 10 msec. In addition, the members are so small that they are enveloped by the shock wave in a similar short length of time.

The total load on the structure is obtained by computing the load on the individual elements, front and back wall, and intermediate framing

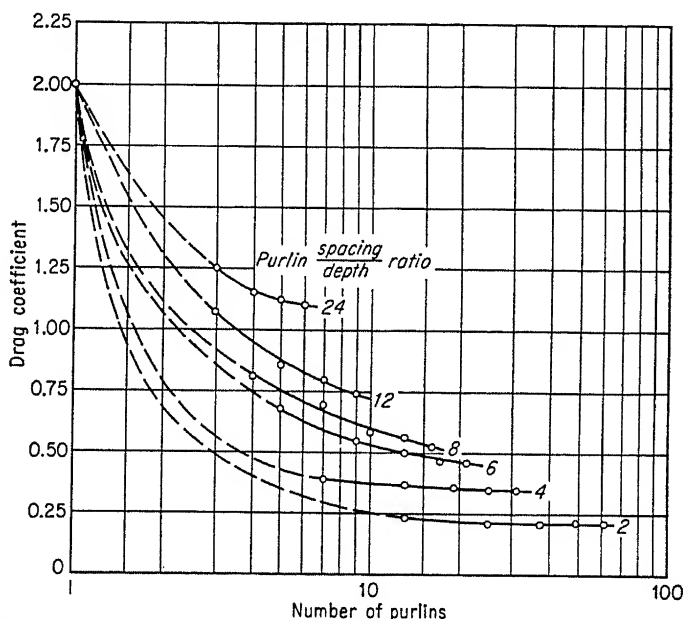


Fig. 11.35. Drag coefficients for roof purlin systems [Chap. 1, Ref. 8].

elements and adding them together on a common time basis. The total drag overpressure on an element can be computed from the formula

$$\text{Drag overpressure} = C_D q \quad (11.17)$$

where C_D = coefficient of drag obtained from Figs. 11.33 and 11.34; this coefficient is applied to individual structural elements
 q = dynamic pressure due to air velocity in incident blast wave at any time

$$q = \frac{\rho u^2}{2} \quad (11.18)$$

and is determined from Fig. 11.13 or 11.22 and Table 11.2.

Shielding is an important factor, and wind-tunnel tests performed at MIT by Biggs [15, 16] on bridge models and by King [9] give useful information. King's data are reproduced as Fig. 11.35.

Figure 11.36 illustrates the net overpressure-time curve for an element located at distance L from the front portion of a structure. The total load on the element is obtained by multiplying the drag overpressure (at any time) by the projected area of the member transverse to the direction of travel of the shock wave. The total load on the structure is obtained by summing the loads on the individual members, based on

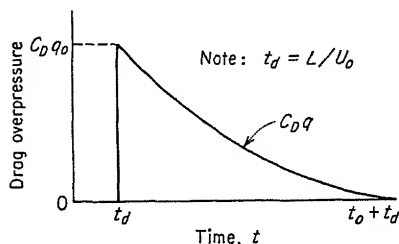


FIG. 11.36. Drag overpressure vs. time on exposed structural elements [Chap. 1, Ref. 8].

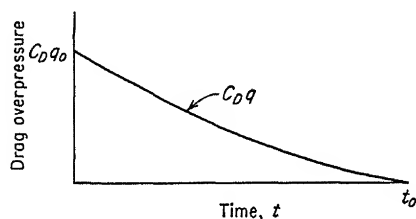


FIG. 11.37. Drag overpressure vs. time on front wall. Elements supporting frangible wall panels [Chap. 1, Ref. 8].

time t referenced to the instant the frontmost elements of the structure are struck by the shock wave.

The overpressure-time curve for the front-wall supporting elements of a frangible wall structure is shown in Fig. 11.37. The overpressure on the front wall prior to the time of failure is determined as previously described for the front wall of a closed rectangular structure. The time of failure is actually a very short time for frangible elements compared with t_o , and

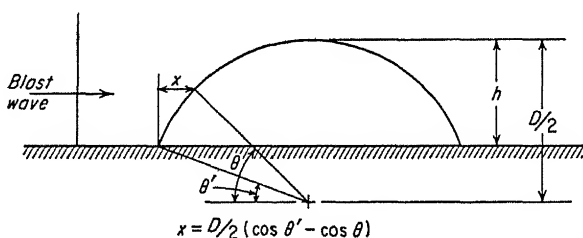


FIG. 11.38. Definition sketch for cylindrical-arch notation [Chap. 1, Ref. 8].

the load transmitted to the supporting elements is subjected to the drag overpressures given by Eq. (11.17).

The overpressure-time curve for the back-wall supporting elements is similar to that for the front wall except that all times are displaced by the appropriate time-displacement factor $t_d = L/U_o$, where L is the distance between the front and back wall. After failure of the back wall the back-wall supporting elements are subjected to the drag overpressures given by Eq. (11.17).

c. *Loading on Cylindrical-arch Surfaces, Cylindrical-arch Overpressure P_{cyl} , Axis Parallel to Shock Front.* Figure 11.38 is a definition sketch for the notation used in the determination of the loads on a cylindrical-arch surface. Structures in this category are illustrated in Fig. 11.39. These consist of exposed arch structures and surface structures of various shapes covered by an earth fill. If the arch or earth-fill surface is not

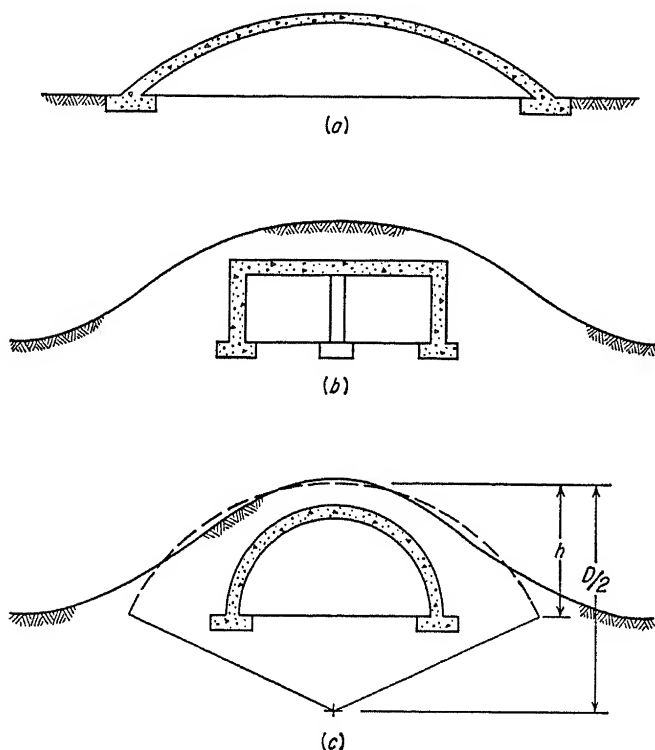


FIG. 11.39. Illustration of structures with cylindrical-arch surfaces [Chap. 1, Ref. 8].

truly circular, it is approximated by an arc of a circle as illustrated by dashed lines in Fig. 11.39, and the loads are computed for the equivalent circular surface. The procedures given in this paragraph determine the air-blast loading as a function of time on the cylindrical-arch surface exposed to the air blast, whether it be the surface of the arch on the exposed structure or the surface of the rounded fill over the covered structure. With this procedure, zero time is the instant at which the incident shock front first strikes the cylindrical-arch surface at its intersection with the horizontal ground surface along the line defined by $\theta = \theta'$.

Figures 11.40 and 11.41 illustrate the variation of the local overpressure P_{cyl} with time on the surface of a cylindrical arch. Each of these figures is valid only within a certain range of θ values, which are determined by the clearing time peculiar to each. These times and the sequence of overpressures within them are defined in Fig. 11.40 for $0^\circ \leq \theta' \leq \theta \leq 90^\circ$ and in Fig. 11.41 for $90^\circ \leq \theta \leq 180^\circ$.

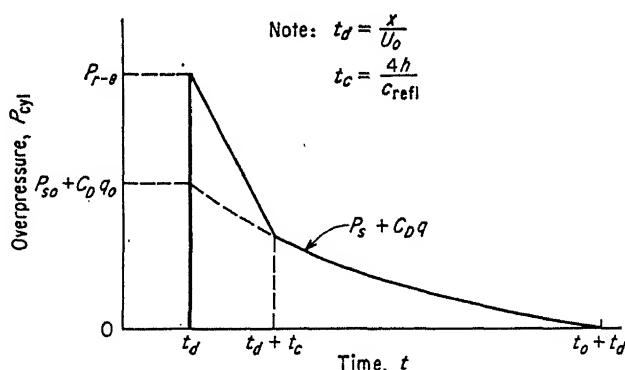


FIG. 11.40. Local overpressure on front surface of cylindrical arch vs. time, axis parallel to shock front. $0^\circ \leq \theta' \leq \theta \leq 90^\circ$. [Chap. 1, Ref. 8]

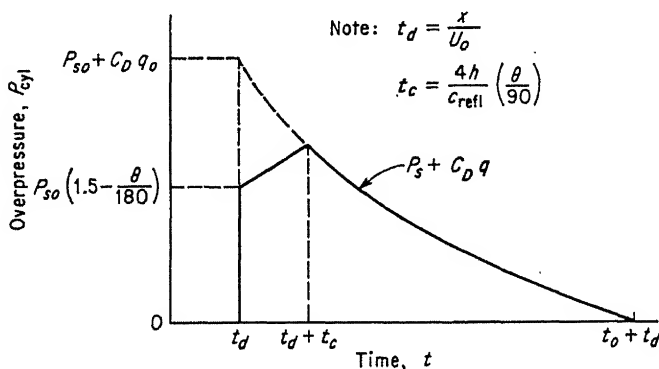


FIG. 11.41. Local overpressure on leeward surface of cylindrical arch vs. time, axis parallel to shock front. $90^\circ \leq \theta \leq 180^\circ$. [Chap. 1, Ref. 8]

The overpressure at a given point on the windward side of the cylinder rises instantaneously from zero to $P_{r-\alpha}$ at time $t_d = x/U_o$. The value of $P_{r-\alpha}$ is given in Fig. 11.12 as a function of α , the angle of incidence of the shock wave. For the cylinder of Fig. 11.38, $\alpha = \theta$. Clearing of reflection effects occurs at time $t = t_d + t_c$, where clearing time t_c is given by

$$t_c = \frac{4h}{c_{\text{refl}}} \quad (11.19)$$

The local overpressure at any point after the clearing of reflection effects is given by Eq. (11.20). P_{eyl} acts normal to the surface of the arch.

$$P_{\text{eyl}} = C_D q + P_s \quad (11.20)$$

where q = dynamic pressure incorporating time-displacement factor t_d

C_D = local drag coefficient, a function of θ , obtained from Figs. 11.42 to 11.46, as discussed below

P_s = overpressure in incident blast wave at any time $t - t_d$

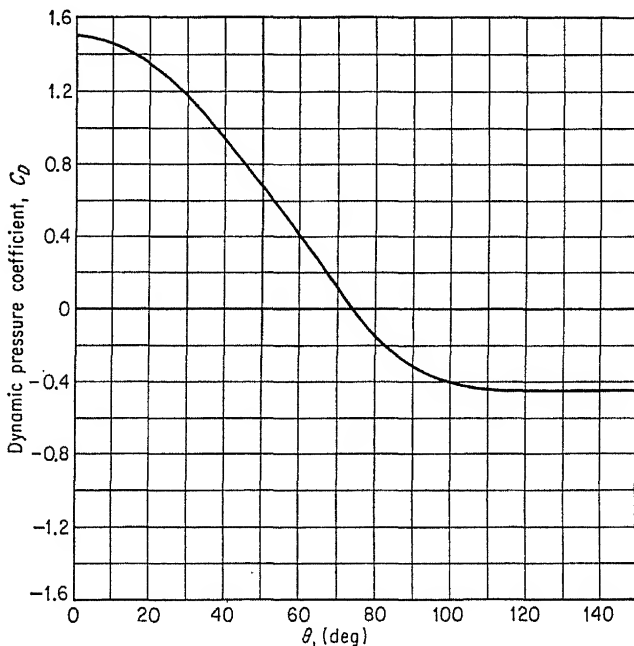


FIG. 11.42. Local-dynamic-pressure coefficient for cylindrical-arch axis parallel to shock front, supersonic Mach numbers [Chap. 1, Ref. 8].

The distribution of dynamic overpressures about an arch is a function of both the Reynolds number Re and the Mach number M of the high-velocity wind in the blast wave [10, 11]. The Reynolds number, a dimensionless quantity of the type $uD\rho/\mu$, is a parameter which characterizes the relative importance of viscous action in steady nonuniform flow. Since the viscosity μ and the density ρ appear as a ratio in the Reynolds number, it is convenient to treat this ratio of fluid properties as a property itself. Thus, the Reynolds number involves only the arch diameter D , a velocity u , and the fluid property ρ/μ . The Mach number, also a dimensionless quantity, is the ratio of the actual velocity to the velocity of sound.

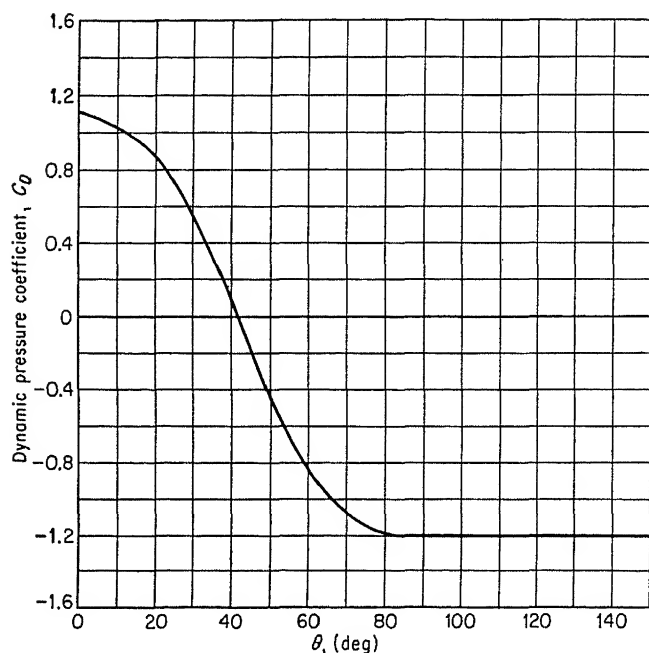


FIG. 11.43. Local-dynamic-pressure coefficient for cylindrical arch, axis parallel to shock front, high subsonic Mach numbers. $0.4 < M < 1$. [Chap. 1, Ref. 8]

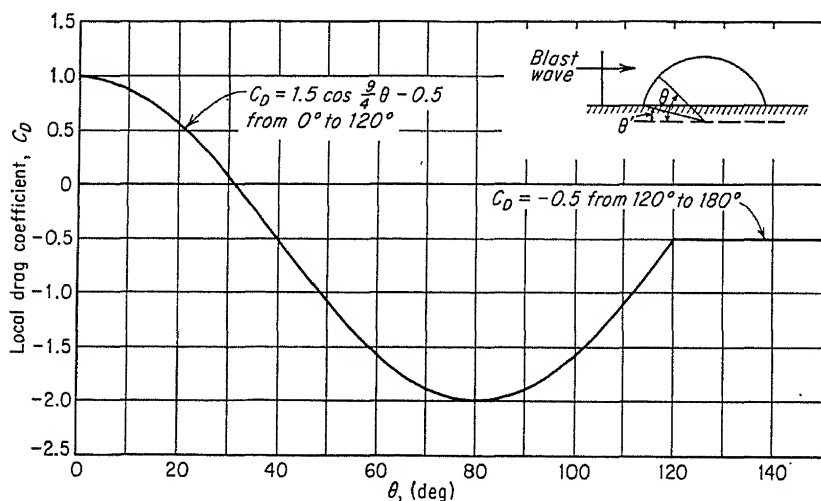


FIG. 11.44. Local-dynamic-pressure coefficient for cylindrical arch, axis parallel to shock front. $Re > 5(10)^5$, and $M < 0.4$. [Chap. 1, Ref. 8]

In the following discussion, the distribution of dynamic pressures about the circular arch is assumed to be the same as the distribution about a circular cylinder having the same diameter. Then the results of experimental studies conducted on flow past circular cylinders can be utilized for this problem. This procedure will introduce some error, but it is believed to be insignificant compared with the uncertainty associated with the basic data.

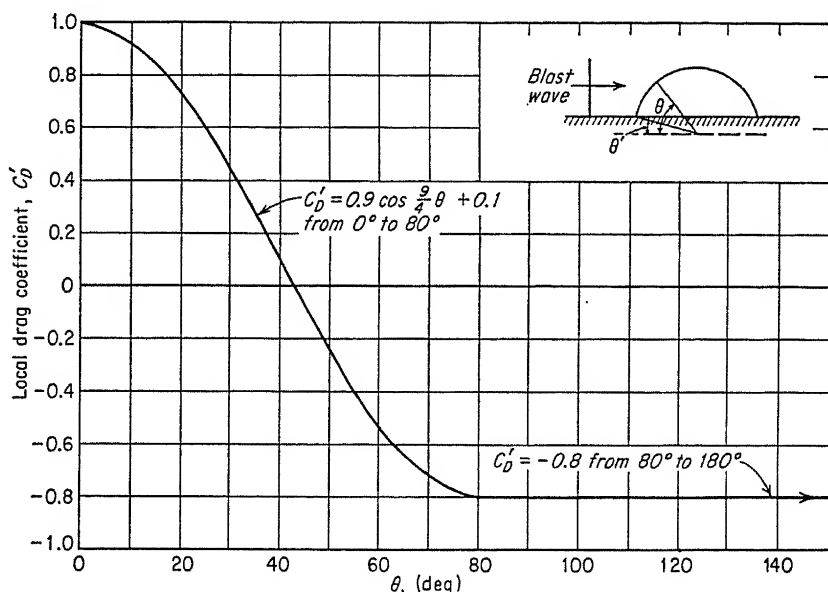


FIG. 11.45. Local-dynamic-pressure coefficient for infinitely long cylindrical arch, axis parallel to shock front. $Re < 5(10)^5$, and $M < 0.4$. [Chap. 1, Ref. 8]

For flow at low Mach numbers, the pressure distribution and the total drag force change abruptly for a Reynolds-number range between $3(10)^5$ and $5(10)^5$. This transition is very sensitive to the smoothness of incident flow, temperature gradients, and roughness of the surfaces. The explanation advanced for this change in pressure distribution and decrease in drag is that the boundary layer changes from laminar to turbulent at this critical Reynolds number and causes the separation point to move farther back, resulting in the redistribution of dynamic pressure.

As the Mach number of the flow is increased, this decrease in total drag and redistribution of pressure at the critical Reynolds number becomes less pronounced, until at a Mach number of about 0.4 it no longer occurs. The separation point does not move when the boundary layer changes from laminar to turbulent and is probably fixed by the presence of shock

waves. For flows with a free-stream Mach number greater than 0.4, the pressure distribution is not influenced by the Reynolds number but it is somewhat dependent upon the Mach number, the distribution being different for supersonic flow than for subsonic flow.

Four pressure distributions are necessary in order that the entire ranges of Reynolds and Mach numbers can be considered. The critical values of Reynolds and Mach numbers are arbitrarily taken as

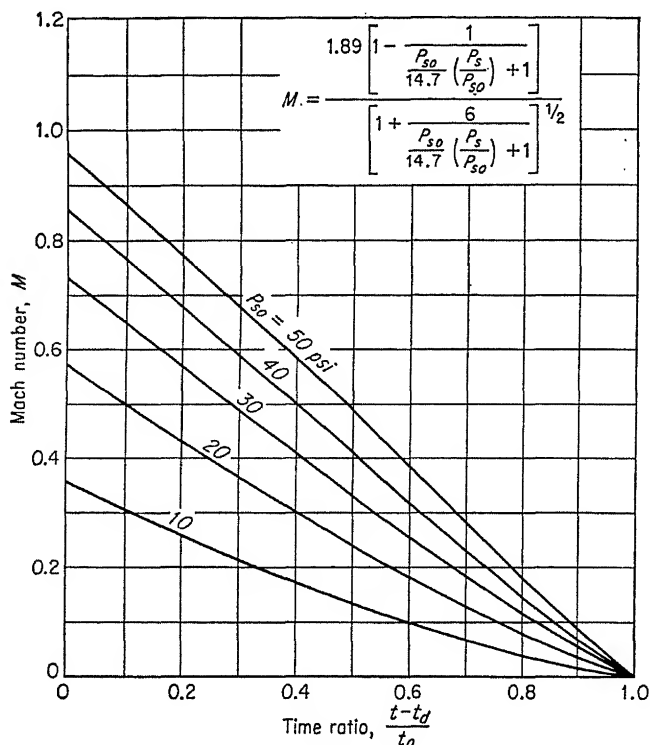


FIG. 11.46. Mach numbers of undisturbed stream vs. time ratio for various peak overpressures [Chap. 1, Ref. 8].

$Re = 5(10)^5$, $M = 0.4$ and 1.0 . These dynamic-pressure coefficients are applicable for steady-flow conditions, and since the flow about the arch is far from steady, their use may introduce some additional error. The order of magnitude of the error could be ascertained by comparing the results obtained by this procedure with direct measurements in field tests in which unsteady effects are present.

The expression for the local-pressure coefficient when $Re < 5(10)^5$ is

$$C_D = \frac{C'_D}{1.2} \left[0.7 + 0.5 \sqrt{1 - \frac{4}{(L/D)^2}} \right] \quad (11.21)$$

where C'_D = local-pressure coefficient for an arch infinitely long when $Re < 5(10)^5$ (Fig. 11.45)

L = length of axis of arch

D = diameter of arch

The Mach number is plotted in Fig. 11.46, and the ratio of Reynolds number to cylinder diameter is plotted in Fig. 11.47 for a range of incident peak overpressures as a function of $(t - t_d)/t_o$.

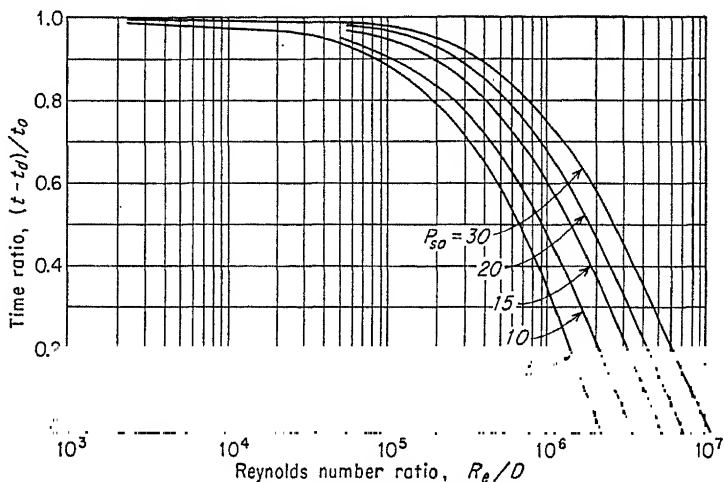


FIG. 11.47. Reynolds-number ratio of undisturbed stream vs. time ratio for various peak overpressures [Chap. 1, Ref. 8].

The overpressure at any point on the leeward side of the cylinder rises instantaneously from zero to a finite overpressure at time $t - t_d = 0$, given by

$$P_{cyl} = \left(1.5 - \frac{\theta}{180}\right) P_{so} \quad (11.22)$$

This initial overpressure clears to the value of P_{cyl} as given by Eq. (11.20) at time $t = t_d + t_c$, where

$$t_c = \frac{4h}{c_{refl}} \frac{\theta}{90} \quad (11.23)$$

The appropriate local dynamic-pressure coefficient C_D is obtained from Figs. 11.42 to 11.45 as discussed above.

AVERAGE END-WALL OVERPRESSURE \bar{P}_{end} , AXIS PARALLEL TO SHOCK FRONT. The average overpressure \bar{P}_{end} , on the ends of a cylinder oriented as in Fig. 11.38, is given in Fig. 11.48. It is assumed that the variation of incident overpressure in the time required for the shock wave to travel across the cylinder is linear and that the average overpressure on the ends is equal to the overpressure in the incident blast wave P_s , with the time-displacement factor $t_d = (D \cos \theta')/2U_o$.

d. Loading on Cylindrical-arch Surfaces, Axis Perpendicular to Shock Front. The local overpressure at any point on the periphery of the cylindrical arch oriented with its axis perpendicular to the shock front is the overpressure in the incident blast wave P_s , with a time-displacement factor $t_d = L'/U_o$, where L' is the distance from the front end to the point at which the overpressure is desired.

The average overpressure on the front and back ends of a cylindrical arch oriented with its axis perpendicular to the shock front can be computed as outlined in Sec. 11.2*a*. The clearing height for the front wall

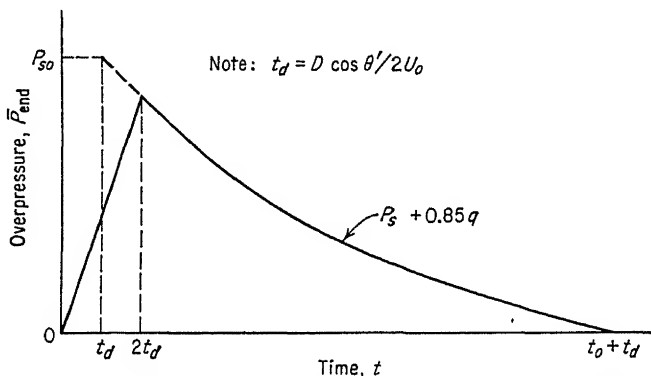


FIG. 11.48. Average overpressure on closed ends of cylindrical arch [Chap. 1, Ref. 8].

and the build-up height for the back wall are equal to h , as shown in Fig. 11.38.

e. Loading on Spherical-dome Surfaces. The notation convention used to designate a point on the surface of a dome is illustrated in Fig. 11.49. With the notation adopted, any point on the periphery of a spherical dome is located by the two angles θ and ϕ . Denoting by p any point on the sphere, θ is the angle between the horizontal diameter parallel to the direction of travel of the shock and radius Op joining the surface point to the geometrical center of the sphere. The elevation of the point above a horizontal plane through the center of the sphere is $R \sin \theta \sin \phi$, where ϕ is the angle between the horizontal plane through the center of the sphere and the inclined plane containing points 0, $0'$, and p .

The variation with time of the local overpressure P_{dome} normal to the surface of the dome is similar to that for a cylinder as shown in Figs. 11.40 and 11.41. The overpressure at a given point rises instantaneously from zero to $P_{r-\alpha}$ at time $t_d = x/U_o$, where $x = d/2 - R \cos \theta$, with d being the distance across the dome at its base, and U_o is the shock-front velocity. The angle of incidence at the impinging shock wave is equal to θ . For values of θ less than 90° the reflected overpressure is obtained from Fig. 11.21; for θ greater than 90° the maximum overpressure is given

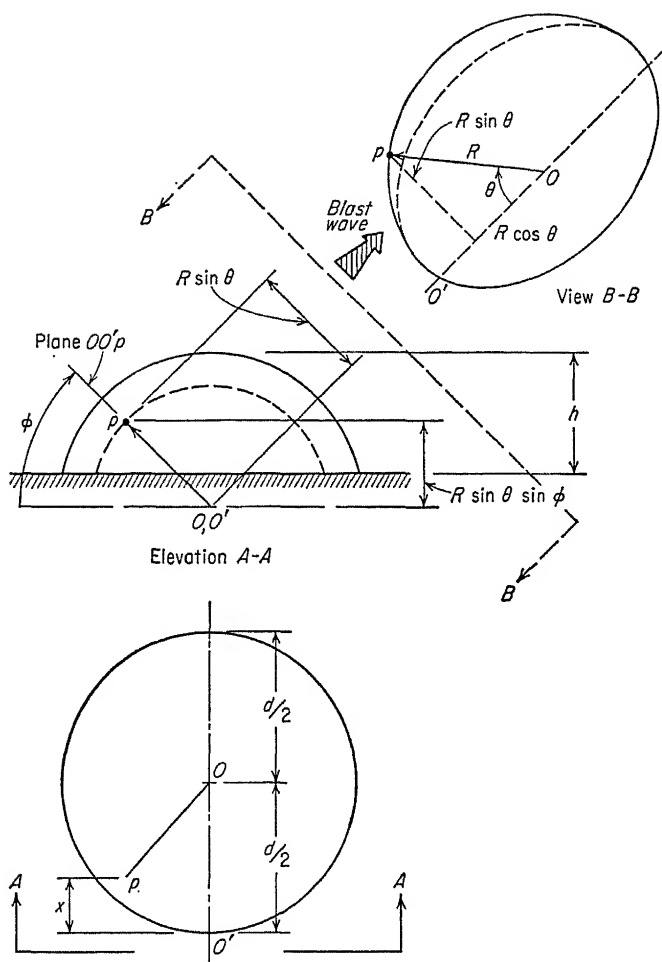


FIG. 11.49. Definition sketch for spherical-dome notation [Chap. 1, Ref. 8].

by the relation

$$P_{\text{dome}} = \left(1.5 - \frac{\theta}{180}\right) P_{so} \quad (11.24)$$

The initial maximum overpressures are cleared in time t_c , as given by Eq. (11.25), where h is the height of the dome above its base.

$$\begin{aligned} t_c &= \frac{3h}{c_{\text{refl}}} & \text{for } \theta < 90^\circ \\ t_c &= \frac{3h}{c_{\text{refl}}} \frac{\theta}{90} & \text{for } \theta > 90^\circ \end{aligned} \quad (11.25)$$

The local overpressure at any point after the clearing of reflected overpressures is given by Eq. (11.26).

$$P_{\text{dome}} = C_D q + P_s \quad (11.26)$$

where q = unit drag pressure incorporating time-displacement factor t_d

C_D = local drag coefficient plotted as a function of θ in Figs. 11.50 and 11.51

The ratio of the Reynolds number of the air-blast wind to the diameter of the sphere is plotted in Fig. 11.47 for various incident overpressures as a

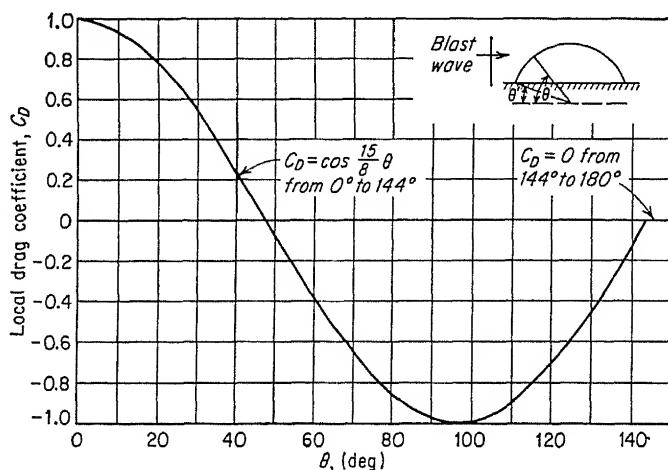


FIG. 11.50. Local drag coefficients for spherical domes, $Re > 10^5$ [Chap. 1, Ref. 8].

function of $(t - t_d)/t_o$. At the Reynolds number $Re = 10^5$, the value of the drag coefficient changes abruptly. The ratio of $(t - t_d)/t_o$ associated with this value of Re determines the applicability of either Fig. 11.50 or 11.51 to obtain C_D for use in Eq. (11.26).

The loading on domes calculated by the methods presented in this paragraph can be in error for overpressures greater than 15 psi. However, use of the present method, with reservations as to its accuracy, for high overpressures is recommended until a more suitable procedure is evolved.

11.3. Radiation. An exploding atomic bomb emits large amounts of thermal and nuclear radiation. The thermal radiation may have serious effects on structures in addition to the destruction caused by the air blast.

The temperatures reached in the explosion are nearly as high as those of the sun, but the distances involved are much less; therefore the resultant thermal radiation causes intense heat on all exposed surfaces. It will cause severe burns to humans and to animal life and will ignite emo-

bustible material, causing fires in structures. Complete or partial shielding is provided by buildings and by clothing.

Nuclear radiation produces a variety of harmful effects in human beings and animals, some of which are not immediately apparent. If a large amount of radiation is absorbed, the consequences can be very serious and often fatal. Some of the nuclear radiation is nearly instantaneous, but the products of fission will emit beta and gamma particles for a long time after the explosion.

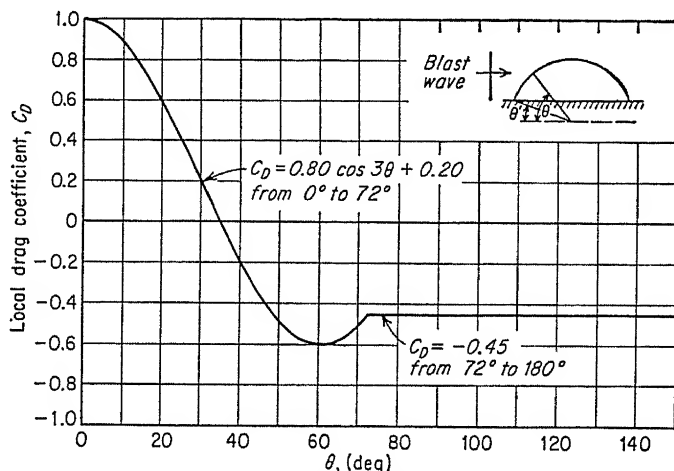


FIG. 11.51. Local drag coefficients for spherical dome, $Re < 10^5$ [Chap. 1, Ref. 8].

a. Thermal Radiation. PHENOMENA. The energy liberated per unit of mass is much greater for an atomic-bomb detonation than for a high-explosive detonation. Therefore the temperatures attained are much higher, resulting in a larger proportion of the energy being emitted as thermal radiation, roughly one-third of the total energy of the atomic bomb. The thermal energy reaching any particular point is a function of the distance from detonation, the yield of the weapon, and the effect of the scattering and absorption caused by the atmosphere. The coefficient of atmospheric attenuation is a function of the visibility, or the horizontal distance at which a large dark object can be seen against the sky at the horizon. The distances at which various thermal-energy levels are delivered for various total-energy yields of a bomb are given in Fig. 11.52 (reproduced from Fig. 7.67 of Ref. 1).

SCALING. If two atomic bombs with total energy yields of W_1 and W_2 are exploded, the proportion of the total energy emitted as thermal radiation is approximately the same for each weapon; therefore the thermal-radiation energy is proportional to the yield. At a given distance from the detonation the total amount of radiant energy on a unit area is also

proportional to the yield and is shown by the expression

$$\frac{Q_2}{Q_1} = \frac{w_2}{w_1} \quad (11.27)$$

where Q_1 and Q_2 = radiant energy on a unit area for the two weapons.

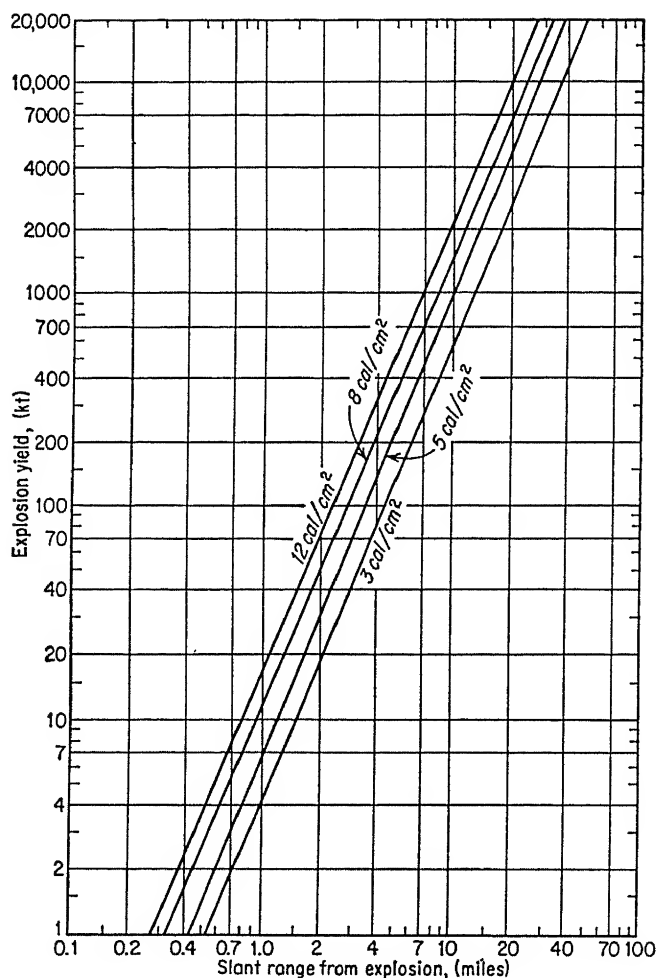


FIG. 11.52. Thermal energy received at various slant ranges [1].

EFFECT ON MATERIALS. A surface exposed to thermal radiation will absorb part and reflect part of this radiation, and in some cases a portion of the radiation will pass through to fall on material beyond. The amount of the absorption depends on the material, and especially upon its color, since the darker-colored materials will absorb a much larger

proportion than light-colored materials. The absorption causes the temperature to rise, and damaging effects may result.

The most important physical effects of the high temperatures due to the absorption of thermal radiation are, of course, charring or ignition of combustible materials and the burning of skin. It is very difficult to establish definite conditions under which these effects will or will not occur and their extent; however, for convenience, it is found necessary to use total energy per unit area as a criterion until such time as it is possible to predict the influence of intensity to include the range available in very-large-yield weapons.

Figure 11.53 shows diagrammatically how the quantity of heat necessary to cause charring of a given species of wood varies with the relationship between the total amount of energy supplied and the rate at which it is supplied. It will be noticed that as the rate of heat supply increases, the total energy necessary decreases rapidly at first and then reaches a nearly constant limiting value called the critical energy. This indicates that for high intensities of thermal radiation, such as occur in an atomic-bomb burst, there is less total energy required to cause charring of wood. This apparently happens to other materials subjected to high surface temperatures.

Although a serious hazard, injury from thermal radiation can be more easily avoided than can some of the other damaging effects of atomic weapons. Shelter behind any object which will prevent direct exposure to rays from the detonation is sufficient protection. A wall or a tree or, unless fairly close to ground zero, even clothing will provide a shield from thermal radiation.

b. Nuclear Radiation. Nuclear radiation has no incendiary effect, but is capable of producing serious harmful effects in human beings and animals. The possibility of exposure to radiation in a damaging amount must be considered in protective construction. Under some conditions, protection against radiation may govern the size of walls and roof of a protective structure.

Nuclear radiation is arbitrarily divided into two types: initial and residual. Initial radiation may be considered as that which occurs during the first minute after detonation, and residual radiation as that which occurs more than one minute after detonation.

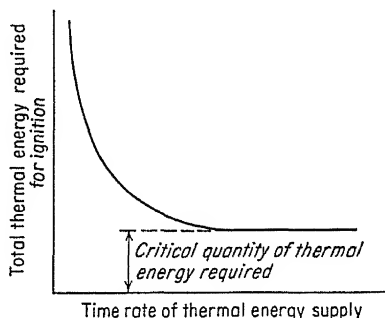


FIG. 11.53. Thermal energy required for ignition of wood as a function of rate of supply [Chap. 1, Ref. 8].

The initial radiation from the detonation of an atomic bomb consists of gamma rays, neutrons, beta particles, and a small proportion of alpha particles. The range of the alpha and beta particles is very limited, but the gamma rays and neutrons are capable of penetrating to appreciable

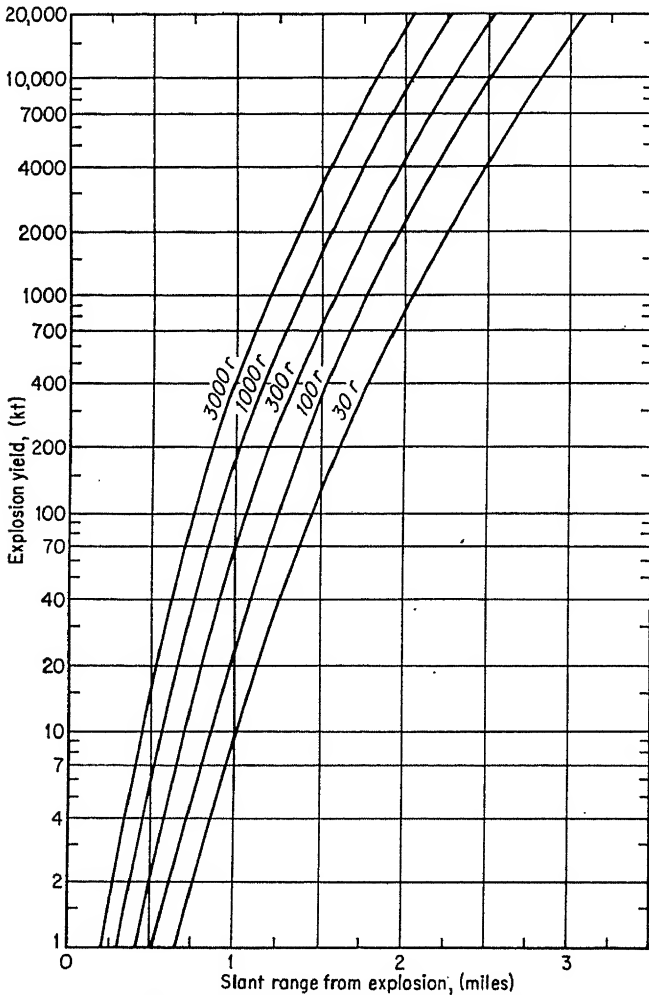


FIG. 11.54. Ranges of specified initial gamma-radiation dosages [1].

distances. Nuclear radiation has no incendiary effect, but both gamma rays and neutrons are capable of causing serious injury to human beings and animal life. At distances close to the bomb it is much more difficult to provide adequate shielding from nuclear radiation than from thermal radiation.

Gamma rays and neutrons are very different in their behavior; however, the relative intensity of these two types of nuclear radiation in the explosion of an atomic bomb is such that exposure to neutrons in addition to gamma rays would not represent an additional hazard, as the range at

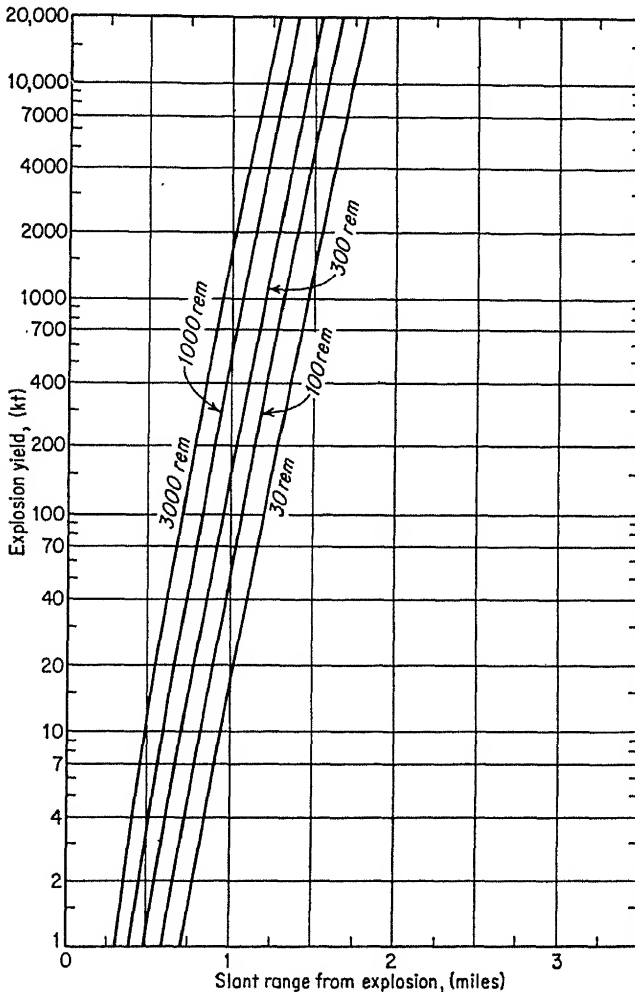


FIG. 11.55. Ranges of specified neutron biological dosages [1].

which the initial neutron intensity is lethal is much less than the range at which the initial gamma rays are lethal. Hence, if one is shielded from the gamma rays, he is also safe from the neutron radiation, but not vice versa.

The nuclear-radiation dosage to which an individual may be exposed is

measured in terms of a unit called the roentgen (r), which is a standard measure of the ionization caused by gamma rays in their passage through matter, and hence of the injury which is caused to the body of living organisms.

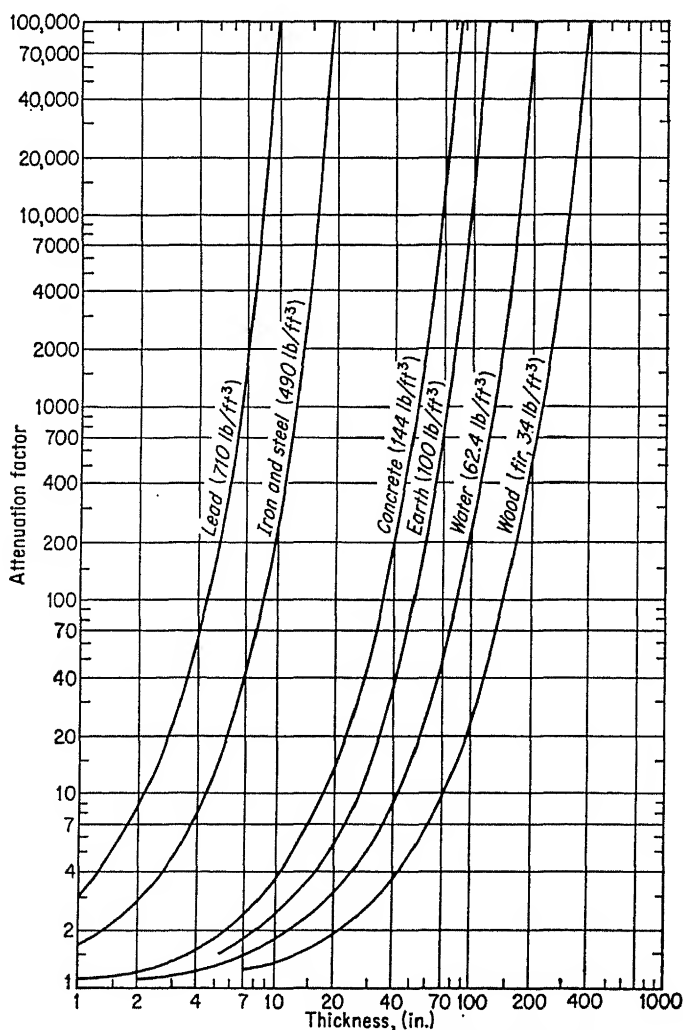


FIG. 11.56. Attenuation of initial gamma radiation [1].

Ranges for various initial gamma-radiation dosages from various-yield weapons are presented in Fig. 11.54 (taken from Fig. 8.39 of Ref. 1).

Ranges for various initial neutron biological dosages from various-yield weapons are presented in Fig. 11.55 (taken from Fig. 8.72 of Ref. 1).

PROTECTION REQUIRED. The effects of gamma radiation on living organisms depend on the total amount of the radiation absorbed, the rate of absorption, and the area of the body exposed. In this section we are interested only in protection from the initial radiation or that occurring within one minute after the explosion; hence the rate of the radiation dosage is very fast and the total amount absorbed by the body is the important criterion in determining its effect on human beings.

Three different degrees of exposure within a short period of time are here defined [1]. They are the lethal dose (600 r or more), which is fatal in nearly all cases; median lethal dose (400 r), which results in death to 50 per cent of those exposed; and moderate dose (100 to 300 r), which is generally not fatal.

The attenuation of initial gamma radiation afforded by various materials is presented in Fig. 11.56 [1].

c. Fallout [1, 12-14]. When an atomic bomb is detonated near the ground a large quantity of pulverized debris is drawn high up into the atmosphere. This dust serves as a collector for the radioactive material by condensing it; slowly the now radioactive dust settles to the earth.

The duration and pattern of fallout is a complex phenomenon, dependent to a large extent on the meteorological conditions. In general, the fallout will be diffused and, if the wind is blowing, will travel in a lateral direction with the wind. Of course, the winds at all altitudes up to about 80,000 ft have an effect on the settling dust.

The fallout radiation can be serious over an area of several thousand square miles from large-yield weapons. Information of particular value on fallout may be found in the testimony of Machta [14] and particularly in Ref. 1.

Protection against radiation from fallout may be supplied by having material between the people and the radiating source. The greater the thickness and the denser the material, the better. A reduction in radiation intensity of about 5,000 will generally give adequate protection from fallout. This would require about 36 in. of earth, 24 in. of concrete, or 3 in. of lead.

It may be practicable to wash off the roof or protective structures with a sprinkler system, carrying away a good per cent of the radioactive fallout, thus lowering the radiation intensities. Such a system may be desirable for particularly critical installations.

REFERENCES

1. "The Effects of Nuclear Weapons," U.S. Government Printing Office, September, 1957.
2. Bleakney, W.: Shock Loading of Rectangular Structures, *Princeton Univ., Dept. Physics, Tech. Rept.* 11-11, Jan. 10, 1952.

3. Feigen, M.: "Air Blast Pressures on a Cantilever Wall," University of California, Los Angeles, December, 1951.
4. Bleakney, W.: Rectangular Block, Diffraction of a Shock Wave around an Obstacle, Princeton University, Department of Physics, Dec. 7, 1949.
5. Bleakney, W.: The Diffraction of Shock Waves around Obstacles and the Transient Loading of Structures, *Princeton Univ., Dept. Physics, Tech. Rept. II-3*, Mar. 16, 1950.
6. White, D. R., D. K. Weimer, and W. Bleakney: The Diffraction of Shock Waves around Obstacles and the Transient Loading of Structures, *Princeton Univ., Dept. Physics, Tech. Rept. II-6*, Aug. 1, 1950.
7. Duff, R. E., and R. N. Hollyer: The Effect of Wall Boundary Layer on the Diffraction of Shock Waves around Cylindrical and Rectangular Obstacles, University of Michigan, Ann Arbor, Mich., June 21, 1950.
8. Uhlenbeck, G.: Diffraction of Shock Waves around Various Obstacles, University of Michigan, Engineering Research Institute, Ann Arbor, Mich., Mar. 21, 1950.
9. King, Jack H.: Steady-state Drag Coefficients for Shielded Member Systems, S.M. thesis, MIT, January, 1955.
10. Gowen and Rerhins: Drag of Circular Cylinders for a Wide Range of Reynolds Numbers and Mach Numbers, *NACA TN 2690*.
11. Modern Developments in Fluid Dynamics, High Speed Flow, vol. II, Great Britain, Aeronautical Research Council.
12. Protection against Fallout Radiation, *Federal Civil Defense Tech. Bull. TB 11-19*.
13. The Radioactive Fallout Problem, *Federal Civil Defense Tech. Bull. TB 19-1*.
14. Committee on Government Operations: Civil Defense for National Survival. Pt. 3, Testimony of Dr. Lester Machta, U.S. Government Printing Office, 1956.
15. Biggs, John M.: Wind Loads on Truss Bridges, *Proc. ASCE*, vol. 79, separate no. 201.
16. Biggs, John M., Saul Namyet, and Jiro Adachi: Wind Loads on Girder Bridges, *Proc. ASCE*, vol. 81, separate no. 587.

CHAPTER 12

BEHAVIOR OF STRUCTURES UNDER BLAST LOADS

12.1. Introduction. The behavior of structures under blast loads can be and has been studied both theoretically and experimentally, but a consideration of the Hiroshima and Nagasaki incidents and the results of a few of the structures tested in the nuclear experiments that have been released publicly will lead to a greater understanding of the requirements of a blast-resistant structure. It is necessary, however, to extrapolate the results of this data to the large-yield (multimegaton) weapons that are likely should a war develop. Extrapolation must be based on sound theoretical principles.

The behavior of a surface structure under blast loading can be visualized in the following manner. If the structure has a strong roof and walls, these elements will serve to transmit the dynamic-blast load to the structural frame. The effect of the pressure wave on the building is similar to that of a heavy blow followed by a more or less steady force. This force acts first on the side of the building nearest the explosion; then, as the blast wave passes, it acts on the remaining sides and roof, loading each of the exterior elements (walls and roof) in an inward direction. The net load on the structure (front-wall minus back-wall loads) acts to distort the frame laterally. Any element in the system (wall, roof, columns, footing, beams) may be deformed so much plastically that it fails ductilely, by buckling, or in a brittle manner, or the building may be separated from its foundation or from the ground if it is insufficiently restrained against sliding or overturning.

If the walls or roof of the structure fail, as would be the case if the walls are of asbestos cement or light sheet metal, then the frame of the building is subjected to severe drag forces, which can distort the frame, causing collapse of the structure if located in a high enough pressure region.

12.2. Hiroshima and Nagasaki Data. The case histories of these two explosions have been recorded in reports prepared by the U.S. Strategic Bombing Survey [1-6]. The bombs dropped on these cities had energy releases of approximately 20 KT. Based on an analysis of the Strategic Bombing Survey reports, the various types of damage and the radii within which they are expected to occur are estimated as for a 20-KT bomb [7]:

Virtually complete destruction will occur out to a radius of approximately one-half mile from ground zero, corresponding to an area of destruction of about three-quarters of a square mile.

Severe damage, defined as major structural damage that would result in collapse or liability to collapse of the building, will occur out to a radial distance which is slightly in excess of 1 mile from ground zero. This corresponds to an area of 4 square miles in which the damage ranges from severe to destructive.

Moderate damage, short of major structural damage but sufficient to render the structure unusable until repaired, will occur out to a radius of about $1\frac{5}{8}$ miles, giving an area of 8 square miles in which the damage ranges from moderate to destructive.

Partial damage will be inflicted out to a radius of approximately 2 miles, adding 4 additional square miles of damage area, and making a total of 12 square miles subject to some degree of damage in excess of plaster damage and window destruction.

Light damage, which is mostly plaster damage and window breakage, may extend out to a radius of 8 miles or more, giving a light damage area of the order of 200 square miles.

Hiroshima suffered, in addition to very extensive blast damage which will be discussed below, an extensive firestorm which developed from some hundreds of fires initiated by direct radiated heat and from secondary sources. Hiroshima was an excellent target for the atomic bomb from the fire standpoint since no rain had fallen for 3 weeks and the city was extensively built up of predominantly combustible buildings over flat terrain. The area suffering fire damage finally extended over 4.4 sq miles. Of a total of 130 buildings which were studied, the floor area of 72 per cent of the fire-resistive buildings, 50 per cent of the noncombustible buildings, and 80 per cent of the combustible buildings was burned in addition to suffering blast and debris damage. Of the buildings within or adjacent to the burned-over area, 58 of 64 fire-resistive buildings, 8 of 12 noncombustible buildings, and 41 of 54 combustible buildings had fire damage. Damage by fire to the interior and contents of the fire-resistive buildings greatly exceeded the damage by blast and debris.

One hundred and seventy-three buildings were included in the Hiroshima study, including practically every reinforced-concrete, every steel-frame, and every load-bearing brick-wall building within the area of blast damage. In addition, a sample of wood-frame structures was included to give evidence on this type of construction. The damage to residential-type construction was also studied. The various construction types were as follows [1]:

a. Because of aseismic design, multistory construction in Hiroshima generally was 50 per cent heavier and 50 to 70 per cent stronger than in comparable United States practice. However, a small number of buildings of substandard design or

construction was found. Concrete was quite variable in quality, some being very poor and the best being about comparable with good United States quality.

b. Light, steel-frame buildings were of excellent workmanship and materials but were slightly lighter than those in United States used for similar occupancies.

c. Load-bearing, brick-wall construction was excellent and compared favorably with better United States and European construction, being if anything, somewhat heavier and stronger than United States construction for similar occupancies.

d. Wood-frame construction, although employing heavier trusses, was weaker than usually found in the United States for similar occupancies because of poor details. Present in Hiroshima was a large number of buildings of weak, wood-pole construction. . . .

Blast damage to buildings spread uniformly in all directions, resulting in an approximately circular area of devastation. Limiting distances to which buildings were damaged depended upon their strength and construction. Thus the heavy, strong, multistory, steel- and concrete-frame structures were damaged only in an area relatively near the point of detonation and their burned-out, but otherwise undamaged, structural frames rose impressively from the ashes of the burned-over section where occasional piles of rubble or twisted steel skeletons marked the location of brick or steel-frame structures. At greater distances steel and brick structures remained undamaged. Blast damage to wood-frame buildings and residential construction beyond the burned-over area gradually became more erratic and spotty as distances were reached at which only the weakest buildings were damaged. In the outer sections of the city there were locations where there was no damage other than breakage of glass or minor disturbances of tile roofs.

In Nagasaki damage to buildings occurred over an area of 1.8 sq miles. "The blast completely demolished dwellings and other structures within a radius of $\frac{5}{8}$ miles of ground zero and caused various degrees of damage to other structures within a radius of $2\frac{1}{2}$ miles" [4]. The area which was damaged was irregular in shape, partly because of the hilly terrain of the city and partly because of the areas which were built up.

The degree of damage to buildings varied according to their relative distance from GZ, the materials of which the buildings were constructed, the design of the buildings, the relation of the long axes of the buildings to GZ, and the shielding effect of hills or man-made structures.

a. The variation in degree of damage depended on distance from GZ. . . .

b. Generally, buildings of reinforced concrete were less susceptible to the effects of the bomb than those of industrial type, steel-frame construction or buildings with load-bearing masonry walls. Wood-frame buildings were the most easily destroyed, and, in addition, had the properties which made entire destruction by fire possible. Steel frame structures, roofed or sided with corrugated asbestos, suffered less structural damage than those covered with corrugated iron or sheet metal. The corrugated asbestos crumbled easily and the blast pressure equalized itself rapidly around the main framing members, while the steel siding transferred the pressure to the structural members, causing general collapse.

c. Variations in design caused different degrees of damage to buildings in the same general building classification. Some specially designed concrete structures built to withstand earthquakes with heavy beams, well-placed steel reinforcing, and haunches between columns and beams withstood the blast pressures at relatively short distances—as close as 1,200 feet from GZ. Steel-frame buildings with pitched monitor-type roofs, especially those with knee braces extending from roof members to a point below the eaves on the columns, suffered less damage than structures with saw-tooth roof framing.

d. Structures of all kinds with their long axes parallel to the force of the blast were less deformed than those which received the pressure on the greater area of their sides.

e. Due to the height of the point of detonation of the bomb (estimated 1,700 feet above sea level), the screening effect of structures within 5,000 feet of GZ was negligible. Buildings in the Nakashima Valley, which extended in a north-easterly direction from Nagasaki Harbor, were shielded from the blast by the intervening hills which rose to heights of 900 feet at a distance of approximately 6,000 feet southeast of GZ [4].

Professor Bowman, who directed the Hiroshima and Nagasaki surveys, has summarized the extent of damage to various types of structures in an *Engineering News-Record* article of Jan. 26, 1950. His interpretation of the data is presented in Fig. 12.1.

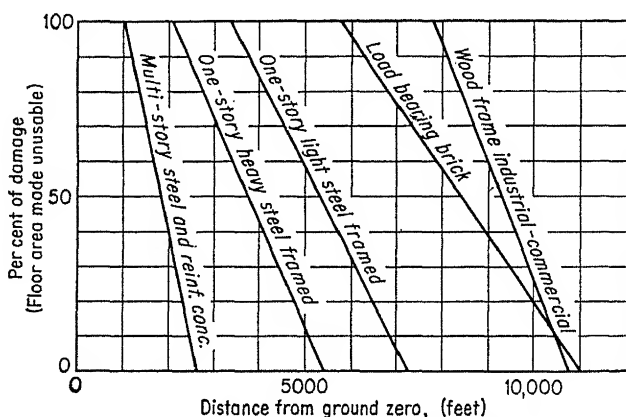


FIG. 12.1. Damage at Hiroshima and Nagasaki from nominal atomic bomb. (Reprint from *Eng. News-Record*, Jan. 26, 1950.)

12.3. Nuclear Experiments. Tests of a variety of structures under various-size atomic bombs have been performed at the Nevada and Pacific Proving Grounds. Specific information has been released on the tests conducted in Nevada by the Federal Civil Defense Administration [8, 9].

In Operation Doorstep, performed in March, 1953, two two-story conventional wood-frame houses were exposed to the blast and radiation

effects of a 15-KT bomb burst 300 ft aboveground. One house located 3,500 ft from ground zero was severely demolished by the blast-pressure wave with a peak incident overpressure of 7 psi. The second house, located at 7,500 ft from ground zero, remained standing under the blast wave, which had a peak incident overpressure of 2 psi. The house was badly damaged and probably would have to be wrecked because of extensive damage to joists and rafters.

In addition to the two houses tested, Operation Doorstep also included a variety of small underground backyard types of shelters which successfully withstood blast pressures from 20 to 45 psi.

Operation Cue, which was completed in the spring of 1955, was a much more extensive test involving houses, utilities, shelters, and small prefabricated metal buildings. A report [9] on the housing summarized the test as follows:

Ten residential structures of wood, brick, lightweight reinforced concrete block, and lightweight precast concrete slabs were exposed in pairs to the effects of a nuclear device . . . of approximately 30 kiloton yield detonated atop a 500-foot tower.

Two houses were two-story and basement structures of wood frame construction redesigned and strengthened on the basis of studies of the findings on similar houses exposed to the effects of a nuclear device in 1953. One of the houses (31.1-b1) was exposed at approximately 4 psi overpressure, the other (31.1-b2) at approximately 2.6 psi overpressure.

Two houses were two-story and basement structures of brick and cinder block exterior walls, cinder block basement walls, and wood-frame floors, partitions and roof, one (31.1-a1) exposed at approximately 5.1 psi overpressure, the other (31.1-a2) at approximately 1.7 psi overpressure. The size and layout of these houses was similar to the strengthened frame houses, but they were of conventional construction.

Two houses were one-story wood-frame rambler type, one (31.1-c1) exposed at approximately 5.1 psi overpressure, the other (31.1-c2) at approximately 1.7 psi overpressure.

Two houses were built of reinforced lightweight concrete blocks with precast lightweight concrete roof slabs, one (31.1-f1) exposed at approximately 5.1 psi overpressure, the other (31.1-f2) at approximately 1.7 psi overpressure.

The final two houses were one-story structures built of precast lightweight concrete wall, partition and roof panels, one (31.1-e1) exposed at approximately 5.1 psi overpressure, the other (31.1-e2) at approximately 1.7 psi overpressure.

Each type of house was tested in a pair; one house at an anticipated overpressure at which collapse or major damage might be expected; the other house, its counterpart, at an anticipated overpressure at which damage without collapse might be expected.

The above ground portion of the two-story brick and cinder block house (31.1-a1) located 4,700 feet from the explosion, was almost completely destroyed, and the first floor system was partially collapsed into the basement. None of the

exterior walls remained standing, and the structure as a whole was beyond repair even for emergency shelter from the elements.

The one-story frame rambler (31.1-c1), located near the two-story brick dwelling 4,700 feet from the explosion, was likewise almost completely destroyed. Only the reinforced concrete bathroom shelter remained intact.

Both the one-story reinforced lightweight concrete block house (31.1-f1) and the one-story precast lightweight concrete house (31.1-e1) suffered only minor structural damage. These houses were also located 4,700 feet from the explosion. With the replacement of doors and window sash, both houses could be made habitable.

At 5,500 feet from the explosion the two-story redesigned frame house (31.1-b1) suffered severe damage and would not be suitable for occupancy without extensive major repairs, which would hardly be economically advisable.

At 7,800 feet from the explosion the two-story redesigned frame house (31.1-b2) suffered relatively heavy damage, but its condition was such that it would be made available for emergency shelter from the elements by shoring and not too extensive repairs.

The two-story brick and cinder block house (31.1-a2) located 10,500 feet from the explosion suffered considerable damage to the roof and second floor ceiling, with minor damage to walls and floors. The masonry appeared to suffer little or no damage, although there was considerable damage to window sash and doors. At a reasonable cost this house could be made suitable for emergency housing.

The one-story precast light aggregate concrete house (31.1-e2) and the one-story reinforced masonry block house (31.1-f2), both located 10,500 feet from the explosion, suffered relatively minor damage. Only minor repairs would be required to make these dwellings suitable for reoccupancy.

The one-story frame rambler (31.1-c2), also located 10,500 feet from the explosion, suffered relatively heavy damage, but nevertheless could be restored to condition suitable for occupancy at moderate costs.

Out of the ten houses included in the test, the condition of seven were such that they could be made habitable for emergency occupancy by shoring and repairs. In practically all of the houses the windows and exterior doors were destroyed. In all except the two collapsed houses, the greatest danger to the occupants would appear to have been from missiles of glass, venetian blinds, furniture and other fragments.

12.4. Extrapolation to Large-yield Weapons. While it is interesting and informative to have estimates of the extent of damage from the low-yield (approximately 20-KT) weapons as detonated at Hiroshima and Nagasaki and in the Nevada Test Site experiments, it is of greater interest to have estimates of radii of damage from the large-yield hydrogen weapons. These estimates can be made by an application of the basic theoretical methods of dynamic analysis, blast-load prediction, and ultimate strengths of structural elements as outlined in Chaps. 1, 2, 7, and 11 and are presented in Table 12.1.

TABLE 12.1. DISTANCES AT WHICH VARIOUS TYPES OF CONSTRUCTION WILL SUFFER DAMAGE FROM 1-MT AND 20-MT WEAPONS

Class of structure	Severe-damage distance, yd		Slight-damage distance, yd	
	1 MT	20 MT	1 MT	20 MT
Single-story light-steel-frame industrial building.....	5,500	17,000	9,000	25,000
Single-story medium-steel-frame industrial building.....	4,600	14,000	9,000	25,000
Single-story heavy-steel-frame industrial building.....	3,700	11,000	9,000	25,000
Multistory steel-frame building.....	4,000	12,000	7,000	19,000
Multistory reinforced-concrete building.....	3,700	11,000	7,000	19,000
Wood-frame housing.....	7,000	19,000	25,000	70,000

REFERENCES

1. U.S. Strategic Bombing Survey: "The Effects of the Atomic Bomb on Hiroshima, Japan," vol. I, May, 1947.
2. U.S. Strategic Bombing Survey: "The Effects of the Atomic Bomb on Hiroshima, Japan," vol. II, May, 1947.
3. U.S. Strategic Bombing Survey: "The Effects of the Atomic Bomb on Hiroshima, Japan," vol. III, May, 1947.
4. U.S. Strategic Bombing Survey: "Effects of the Atomic Bomb on Nagasaki, Japan," vol. I, June, 1947.
5. U.S. Strategic Bombing Survey: "Effects of the Atomic Bomb on Nagasaki, Japan," vol. II, June, 1947.
6. U.S. Strategic Bombing Survey: "Effects of the Atomic Bomb on Nagasaki, Japan," vol. III, June, 1947.
7. Los Alamos Scientific Laboratory: "The Effects of Atomic Weapons," U.S. Government Printing Office, September, 1950.
8. Federal Civil Defense Administration: "Operation Doorstep," U.S. Government Printing Office, Mar. 17, 1953.
9. Federal Civil Defense Administration: "Operation Cue," U.S. Government Printing Office, May, 1955.

BLAST-RESISTANT-DESIGN CONSIDERATIONS

13.1. The Problem. The principal objective of the architect-engineer of a blast-resistant structure, as stated in Chap. 10, is to design the building so that the structure itself, its equipment, contents, and occupants are as invulnerable to the various effects of atomic weapons as is physically and economically practicable.

This chapter presents the problems that face the designers and acquaints them with factors which will assist in determining the degree of protection that it is practical to attempt. It deals with general methods of attaining resistant construction and with the importance of good planning through site selection, type of structural framing, the external geometry or shape of the building, internal arrangement, and selection of materials, all of which are directly related to the problem of achieving the protection required. It does not attempt to tell the architect or engineer how to design a specific building but rather to show him the way toward a solution which is as economical as is consistent with the more severe design requirements which are imposed.

13.2. Criteria for the Building Program. The various criteria of the building program must be established by the owner with the advice of his architect-engineer. A number of questions may be posed which will assist in delineating the program. They are as follows:

1. What are the possible sites for building? How far are they from target areas? Is it possible to locate the building at great distances from such areas and out of the possible fallout areas?
2. Is it intended that all contents of the structure are to be protected, or only a certain number of types, or are the contents expendable?
3. Are some or all of the occupants to be protected at their normal work locations, or are central areas required within the building?
4. Is it possible to take advantage of terrain features, tunnels, or abandoned mines?
5. Is it possible and feasible to construct the structure underground?
6. Will emergency housing of personnel be required for extended periods of time?

The answers to these questions will be affected by a number of factors including:

1. The relative importance of the structure, its function, contents, and occupants to the continued ability of the community to operate during and after exposure to the effects of atomic explosion.

2. The economic practicability of building resistant construction of the resistance required to give reasonable protection.

3. The probability of successfully resisting determined enemy attack.

13.3. Type of Construction. The functional requirements of the proposed project form a primary basis for selection of type of construction. However, the requirements imposed on the structural frame, wall and roof panels, entrances, etc., by the air-blast wave and radiation loads may and probably will serve to modify the normal solution to the design problem. Many of the requirements of normal construction will be compromised, and the resulting structure may not be as desirable in some respects as a conventional building. However, the severe "design loads" will necessitate compromises with normal building practice.

Several types of construction may be used. Probably the greatest level of protection can be secured in buried or semiburied construction.

a. Buried or Semiburied Construction. If practicable, advantage should be taken of the high blast resistance of earth-covered structures either above or below ground since this form of construction is extremely resistant to high blast pressures. Factors which contribute to this resistance are:

1. Reduction in the blast loading on the structure occurs because of the streamlining effect of the earth cover.

2. A further reduction in the blast load will result if the structure is below ground, because of the elimination of reflected pressures and also because of the attenuation of pressure in the earth.

3. The mass of the earth increases the inertia of the structure and accordingly may reduce the net loads on the structure, thus reducing stresses and deformation.

4. The soil can act as an earth arch over the structure, carrying a good portion of the blast load and reducing the required structural strength.

The earth cover will add to the shielding material for protection of personnel against nuclear radiation. The shielding thus provided applies to the entire structure, and separate or specially shielded areas are not required, as may be necessary in aboveground structures.

The function of the structure or ground conditions may prohibit buried construction or even semiburied construction, in which case one of several forms of surface structure may be considered.

b. Shear-wall Construction. For surface structures the shear-wall system should be used whenever possible since this type is superior to the conventional rigid-frame system in regard to strength and cost. The shear walls, floors, and roof should preferably be of reinforced concrete.

However, shear walls of reinforced-brick masonry may find some applications, and floor and roof may be of steel construction provided they are detailed to transmit the lateral blast forces from the exterior walls to the shear walls.

c. Arch and Dome Construction. This type of construction possesses two advantages which can be exploited to obtain a high level of blast resistance. The first advantage is a reduction in load, which results because a curved surface is presented to the incident blast wave. The second advantage is in the high efficiency which such structures possess from the standpoint of strength.

Disadvantages of this type of construction arise from restricted space arrangements and the higher cost of constructing curved or warped surfaces.

d. Rigid-frame Construction. The rigid-frame system of construction should be used only when the shear wall or arch or dome forms of construction cannot be used. Such situations might arise because of severe space requirements. However, even if this is the case, it may be possible to secure some of the economy of shear-wall construction by incorporating shear walls in portions of the structure.

e. Single-story vs. Multistory Construction. Single-story construction is generally preferable to multistory construction although cost comparisons may be necessary to establish priority in some cases. The economy of single-story construction arises because very great lateral loads are developed on exposed vertical surfaces, requiring greater lateral-resistance capabilities in the lower stories of multistory structures.

f. Exterior Walls. A fundamental planning decision must be made with respect to type of walls. Either they should be strong enough to keep the blast out at the desired degree of resistance, or they should be designed to fail readily, preferably breaking into small pieces that will not form dangerous missiles. If these are to be frangible, a wall of corrugated asbestos cement is probably preferable.

If the walls are to be blast-resistant, they probably should be windowless because of the great difficulty in securing the necessary blast resistance in a fenestrated wall.

Reinforced concrete is probably the best material, although carefully designed reinforced masonry may find application for lower-pressure levels. Some types of metal siding, if properly attached to closely spaced girts, can also be used. Structurally weak materials such as unreinforced-brick or concrete-block masonry, asbestos cement siding, weak steel siding, etc., cannot be used.

g. Windowless Construction. Windowless construction is recommended for all structures planned for pressure levels above 10 psi.* For

* It is possible that inswinging sash can be developed, permitting the glass to remain unshattered at pressure levels up to 10 psi.

certain types of blast-resistant construction there may be an advantage in the use of frangible exterior walls or windows, with an interior area of the structure of blast-resistant construction.

There may be objections to windowless buildings by certain users who would like to have blast resistance and daylight too. This cannot be done for an entire structure except for relatively low pressure levels as mentioned above. Accordingly, a consideration of the advantages of windowless construction may offset the disadvantages:

1. Windowless blast-resistant construction provides resistant areas for the entire area of the building.

2. The elimination of windows means more usable wall space.

3. There will be less heat loss in the winter and less heat gain in the summer.

4. Illumination can be made more uniform, with all areas becoming equally desirable from this standpoint.

5. The cost of windows is generally greater than the cost of a blank wall.

6. The very *great* hazard from window breakage from blast is eliminated. The area of glass breakage around an exploding atomic or hydrogen bomb is so much greater than that for structural damage from blast, or personnel injury from nuclear or thermal radiation, that the elimination of this hazard is a very real gain.

Of course, there are obvious disadvantages to windowless construction, including the following:

1. Mechanical ventilation and probably air conditioning are required.

2. The loss of daylight is aesthetically undesirable in many cases.

3. For certain types of buildings, particularly industrial structures, a more economical blast-resistant structure could result if frangible wall construction were used along with a strengthened frame. The use of such construction would entail the loss of the weather covering should an attack develop.

h. Geometry. In all protective construction, wall heights should be kept to a minimum. This reduces the area exposed to lateral blast load, and accordingly the total lateral load, and also further reduces the bending moments in columns or shear walls by the reduction in height.

Long-span construction becomes very costly when blast resistance is required. Thus hangars, auditoriums, armories, etc., will be costly and difficult to construct for high levels of blast resistance. The arch or dome shapes may be more economical for hangars.

Building heights greater than three stories can be designed without serious difficulty but probably will be costly in comparison with lower buildings. However, the cost will be related to the proportions of the building, for buildings of slender proportions will be more costly than those with broader proportions and therefore must be avoided if possible.

i. Doors and Openings. All access openings must be protected by blast-resistant doors or covers. Such elements must be capable of resisting the incident blast pressures, both positive and negative. The hinge and lock details must be carefully designed so that permanent deformations will not occur at the design load, to preclude the possibility of jamming. Additional sealing doors may be required to exclude radioactive contamination.

Covers for ventilation openings may have to be automatically closing, actuated by the blast itself or by the light from the explosion.

j. Foundations. Foundations must be capable of resisting much larger vertical loads than normal, but loads of a transient nature. Soils are generally able to resist much larger dynamic loads than static loads, but the relationships are incompletely defined at the present time. In addition to the transient vertical load there is a transient horizontal load and an overturning effect imposed on the foundation. The tendency of the structure to overturn and slide under the large transient forces must be checked (Sec. 13.7).

13.4. Functional Considerations. *a. Space Arrangement.* Normal arrangements of space might be affected. Some of the causes might include the following:

1. The requirement of shelter areas for personnel in specific locations may alter normal arrangement of space.

2. The possibilities of reducing the amount of blast load on a structure through the use of domed or other specially shaped surface structures may impose special limitations on ceiling heights near the periphery of the building.

3. The requirement of providing strength in the framing of the structure against lateral loads may impose certain limitations on arrangements of space.

b. Shelter Areas. The provision of a shelter area which may consist of only a small fraction of the area of the building to essentially the entire building is a basic requirement for a blast-resistant structure housing personnel, unless shelter facilities external to the building are to be provided.

c. Building Services. Building services such as gas, water, steam lines, electrical connections, elevators, stand-by water should all be designed so that possibilities of failures are minimized. Location of connections from the outside to the building is a particularly critical point. The avoidance of having connections in areas where differential displacements are likely to occur is of paramount importance.

The provision of stand-by water supplies for fire fighting and for the maintenance of pressure in sprinkler systems demands primary consideration because of the very great danger of fire resulting from secondary effects.

Shelter areas should, in general, not house any of the utility lines mentioned in the previous paragraph, which would offer hazards if broken. High-pressure steam, gas, and water in large quantities may offer potential hazards, which should be avoided.

13.5. Structural Design. The evolution of the design of a protective structure after the level of protection has been established involves several steps:

Step 1: Selection of type of construction

Step 2: Preliminary layout of the structure, including size and shape

Step 3: Determination of type of behavior—elastic, elasto-plastic, or plastic—and amount of plastic deformation permitted on the various structural elements

Step 4: Determination of the blast-pressure-vs.-time curves for all surfaces of the structure

Step 5: Dynamic design of the various structural elements

a. Preliminary Layout. After the type of construction has been selected a preliminary layout must be made of clearance required, framing arrangements, and minimum allowable sizes of the structural elements. The minimum sizes may be based upon the required static-load capacity, building-code specifications, or practical-construction requirements.

b. Type of Behavior. It is recommended for reasons of economy that designs be based on plastic behavior whenever possible. Some permanent deformation and cracking of the concrete or steel may be tolerated where no harm would be done to the contents of the structure and its usefulness for its major function would not be impaired (Sec. 13.7).

Elastic design may be required for certain important structures or in cases where personnel will be sheltered in relatively confined areas.

c. Blast-pressure Loading Curves. The blast loading on all exterior surfaces of the proposed structure must be determined for the given "design loads," which include an initial blast overpressure P_s and duration t_0 , consistent with a given atomic weapon and distance from point of detonation. The selected P_s and t_0 effectively determine the level of protection.

Procedures for calculating the blast-loading curves for various types of surfaces are given in Chap. 11.

d. Dynamic Structural Design. Since the applied loads are dynamic in character and of high intensities it is necessary that the structural-design procedure involve (1) a consideration of the acceleration and motion of the elements and (2) the ultimate strength of elements. Such design procedures are inherently more complex than the conventional static-design procedures (Chaps. 7 and 14).

The ultimate strengths of structural elements of steel or reinforced

concrete can be predicted easily following methods outlined in Chaps. 1 and 2. Since the response of elements of the structure is dynamic, and accordingly rapid, advantage is taken of higher yield stresses under rapid response of steel and reinforced concrete.

13.6. Personnel Shelters. Personnel shelters may be separate complete structures or strengthened areas within a partially resistant building. In either case there are no special structural-design problems.

Considering the separate shelter, blast doors are required for all entrances and access openings to exclude radiation, heat, and blast. Because of possible prolonged occupancy due to the fallout hazard, ventilation and filtering systems will be required.

For shelter areas within buildings, the blastproof doors and air-filtering systems may not be required.

For all shelter areas the following criteria must be met:

1. Shielding must be sufficient to reduce the dosage from initial gamma radiation to between 25 and 100 r.

2. Blast, heat, and radioactive particles must be excluded from the shelter area.

3. The structural system must be capable of sustaining the design blast loads with elastic behavior only.

4. Prolonged occupancy must be considered a possibility.

Elastic behavior of the structural system is recommended to preclude the possibility of injury to personnel from concrete spalling (which is not significant structural damage) and from excessive movements which might develop if plastic action were permitted.

13.7. Deflection Criteria for Plastic Design. The allowable maximum deflection of a building frame may be dependent upon its function or the contents, such as mechanical equipment or instruments which cannot be isolated from the building. Mechanical equipment and utilities would require special design consideration to provide sufficient flexibility to prevent failure if large displacements are permitted.

Perhaps more important and difficult to evaluate is the amount of plastic deformation that a structural system or element can be subjected to and still be able to perform its normal structural function.

The structural adequacy of reinforced-concrete and steel structures to carry conventional dead and live loads may not be affected seriously by permanent distortions of limited magnitudes. Tests of reinforced-concrete and steel structures in the atomic tests conducted by the United States have shown that they can withstand relatively large permanent distortions without seriously affecting their ability to carry normal loads.

The results of static tests [1-4] that have been carried to the point of failure will provide a guide to the establishment of design criteria for plastic behavior. The results of these tests are presented in terms of a

ductility ratio. For any element this ductility ratio β is defined as the ratio of the maximum deflection of the member at the point of collapse to the maximum elastic deflection:

$$\beta = \frac{x_c}{x_e} \quad (13.1)$$

For plastic design, a deflection greater than x_e and less than x_c should be used. If a design factor α having a value less than 1.0 is introduced, the design maximum deflection is

$$x_m = \alpha \beta x_e \quad (13.2)$$

The factors α and β vary with type of element and material of construction. Considerations which play an important part in determining values of α are the economics of construction, the sensitivity to dynamic loads, the function and content of the structure, etc.

Although considerable investigating remains to be done before the variation in cost of construction can be used as a firm guide for choosing α for all types of elements, it is clear from a limited study that for all elements there is a minimum value of α above which there is no significant reduction in the cost of construction for a given design overpressure. Slight variations in magnitude and duration of the applied load, as well as in the magnitude of the yield stress, mass, and spring constant of the element, may lead to changes of considerable magnitude in the maximum displacement. For this reason, deflection criteria should be given by a range of values rather than by a particular value.

Pending further investigation, it is recommended that the value of α be permitted to vary from one-half to one-third. The maximum deflection would then be

$$\frac{\beta x_e}{2} > x_m > \frac{\beta x_e}{3} \quad (13.3)$$

Results of tests on a large number of reinforced-concrete beams using a structural grade of steel yield the following conclusions in regard to the ductility ratios β of such members [2]:

1. Concrete strength has little effect on the energy-absorbing capacity of beams failing initially in tension but does have an effect on the energy-absorbing capacity of beams failing in compression.

2. The ductility of a beam depends on the per cent of reinforcing steel.

3. The compression reinforcement adds to the ductility of a beam. The addition of compression reinforcement enables a larger-angle change to take place before the concrete crushes, and thereby increases the deflection which the beam can undergo before collapse.

4. To be most effective, the compression reinforcement must be well tied.

5. For rectangular beams reinforced in tension only,

$$\beta = \frac{0.1}{p} \quad (13.4)$$

where p is the ratio of tension reinforcement to the area bd . A limiting value of β is 50.

6. For doubly reinforced rectangular beams,

$$\beta = \frac{0.1}{p - p'} \quad (13.5)$$

where p and $p' =$ the ratios of area of tension and compression reinforcements, respectively, to area bd . A limiting value of β is 50 for the case in which $0 \leq (p - p') \leq 0.002$.

A short series of tests of I beams [3] subjected to concentrated load at mid-span was conducted in which the specimens were loaded to destruction. In long spans, local buckling preceded lateral buckling. The average ductility ratio was 26.4 for specimens loaded in the strong direction. In similar tests with superimposed axial load equal to three-fourths the ultimate lateral load, the ductility ratio β was 8.1. The combination of axial load and lateral load on a beam reduces the elastic stiffness, decreases the maximum lateral load, decreases lateral-load resistance after reaching maximum load, and decreases the ductility ratio β . Comparative tests of beams loaded in either the strong or weak direction indicated little difference in ductility ratio.

Welded portal frames [4] tested to ultimate under vertical load with sidesway and lateral buckling prevented by special supports showed a range of ductility ratios from 6 to 16. The ratio of failure deflections to the span varied from 0.036 to 0.068. The range of values resulted from varying the size of component elements.

Composite concrete and steel T beams [5] with channel shear connectors subjected to a concentrated load at mid-span produced an approximate ductility ratio of 8 and an approximate ultimate-deflection ratio to a span of 0.016. This latter ratio indicates the stiffness of composite-beam construction.

A summary of these test data is tabulated below:

Test	Ductility ratio	Ultimate-deflection-to-span ratio	Ref.
Reinforced-concrete beams.....	$\frac{0.1}{p}, \frac{0.1}{p - p'}$	2
Steel beams, lateral load.....	26.4	0.097	3
Steel beams, lateral and axial load.....	8.1	0.025	3
Welded portal frames, vertical load.....	6-16	0.068-0.036	4
Composite T beam.....	8	0.016	5

The data summarized are intended only as a guide to the designer. Indicated therein is the order of magnitude of collapse deflection for certain specific loading conditions. In a particular design condition, the loading and response must be considered very carefully in determining the allowable deflection. Very few buildings will be designed to collapse under the design load, so it is necessary to utilize a reduction factor, designated herein as α , to modify the test value β in determining the plastic-design deflection.

13.8. Design of Foundations. Buildings which are subjected to large horizontal blast loads from atomic weapons will tend to slide laterally and rotate. The primary consideration in the design of foundations for such structures is to prevent both of these motions, or at least to limit these motions to reasonable magnitudes.

The sliding of buildings is resisted by passive pressure on the rear vertical faces of the foundations and by friction between the soil and the foundation. In buildings on pile foundations, lateral movements of the foundation are resisted by lateral shearing and bending forces in the piles. Batter piles may be required in some cases.

To limit the sliding of the foundation it is necessary to utilize all the available resistance forces. This requires the use of foundation struts or floor slabs acting as deep beams to distribute the lateral forces to the points where resistance can be provided. In all types of buildings the horizontal blast loads tend to overturn the building, thus causing unequal distribution of foundation pressure, with the higher pressures occurring at the rear of the building. Since the friction forces under the footings are proportional to the vertical foundation pressure, the available frictional resistance at the front of the building is generally small. This lack of sufficient frictional resistance at the base of footings for the walls and columns near the front of buildings makes it necessary to utilize the lateral resistance furnished by the passive pressure on the back of these footings, or to provide footing struts or floor-slab diaphragms connected to the rear footings where the bearing pressures are high and large friction forces can be developed. The resistance to passive pressure on the rear vertical face of rear-wall footings is also much higher than for the front-wall footings because of the effect of the blast pressure on the ground surface at the rear of the structure.

In the case of shear-wall buildings with interior columns carrying large vertical loads but no lateral loads, the large column loads permit development of large frictional forces which may possibly be needed to resist the lateral loads on the shear walls. In this case the column footings may be tied to the shear walls by horizontal floor-slab deep beams, or a mat foundation may be used.

For buildings which resist horizontal blast loading through rigid-frame action, it is advantageous to provide maximum restraint against rotation

at the bottoms of the frame columns. This requires that individual footings for these columns be rather large by conventional standards. This condition makes it advantageous in some cases to use continuous strap footings or mat foundations.

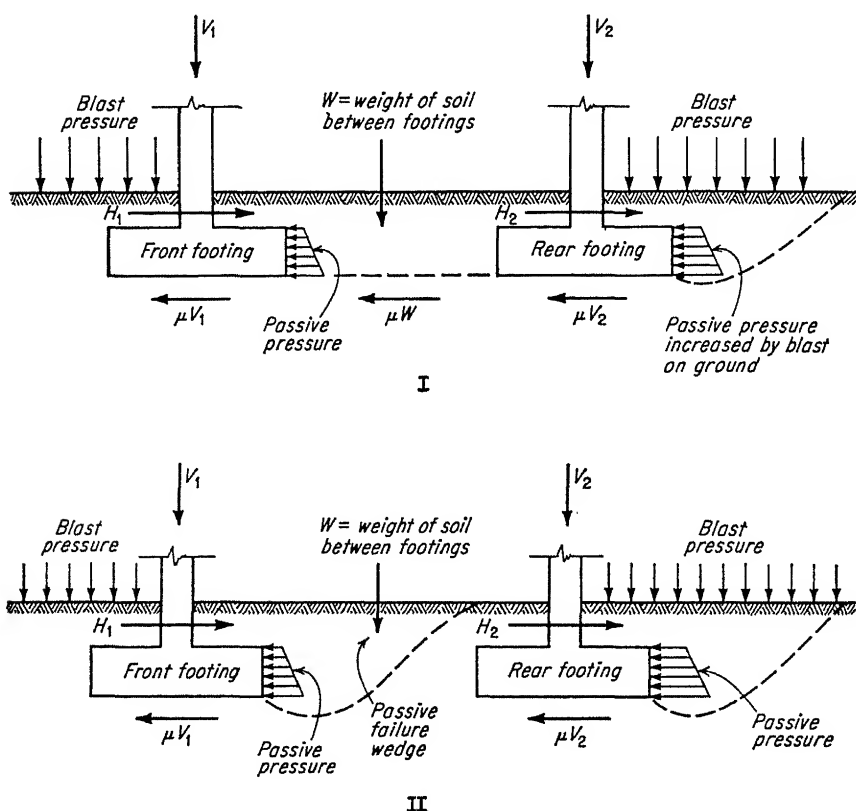


FIG. 13.1. Sources of lateral resistance on spread footing foundations. Case I: $\mu W < \text{potential passive pressure behind front footing}$. Case II: $\text{passive pressure behind footing} < \mu W$.

If a footing moves laterally against the soil, the soil develops passive pressure on the rear face of the footing, as indicated in Fig. 13.1. In the case of interior- or front-wall footings, the resistance available due to passive pressure is a function of the depth to the surface of the soil and the weight of the soil enclosed between the footings. The maximum resistance that the soil enclosed between the footings can provide is the lesser of (1) the resistance due to passive pressure of the soil, or (2) the frictional resistance approximated by the product of the coefficient of friction and the weight of the soil between footings. Wherever backfill is

necessary in the construction of the footing, it is recommended that compacted sand and gravel be used so that the frictional resistance may be a maximum. For the development of maximum frictional resistance it is preferable to pour foundations against undisturbed soil. The resistance to passive pressure on the rear face of the foundation is increased by the blast pressure acting on the ground surface at the rear of the building. The increase is determined by assuming a depth of overburden sufficient to cause the same pressure on the ground surface and applying the standard soil-mechanics procedures [6]. The blast pressure on the ground also causes soil pressures to develop on the front face and top surface of the front footings. The pressure on the top of the footings at the front of the building due to the blast pressure on the ground surface is a very important source of resistance to overturning. It may be found necessary in some cases to increase the projection of the footings in front of the building so that a large downward load will be developed along the front wall or column footings. If a building is subject to blast from any direction, it is of course necessary to provide the same footings projection on both the front and rear, and possibly on the ends of the building. The blast pressure on the ground and the projecting footings is identical with that on the wall directly above the footing.

A study of typical foundations based on assumed soil data indicated that (1) if friction equal to or greater than the net lateral force can be developed, the lateral motion of the foundation will be negligible; and (2) if friction alone is not great enough but if friction plus passive pressure equal to or greater than the net lateral force can be developed, the footing motion will be limited to an order of magnitude approximating 4 per cent of the footing depth. To design a foundation by a conservative quasi-static approach so that its lateral motion will be small, it is recommended that the resistance available from passive pressure at any time be made equal to, or greater than, twice the difference between the total lateral load on the footing and the available friction.

In many foundation designs it will be found uneconomical to prevent lateral motion of the structure by providing friction and passive pressures to resist the total lateral dynamic reactions on the footings. In these cases, a dynamic analysis should be performed to determine the magnitude of the footing motion.

REFERENCES

1. MIT Department of Civil and Sanitary Engineering: "Behavior of Structural Elements under Impulsive Loads," June, 1949.
2. Gaston, J. R., C. P. Siess, and N. M. Newmark: An Investigation of the Load-deformation Characteristic of Reinforced Concrete Beams Up to the Point of Failure, *Univ. Illinois Structural Research Ser.*, no. 40, December, 1952.

3. Howland, F. L., and N. M. Newmark: Static Load Deflection Tests of Beam-columns, *Univ. Illinois Civil Eng. Studies, Structural Research Ser.*, no. 65, December, 1953.
4. Ruzik, J. M., K. E. Knudsen, et al.: "Welded Portal Frame Tested to Collapse," Lehigh University, February, 1952.
5. Viest, I. M., C. P. Siess, et al.: Full Scale Test of Channel Shear Connectors and Composite T-beams, *Univ. Illinois Eng. Expt. Sta. Bull.* 405, December, 1952.
6. Taylor, D. W.: "Fundamentals of Soil Mechanics," John Wiley & Sons, Inc., New York, 1948.

CHAPTER 14

EXAMPLES OF BLAST-RESISTANT DESIGN

14.1. General. Two examples are presented of buildings designed to resist a 10-psi blast wave from a small-size atomic bomb (18 to 20 KT). The first example presented is that of a steel-frame one-story building, while the second is a one-story reinforced-concrete shear-wall building. The various steps in the structural design of the one-story steel-frame building are described, and some of the computations are presented for purposes of illustration.

14.2. Single-story Steel-frame Building. As an illustration, the first example presented is that of one bay of a windowless, one-story, rigid-frame building. Figure 14.1 illustrates the cross section and plan view of the building with some of the finally designed sizes indicated.

The arbitrarily selected design overpressure is 10 psi from an 18-KT weapon. Other pressure levels from other sizes of weapons could have been chosen, but the design steps outlined would have been essentially the same.

Other structural arrangements, such as an arch or dome, or a shear-wall type of framing or underground construction could have been used. The proper selection will, of course, be based on a number of considerations (Sec. 13.3).

In this example, it is contemplated that resistant, rather than frangible, walls will be used. One-way reinforced-concrete slabs are used for the roof and walls, while the purlins, columns, and girders are wide-flange structural shapes.

Various steps are involved in the structural design. They are described in the following sections.

a. Loading. The incident-overpressure-vs.-time curve along with the front-face-, rear-face-, net-lateral-, and average-roof-overpressure-vs.-time curves are constructed following procedures outlined in Sec. 11.2a. The results of such computations give the curves of Figs. 14.2 to 14.6.

b. Design of Wall Slabs. All slabs are generally designed for the front-face-overpressure curve since the direction to ground zero is generally uncertain. In this particular case the wall is designed as a one-way reinforced-concrete slab which is permitted to deform into the plastic

region. The pressure-time curve given in Fig. 14.3 is idealized into a triangular load-time curve so that the design coefficients given in Secs. 7.6 and 7.7 may be used. The extent of plastic action permitted is established. In this case an x_m/x_{el} value of 5 is adopted. Based on this, a wall section 11 in. thick with a depth to steel of 9.5 in. is selected. Checks

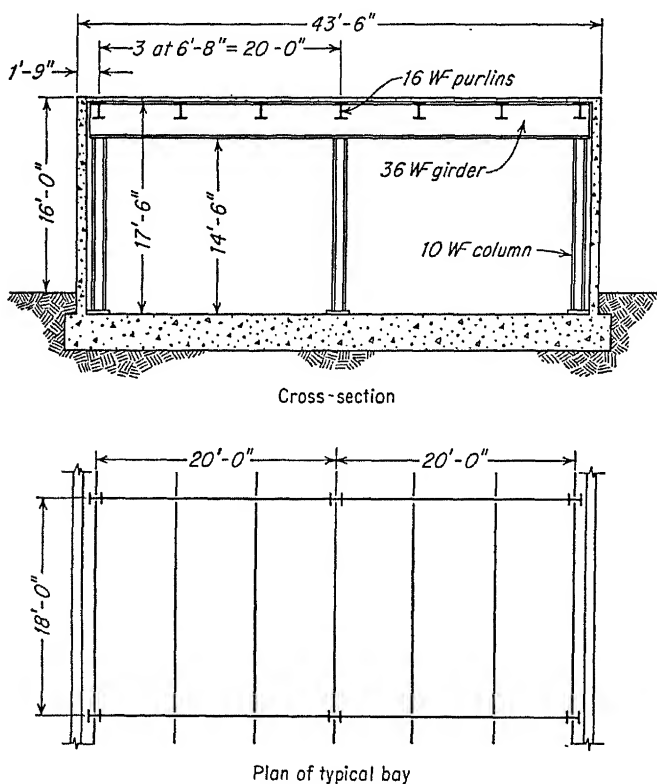


FIG. 14.1. Plan and section of steel-frame building for 10 psi from an 18-KT bomb [Chap. 1, Ref. 8].

on the bond and shear stress are made for selected reinforcing, using dynamic reactions calculated from the formulas of Sec. 7.6. An actual check of the deflection of the element may be made, using the numerical-analysis procedures outlined in Chap. 8.

c. Design of Roof Slab. The roof slab is the next element to be designed. In this case it is designed as a one-way reinforced-concrete slab spanning continuously over purlins located at the third points of the supporting girder. Other structural arrangements could be used.

The slab is permitted to deform into the plastic range, developing plastic hinges at both supports and mid-span.

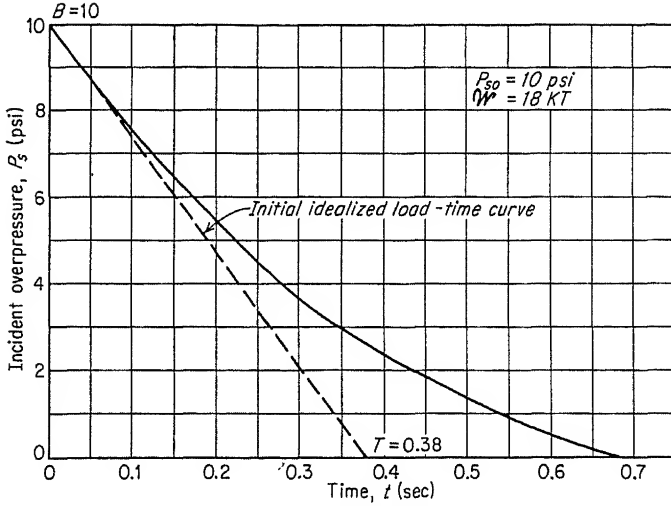


FIG. 14.2. Incident-overpressure-vs.-time curve [Chap. 1, Ref. 8].

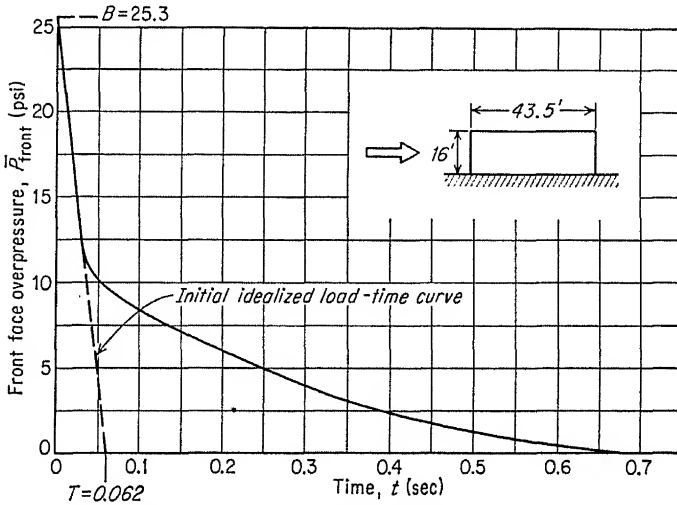


FIG. 14.3. Front-face-overpressure-vs.-time curve [Chap. 1, Ref. 8].

The critical roof-slab loading is the incident-overpressure-vs.-time curve (Fig. 14.2). This loading results from the blast wave moving parallel to the long axes of the rather narrow building. Since the slab is framed perpendicular to the direction of the blast wave, the load is uniformly distributed along each slab span. The individual 1-ft-slab elements along the purlin reach their maximum deflections at different times; however, they provide little restraint to adjacent elements, and this effect

is neglected. The roof loading for a blast wave moving perpendicularly to the long axis of this building would be less.

The blast-loading curve of Fig. 14.2 is idealized to a triangular load of 10 psi peak value and a duration of 0.38 sec.

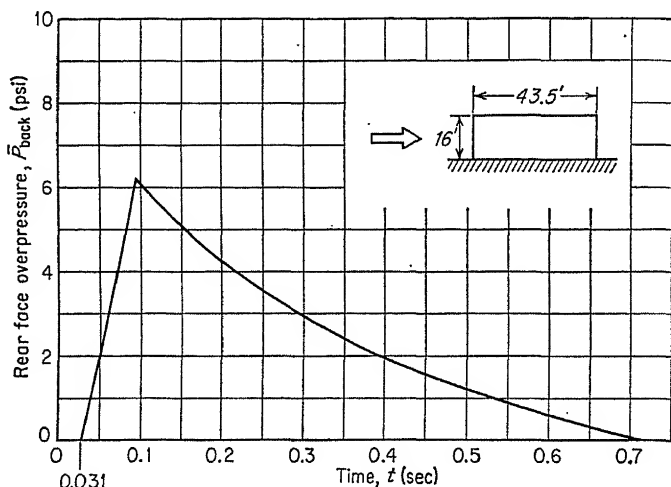


FIG. 14.4. Rear-face-overpressure-vs.-time curve [Chap. 1, Ref. 8].

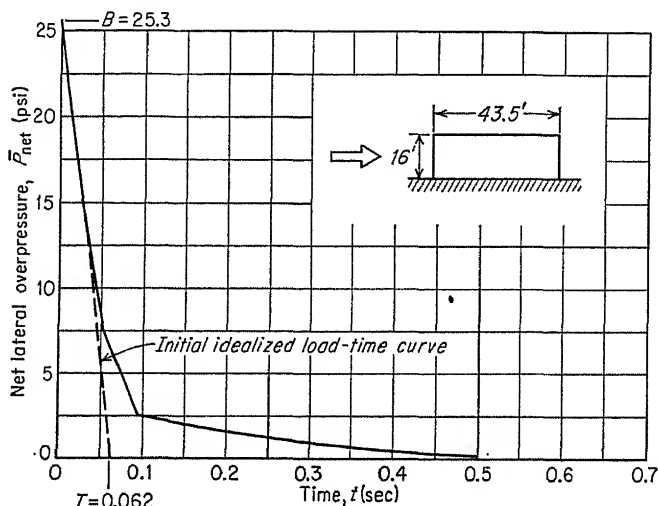


FIG. 14.5. Net-lateral-overpressure-vs.-time curve [Chap. 1, Ref. 8].

Following the dynamic-design procedure of Sec. 7.3, a slab thickness of $3\frac{3}{4}$ in. is determined. A numerical-integration procedure is used then to actually determine the reactions of the slab for use in the next design step.

d. Design of Roof Purlins. The purlins are framed flush with the tops of the girders and are provided with moment-resisting connections to the girders. Connectors attached to the top flanges of the purlins are imbedded in the concrete slab to provide lateral support to the top compression flange and to prevent separation of the slab from the purlins during reversals in stress.

The purlins are designed for plastic behavior so that plastic hinges are developed at mid-span and at the supports, with an x_m/x_{el} of 6 allowed.

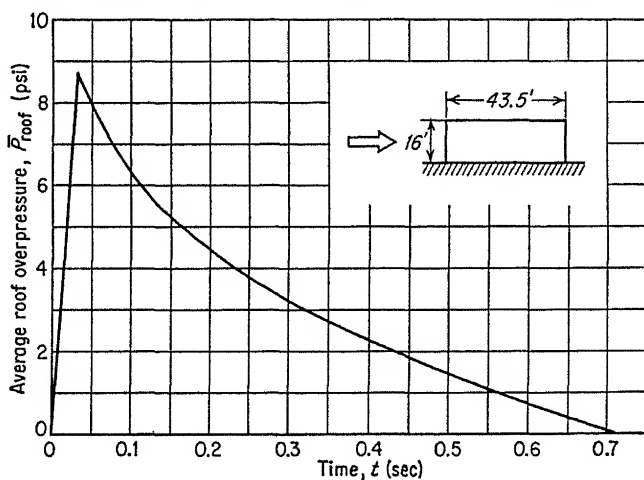


FIG. 14.6. Average roof overpressure vs. time curve [Chap. 1, Ref. 8].

The loading for the purlins is a little more complicated than in previous cases.

For the blast wave moving normal to the long axis of the building, and thus normal to the axis of the purlin, the loading may be considered to be uniformly distributed along the length of the purlin. For this condition the pressure-vs.-time variation at each point along the roof is a function of its position. In addition, the load on a purlin is a function of the length of the slab spans because the load on the purlin builds up to a maximum value in the time required for the blast wave to traverse the two adjoining slabs. In the preliminary design of the purlins the design load is the simplest form of the roof load obtained from the incident-overpressure-vs.-time curve. The rise time, slab dynamic reactions, and local variation are all neglected in this preliminary step.

For the blast wave moving parallel to the long axis of the building, and thus parallel to the axis of the purlin, the load varies along the span as a result of the time required for the blast wave to traverse the purlin span. At any point along the purlin the time variation of the load is the same and defined by the incident-overpressure-vs.-time curve.

The local overpressures on the roof are plotted for the middle third points of the purlin in Fig. 14.7, following procedures of Chap. 11.

The roof slab is analyzed for the local overpressure curves of Fig. 14.7,

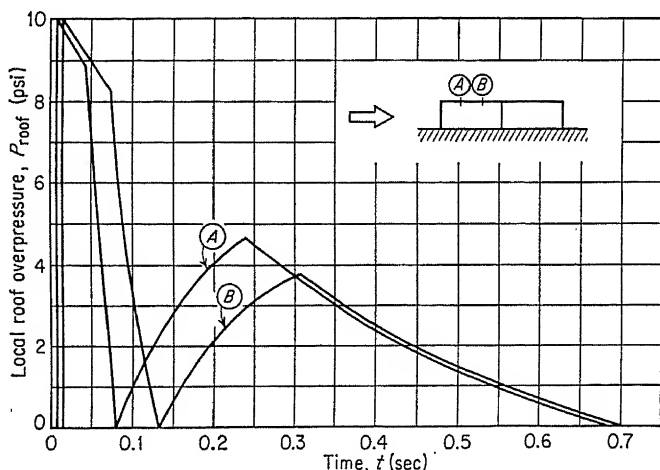


FIG. 14.7. Local roof overpressure for purlin [Chap. 1, Ref. 8].

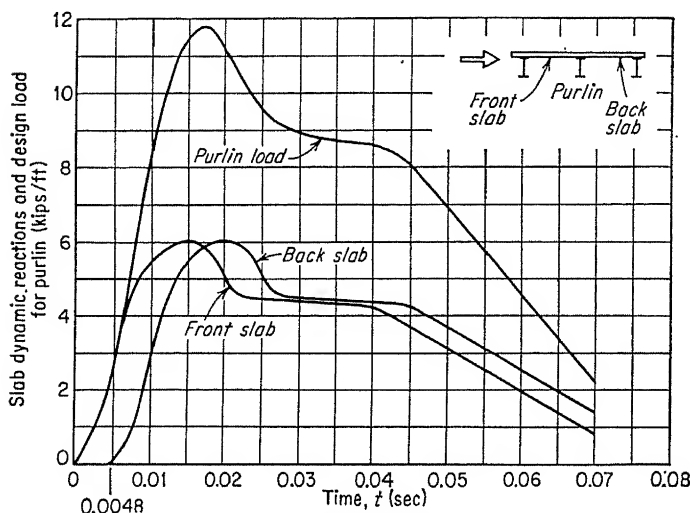


FIG. 14.8. Dynamic reactions of roof slab [Chap. 1, Ref. 8].

and the reactions are plotted in Fig. 14.8 and combined to give the purlin load.

Based on these loads a purlin is selected following the dynamic-design procedures of Sec. 7.3, allowing plastic deformation with a deflection ratio x_m/x_{el} of 6. Based on these criteria a 16WF36 purlin is selected.

e. Preliminary Column Design. A single-story frame subject to lateral load behaves essentially as a single-degree-of-freedom system if the load is applied at the level of the girder. The columns act as the spring in the dynamic system. It is therefore unnecessary to substitute an equivalent system for the original structure, and the mass and load factors (Chap. 7) which are necessary in the design of beams and slabs are not used in the design of single-story frames.

For purposes of preliminary design the frame girders are assumed to be infinitely rigid, thus simplifying the determination of the column spring constant. It is desirable that the energy-absorption capacity of the columns be greater than the work done to provide an allowance for factors which are neglected in preliminary design. These factors include (1) the effect of direct stress on the plastic-hinge moment, (2) the effect of lateral deflection of the column on its resistance, and (3) effect of girder flexibility.

The design lateral load on the frame is obtained from the dynamic reactions at the top of the front wall minus the reactions of the rear-wall slab if they are important at the proper time. However, for preliminary-design computations it is satisfactory to use the net-lateral-overpressure curve of Fig. 14.5. The net lateral load applied to the walls is assumed to be divided equally between the foundation at the base of the walls and the frame at the top. This results in a conservative load for the frame since the dynamic-reaction equations for the wall slab result in footing reactions that are larger than the roof reactions.

The design load may be idealized as shown in Fig. 14.5 so that the design charts of Chap. 7 may be used. The mass used in the dynamic calculation includes the total roof-system mass plus one-third (mass of columns plus walls).

Plastic deformation of the columns is permitted with a deflection ratio x_m/x_{el} of 12 allowed. A column section is selected and tested for adequacy, and then checked to see that it satisfies allowable shear stresses, local-buckling criteria (Sec. 1.4c), and the slenderness criteria for beam-columns (Sec. 1.4d).

f. Design of Roof Girder. The girder is designed for elastic behavior, even though the rest of the structure is permitted to undergo plastic deformation. This is desirable since the lateral strength of the frame depends upon restraint at the tops of the columns. If plastic hinges were formed in the girders because of vertical loads, these members probably would not provide the restraint necessary for the columns to carry lateral loads at the same time.

The preliminary column design which was mentioned in the section above revealed that the plastic moment in the columns at the upper ends would be approximately 318 kip-ft. The purlins have been previously

designed, and the dynamic reactions determined by numerical integration. From the latter it was concluded that the blast load on the girder by the two purlins in one girder span could be idealized as shown in Fig. 14.9. The total dead reaction from the same two purlins is 15.3 kips.

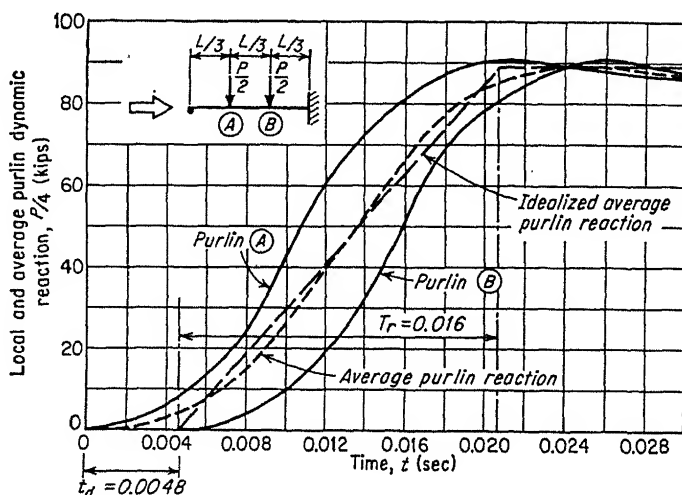


FIG. 14.9. Design blast load for girder [Chap. 1, Ref. 8].

Thus the total stress in the girder is the sum of three effects:

1. The static purlin reactions and the weight of the girder itself
2. The dynamic purlin reactions
3. The dynamic moments introduced by the columns and caused by the lateral blast loads

The design criteria are that the total stress due to the maximum moment which occurs at the center column shall equal the dynamic yield stress of 41.6 ksi. The computations are given in some detail below.

Since the two spans of the girder are loaded almost simultaneously, and since the exterior columns are relatively slender, it is permissible to consider each span as a beam fixed at one end and pinned at the other. Referring to Table 7.3 we obtain the following factors:

For the concentrated mass and loads,

$$K_L = 0.81 \quad K_M = 0.67 \quad R_m = \frac{6M_P}{L} \quad k = \frac{132EI}{L^3}$$

For the uniform mass,

$$K_M = 0.45$$

A preliminary-design trial indicates that a 33WF160 section might be satisfactory. We shall proceed to check the adequacy of this selection.

33WF160:

$$I = 9,739 \text{ in.}^4$$

$$S = 541 \text{ in.}^3$$

$$M_P = 1.05 f_{dy} S = (1.05)(41.6)(541/2) = 1,970 \text{ kip-ft}$$

$$k = \frac{132EI}{L^3} = \frac{(132)(30,000)(9,739)}{(20)^3(144)} = 33,300 \text{ kips/ft}$$

$$\text{Concentrated mass} = \frac{15.3}{32.2} = 0.475 \text{ kip-sec}^2/\text{ft}$$

$$\text{Uniform mass} = \frac{(0.16)(20)}{32.2} (1.15 \text{ for details}) = 0.114 \text{ kip-sec}^2/\text{ft}$$

$$\begin{aligned} \text{Total equivalent mass} &= m_{te} = (0.475)(0.67) + (0.114)(0.45) \\ &= 0.37 \text{ kip-sec}^2/\text{ft} \end{aligned}$$

$$k_e = (33,300)(0.81) = 27,000 \text{ kips/ft}$$

$$T_n = 2\pi \sqrt{\frac{m_{te}}{k_e}} = 2\pi \sqrt{\frac{0.37}{27,000}} = 0.0232 \text{ sec}$$

$$\frac{T_r}{T_n} = \frac{0.016}{0.0232} = 0.69$$

From Fig. 7.13,

$$\text{DLF}_{\max} = 1.38$$

Maximum moment at center column due to dynamic

$$\begin{aligned} \text{purlin reactions} &= \text{DLF} \left(\frac{PL}{6} \right) = \frac{(1.38)(356)(20)}{6} \\ &= 1,640 \text{ kip-ft} \end{aligned}$$

$$\begin{aligned} \text{Moment due to concentrated dead loads} &= \frac{(15.3)(20)}{6} \\ &= 51 \text{ kip-ft} \end{aligned}$$

$$\text{Moment due to distributed dead load} = \frac{(0.16)(20)^2}{8} (1.15) = 9 \text{ kip-ft}$$

Moment due to plastic moment in column

$$= \frac{1}{2}(M_P)_{\text{col}} = \frac{1}{2}(1,970) = 985 \text{ kip-ft}$$

$$\text{Total moment} = 1,859 \text{ kip-ft} < 1,970 \quad \therefore \text{OK}$$

Thus the section is adequate for bending moment. In order to check the shear we must compute the maximum dynamic reaction.

From Fig. 7.13 we note that $t_m/T_r = 1.19$; thus t_m is equal to 0.016×1.19 , or 0.019 sec. Since t_m is greater than T_r , the maximum resistance and maximum load occur simultaneously and the two should be combined for maximum dynamic reaction. From Table 7.3

$$V_2 = 0.33R + 0.33P$$

where V_2 = shear due to dynamic load

$$R = 1.38P$$

$$\text{Thus,} \quad V_2 = (0.33)(1.38)(356) + (0.33)(356) = 280 \text{ kips}$$

The shear due to dead load is 12 kips and the shear due to the lateral blast load on the frame is 48 kips. Thus the total shear-stress intensity is

$$v = \frac{V}{A_w} = \frac{340}{(36)(0.653)} = 14.5 \text{ ksi} < 21 \quad \therefore \text{OK}$$

We must now check the possibility of local buckling according to the criteria of Sec. 1.4c. When the design is completely elastic the conventional width-thickness requirements are adequate. However, in this

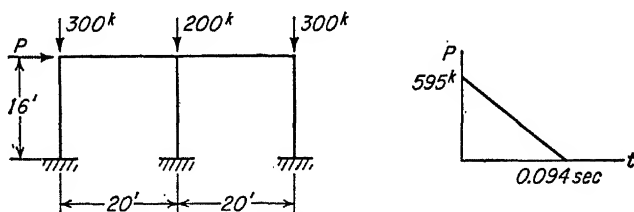


FIG. 14.10. Loading for column design.

case, we anticipate the development of the full plastic resisting moment at the center column. Since this requires some plastic redistribution of stress on the cross section, the requirements of Sec. 1.4c should be followed in this region.

$$\frac{b}{t_f} = \frac{12}{1.02} = 11.8 < 17 \quad \therefore \text{OK}$$

$$\frac{a}{t_w} = \frac{33.96}{0.653} = 52 < 70 \quad \therefore \text{OK}$$

g. Final Column Design. The preliminary column design of Sec. 14.2e above may at this time be defined to account for the variation of plastic-hinge moment with direct stress, the variation of column resistance with lateral deflection, the effect of girder flexibility on the stiffness of the columns, and the difference between the load on the wall slab and the dynamic reactions from the wall, which are used as the lateral design load for the frame columns.

The final design of the columns should be done by numerical integration because of the variety of time-varying loads involved. However, we shall limit our discussion to an approximate solution based on the curves of Chap. 7, which are often adequate for practical purposes.

The horizontal load is equal to the dynamic reaction at the top of the side walls. The analysis of these elements indicates that the frame load may be idealized as shown in Fig. 14.10. The vertical-column loads are the dead and dynamic reactions of the girders. For this approximate analysis it may be assumed that these loads are constant as shown in Fig. 14.10. It is also assumed that the three column loads are equal.

This simplifies the analysis since it enables us to consider only the total lateral resistance of the frame rather than that of the three columns separately. It does not introduce serious error since the resulting decrease in the resistance of the exterior columns is essentially balanced by the increase for the interior columns. All these columns are of the same cross section. The permissible lateral deflection of the frame is taken between 1.25 and 1.50 ft, which implies considerable plastic deformation.

The mass of the equivalent one-degree system taken as the total mass at the roof level plus one-third the mass of the walls and columns is equal to 2.64 kip-sec/ft. In order to determine the spring constant the lateral deflection at the top of the frame due to a unit load at the same point is computed by conventional methods. The spring constant is thus computed to be 815 kips/ft. The detailed computations for the maximum frame deflection follow:

$$\text{Assume } C_R = 0.2 \quad \text{Required } R = 0.2 \times 595 = 119 \text{ kips}$$

The total resistance when plastic hinges have been formed at both ends of all three columns is equal to $3(2M_D/h)$, where M_D is the maximum moment, taking into account direct stress. The height of column h is taken as the clear height to the bottom of the girder, or 14.5 ft. Thus,

$$\text{Required } M_D = \frac{Rh}{6} = \frac{(119)(14.5)}{6} = 287 \text{ kip-ft}$$

Try 10WF77:

$$\begin{aligned} S &= 86.1 \text{ in.}^3 \\ I &= 457.2 \text{ in.}^4 \\ A &= 22.67 \text{ in.}^2 \end{aligned}$$

Check for local buckling according to Sec. 1.5a:

$$\begin{aligned} \frac{a}{t_w} &= \frac{8.89}{0.535} = 16.6 < 43 & \therefore \text{OK} \\ \frac{b}{t_f} &= \frac{10.195}{0.868} = 11.75 < 17 & \therefore \text{OK} \end{aligned}$$

Compute M_D according to Sec. 1.6a:

$$\begin{aligned} M_P &= (1.05)(41.6) \left(\frac{86.1}{12} \right) = 314 \text{ kip-ft} \\ P_P &= (41.6)(22.67) = 945 \text{ kips} \end{aligned}$$

$$\text{Eq. (1.14), } M_1 = 296 \text{ kips}$$

$$\text{Eq. (1.15), } P_1 = 175 \text{ kips}$$

$$\text{Eq. (1.17), } M_D = 314 - {}^{300}_{175}(314 - 296) = 283 \text{ kip-ft} \quad \therefore \text{OK}$$

Now, check the original assumptions for C_R by an analysis of the equivalent system. Note that the load and mass factors are both unity.

$$R_{me} = \frac{6M_D}{h} = \frac{(6)(283)}{14.5} = 117 \text{ kips}$$

$$x_{el} = \frac{R_{me}}{k_e} = \frac{117}{815} = 0.144 \text{ ft}$$

$$T_n = 2\pi \sqrt{\frac{m_{te}}{k_e}} = 2\pi \sqrt{\frac{2.64}{815}} = 0.36 \text{ sec}$$

$$\frac{T}{T_n} = \frac{0.094}{0.360} = 0.26 \quad C_R = \frac{117}{595} = 0.197$$

From Fig. 7.11,

$$\frac{x_m}{x_{el}} = 8.0$$

$$x_m = (8.0)(0.144) = 1.15 \text{ ft} \quad \therefore \text{OK}$$

Having satisfied the deflection criteria, we should now check the possibility of lateral-torsional buckling of the columns. Using Eq. (1.18) and Tables 1.1 and 1.2,

$$\frac{K' L d}{100 b t_f} = \frac{(0.14)(14.5)(12)(10.62)}{(100)(10.195)(0.868)} = 0.292$$

$$\frac{K'' L}{15 r} = \frac{(0.50)(14.5)(12)}{(15)(2.60)} = 2.23$$

Note that the columns are assumed to be fully fixed in both directions at both ends.

$$283\%_{14}(0.292) + 30\%_{45}(2.23) = 0.98 < 1 \quad \therefore \text{OK}$$

Thus the 10WF77 columns are completely satisfactory by this approximate analysis.

As mentioned previously, the column design in some cases should be finally checked by numerical integration. This would differ from the above approximate analysis in the following aspects:

1. In each time interval the horizontal load on the frame is taken as the actual dynamic reaction from the side walls rather than the idealized value.

2. The time-varying dynamic reaction from the purlins is used rather than the constant value assumed above.

3. The buckling criteria [Eq. (1.18)] are checked at each time interval to ensure that the left side of the equation at no time exceeds unity.

4. The effect of the moment caused by the horizontal movement of the points of application of the vertical loads is taken into account. As these loads move they produce a sidesway effect, which augments the

lateral deflection due to the horizontal blast force. In effect, the resistance of the frame is reduced by an amount equal to Fx/h , where F is the total vertical load. This is an appreciable effect, and for this reason the approximate analysis probably underestimates the lateral deflection.

h. Frame Connections. The connections form an important part of any structural design. This is particularly true under dynamic loads because of the uncertainties regarding stress concentrations. It is also significant that the material in connections tends to be more brittle than that in the body of the member. Allowable stresses for connection material is given in Sec. 1.7. It is recommended that connections be designed conservatively.

No new analysis is required for connection design since the gross forces are simply those at the end of the connected members. Referring to the frame design given above, the column-girder connection and the column-base detail are both designed for the maximum bending moment and direct stress carried by the columns. This frame design anticipated the formation of plastic hinges at both ends of the columns, and the question is raised as to whether the hinge forms in the connection or in the body of the member. However, the ductility of the connection is questionable because the stress paths are not straight, the stress distribution is uncertain, and the quality of the welds cannot be completely controlled. For this reason, and because the frame design requires considerable ductility, it is recommended that the connection be made slightly stronger than the member itself. Thus the plastic hinge will form in the member itself where the desired ductile behavior is more certain.

Figures 14.11 and 14.12 show welded details which were designed for the building frame under discussion. As in conventional design welded connections are more easily adapted to rigid-frame construction than are riveted or bolted details. Actually, the details shown are little different from those that would be used in conventional design, and no unusual problems are encountered.

Since ultimate-strength theory is used for both connection and member, the capacity of the former is little more than would be required to connect the same members in a conventional structure.

i. Design of Foundation. The design of a foundation is subject to a number of uncertainties: first, the dynamic capacity of soils is very uncertain; second, the dynamic problem is sufficiently complex so that extensive calculations are required, making it almost an impractical design procedure. Because of this uncertainty regarding soil strengths and the complexity of an accurate dynamic analysis, a quasi-static-analysis procedure has been evolved (Sec. 13.7). The first requirement of the quasi-static analysis is a tabulation of all the lateral and vertical loads on the foundation. To assist in this tabulation a preliminary plan of one bay

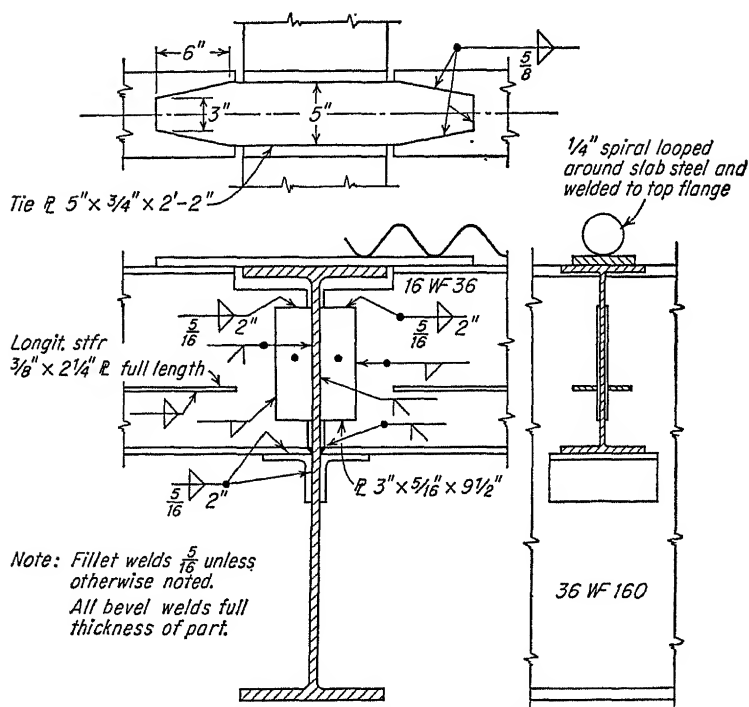


FIG. 14.11. Purlin-to-girder connection [Chap. 1, Ref. 8].

of the foundation is prepared as indicated in Fig. 14.13. The locations of the forces on the foundation are shown in Fig. 14.14. The vertical loads include the column and footing blast loads and the dead load of the entire structure. The front-wall-footing projection is subjected to vertical blast forces (front-face overpressure) and assists the foundation to resist overturning. The total load on all these columns is given in Fig. 14.15, and Fig. 14.16 presents the sum of the total column load and the blast load on the front-footing projection.

The lateral loads on the footing include the shear in the columns and the front- and rear-wall-slab reactions at the wall footings. The total lateral load is given in Fig. 14.17.

Based on the above loads the footing-plan size is determined. The required plan area is determined by using the dynamic-design-bearing capacity of the soil.

The size of the wall footing is determined using the maximum value of the blast load on the footing projection and adding to it the dead load of the wall and the overburden.

The depth of the foundation is set by first determining the unbalanced lateral load, determined by subtracting the available frictional force

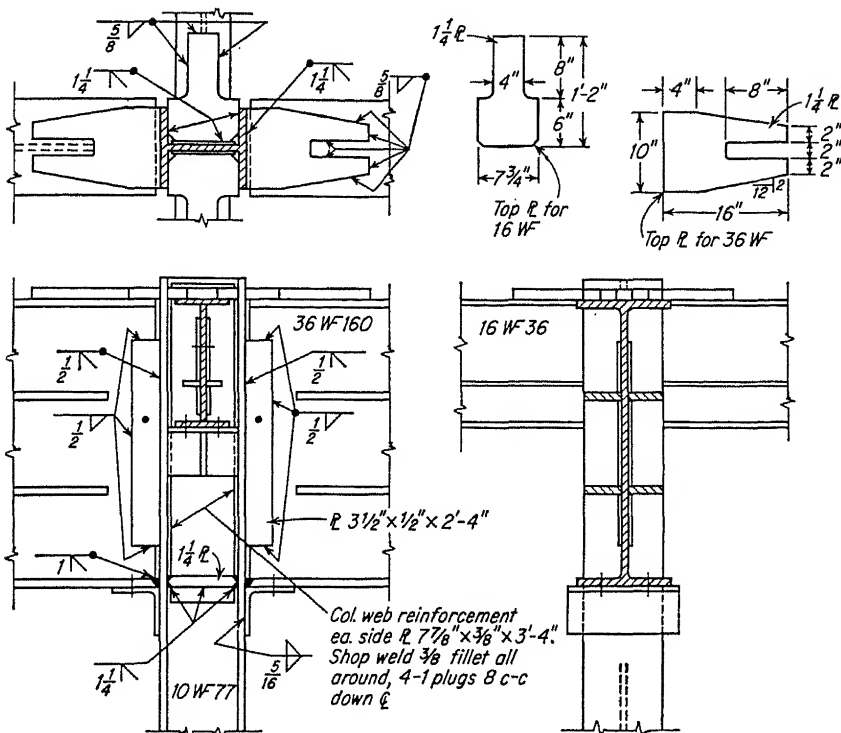


FIG. 14.12. Girder-to-column connection [Chap. 1, Ref. 8].

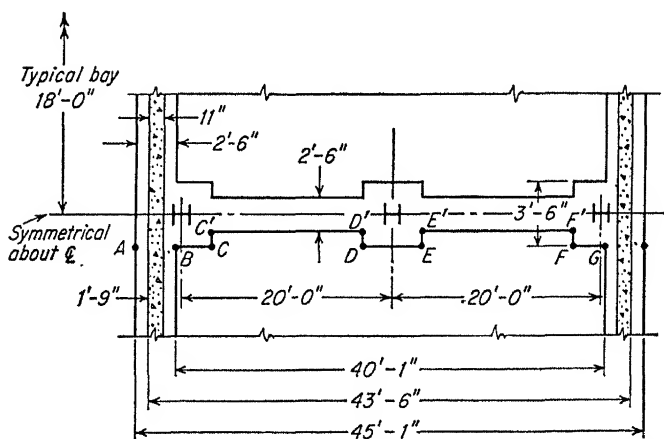


FIG. 14.13. Preliminary foundation plan for one bay [Chap. 1, Ref. 8].

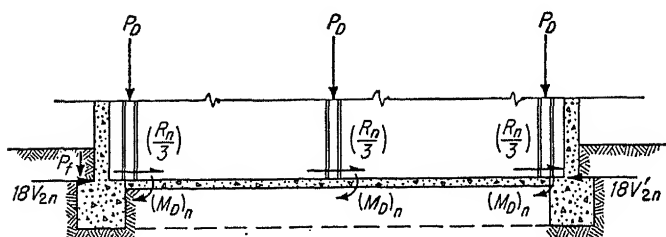


FIG. 14.14. Force on foundation [Chap. 1, Ref. 8].

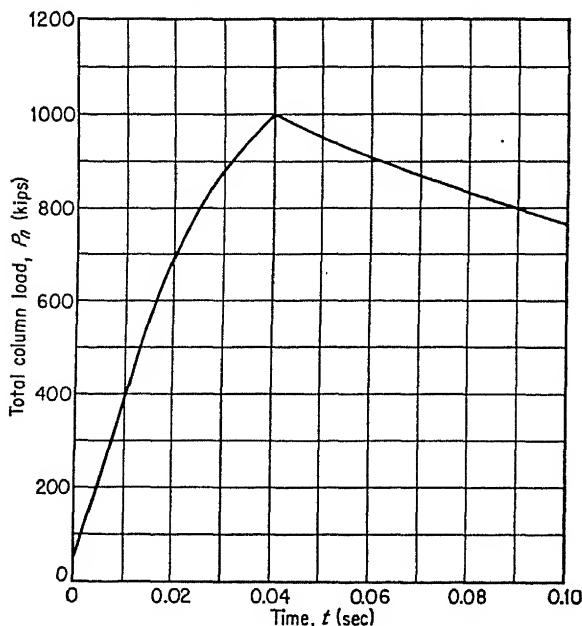


FIG. 14.15. Total column load [Chap. 1, Ref. 8].

from the total lateral load. Figure 14.17 gives the total lateral load, and from this is subtracted the frictional resistance to sliding. (Frictional resistance to sliding equals total vertical load times friction coefficient.) The total vertical load includes the dead load of the structure.

The procedure of Sec. 13.7 requires that the depth of footing be that necessary to develop sufficient passive-pressure resistance to equal twice the unbalanced lateral load at any time.

The foundation is checked for adequacy against overturning. Figure 14.18 illustrates the load positions which are active in this case. The overturning moment is determined as a function of time and combined with the total vertical forces to determine whether the allowable dynamic soil stresses are exceeded. Following the above, the structural elements of the foundation are designed by conventional procedures.

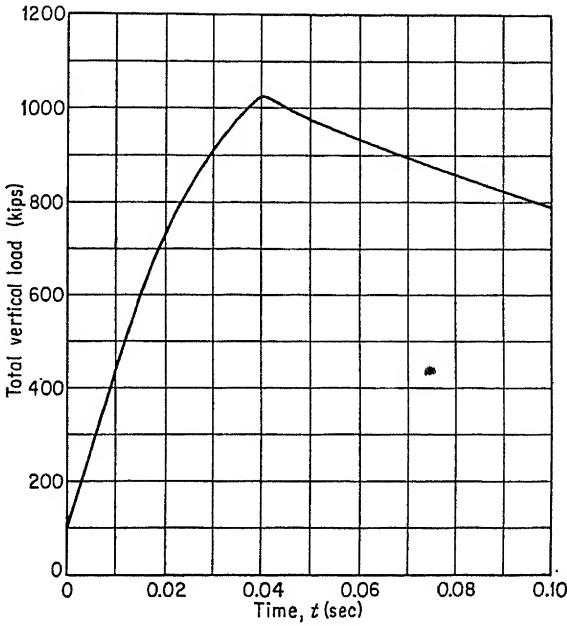


FIG. 14.16. Total vertical load on footing [Chap. 1, Ref. 8].

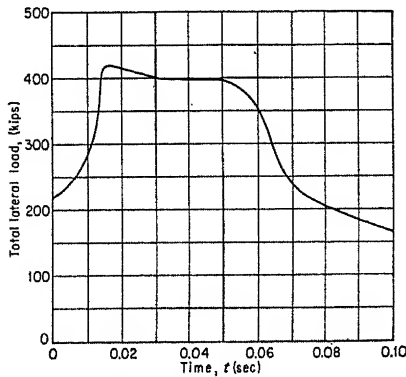


FIG. 14.17. Total lateral load on footing [Chap. 1, Ref. 8].

14.3. Single-story Reinforced-concrete Shear-wall Building. This section presents illustrations of portions of the design of a windowless one-story reinforced-concrete shear-wall building designed to resist a peak air-blast pressure of 10 psi from a 20-KT atomic-bomb burst. The steps in design are similar to those described in Sec. 14.2, except for the manner of handling the shear wall.

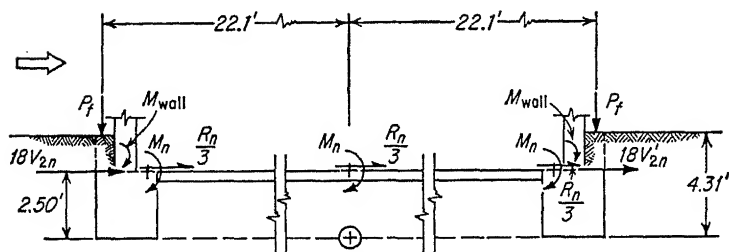


FIG. 14.18. Overturning forces [Chap. 1, Ref. 8].

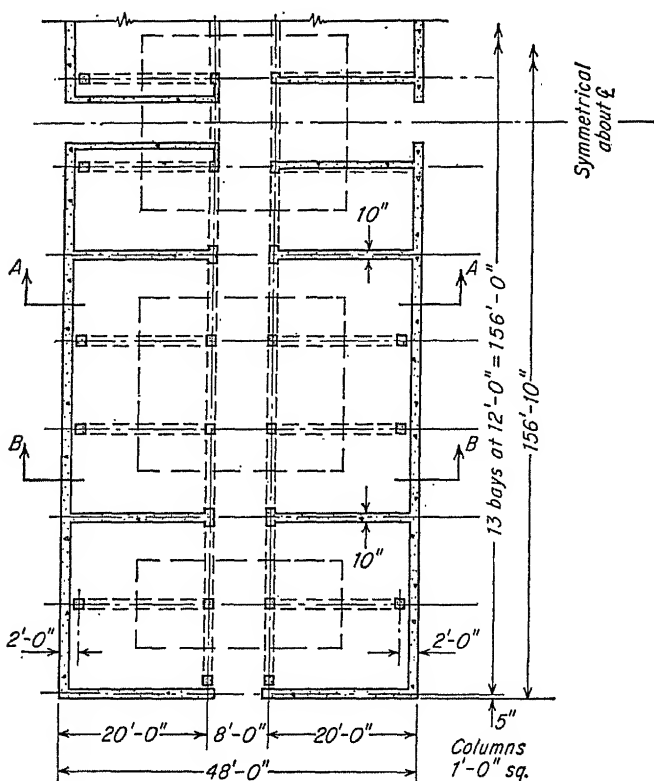


FIG. 14.19. Plan of one-story reinforced-concrete shear-wall building [Chap. 1, Ref. 8].

Figure 14.19 illustrates the plan of the building showing locations of shear wall. The columns are used to carry vertical load only. Sections of the building and also a partial foundation plan are indicated in Fig. 14.20.

The properties of various sections of the building have been designed for locations as indicated in Fig. 14.21.

The various sections A-A to E-E are indicated in Figs. 14.22 to 14.26.

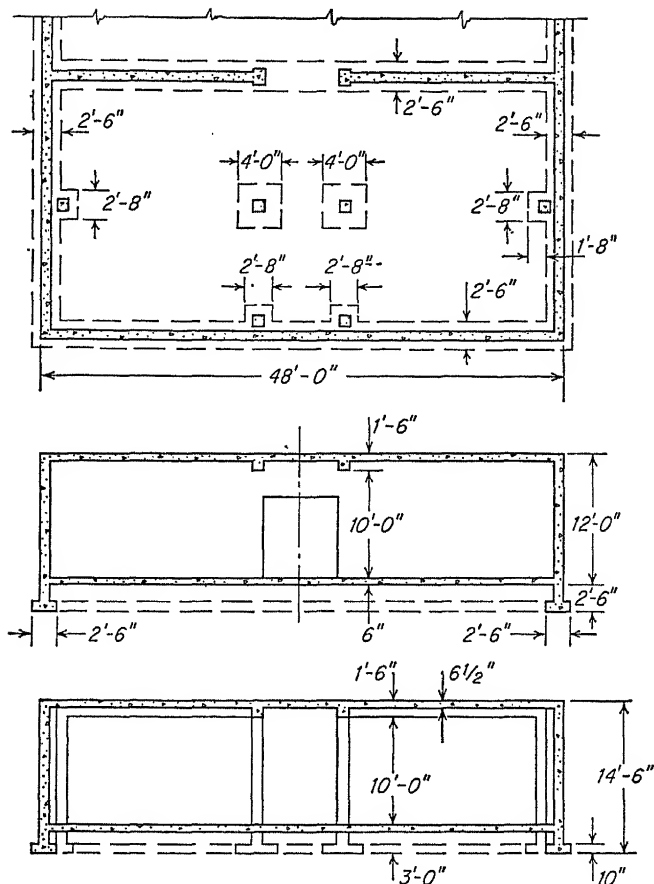


FIG. 14.20. Foundation plan and section of building [Chap. 1, Ref. 8].

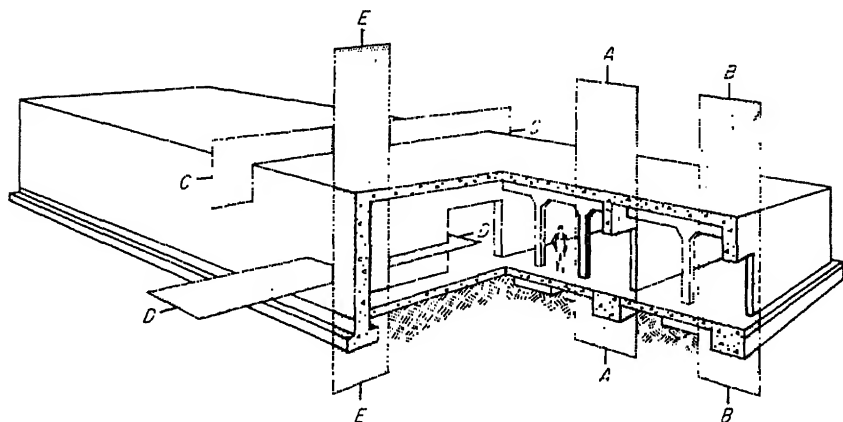
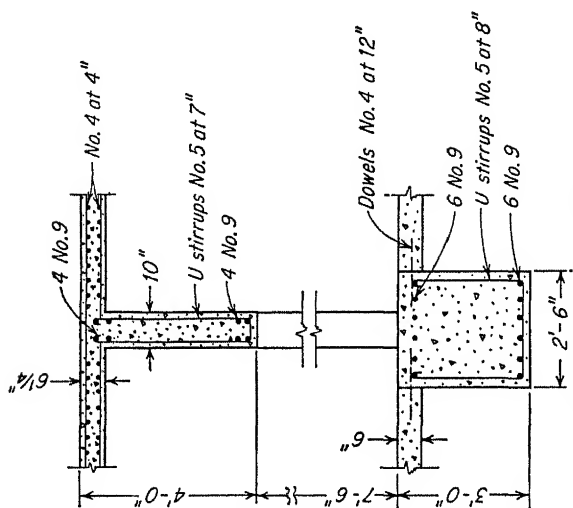
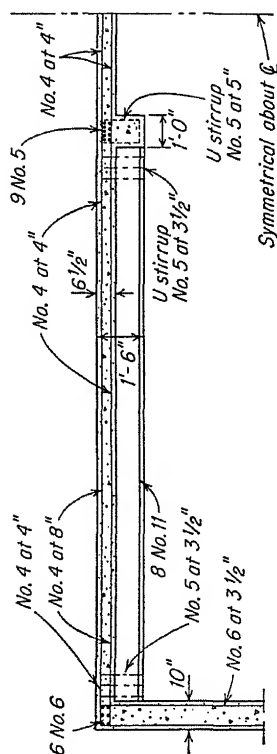
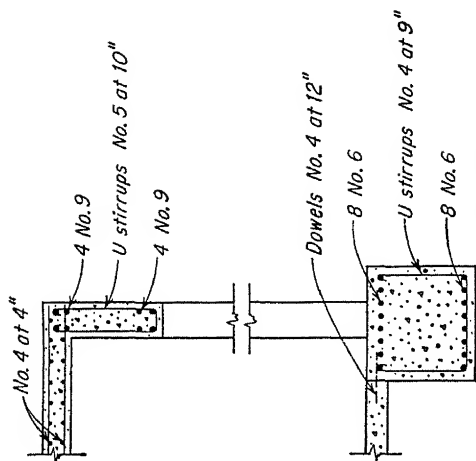


FIG. 14.21. Perspective showing locations of designed sections [Chap. 1, Ref. 8].



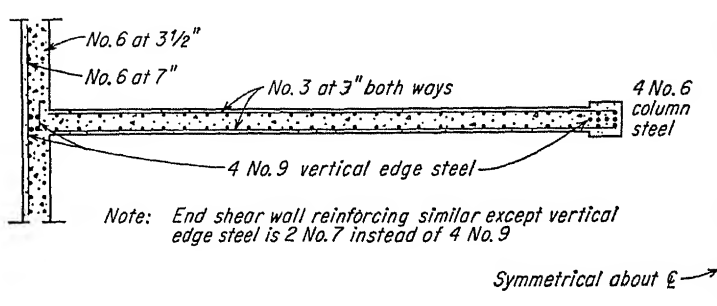


FIG. 14.25. Section D-D [Chap. 1, Ref. 8].

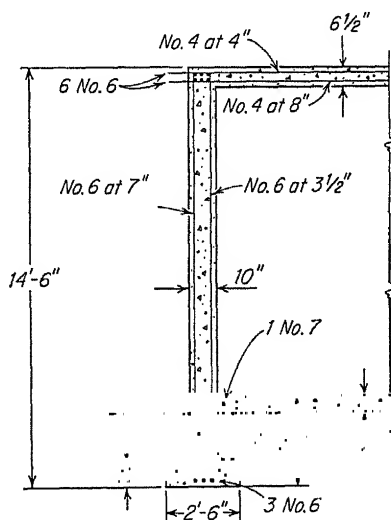


FIG. 14.26. Section E-E [Chap. 1, Ref. 8].

CHAPTER 15

DISCUSSION OF LABORATORY AND THEORETICAL DEVELOPMENTS FOR IMPROVED BLAST-RESISTANT DESIGN

15.1. Introduction. Three general areas of information relating to blast-resistant design have been developed in the past ten years by theoretical and laboratory investigations. These areas have included blast loads on buildings by means of shock tubes, static and dynamic properties of structural elements by laboratory investigations using specially devised loading machines, and theoretical developments of dynamic-analysis and -design procedures. Many investigators have participated in these developments, a number under the sponsorship of government agencies and some under private sponsorship.

15.2. Laboratory Studies of Blast Loading. The important problem of predicting the time character of dynamic loading on a structure, given the initial peak overpressure and the duration and shape of the positive and negative phases of the blast wave, can be approached in four ways: the laboratory shock tube, theoretical analysis, the use of high-explosive charges to develop blast waves, and lastly, the full-scale nuclear test. The principal developments have been made, however, in the laboratory shock tube, with additional investigations using high-explosive charges, both results being confirmed by the relatively full-scale nuclear tests in Nevada and at the Pacific Proving Grounds.

Pioneering in the shock-tube studies were the group at Princeton University under the leadership of Professor Walker Bleakney and the group at the Ballistics Research Laboratory, Aberdeen Proving Grounds, under Dr. Curtis Lampson. The field of investigators expanded to include groups at the University of Michigan, Armour Research Foundation, Massachusetts Institute of Technology, and others.

The shock tube is admirably suited to studies of this nature, although it has some disadvantages. On the plus side, it provides a laboratory-controlled method for obtaining shock waves of desired peak pressures in a relatively inexpensive manner. These shock waves may be imposed on structural models of arbitrary shapes but of limited dimensions. Accurate pressure-time measurements can be made on each face of the model.

Disadvantages of the shock tube relate to the following: limited control of the shape of the pressure pulse following the initial peak; limited duration of pressure pulse, particularly as higher peak pressures are used; limited time of observation due to reflections from sides of shock tube; limited peak pressures. However, despite these disadvantages it has been an extremely powerful tool.

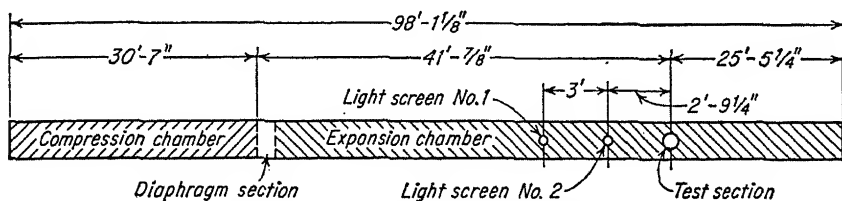


FIG. 15.1. MIT shock-tube dimensions.

The shock tube may consist of a straight tube of arbitrary but generally of uniform cross section separated into high- and low-pressure portions by a diaphragm. Figure 15.1 illustrates the dimensions of the MIT shock tube which was constructed under Air Force sponsorship (Contract AF33-038-8906). Bursting of the diaphragm permits the propagation of first a compression wave into the low-pressure region and a rarefaction

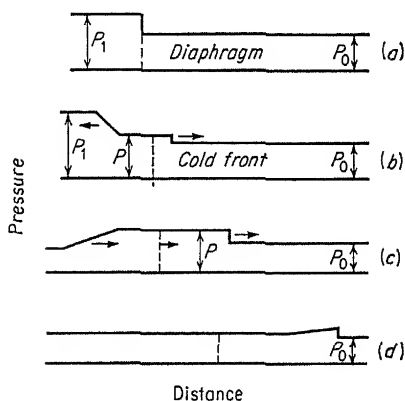


FIG. 15.2. Pressure distribution in shock tube at different times.

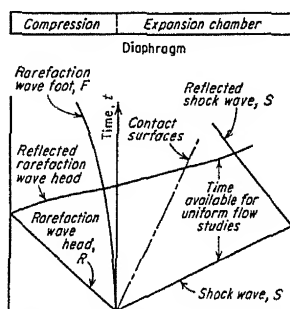


FIG. 15.3. X-T diagram of shock-tube wave motion in a finite tube.

wave into the high-pressure region. The compression wave rapidly becomes a shock wave as it progresses down the tube. Figure 15.2, drawn from Ref. 15.1, indicates diagrammatically the propagation of the pressure and rarefaction waves. The interaction of the rarefaction wave with the closed high-pressure end of the tube and the compression wave with the closed or open low-pressure end of the tube will cause reflections which will eventually alter the character of the shock front. However,

prior to this time there will exist for a short period of time stable flow conditions at the test section. Figure 15.3 illustrates the shock-tube wave motion.

For the purpose of studying the force-time characteristics of the loading on the various faces of a structure, nondeformable models of proper size may be inserted in the test section of the shock tube. Pressure measurements may be made using very small pressure gauges made of quartz crystals,

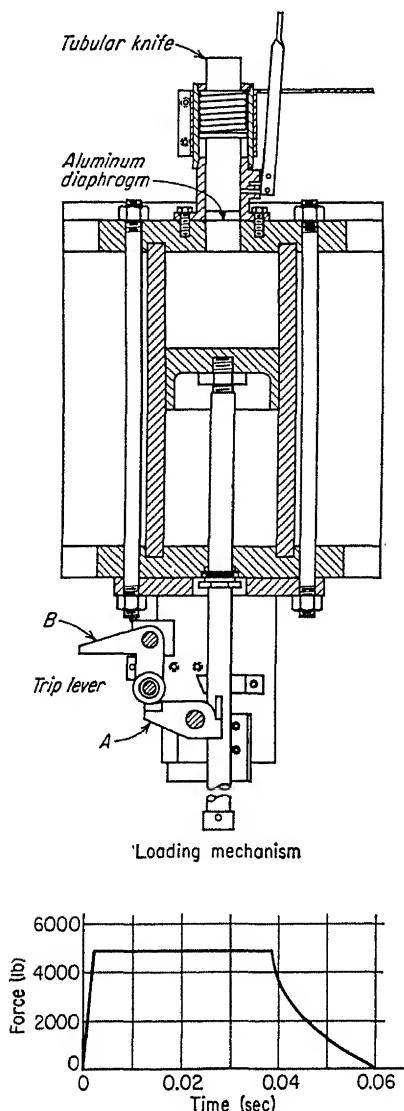


FIG. 15.4. MIT rapid-load machine-loading mechanism and typical load-time curve.

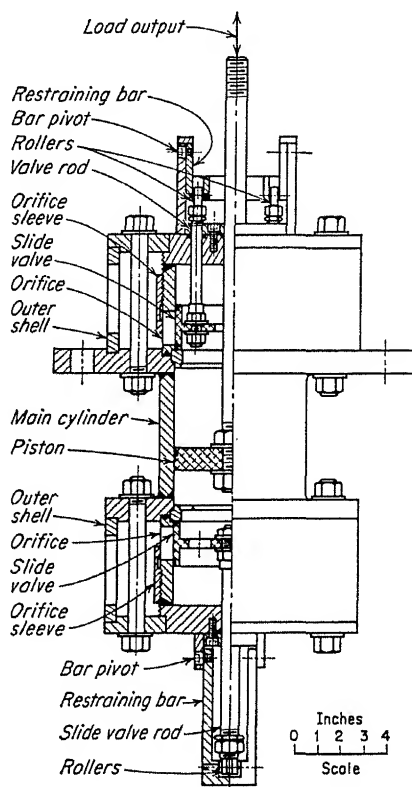


FIG. 15.5. University of Illinois pulse loading machine.

barium titanate, or other types of transducers, or by the use of the optical interferometer, which will determine the density of the air, and accordingly may be used to determine pressure distributions.

Many reports have been published [2-14] on the diffraction of shock waves around two- and three-dimensional objects and have served as a partial basis for the loading equations presented in Chap. 11.

15.3. Strength Properties of Structural Elements. As in the case of the blast-loading problem extensive investigations of both the static- and dynamic-strength properties of structural elements have been conducted under the sponsorship of various government agencies and private organizations. Properties of materials, steel and concrete, and structural elements of steel and reinforced concrete have been determined at a number of institutions, the Bureau of Standards, California Institute of Technology, Lehigh University, Stanford University, the University of Illinois, and the Massachusetts Institute of Technology, as well as at other locations.

Preliminary work on the dynamic behavior of reinforced-concrete beams under impact was conducted by Richart and Newmark during World War II [15-17]. Following the advent of the atomic bomb the Massachusetts Institute of Technology under contract to the Corps of Engineers conducted an extensive study of the behavior of reinforced-concrete elements under dynamic loads. Figure 15.4 illustrates diagrammatically the machine and the character of the load-time pulse which was used to deform reinforced-concrete beams and frames and steel beams both elastically and plastically. Results of these studies [18-27] have been extensively used in establishing the dynamic yield stresses which were presented in Chaps. 1 and 2. More recently additional studies have been conducted at the University of Illinois under contract to the Corps of Engineers and U.S. Air Force. Most of these have been concerned with the static-strength characteristics of structural elements [28-39], but a new type of dynamic-loading machine of 50 kips capacity has been developed and is just now being used in a new series of dynamic tests on beams and beam-column connections. Figure 15.5 illustrates diagrammatically the machine, which utilizes compressed gas as the actuating force. No results of these studies are as yet available.

The Massachusetts Institute of Technology under contract to the Corps of Engineers has constructed a dynamic-loading machine with a 300-kip capacity to be used in a study of the dynamic characteristics of shear walls and columns. This machine will utilize a hydraulic system, with accumulators supplying the necessary power. Figure 15.6 illustrates the system under construction.

The dynamic-strength characteristics of plain concrete have been studied by the Bureau of Standards [40], using an impact pendulum.

The static-strength characteristics of shear walls have been studied at MIT [41] and more recently at Stanford [42-50].

The static-strength characteristics of structural-steel connections have been studied by the University of Michigan [51].

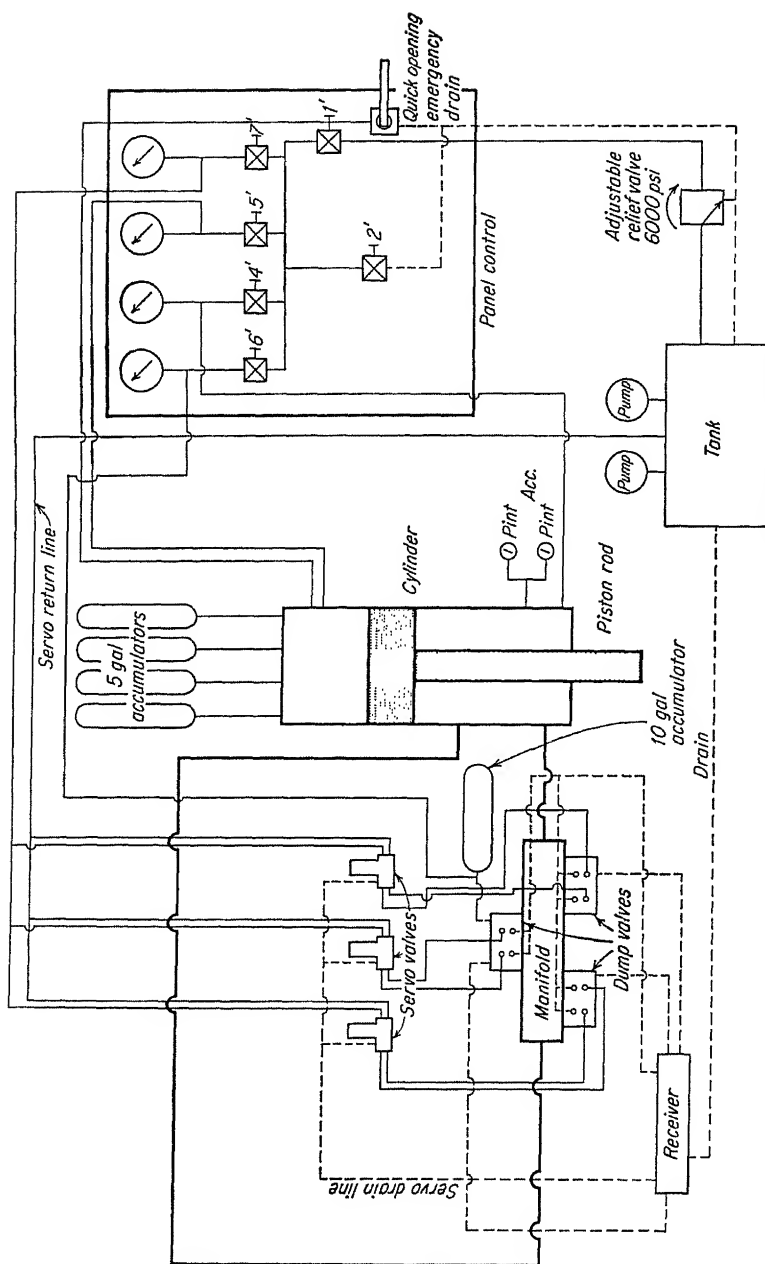


Fig. 15.6. Schematic of hydraulic system of MIT shear-wall machine.

A unique rapid-load machine was developed at the California Institute of Technology by Wood and Clark [52] which has been used to run dynamic-tension tests on specimens of various materials [53].

15.4. Dynamic-analysis and -design Procedures. The material presented in Chaps. 3 to 8 summarizes in essence the dynamic-analysis and -design procedures currently in use. Much of this material has been based on developments made by the MIT group under contract to the Corps of Engineers. However, many other groups have contributed to the analysis procedures used in blast-resistant design, including the University of Illinois [54-56], the University of Michigan [57-60], the consulting firm of Ammann and Whitney in New York City [61], and Armour Research Foundation [62].

Some of the development has been simplification of classical dynamic analysis, the application of numerical-analysis techniques (Chap. 8), and the application of analog and digital computers to the numerical problems involved in dynamic analysis.

REFERENCES

1. Bleakney, W., D. K. Weimer, and C. H. Fletcher: The Shock Tube: A Facility for Investigations in Fluid Dynamics, *Rev. Sci. Instr.*, vol. 20, no. 11, November, 1949.
2. White, Weimer, and Bleakney: The Diffraction of Shock Waves around Obstacles and the Resulting Transient Loading of Structures, Princeton University, Princeton, N.J., Aug. 1, 1950.
3. Bleakney, Walter: The Diffraction of a Shock Wave around a Hollow Rectangular Block-opening Facing Shock, Armed Forces Special Weapons Project, Oct. 25, 1950.
4. Shock Loading of Rectangular Structures, Princeton University, Jan. 10, 1952.
5. Brickl, D., and W. Bleakney: The Diffraction of Shock Wave over a 3-dimensional Object, Princeton University, April, 1953.
6. Griffith, Weimer, Brickl, and Bleakney: The Effect of Reynolds Number on the Diffraction of a Shock Wave, Princeton University, February, 1951.
7. Uhlenbeck, George: Diffraction of Shock Waves around Various Obstacles, University of Michigan, Mar. 21, 1950.
8. Duff, R., and R. Hollyer: Diffraction of Shock Waves through Obstacles with Various Openings in Their Front and Back Surfaces, University of Michigan, Nov. 7, 1950.
9. Hollyer, R., and A. Hunting: The Passage of Shock Waves over Oblique Obstacles, University of Michigan, Aug. 27, 1951.
10. Turner, E. B., A. C. Hunting, and A. C. Kolb: The Passage of Shock Waves over a Rectangular Block at Various Angles, University of Michigan, August, 1953.
11. Turner, E., A. Hunting, and W. Johnson: Three-dimensional Observations on the Passage of Shock Waves over a Rectangular Block, U.S. Navy Department, February, 1954.
12. Coulter, G., and James Allen: Diffraction of Step Shocks through a Double Slit, Aberdeen Proving Ground, January, 1954.
13. Taylor, William J.: Shock Tube Tests of Model Communal Shelter, Aberdeen Proving Ground, January, 1954.

14. Ferguson and Kingery: Air Blast Loading on Three-dimensional Scale Models of Dome Shape Rings, Aberdeen Proving Ground, April, 1955.
15. Richart, F. E., and N. M. Newmark: Impact Tests of Reinforced Concrete Beams, *NDRC Rept. A-125*.
16. Richart, F. E., and N. M. Newmark: Impact Tests of Reinforced Concrete Beams, *NDRC Rept. A-213*, vol. II.
17. Munse, W. H., and F. E. Richart: Impact Tests of Reinforced Concrete Beams, *NDRC Rept. A-304*, vol. III.
18. Hansen, R. J.: Behavior of Reinforced Concrete Structural Elements under Long Duration Impulsive Loads, *Summary Rept.*, pt. I, MIT, September, 1949.
19. Steyn, K.: Behavior of Reinforced Concrete Structural Elements under Long Duration Impulsive Loads, pt. III, Behavior within the Plastic Range, MIT, June, 1949.
20. Penzien, J.: Behavior of Reinforced Concrete Structural Elements under Long Duration Impulsive Loads, pt. II, Behavior within the Elastic Range, MIT, September, 1949.
21. Wells, W. M.: Behavior of Reinforced Concrete Structural Elements under Long Duration Impulsive Loads, pt. IV, Design, Construction and Operation of Slab Machine, September, 1949.
22. Hansen, R. J., et al.: Behavior of Structural Elements under Impulsive Loads, pt. I, MIT, April, 1950.
23. Hansen, R. J., et al.: Behavior of Structural Elements under Impulsive Loads, pt. II, MIT, July, 1951.
24. Hansen, R. J., et al.: Behavior of Structural Elements under Impulsive Loads, pt. III, MIT, July, 1951.
25. Hansen, R. J., et al.: Behavior of Wall Panels under Static and Dynamic Loads, pt. I, MIT, August, 1952.
26. Hansen, R. J., et al.: Behavior of Wall Panels under Static and Dynamic Loads, pt. II, MIT, January, 1954.
27. Penzien, Joseph, and Robert J. Hansen: Static and Dynamic Elastic Behavior of Reinforced Concrete Beams, *J. ACI*, vol. 25, no. 7, March, 1954.
28. Yen, C. S., and T. J. Dolan: A Critical Review of the Criteria for Notch-sensitivity in Fatigue of Metals, University of Illinois, March, 1952.
29. McCollister, H., C. Siess, and N. Newmark: Load Deformation Characteristics of Simulated Beam Column Connections in Reinforced Concrete, University of Illinois, June, 1954.
30. Laupa, A.: The Shear Strength of Reinforced Concrete Beams, University of Illinois, for U.S. Corps of Engineers, September, 1953.
31. Laupa, A., C. P. Siess, and N. M. Newmark: The Shear Strength of Simple-span Reinforced Concrete Beams without Web Reinforcement, University of Illinois, for Office of the Chief of Engineers, April, 1953.
32. Egger, W.: Notes on the Analysis of Obliquely Loaded Beams in the Inelastic Range, *Univ. Illinois SRL 98*, April, 1955.
33. Wilkinson, C. L., and F. L. Howland: The Response of Model Frames Subjected to Dynamic Lateral Loads, *Univ. Illinois SRL 99*, June, 1955.
34. Wojcieszak, R. F., and F. L. Howland: The Response of Beam Columns Subjected to Dynamic Lateral Loads, *Univ. Illinois SRL 100*, June, 1955.
35. Howland, F. L.: Inelastic Behavior of Mild Steel Beams Subjected to Transverse Impact, *Univ. Illinois SRL 106*, August, 1955.
36. Mayerjak, R. J.: The Study of the Resistance of Model Frames to Dynamic Lateral Loads, *Univ. Illinois SRL 108*, August, 1955.

37. Howland, F. L., and W. Egger: Correlations of Results of Dynamic Tests of Beams in Model Frames, *Univ. Illinois SRL* 109, September, 1955.
38. Bernaert, S., and C. P. Siess: Strength in Shear of Reinforced Concrete Beams under Uniform Load, *Univ. Illinois SRL* 120, June, 1956.
39. Baron, M. J., and C. P. Siess: Effect of Axial Load on the Shear Strength of Reinforced Concrete Beams, *Univ. Illinois SRL* 121, June, 1956.
40. Watstein, D.: Effect of Straining Rate on the Compressive Strength and Elastic Properties of Concrete, *J. ACI*, April, 1953.
41. Galletly, Gerard D.: Behavior of Reinforced Concrete Shear Walls under Static Loads, MIT, August, 1952.
42. Williams, H. A., and J. R. Benjamin: Investigation of Shear Walls. Pt. 1, Experimental Behavior and Empirical Results of Plain Concrete and Brick Walled Bents under Static Shear Loading, *Stanford Univ. Tech. Rept.* 1, pt. 1, April, 1952.
43. Benjamin, J. R.: Investigation of Shear Walls. Pt. 2, Prediction of Behavior of Plain Concrete and Brick Walled Bents under Static Shear Loading by Lattice Analogy, *Stanford Univ. Tech. Rept.* 1, pt. 2, April, 1952.
44. Williams, H. A., and J. R. Benjamin: Investigation of Shear Walls. Pt. 3, Experimental and Mathematical Studies of the Behavior of Plain and Reinforced Concrete Walled Bents under Static Shear Loadings, *Stanford Univ. Tech. Rept.* 1, July, 1953.
45. Williams, H. A., and J. R. Benjamin: Investigation of Shear Walls. Pt. 4, Experimental and Mathematical Studies of the Behavior of Brick Walled Bents under Static Shear Loading, *Stanford Univ. Tech. Rept.* 2, August, 1953.
46. Williams, H. A., and J. R. Benjamin: Investigation of Shear Walls. Pt. 5, Prediction of the Behavior of Plain Concrete, Reinforced Concrete, and Brick Walled Bents under Static Shear Loading, *Stanford Univ. Tech. Rept.* 3, August, 1953.
47. Benjamin, J. R., and H. A. Williams: Investigation of Shear Walls. Pt. 6, Continued Experimental and Mathematical Studies of Reinforced Concrete Walled Bents under Static Shear Loading, *Stanford Univ. Tech. Rept.* 4, August, 1954.
48. Walter, J. K., J. R. Benjamin, and H. A. Williams: Investigation of Shear Walls. Pt. 7, Continued Experimental and Mathematical Studies of the Behavior of Brick Walled Bents under Static Shear Loading, *Stanford Univ. Tech. Rept.* 5, August, 1954.
49. Stivers, R. M., J. R. Benjamin, and H. A. Williams: Investigation of Shear Walls. Pt. 8, Stresses and Deflections in Reinforced Concrete Shear Walls Containing Rectangular Openings, *Stanford Univ. Tech. Rept.* 6, August, 1954.
50. Benjamin, J. R., and H. A. Williams: Investigation of Shear Walls. Pt. 9, Continued Experimental and Mathematical Studies of Reinforced Concrete Walled Bents under Static Shear Loading, *Stanford Univ. Tech. Rept.* 7, September, 1955.
51. Shenker, Salmon, and Johnston: Structural Steel Connections, University of Michigan, June, 1954.
52. Clark and Wood: The Design and Construction of a Hydro-pneumatic Machine for Rapid Load Tensile Testing, California Institute of Technology, May, 1947.
53. Clark and Wood: The Influence of Rapid Load and Time at Load on the Tensile Properties of Several Alloys, California Institute of Technology, June, 1948.
54. Tung, T. P., and N. M. Newmark: A Review of Numerical Integration Methods for Dynamic Response of Structures, *Univ. Illinois SRL* 69, March, 1954.
55. Newmark, N. M.: Methods of Analysis for Structures Subjected to Dynamic Loading, Report to Physical Vulnerability Division, Directorate of Intelligence, U.S. Air Force, December, 1949. Revised December, 1950.

56. Analysis and Design of Structures to Resist Atomic Blast, *Virginia Polytechnic Inst. Eng. Expt. Sta. Bull.* 106, pt. II, January, 1956.
57. Johnston, B. G.: Structural Steel Members and Frames, *Proc. Symposium on Earthquake and Blast Effects on Structures*, University of California, 1952.
58. Johnston, B. G. (with R. C. Byce, L. S. Hu, C. Muktabhant, and H. H. Tung): Steel Frames for Industrial Buildings, in symposium, "Building in Atomic Age," MIT, 1952.
59. Johnston, B. G.: Blast-resistant Buildings, *Architectural Forum*, vol. 101, no. 1, July, 1954.
60. Johnston, B. G. (with Archie Mathews): Blast Resistant Building Frames, *Proc. ASCE*, separate no. 695, May, 1955.
61. Whitney, G. S., B. G. Anderson, and E. Cohen: Design of Blast Resistant Construction for Atomic Explosion, *J. ACI*, vol. 26, no. 7, March, 1956.
62. Armour Research Foundation: "A Simple Method for Evaluating Blast Effects on Buildings," rev. ed., July, 1954.

EARTHQUAKES AND EARTHQUAKE EFFECTS ON STRUCTURES

16.1. Earthquakes. Much more is known concerning the immediate causes of earthquakes than about the processes which lead up to the event. Earthquakes may be of tectonic or volcanic origin. For tectonic earthquakes, the elastic-rebound theory proposed by Professor H. F. Reid offers a reasonable explanation. Because of such causes as thermal contraction of the earth, isostasy, drifting continents, and/or radioactivity and convection currents, there is constant geological activity in the interior of the earth, resulting in accumulation of strains in the faults of earth blocks. When the strains become greater than it can endure, the earth crust ruptures and the strained crust blocks rebound until the strains are wholly or partially relieved. In this process, seismic waves are created which propagate in different directions, sometimes to great distances, depending on the amount of energy released. Displacements on fault planes cause vibrations to be propagated as elastic waves to the surface and cause damage to structures near the source of disturbance.

The building up of stress differences may be a slow process, and there may be a long period of unstable equilibrium which may be terminated abruptly by forces such as those resulting from atmospheric disturbances during storms. Such forces which are not directly related to the forces to be released, and possibly insignificant compared with them, are known as *trigger forces*. Before and after the main shock, there are frequently shocks to complete the adjustments within the earth crust. Those occurring before the major disturbance are called *foreshocks* and those occurring later *aftershocks*. These shocks are believed to be due to partial or excessive rebound of the earth masses. Earthquakes ordinarily originate at depths of 7 to 30 miles from the surface, although some deep-seated earthquakes have originated at depths greater than 400 miles. The point of origin of an earthquake is called the *focus*, and the point on the earth surface directly above the focus is the *epicenter*. Volcanic eruptions such as the one which blew off the top of the island of Krakatoa near Java in 1887 can be violent and produce high sea waves and nearby destruction, but the energy release is small compared with earthquakes of tectonic origin [1].

16.2. Geographical Distribution of Earthquakes. Most of the world's destructive earthquakes occur in well-defined seismic zones. One is the Circum-Pacific *seismic zone*, which forms an almost continuous circle surrounding the Pacific Ocean. It extends from New Zealand, the Philippines, Japan, the Aleutians, the coast of North, Central, and South Americas, almost to the tip of Cape Horn. Another is the *Alps-Caucasus-Himalaya seismic zone*, or the *Alpide belt*, which extends from the Azores across the Alpines of Mediterranean Europe and across Asia to Burma along the front of the Himalayan range. One branch shoots northward toward the upper course of the Yellow River in China, and the other branch turns southward, passing through Sumatra and Java, and merges with the Circum-Pacific belt. There are other minor active zones in the Arctic, Atlantic, and Indian Oceans, and earthquakes of considerable magnitude occur occasionally in areas considered to be stable.

In the United States, the Pacific Coast is most active seismically, although the greatest earthquakes have occurred in southern Missouri in the Mississippi Valley in 1811-1812. Professor P. Byerley lists the seismicity of the western states in the following order: California, 10.0, maximum reference; Nevada, 1.17; Utah, 1.14; Washington, 1.08; Montana, 0.57; New Mexico, 0.33, according to his evaluation scale. Oregon 0.27 presents an anomaly because the seismic belt is 100 miles or more at sea off the coast of Oregon [2].

Japan is also located on the Circum-Pacific belt, and with the exception of certain regions in the northern island of Hokkaido and the southern island of Kyushu, all structures are vulnerable to earthquake damage.

16.3. Earthquake Waves. The complex ground motion resulting from an earthquake is composed of body waves and surface waves. Two well-known types of body waves are (1) the longitudinal and (2) the transverse waves. Surface waves are (3) the Rayleigh and (4) the Love waves. Other types have been discovered and reported by Leet on detonating the atomic bomb on July 16, 1945, in New Mexico [3]. The speed with which any wave travels through earth medium is controlled by the elastic properties of the medium and by its density. The intensity of ground motion is affected by the physical characteristics of the ground near the surface and is intimately related to earthquake damage of man-made structures.

1. *Longitudinal (compressional, irrotational) P waves.* The symbol *P* is used to denote this fast wave as it arrives first to be recorded on seismographs. These stress waves are created by motion of particles moving back and forth (tension and compression) in the direction of propagation, characterized by change in volume but free from rotation. The velocity range is between 4.3 and 8.6 miles/sec.

2. *Transverse (shear, rotational) S waves.* The symbol *S* for secondary is used to denote this wave, which is slower than *P* waves. A particle in the path of a transverse wave may oscillate in any direction in the plane normal to the direction of advance of the wave, characterized by no change in volume, but possesses rotational quality. Although slower than longitudinal waves, transverse shear waves transmit more energy than *P* waves. When the body waves strike the ground surface, they are reflected and set up surface waves which propagate along the surface of the ground.

3. *Rayleigh R waves.* The symbol *R* is used in honor of Lord Rayleigh, who showed that this type of wave motion could be propagated along the

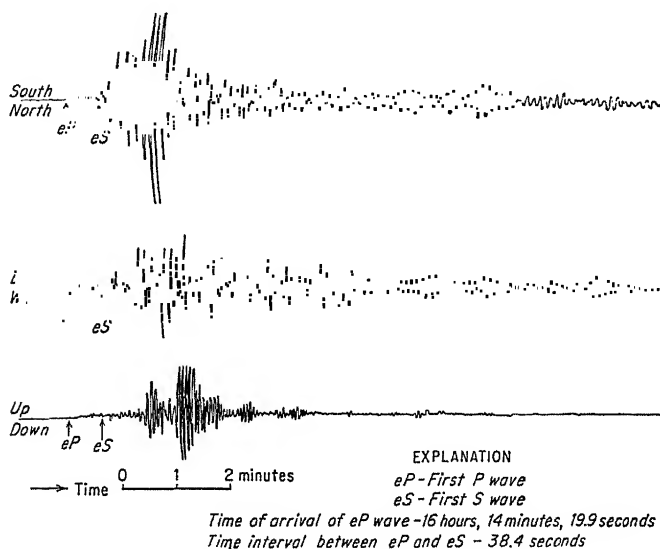


FIG. 16.1. Tokyo seismograms. (Central Meteorological Observatory, Tokyo.)

surface of a homogeneous elastic solid. This wave is a combination of the two wave types mentioned above.

4. *Love Q waves.* The symbol *Q* is ordinarily used to denote this type of wave. Love showed that such waves could be propagated under certain conditions. These waves vibrate transversely to the direction of wave travel without a vertical component.

Because of reflection, refraction, and dispersion of seismic waves, seismograms disclose complex oscillations. These records are necessary to understand the characteristics of the exciting force of earthquakes and in the development of more rational methods to resist such forces. The seismogram recorded at Tokyo at the time of the Fukui earthquake, June 28, 1948, is shown in Fig. 16.1. Tokyo is located almost 200 miles approximately east of Fukui.

16.4. Earthquake Magnitude and Intensity. The *magnitude of an earthquake* is measured by the quantity of kinetic energy released by the shock. The earthquake magnitude, as defined by Richter for California earthquakes, is the logarithm of the maximum trace amplitude expressed in thousandths of a millimeter with which the standard short-period torsion seismometer (having a free period of 0.8 sec, static magnification of 2,800, and nearly critical damping) would register an earthquake at an epicentral distance of 100 km. When the focus is 18 km, the relation between the energy E released by the shock, in ergs, and the magnitude of the earthquake M is given by Richter-Gutenberg [5] as follows:

$$E = (10)^{11.3}(10)^{1.8M} \quad (16.1a)$$

Expressing the energy in foot-pounds, the expression becomes

$$E = (74,000)(10)^{1.8M} \quad (16.1b)$$

The magnitude assignment based on instrumental records enables the determination of the total strain energy released by any earthquake, which equals the total energy dissipated in vibrations and other energy losses. The magnitude of earthquakes varies as the logarithm of the energy released.

The *earthquake intensity* is estimated on the basis of noninstrumental observation of damage to structures caused by any particular earthquake. The intensity will vary depending on the distance from the epicenter, geologic conditions, and type and quality of construction at any locality. The Modified Mercalli (MM) scale, having 12 divisions, as described in Table 16.1, was adopted by the U.S. Coast and Geodetic Survey in 1931 to describe the intensity of earthquakes.

In Japan, earthquake intensity is evaluated by the scale used by the Central Meteorological Observatory, Tokyo (CMO), which is shown in Table 16.2.

An addition of grade VII to indicate exceptionally strong and destructive earthquakes has recently been put into effect.

Of approximately 40 intensity scales existing, the Rossi-Forel scale consisting of 10 divisions (1884) and the Mercalli II scale consisting of 9 divisions (1902), which are adapted to Italian earthquakes, are the better known.

Observation of earthquake damage and evaluation of intensity are necessary to supplement instrumental records to further the understanding of earthquakes and their effects on structures.

16.5. Earthquake Spectra and Spectrum Intensity. The determination of earthquake spectra for records of ground motion obtained from Pacific Coast earthquakes through 1938 by M. A. Biot and of the El Centro, Calif., earthquake of 1940 by E. C. Robison marks a significant

TABLE 16.1. THE MODIFIED MERCALLI INTENSITY SCALE (CONDENSED)

- I. Not felt except by a few under especially favorable conditions.
- II. Felt only by a few persons at rest. Delicately suspended objects may swing.
- III. Felt quite noticeably under favorable circumstances, but many people do not recognize seismic nature of the disturbance and many do not notice it. Standing automobiles may rock slightly. Like passing of a truck. Duration estimated.
- IV. Felt by many or most. Some awakened. Dishes, windows, doors disturbed; walls crack. Sensation like heavy truck striking building.
- V. Felt by nearly everyone; many awakened. Some dishes, windows, etc., broken; a few instances of cracked plaster; unstable objects overturned. Disturbance of trees, poles, and other tall objects sometimes noticed. Pendulum clocks may stop.
- VI. Felt by all; many frightened and run outdoors. Some heavy furniture moved; a few instances of fallen plaster or damaged chimneys. Damage slight.
- VII. Everybody runs outdoors. Damage negligible in buildings of good design and construction; slight to moderate in well-built ordinary structures; considerable in poorly built or badly designed structures; some chimneys broken. Noticed by people driving motor cars.
- VIII. Damage slight in specially designed (brick) structures; considerable in ordinary substantial buildings with partial collapse; great in poorly built structures. Panel walls thrown out of frame structures. Fall of chimneys, factory stacks, columns, monuments, and walls. Heavy furniture overturned. Sand and mud ejected in small amounts. Changes in well water. Disturb persons driving motor cars.
- IX. Damage considerable in specially designed (masonry) structures; well-designed frame structures thrown out of plumb; great in substantial (masonry) buildings, with partial collapse. Buildings shifted off foundations. Ground cracked conspicuously. Underground pipes broken.
- X. Some well-built wooden structures destroyed; most masonry and frame structures destroyed with foundations; ground badly cracked. Rails bent. Landslides considerable from river banks and steep slopes. Shifted sand and water. Water splashed (slopped) over banks.
- XI. Few if any (masonry) structures remain standing. Bridges destroyed. Broad fissures in ground. Underground pipelines completely out of service. Earth slumps and land slips in soft ground. Rails bent greatly.
- XII. Damage total. Waves seen on ground surfaces. Lines of sight and level distorted. Objects thrown into the air.

TABLE 16.2. JAPANESE EARTHQUAKE-INTENSITY SCALE

- I. Felt by persons at rest. Acceleration 0.5 to 2 gals (980 gals equals gravity acceleration g).
- II. Felt by everyone. Acceleration 2 to 8 gals.
- III. Rattling of latticed sliding doors (partitions); swinging of chandeliers and other hanging objects; movement of liquids. Acceleration 8 to 32 gals.
- IV. Overturning of unstable objects; spilling of liquids; motion severe enough to cause fear. Acceleration 32 to 128 gals.
- V. Overturning of stone lanterns and tombstones; damage to old houses and to mud-plastered warehouses; cracking of masonry chimneys. Acceleration 128 to 512 gals.
- VI. Landslides; partial or total destruction of houses. Acceleration greater than 512 gals.

development in engineering seismology. An earthquake spectrum is a curve showing how the maximum response of an elastic one-degree-of-freedom structure produced by the actual ground motion of a particular earthquake varies for various values of the fundamental period of such a structure. The spectrum curves determined by Biot and Robison represented acceleration response, and the two curves showed remarkable similarity in shape with peak response at 0.2 and 0.25 sec, respectively (Fig. 17.3). These spectrum curves also represent the variation of the base shear of an undamped one-mass system. In the formulation of the Lateral Force Code by the Joint Committee of the San Francisco Section, ASCE, and Structural Engineers Association of Northern California [4],

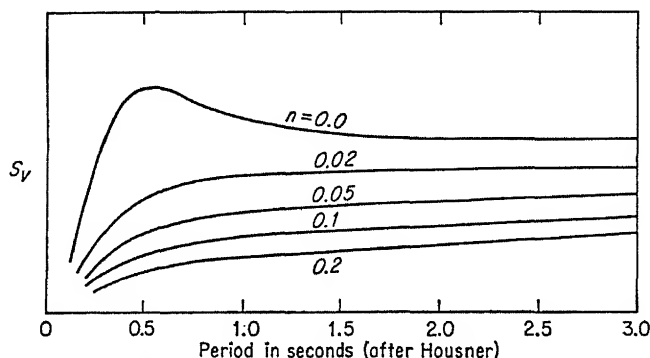


FIG. 16.2. Average-velocity spectrum.

great importance was attached to the significance of these acceleration spectra.

Earthquake-spectra technique has further been improved by Professors Martel, Housner, Hudson, and others at California Institute of Technology for practical engineering application to structural analysis for problems involving seismic forces [8]. The spectrum for the maximum-relative-velocity response (or for brevity, the *response spectrum*) is considered to be most useful for application in engineering seismology and is denoted by S_v in view of the fact that the physical dimensions of this quantity are those of velocity. Housner defines the *spectrum intensity* of an earthquake to be the area under the response-spectrum curve between the periods 0.1 and 2.5 sec. As buildings possess appreciable damping, the spectrum curve for 0.2 of critical damping (that is, $n = 0.2$) may be taken as a better measure of damage than the undamped curve, $n = 0$.

The family of curves shown in Fig. 16.2 represents the average shapes of the response-spectrum curves obtained by Housner based on data for the El Centro, 1934; El Centro, 1940; Olympia, 1949; and Taft, 1952, earthquakes [8].

The response spectrum S_V is related to the seismic coefficient C in the expression for determining the earthquake force F as follows:

$$F = CW = \frac{\ddot{x}_{\max}}{g} W = \frac{(2\pi/T)S_V}{g} W = \frac{2\pi}{Tg} S_V W$$

Hence

$$C = \frac{2\pi}{Tg} S_V \quad (16.2)$$

The use of the response spectrum to show the physical characteristics of ground motion and establish seismic coefficients for structural behavior is fully explained in papers by Hudson and Housner [7, 8].

16.6. Period of Vibration of Buildings. The period of vibration of simple idealized structures may readily be calculated. The application of theory to actual buildings and structures is more difficult. Consequently, recourse to actual observation of vibration of buildings has been made. The Coast and Geodetic Survey has measured the period of vibration of hundreds of buildings, water-tank towers, and ground vibrations. Some of the results of the work done by the Survey have been reported [9], and the Joint Committee on Lateral Force considered available data on the subject in proposing an empirical relation for the period of vibration of buildings, taking into consideration the height and width of buildings, as follows:

$$T_n = 0.06 \frac{H}{\sqrt{b}} \quad \text{sec} \quad (16.3)$$

where H = height, ft

b = width, ft, in direction of motion considered

The Joint Committee has, however, recommended the use of a more conservative coefficient of 0.05 in the above equation in the computation of the seismic coefficient $C = 0.015/T$. The total lateral seismic force V is determined from the relation $V = CW$, where W represents the weight of the building considered in seismic computations.

Similar observations have been made for certain buildings in large cities in Japan. Based on his numerous observations, Dr. T. Taniguchi of Tokyo Institute of Technology has suggested the following empirical relation for the fundamental period of buildings, where N is the number of stories:

$$T_n = (0.07 \text{ to } 0.09)N \quad \text{sec} \quad (16.4)$$

In addition to the proportions of buildings, relative rigidity influences the period. The effect of rigidity on the period may be illustrated by the following observations on the Marunouchi Building facing Tokyo Station. When the building was completed, its period was 0.94 sec; after the semi-destructive earthquake of Apr. 26, 1922, when the building suffered slight damage, the period increased to 1.01 sec. Repairing and strengthening

of the building (eight stories aboveground with one basement story) reduced the period to 0.71 sec. The building again suffered serious damage in the 1923 earthquake and in this condition had a period of 1.18 sec. After rehabilitation, the period of free vibration is 0.48 sec, which is indicative of its high rigidity. Japanese buildings, limited to a maximum of nine stories because of height restriction of 102 ft (31 m), generally have periods ranging from 0.1 to 1.3 sec. The period of vibration of buildings in an actual earthquake may be somewhat higher because of yielding of the ground under the foundations.

Detailed investigations on certain buildings, such as the Alexander Building in San Francisco, have been performed by Blume [10], Clough [11], and others, covering the numerous phases of dynamic response under earthquake motion, which shed considerable enlightenment on the subject.

16.7. Strong-motion Programs. Accurate records of ground motion due to strong earthquakes are necessary to further our knowledge of earthquake characteristics. The strong-motion program, initiated in 1932 by the U.S. Coast and Geodetic Survey, succeeded in obtaining useful records of the Long Beach earthquake of Mar. 10, 1933, and complete records of strong motions of the El Centro, Calif., earthquake of May 18, 1940, and subsequent earthquakes. Strong-motion seismographs, which usually register the ground-acceleration components in two horizontal directions perpendicular to each axis and one vertical direction, are of sturdy construction. The accelerographs and other instruments used in the early stage of the program and other phases of the program are described in a special publication of the Survey [12].

The types of strong-motion seismographs and supplementary instruments currently used were described by Cloud at the World Conference on Earthquake Engineering, June, 1956 [13]. Approximately 60 strong-motion seismographs are distributed in the Pacific Coast states of California, Washington, Montana, Nevada, Utah, and Oregon.

In spite of frequent and often calamitous earthquakes that occur in Japan, only limited records of ground motion have been obtained. The Strong-Motion Acceleration Committee, which was established in 1951, has developed the strong-motion accelerograph known as SMAC, shown in Fig. 16.3. These SMAC instruments have been installed in various buildings in Tokyo, Osaka, and Nagoya, and they will be installed in increasing numbers as funds for the program become available. The accelerograph consists essentially of three pendulums set at right angles to each other; a spring motor for driving the recording paper; a time-marking clock; and an electric starter. These instruments begin operating automatically at accelerations greater than 10 gals and run for 3 min and stop. They are geared to repeat the above operation three times.

Special-purpose instruments for studying microtremors of different soil types, direct-reading instruments for measuring the amplitude distribution and mode of vibration of buildings, inexpensive accelerographs not recording the acceleration in the vertical direction, and other instruments are described in a paper by Takahasi of the Earthquake Research Institute, Tokyo University [14].

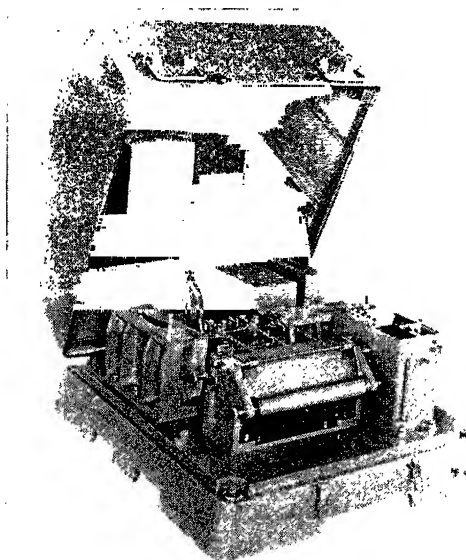


FIG. 16.3. SMAC accelerograph.

16.8. Earthquake Effects on Structures. The history of past great earthquakes records amazing loss of life and damage to property. It is recorded that 830,000 lives were lost in the earthquake of Feb. 2, 1556, affecting the three provinces of Shensi, Shansi, and Honan in China. A more recent and minor earthquake of Dec. 16, 1920, which affected only the province of Kansu, caused the death of 100,000 persons [15]. The Kanto earthquake of Sept. 1, 1923, which occurred a few seconds before noon, nearly wiped out Tokyo and Yokohama. The resulting conflagration caused most of the loss of property and approximately 100,000 lives. The Fukui earthquake of June 28, 1948, resulted in the death of approximately 5,000 persons, mostly due to persons being caught in falling debris and engulfed in flames by the fires that followed after the shocks. Well-documented reports of earthquake-damage investigations are available for recent earthquakes.

From the point of view of contributing to earthquake engineering, the following earthquakes may be selected as being of significance: the San

Francisco earthquake of Apr. 18, 1906, which put to actual test buildings of modern construction; Kanto earthquake of 1923, resulting in the adoption of a seismic coefficient of 0.1; Santa Barbara earthquake, which contributed to the formulation of the Uniform Building Code; Long Beach earthquake of Mar. 10, 1933, which resulted in the enactment of the Riley and Field Acts and also yielded useful records of strong ground motion; El Centro earthquake of May 18, 1940, which yielded the first complete record of the strong ground motion; and the Fukui earthquake of 1948, which caused the structural collapse of a four-story reinforced-concrete building.

Experience from past earthquakes in Japan indicates that damage to buildings and other types of structures is closely related to design, construction, types of construction, and soil or geologic conditions. Based on statistical studies of earthquake damage, certain generalized conclusions may be drawn.

For wooden-frame buildings, often with heavy roof tiles, high degree of damage is suffered when they are located on soft alluvial soil. Less damage occurs for locations on firm soil. Frequently, two-story houses become one-story, the first story being crushed between the ground and the second story, which sways excessively and falls. The deformation of the first story is great in any case. Wooden buildings are inherently flexible, as constructed in Japan, and the large amplitude and greater period of ground motion in soft soils adversely affect this type of construction.

For masonry construction of brick or for bamboo-reinforced-mud construction, a high degree of damage is suffered for locations on firm soil. The damage is less for locations on soft soil. The lack of elastic give and the vulnerability to shock in this type of construction are believed to be important. A group of brick buildings in downtown Tokyo (alluvial soil) that were built prior to the 1923 Kanto earthquake with great care have survived the numerous subsequent earthquakes with little damage.

Reinforced-concrete buildings of good design and construction usually give fine performance, although there are exceptions when design, construction, or other factors detract from the quality. The Daiwa Department Store building is the case in point. It had suffered wartime fire and possessed structural weakness and collapsed in the Fukui earthquake. The Fukui Broadcasting Station building, although of a smaller scale, of reinforced concrete rode through the same earthquake without damage.

The steel frame encased in reinforced concrete for fire protection, durability, and strength is another type of construction which has given satisfactory performance. The structural-steel members have built-up sections, consisting of nominal-size angles and plates.

Steel-frame buildings with brick or tile walls have suffered badly

Those provided with seismic walls of reinforced concrete deform less and consequently suffer less damage. Attention to structural details and construction is important to minimize damage.

16.9. Failure of Daiwa Department Store Building. The site of this building consisted of deep, soft alluvium with a high water table near the surface. The north and west elevations of the building before the earthquake are shown in Fig. 16.4. The $X-X'$ and $Y-Y'$ sections through the building, indicated in Fig. 16.7, are shown in Fig. 16.5. The foundation plan and the view at section $Z-Z'$ are shown in Fig. 16.6. The floor plans are shown in Figs. 16.7 to 16.9.

The long axis of the building extended north and south. The building may, for convenience, be considered to consist of three portions: (1) the front (north) triangular portion with the main entrance and tower, (2) the six-story sales portion, and (3) the rigid eight-story portion with a basement that contained elevator shafts, stairways, and toilets. Portion 3 was the most rigid, having in addition a mat foundation, and portion 2 the least rigid, having footings connected in two directions by nominal tie beams. Continuous footings were provided under the exterior walls of the building.

As evident from Fig. 16.6 there was foundation discontinuity between portions 2 and 3 where structural distress from the earthquake was most pronounced. The building sagged at column row 7, pulling portion 3 a distance of 13 in. at the top and portion 1 a distance of 18 ft 4 in. at the top as indicated in Fig. 16.10.

The appearance of the damaged building from the outside and inside after the earthquake is sketched in Fig. 16.12.

At the time this building was built (May to December, 1937), reinforcing bars were becoming scarce because of the demands of the military, and restrictions on new department-store construction were beginning to be enforced. These circumstances contributed to the speed-up of the construction, which may well have influenced structural planning and design as well as construction.

As mentioned previously, portion 3 was provided with a basement and a mat foundation, creating a differential of 8.75 ft in the foundation depth between portion 3 and the adjoining portions 1 and 2. Wooden piles of 15-ft length were driven under portions 1 and 2, and piles of 12-ft length under portion 3. The connection of the foundation between portions 2 and 3 in the longitudinal direction was by nominal tie beams without due consideration for earthquake effects.

There was also a lack of symmetrical placement of seismic shear walls in the building, as is evident from the inspection of the floor plans. The lack of uniform rigidity could cause large deformations in the flexible portion 2. The interior columns in row 3 in the fifth and sixth stories

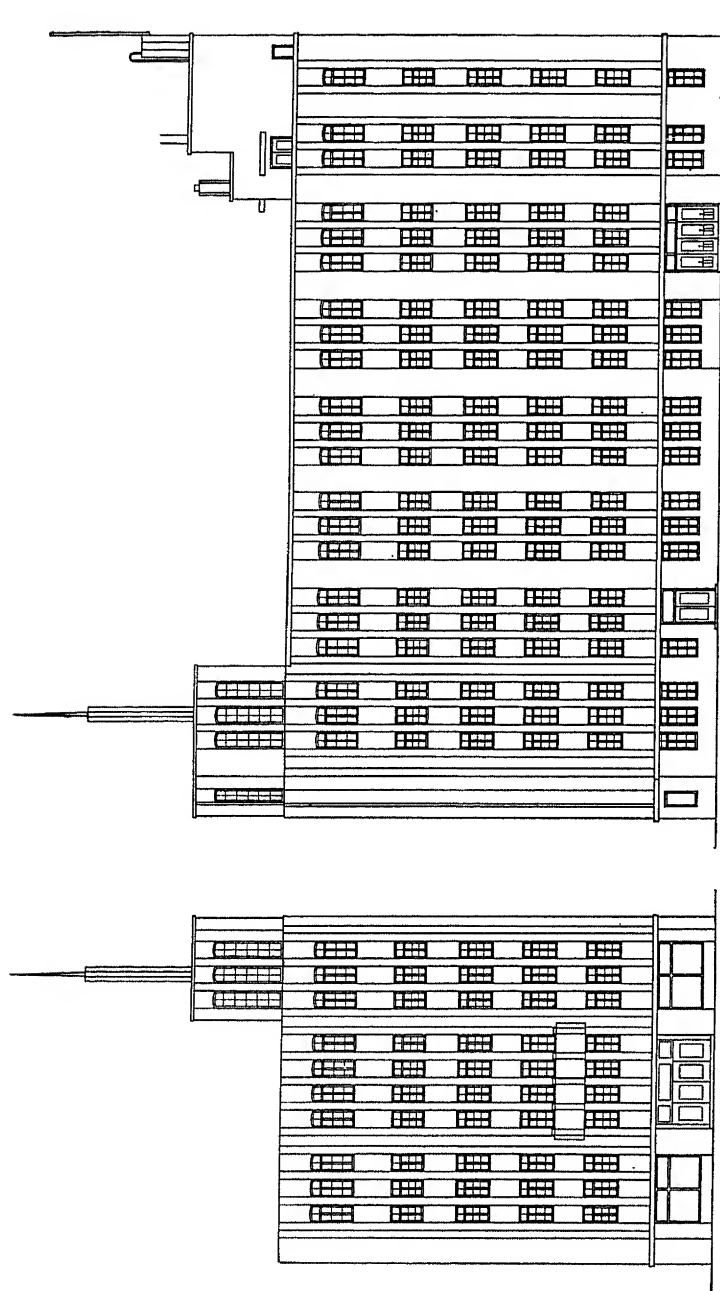


FIG. 16.4. Elevations, Daiwa Department Store, Fukuji, Japan.

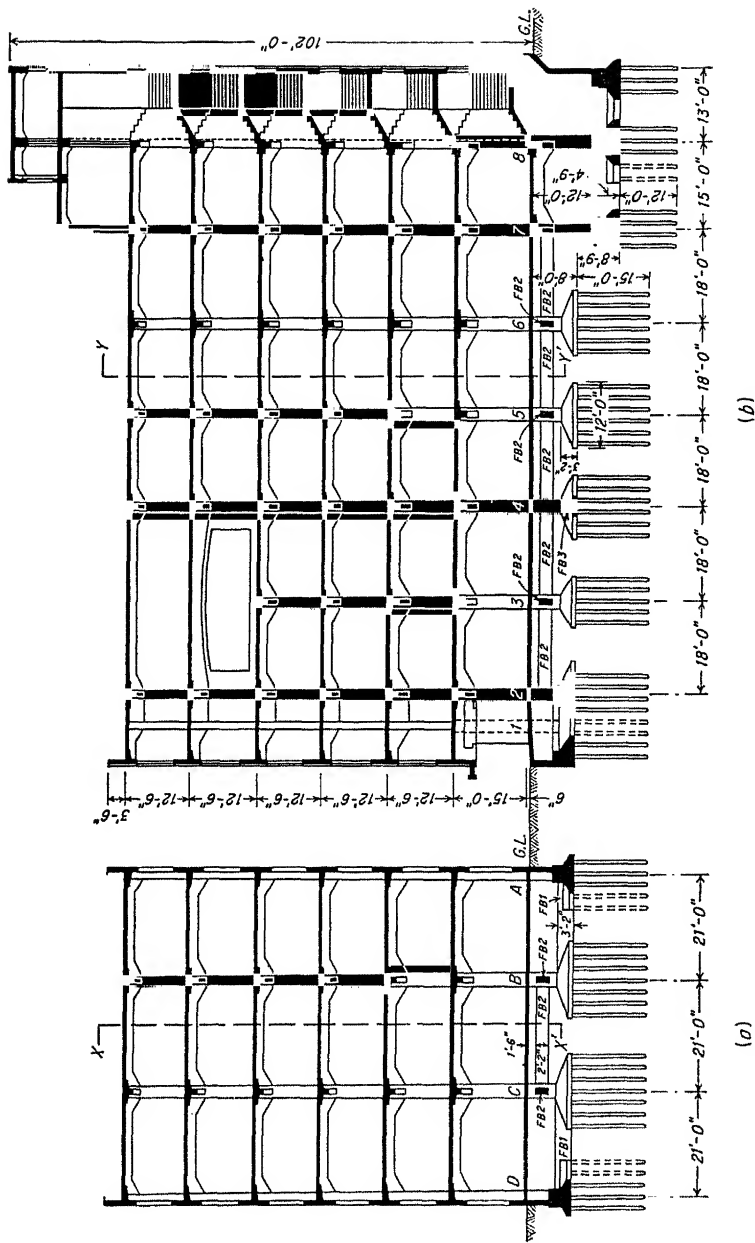


Fig. 16.5. Sections, Daiwa Department Store. (a) Section Y-Y'; (b) section X-X'.

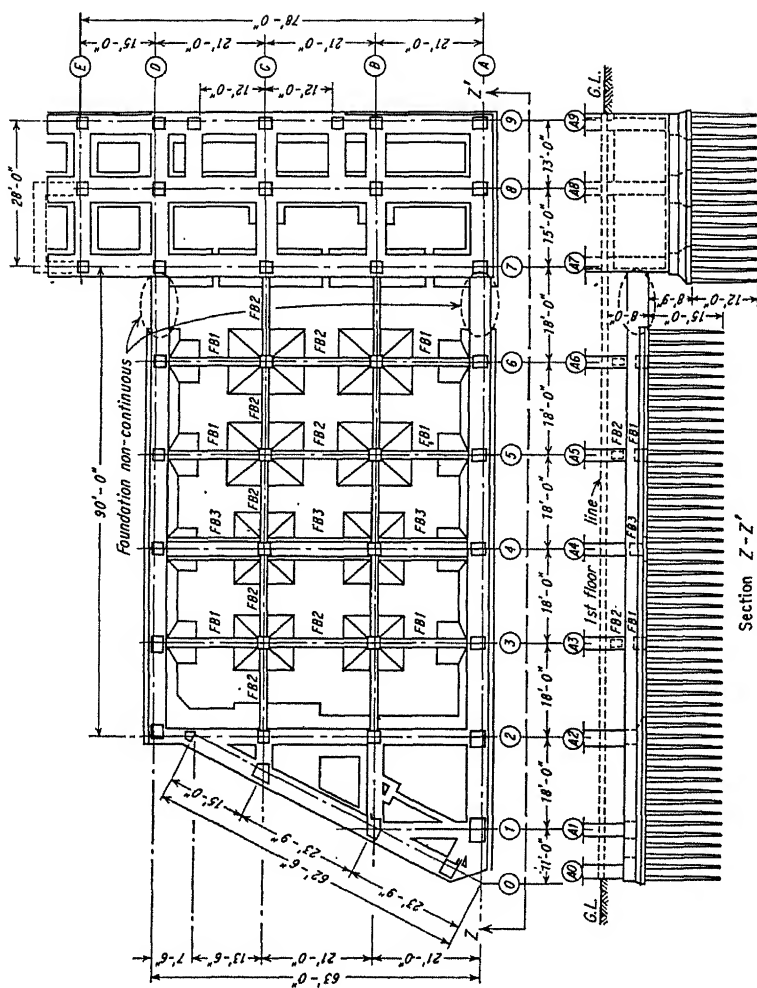


Fig. 16.6. Foundation plan, Daiwa Department Store.

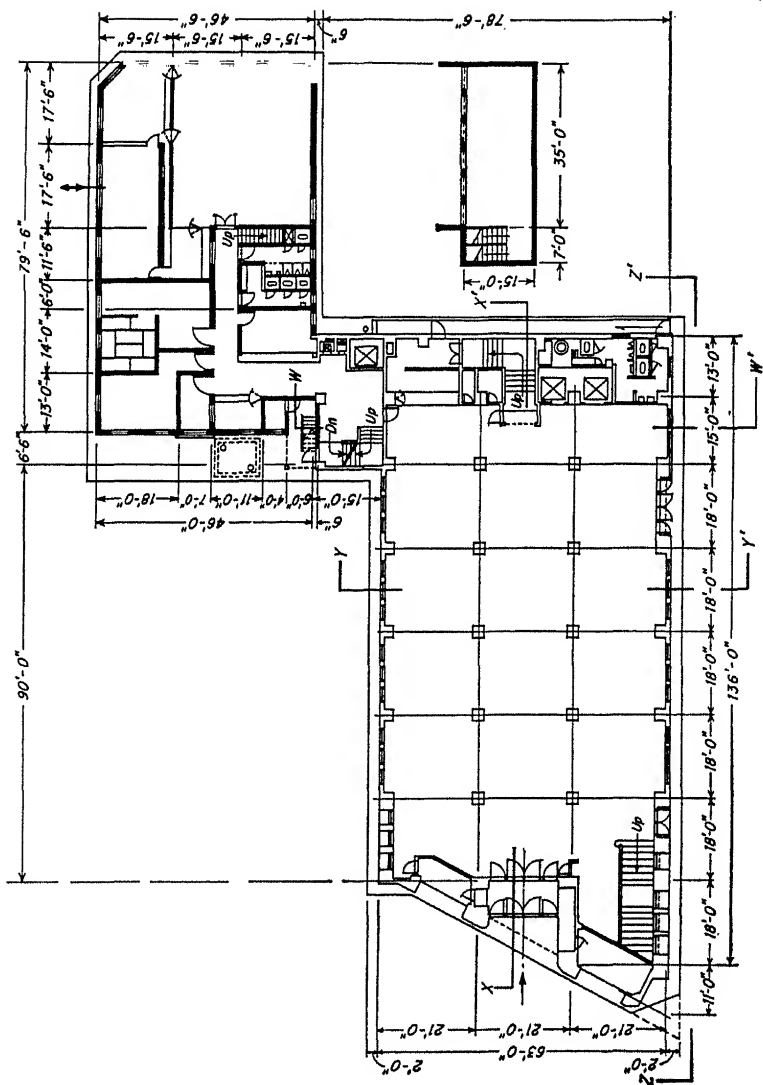


FIG. 16.7. First-floor plan.

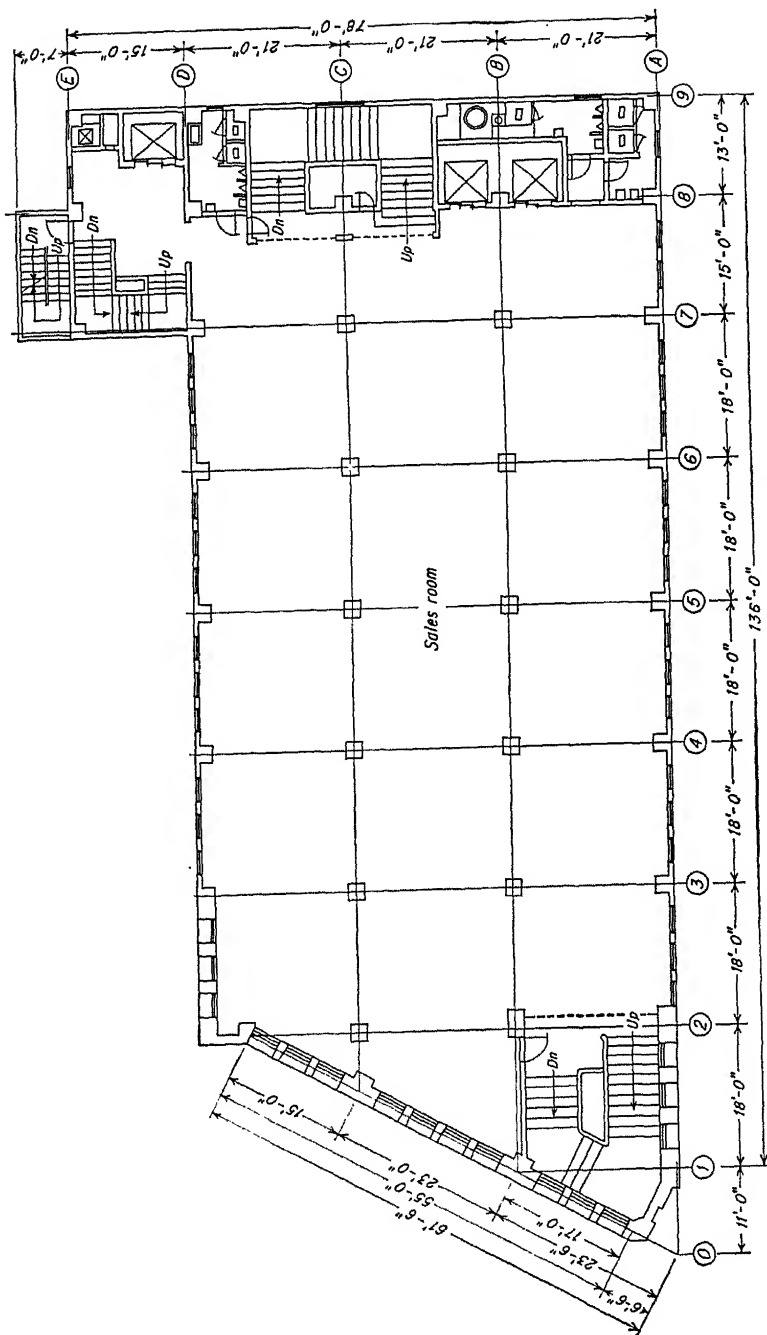


FIG. 16.8. Typical (second-, third-, fourth-) floor plan.

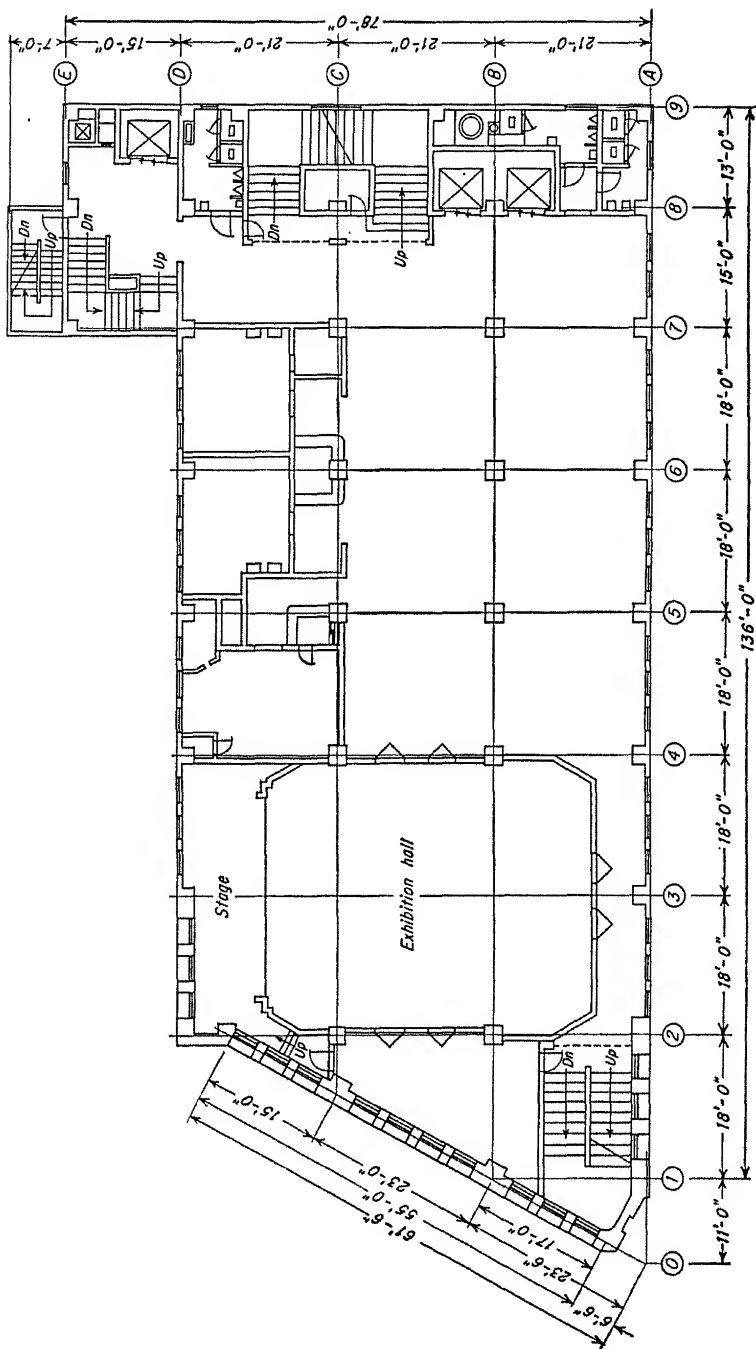


FIG. 16.9. Fifth-floor plan.

were eliminated to provide large exhibition space, which contributed further to the weakening of portion 2.

In August, 1945, this building suffered serious fire damage. The one-story wooden wing (Fig. 16.7) was destroyed, and the main building was gutted by fire. After the war, the main building was rehabilitated, but

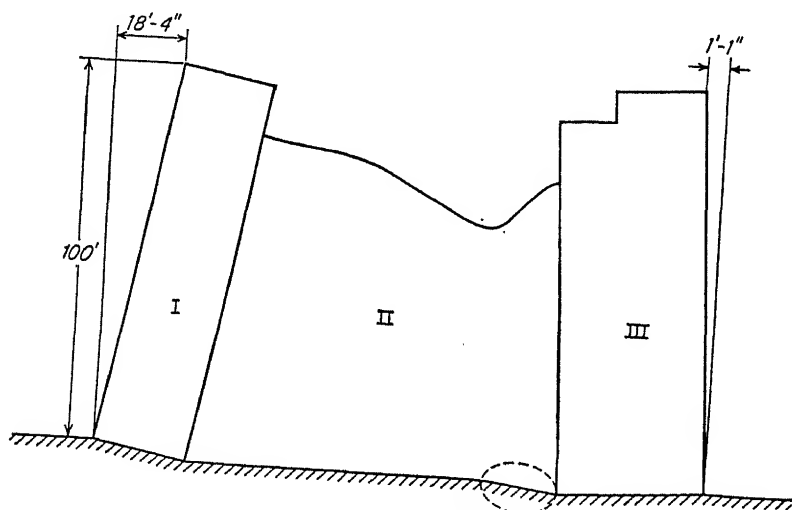


Fig. 16.10. Deformation of building, west view.

in a manner not entirely satisfactory. In some instances, the reinforcing bars exposed by spalled concrete were barely covered with plaster.

The Fukui earthquake caused the connections between columns and girders to fail. In practically all cases, the failure was noted at the beginning of the haunches in the girders. The bent between column rows

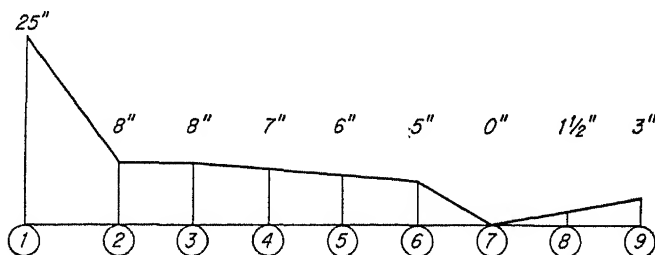


Fig. 16.11. Ground-floor elevation after earthquake.

6 and 7 practically disappeared because of crushing together of portions 2 and 3.

Inspection of the original design disclosed that the exterior wall girders were given a value of the seismic-distribution coefficient D of 3, whereas the actually designed members were found incapable of taking the stresses

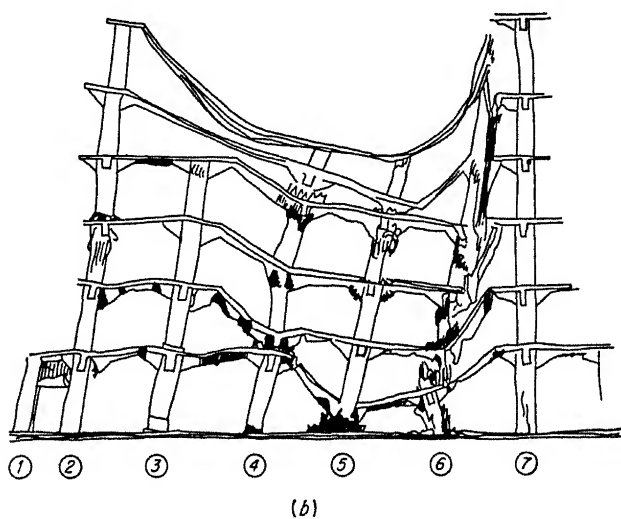
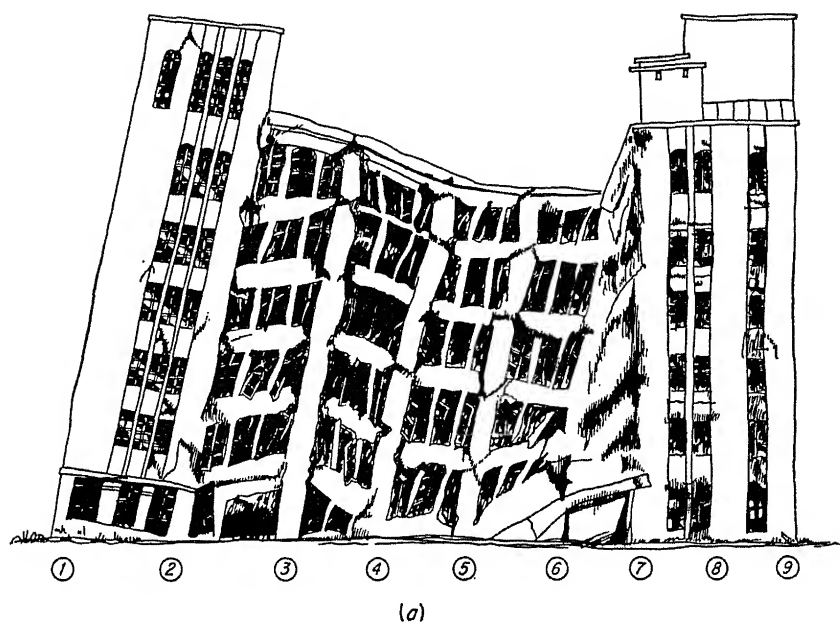


FIG. 16.12. Collapse of Daiwa Department Store. (a) West elevation; (b) section X-X' (see Fig. 16.7).

developed under the design assumption. Insufficient consideration was accorded the discontinuity existing between portions 2 and 3 from the foundations to the top of the building. To ensure unified action of a shear-type building such as this building, the members at this junction should have been made much stronger and rigid than was the actual case. Wartime fire also had an adverse effect on concrete properties, which did not benefit from the careless rehabilitation after the war. Unfavorable site conditions, an exceedingly high-intensity quake, and indifferent structural planning, design, and construction caused the failure of this building.

Although the failure of the Daiwa building in the Fukui earthquake was the most impressive, damage to water, gas and electric systems, roads, bridges, levees and chimneys, and elevated water tanks was widespread. As has been well substantiated from past earthquake experience, there were buildings and other structures of sound design and construction that survived the severe ground motions of this earthquake with slight or no structural damage. A detailed report, fully illustrated, of this earthquake is available in Ref. 16.

A careful study of comprehensive reports on the engineering aspects of the 1933 Long Beach earthquake by Binder [17] and of the earthquake lessons from the Pacific Northwest by Miller [18] and others will help to develop an appreciation of earthquake effects on all types of structures.

REFERENCES

1. Heck, N. H.: "Earthquakes," Princeton University Press, Princeton, N.J., 1936.
2. Byerly, P.: Seismicity of the Western United States, "Proceedings of World Conference on Earthquake Engineering," Earthquake Engineering Research Institute and University of California, Berkeley, June, 1956.
3. Leet, L. D.: "Earth Waves," Harvard University Press, Cambridge, Mass., 1950.
4. Joint Committee of San Francisco, Calif. Section, ASCE and Structural Engineers Assoc. of Northern California: Lateral Forces of Earthquake and Wind, *Proc. ASCE*, vol. 77, separate no. 66, April, 1951.
5. Gutenberg, B., and C. F. Richter: Earthquake Magnitude, Intensity, Energy and Acceleration, *Bull. Seismological Soc. Am.*, vol. 32, no. 3, July, 1942.
6. Housner, G. W.: Spectrum Intensities of Strong-motion Earthquakes, in "Proceedings of Symposium on Earthquake and Blast Effects on Structures," EERI and University of California, Los Angeles, June, 1952.
7. Hudson, D. E.: Response Spectrum Technique in Engineering Seismology, in "Proceedings of World Conference on Earthquake Engineering," EERI and University of California, Berkeley, June, 1956.
8. Housner, G. W.: Limit Design of Structures to Resist Earthquakes, in "Proceedings of World Conference on Earthquake Engineering," EERI and University of California, Berkeley, June, 1956.
9. Ulrich, F. P., and D. S. Carder: Vibrations of Structures, in "Proceedings of Symposium on Earthquake and Blast Effects on Structures," EERI and University of California, Los Angeles, June, 1952.

10. Blume, J. A.: Period Determinations and Other Earthquake Studies of a Fifteen-story Building, in "Proceedings of World Conference on Earthquake Engineering," EERI and University of California, Berkeley, June, 1956.
11. Clough, R. W.: On the Importance of Higher Modes of Vibration in the Earthquake Response of a Tall Building, *Bull. Seismological Soc. Am.*, October, 1955. Also, Earthquake Forces in a Tall Building, *Civil Eng.*, January, 1956.
12. Earthquake Investigations in California 1934-1935, *U.S. Dept. Commerce, Coast and Geodetic Survey, Spec. Publ.* 201.
13. Cloud, W. K., and D. S. Carder: The Strong-motion Program of the Coast and Geodetic Survey, in "Proceedings of World Conference on Earthquake Engineering," EERI and University of California, Berkeley, June, 1956.
14. Takahasi, R.: The SMAC Strong-motion Accelerograph and Other Latest Instruments for Measuring Earthquakes and Building Vibrations, in "Proceedings of World Conference on Earthquake Engineering," EERI and University of California, Berkeley, June, 1956.
15. Imamura, A.: "Theoretical and Applied Seismology," Maruzen Co., Tokyo, 1938.
16. "The Fukui Earthquake, Hokuriku Region, Japan," Far East Command, General Headquarters, Office of the Engineer, February, 1949.
17. Binder, R. W.: Engineering Aspects of the 1933 Long Beach Earthquake, in "Proceedings of Symposium on Earthquake and Blast Effects on Structures," EERI and University of California, Los Angeles, June, 1952.
18. Miller, A. L.: Earthquake Lessons from the Pacific Northwest, in "Proceedings of Symposium on Earthquake and Blast Effects on Structures," EERI and University of California, Los Angeles, June, 1952.

CHAPTER 17

EARTHQUAKE PROVISIONS IN BUILDING CODES

17.1. Introduction. Building codes specify design and construction requirements which are intended to protect buildings from major structural damage and the public from loss of life and injury from earthquakes, based to a large extent on past earthquake experience and judgment. Because of differences in the magnitude of earthquakes, geological formations, types of construction, and other factors, the philosophy of aseismic design among different groups of engineers might naturally differ in several respects. The earthquake provisions in the Uniform Building Code (UBC), the national Japanese Building Code (JBC), and the Joint Committee Code (JCC) on Lateral Forces of Earthquake and Wind are presented and briefly discussed.

17.2. Uniform Building Code. The first edition of the Uniform Building Code was published as the 1927 edition, which was prepared by the Pacific Coast Building Officials Conference after the Santa Barbara earthquake of June 29, 1925, that caused considerable damage to buildings in swampy and filled ground. As experience and usage increased, provisions were modified, and revised editions have appeared as the 1937 edition, 1949 edition, 1952 edition, and the current 1955 edition. The historical development of this code has been described by Andrus [1].

The 1927 edition of the code required that all buildings more than 20 ft in height, except exposed-steel-frame and wood-frame buildings, be designed for earthquake forces using 7.5 per cent of the specified vertical loads as the seismic coefficient when the allowable bearing capacity of the soil was 2 or more tons per square foot, and 10 per cent for soils of lesser bearing capacity. An increase of $33\frac{1}{3}$ per cent in the allowable unit stresses was permitted for all materials, except for structural steel, which was allowed a 50 per cent increase.

The 1937 edition adopted a new formula for the lateral force F :

$$F = CW \quad (17.1)$$

where C = seismic coefficient

W = total dead load plus half the live load

In the case of warehouses, the full live load was to be used. A seismic-probability map of the 11 Western states was included and made a part

of the code, which designated different areas into zones 1, 2, and 3. Seismic coefficients were established for zone 1, the least active zone, and these were multiplied by 2 for zone 2 and by 4 for zone 3, the most seismically active zone. Aside from the building proper, seismic-coefficient values were established for walls, parapet walls, ornamentations, stacks, and tanks. The allowable increase in the unit stresses for materials was generally $33\frac{1}{3}$ per cent, with a maximum of 20,000 psi for reinforcing steel. Under this code, for an area in zone 3, the coefficients were 8 per cent for buildings resting on soil with bearing capacity greater than 1 ton/ft² and 16 per cent for soil with lesser capacity.

The 1949 edition replaced the seismic-probability map of the Western states with a map of the 48 states prepared by the Coast and Geodetic Survey, and an expression for determining the seismic coefficient, known as the Los Angeles formula, was adopted, where N is the number of stories above the story under consideration, as follows:

$$C = \frac{0.15}{N + 4.5} \quad (17.2)$$

for zone 1, twice this value for zone 2, and four times this value for zone 3, thus giving a maximum value of 13.3 per cent for a single-story building. The live load was disregarded in computing the weight of the building for seismic computations, except for warehouses and tanks, for which full live load was considered. The above expression for C has been retained in the later editions of this code. The effect of local soil conditions on earthquake intensity originally considered has been discarded in later editions, and seismicity alone is considered.

The earthquake-resistant-design provisions of the Uniform Building Code, 1955 edition, in the Appendix on Lateral Bracing, Sec. 2312, and related provisions are extracted below. Figures and tables extracted are numbered as in the source material.

Sec. 2303 (Method of Design). . . . All allowable stresses and soil bearing values specified in this Code may be increased one-third due to wind or earthquake either acting alone or when combined with vertical loads. No increase shall be allowed for vertical loads acting alone.

Wind and earthquake loads need not be assumed to act simultaneously. . . .

Sec. 2305 (Roof Loads). Roofs shall sustain, within the stress limitations of this Code, all "dead loads" plus unit "live loads" as set forth in Table No. 23-B. . . .

Snow load, full or unbalanced, or wind load shall be considered in place of loads as set forth in Table No. 23-B, where such loading will result in larger members or connections.

Sec. 2306 (Reduction of Live Loads). . . . Reductions in unit live loads as set forth in Table No. 23-A for floors shall be permitted in the designing of columns, piers, walls, foundations, trusses, beams, and flat slabs.

Except for places of public assembly, and except for live loads greater than 100 pounds per square foot, the design live load on any member supporting 150 sq. ft. or more may be reduced at the rate of 0.08 per cent per square foot of area supported by the member. The reduction shall not exceed 60 per cent nor "*R*" as determined by the following formula:

$$R = 23.1 \left(1 + \frac{D}{L} \right)$$

where *R* = Reduction in per cent

D = Dead load per square foot of area supported by the member

L = Unit live load per square foot of area supported by the member

For storage live loads exceeding 100 pounds per square foot, no reduction shall be made except that design live loads on columns may be reduced 20 per cent. . . .

Sec. 2312 (Lateral Bracing). The following provisions are suggested for inclusion in the Code by cities located within an area subject to earthquake shocks:

(a) **General.** . . . The [lateral] force shall be assumed to come from any horizontal direction.

All bracing systems both horizontal and vertical shall transmit all forces to the resisting members and shall be of sufficient extent and detail to resist the horizontal forces . . . and shall be located symmetrically about the center of mass of the building or the building shall be designed for the resulting rotational forces about the vertical axis.

(b) **Horizontal Force Formula.** In determining the horizontal force to be resisted, the following formula shall be used:

$$F = CW$$

where "*F*" equals the horizontal force in pounds, "*W*" equals the total dead load, tributary to the point under consideration.

Exceptions: 1. For warehouses, "*W*" shall equal the total dead load plus 50 per cent of the vertical design live load tributary to the point under consideration.

2. For tanks, "*W*" shall equal the total dead load plus the total live load.

Machinery or other fixed concentrated loads shall be considered as part of the dead load.

"*C*" equals a numerical constant as shown in Table No. 23-C [Table 17.1].

(c) **Foundation Ties.** . . . In the design of buildings of Types I, II, and III, where the foundations rest on piles or on soil having a safe bearing value of less than 2000 pounds per square foot, the foundations shall be completely interconnected in two directions approximately at right angles to each other. Each such interconnecting member shall be capable of transmitting by both tension and compression at least 10 per cent of total vertical load carried by the heavier only of the footings or foundations connected. The minimum gross size of each such member if of reinforced concrete shall be twelve inches by twelve inches . . . and shall be reinforced with not less than the minimum reinforcement specified in Section 2620. . . .

Interconnecting slabs shall be reinforced with not less than .11 sq. in. of steel

TABLE 17.1. HORIZONTAL FORCE FACTORS [UBC TABLE 23-C]

Part or portion	Value of " <i>C</i> "*	Direction of force
Floors, roofs, columns, and bracing in any story, or the structure as a whole†	$\frac{.15}{N\ddagger + 4.5}$	Any direction horizontally
Exterior bearing and non-bearing walls, interior bearing walls and partitions, interior non-bearing walls and partitions over 10 ft in height, masonry fences over 6 ft in height	.05 with a minimum of 5 psf	Normal to surface of wall
Cantilever parapet and other cantilever walls, except retaining walls	.25	Normal to surface of wall
Exterior and interior ornamentations and appendages	.25	Any direction horizontally
When connected to or a part of a building: towers, tanks, towers and tanks plus contents, chimneys, smokestacks, and penthouses	.05	Any direction horizontally
Tanks, elevated tanks, smokestacks, standpipes, and similar structures not supported by a building	.025	Any direction horizontally

* See inside back cover [of Appendix to UBC] for zones. [The *C* values given are minimum values which are applicable only for Zone 1 (infrequent earthquakes).] For locations in Zone 2, "*C*" shall be doubled. For locations in Zone 3, "*C*" shall be multiplied by 4.

† Where wind load as set forth in Section 2307 would produce higher stresses, this load shall be used [instead of the seismic load].

‡ *N* is number of stories above the story under consideration, provided that for floors or horizontal bracing, *N* shall be only the number of stories contributing loads.

[in both longitudinal and transverse directions]. The bottom of such slab shall be not more than twelve inches above the tops of at least 80 per cent of the piers or foundations. The footings and foundations shall be tied to the slab [so] as to be restrained in all horizontal directions.

(d) **Plans and Design Data.** With each set of plans filed, a brief statement of the following items shall be included:

1. A summation of the dead and live load of the building, floor by floor, which was used in figuring the shears for which the building is designed.

2. A brief description of the bracing system used, the manner in which the designer expects such system to act, and a clear statement of any assumptions used. Assumption as to location of all points of counterflexure in members must be stated.

3. Sample calculation of a typical bent or equivalent.

(e) **Detailed Requirements.** 1. **Bonding and tying.** Cornices and ornamental details shall be bonded in the structure. . . . This applies to the interior as well as to the exterior of the building.

2. **Overturning moment.** . . . Calculated overturning moment . . . due to [earthquake] forces [not to] exceed two-thirds of the moment of stability. . . . Moment of stability shall be calculated using the same loads as used in calculating the overturning moment.

3. **Additions.** . . . To resist and withstand the [earthquake] forces. . . .

4. **Alterations.** . . . Resistance [not to be] less than that before such alteration.

5. **Building separations.** All portions of buildings and structures shall be designed and constructed to act as an integral in resisting lateral forces unless structurally separated by a distance of at least one inch, plus one-half inch for each ten feet of height above twenty feet. . . .

(f) **Lime Mortars.** Lime mortars shall not be used in any unit masonry construction forming a part of a building.

(g) **Intention or Interpretation of Lateral Force Provisions.** . . . The provisions incorporated in this Section are general and, in specific cases, may be interpreted or added to as to detail by rulings of the Building Official in order that the intent shall be fulfilled.

17.3. Japanese Building Code. As a consequence of the 1923 Kanto earthquake experience, a national building code was adopted which established a seismic coefficient of 0.1 together with low allowable stresses (17,000 psi for steel and others correspondingly low) without any provision for allowable increases in the stresses for combined stresses resulting from vertical and horizontal loadings. In subsequent years, the allowable unit stresses were increased by moderate amounts for steel up to 20,000 psi and correspondingly for other materials because of improved quality and properties.

A radical change was made in 1950 when the new Japanese Building Code was adopted. The basic seismic coefficient of 0.2 and allowable unit stresses approaching the yield or creep values of different materials were specified. The allowable steel stress was increased to 34,000 psi for combined stresses resulting from sustained and temporary loads. The bearing capacity of soils under seismic loading was doubled for all soil types, although there was some dissent among the members of the Structural Standards Committee of the Architectural Institute of Japan, which was entrusted with the task of preparing structural-design standards for construction in timber, steel, reinforced concrete, masonry, and foundations in harmony with the basic requirements of the new code. The need of structural criteria for everyday design often compels setting up provisions which are difficult to reconcile with true situations.

The structural provisions of the current code are compiled as a Japanese

Industrial Standard for Buildings, designated JIS 3001 and entitled Structural Calculations for Buildings. JIS 3001 specifies the design loads, allowable unit stresses, and other basic matters pertaining to structural design. The provisions are revised from time to time as results of research, investigations, and experience warrant such modifications. A more detailed background in the development of earthquake provisions in Japanese codes is given in the paper by Otsuki [2].

Provisions relating to earthquake-resistant design in JIS 3001 have been extracted below:

Chapter 1. General Provisions

Art. 1. This standard establishes the method of structural calculations as well as the loads, the allowable unit stresses, and other basic matters pertaining to structural calculations. This standard need not be used for buildings designed on the results of special investigations, and for temporary and small buildings.

Art. 2. Every portion of the structure shall be designed so that the unit stresses as determined in the prescribed manner of Art. 3 shall be less than the allowable unit stresses for the materials used, and the allowable bearing capacity of the soils.

Art. 3. The design stresses for each portion of the structure shall, under ordinary conditions, be the stresses resulting from the loads prescribed in Chapter 2, and the most unfavorable stresses resulting from special loads in addition to those prescribed above shall also be considered.

TABLE 17.2. COMBINATION OF STRESSES [JBC TABLE 1]

Loading	General areas	Heavy-snow districts	Remarks
Sustained . . .	Ordinary, $C + P$	$C + P + S$	When considering overturning of the building, pulling out of columns, etc., the live load may be somewhat reduced
Temporary . .	Snow, $C + P + S$	$C + P + S$	
	Storm, $C + P + W$	$C + P + S + W$	
	Earthquake, $C + P + K$	$C + P + S + K$	

C = stresses resulting from dead loads, as prescribed in Chap. 2, Sec. 2

P = stresses resulting from the live loads in Chap. 2, Sec. 3

S = stresses resulting from the snow loads in Chap. 2, Sec. 4

W = stresses resulting from wind loads in Chap. 2, Sec. 5; in heavy snow districts, when snow is considered as a sustained load, the wind load values due to cyclones are to be taken

K = stresses resulting from earthquake forces as prescribed in Chap. 2, Sec. 6

Art. 4. Portions of structures shall be strengthened or sections enlarged, taking into consideration errors resulting from assumptions in the design, improper construction, defective materials, rotting, and wearing of the materials which may be incorporated in the building.

Chapter 2. Loads

Section 1. General Provisions

Art. 5. Loads on buildings, under ordinary conditions, shall be the following: Dead load, live load, snow load, wind pressure, earthquake force. Depending on the use of the building, special loads other than those provided for herein must be considered.

Art. 6. For buildings of special importance, the loads established in this chapter must be increased appropriately.

Section 2. Dead Loads

Art. 7. Dead loads shall be established considering actual conditions.

Art. 8. Weight of different materials shall, under ordinary conditions, be taken from Table 2.

Table 2. Weight of Materials (omitted). Values for soils, stones, roof tiles, terra cotta, lightweight concrete, special concretes, ordinary concrete, metals, and woods listed.

Art. 9. Weight of different portions of a building shall be taken from Tables 3 through 8, unless calculated.

Table 3. Weight of Roof (omitted). Values for roofs of tile, asbestos slate, corrugated sheets, wooden purlins given.

Table 4. Weight of Roof Trusses, on horizontal plane, in kg/sq m. Wooden construction . . . $10 + L$. Steel construction . . . $10 + 0.8L$. Note: L is span in meters.

Table 5. Weight of Ceiling (omitted).

Table 6. Weight of Floors (omitted).

Table 7. Weight of Walls (omitted).

Table 8. Weight of Windows and Doors (omitted).

Section 3. Live Loads

Art. 10. Live loads shall be determined based on the following provisions:

1. Live load shall be determined on the basis of use of the floor and estimation of the loading conditions. When the weight of the materials on the floor is not actually computed, weights may be taken from Tables 9 and 10. For materials other than those listed, the live load is to be determined by referring to Section 2.

2. In determining the live load, load concentration must be considered taking into account the size of the tributary area.

3. Where vibration or impact action is involved, the live load should be increased appropriately.

Table 9. Average Weight of Persons and Furniture (omitted).

Table 10. Weight of Materials Other than Building Materials (omitted).

Art. 11. The live loads for use in the structural design of various members or portions, unless actually computed, may be taken from Table 11 [Table 17.3].

In computing the axial load on columns and footings due to vertical loads, the values given in Table 11 [Table 17.3], Column 2, may be reduced depending on the number of floors supported by them, according to Table 12 [Table 17.4].

TABLE 17.3. DESIGN LIVE LOADS [JBC TABLE 11]
In pounds per square foot

Type of occupancy	(1) Floor construction	(2) Girders, columns, and footings	(3) Earthquake analysis	(4) (3) ÷ (1)
<i>a.</i> Residences, hospital wards.	36	26	12	0.33
<i>b.</i> Office space.....	60	36	16	0.27
<i>c.</i> Stores, department stores..	60	48	26	0.43
<i>d.</i> Classrooms.....	46	42	22	0.48
<i>e.</i> Auditoriums, theatres with fixed seats.....	60	54	32	0.53
<i>f.</i> Same as <i>e</i> but with seats not fixed.....	72	66	42	0.58
<i>g.</i> Garages.....	110	80	40	0.36
<i>h.</i> Corridors, vestibules, and stairways	For types <i>d</i> , <i>e</i> , and <i>f</i> , the loads prescribed for type <i>f</i> are to be used; for other types, the loads for adjacent type of occupancy are to be used			
<i>i.</i> Roofs and balconies.....	Loads for type <i>a</i> are to be used; where congestion of people is likely, use loads for type <i>f</i>			

TABLE 17.4. VERTICAL AXIAL LOAD FOR COLUMNS AND FOOTINGS
[JBC TABLE 12]

	Number of floors supported			
	1	2	3	More than 4
Percentage of the loads given in Table 11 [Table 17.3], Col. 2	100	95	90	5% reduction for each floor supported with 60% as the minimum

Section 4. Snow Loads

Art. 12. Snow loads shall be computed on the basis of the following provisions:

1. Snow load is to be determined from maximum depth of snowfall and its unit weight.

2. Maximum vertical depth of snow on roofs shall be taken as the snow depth on flat ground, multiplied by the factors indicated in Table 13 [Table 17.5].

TABLE 17.5. ROOF SLOPE AND SNOW LOAD [JBC TABLE 13]

Slope	30° or less	30 to 60°	More than 60°
Value to be used.....	100 %	To be interpolated in direct proportion	0 %

For roofs having snow stops or for roofs where it is difficult to remove snow, special consideration of these factors is necessary.

3. Unit weight of snow in general is to be taken as 2 kg/sq m for 1 cm depth of snow, and more than 3 kg/sq m/cm in heavy snow areas.

4. When snow load is considered as a sustained load or also in combination with strong winds, earthquakes, etc., the value of the snow load may be reduced appropriately.

5. When the depth of snow deposit on each side of a pitched roof is considerably different, the effect of one-side loading is to be considered.

6. When snow is removed periodically from the roof, the design snow load may be reduced in consideration thereof.

7. At portions of the building where snow is likely to accumulate, the design snow load is to be increased in consideration thereof.

Section 5. Wind Pressure

Art. 13. Wind pressure for design is to be determined from the following equation when based on velocity pressure and wind pressure coefficients:

$$P = cq$$

P = wind pressure intensity in kg/sq m

c = wind pressure coefficient

q = velocity pressure in kg/sq m

The velocity pressures are values obtained from the following equation (see Fig. 1) [Fig. 17.1]:

$$q = 60 \sqrt{H}$$

where H is height from ground level in meters. However, under ordinary conditions, the step loadings indicated in Table 14 [Table 17.6] may be used.

TABLE 17.6. VELOCITY PRESSURES AND HEIGHT FROM THE GROUND SURFACE
[JBC TABLE 14]

<i>Height from the ground surface, m</i>	<i>Velocity pressure, kg/sq m</i>
0-8 (0-26.4 ft)	120 (24 psf)
8-15 (26.4-50 ft)	210 (42 psf)
15-30 (50-100 ft)	300 (60 psf)

Art. 14. Velocity pressures due to typhoons may be reduced depending on the locality (see Fig. 2) [Fig. 17.1].

Art. 15. Velocity pressures due to cyclones may be reduced depending on the locality (see Fig. 3) [see Fig. 17.1]. Note: Cyclone is defined as strong winds blowing mainly from the northwest direction during winter and spring months.

Art. 16. Velocity pressures referred to in Arts. 14 and 15 may be increased or reduced according to the following provisions:

1. A reduction may be made in areas removed from the sea coast or where the wind velocity is known definitely to be small.

2. A reduction may be made where wind impact is known definitely to be weak.

3. At sites where there are near obstacles, the velocity pressure may be reduced for wind coming from that direction.

4. An increase must be made on mountain tops, cliffs, etc., and wind channels where the impact of the wind is strong.

Art. 17. Wind pressure coefficients, under ordinary conditions, may be taken from Fig. 4 [Fig. 17.2].

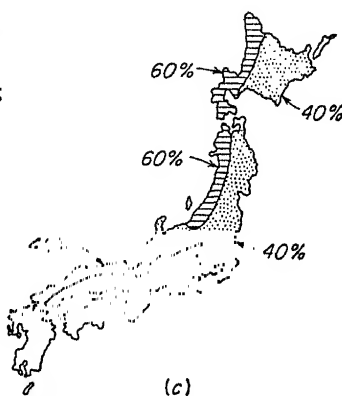
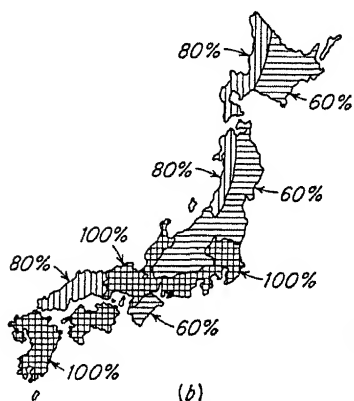
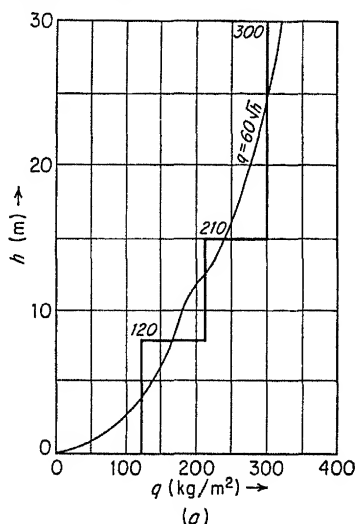


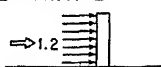
FIG. 17.1. Figures extracted from Japanese Building Code. (a) Relation of velocity pressure and height from standard. [JBC Fig. 1.] (b) Typhoon. Percentage of standard velocity pressure for design. [JBC Fig. 2.] (c) Cyclone. Percentage of standard velocity pressure for design. [JBC Fig. 3.]

Art. 18. Caution must be exercised where large negative pressures may build up on portions of a building.

Section 6. Earthquake Forces

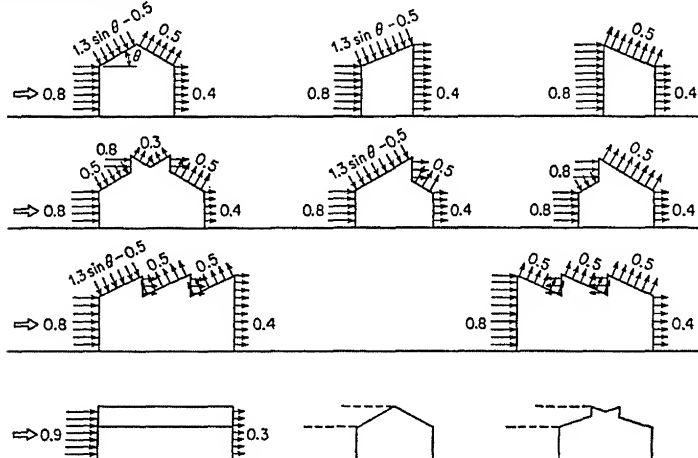
Art. 19. Earthquake forces must be determined by multiplying the horizontal seismic coefficient and the sum of the dead load and live load. In heavy snow districts, snow load must also be added to the above loads.

1. VERTICAL SURFACE



⇒ = Direction of wind

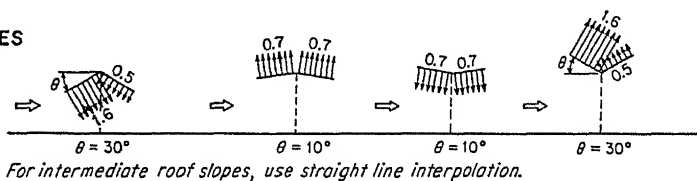
2. COVERED STRUCTURES



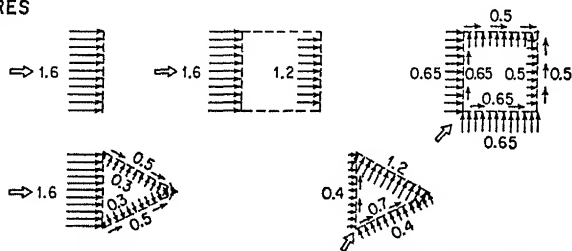
3. OPEN STRUCTURES



4. CANOPIES



5. LATTICED STRUCTURES



The area of lattice members to be subject to wind pressure shall be the area visible from a position normal to such members.

FIG. 17.2. Wind-pressure coefficients. [JBC Fig. 4.]

Art. 20. Horizontal seismic coefficients shall be determined as follows:

1. 0.2 or more on ordinary structures. In multistory buildings and structures projecting above the roof, the seismic coefficient must be increased.

2. 0.3 or more for wooden buildings resting on filled ground, built-up ground and other weak soils.

3. 0.3 or more for independent chimneys and chimneys extending above the roof level. However, with regard to overturning of the footings of chimneys the above values may be reduced by $\frac{1}{2}$.

4. The seismic coefficient values may be reduced where the earthquake force is known definitely to be small.

Chapter 3. Allowable Unit Stresses

Section 1. Wooden Construction

Articles 21 to 26 omitted.

Section 2. Steel Construction

Art. 27. The allowable stresses for steel, under ordinary conditions, shall be as shown in Table 19 [Table 17.7].

TABLE 17.7. ALLOWABLE UNIT STRESSES FOR STEEL [JBC TABLE 19]
In pounds per square inch

Material	Under sustained loading						Temporary loading
	Comp.	Tens.	BM	Shear	Bear.	Contact	
Structural steel...	22,700	22,700	22,700	11,350	42,500	65,200	1.5 times the values of the allowable stresses for sustained loading
Rivet steel.....		22,700	17,000	
Bolts:							
Unfinished.....		11,350	
Finished.....		14,200	17,000	
Cast steel.....	22,700	22,700	22,700	11,350	42,500	65,200	
Cast iron.....	14,200	39,600	

NOTE: Allowable rivet strength is to be computed on the basis of the diameter of the rivet hole. Allowable bolt strength in tension is to be based on the cross section of the bolt.

Art. 28. The allowable stresses of welded connections, based on throat thickness, shall be as shown in Table 20 [Table 17.8].

Art. 29. The allowable buckling stress in compression members shall be determined from the following equations, based on the effective slenderness ratio of the members:

$$\begin{aligned}
 \lambda &\leq 30 & f_x &= f_c \\
 30 &\leq \lambda \leq 100 & f_x &= f_c \left[1 - 0.4 \left(\frac{\lambda}{100} \right)^2 \right] \\
 \lambda &> 100 & f_x &= \frac{0.6f_c}{(\lambda/100)^2}
 \end{aligned}$$

where f_x = allowable buckling stress

f_c = allowable compressive stress

λ = effective slenderness ratio

Art. 30. Constants for structural steel shall be taken as indicated in Table 21 [Table 17.9].

TABLE 17.8. ALLOWABLE UNIT STRESSES FOR WELDED CONNECTIONS
[JBC TABLE 20]

In pounds per square inch

Welding	Type of joint	Sustained loading				Temporary loading
		Comp.	Tens.	BM	Shear	
Shop	Butt	19,700	19,700	19,700	9,850	1.5 times the values of the allowable stresses for sustained loading
	Fillet		11,380			
Field	Butt	17,000	17,000	17,000	8,500	
	Fillet		9,850			

TABLE 17.9. CONSTANTS FOR STRUCTURAL STEEL [JBC TABLE 21]

In pounds per square inch

Material	Young's modulus	Shear modulus	Poisson's ratio
Steel and cast steel	30×10^6	11.5×10^6	0.3

Section 3. Reinforced Concrete Construction

Art. 31. Allowable stresses for reinforced concrete, under ordinary conditions, shall be as indicated in Table 22 [Table 17.10].

TABLE 17.10. ALLOWABLE UNIT STRESSES FOR REINFORCED CONCRETE
[JBC TABLE 22]

In pounds per square inch

Material	Sustained loading				Temporary loading
	Comp.	Tens.	Shear	Bond	
Steel	22,700	22,700	1.5 times the allowable values for sustained loading
Concrete	$\frac{1}{8} F_c$; less than 1,000	$\frac{1}{50} F_c$; less than 100	...	100	2 times the allowable values for sustained loading

NOTE: F_c denotes ultimate compressive strength of concrete cylinders at 4 weeks.

Art. 32. Constants for reinforced concrete, under ordinary conditions, shall be taken from Table 23 [Table 17.11].

TABLE 17.11. CONSTANTS FOR REINFORCED CONCRETE [JBC TABLE 23]

	Young's modulus, psi		Modular ratio
	Steel	Concrete	
Frame analysis.....	30×10^6	3×10^6	10
Member design.....	30×10^6	2×10^6	15

Art. 33. When the minimum diameter of a rectangular compression member is less than 115 of the clear length of the member, consideration for buckling is required.

Section 4. Foundation Construction

Art. 34. The allowable bearing capacity of soils, under ordinary conditions, may be taken from Table 24 [Table 17.12]. However, for soils not included in the table, the presumptive bearing capacity shall be determined by reference to Table 24 [Table 17.12].

TABLE 17.12. ALLOWABLE BEARING CAPACITY OF SOILS [JBC TABLE 24]
In tons per square foot, approximately

Description	Sustained loading	Temporary loading
Hard rock.....	40	2 times the values for sustained loading
Soft rock.....	25-10	
Gravel, mixtures of sand and gravel, compact and loose	6-2	
Sand, compact and loose.....	4-1	
Mixtures of sand and clay, loam.....	3-1.5	
Clays, hard, medium, and soft.....	3-1	
Silt.....	0	To be determined according to actual conditions
Special soils.....		

Art. 35. Values given in Table [17.12] need not be used when the bearing capacity is determined by soil loading tests. Note: Bearing plates for the loading test of 45 cm square is standard, and the load producing a total settlement of 2 cm shall be considered the allowable bearing capacity for temporary loads and $\frac{1}{2}$ of this value as the bearing capacity under sustained loads. The total settlement is defined as the amount of settlement resulting from the applied load when the increment of the settlement in 24 hours becomes less than 0.1 mm.

Art. 36. The allowable bearing capacity of a pile, under ordinary conditions, shall be determined from the equations given in Table 25 [Table 17.13]. However, the stresses developed in the pile shall not exceed the allowable stresses of the pile material.

TABLE 17.13. ALLOWABLE BEARING CAPACITY OF PILES [JBC TABLE 25]
In metric tons

Driving equipment	Sustained loading	Temporary loading
Drop hammer.....	$R = \frac{0.15WH}{S+k} \frac{W}{W+P}$	2 times the values for sustained load- ing
Single-acting steam hammer.....	$R = \frac{0.18WH}{S+k} \frac{W}{W+P}$	
Double-acting steam hammer.....	$R = \frac{0.2F}{S+k} \frac{W}{W+P}$	

R = allowable bearing capacity of pile, metric tons

W = weight of hammer, metric tons

H = height of drop of hammer, cm

S = final penetration of pile under final blows of hammer, cm

P = weight of pile, metric tons

F = energy of impact of steam hammer, metric ton-cm

$k = 5RL/2AE + 0.15$ cm

L = pile length, cm

A = average cross-sectional area of pile, cm²

E = Young's modulus of pile material, metric tons/cm²

Art. 37. Provisions of the previous article need not be applied when the supporting power of the pile is determined from loading tests. Note: When the total settlement is 1.5 cm, the load causing this settlement may be taken as the allowable supporting power under temporary loading and $\frac{1}{2}$ of this value may be taken as the supporting power under sustained loading. Total settlement is defined as the amount of settlement resulting when the settlement increment in 24 hours becomes less than 0.1 mm.

17.4. Proposed Modifications in the Japanese Seismic Factors. The Architectural Institute of Japan, as of August, 1955, has proposed certain modifications with reference to seismic factors by taking into consideration the height of buildings, the relation between the type of construction and soil conditions, and the frequency expectation of destructive earthquakes in different regions in Japan, as follows:

1. Basic seismic factors for buildings:

Height above the ground, ft	Basic seismic factor C_o
Up to 52.5 (approx.).....	0.20
52.5-66.....	0.21
66-79.....	0.22
79-92.....	0.23
92-102 (limiting height).....	0.24

2. Modification of C_o for construction type and soil conditions (coefficient A):

Soil	Wood	Steel	Reinforced concrete	Masonry
Tertiary (old and firm formations)	0.6	0.6	0.8	1.0
Diluvium (thick gravel beds)	0.8	0.8	0.9	1.0
Alluvium (soft and recent formations)	1.0	1.0	1.0	1.0
Exceedingly soft	1.5	1.0	1.0	1.0

3. Modification of C_0 for different regions (coefficient B):

Regions

Kanto, Chubu, Kinki, which include cities of Tokyo, Yokohama, Kyoto, Osaka, Nagoya	1.0
Northeastern region, central region, island of Shikoku, and southern Hokkaido	0.9
Kyushu, northern Hokkaido	0.8

The design seismic factor C is to be determined from

$$C = C_0(\text{coefficient } A)(\text{coefficient } B)$$

When the product of the coefficients A and B is less than 0.5, it should be taken as 0.5.

17.5. Joint Committee Code for Lateral Forces. The Lateral Force Code prepared by the Joint Committee of San Francisco, California Section, ASCE, and Structural Engineers Association of Northern California and published in the *ASCE Proceedings*, vol. 77, separate no. 66, April, 1951, represents a work of outstanding significance and value in pointing toward a rational approach to the dynamic problem of earthquake-resistant design. For the first time, the determination of the seismic coefficient C takes into consideration the dynamic behavior of buildings. The qualitative variation of the dynamic shear acting on buildings is based on the characteristic properties of earthquakes as represented by the acceleration spectra determined by Biot and Robison based on past earthquakes for undamped one-mass systems with varying fundamental periods T as shown in Fig. 17.3. The distribution of the base shear V to different floor levels assumes an inverted triangular loading with twice the average load at the top and zero load at the base on the assumption that buildings deflect half in bending and half in shear.

A maximum seismic coefficient of 6 per cent for buildings with low periods of vibration in the fundamental mode up to 0.25 sec and a minimum seismic coefficient of 2 per cent for buildings with periods of vibration greater than 0.75 sec have been designated, based on past earthquake experience on the West Coast as shown in Fig. 17.4. The permissible unit stresses may be increased by one-third for combined stresses due to sustained and temporary loads of earthquake or wind.

As pointed out by the Joint Committee [3], this code specifies design and construction provisions which will guard against major structural damage and loss of life and does not attempt more than this. J. E. Rinne, chairman of the Joint Committee, discusses the various considerations leading to the Lateral Force Code development in another paper

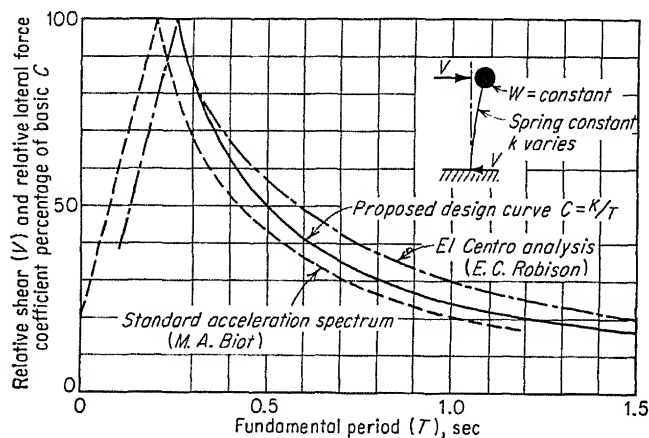


FIG. 17.3. Response of simplified structures to earthquakes.

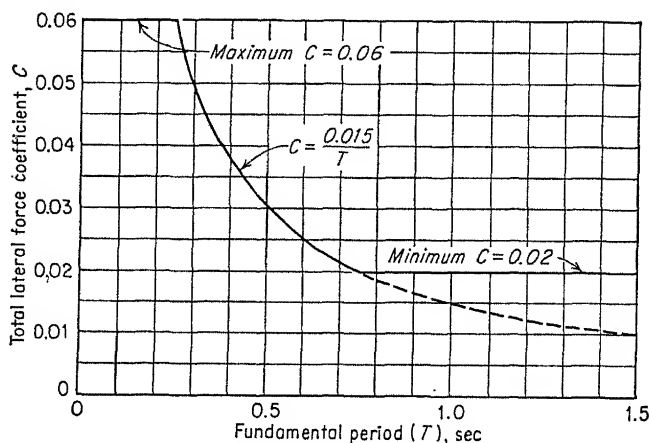


FIG. 17.4. Lateral-force coefficients for buildings.

[4] which indicates the numerous difficulties and complications inherent in the problem of practical aseismic design.

San Francisco had adopted a building code based on the Joint Committee Code with slight modifications, on the side of safety, as follows:

$$C = \frac{0.02}{T} \quad (17.3)$$

for the building as a whole, and C is to be not less than 0.035 or more than 0.075.

$$C = \frac{0.035}{T} \quad (17.4)$$

for all structures other than buildings, and C is to be not less than 0.04 or more than 0.10.

The Joint Committee Code for lateral forces is reproduced below.

SECT. 01.—GENERAL REQUIREMENTS

Every building and other structure, in all its parts and details, shall be designed and constructed to resist and withstand lateral forces herein described from any direction due to wind forces or earthquake forces, whichever are greater. The forces considered shall be not less than those described in Sections 02, 03, and 04. In general, every building or structure shall be so designed that all its elements calculated to resist lateral forces are tied and bonded together.

SECT. 02.—WIND PRESSURE

(a) For purposes of design the wind pressure shall be taken on gross area of the vertical projection of buildings and structures at not less than 15 lb per sq ft for those areas of the building or structure less than 60 ft above ground and at not less than 20 lb per sq ft for areas more than 60 ft above ground. Roofs and their anchorages shall be designed for an uplift force of 10 lb per sq ft.

(b) The wind pressure on roof tanks, roof signs, or other exposed roof structures and their supports, shall be taken as not less than 30 lb per sq ft of the gross area of the plane surface, acting in any direction.

(c) In calculating the wind pressure on circular tanks, towers, or stacks, these pressures shall be assumed to act on six-tenths of the projected area.

(d) On open-framed structures the area used in computing wind pressure shall be one and one-half times the net area of the framing members in the side exposed to the wind using a base pressure of 30 lb per sq ft.

SECT. 03.—MINIMUM EARTHQUAKE FORCES FOR BUILDINGS

(a) *Total Lateral Force.*—Every building shall be designed and constructed to withstand minimum total lateral forces, determined independently in the directions of the principal axis of the building, as given by the formula,

$$V = CW$$

in which V is the total lateral force or shear at the base; C is the numerical coefficient as given hereafter; and W is the total weight of the building above the base, including dead load plus a percentage of the live load hereinafter specified.

(b) *Coefficient C .*—

1. In the building as a whole the coefficient C shall be

$$C = \frac{0.015}{T}$$

in which T is the fundamental period of vibration of the building in seconds in the direction considered. The required value of C shall not be less than 0.02 nor more than 0.06.

2. Qualified persons may submit technical data to substantiate the period T obtaining for a contemplated building. In the absence of such data, it may be assumed that

$$T = 0.05 \frac{H}{\sqrt{b}}$$

in which H is the height of the main portion of the building, in feet, measured above the base which shall be the level at which the structure is positively connected to the ground; and b is the width, in feet, of the main portion of the building in the direction considered.

(c) *The Weight W .*—The weight W of buildings shall include all dead load plus 50% of the design live load for storage and warehouse floors, 25% of the design live load for all other floors, and no live load for roofs.

(d) *Applied Lateral Forces.*—

1. The total lateral force V shall be distributed over the height of the building in accordance with the following formula:

$$F_x = V \frac{w_x h_x}{\Sigma(wh)}$$

in which F_x is the lateral force applied to any level x ; w_x is the weight at level x ; h_x is the height of level x above the base; and $\Sigma(wh)$ is the summation of the products wh for the building.

2. At each level x , the force F_x shall be applied over the area of the building, in accordance with the mass distribution on that level.

(e) *Lateral Forces on Parts of the Building.*—

1. Parts of buildings and their anchorage shall be designed for lateral forces determined from the formula,

$$F_P = C_P W_P$$

in which F_P is the lateral force on the part and in the direction under considera-

TABLE 17.14. COEFFICIENTS C_P FOR USE IN SECT. 03(e)1

Part	C_P	Comment	Direction
Exterior walls and other nonresisting elements not otherwise classified	0.20	With a minimum of 15 lb per sq ft	Normal to surface of wall
Interior walls and partitions	0.10	With a minimum of 5 lb per sq ft	
Parapet walls, exterior and interior ornamentalations	0.50	Any direction horizontally
Towers and tanks, including contents, chimneys, smokestacks, and penthouses when connected to or part of a building	0.20	Any direction horizontally

tion; W_P is the weight of the part; and C_P is a coefficient selected from [Table 17.14].

2. The distribution of these forces shall be according to the gravity loads pertaining thereto.

SECT. 04.—MINIMUM EARTHQUAKE FORCES FOR OTHER STRUCTURES

(a) All structures other than buildings, except tower-supported structures, shall be designed and constructed to withstand minimum total lateral forces determined as for buildings (Sect. 03) except that C shall be determined by

$$C = \frac{0.025}{T}$$

in which the required value of C shall not be less than 0.03 nor more than 0.10. Qualified persons may submit technical data to substantiate the period T obtaining for a contemplated structure; otherwise T shall be calculated by recognized methods assuming fixed base conditions.

(b) In all tower-supported structures, such as elevated tanks, C shall not be less than 0.10.

(c) The total lateral force shall be distributed over the height of the structure in the same manner as for buildings, Sect. 03(d).

(d) The weight W shall include all dead load plus normal operating live load.

(e) The provisions of Sect. 03(e) shall apply also to parts of structures other than buildings. . . .

SECT. 05.—DISTRIBUTION OF HORIZONTAL SHEAR

The total horizontal shear at any horizontal plane shall be distributed to the various resisting elements in proportion to rigidities.

SECT. 06.—HORIZONTAL TORSIONAL MOMENTS

Proper provision shall be made for horizontal torsional moments unless the center of rigidity of the resisting structural units is coincident with the center of gravity of the vertical loads in the building or other structure.

SECT. 07.—PROVISIONS AGAINST OVERTURNING

(a) The dead load moment of stability of every building or other structure shall not be less than one and one-half times the overturning moment caused by wind pressure.

(b) Provision for overturning moment shall be made for the specified earthquake forces in the top ten stories of buildings or the top 120 ft of other structures, and the moments shall be assumed to remain constant from these levels into the foundations.

SECT. 08.—BUILDINGS HAVING SETBACKS

(a) Buildings with setbacks shall be designed by the methods previously specified in Sect. 03 except that, for purposes of determining the period T , the coefficient C , and the base shear V , the height H shall be the average derived

by dividing the area of the elevation of the building, as projected on a plane parallel to the direction considered, by the base width b .

(b) Towers having a plan area less than 25% of the plan area of the lower part of the building may be designed as separate structures for their own height, width, and weight. In this case the resulting total shear from the tower is to be applied at the top of the lower part of the building which shall be otherwise considered separately for its own height, width, and weight.

SECT. 09.—DESIGN REQUIREMENTS

(a) *Structural Frames*.—The lateral force-resisting capacity of any moment-resisting structural frame may be deducted from the total required lateral force to determine the required resistance of other lateral force-resisting elements, provided that such a frame has a resistance of at least 25% of the total lateral forces hereinbefore required, and provided that the building or structure as a whole shall be designed to resist a lateral force resulting from a coefficient C equal to not less than 0.02.

(b) *High Buildings*.—In buildings higher than 135 ft a moment-resisting frame shall be provided, designed to resist a lateral force resulting from a coefficient C equal to 0.01, or the wind force specified in Sect. 02, whichever is the greater.

(c) *Increase of Unit Stresses for Horizontal Forces*.—

1. For combined stresses due to lateral loads caused by earthquakes or wind, and for the vertical design dead and live loads as defined elsewhere, the permissible unit stresses may be increased one third, provided the section thus required is not less than that required for dead and live loads alone. For members carrying stresses due only to lateral forces caused by earthquakes or wind the permissible unit stresses may be increased one third.

2. In foundations due consideration shall be given to the capacity of the soil under combined vertical and short time lateral loading, but any increase shall not exceed 100% of the normal bearing value.

(d) *Combined Axial and Bending Stresses in Columns*.—

1. Maximum allowable extreme fiber stress in columns at the intersection of a column with floor beams or girders, for combined axial and bending stresses, shall be the allowable bending stress for the material used. Within the center one-half of the unsupported length of the column, the combined axial and bending stresses shall be such that

$$\frac{f_a}{f_{sa}} + \frac{f_b}{f_{sb}} \leq 1$$

in which f_a is the axial stress; f_{sa} is the allowable axial stress; f_b is the bending stress; and f_{sb} is the allowable bending stress.

2. When stresses are due to a combination of vertical and lateral loads, the allowable unit stresses may be increased as provided in Sect. 09(c).

REFERENCES

1. Andrus, F. M.: Earthquake Design Requirements of the Uniform Building Code, in "Proceedings of Symposium on Earthquake and Blast Effects on Structures," EERI and University of California, Los Angeles, June, 1952.

2. Otsuki, Y.: Development of Earthquake Building Construction in Japan, in "Proceedings of World Conference on Earthquake Engineering," EERI and University of California, Berkeley, June, 1956.
3. Lateral Forces of Earthquakes and Wind, *Proc. ASCE*, vol. 77, separate no. 66, April, 1951.
4. Rinne, J. E.: Building Code Provisions for Aseismic Design, in "Proceedings of Symposium on Earthquake and Blast Effects on Structures," EERI and University of California, Los Angeles, June, 1952.

CHAPTER 18

EARTHQUAKE-RESISTANT-DESIGN METHODS AND PRACTICE

18.1. Introduction. Day-to-day design of buildings for earthquake forces usually employs equivalent static loads that are determined in accordance with provisions in the applicable building code. The determination of earthquake forces by the Uniform Building Code and the modified Japanese Building Code is based on the constant-acceleration concept, while the Joint Committee Code is based on consideration of the earthquake spectra of past Pacific Coast earthquakes. The constant-acceleration concept is generally justifiable for rigid, shear-type buildings with short periods of vibration. The velocity-spectrum technique of Housner and Hudson may be applied expediently to moderately flexible structures such as high stacks and elevated water-tank towers. For tall buildings with long periods of vibration, perhaps another design criterion such as constant displacement may be indicated.

Dynamic methods of analysis applicable to earthquake-resistant design and some examples of such application are briefly referred to without attempting to explain the methods fully. Statical methods of design which are used in ordinary design offices are more fully described with examples, and a comparative study of aseismic designs by three different building codes is included.

18.2. Dynamic Methods of Analysis. The theory of structural dynamics (Chaps. 3 to 6) may be applied to actual buildings by representing the prototypes by idealized systems and obtaining solutions by simplified analysis (Chap. 7). The application of the theory to cases other than one-mass or several-mass systems involves a great deal of calculations and for actual situations becomes impractical as a normal design procedure. Cheney shows an application of the normal-mode method of analysis for a two-story building for earthquake loading which involves the determination of participation factor, dynamic-load factor, and characteristic values, as developed in Chap. 4 of this book [1]. Housner shows an application of the response-spectrum method of analysis for earthquake-resistant design of tall stacks [2], and others have employed methods combining the normal-mode and earthquake-

spectra technique in the studies of the behavior of elevated water-tank towers and refinery vessels [3].

Three different dynamic methods of analysis applicable to the earthquake problem were presented by Housner, Jacobsen, and Newmark at the Symposium on Earthquake and Blast Effects on Structures held at UCLA in June, 1952 [4-6]. Newmark presented another paper complementary to the above at the Conference on Building in the Atomic Age, Massachusetts Institute of Technology, June, 1952 [7]. At the World Conference on Earthquake Engineering, University of California, Berkeley, June, 1956, Hudson and Housner [8, 9] further elaborated on their response-spectra technique and Ayre [10] discussed the dynamic response of shear-type buildings, using, in part, the phase-plane-delta method.

a. Earthquake-spectrum Technique. The technique developed at California Institute of Technology employs a direct electric analog computer for the determination of earthquake-response spectra. A series electrical circuit consisting of an inductance, a capacitance, and a resistance forms a direct analogy to the mechanical single-degree-of-freedom system. The ground-acceleration record is reproduced, and the response characteristics are measured as voltages at various points in the circuit. By this technique, response spectra have been determined for strong-motion earthquakes on the Pacific Coast, and characteristics of these earthquakes have been studied. Practical applications of this technique to determine the dynamic response of structures subjected to ground disturbances by Hudson and Housner demonstrate the significance of this new development [8, 9].

b. Phase-plane-delta Method. The method described by Jacobsen is an expedient graphical method for obtaining the dynamic response of structures subjected to blast or earthquake loadings and involving deformations from the elastic into the plastic range. The ground-acceleration-time function is approximated by rectangular block doublets, and a first-order differential equation of motion is obtained with displacement and velocity as the variables which are plotted in the phase plane. Several examples in the paper illustrate the use of the method in one-mass systems.

c. Numerical-integration Methods. The method presented by Newmark is completely general in determining the response of structures under any type of dynamic loading. The structure is represented by an idealized lumped-mass system in the usual manner, and the relationship between force and displacement is assumed at the beginning. Numerical step-by-step integration is carried out on the basis of assumed displacements which are checked and modified until compatibility is satisfied. This procedure is applicable in all ranges of deformation. The use of

rapid electronic computing equipment facilitates obtaining solutions for complicated structures such as multistory buildings.

A numerical method for use in the design office has been proposed by Whitney, Anderson, and Salvadori (*J. ACI*, September, 1951) for the analysis of shear buildings under sinusoidal pulses which considers structural stiffness and rocking of buildings about the foundation.

18.3. Statical Methods of Design. The highly indeterminate multi-story building frames subjected to horizontal static loads require involved calculations by the so-called exact methods such as the slope-deflection method. Consequently, convenient approximate methods have been developed ranging from crude approximations to more rational approximations.

a. Approximate Methods. The cantilever and portal methods are the better-known approximate methods widely used in the past. Certain modifications in the above methods have been proposed from time to time such as the modified portal method by Naito. Another method based on the study of numerous bents by the slope-deflection method is the one suggested by Bowman [12]. The factor method, developed by Wilbur, which considers the stiffness of the members of building frames [13], and the AIJ (Architectural Institute of Japan) method, based on investigations of Muto, which also considers the member stiffnesses [14], are representative of the more rational approximate methods. The factor method, the AIJ method, and the Bowman method can be expected to give generally good results for regular building frames. The assumptions and procedures to be followed in these methods are outlined briefly.

In the *cantilever method*, the following assumptions are made in order to render the building frames statically determinate:

1. Points of inflection are located at the mid-span of girders.
2. Points of inflection are located at the mid-height of columns.
3. Unit direct stresses in the columns vary as the distances of the columns from the center of gravity of the bent. (It is usually assumed that all columns in a story are of equal area. In this case, the total axial forces in the columns will vary as the distances from the center of gravity of the bent.)

In the *portal method*, the following assumptions are made:

1. Same as in the cantilever method.
2. Same as in the cantilever method.
3. The shear in the exterior columns is the same and is equal to one-half the shear in the interior columns, which is the same for all interior columns in a given story.

In the *modified portal method*, the following modifying assumptions are made:

1. Same as in the portal method except in the lower stories, which are determined by the requirements of statical equilibrium.

2. Same as in the portal method except in the top story, where the points of inflection are located 0.4 of the story height measured from the bottom, and in the bottom story, where they are located 0.6 of the story height from the bottom.

3. Same as in the portal method, except for the bottom story, where the shear in the exterior column is 0.8 of the shear in the interior column.

In the *Bowman method*, the following assumptions are made:

1. Points of contraflexure in exterior girders are located at 0.55 of their length from their outer ends and in other girders at their mid-points except (a) in the center bay, where the total number of bays is odd, and (b) in the two bays nearest the center, where the total number of bays is even. In these excepted cases the points of contraflexure in girders will be located as required by conditions of symmetry and equilibrium.

2. In bents of one or more stories, the points of contraflexure in bottom-story columns are at 0.60 height from the base; in bents of two or more stories, the points of contraflexure in top-story columns are at 0.65 height from the top; in bents of three or more stories, the points of contraflexure in the columns of the story next to the top are at 0.60 height from the upper end; in bents of four or more stories, the points of contraflexure in the columns of the second story from the top are located at 0.55 height from the upper end; and in bents of five or more stories the points of contraflexure in the columns of stories not provided for above are at 0.50 height.

3. There is divided equally* among the columns of the bottom story an amount of shear equal to $(\text{number of bays} - \frac{1}{2})/(\text{number of columns})$ times the total shear in the story; the remaining shear in the bottom story is divided among the bays inversely as their widths;† and the shear in a bay is divided equally between the two columns adjacent to the bay. There is divided equally* among the columns of other stories an amount of shear equal to $(\text{number of bays} - 2)/(\text{number of columns})$ times the total shear in the story; the remaining shear in the story is divided among the bays inversely as their widths;† and the shear in a bay is divided equally between the two columns adjacent to the bay.

b. *The Factor Method.* This method may be considered as an approximate slope-deflection method using correct relative-stiffness values of

* Where the column moments of inertia of a story are not equal, as when investigating an existing building, this part of the shear is to be divided among the columns in proportion to their moments of inertia.

† Where the moments of inertia of the girders above any story are not equal, this part of the shear should be divided among the bays directly as the stiffnesses of the girders above the bays.

the members of the frame. The following six steps are involved in this method:

1. For each joint, compute the girder factor g by the following: $g = \Sigma K_c / \Sigma K$, where ΣK_c denotes the sum of the K values for the columns meeting at that joint, and ΣK denotes the sum of the K values for all members of that joint. Write each value of g thus obtained at the near end of each girder meeting at the joint where it is computed.

2. For each joint, compute the column factor c by the following: $c = 1 - g$, where g is the girder factor for that joint as computed in step 1. Write each value of c thus obtained at the near end of each column meeting at the joint where it is computed. For the fixed column bases of the first story, take $c = 1$.

3. From steps 1 and 2, there is a number at each end of each member of the bent. To each of these numbers, add half of the number at the other end of the member.

4. Multiply each sum obtained from step 3 by the K value for the member in which the sum occurs. For columns, call this product the column moment factor C ; for girders, call this product the girder moment factor G .

5. The column moment factors C from step 4 are actually the approximate relative values for column end moments for the story in which they occur. The sum of the column end moments in a given story may be shown by statics to equal the total horizontal shear on that story multiplied by the story height. Hence, the column moment factors C may be converted into column end moments, by direct proportion, for each story.

6. The girder moment factors G from step 4 are actually approximate relative values for girder end moments at each joint. The sum of the girder end moments at each joint equals, by statics, the sum of the column end moments at that joint, which can be obtained from step 5. Hence, the girder moment factors G may be converted to girder end moments, by direct proportion, for each joint.

c. AIJ (Architectural Institute of Japan) Method. The provisions of this method are as follows:

1. The analysis of rectangular frames acted on by horizontal loads is based on the following assumptions:

- (a) The horizontal loads are considered to act in the longitudinal and transverse directions, separately.

- (b) The deflection of any given story of a building consisting of various bents is considered to be the same, except in special cases.

2. If an exact method of analysis is not used, an approximate method embodying the provisions of items 3 and 4 below and one which takes into consideration the relative stiffness of the members of the frame is to be used.

3. For frames in which the lower ends of the bottom-story columns may

be considered as fixed and the horizontal forces acting at each floor level are approximately of the same magnitude, the shears, bending moments, and direct axial loads are to be computed in the order indicated below.

(a) Shear distribution in columns. The shear is divided among the columns of any story in proportion to the value of D , to be determined from the relation

$$D = ak_c$$

where $a = \bar{k}/(2 + \bar{k})$, for all stories except lowest

$a = (1 + \bar{k})/(2 + \bar{k})$, for lowest story

k_c = column-stiffness ratio

$\bar{k} = \frac{1}{2}(\text{sum of girder stiffnesses at top and bottom})/(\text{column stiffness})$, for columns of all stories except lowest

$\bar{k} = (\text{sum of girder stiffnesses at top of column})/(\text{column stiffness})$, for columns in lowest story

(b) Location of points of inflection in columns. The point of inflection of each column is to be determined from the following relation, where y is measured from the base of a column:

$$y = (y_0 + y_1 + y_2 + y_3)h$$

where y_0 = standard point of inflection (AIJ-1 to AIJ-12)

y_1 = correction for differences in stiffness of girders framing into column at top and bottom; need not be considered for lowest story (AIJ-13)

y_2 = correction for difference in story height above column under consideration; need not be considered for top story (AIJ-14)

y_3 = correction for differences in story height below column under consideration; need not be considered for lowest story (AIJ-14)

h = story height

(c) Column and girder bending moments. The column bending moments to be computed from the calculated column shears and points of inflection of columns. Girder bending moments to be obtained from column moments at the joint in question in proportion to the stiffness of the girders.

(d) Girder shears and column direct loads. The girder shears to be determined from the bending moments acting at the ends of the girder under consideration, and the column direct loads by algebraic summation of girder shears, starting from the top story.

d. Exact Methods. The slope-deflection method and moment-distribution method represent practically usable methods for the solution of multistory-building frames. The adequacy of any approximate method is judged by the degree of agreement obtained in the results by the approximate and exact methods.

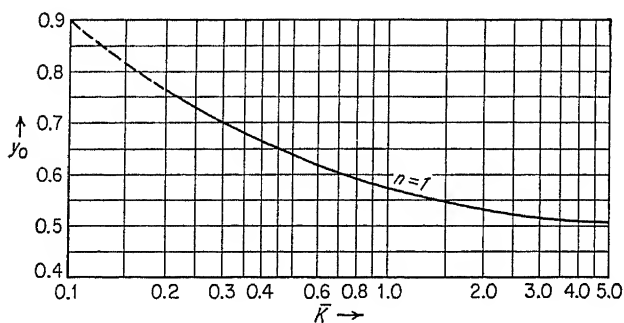


FIG. 18.1. Chart AIJ-1. y_0 for one-story frame. n denotes location of story.

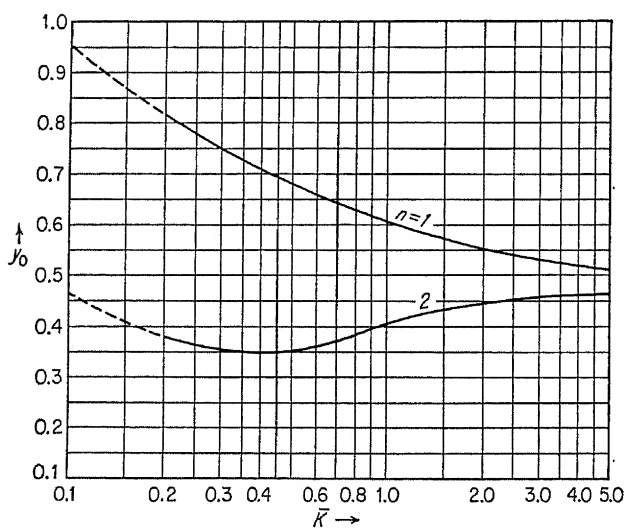


FIG. 18.2. Chart AIJ-2. y_0 for two-story frame. n denotes location of story.

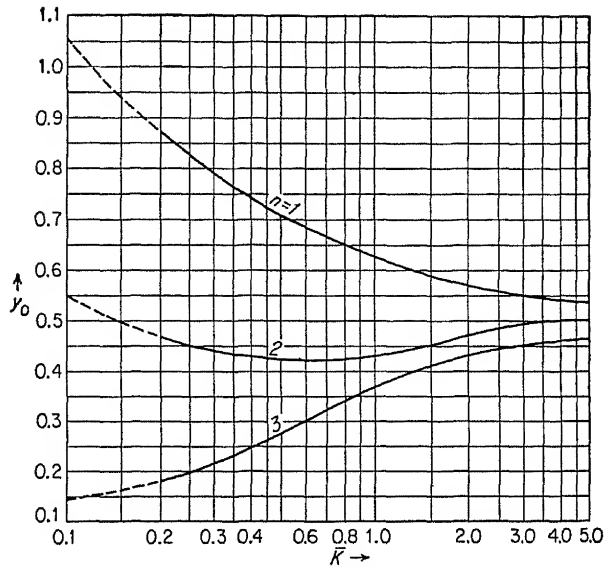


FIG. 18.3. Chart AIJ-3. y_0 for three-story frame. n denotes location of story.

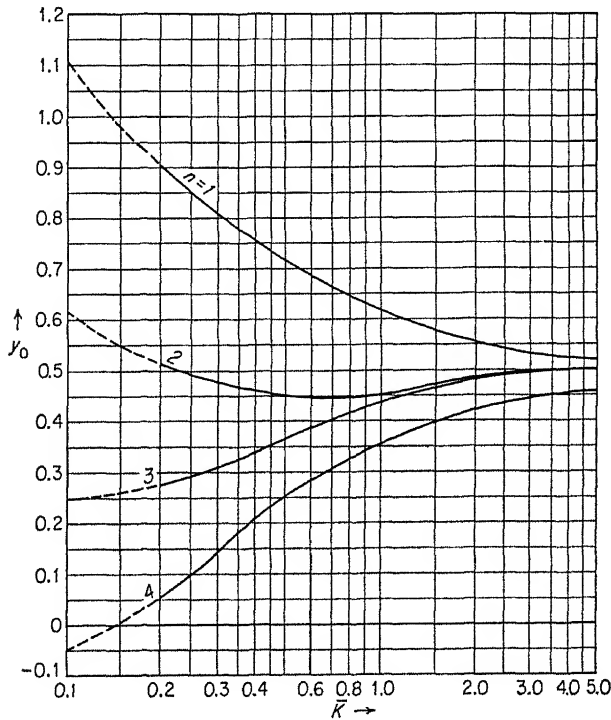


FIG. 18.4. Chart AIJ-4. y_0 for four-story frame. n denotes location of story.

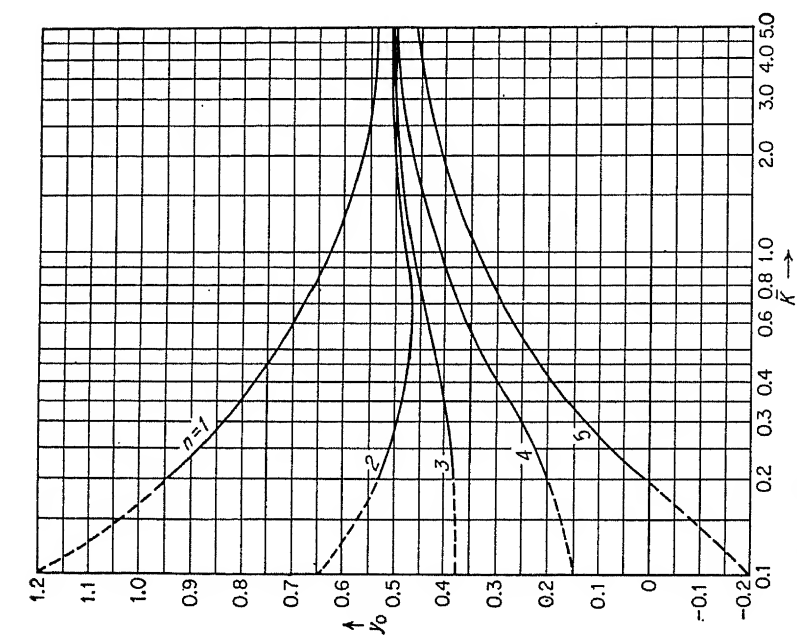


Fig. 18.5. Chart AIJ-5. y_0 for five-story frame. n denotes location of story.

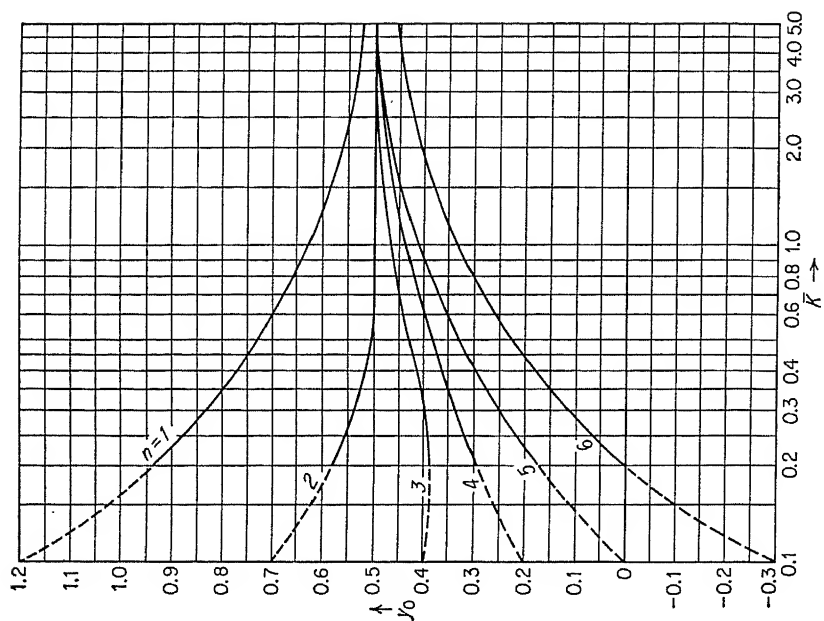


Fig. 18.6. Chart AIJ-6. y_0 for six-story frame. n denotes location of story.

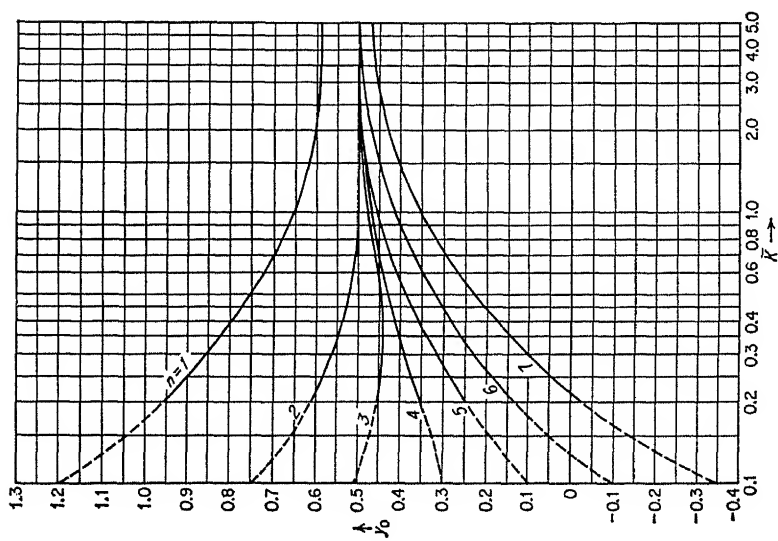


Fig. 18.7. Chart AIJ-7. y_0 for seven-story frame. n denotes location of story.

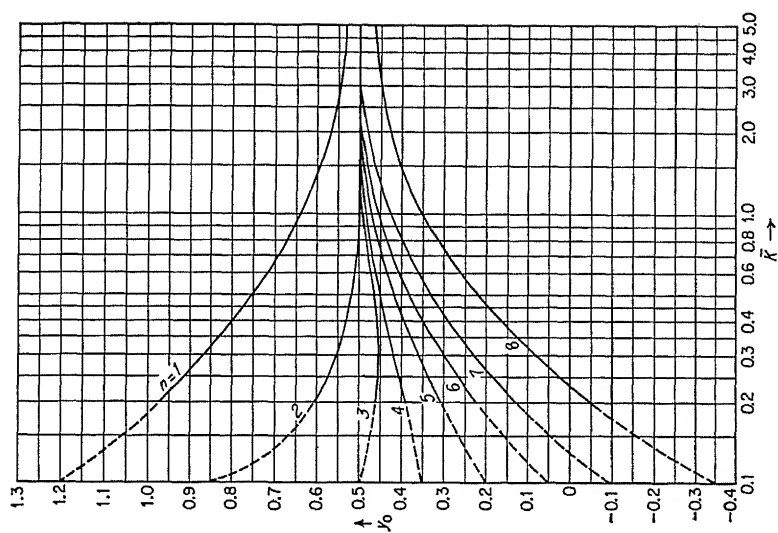


Fig. 18.8. Chart AIJ-8. y_0 for eight-story frame. n denotes location of story.

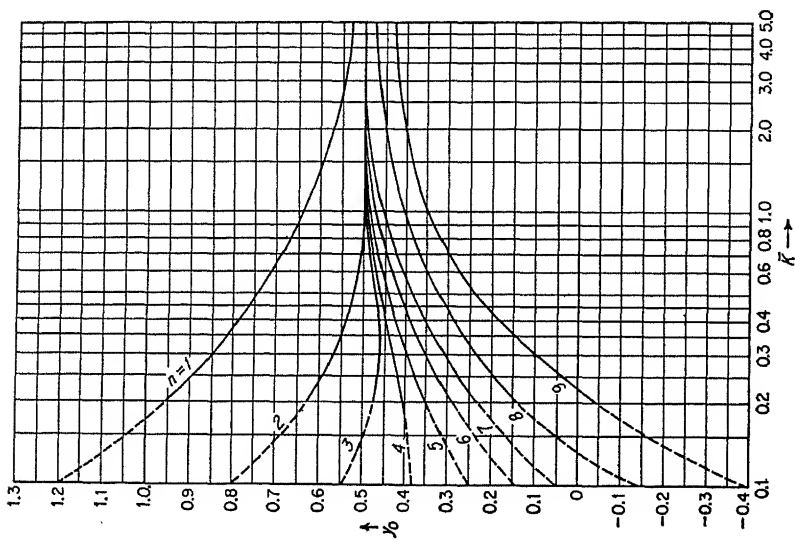


Fig. 18.9. Chart AIJ-9. y_0 for nine-story frame. n denotes location of story.

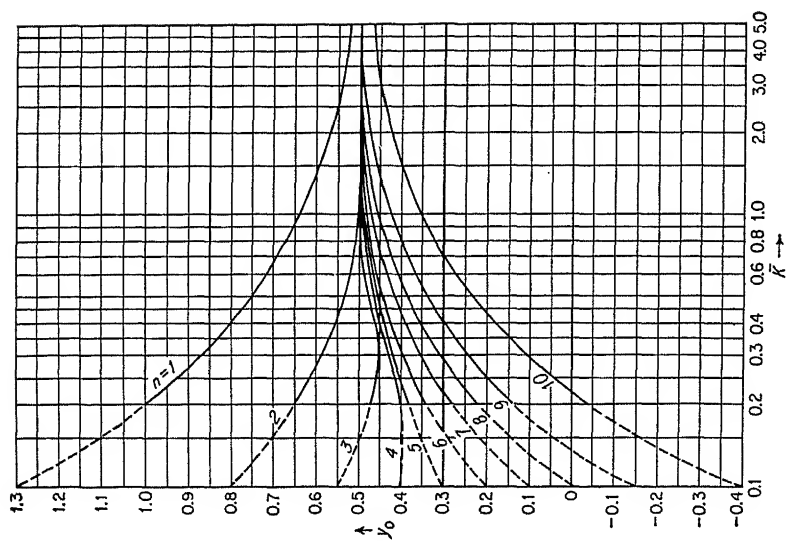


Fig. 18.10. Chart AIJ-10. y_0 for 10-story frame. n denotes location of story.

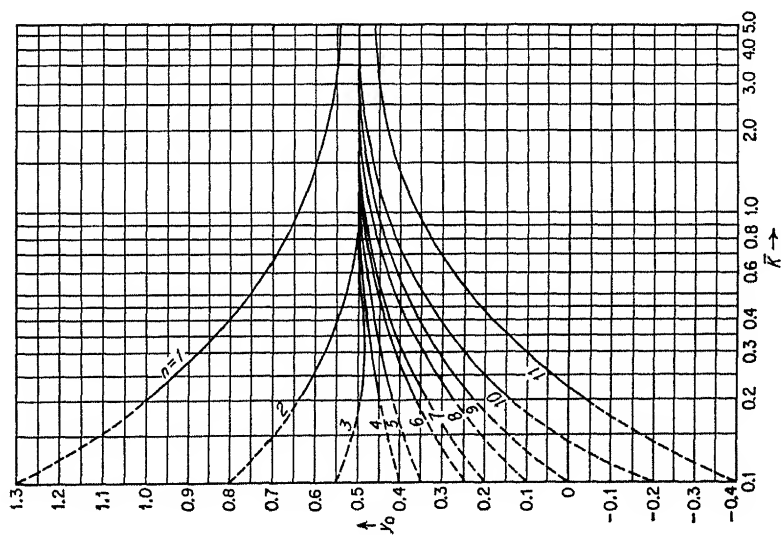


Fig. 18.11. Chart AIJ-11. y_0 for 11-story frame. n denotes location of story.

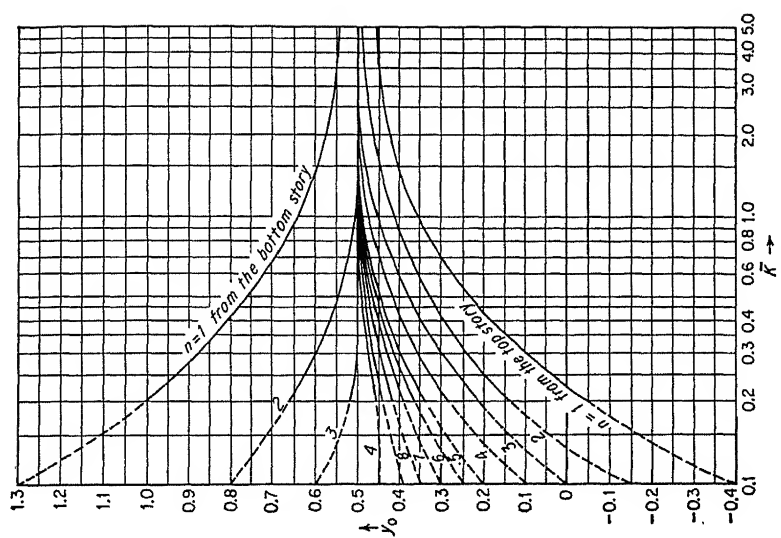
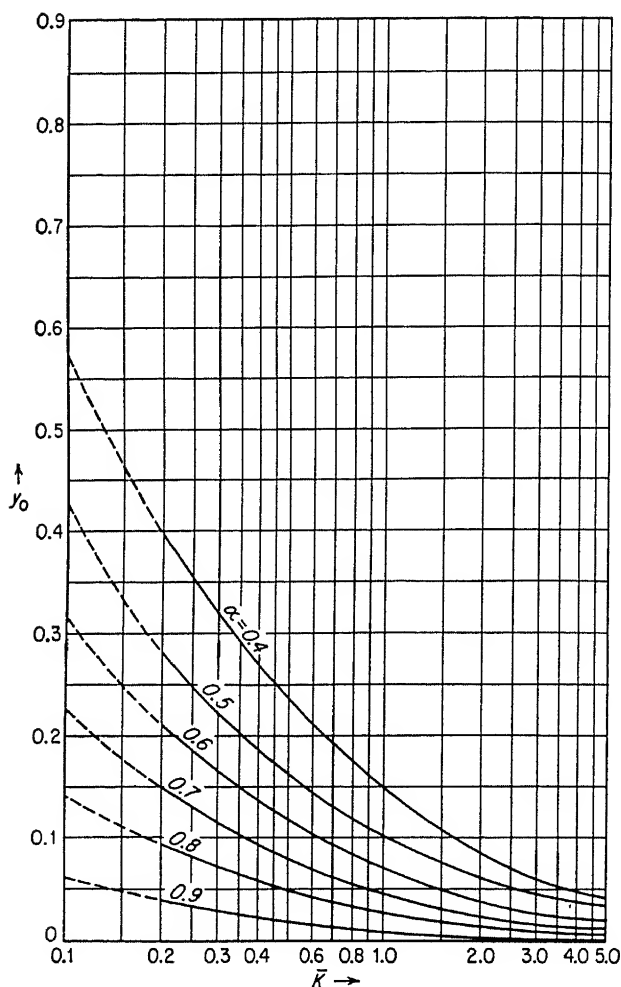


Fig. 18.12. Chart AIJ-12. y_0 for 12-story or more frame. n denotes location of story.



NOTE: Need not be considered for the lowest story.

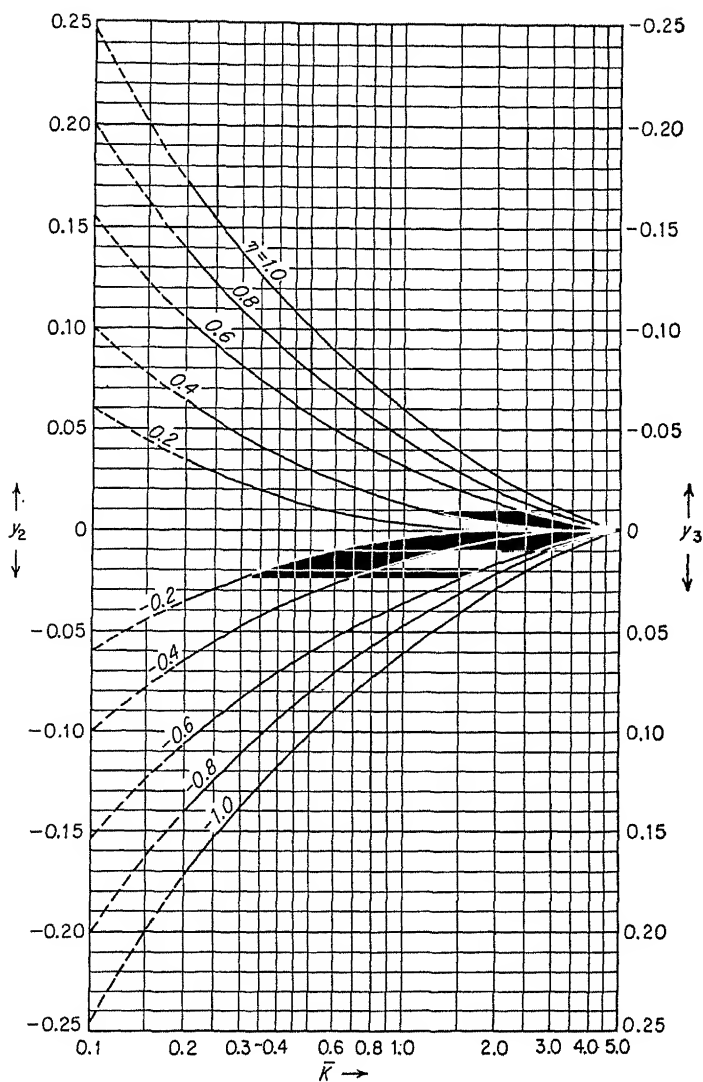
$$\alpha = \frac{\Sigma K \text{ of girders above}}{\Sigma K \text{ of girders below}}$$

When the stiffness of the girders below the column is less than that of the girders at the top, take

$$\alpha = \frac{\Sigma K \text{ of girders at bottom}}{\Sigma K \text{ of girders at top}}$$

and use the negative sign of the value thus obtained.

FIG. 18.13. Chart AIJ-13. Correction value y_1 due to variation in girder stiffness.



NOTE:

$$\eta = \frac{h \text{ (above)}}{h} - 1 \quad \text{in reading } y_2$$

$$\eta = \frac{h \text{ (below)}}{h} - 1 \quad \text{in reading } y_3$$

y_2 need not be considered for the top story. y_3 need not be considered for the bottom story.

FIG. 18.14. Chart AIJ-14. Correction values y_2 and y_3 due to variation in story heights.

18.4. Design of Actual Buildings. A reinforced-concrete eight-story building, seven stories aboveground with one basement story, will be used to illustrate the application of different methods of solution and to make certain comparisons. This building was designed in the office of Dr. T. Naito during the author's association in this office between 1933 and 1937. The north elevation of this department store is shown in Fig. 18.15. A typical section through columns A_3-E_3 is shown in Fig. 18.16. Beam plans and foundation plan and sections are shown in Fig. 18.17, and it will be noted that footings are interconnected with strong tie beams and a foundation slab is provided under the entire building. The design loads for the slabs, beams (girders), and columns and for seismic loading are assembled in Table 18.1. When this building was designed, the seismic coefficient then used was 0.1, and 50 per cent of the floor live load was taken for seismic computations with the allowable unit stress for steel of 17,000 psi without any permissible increase in this value for combined stress resulting from sustained and temporary-earthquake loadings. Based on the study of architectural drawings, the seismic-distribution coefficients D^* were evaluated for each bay for all stories in two principal directions, which are indicated in Fig. 18.18 for each story. The value of $D = 1$ is assigned to a normal open bay, and a maximum value of $D = 8$ or 9 has been assigned to a walled bay without openings, and intermediate values for other bays, depending on the relative rigidities of the bays. The evaluation of these D values is based mostly on experience and judgment.

The modified portal method was used in the original design. The weight of the building for seismic design is computed from the top to the basement for each story separately and is shown in the column under heading W in Table 18.2. The total weight above the plane considered is shown in the column under heading ΣW , and the total earthquake shear in the column under the heading $\Sigma S = 0.1\Sigma W$. Computations of the column and girder moments, the girder shears, and the column direct stresses for frame A_3-E_3 are summarized in Table 18.3.

The frame under consideration through columns A_3-E_3 is shown in plan in Fig. 18.17. The amount of horizontal shear acting on this frame at each floor level is obtained from the relation: sum of the D values for the frame divided by the total D values for the entire building for each story in the direction considered. The force of 6.5 metric tons acting at the roof level is obtained as follows: the D value for the top story is 4, which is multiplied with a unit shear value in the vertical direction for this story of 1.62 (Table 18.3), giving 6.5 tons, approximately. The horizontal forces at other floor levels are obtained similarly. It is to be noted that at the first-floor level, a force of 7.6 tons must be applied

* Note that D as used here is similar to, but not specifically the same as, D used in the AIJ method described in the previous section.

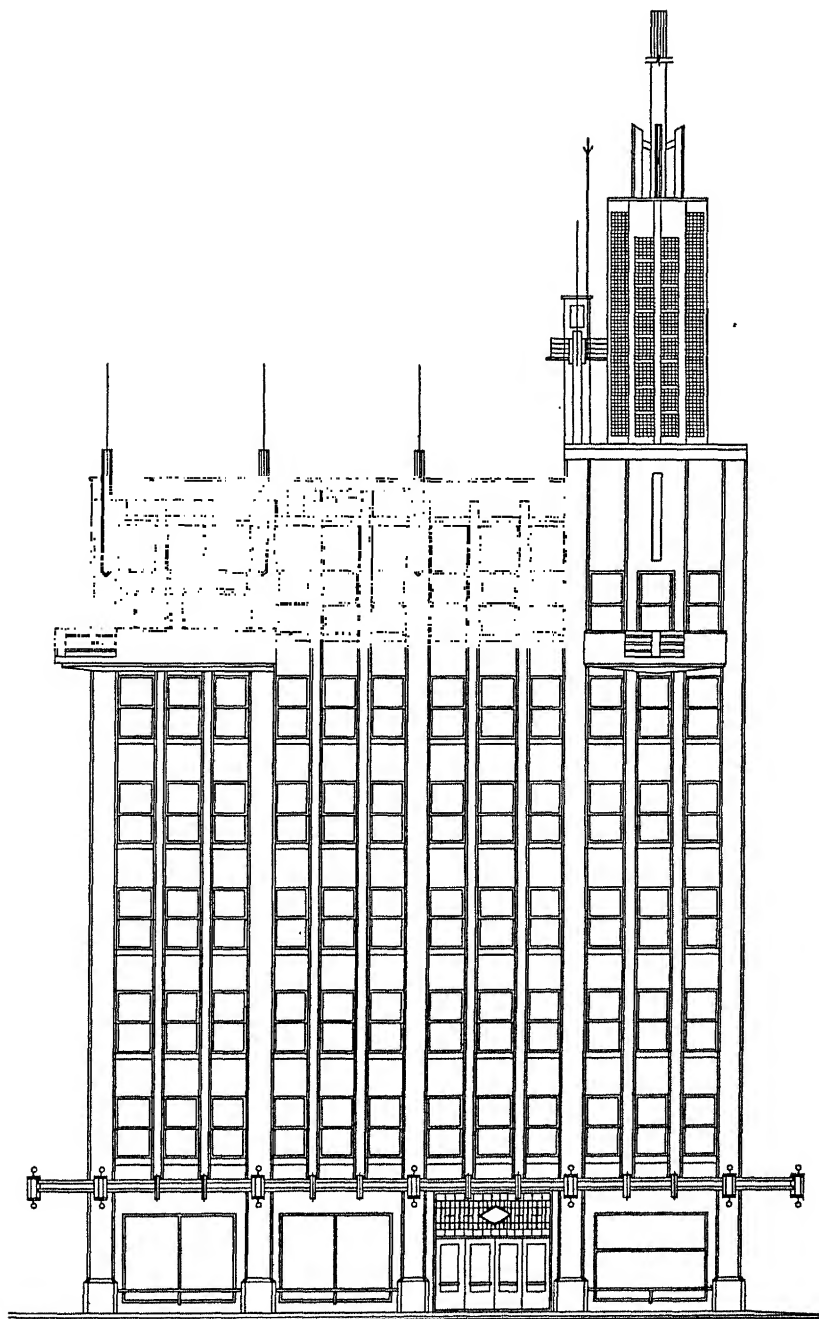


FIG. 18.15. R.C. Department Store, north elevation.

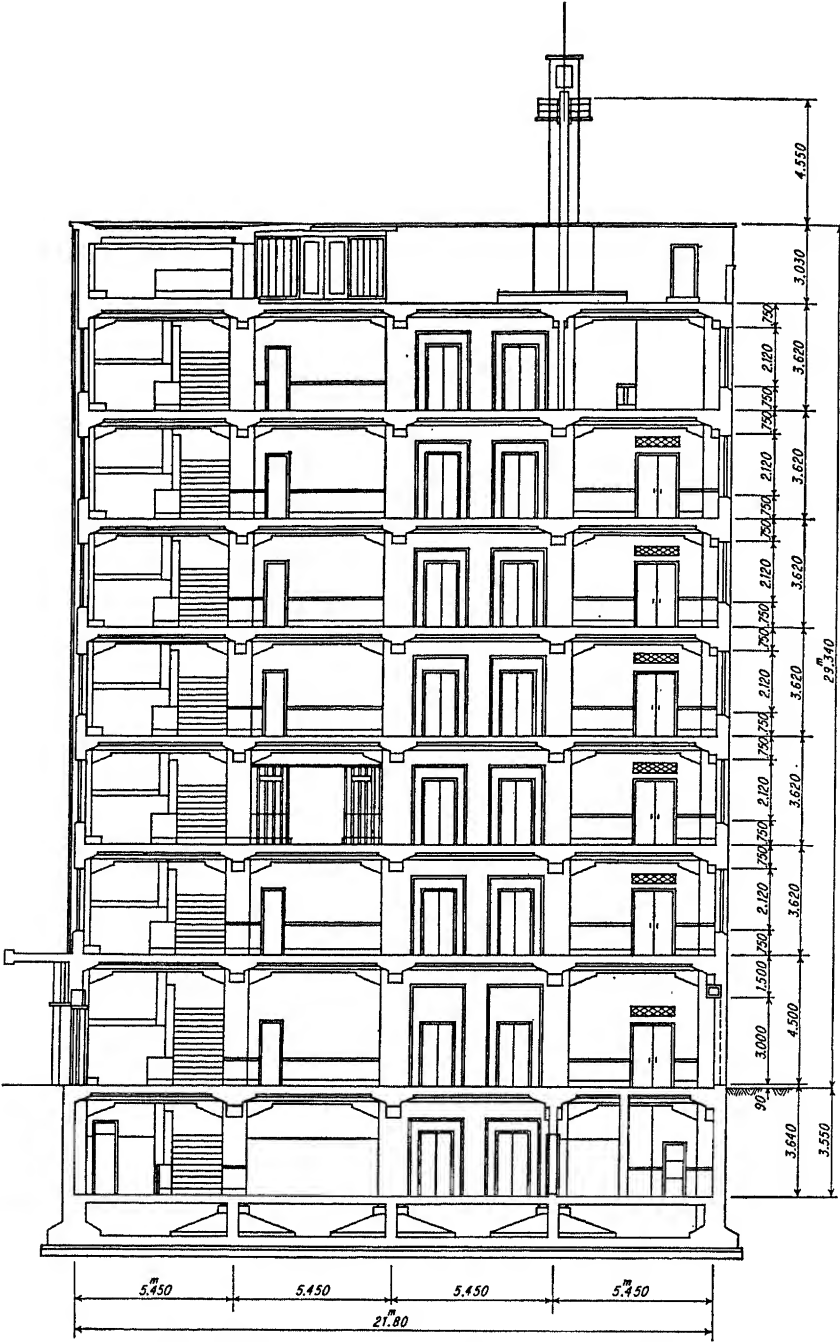
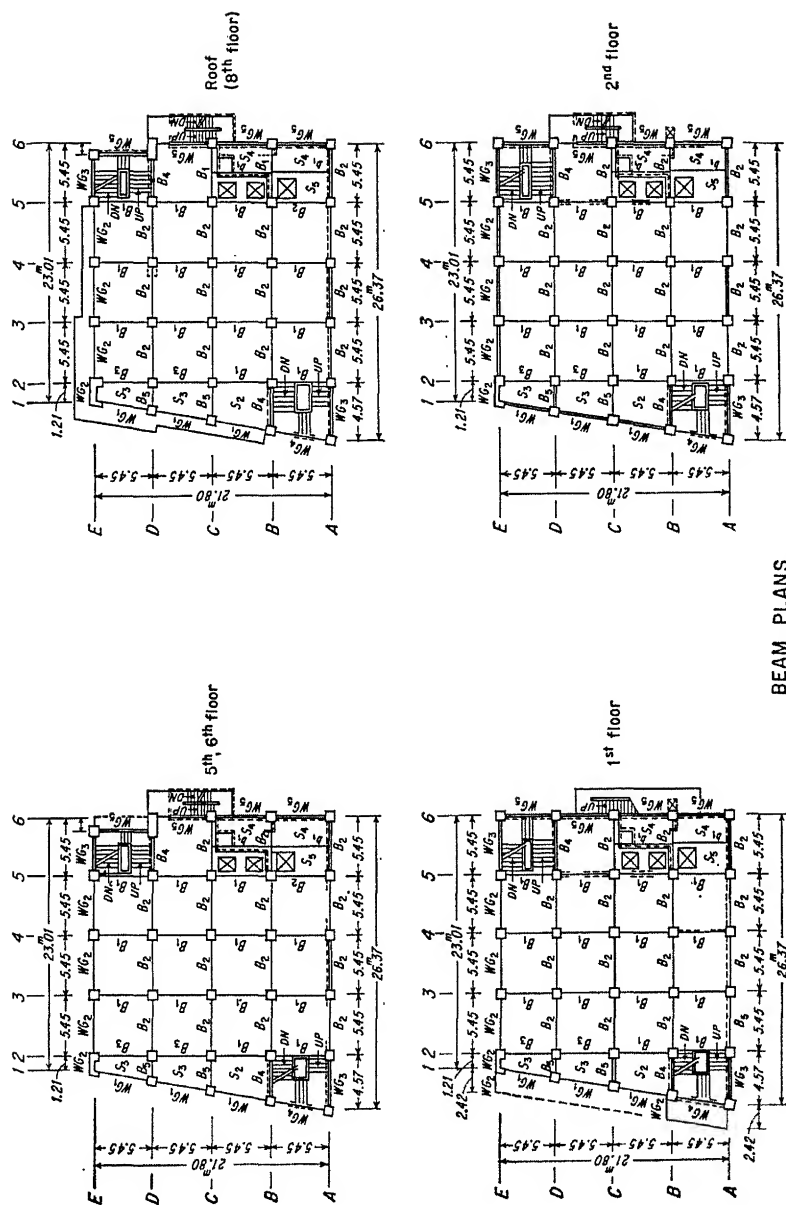


FIG. 18.16. R.C. Department Store, section A₃-B₃.



BEAM PLANS
Fig. 18.17a. Foundation plan.

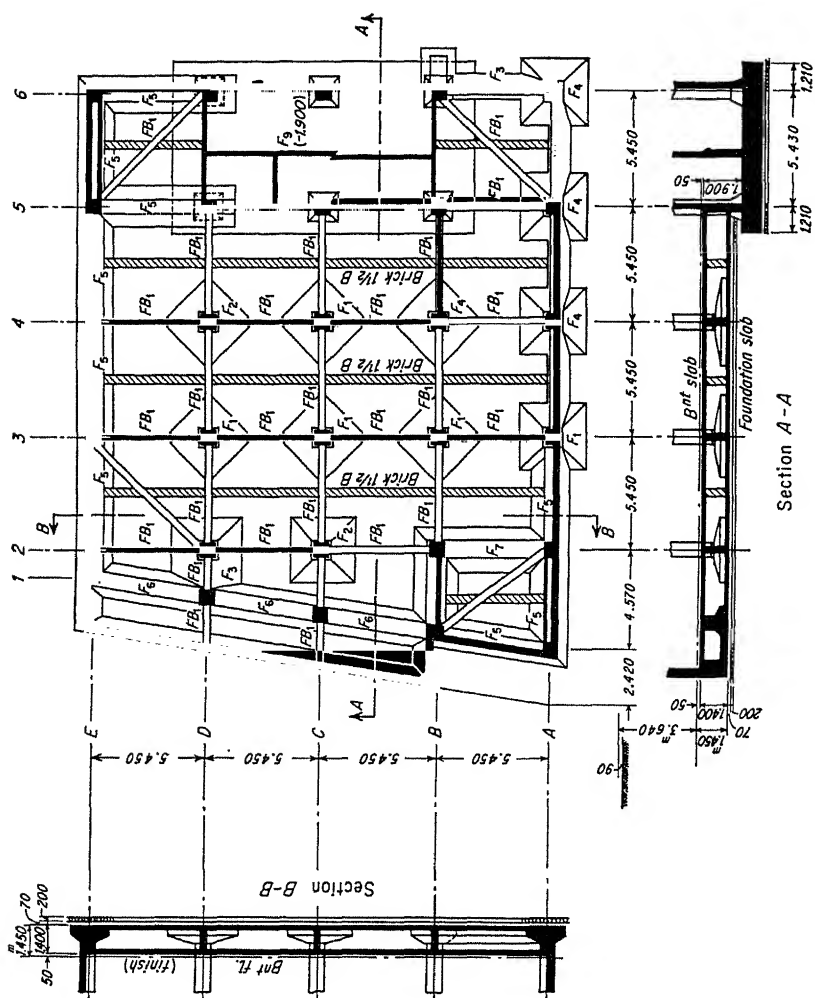


FIG. 18.17b. Sections.

in a direction opposite to the forces above in order to satisfy the shear value for the basement story, a situation frequently occurring when there are more seismic walls or other resisting elements than in the stories above. The moments at the ends of columns for the frame are indicated in Fig. 18.19*a*, and those for girders in Fig. 18.19*b*. The dashed lines indicate moment variations by the slope-deflection solution. The discrepancies in the moment values in the lower stories are considerable.

The solution of the same frame by Bowman's method is shown in Fig. 18.20*a* and *b*.

The solution by the AIJ method or the factor method requires that the relative stiffness of the members in the frame be known. The dimensions of the frame, stiffness of members, and the forces acting at different floor levels are shown in Fig. 18.21*a*. Following the procedure outlined for the AIJ method, the moment values at the ends of columns and girders are obtained as illustrated in Fig. 18.21*b* and *c*, respectively. The solution of the same frame under a different loading condition by the factor method is indicated in the following article.

As is evident from the moment values obtained by different methods, it is necessary to exercise sound judgment to ensure that the stresses be routed from the foundation to the roof, and vice versa, smoothly, in designing the separate members comprising each frame of the building. Attention to structural details is equally important.

TABLE 18.1. ASSUMED DESIGN LOADS
In tons per square meter

		Load	Slab	Beam	Column	Earthquake
Penthouse	Roof	Live load	0.20	0.16	0.14	0.10
		Dead load	0.40	0.492	0.56	0.56
		Total	0.60	0.652	0.70	0.66
	8th	Live load	0.75	0.60	0.527	0.375
		Dead load	0.36	0.45	0.51	0.51
		Total	1.11	1.05	1.037	0.885
7th roof		Live load	0.55	0.44	0.387	0.275
		Dead load	0.55	0.67	0.713	0.713
		Total	1.10	1.11	1.1	0.988
General floors (2d to 7th)		Live load	0.55	0.44	0.387	0.275
		Dead load	0.55	0.67	0.863	0.86
		Total	1.10	1.11	1.25	1.135
1st floor		Live load	0.55	0.44	0.387	0.275
		Dead load	0.60	0.71	0.863	0.86
		Total	1.15	1.15	1.25	1.135

TABLE 18.3. ANALYSIS OF FRAME A_3-E_3 BY NAITO'S MODIFIED
PORTAL METHOD
In metric tons

<div>Plan</div> <div>↕</div> <div>↔</div>		Roof	ΣS , tons	ΣD		$s = \frac{\Sigma S}{\Sigma D}$, tons		Interior- column moment, ton-meters		Exterior- column moment, ton-meters		Girder moment, ton-meters		Girder* shear, tons		Column direct stress, tons	
				↑	↔	↑	↔	↑	↔	↑	↔	↑	↔	↑	↔	↑	↔
3.62 m	0.6h	7	82.6	51	61	1.62	1.35	3.5	2.93	1.75	1.47	1.75	1.47	0.64	0.54	0.64	0.54
3.62 m	0.5h	6	156	41	63	3.8	2.46	6.9	4.45	3.45	2.23	8.6	5.58	3.15	2.04	2.34	1.71
3.62 m	0.5h	5	233	41	63	5.7	3.7	10.3	6.7	5.15	3.35	12.0	7.75	4.4	2.84	5.49	3.75
3.62 m	0.5h	4	311	41	64	7.6	4.85	13.7	8.8	6.85	4.4	15.45	9.8	5.65	3.6	9.89	6.59
3.62 m	0.5h	3	390	41	64	9.5	6.1	17.2	10.8	8.6	5.4	19.1	12.05	7.0	4.4	15.54	10.19
3.62 m	0.5h	2	470	41	64	11.5	7.35	21.0	13.3	10.5	6.65	24.4	16.15	8.9	5.9	22.54	14.59
4.5 m	0.5h	1	553	45	66	12.2	8.4	27.8	19	13.9	9.5	21.3	14.05	7.8	5.16	31.44	20.49
4.10 m	0.6h	B	644	63	104	8.98†	5.52†	14.8	9.1	11.8	7.3					39.24	25.65
																43.31	28.15

* Span 5.45 m.

$$\dagger s = \frac{\Sigma S}{\Sigma D} \times \frac{4}{4.6} = \frac{644}{63} \times 0.87 = 8.98 \text{ tons} \quad s = \frac{\Sigma S}{\Sigma D} \times \frac{5}{5.6} = \frac{644}{104} \times 0.89 = 5.52 \text{ tons}$$

Shear of exterior columns assumed 80 per cent of that of interior columns.

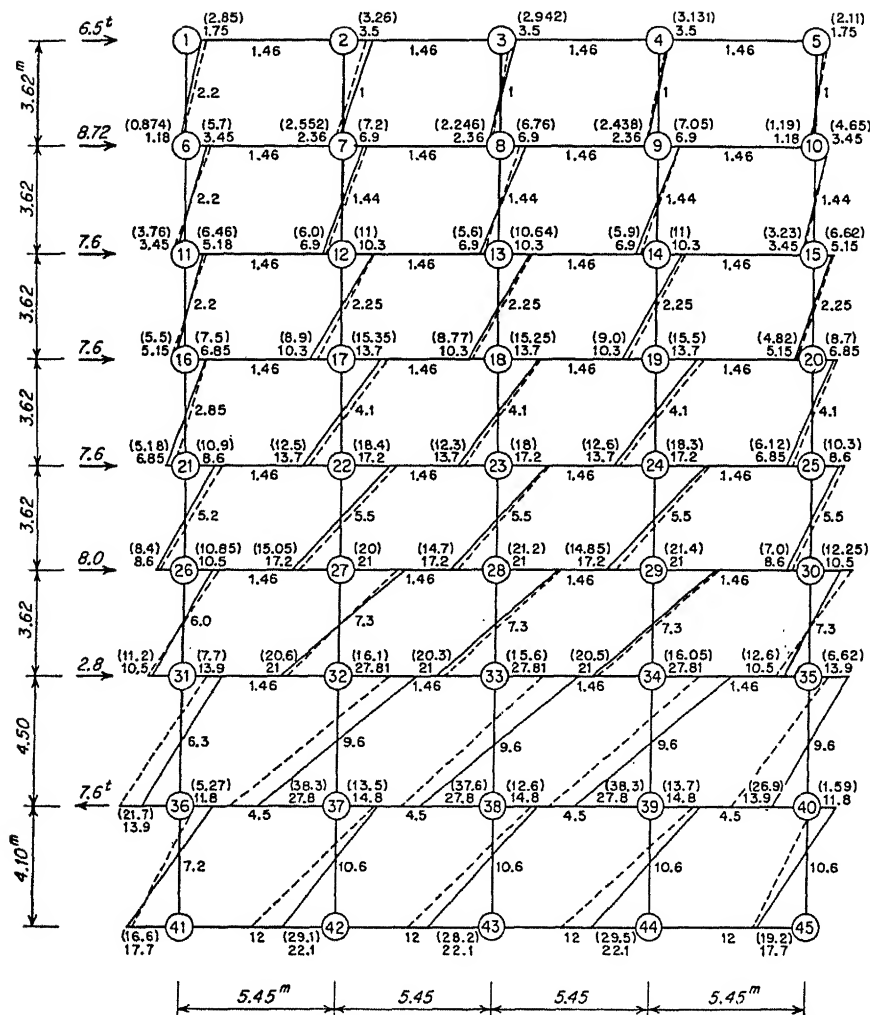


FIG. 18.19a. Moment values by Naito's modified portal method. Column moments in ton-meters. Moment values by slope-deflection method shown by dashed lines and numbers in parentheses. Moment values by Naito's modified portal method shown by solid lines.

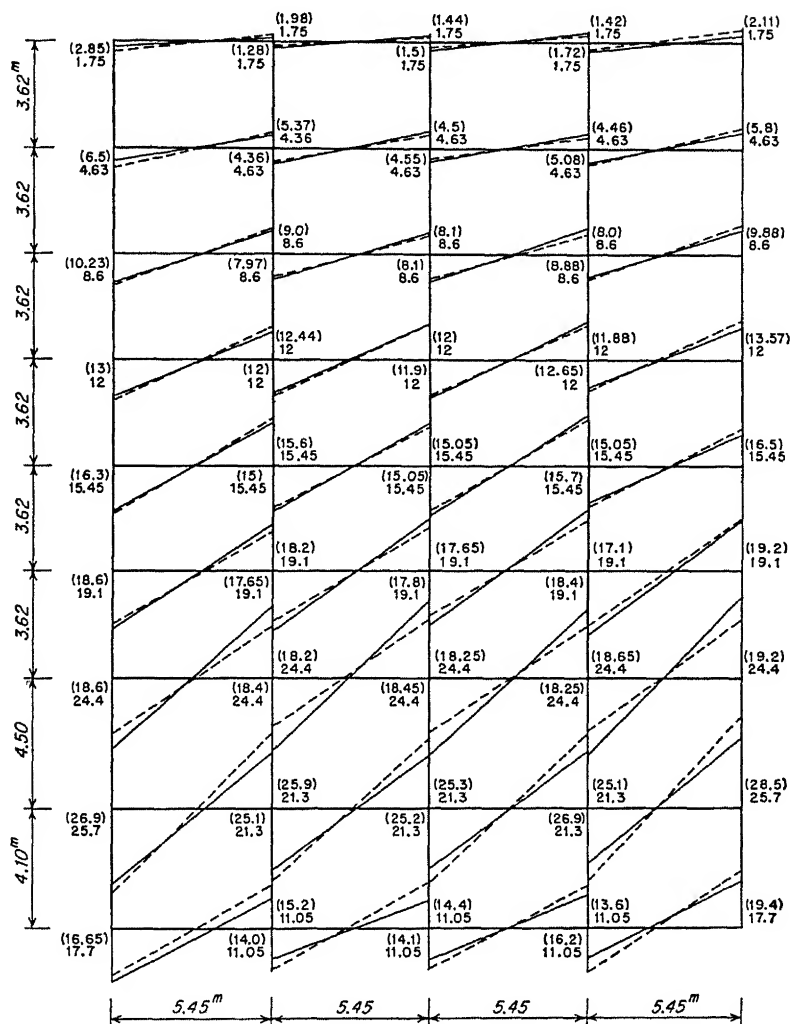
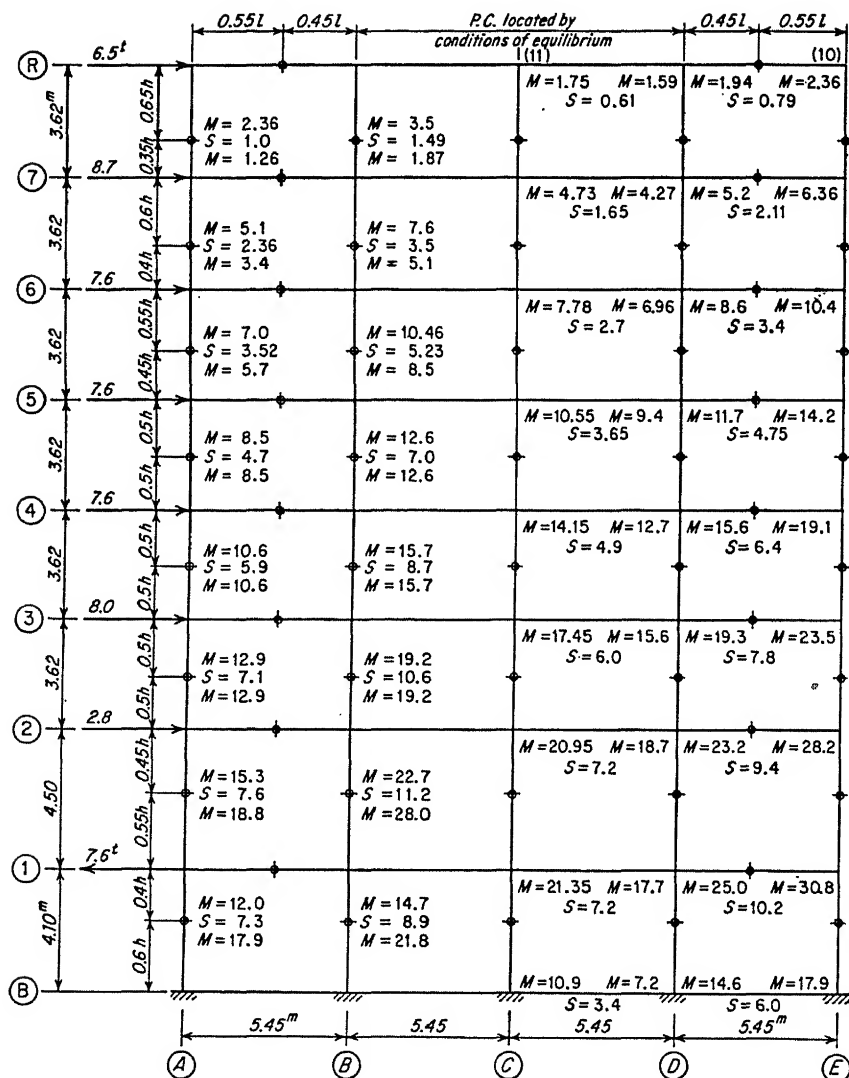


FIG. 18.19b. Moment values by Naito's modified portal method. Girder moments in ton-meters. Moment values by slope-deflection method shown by dashed lines and numbers in parentheses. Moment values by Naito's modified portal method shown by solid lines.



NOTE:

- Points of contraflexure in girders and columns as shown.
- Distribution of shear.
 - Bottom story: divide [(no. of bays - 0.5)/(no. of columns)] \times total story shear equally among columns, and remaining shear to bays inversely as their width.
 - Other stories: divide [(no. of bays - 2)/(no. of columns)] \times total story shear equally among columns, and remaining shear to bays inversely as their width.

FIG. 18.20a. Solution by Bowman's method.

Story	(1)	(2)	(3)	(4)	(5)	(6)	(7)	(8)	(9)	(10)	(11)
	Story shear $Q(t)$	Total shear $\Sigma Q(t)$	$\frac{(\text{Boys}-2) \Sigma Q}{(\text{No. of cols})^2}$	Remaining ΣQ No. of bays	Int col shear $S(t)$	Ext col shear $S(t)$	P.I. (m)	Int. col. moment (t m)	Ext. col. moment (t m)	Ext. girder $M(t m)$	Int. girder $M(t m)$
7	6.5 →	6.5	$\frac{(4-2) \times 6.5}{5 \times 5} = 0.52 \text{ t/col.}$	$(1-0.4) \times \frac{6.5}{4} = 0.97 \text{ t/bay}$	$(3) + (4) = 0.52 + 0.97 = 1.49$	$(3) + (4)/2 = 0.52 + 0.48 = 1.0$	2.36	3.5	2.36	2.36	1.75
6	8.7 →	15.2	1.22	2.28	3.5	2.36	2.17	7.6	5.1		
5	7.6 →	22.8	1.82	3.4	5.23	3.52	2.00	10.46	7.0		
4	7.6 →	30.4	2.44	4.54	7.0	4.7	1.62	8.5	5.7	14.2	10.55
3	7.6 →	38.0	3.03	5.7	8.7	5.9	1.81	12.6	8.5	19.1	14.15
2	8.0 →	46.0	3.7	6.9	10.6	7.1	1.81	15.7	10.6	23.5	17.45
1	2.8 →	48.8	3.9	7.3	11.2	7.6	1.81	15.7	10.6	28.2	20.95
B	7.2 ←	41.2	$\frac{(\text{Boys}-0.5) \Sigma Q}{(\text{No. of cols})^2} = \frac{(4-0.5) \times 41.2}{5 \times 5} = 5.8$	$(1-0.7) \times \frac{41.2}{4} = 3.1$	8.9	7.3	2.02	22.7	15.3		
							2.48	28.0	18.8	30.8	21.35
							1.65	14.7	12.0		
							2.45	21.8	17.9	17.9	10.9

FIG. 18.20b. Solution by Bowman's method.

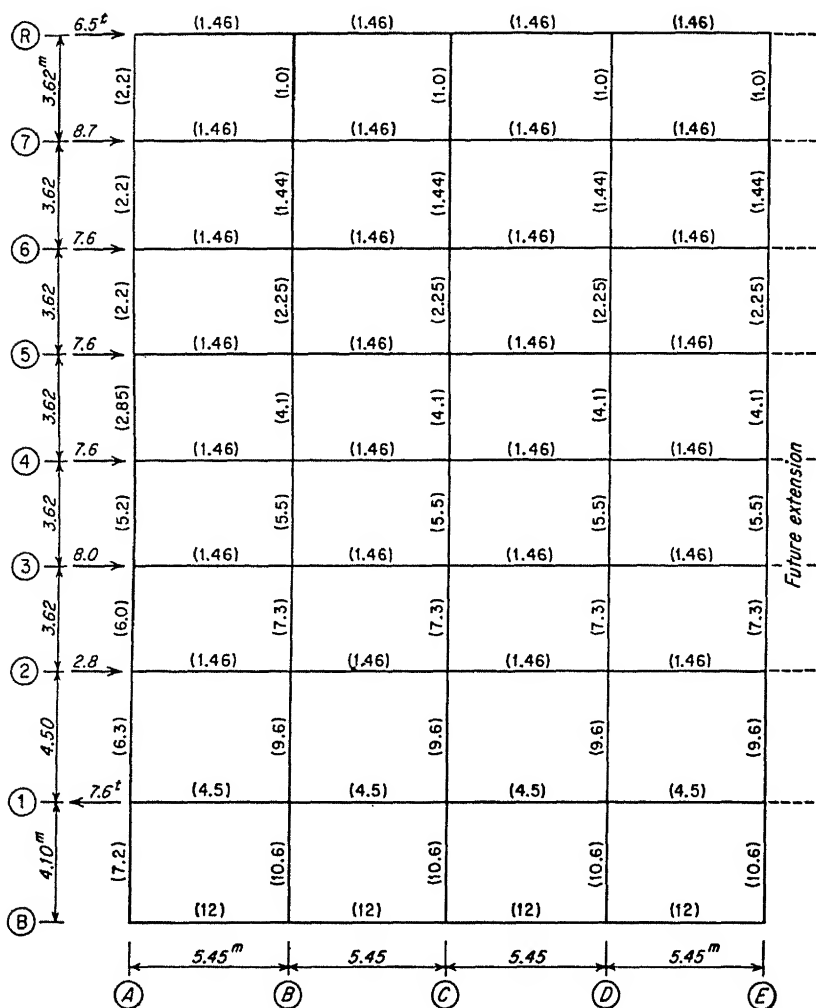


FIG. 18.21a. Dimensions. Stiffness of members and horizontal forces acting on the frame selected. Figures in parentheses are relative-stiffness values.

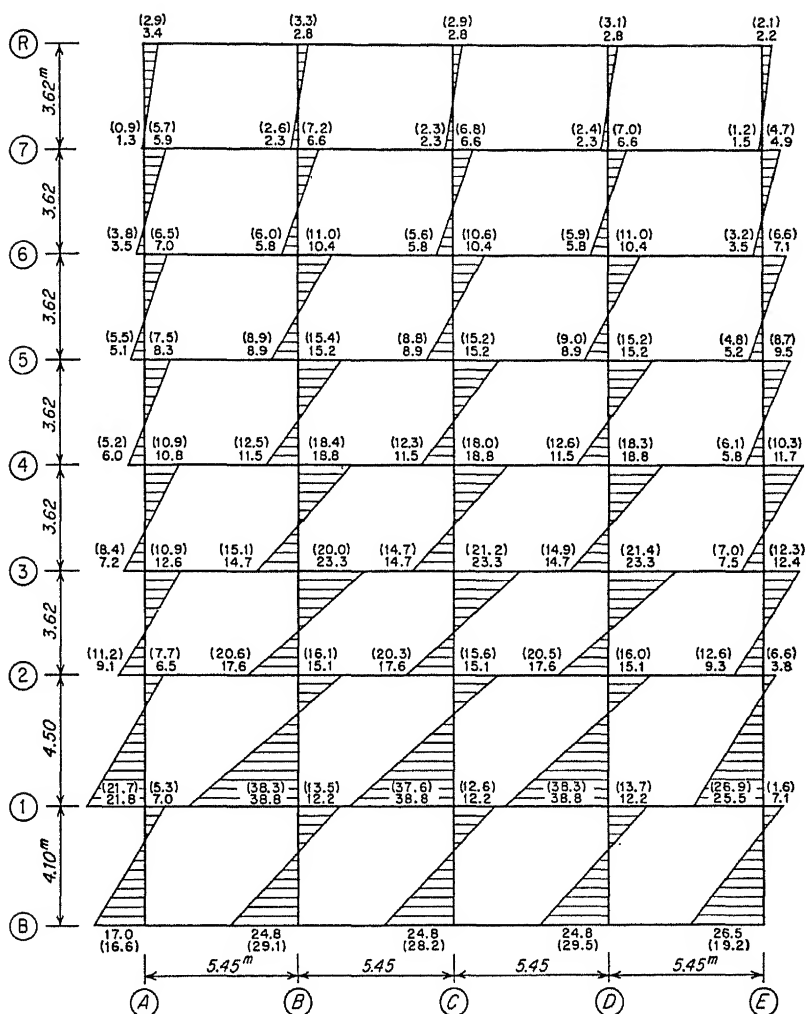


FIG. 18.21b. Moment values by the Architectural Institute of Japan method. Column moments in ton-meters. Figures in parentheses are nearly correct values obtained by the slope-deflection method.

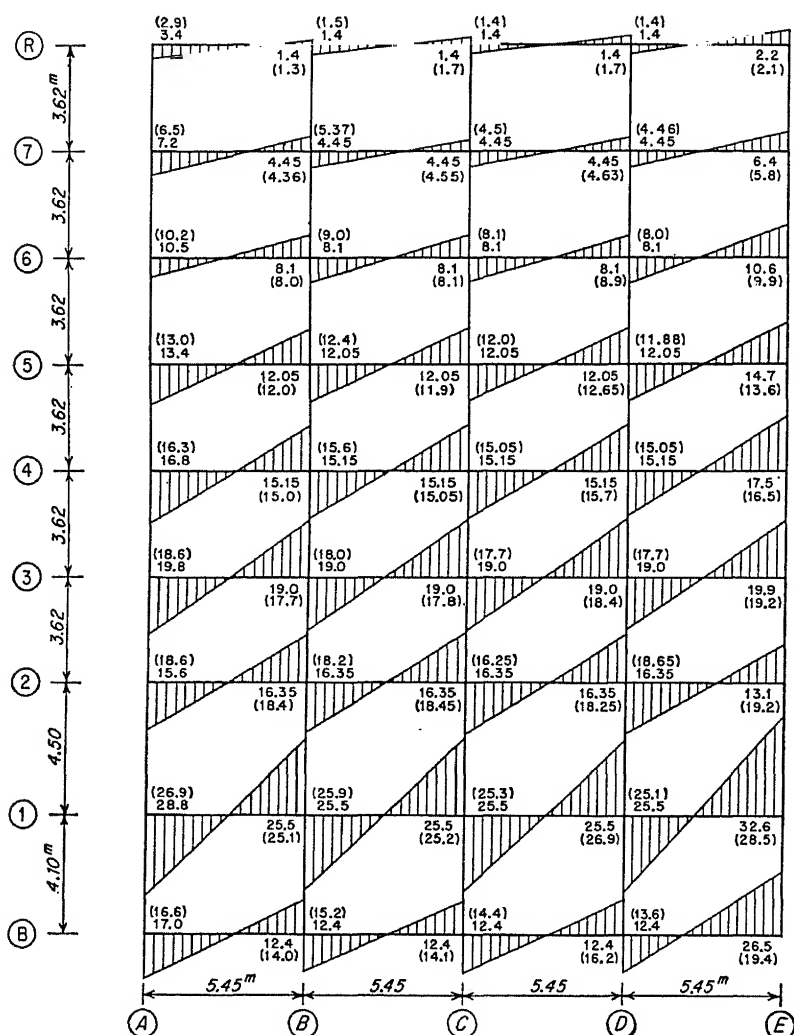


FIG. 18.21c. Moment values by the Architectural Institute of Japan method. Girder moments in ton-meters. Figures in parentheses are nearly correct values obtained by the slope-deflection method.

18.5. A Comparison of Aseismic Designs by Different Codes. The earthquake provisions of the Uniform Building Code (UBC), the Joint Committee Code (JCC), and the Japanese Building Code (JBC) have been applied to the study of the frame described in the previous article. The loads used in the original design, tabulated in Table 18.1, for earthquake computations are used in making rough comparisons in this study. At the time this building was designed, a reduction in the floor live load up to 20 per cent for girders, 30 per cent for columns, and 50 per cent for earthquake design was permitted. In addition to the 50 per cent live load, the total dead weight of the building must be considered. The weight of the building computed on this basis is shown in Table 18.2. As previously mentioned, the seismic coefficient was 0.1, and the allowable steel stress was 17,000 psi at the time this building was designed, without any increase in the stress being permitted for earthquake consideration. Under the present code, the basic seismic coefficient is 0.2, the allowable unit stress for steel is 34,000 psi, and the live loads have been revised to give a more economical design. Consequently, the weight of the building used in the present study is somewhat greater than would be the case under the current JBC provisions, but no increase in the seismic coefficients for increasing height has been made which is compensating.

Applying the provisions of the three building codes mentioned above, the earthquake forces acting at each floor level of the subject are summarized in Table 18.4. The total earthquake shear at each story is shown as a percentage of the JBC value taken as 100 per cent. It is obviously necessary to take into consideration the allowable unit stresses permitted by the three codes and compute the required section modulus at the ends of members for seismic stresses to make a comparison.

The factor method has been selected as the method of obtaining seismic moments for the loadings required by the three codes. The effect of the heavy foundation girders has been considered in computing the column- and girder-moment factors. The column- and girder-moment factors are indicated in Fig. 18.22 obtained by slide-rule computation. The bending moments and the required section moduli at the ends of columns are shown in Table 18.5*a* and for girders in Table 18.5*b*.

Although this study is approximate and crude, it does show glaring discrepancies in the results obtained by the three building codes and reflects the philosophy of aseismic design among different groups of engineers. These discrepancies may be due to different earthquake intensities resulting from dissimilar geological conditions at different locations and different dynamic characteristics of buildings resulting from construction practices which differ in important respects. More study of frames such as the eight-story subject frame is indicated which cannot be considered as a rigid shear-type structure or a flexible bending-type

TABLE 18.4. SUMMARY OF EARTHQUAKE FORCES
In metric tons

Floor	Uniform Building Code		Joint Committee Code		Japanese Building Code	
	Story force	Total shear	Story force	Total shear	Story force	Total shear
R	8.6 →		2.9 →		13.0 →	
7		8.6 (66%)		2.9 (22%)		13 (100%)
6	8.0 →		3.5 →		17.4 →	
		16.6 (55%)		6.4 (21%)		30.4 (100%)
5	4.4 →		2.6 →		15.0 →	
		21.0 (46%)		9.0 (20%)		45.4 (100%)
4	3.3 →		2.1 →		15.4 →	
		24.3 (40%)		11.1 (18.5%)		60.8 (100%)
3	2.5 →		1.9 →		15.2 →	
		26.8 (35%)		13.0 (17%)		76.0 (100%)
2	2.2 →		1.4 →		15.5 →	
		29.0 (32%)		14.4 (16%)		91.5 (100%)
1	0.9 ←		0.4 ←		7.1 →	
		28.1 (28.5%)		14 (14%)		98.6 (100%)
B	6.7 ←		3.6 ←		16.6 ←	
		21.4 (26%)		10.4 (13%)		82.0 (100%)

		1.06	0.56	0.56	0.67		
R	→	1.16	0.81	1.01	0.56	1.01	0.78
	→ 0.99	1.43	0.91	1.04	0.91	1.04	0.67
7	→	0.82	1.22	1.10	1.04	1.10	1.26
	→ 0.82	1.50	1.02	1.23	1.02	1.23	0.67
6	→	0.79	1.37	1.34	1.23	1.34	1.46
	→ 0.76	1.54	1.19	1.54	1.19	1.54	0.74
5	→	0.84	1.58	1.74	1.54	1.74	1.68
	→ 0.74	1.80	1.58	1.68	1.58	1.77	0.92
4	→	1.09	1.74	1.78	1.68	1.78	1.83
	→ 1.03	1.88	1.68	1.78	1.68	1.84	0.91
3	→	1.02	1.82	1.94	1.78	1.94	1.90
	→ 0.96	1.94	1.79	1.86	1.79	1.92	0.95
2	←	1.42	1.90	2.92	1.86	2.92	1.97
	← 1.89	4.92	3.70	4.65	3.70	4.95	2.10
1	←	4.05	4.80	7.00	4.65	7.00	3.23
B		5.40	9.00	5.50	9.00	6.50	6.60
		5.92	5.50	5.50	7.30		
		Col. A	B	C	D	E	

FIG. 18.22. Solution by factor method. For stiffness of members, see Fig. 18.21a. Numbers are column- and girder-moment factors.

structure. JBC is perhaps too severe, and the discrepancies noted should not be construed as indicating lack of safety in buildings designed according to American practice, which is based on past earthquake experience and rational reasoning.

TABLE 18.5a. BENDING MOMENTS AT ENDS OF MEMBERS
 Column moments in ton-meters and required section moduli in cubic centimeters

Story	End	Code*	Col. A		Cols. B, C, D		Col. E	
			Moment	Sec. mod.	Moment	Sec. mod.	Moment	Sec. mod.
7	Top	1	3.80	202	3.40	181	2.60	139
		2	1.30	69	1.14	61	0.88	46
		3	5.80	241	5.10	212	3.90	162
	Bottom	1	3.30	176	3.10	165	2.20	117
		2	1.10	59	1.03	55	0.75	40
		3	5.00	208	4.50	187	3.40	142
6	Top	1	5.10	272	7.10	378	4.70	250
		2	2.00	109	2.73	146	1.84	98
		3	9.60	400	12.80	533	8.50	355
	Bottom	1	4.90	261	6.60	351	4.20	224
		2	2.04	108	2.55	136	1.67	89
		3	9.60	400	12.00	500	7.80	325
5	Top	1	5.60	298	9.50	507	5.80	309
		2	2.40	129	4.10	218	2.60	136
		3	12.00	500	20.50	855	12.80	536
	Bottom	1	5.40	288	8.50	453	5.10	272
		2	2.33	124	3.65	194	2.24	120
		3	11.60	483	18.20	758	11.40	475
4	Top	1	5.50	293	11.30	607	6.70	357
		2	2.55	136	5.27	281	3.08	164
		3	13.70	570	28.40	1,180	17.00	710
	Bottom	1	4.80	256	10.30	553	6.10	325
		2	2.26	120	4.78	255	2.75	146
		3	12.00	500	25.70	1,070	15.00	625
3	Top	1	7.10	378	12.10	650	6.80	362
		2	3.60	193	5.85	312	3.28	175
		3	20.90	870	34.00	1,420	19.00	790
	Bottom	1	6.70	357	11.20	602	6.20	330
		2	3.26	174	5.43	290	3.01	160
		3	19.70	820	32.0	1,330	17.40	720
2	Top	1	7.00	373	13.20	709	7.20	384
		2	3.53	188	6.65	354	3.63	194
		3	22.30	930	42.50	1,770	22.30	930
	Bottom	1	6.80	362	12.20	655	6.40	341
		2	3.46	185	6.15	328	3.33	177
		3	21.00	874	39.10	1,630	20.70	860
1	Top	1	7.20	384	14.20	762	8.00	427
		2	3.36	180	6.90	370	3.85	205
		3	23.40	970	48.00	2,000	26.80	1,110
	Bottom	1	9.40	501	18.00	966	10.40	558
		2	4.48	239	8.76	467	4.96	265
		3	31.40	1,300	61.00	2,540	34.60	1,440
B	Top	1	5.20	277	8.90	474	6.10	325
		2	2.54	136	4.38	234	2.96	158
		3	19.80	825	34.20	1,420	23.10	960
	Bottom	1	6.90	368	11.50	617	8.40	448
		2	3.40	182	5.62	300	4.14	220
		3	26.30	1,090	44.00	1,830	32.30	1,350

* Code 1 refers to the Uniform Building Code (UBC). Code 2 refers to the Joint Committee Code (JCC). Code 3 refers to the Japanese Building Code (JBC).

TABLE 18.5b. BENDING MOMENTS AT ENDS OF MEMBERS
Girder moments in ton-meters and required section moduli in cubic centimeters

	Code	Girder AB		Girder BC		Girder CD		Girder DE	
		Left	Right	Left	Right	Left	Right	Left	Right
R	1. Moment	3.8	2.0	1.4	1.7	1.7	1.5	1.9	2.6
	Sec. mod.	202	107	75	91	91	80	101	139
	2. Moment	1.3	0.68	0.47	0.57	0.57	0.52	0.62	0.88
7	Sec. mod.	69	37	15	31	31	28	33	47
	3. Moment	5.8	3.0	2.1	2.55	2.55	2.3	2.8	3.9
	Sec. mod.	242	125	87	106	106	96	116	162
6	1. Moment	8.4	5.5	4.6	5.2	5.2	4.9	5.5	6.9
	Sec. mod.	448	394	246	278	278	262	394	368
	2. Moment	3.15	2.1	1.7	1.9	1.9	1.8	2.0	2.5
5	Sec. mod.	168	112	91	102	102	96	107	134
	3. Moment	14.6	9.3	8.0	8.65	8.65	8.3	9.0	11.9
	Sec. mod.	608	387	333	360	360	345	375	495
4	1. Moment	10.5	8.5	7.7	8.1	8.1	7.5	8.5	10.0
	Sec. mod.	560	453	412	432	432	400	453	534
	2. Moment	4.4	3.5	3.1	3.3	3.3	3.2	3.4	4.2
3	Sec. mod.	235	186	166	176	176	170	182	224
	3. Moment	21.6	17.1	15.4	16.25	16.25	15.5	17.0	20.6
	Sec. mod.	900	712	640	675	675	645	710	855
2	1. Moment	10.9	10.1	9.7	9.9	9.9	9.6	10.2	11.8
	Sec. mod.	582	540	518	528	528	512	544	630
	2. Moment	4.9	4.6	4.4	4.5	4.5	4.3	4.6	5.3
1	Sec. mod.	262	246	235	240	240	230	246	283
	3. Moment	25.3	23.6	23.0	23.3	23.3	23.0	23.6	28.4
	Sec. mod.	1,050	980	960	970	970	960	980	1,180
B	1. Moment	11.9	11.0	11.4	11.2	11.2	11.0	11.4	12.9
	Sec. mod.	635	588	608	598	598	588	608	688
	2. Moment	5.9	5.4	5.2	5.3	5.3	5.2	5.4	6.0
B	Sec. mod.	315	288	277	283	283	277	288	320
	3. Moment	32.9	30.4	29.3	29.85	29.85	29.0	30.7	34.0
	Sec. mod.	1,370	1,260	1,220	1,240	1,240	1,210	1,180	1,420
B	1. Moment	13.7	12.4	12.0	12.2	12.2	12.0	12.4	13.4
	Sec. mod.	732	662	641	651	651	641	662	716
	2. Moment	6.8	6.15	5.9	6.0	6.0	5.9	6.2	6.6
B	Sec. mod.	362	328	315	320	320	315	330	352
	3. Moment	42.0	37.7	36.8	37.25	37.25	36.6	37.9	39.7
	Sec. mod.	1,750	1,570	1,535	1,550	1,550	1,520	1,580	1,650
B	1. Moment	14.0	13.3	13.1	13.2	13.2	13.0	13.4	14.4
	Sec. mod.	748	710	700	705	705	694	716	769
	2. Moment	6.82	6.6	6.45	6.53	6.53	6.45	6.6	7.18
B	Sec. mod.	364	352	345	350	350	344	352	383
	3. Moment	44.4	44.0	43.1	43.55	43.55	43.0	44.1	47.5
	Sec. mod.	1,840	1,830	1,800	1,810	1,810	1,790	1,830	1,980
B	1. Moment	16.6	13.6	13.3	13.4	13.5	13.1	13.8	16.5
	Sec. mod.	886	728	710	716	721	700	737	882
	2. Moment	7.02	6.7	6.44	6.57	6.57	6.4	6.74	7.92
B	Sec. mod.	375	357	344	350	350	341	360	423
	3. Moment	51.0	48.3	46.9	47.6	47.6	46.1	49.1	57.7
	Sec. mod.	2,120	2,010	1,800	1,980	1,980	1,920	2,050	2,400
B	1. Moment	6.9	6.0	5.5	5.7	5.8	5.3	6.2	8.4
	Sec. mod.	368	320	294	304	309	283	331	448
	2. Moment	3.4	2.92	2.7	2.81	2.81	2.6	3.02	4.14
B	Sec. mod.	182	156	144	150	150	138	161	220
	3. Moment	26.3	23.0	21.0	22.0	22.0	20.0	24.0	32.3
	Sec. mod.	1,090	960	870	915	915	830	1,000	1,340

18.6. Miscellaneous Considerations. In practical design of buildings in seismic regions, effort should be made so far as practicable to obtain coincidence of the centers of mass and rigidity about the vertical axis of the building. This coincidence is disturbed by nonuniform location of seismic walls and other resisting elements in plan. Torsional effects if present should be taken into consideration, though extremely fastidious attention would be uncalled for in many instances. Rational procedures for distributing the lateral forces to columns, walls, and other structural elements should be followed, such as the rigidity-center method of Lin [15] or the Japanese method described by Muto [14].

Connection of members in structural framing should be made strong and rigid to reduce excessive deformation. It is customary in Japan to provide rib plates welded to the top connecting angle or plate in girder-column connections in order to maintain the initial shape under high seismic stresses.

The importance of adequate foundations and interconnection of footings by strong moment-resisting tie beams cannot be overemphasized. It becomes an item of additional cost, but in many instances provides insurance against serious damage in severe earthquakes, particularly when soil conditions are unfavorable.

Separation of buildings in congested areas to prevent the danger of mutual pounding by providing sufficient space around each structure may require attention. A minimum of 3 in. for several-story buildings and 8 or more inches for tall buildings may be required, depending on the dynamic properties of the building and the site soil [16].

REFERENCES

1. Cheney, J. A.: Structural Analysis by Dynamic Load Parameters, *J. ACI*, vol. 28, no. 1, July, 1956.
2. Housner, G. W.: Earthquake Resistant Design Based on Dynamic Properties of Earthquakes, *J. ACI*, vol. 28, no. 1, July, 1956.
3. Moran, D. F., and K. V. Steinbrugge: Earthquake Response of Elevated Water Tanks and Refinery Vessels, Technical Meeting, Structural Engineers Assoc. of Northern California, San Francisco, Nov. 1, 1955.
4. Housner, G. W.: Spectrum Intensities of Strong-motion Earthquakes, in "Proceedings of Symposium on Earthquake and Blast Effects on Structures," EERI and University of California, Los Angeles, June, 1952.
5. Jacobsen, L. S.: Dynamic Behavior of Simplified Structures Up to the Point of Collapse, in "Proceedings of Symposium on Earthquake and Blast Effects on Structures," EERI and University of California, Los Angeles, June, 1952.
6. Newmark, N. M.: Computation of Dynamic Structural Response in the Range Approaching Failure, in "Proceedings of Symposium on Earthquake and Blast Effects on Structures," EERI and University of California, Los Angeles, June, 1952.

7. Newmark, N. M.: Analysis and Design of Structures Subjected to Dynamic Loading, in "Proceedings of Conference on Building in the Atomic Age," MIT, June, 1952.
8. Hudson, D. E.: Response Spectrum Technique in Engineering Seismology, in "Proceedings of World Conference on Earthquake Engineering," EERI and University of California, Berkeley, June, 1956.
9. Housner, G. W.: Limit Design of Structures to Resist Earthquakes, in "Proceedings of World Conference on Earthquake Engineering," EERI and University of California, Berkeley, June, 1956.
10. Ayre, R. S.: Methods for Calculating the Earthquake Response of Shear Buildings, in "Proceedings of World Conference on Earthquake Engineering," EERI and University of California, Berkeley, June, 1956.
11. Zeevaert, L., and N. M. Newmark: Aseismic Design of Latino Americana Tower in Mexico City, in "Proceedings of World Conference on Earthquake Engineering," EERI and University of California, Berkeley, June, 1956.
12. Sutherland, H., and H. L. Bowman: "Structural Theory," 4th ed., art. 9.6, John Wiley & Sons, Inc., New York, 1950.
13. Wilbur, J. B., and C. H. Norris: "Elementary Structural Analysis," art. 12.13, McGraw-Hill Book Company, Inc., New York, 1948.
14. Muto, K.: Seismic Analysis of Reinforced Concrete Buildings, in "Proceedings of World Conference on Earthquake Engineering," EERI and University of California, Berkeley, June, 1956.
15. Lin, T. Y.: Lateral Force Distribution in a Concrete Building Story, *J. ACI*, vol. 23, no. 4, December, 1951.
16. Engle, H. M., and J. E. Shield: "Recommendations, Earthquake Resistant Design of Buildings, Structures and Tank Towers," rev., Pacific Fire Rating Bureau, 1950.
17. Rinne, J. E.: Aseismic Design Criteria for a 450 Foot Reinforced Concrete Stack, Technical Meeting, Structural Engineers Assoc. of Northern California, San Francisco, Nov. 1, 1955.

CHAPTER 19

VIBRATION OF GIRDERS UNDER MOVING TRAFFIC LOADS

19.1. Introduction. This chapter is concerned almost entirely with certain aspects of the problem of highway-bridge response to moving traffic loads. It is included in the present volume, first, because the subject is of wide interest to civil engineers; second, because the methods used in attacking this problem may be applicable to other problems in the broad field of structural analysis and design for dynamic loading.

19.2. Background to the Problem. It is obvious that both deflections and stresses in a bridge subjected to a moving load will differ from the deflections and stresses which would be caused by the same load applied statically. It is apparent that there is a twofold dynamic character to the loading. First, the load is brought on, and then removed from, the structure in a relatively short time. Second, the load itself is time-varying because it is caused by a complex spring-and-mass system (that is, the vehicle with its masses, springs, shock absorbers, etc.).

For years highway-bridge designers have acknowledged the fact of dynamic stresses by adding to the dead and (static) live-load stresses an "impact" fraction of the latter. Thus we have the expression

$$f_{\text{impact}} = f_{\text{live}} \frac{50}{L + 125} \quad (19.1)$$

where L = length of span subjected to live load. In a review of the history of impact provisions, Goodman [1] points out that early bridge engineers were more concerned with the fatigue aspects of live loading than with the dynamic amplifications of stress. Impact fractions of the type given by Eq. (19.1) were developed for the purpose of limiting the range of repeated stress. Thus for large values of L (long span), the dead-load stress is a substantial fraction of the total permissible working stress; therefore the range of repeated (live) stress is relatively small. Since this condition is favorable from the standpoint of fatigue a smaller "impact" allowance was deemed necessary.

Whatever the original basis for Eq. (19.1) engineers have for many years recognized that dynamic increases in live-load stresses do in fact occur and have utilized the impact fraction as a means of accounting for them. Although actual ratios of dynamic-stress increment to static-live-load stress cannot possibly be expressed in any such simple fashion as indicated by Eq. (19.1), the insignificant number of highway-bridge failures over the past several decades indicates that the over-all design process, including the use of Eq. (19.1), has been conservative. No doubt the impact fraction has been much in error on the high side in some cases and on the low side in others. The fact that failures have not taken place in those bridges for which the impact fraction was underestimated may be due in large measure to the fact that the basic live loading was much overestimated.

Engineers have long recognized that, apart from the safety of bridges, which may be handled in terms of stresses, it is desirable to avoid excessive dynamic deflections because of the discomfort and apprehension which these may cause the public, particularly the pedestrian public. In the past they have attempted to prevent excessive deflection effects by means of limitations on depth/span ratios and deflection/span ratios. These criteria are crude at best, for while the relations between characteristics of the motion and human discomfort are obscure, it is known that acceleration and probably changes in acceleration are important factors. It is apparent that specification of limiting deflection/span ratios and depth/span ratios cannot guarantee satisfactory control of these characteristics.

While railway-bridge vibration was the subject of intensive studies as much as half a century ago, major effort has been directed to highway-bridge vibration only within the very recent past. This is not surprising since the railways represented a well-developed transportation system at a time when automotive transportation was in its infancy. Railway-bridge engineers had to design for very heavy locomotive loadings, aggravated by the hammer-blow effect peculiar to steam locomotives, long before the advent of massive truck-and-trailer combinations which are now so common on the nation's highways. In contrast, the highway system has been steadily increasing in size, and the number of highway bridges, for replacement as well as on new routes, continues to increase at a rapid rate. It is worthy of note that a large percentage of these new bridges involve grade separations. They are mainly of short span (say, <200 ft), and many of them are of relatively shallow proportions. This may be traced in part to the need to minimize the cost of approaches and in part to aesthetic considerations. Whichever the reason, plate girders are being used on sites which formerly would have seen trusses, and rolled beams are used at spans which formerly would have called for

plate girders. Another factor in the trend toward smaller depth/span ratios has been the rapid adoption of prestressed concrete, which has been used at longer spans and larger span/depth ratios than appeared to be feasible with ordinary reinforced concrete. Some of these slender spans have evidenced considerable motion due to the passage of heavy vehicles. Although this motion is mainly evident to pedestrians, and to passengers in cars which are stationary or slowly moving in adjacent lanes, it has been a cause for some concern. First, there is the natural desire on the part of highway-department personnel to avoid the unfavorable public reaction. Second, the existence of motion sufficient to be uncomfortable raises questions as to whether actual stresses may not be greater than the designer supposed.

The present considerable interest in highway-bridge vibration is thus concerned with two needs: namely, a means to predict vibration for a given design, so as to avoid designs which would vibrate excessively, and a means to predict dynamic-live-load stresses, so that materials of construction can be used safely but with economy. Much of the discussion in this chapter is concerned with the problem of bridge deflections, which has been the subject of a continuing program of research at MIT since 1953. This research is part of a Joint Highway Research Project undertaken by the Department of Civil and Sanitary Engineering, MIT, and the Commonwealth of Massachusetts Department of Public Works. As will be evident from the partial list of references at the end of this chapter, however, both aspects of the problem (deflections and stresses) are receiving attention by a number of different research organizations here and abroad. Aided by modern methods for measuring and recording strain, and by recently developed computers which facilitate analytical attack on the problem, these several groups may be expected to make significant progress within the next few years.

19.3. Physical Concepts. If the weight of the vehicle were very gradually applied, the bridge deflection would likewise gradually increase, the deflection at any instant of time being simply the static value corresponding to the load at the same instant. The slow passage of a vehicle across a bridge involves the steady movement of a force to successive positions with which are associated successively larger (static) deflections of the structure, and after passing mid-span, to successive positions causing smaller deflections. Thus the slow passage of a constant force across the span is equivalent to applying to an elastic system a force which increases to a maximum value and then decreases to zero. Since the actual passage is not, in fact, gradual, the load may be expected to cause vibration, and this vibration continues even after the vehicle has left the span.

Although real bridges may experience the effects of several vehicles concurrently, it is necessary, at the present time, to limit consideration to a single vehicle. This is not an unrealistic restriction because maximum vibrations usually are due to very heavy trucks, of which not more than one is apt to be on a single (simple) span at any one time. When the investigations are extended to continuous structures, the probability of more than one heavy truck being on the structure at the same time will, of course, increase. However, if a good understanding is achieved for the effect of a single vehicle, it should be possible to extend our knowledge to the multivehicle case.

A modern truck on its mechanical springs and tires, and with its shock absorbers, is a very complex elastic system. Joints, bumps, cracks, and other forms of pavement roughness may cause it to vibrate in any one of a number of vibration modes, or simultaneously in several modes. Fortunately, field measurements correlated with theory indicate that practical results are obtained when the vehicle is idealized to a single-degree mass-and-spring system. It will be apparent, however, that the force which this idealized vehicle exerts on the bridge depends not only on the vertical motion of the vehicle mass but likewise on the motion of the bridge itself. Thus the vehicle and bridge comprise a complex elastic system.

Field measurements reported in Ref. 2 indicate that the vertical oscillation of the vehicle on its springs is a major cause of bridge vibration. This was confirmed by subsequent tests in which records were made not only of the bridge motion but also of the varying force transmitted by the main axle of the test vehicle.

19.4. Theoretical Expressions. *a. Simply Supported Beam; Constant Force Moving at Constant Velocity; Including Damping.* In 1847 Willis derived the differential equation for the deflection under the point of loading for a beam of negligible mass and damping subjected to a moving mass loading. At a later date Stokes obtained an exact solution to Willis's equation by means of power series. While this equation was of value in the analysis of railway bridges, the assumption of negligible beam mass rendered it inapplicable to the highway-bridge problem.

In 1905 Krylov obtained a solution in which the mass of the load was assumed negligible in comparison with the mass of the bridge, that is, the case of a constant force moving with uniform velocity. This case was likewise treated, at later dates, by Sir Charles Inglis and by S. Timoshenko. The state of oscillation of a simply supported beam, subjected to a constant force P , moving at a uniform velocity, may be expressed as follows:

$$y = \frac{2PL^3}{EI\pi^4} \left\{ \sum_{i=1}^{i=\infty} \frac{\sin(i\pi x/L)}{i^2[(i^2 - \alpha^2)^2 + (2Si\alpha)^2]^{1/2}} \sin(i\omega t - \Psi_i) \right. \\ \left. + \sum_{i=1}^{i=\infty} \frac{\sin(i\pi x/L)}{i^2[(i^2 - \alpha^2)^2 + (2Si\alpha)^2]^{1/2}} \frac{\alpha}{i} \frac{e^{-S p_i t}}{\sqrt{1 - S^2}} \sin(\sqrt{1 - S^2} p_i t - \Phi_i) \right\} \quad (19.2)$$

where y = deflection of beam at point x from end of span

w = weight per unit length of beam

L = span

t = time, sec

$\alpha = \frac{\pi V}{p_i L}$

V = velocity of force along span

S = damping coefficient

ω = forcing circular frequency = $\frac{\pi V}{L}$

p_i = natural circular frequency = $\frac{i^2 \pi^2}{L^2} \sqrt{\frac{EIg}{w}}$

EI = flexural rigidity of beam

$\Psi_i = \tan^{-1} \frac{2Si\alpha}{i^2 - \alpha^2}$

$\Phi_i = \tan^{-1} \frac{-\sin \Psi_i}{(S/\sqrt{1 - S^2}) \sin \Psi_i - (\alpha/iS) \cos \Psi_i}$

The first term in Eq. (19.2) represents the forced vibration, and for practical velocities it reduces to an expression giving essentially the static deflection of the beam, that is, the deflection which would result from a very slow passage. Accordingly, the net dynamic effect is given by the second term of Eq. (19.2), which represents the free vibrations of the beam. Note that the damping term causes suppression of the free vibrations with time.

When the moving force passes off the beam, a new solution must be used for the free vibration of the unloaded beam. This solution is given by

$$y = \sum_{i=1}^{i=\infty} C_i e^{-S p_i t} (\sin \sqrt{1 - S^2} p_i t - \gamma_i) \quad (19.3)$$

where C_i and γ_i = constants which must be chosen to satisfy conditions of motion at the instant when the force leaves the span.

An illustrative solution of the constant-force case given by Eq. (19.2) is shown in Fig. 19.1, where the mid-span deflection has been plotted vs. position of the force. Damping has been neglected, and the values of the other parameters were assumed as indicated.

b. Simply Supported Beam; Sinusoidal Alternating Force at Constant Velocity; Neglecting Damping. In 1928 Sir C. E. Inglis represented the "hammer blows" due to unbalanced weights on the driving wheels of a locomotive by a sinusoidal alternating force moving at a constant velocity

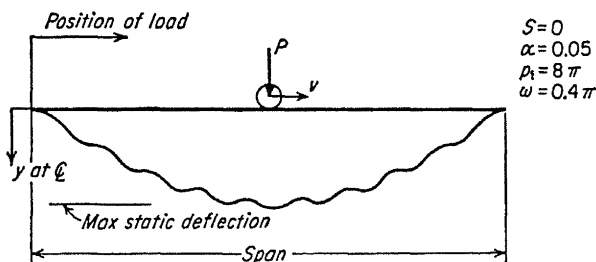


FIG. 19.1. Mid-span deflection produced by constant moving load.

across a beam. Expressing the alternating force by $P \sin nt$, and considering only the first mode of beam response, he presented the following expression:

$$y = \frac{PL^3}{EI\pi^4} \left[\frac{\cos(n - \omega)t - \sin pt}{1 - \left(\frac{n - \omega}{p}\right)^2} - \frac{\cos(n + \omega)t - \cos pt}{1 - \left(\frac{n + \omega}{p}\right)^2} \right] \sin \frac{\pi x}{L} \quad (19.4)$$

Equation (19.4) indicates that the most severe beam oscillations occur when the force frequency n is equal to the beam frequency p . Equation (19.4) does not include the effect of the constant portion of the force. A complete solution for the combined effect of a constant force plus an alternating force would be obtained by adding Eq. (19.2) to Eq. (19.4).

A particular solution of Eq. (19.4) is illustrated in Fig. 19.2, which is a plot of mid-span deflection vs. position of force. Note that the beam vibrates at the frequency of the alternating force. For this particular example the maximum amplitude is about 1.9 times the static deflection which would be caused by the same force positioned at mid-span. If it had been assumed that $p = n$, maximum deflection would have occurred as the force leaves the span and would have equaled $1/\alpha$ times the static deflection.

In 1937, Schallenkamp presented a rigorous solution for a smoothly running load which took account of the masses of both beam and load, but his solution is not in a form convenient for computations. Furthermore, in view of the predominant effect of alternating-force components

the application of a complex solution for the relatively less important contribution of the nonalternating force seems not to be necessary.

c. Simplified Deflection Analysis. Using the basic equations developed by Inglis, Hillerborg, and others, Biggs, Suer, and Louw have developed

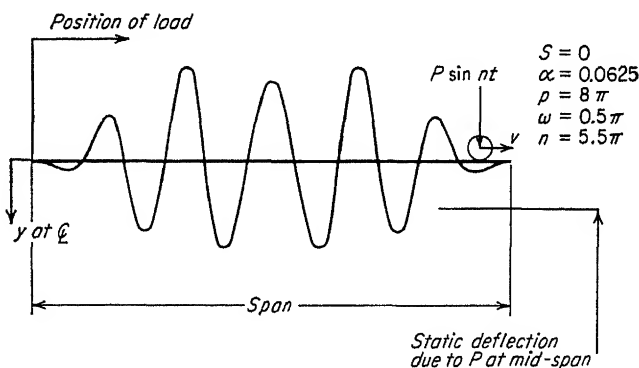


FIG. 19.2. Mid-span deflection produced by sinusoidal moving load.

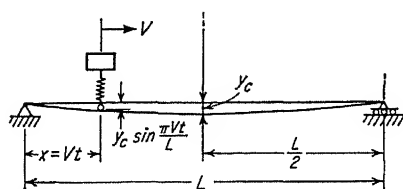


FIG. 19.3. Idealized dynamic system.

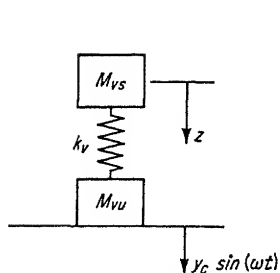


FIG. 19.4. Idealized vehicle.

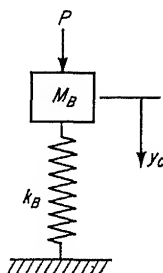


FIG. 19.5. Idealized bridge.

an approximate solution which is particularly suitable for computational techniques. Major assumptions are as follows:

1. The bridge is represented by a simple beam, of which only the first-mode behavior is considered. Thus, a single-degree-of-freedom system is assumed for the bridge.

2. The vehicle is treated as a single-degree-of-freedom system.

3. Viscous damping is assumed in both bridge and vehicle.

Figure 19.3 shows the idealized dynamic system, and Figs. 19.4 and

19.5 show the idealized vehicle and bridge, respectively. Notation is as follows:

- V = velocity of vehicle
- L = span of bridge
- y_c = mid-span deflection at any time
- x = distance of vehicle from end of span
- ω = crossing frequency = $\pi V/L$
- M_B^T = actual total mass of bridge
- M_B = effective mass in bridge equivalent system
- k_B = stiffness of bridge equivalent system
- c_B = damping in bridge equivalent system
- p_B = bridge natural frequency (first mode only)
- Δ = distortion of vehicle spring
- z = absolute deflection of sprung mass, from neutral position
- M_{vs} = sprung mass of vehicle
- M_{vu} = unsprung mass of vehicle
- M_v = total mass of vehicle
- k_v = stiffness of vehicle springs
- c_v = damping of vehicle springs

The stiffness and mass, k_B and M_B , for the bridge equivalent system are given by

$$k_B = \frac{\pi^4 EI}{2L^3} \quad (19.5)$$

$$M_B = \frac{1}{2}M_B^T + M_{vu} \sin^2 \omega t \quad (19.6)$$

The differential equations of motion for the sprung mass and for the bridge are given by

$$-k_v \Delta - c_v \dot{\Delta} = M_{vs} \ddot{z} \quad (19.7)$$

$$(M_v g + k_v \Delta) \sin \omega t - k_B y_c - c_B \dot{y}_c = M_B \ddot{y}_c \quad (19.8)$$

Also, Δ and z are related as follows:

$$\Delta = z - y_c \sin \omega t \quad (19.9)$$

Equations (19.7) to (19.9) may readily be reduced to a pair of simultaneous differential equations in terms of y_c , z , and their derivatives. This pair of equations may be solved by numerical integration, utilizing a digital computer, or by means of an analog computer. In the investigation conducted by Biggs et al., the equations were solved by digital computer.

It may be noted that assumed initial vibrations of the sprung mass of the vehicle itself are taken into account by initial values Δ_0 , $\dot{\Delta}_0$, \dot{z}_0 at time $t = 0$.

19.5. Verification of Simplified Deflection Analysis by Model Study and by Field Measurements. *a. Verification by Model Study.* As described in Ref. 9, a simple-beam model bridge was built to represent a typical two-lane 90-ft-span girder bridge. Natural frequency and static deflection of the model are the same as for the prototype: The model vehicle, which simulated a 20-ton two-axle truck, had a spring-mounted and damped mass which could be excited at the start of each passage. Vehicle velocity and the natural frequency, damping, and initial oscillation of the mass were varied in a series of tests.

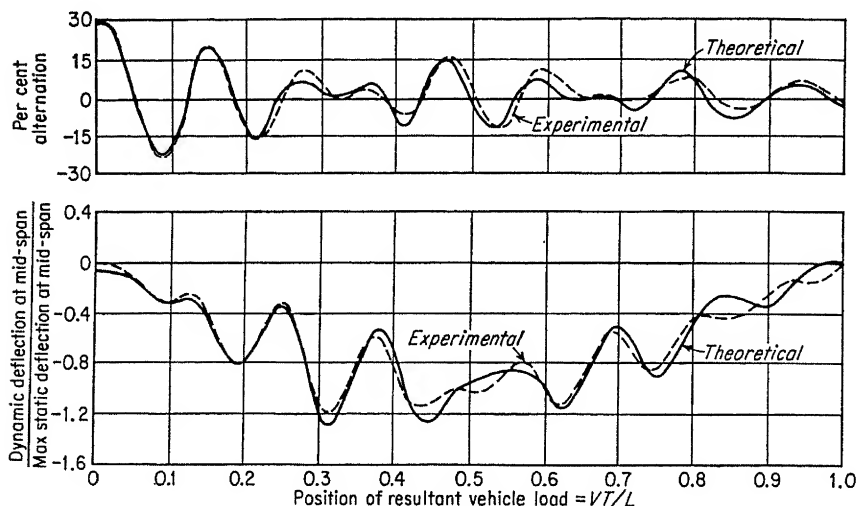


FIG. 19.6. Comparison of mid-span deflections: theoretical and experimental (model run 37).

During each test run mid-span deflection of the beam and force in the vehicle spring were simultaneously measured and recorded. The dashed-line curves in Figs. 19.6 and 19.7 are typical results obtained in the model tests. The corresponding solid-line curves were obtained by theoretical analysis as outlined above. In each case the upper curves show the variation in vehicle spring force and the lower curves show variation in the ratio of dynamic to static deflection. In both cases the beam natural frequency (first mode) was 4.05 cps and the vehicle velocity corresponded to a prototype vehicle velocity of 30 mph. For the run shown in Fig. 19.6 the vehicle natural frequency was 3.87 cps, and for the run shown in Fig. 19.7 the vehicle natural frequency was 3.07 cps.

b. Verification by Field Measurements. Figures 19.8 and 19.9 show cross sections of the two bridges selected for field tests. The structures at Main Street and at South Street in Townsend, Mass., are a stringer bridge and a through girder bridge, respectively [10].

The test vehicle, a 1952 two-axle (six-wheel) Sterling White 10-ton dump truck, has a wheel base of 13 ft. The suspension system is comprised of leaf springs plus auxiliary springs on the rear axle which are engaged only under heavy load. The truck was loaded to a total weight

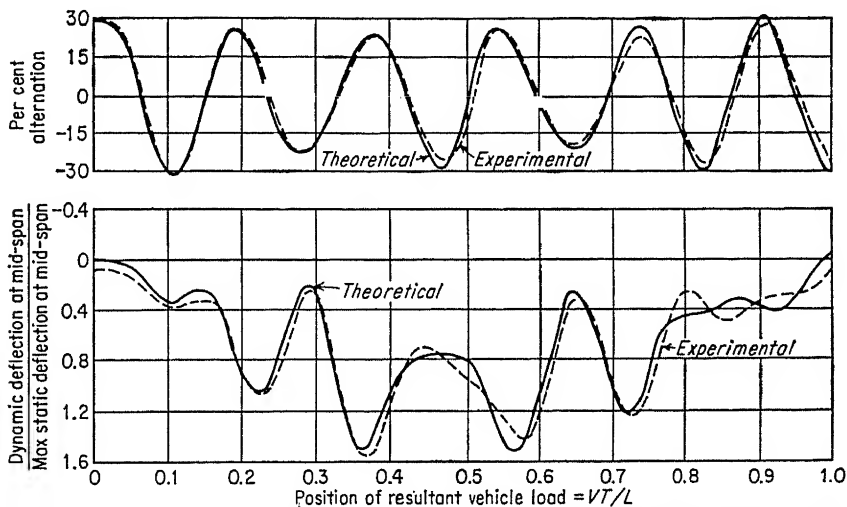


FIG. 19.7. Comparison of mid-span deflections: theoretical and experimental (model run 43).

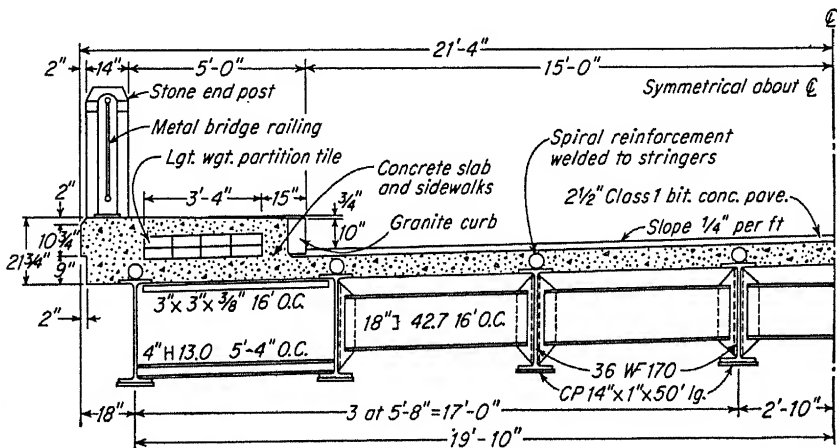


FIG. 19.8. Townsend Main Street Bridge. Span, 88 ft 8 in.; weight, 7,830 lb/ft; design EI , 7.44×10^{12} lb-in.²; composite EI , 9.12×10^{12} lb-in.²

of 41,600 lb, of which 33,900 lb was on the rear axle. By running the truck over an obstruction and recording the resulting free vibration the natural frequency of rear-axle-load variation was found to be about 2.3 cps and the average viscous damping was found to be about 0.07 lb-sec/in.

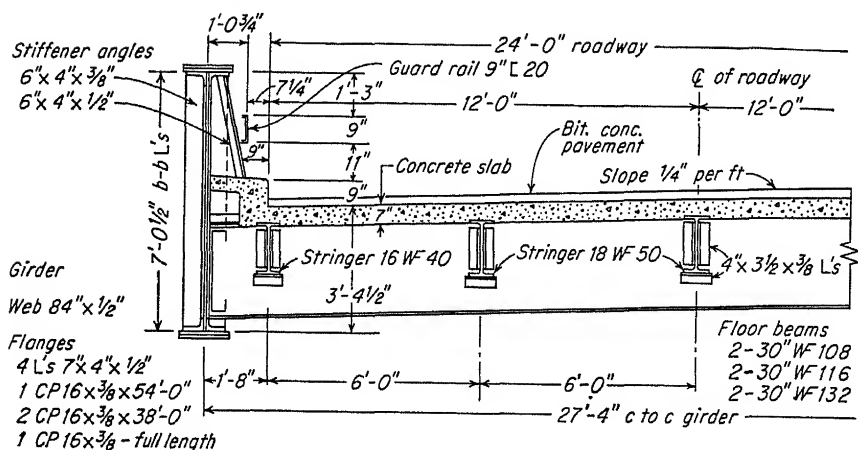


FIG. 19.9. Townsend South Street Bridge. Span, 86 ft; weight, 5,120 lb/ft; design EI , 6.27×10^{12} lb-in.²; composite EI , 7.20×10^{12} lb-in.²

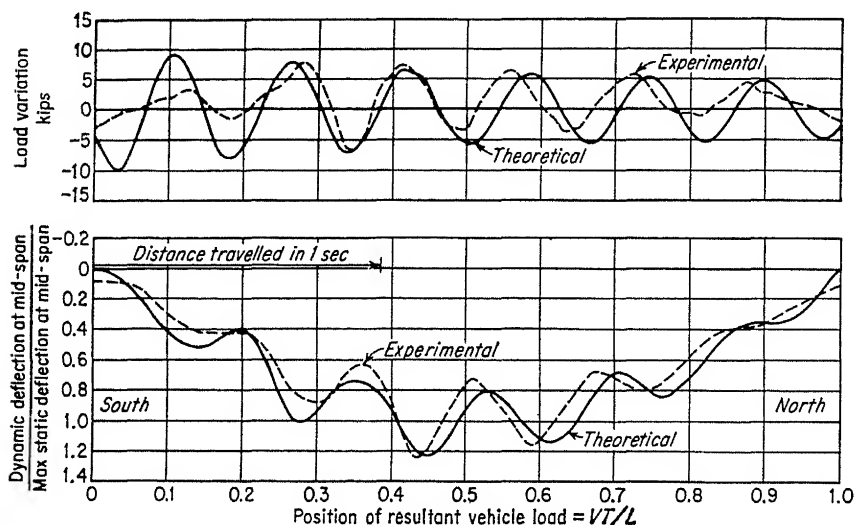


FIG. 19.10. Comparison of mid-span deflections: theoretical and experimental. Townsend Main Street Bridge, run 3. Static deflection, 0.162 in.; velocity, 37.0 ft/sec; span, 88.67 ft.

Natural frequencies of the test bridges, from observed vibrations after the truck had passed off the span, were 3.77 cps for the Main Street Bridge and 4.17 cps for the South Street Bridge.

Instrumentation provided simultaneous measurement of mid-span bridge deflections, force applied by truck rear axle, and vertical acceleration of truck rear axle.

Figures 19.10 and 19.11 show dashed-line plots of results obtained

experimentally for the Main Street Bridge. The experimental load-variation plots are based on the rear-axle force data and rear-axle acceleration data. The theoretical plots of load variation and bridge deflection are the result of an analog-computer solution of the basic equations. In this solution the initial values of Δ_0 and $\dot{\Delta}_0$ were arbitrarily chosen to provide a good matching of the experimental and theoretical load-variation curves. It is apparent that the resulting theoretical plots of bridge deflection are in quite good agreement with the experimental results.

Figures 19.12 and 19.13 present similar information with respect to the South Street Bridge. In each of these figures there are plots of measured

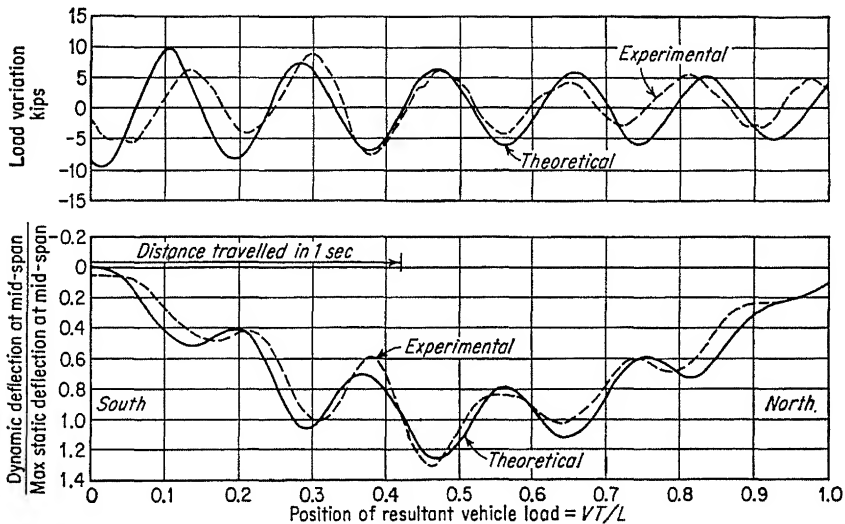


FIG. 19.11. Comparison of mid-span deflections: theoretical and experimental. Townsend Main Street Bridge, run 14. Static deflection, 0.162 in.; velocity, 33.9 ft/sec; span, 88.67 ft.

bridge deflection for each of two adjacent stringers which straddle the bridge axis. The phase shift between these two records is caused by skew of the bridge axis. While the agreement between theory and experiment is satisfactory for the South Street Bridge, it is not quite so good as agreement obtained for the Main Street Bridge.

Figure 19.14 (Main Street) and Fig. 19.15 (South Street) are for the same test runs as were presented in Figs. 19.10 and 19.12, respectively, but with the theoretical deflections computed directly from the experimentally determined load-variation data. As would be expected, this procedure gives better agreement between theoretical and experimental deflections. It should be noted that much of the discrepancy between theoretical- and experimental-deflection plots is due to phase shifts, probably caused by skew of the bridge axis. These phase shifts are of no

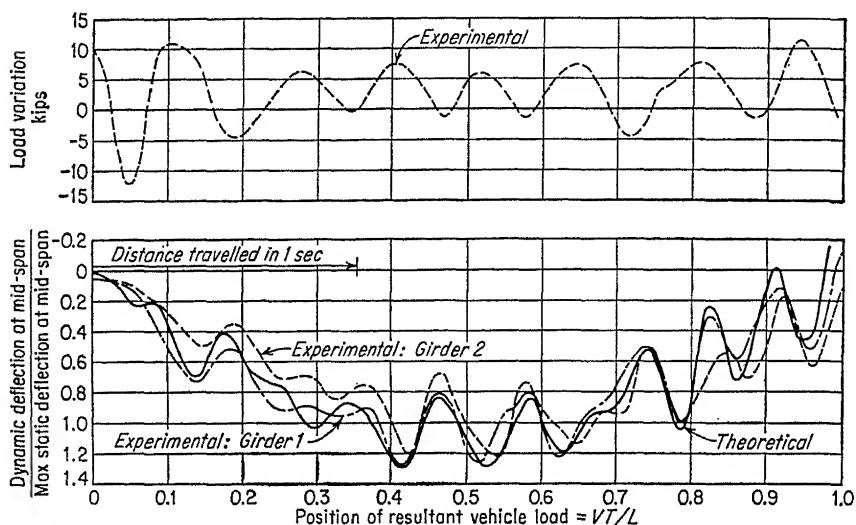


FIG. 19.12. Comparison of mid-span deflections: theoretical (based on measured-load variation) and experimental. Townsend South Street Bridge, run 15. Static deflection, 0.125 in.; velocity, 30.3 ft/sec; span, 86 ft.

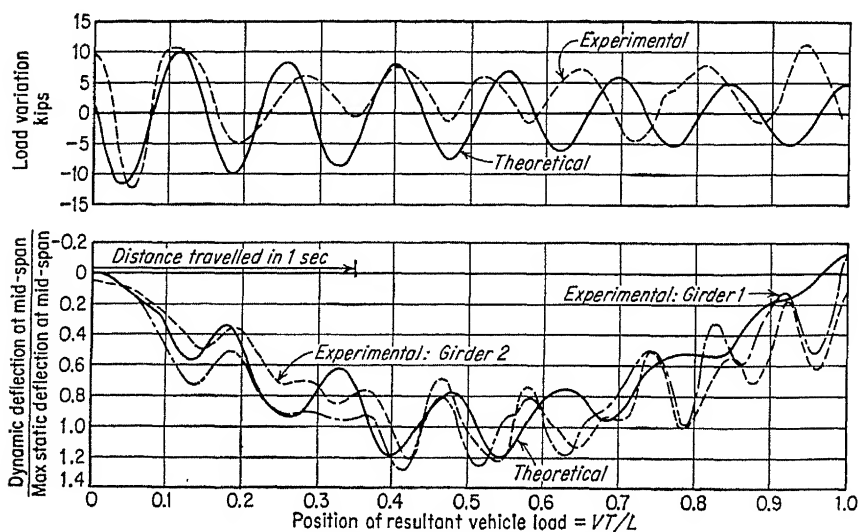


FIG. 19.13. Comparison of mid-span deflections: theoretical and experimental. Townsend South Street Bridge, run 11. Static deflection, 0.125 in.; velocity, 28.0 ft/sec; span, 86 ft.

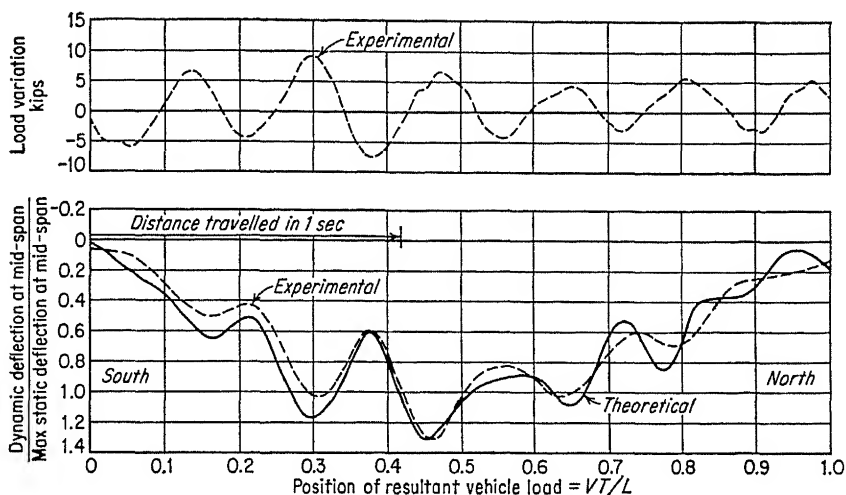


FIG. 19.14. Comparison of mid-span deflections: theoretical (based on measured-load variation) and experimental. Townsend Main Street Bridge, run 3. Static deflection, 0.162 in.; velocity, 37.0 ft/sec; span, 88.67 ft.

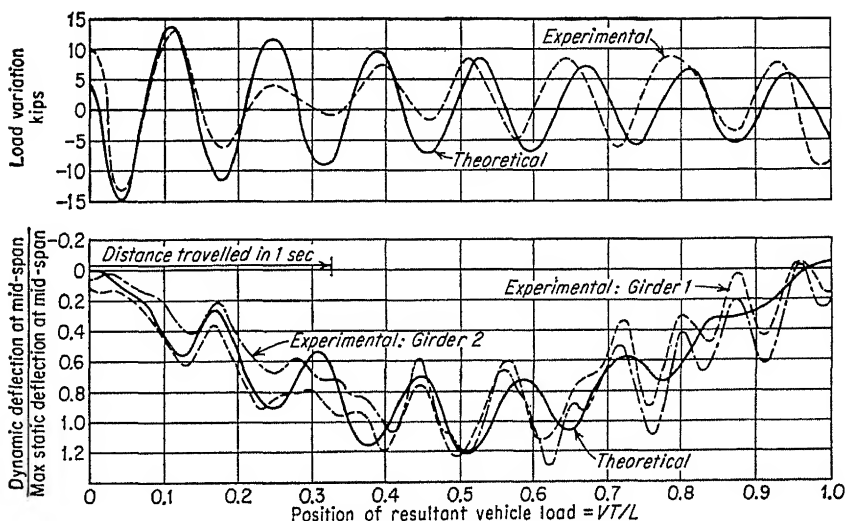


FIG. 19.15. Comparison of mid-span deflections: theoretical and experimental. Townsend South Street Bridge, run 15. Static deflection, 0.125 in.; velocity, 30.3 ft/sec; span, 86 ft.

significance from the standpoint of the practical usefulness of the theoretical prediction.

It was concluded that the simplified method of analysis permitted prediction of bridge deflections with an accuracy quite sufficient for practical design purposes. Refinements, to take account of additional factors such as surface roughness, seem not to be warranted.

19.6. Theoretical Effects of Varying the Major Parameters. The bridge natural frequency p_B and the vehicle natural frequency p_v are given by

$$p_B^2 = \frac{k_B}{M_B} = \frac{M_v g}{M_B \delta_{st}} \quad \text{and} \quad p_v^2 = \frac{k_v}{M_v} \quad (19.10)$$

where δ_{st} is the mid-span static deflection caused by the vehicle and g is the gravity acceleration. Substituting Eq. (19.10) into Eqs. (19.7) to (19.9) and eliminating the damping terms, we obtain

$$\frac{\ddot{y}_c}{\delta_{st}} = p_B^2 \left(\sin \omega t - \frac{y_c}{\delta_{st}} \right) + p_v^2 \frac{M_v}{M_B} \left(\frac{z}{\delta_{st}} - \frac{y_c}{\delta_{st}} \sin \omega t \right) \sin \omega t \quad (19.11)$$

$$\frac{\ddot{z}}{\delta_{st}} = -p_v^2 \left(\frac{z}{\delta_{st}} - \frac{y_c}{\delta_{st}} \sin \omega t \right) \quad (19.12)$$

The magnitude of dynamic deflection is seen to depend upon the magnitude of parameters ω , M_v/M_B , p_v , p_B/p_v , and the initial conditions z_0 , \dot{z}_0 , y_{c0} , \dot{y}_{c0} . The initial bridge conditions are $y_{c0} = \dot{y}_{c0} = 0$, and the initial vehicle conditions are given by

$$z_0 = z_m \sin \phi \quad (19.13)$$

$$\dot{z}_0 = z_m p_v \cos \phi \quad (19.14)$$

where z_m = amplitude of initial vehicle oscillation

ϕ = a phase angle

For convenience z_m is replaced by

$$\beta = \frac{k_v z_m}{M_v g} = \left(\frac{p_v}{p_B} \right)^2 \frac{M_v}{M_B} \frac{z_m}{\delta_{st}} \quad (19.15)$$

The several parameters were varied over the following ranges:

$$\begin{aligned} 0.1 &\leq \beta \leq 0.6 \\ 0.05 &\leq \frac{M_v}{M_B} \leq 0.5 \\ 0.67 &\leq \frac{p_B}{p_v} \leq 8.0 \end{aligned} \quad (19.16)$$

For each combination of the above parameters critical values of ω (in the range $0.04p_B$ to $0.10p_B$) and ϕ (0 to 2π) were estimated by analog-computer studies. In studying the effects of varying β , p_B/p_v , and M_v/M_B , the critical combinations of ω and ϕ were assumed to apply in all cases.

a. *Influence of β .* It was found that y_m/δ_{st} increases essentially linearly with β . This is not surprising in view of the fact that β is a direct measure of the amplitude of initial vehicle oscillation.

b. *Influence of p_B/p_v .* It was found that y_m/δ_{st} is maximum when p_B/p_v is equal to unity. It should be noted, however, that a unity frequency ratio does *not* signify deflections increasing without limit, as would be the case if an external force were resonant with the bridge frequency. The vibration energy in the bridge is limited by the initial energy in the oscillating vehicle. It was noted also that the influence of frequency ratio p_B/p_v diminishes with increasing mass ratio.

c. *Influence of M_v/M_B .* For high-frequency ratios p_B/p_v it was found that variations in M_v/M_B had practically no effect on y_m/δ_{st} . At smaller-frequency ratios, and particularly at unity-frequency ratio, the mass ratio was found to have a pronounced effect, increases in mass ratio causing decreases in y_m/δ_{st} .

It may be noted that δ_{st} is itself directly proportionate to M_v . Thus for a given bridge the absolute deflection increases with M_v/M_B , even though the ratio y_m/δ_{st} decreases.

19.7. Practical Application of Theory. From studies of the influence of variations of parameters it was possible to produce curves useful for design applications. These are presented in Fig. 19.16. Figure 19.16a gives the relationship between y_m/δ_{st} and p_B/p_v for constant values of β ($= 0.30$) and M_v/M_B ($= 0.20$). Figure 19.16b gives correction factors $(CF)_\beta$, for values of β other than 0.30. Figure 19.16c gives correction factors $(CF)_M$ for values of M_v/M_B other than 0.2.

For an actual bridge the mid-span deflection which may be anticipated to occur, because of the passage of a single heavy vehicle, can be estimated by the following steps.

1. Compute the static deflection δ_{st} caused by a single vehicle at mid-span on the roadway centerline. Moment of inertia to be used is the composite value, including all elements which could conceivably contribute to stiffness.

2. Compute the bridge natural frequency using

$$f_B = \frac{1.2\pi}{2L^2} \sqrt{\frac{EI}{w}} g \quad (19.17)$$

where 1.2 = a factor based on field measurements

EI = flexural stiffness for composite section

w = weight of bridge per foot of span

3. Assume a value of β . It appears, from the limited field-test data, that an assumption $\beta = 0.5$ would not be unduly conservative.

4. Assuming a vehicle natural frequency within the range 1 to 2.5 cps, compute the range of possible frequency ratios p_B/p_v ($= f_B/f_v$).

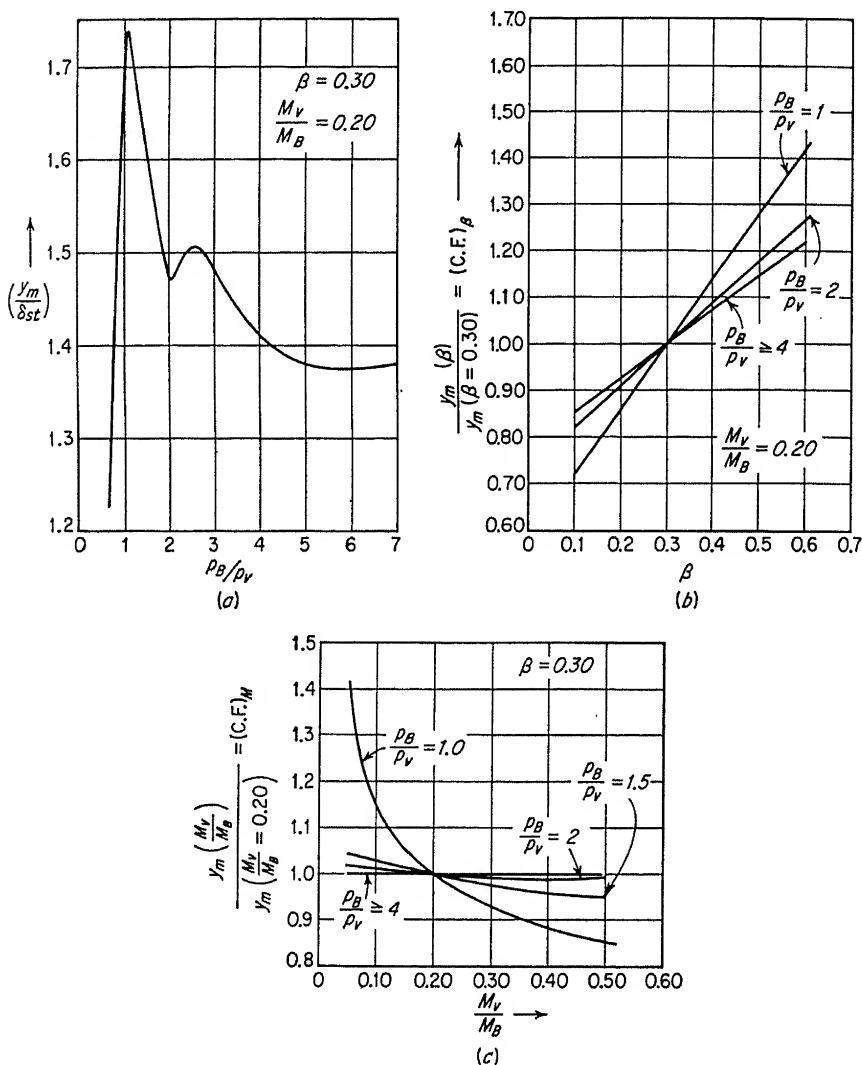


FIG. 19.16. Design curves for maximum dynamic deflection.

5. Compute the mass ratio M_v/M_B , keeping in mind that M_B is only one-half the total bridge mass.

6. Enter Fig. 19.16a to find a value of y_m/δ_{st} , for $\beta = 0.30$, and a frequency ratio within the range computed in step 4.

7. Enter Fig. 19.16b and c to obtain values of $(\text{C.F.})_\beta$ and $(\text{C.F.})_M$.

8. Compute the deflection y_m according to

$$y_m = \delta_{st} \frac{y_m}{\delta_{st}} (\text{C.F.})_\beta (\text{C.F.})_M \quad (19.18)$$

The deflection ratio for a single vehicle not on the bridge centerline, or for more than one vehicle, would be somewhat less than the ratio y_m/δ_{st} obtained above.

REFERENCES

1. "Proceedings of the Second Illinois Structural Engineering Conference," University of Illinois, November, 1952.
2. Biggs, J. M., and H. S. Suer: Bridge Vibration: An Experimental Investigation of the Vibration of Simple-span Highway Bridges, *MIT, Dept. Civil and Sanitary Eng., Progr. Rept. 1*, September, 1954.
3. Chen, W. L., and E. L. Koetjé: "Model Investigation of the Vibration of Continuous Three-span Steel Bridges," unpublished thesis, MIT, Dept. of Civil and Sanitary Engineering, May, 1956.
4. "Vibration and Stresses in Girder Bridges," *Highway Research Board Bull. 124*, 1956, contains the following six papers:
 Biggs, J. M., and H. S. Suer: Vibration Measurements on Simple Span Bridges
 Scheffey, C. F.: Dynamic Load Analysis and Design of Highway Bridges
 Edgerton, R. C., and G. W. Beecroft: Dynamic Studies of Two Continuous Plate-girder Bridges
 Hayes, J. M., and J. A. Sbarounis: Vibration Study of Three-span Continuous I-beam Bridge
 Foster, G. M., and C. T. Oehler: Vibration and Deflection of Rolled-beam and Plate-girder Bridges
 Tung, T. P., L. E. Goodman, T. Y. Chen, and N. M. Newmark: Highway-bridge Impact Problems
5. Inglis, E. E.: A Mathematical Treatise on Vibrations in Railway Bridges, Cambridge University Press, New York, 1934.
6. Timoshenko, S. P.: "Vibration Problems in Engineering," D. Van Nostrand Company, Inc., Princeton, N.J., 1937.
7. Hillerborg, A.: "Dynamic Influences of Smoothly Running Loads on Simply-supported Girders," Institute of Structural Engineering and Bridge Building of the Royal Institute of Technology, Stockholm, 1951.
8. Lin, T. Y., R. Horonjeff, R. W. Clough, and C. F. Scheffey: "Investigation of Stresses in the San Leandro Creek Bridge," *Univ. California, Inst. Transportation and Traffic Eng., Research Rept. 13*, 1953.
9. Connell, R. M., and R. J. Lamp: Model Investigation of Effects of Vehicular Vibrations on Simple Span Bridges, unpublished thesis, MIT, Dept. of Civil and Sanitary Engineering, June, 1955.
10. Suer, H. S.: Dynamic Response of Simple Span Highway Bridges to Moving Vehicle Loads, unpublished doctor's thesis, MIT, Dept. of Civil and Sanitary Engineering, September, 1955.

CHAPTER 20

DYNAMIC EFFECTS OF WIND LOAD

20.1. Introduction. All wind forces are dynamic in the sense that they are effects of a moving fluid. However, under certain ideal circumstances a body immersed in a wind stream of constant velocity (magnitude and direction) experiences forces which do not vary with time, and these might logically be termed static wind forces. These ideal conditions are rarely developed. Fluctuations in the general wind, as well as in its local characteristics, and influences of the shape (and sometimes the motion) of the body are factors which cause time variations of actual wind forces.

The common design assumption that wind forces are static can be justified as a useful simplification in the majority of cases of wind loading encountered by structural engineers. There are certain cases, however, where the dynamic character of wind forces is of great importance, and in some of these cases the response to wind loading cannot possibly be explained otherwise than on the basis of time variations of wind force.

In some instances possible dynamic effects of wind load can be anticipated at the design stage. More often, these effects cannot be predicted with sufficient certainty to warrant accounting for them in the design, and the engineer's problem is to devise corrective measures after the dynamic effects have appeared in an existing structure.

It is the purpose of this chapter to outline the main types of time-varying wind forces, to indicate kinds of structures in which the dynamic effects of such forces may be important, and to note preventive and corrective measures which have been employed or proposed.

20.2. Factors Justifying the Common Design Assumption That Wind Forces Are Static. Since natural winds rarely can cause truly static forces it is desirable to point out factors which tend to justify the common design assumption that wind loads may be treated as static forces.

a. Nonperiodic Character of Common Wind Loadings. For many structural elements subject to wind forces these forces, although time-varying, do not involve sustained periodic components. Moreover, where periodic variations do occur, they may be limited to local pressures rather than to over-all forces. Thus one member of a truss may experience periodic wind pressures, but the primary wind stresses in this and

other members may depend upon the total wind loading on the entire structure.

b. Insensitivity of Wind-load Stresses to Local-force Variations. As indicated in the above section, primary wind stresses often depend more upon over-all wind loads than upon local pressures. Thus the bending stresses in a bridge chord due to wind forces on the chord itself may not be as important as direct stresses in the chord due to wind forces upon the entire structure. If a sudden increase in wind load on the chord causes dynamic magnification of the bending stresses, they still may be of secondary magnitude.

c. General Insensitivity to Rapid Changes of Wind Force. Undoubtedly many structures or structural elements subjected to rapid changes of wind load possess natural frequencies and degrees of damping such that they experience very little dynamic magnification of the applied forces.

d. Concurrent Existence of Nonwind Forces of Significant Magnitude. For many structures there are other important sources of loading in addition to the wind. For example, gravity forces, associated with the mass of the structure and with superimposed masses, frequently cause stresses as large as, or larger than, the stresses due to wind. Thus any underestimation of wind stresses due to treatment of wind loads as static forces may imply a much smaller underestimation of the combined stresses due to all causes.

e. Existence of Sources of Potentially Greater Error Than Is Due to Neglect of Dynamic Effects. There are several factors which affect the maximum wind forces experienced by a structure within its service life. These include direction and magnitude of the most severe winds, shape and orientation of structure and its members, surrounding topography, exposure, and dynamic characteristics of the structure.

Since basic wind forces vary in proportion to velocity squared, a 20 per cent error in estimated maximum velocity would cause a 40 per cent error in wind forces. The maximum wind velocity which will occur within a service life of several years cannot be predicted (with any degree of certainty) within 20 per cent.

In most cases the shape of structure, surrounding topography, exposure, etc., do not correspond to any of the idealized forms for which wind-tunnel tests have established the relations between force and velocity. Therefore these factors may introduce additional error of 25 per cent, 50 per cent, or more.

Neglect of the dynamic effects of rapidly changing wind forces would not, in theory, introduce an error in excess of 100 per cent, and in most practical cases the error probably would not exceed about 25 per cent. (Exceptions will be noted later.)

From the foregoing it is apparent that the potential error in predicted

wind forces due to other factors might easily exceed the error associated with neglect of dynamic effects. If the loss of a structure due to wind forces in excess of predicted values would result in great loss of life or property, or interruption of a critical function, then a careful study of *all* factors may be justified. Such a study should include not only estimates of the dynamic effects of rapidly changing wind forces, but in addition wind-tunnel tests, statistical evaluations of meteorological data, etc. On the other hand, if the project does not warrant the time and expense that would be involved in a study of all the factors that influence wind forces, there may be no justification for intensive study of a single aspect of the problem, namely, the dynamic response of the structure. From this point of view the use of static wind forces, of a magnitude reflecting previous successful performance of similar structures in comparable geographic zones, appears to be entirely logical.

20.3. Conditions Requiring Consideration of Dynamic Effects of Wind Load. *a. Structures Sensitive to Gusts.* In Sec. 20.2 a number of factors were mentioned justifying the almost universal practice of neglecting the dynamic effects of wind gusts. There are certain special cases, however, for which these effects may be sufficiently important to warrant their inclusion in the design computations. If wind forces represent the major loading, if dimensions are such that gust effects can occur concurrently over major portions of the structure, if the structure has a fundamental period which is not small in comparison with typical gust-acceleration times, and if the structure has small damping, the dynamic magnification of applied wind forces may be very large.

As an illustration of structures for which the dynamic effect of gusts may be significant, one may cite the examples of radio and television towers, particularly those which are of the free-standing (that is, non-guyed) type. In such towers the gravity-load effects are very small and stresses are due virtually entirely to the effects of wind load. Because even very tall towers are relatively narrow (particularly in the critical zone near the top) all members may experience a wind-velocity change almost simultaneously; thus the resultant wind loading may be expected to change rapidly during gusts. It will be found that the fundamental period of free-standing towers, particularly very tall towers, is rather long. Most structures of this kind are assembled by field-bolted joints, and the connections of this kind provide a degree of damping. However, the total damping, including friction damping due to slipping in the joints, may not be sufficient to modify the response to gusts to any important degree.

In Sec. 20.5a numerical examples are presented indicating the range of fundamental periods which might be expected in tall, slender, nonguyed radio towers and showing the dynamic magnification corresponding to

assumed gust conditions. It should be noted at this time that the result of neglecting dynamic response is an overestimation of the wind velocity which would cause failure. This has no great design significance because all tower manufacturers follow the same practice. It is customary to specify tower design loadings in pounds per square foot of exposed area (as a 20-lb, 30-lb, or 40-lb tower) without too much concern regarding definition of equivalent wind velocity. Should experience motivate a customer to desire a tower resistant to higher velocities (perhaps as a result of loss of a previous tower), he can achieve this end by specifying a higher design loading. Thus a specific provision for the dynamic effects of gusts is not essential from the standpoint of the design process. Perhaps the greatest value of an understanding of the gust effect is in rationalizing the occasional failure of this kind of structure with the wind velocities at time of failure. If a survey of such failures were to reveal maximum

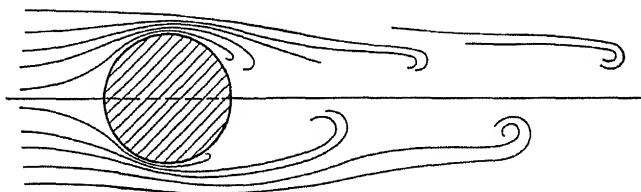


FIG. 20.1. Karman vortex trails.

velocities consistently lower than anticipated, this might result in a general increase in design loading values.

b. Structures Subject to the Periodic Forces Associated with Karman Vortices. Fluid flow past a cylindrical body generally results in the formation of vortices of the pattern shown in Fig. 20.1. While the body shown has a circular cross section, the vortex formation occurs in the flow past any blunt section. This phenomenon, known as the *Karman vortex trail*, has been studied experimentally, and the following relationship between velocity V , transverse dimension d , and frequency of shedding f has been established:

$$\frac{fd}{V} = S \quad (20.1)$$

where S is termed the *Strouhal number*.

Over a wide range of Reynolds number ($R = Vd/\nu$, velocity times diameter, divided by kinematic viscosity), it was found that S is constant for a given shape. Until recently it was believed that the range of constant extended to a critical Reynolds number ($\approx 200,000$) and that for larger values of Reynolds number the periodic vortex shedding would not occur. Field observations of vibrating stacks indicate that the phenomenon must exist at very much larger values of Reynolds number,

and there is evidence that above $R = 200,000$ the Strouhal number increases. If f , d , and V are expressed in cycles per second, feet, and feet per second, the Strouhal number for $R < 200,000$ is approximately 0.2 for circular cylindrical bodies. Relatively few tests have been made at higher Reynolds number, but Delaney and Sorensen [4] found $S = 0.43$ at $R = 1,500,000$.

Corresponding to the periodic Karman vortices the body experiences a periodic transverse force, which may be expressed as

$$F_K = C_K(1/2\rho V^2 A) \sin 2\pi ft \quad (20.2)$$

where F_K = periodic transverse force

C_K = coefficient (dimensionless)

ρ = air density (mass/unit volume)

V = air velocity

A = area of body projected on air stream

f = frequency of vortex shedding, cps

t = time

There is uncertainty regarding the value of the coefficient C_K , but it appears to be approximately $C_K = 1.0$. It will immediately be apparent that the periodic force associated with this phenomenon is relatively large (compare with the drag coefficient for cylinders, $C_D = 1.2$ in range $R < 200,000$ and $C_D \approx 0.4$ in range $R > 200,000$).

It should be noted that Eq. (20.1) implies a vortex-shedding frequency which depends upon the dimension D and velocity V only. In reality there is evidence suggesting that the periodic effect may not be independent of the stiffness and natural frequency of the body, when finite oscillations are permitted [6]. Under some circumstances it seems that the body will oscillate at its natural frequency even though this is quite different from the frequency called for by the Strouhal number and that the frequency of vortex shedding may likewise be altered to the natural frequency of the body [6].

Additional research is necessary to establish definitely influences of Reynolds number and dynamic properties of the body on the frequency of vortex shedding and on the coefficient C_K in Eq. (20.2). However, even in the present state of knowledge it is possible to identify a number of practical cases in which the phenomenon is a predominant factor, as well as others for which it is at least a contributing factor. Vibration of transmission lines, industrial stacks, tubular members of a space truss, and the original Tacoma Narrows suspension bridge are among the cases in which serious vibrations have been attributed to Karman vortices. Some of these cases are discussed briefly in Sec. 20.5. In addition, one might mention singing blades of ship propellers and hydraulic turbines as well as vibrations of submarine periscopes. There are also cases in

which the effects of Karman vortices are believed to initiate a vibration after which the behavior is associated with different phenomena, such as are described in Sec. 20.3c or 20.3d.

If one takes the point of view that the frequency of trailing vortices (and thus also the frequency of periodic force, F_K) is independent of the dynamic characteristics of the body, the effect can be treated like any other case of a periodic external exciting force. The possible preventive or corrective measures are (1) to prevent the development of periodic vortices by streamlining, shrouding, or spoilers, (2) to change the natural frequency of the body so that resonance or near resonance is avoided, (3) to supply sufficient damping to assure that resonant vibrations will not involve excessive amplitudes.

If it appears that the periodic forces are a function of the body's motion, the analysis of behavior and the design of corrective measures may be more difficult. However, the measures suggested in the above paragraph, particularly item 1 or 3, still are indicated.

c. Structures Having Negative Slope of Curves of Lift or Moment vs. Angle of Attack. By wind-tunnel tests it is possible to establish curves of the forces which the wind exerts on a cylindrical body of given cross section in terms of the stagnation pressure $\frac{1}{2}\rho V^2$, a transverse dimension, and the angle of attack α . Thus for *lift* (force normal to the wind) and *drag* (force in the direction of wind) we can write

$$L = C_L(\frac{1}{2}\rho V^2 A) \quad (20.3)$$

$$D = C_D(\frac{1}{2}\rho V^2 A) \quad (20.4)$$

The dimensionless coefficients C_L and C_D as well as a corresponding coefficient C_M (for moment) depend upon Reynolds number but are essentially constant for wide ranges of velocity. The coefficients C_L , C_D , and C_M vary with the shape of section and with the angle of attack α .

Figure 20.3 illustrates the lift and drag forces and defines the angle of attack α . Figure 20.4 shows (in a qualitative form only) typical curves of C_L and C_D which might be obtained for an airfoil section. Notice that the lift coefficient C_L in Fig. 20.4 has a positive slope over a wide range of α . This stable condition is in contrast to the unstable condition represented by the negative slope for the curves C_L and C_M in Fig. 20.2 in the vicinity of $\alpha = 0$.

Now consider what may happen to a section having a negative slope C_L when it is subjected to a horizontal wind velocity V . If the section moves downward, as in Fig. 20.5, the angle of attack for the relative wind velocity increases. If the section curve of C_L versus α has a negative slope, as in Fig. 20.2, the effect of downward motion will be to increase the *downward* lift component of force. Similarly, if the body has an

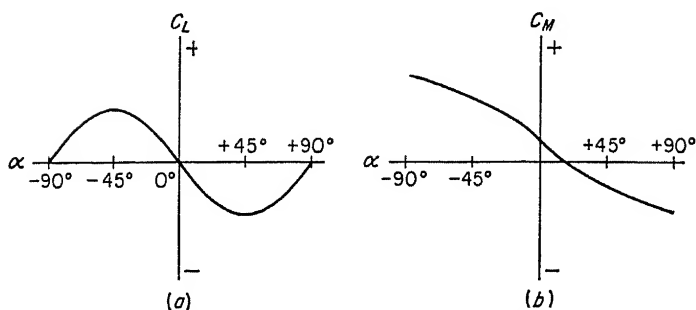


FIG. 20.2. Static-lift and static-moment curves, showing regions of negative slope.

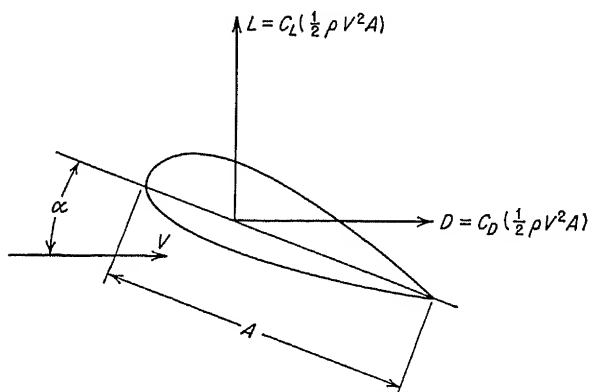


FIG. 20.3. Lift, drag, and angle of attack.

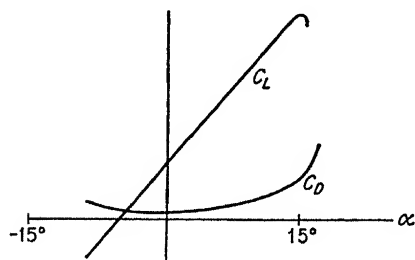
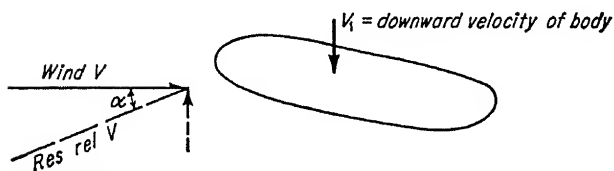
FIG. 20.4. Typical curves of C_L and C_D versus α .

FIG. 20.5. Effect of downward velocity of body on angle of attack.

upward velocity and the section has a negative sloping curve of C_L , the effect will be to increase the upward lift component.

Noting in Fig. 20.3 that L and D are taken parallel and perpendicular to the direction of relative wind, and denoting by L_1 the force component in the direction of body motion, we write

$$L_1 = L \cos \alpha + D \sin \alpha \quad (20.5)$$

and for small values of α ,

$$\frac{dL_1}{d\alpha} = \frac{dL}{d\alpha} + D \quad (20.6)$$

$$\frac{dL_1}{d\alpha} = \left(\frac{d}{d\alpha} C_L + C_D \right) \left(\frac{1}{2} \rho V^2 A \right) \quad (20.7)$$

From Eq. (20.7) we see that the criterion for stability is really not the slope of the C_L curve, but the slope of C_L plus the value of C_D . When this sum is negative, an unstable condition results and oscillation must result.

For an unstable value of $(dC_L/d\alpha + C_D)$ it is apparent that energy is pumped into the moving body in every cycle of oscillation. Thus the amplitude of motion increases until the energy change per cycle is zero. This point may be reached in part through a change to positive slope of C_L (as at the larger angles α of Fig. 20.2a) so that in part of each cycle energy is being pumped in and in the rest of the cycle energy is being dissipated. The maximum amplitude reached will likewise be limited by the amount of damping (internal or otherwise) which exists apart from the aerodynamic phenomenon.

What has been described above with respect to body motion normal to the wind stream may also occur with respect to angular oscillation. Imagine a section prevented from moving transversely but free to rotate. The moment of aerodynamic forces, with respect to the axis of rotation, can be expressed as

$$M = C_M \left(\frac{1}{2} \rho V^2 A^2 \right) \quad (20.8)$$

where C_M , a dimensionless coefficient, is a function of α . For an unfavorable slope of C_M torsional oscillations of the body may build up in a manner analogous to that described above for transverse oscillations.

To determine whether a given section is stable or unstable with respect to negative slope effects, it usually is necessary to make tests. In general, long elongated sections are stable when the long axis is parallel to the wind and unstable when the long axis is across the wind. The negative slope effect is particularly strong in a semicircular section held with flat side toward the wind and almost nonexistent when the curved side is toward the wind.

d. Structures Subject to Flutter. Flutter is an unstable oscillation which occurs as the result of coupled transverse and angular motions of an object in a wind stream. It differs from the phenomenon described in Sec. 20.3c in that flutter vibration can occur with a section having positive slopes for both the curves C_L and C_M versus α . A qualitative explanation may be given with the aid of Fig. 20.6, according to Den Hartog [1].

The section is capable of both transverse (vertical) motion and angular motion, against elastic restraint. A flutter mode involves angular and vertical motion occurring at a common frequency, and in such phase that the lift and moment components of force pump work into the system during every cycle. For example, suppose that during a portion of the cycle the section has a downward component of velocity and a clockwise angular velocity. Both of these velocity components would cause increasing angle of attack. If at the given instant both M and L are positive, the

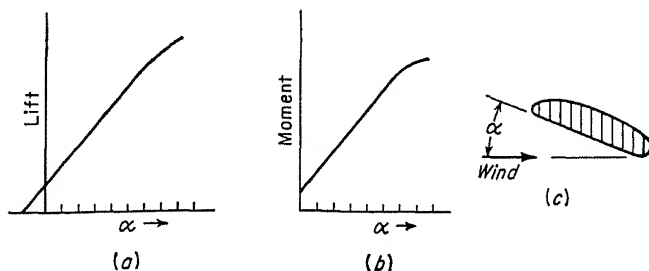


FIG. 20.6. Lift and moment diagrams at small angle of attack.

moment M will put energy in the system (because it acts in the direction of angular velocity) and L will take energy out of the system (because it opposes the downward motion). The mathematics of flutter phenomena [11] is complex and beyond the scope of this presentation. Given the aerodynamic and dynamic characteristics of a particular section, however, analysis to determine the critical wind velocity at which flutter will occur is feasible.

It is of interest to note that flutter vibration occurs not at either natural frequency of the system, but at a flutter frequency which depends not only upon mass and stiffness but upon the aerodynamic characteristics of the system as well.

It is also important to note that true flutter generally results in very rapid amplitude increases to catastrophic proportions. It is a major problem in the field of aircraft structures, but is not often encountered in the field of civil-engineering structures. Apparently this phenomenon can be important in the vibration of certain types of suspension bridges (Sec. 20.5c).

20.4. Sources of Positive Damping. It is apparent that the seriousness of the kinds of dynamic behavior described in Sec. 20.3 depends in some instances upon the amount of positive damping which is available to dissipate energy. Excluding special damping devices (viscous or friction) which may be added to the system deliberately, there is some inherent damping in every vibrating system.

When it is feasible to do so the amount of damping in an elastic system is easily measured by displacing the system from equilibrium and observing the resulting free vibration upon release. If in the course of this diminishing free vibration we observe the magnitudes x_{n+1} and x_n of successive peak displacements, we can write

$$\frac{x_n - x_{n+1}}{x_n} = \delta = \frac{2\pi c}{c_c} \quad (20.9)$$

where c = damping coefficient

c_c = critical damping = $2 \sqrt{mk}$

m = mass term

k = stiffness term

δ = logarithmic decrement

The logarithmic decrement frequently is used as a means of specifying the degree of damping. If the damping is truly viscous (damping force equals constant times velocity), the logarithmic decrement will have a value independent of amplitude of motion; that is, the ratio of successive peaks in the free-vibration curve will be constant.

Damping sometimes may be determined by application of an external force tuned to be in resonance with a natural mode of vibration of the system. For this condition the damping factor c can be computed from the relationship

$$c = \frac{P}{\omega x_o} \quad (20.10)$$

where ω = resonant frequency

x_o = amplitude of motion

P = amplitude of external force

Internal damping originates in the imperfect elasticity of the structural materials, in plastic yielding and friction due to small movements in riveted or bolted joints, in friction bearings, and in other kinds of articulations. For steel beams at stresses of 2 and 10 ksi, corresponding logarithmic decrements of 0.003 and 0.007 have been reported [8]. Obviously, these values are small, as is the value of δ for structural metals in general, at moderate stresses. Where friction, in joints and bearings, is a factor, it may well contribute 10, 20, or 50 times as much damping as is obtained through imperfect elasticity. It often has been noted that welded structures possess significantly smaller damping than do their

riveted counterparts, particularly at higher stress levels. For concrete the hysteresis effect presumably is more pronounced, and a logarithmic decrement of 0.100 has been reported at stresses of 200 psi.

From the foregoing it is apparent that internal damping is not insignificant, but in many practical cases involving resonance internal damping alone will be unable to limit amplitudes to acceptable values.

20.5. Examples of Dynamic Response to Wind. In this, the concluding article, several interesting examples of dynamic response to wind loading will be mentioned. In virtually every case the problem has been extensively discussed in the literature. Consequently, the present discussion will be limited to a few brief comments.

a. Nonguyed Towers Subject to Gusts. Consider a nonguyed radio tower of height L (feet), having three legs of area A (square feet) each, with leg spacing S (feet) on each face. Further assume (although this is not generally so) that A and S are constant throughout the entire height. Denoting the flexure stiffness by EI and assuming the mass per foot of height is four times the mass of a single leg,

$$m = 4A \left(\frac{490}{32.2} \right) = 61A \quad (20.11)$$

$$EI = (3)(10)^7(144) \left(\frac{AS^2}{2} \right) = (216)(10)^7 AS^2 \quad (20.12)$$

The expression for fundamental period of a uniform cantilever beam is

$$T_n = \frac{\pi}{1.75} \sqrt{\frac{mL^4}{EI}} \quad (20.13)$$

Substituting Eqs. (20.11) and (20.12) into Eq. (20.13), we obtain

$$T_n = 0.0003 \frac{L}{S} L$$

Based on values of $L/S = 10, 20, 30$ and values of $L = 100, 200, 300$ ft, the corresponding periods T_n are as follows:

L	T_n , sec		
	$L/S = 10$	$L/S = 20$	$L/S = 30$
100	0.3	0.6	0.9
200	0.6	1.2	1.8
300	0.9	1.8	2.7

From data in Ref. 2 it appears that wind-velocity increases from, say, $0.5V$ to V in 1 sec are entirely possible. This would correspond to wind-

force increases from $0.25F$ to F in 1 sec. For practical purposes this may be approximated by a linear increase from zero to F in 1 sec. Assume $T_r = 1.0$ and $T_n = 1.8$ sec. Then $T_r/T_n = 0.56$. From Fig. 7.13 we find a dynamic factor of 1.57; that is, the stresses in the tower would correspond to static forces 1.57 times larger than those associated with velocity V .

It seems quite possible that the maximum value of dynamic-load factor (DLF = 2.0) might be approached in actual towers. There is the further possibility, difficult to predict, that a gust might strike in phase with residual motion from previous gusts, in which case the factor 2.0 might be exceeded.

b. Singing Transmission Lines. Under sustained steady winds it has long been known that transmission lines develop high-frequency vibration. Resonance takes place at a high harmonic of the fundamental. According to Den Hartog [1], this is solely a case of trailing Karman vortices, with close correspondence between observed frequencies and frequencies computed on the basis of constant Strouhal number. It may be noted that singing of transmission lines occurs at Reynolds numbers generally $< 50,000$.

This kind of vibration, though small in amplitude, may involve numerous cycles of stress, and it appears to have been the cause of fatigue failure in several cases. A device known as the *Stockbridge damper* has been found to be quite effective in stopping or greatly reducing motion. Motion of the line excites motion of the damper, and energy is dissipated via friction within the damper. It has been found that these dampers should be located to avoid coincidence with nodal points of the motion.

c. Industrial Stacks. A fairly large number of industrial smokestacks have exhibited vibration attributed to the effects of Karman vortices. In some instances the motion (in cantilever-bending mode) has been so violent as to cause an actual rupture of the stack. While most reported cases have involved the cantilever mode, there have been instances of an ovaling mode in which a stack cross section becomes oval first in one direction and then at 90° thereto. It is of interest to note that for a given vortex-shedding frequency f , the exciting frequency for ovaling mode is $2f$. This is because each vortex acts in the same sense on the ovaling mode, whereas successive vortices act in opposite senses on the cantilever mode.

It has been observed that riveted stacks fare better than welded stacks. This is believed to be due to the greater internal damping of riveted constructions. Stacks which contain concrete or brick lining (as well as concrete and brick stacks) appear far less susceptible to this kind of vibration.

Model tests by Price [6] indicate that stack vibration could be pre-

vented by shrouding the stack with a separate perforated shell. It seems very doubtful that this solution would prove to be economical, either for a new installation or as a preventive measure. Dockstader et al. [5] conclude that stacks designed to be nonresonant with the vortex-shedding frequency (based on $S = 0.2$) for all wind velocities below 70 mph should be satisfactory. If a stack is to be lined with concrete, it appears wise to provide temporary stays for the period when the steel shell is without lining. On the basis of installations reported in Refs.

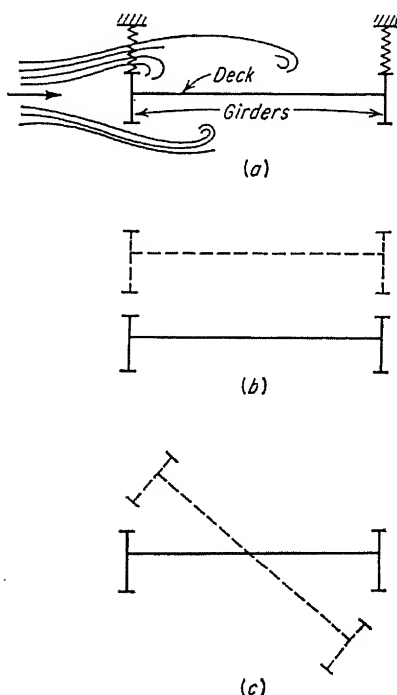


FIG. 20.7. Girder-stiffened suspension bridge. (a) Formation of Karman vortices; (b) vertical modes; (c) torsional modes.

slender proportions. It should be noted that the form, comprised of girders and deck, possesses little inherent torsional stiffness. About a year after the bridge went into service it developed catastrophic motion and was thereby destroyed.

As the result of years of experimental and analytical studies it appears to have been established that the predominant factor in the failure at Tacoma Narrows was the formation of Karman vortices shedding from the top and bottom edges of the windward stiffening girder. This is illustrated in Fig. 20.7a. Under the periodic forces associated with vortex

1 and 5 it appears feasible to eliminate severe vibration by adding damping, in the form of either friction devices or hydraulic shock absorbers. Since mechanical devices of this kind present a maintenance problem, they do not represent an ideal solution.

d. Girder-stiffened Suspension Bridges. The disastrous failure of the first Tacoma Narrows suspension bridge stimulated a considerable volume of experimental and theoretical research. In particular, the analytical contributions of Bleich [8, 9] and the extensive tests at the University of Washington [10, 12, 13] have thrown much light on this complex subject.

The first Tacoma Bridge consisted of two shallow (8-ft) stiffening plate girders spaced 39 ft apart and supporting a solid deck near girder mid-depth. For the main span length (2,800 ft) the foregoing depth and width figures imply extraordinarily

shedding the bridge may vibrate in a vertical or torsional mode (Fig. 20.7*b* and *c*). The failure at Tacoma Narrows resulted from resonance between vortex action and a torsional mode of vibration.

It is by no means established that girder-stiffened suspension bridges cannot be designed to perform satisfactorily under all conditions. By providing slot openings in the otherwise solid deck structure, by locating the deck nearer to the top flange of the girder and adding a bottom lateral truss (for increased torsional rigidity), the girder-stiffened type may be found to be satisfactory. On the basis of tests to date, however, the truss-stiffened type seems to have important advantages.

e. Truss-stiffened Suspension Bridges. In the truss-stiffened suspension bridge, the plate girders (Fig. 20.7*a*) are replaced by open trusses having top and bottom chords which are, relatively, much shallower than the stiffening girders which they replace. It is convenient to make the trusses much deeper than the plate girders, thereby achieving a large gain in stiffness.

Elimination of the large blunt girders reduces the vortex phenomenon to a secondary, though not insignificant, role. It was discovered in tests and verified in an analytical development by Bleich [9] that the truss-stiffened bridge may experience the flutter phenomenon. Apparently the shallow deck approximates the flat-plate flutter behavior, with some modification to include the effect of small (vortex-induced) periodic forces at the leading edge.

By adding a bottom-chord lateral-truss system to the deep-truss-stiffened type of suspension system, a very great gain in torsional stiffness is achieved. It appears that this arrangement (deep-truss-stiffened, with bottom lateral truss) can provide complete safety from dangerous vibrations due to wind load.

REFERENCES

1. Den Hartog, J. P.: "Mechanical Vibrations," 4th ed., McGraw-Hill Book Company, Inc., New York, 1956.
2. Sherlock, R. H.: Variation of Wind Velocity and Gusts with Height, *Trans. ASCE*, vol. 118, 1953.
3. Roshko, A.: On the Drag and Shedding Frequency of Bluff Cylinders, *NACA TN* 3169, July, 1954.
4. Delaney, N. K., and N. E. Sorensen: Low Speed Drag of Cylinders of Various Shapes, *NACA TN* 3038, November, 1953.
5. Dockstader, E. A., W. F. Swiger, and E. Ireland: Resonant Vibration of Steel Stacks, *Proc. ASCE*, separate no. 541, November, 1954.
6. Price, P.: Suppression of the Fluid-induced Vibration of Circular Cylinders, *J. Eng. Mech.*, July, 1956.
7. Dickey, W. L., and G. B. Woodruff: The Vibration of Steel Stacks, *Proc. ASCE*, separate no. 540, November, 1954.

8. Bleich, F., and L. W. Teller: Structural Damping in Suspension Bridges, *Trans. ASCE*, vol. 117, 1952.
9. Bleich, F.: Dynamic Instability of Truss-stiffened Suspension Bridges under Wind Action, *Trans. ASCE*, vol. 114, 1949.
10. Aerodynamic Stability of Suspension Bridges, Progress Report of the Advisory Board on the Investigation of Suspension Bridges, *Trans. ASCE*, vol. 120, 1955.
11. Theodorsen, T.: General Theory of Aerodynamic Instability and the Mechanism of Flutter, *NACA TN* 496, 1935.
12. Vincent, G. S.: Mathematical Prediction of Suspension Bridge Behavior in Wind from Dynamic Section Model Tests, *Intern. Assoc. Bridge and Structural Eng.*, vol. 12, 1952.
13. Aerodynamic Stability of Suspension Bridges, *Univ. Washington Eng. Expt. Sta. Bull.* 116 (in several parts).

INDEX

- Absolute maximum work, 138
- Aerodynamic lift forces, 439
 - effect on structures of negative slope of curves for, 439-441
- Air blast, 234, 239, 240
 - clearing time, 253
 - duration, 246
 - dynamic pressure, 247, 248, 255
 - loading on structures, 249-278
 - diffraction, 239, 250
 - drag, 239, 267, 268
 - Mach numbers, 274
 - Mach stem, 244, 245, 249
 - overpressure, versus distance, 245
 - reflected, 247, 252
 - versus time, 243
 - Reynolds number ratio, 275
 - scaling, 247, 248
 - shock-front formation, 241
 - shock-front velocity, 242, 246
 - vortex formation, 250, 251
- Analog computers, 214-219
- Atomic bomb, 233
 - air blast, 234, 239
 - detonation of, 234
 - fire hazard from, 236
 - nuclear radiation, 235-285
 - thermal radiation, 234, 279-281
- Beam-bridge vibration, due to constant force moving at constant velocity, 419-421
 - due to sinusoidal force moving at constant velocity, 421-422
 - effect of major parameters on, 430-431
- Beam-bridge vibration, field test verification of, 424-430
 - model study verification of, 424
 - simplified deflection analysis of, 422-423
- Beams, determination of normal modes of vibration of, 113-114
 - characteristic loading for, 118
 - characteristic shapes for, 114-119
 - important properties of, 117-119
 - normalizing condition for, 118
 - orthogonality condition for, 118
 - simple end-supported beam, 114-116
 - two-span continuous beam, 116-117
- participation factor, 120
- reduced equation of motion, 121-122
 - use of characteristic shape functions to represent deflection and load functions, 119-120
- steel (*see* Bending strength of beams)
- transformation factors for, 160-162
- Behavior of reinforced concrete
 - columns, 37-40
 - concentric rapid loading, 40
 - concentric static loading, 37
 - eccentric rapid loading, 40
 - eccentric static loading, 38
- Bending strength of beams, steel, 8-9, 13
 - effect on, of direct stress, 15-16
 - of shear, 9
- Blast damage, 287-293
 - at Hiroshima, 287-289

- Blast damage, from large-yield weapons, 292-293
 - at Nagasaki, 289-290
 - in Nevada tests, 290-292
- Blast-resistant construction, 295
 - arch and dome, 296
 - buried, 295
 - column design, 313, 316-318
 - connection details, 319
 - foundations, 303-305, 319-322
 - personnel shelters, 300
 - program of, criteria for, 294
 - rigid frame, 296
 - roof girder, 313-316
 - roof purlin, 311-312
 - roof slab, 308-310
 - semiburied, 295
 - wall slab, 307-308
- Bolts, strength of, 17
- Bond between reinforcing bars and concrete, 44
- Buckling, beam-columns, 16
 - columns, 13-14
 - lateral (beams), 10-13
 - local, 9-10, 13
- Building codes (*see* Earthquake provisions in building codes)
- Characteristic loading, defined, 86
 - use of, to represent dynamic loadings, 95-101
 - to represent static loadings, 92-95
- Characteristic shape of mode defined, 82, 104
 - (*See also* Beams)
- Circular frequency defined, 56
- Columns, steel, 13-16
 - axially loaded, 13-15
 - beam-, 15-16
- Compressive strength of concrete, 21
 - for rapid loading, 23
 - for repeated loading, 23
 - for static loading, 21
- Concentrated-mass systems defined, 73
- Connections, steel, 17
 - fatigue of, 18
- Damped forced vibration, defined, 54
 - of one-degree system, 59
- Damped free vibration defined, 54
- Damped vibration, steady-state, 63
 - transient-state, 63
- Damping, effect on structural response, 126
 - sources of, 443
 - viscous, 59
- Deflection equations for concentrated-mass systems, 81, 105
- Deflection method, 143-146
- Deflection ratio, 143
- Degree of freedom, 53
- Detonation of atomic bomb, 234
- Difference equations, 202-206
- Differential equation of motion for beams, 111-113
- Diffraction loading, air blast, 239, 250
- Digital computers, 219-229
- Drag coefficients, 265
 - for arches, 271-274
 - for domes, 278
- Drag loading, 239, 267-268
- Ductility ratio, 301-302
 - test data, 302
- Dynamic air-blast pressure, 247, 248, 255
- Dynamic coupling, 74
- Dynamic-load factor, 58, 145
 - for gradually applied load, 67
 - for rectangular pulse load, 67
 - for suddenly applied load, 66
 - for triangular pulse load, 68
- Dynamic reactions, 149, 153
- Earthquake effects on structures, on Daiwa department store, 347-356
 - general, 345-346
- Earthquake provisions in building codes, 358-362
 - Japanese Building Code, 362-372
 - Joint Committee Code for Lateral Forces, 373-378
 - Uniform Building Code, 358-362

- Earthquake-resistant design methods, 380-385
 - comparison of aseismic design by different codes, 409-413
 - dynamic, 380-382
 - earthquake-spectrum technique, 381
 - numerical-integration method, 381
 - phase-plane-delta method, 381
 - example of design of actual building, 394-408
 - miscellaneous design considerations, 414
 - statical, 382-385
 - Architectural Institute of Japan (AIJ) method, 384-385
 - cantilever method, 382
 - factor method, 383-384
 - modified portal method, 382-383
 - portal method, 382
- Earthquakes, description of, 337
 - geographical distribution of, 338
 - intensity of, 340
 - intensity scales, Japanese, 341
 - modified Mercalli, 341
 - magnitude, 340
 - spectrum and spectrum intensity, 342
 - waves, 338
- Endurance limit, 18
- Energy, absorbed, 141
 - kinetic, 137
 - strain, 141
- Energy method, 135-143
- Equations of motion for concentrated-mass systems, 84, 105
- External work done, 136
- Fatigue, 17-18
- Flat slabs, 164, 167
- Flexibility coefficients defined, 81
- Flexural behavior of reinforced concrete, 27
 - bending strength, rapid loading, 33
 - static loading, 31
- Flutter, structures subject to, 442
- Forced part of response solution, 57
- Foundations, 303-305, 319-322
- Frames, 164
- Free part of response solution, 57
- Frequency defined, 56
- Frequency equation, 77, 82
- Idealized systems, 132-135, 146-153, 158-167
 - accuracy of, 156-158
- Impact, dynamic response caused by, 127-130
 - elastic, 127
 - energy-absorbed ratio, 129
 - plastic, 128
- Impact factor (or fraction), 416-418
- Karman vortex trail, 437
 - effect on structures, 437-439
- Kinetic energy, 137
- Limit design of steel structures, xviii
- Limitations of response theory, 51-52
- Load, dynamic, various types, im-
 - pactive, 54
 - impulsive, 54
 - nonperiodic, 54
 - periodic, 54
 - pure impulsive, 136
- Load factor, 148-150
- Loading, from air blast, 249
 - on arches, 269
 - on back wall, 257-258
 - diffraction, 239, 250
 - on domes, 276-278
 - drag, 239, 267-268
 - on front wall, 257
 - on open structures, 266
 - on roof, 260
 - on side walls, 265
 - as compared to load, 85*n*.
- (See also Characteristic loading)
- Loading machines, 331-333

- Mach numbers, 274
- Mach stem, 244, 245, 249
- Mass factor, 148, 151
- Modulus of elasticity of concrete, 22
- Multidegree systems, 177-179

- Natural period, 176-177
- Normal mode of vibration, definition of, 75
 - determination of, for beams (*see* Beams)
- Normalized amplitudes, 79
- Normalized characteristic loads defined, 87, 105
- Normalizing condition, 87, 105
- Nuclear radiation, 235, 282-285
 - fallout, 285
 - gamma rays, 282
 - attenuation of, 284
 - neutrons, 283
 - protection required, 285
- Numerical integration, 185-212
 - acceleration methods, 185-195
 - acceleration-pulse, 195
 - constant-acceleration, 187
 - constant-velocity, 190
 - linear-acceleration, 188
 - Newmark β , 193
- checking procedures, 209-210
- errors, 207-209
- other methods of, for second-order differential equations, 196-207
 - Adams-Stormer, 206
 - Euler, 202
 - finite differences, 206
 - Gill, 200
 - Heun, 200
 - Kutta, 199
 - Milne, 198
 - Runge, 199
 - Taylor series, 197
- selection, of method, 211-212
 - of time intervals, 210-211
- starting procedure, 207

- Orthogonality condition, 79, 86, 105

- Participation factor defined, 93, 105
- Period, defined, 56
 - of vibration of buildings, 343
- Personnel shelters, 300
- Plastic modulus, 9
- Plastic theory of reinforced-concrete design, xvii

- Radioactive fallout, 285
- Reduced equation of motion, 101
- Resistance factor, 148, 152
- Response, computed by step-by-step procedures, 70-72
 - defined, 54
 - produced by support vibration, 108-110
- Response solution, forced part of, 57
 - free part of, 57
- Response theory, limitations of, 51-52
 - recapitulation for concentrated-mass systems, 103-108
- Reynolds-number ratio, 275
- Rivets, strength of, 17

- Shear behavior of reinforced concrete, 34
 - shear strength, 35
 - web reinforcement, 35
- Shear strength, of beams, steel, 9
 - of concrete, 25
- Shear walls and deep beams, 40
- Shear yield stress of steel, 5, 7
- Shock tubes, 328, 329
- Smokestacks, vibration of, 445
- Spring constant, 148, 152
 - effective, 163
- Static coupling, 74
- Static-mode loadings defined, 95, 105
- Stiffness coefficients defined, 84
- Stodola's procedure, 87-92
- Strain, ultimate, of concrete, 22
- Strain energy, 141

- Strength, of bolts, 17
 of reinforcing steel, 25
 for rapid loading, 27
 for repeated loading, 26
 for static loading, 25
of rivets, 17
ultimate, structural design for, xvii
of welds, 17
- Stress-strain curve for steel, dynamic
 loading, 6
 static loading, 4
- Strouhal number, 437
- Structural design defined, xvi
- Suspension bridges, girder stiffened,
 vibration of, 446
 truss stiffened, vibration of, 447
- Tensile strength of concrete, 24
 for rapid loading, 25
 for repeated loading, 25
 for static loading, 24
- Thermal radiation, 234, 279-281
 effect on materials, 280-281
 levels of, 280
- Time factor associated with response
 caused by initial motion, 98
- Towers (nonguyed) subject to wind
 gusts, 444-445
- Transformation factors, 146-153, 158-
 167
 for beams, 160-162
 for flat slabs, 164
 for frames, 164
 for two-way slabs, 164-166
- Transmission lines, singing of, 445
- Two-way slabs, 164-166
- Ultimate strain of concrete, 22
- Ultimate strength, structural design
 for, xvii
- Undamped forced vibration, defined,
 54
 of one-degree system, 56
- Undamped free vibration, defined, 54
 of one-degree system, 55-56
 of two-degree system, 74-79
- Undamped one-degree system,
 response due to support vibra-
 tions of, 69
- Vibration defined, 54
- Viscous damping, 59
- Welds, strength of, 17
- Wind forces, characteristics of,
 dynamic, 436-442
 static, 434-436
- Wind gusts, nonguyed towers subject
 to, 444-445
 structures sensitive to, 436-437
- Work, absolute maximum, 138
- Work-done ratio, 138
- Yield stress of steel, 4-5
 effect of rate of strain on, 6-7



"A book that is shut is but a block"

CENTRAL ARCHAEOLOGICAL LIBRARY

GOVT. OF INDIA
Department of Archaeology
NEW DELHI.

Please help us to keep the book
clean and moving.

S. B. 148. N. DELHI.